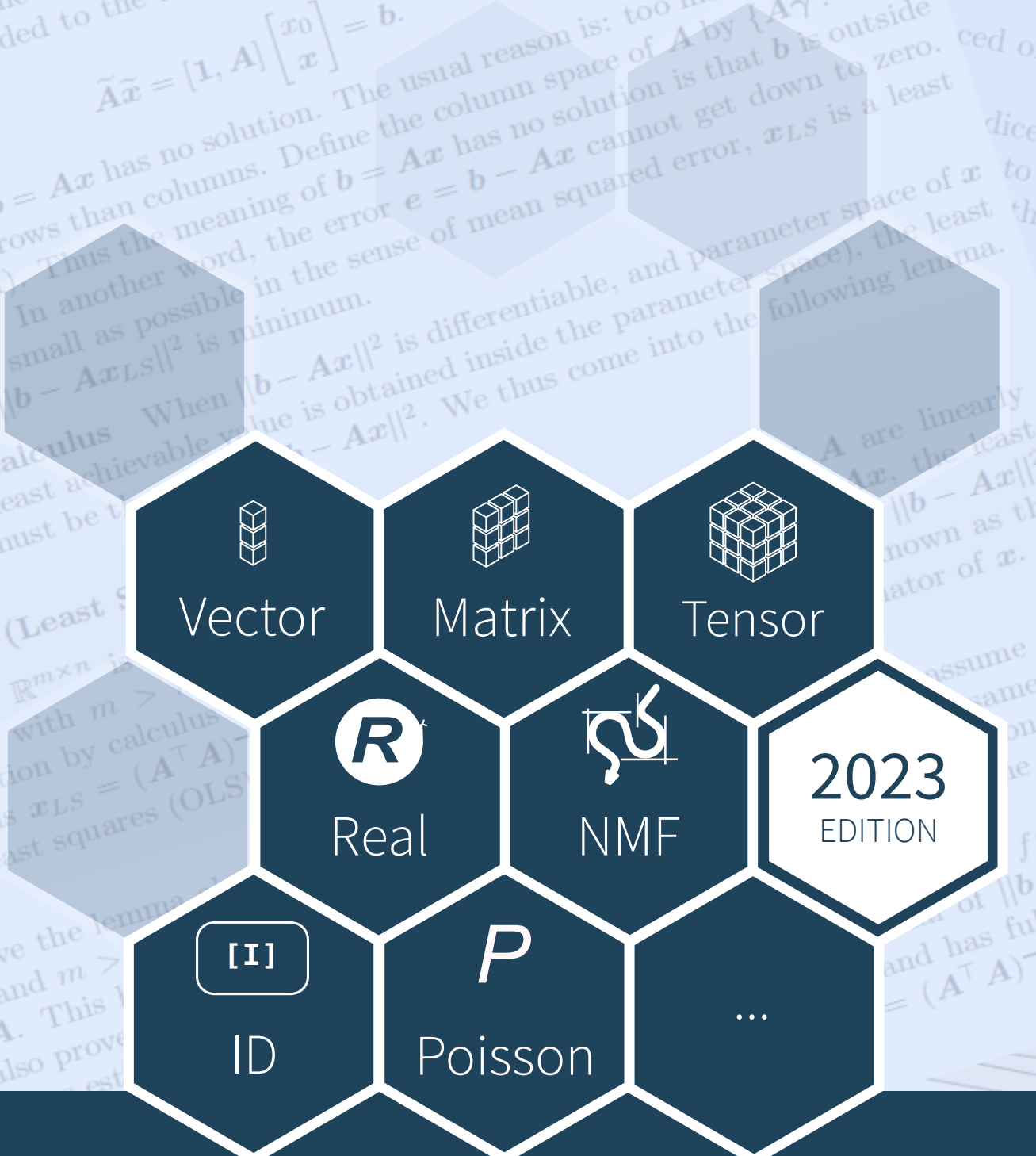


arXiv:2302.11337v2 [math.NA] 21 Jan 2024

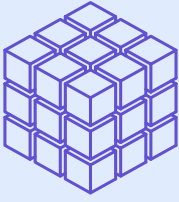


Bayesian Matrix Decomposition and Applications

Jun Lu

License by





Bayesian Matrix Decomposition and Applications

Jun Lu

JUN.LU.LOCKY@GMAIL.COM

© 2023 JUN LU

VERSION 0.1

In 1954, Alston S. Householder published *Principles of Numerical Analysis*, an early and influential work on matrix decomposition, specifically favoring (block) LU decomposition—a method that factorizes a matrix into the product of lower and upper triangular matrices. Today, matrix decomposition stands as a foundational technology in machine learning, driven significantly by the backpropagation algorithm’s development for neural network fitting. It plays a crucial role in reducing data dimensionality and representing it in a format more amenable to machine learning algorithms.

Bayesian matrix decomposition is a relatively new field within the broader area of matrix decomposition and machine learning. The concept of Bayesian matrix decomposition is rooted in Bayesian statistics, in which case it integrates the principles of Bayesian statistics with matrix decomposition methods to perform matrix factorization. The use of Bayesian methods in matrix decomposition was first introduced in the early 2000s, with the aim of addressing the limitations of traditional matrix factorization techniques, e.g., limited explanatory and predictive performance.

The sole aim of this book is to provide a self-contained introduction to concepts and mathematical tools in Bayesian matrix decomposition in order to seamlessly introduce matrix decomposition techniques and their applications in subsequent sections. However, given the limited scope to provide this discussion, we clearly recognize our inability to cover all the fascinating and useful conclusions regarding Bayesian matrix decomposition, such as the separated analysis of variational inference for carrying out the optimization. We refer the reader to literature in the field of Bayesian analysis for a more detailed introduction to the related fields.

Primarily, this book serves as a summary of the purpose and significance of key Bayesian matrix decomposition methods, including real-valued decomposition, nonnegative matrix factorization, and Bayesian interpolative decomposition. It delves into the origin and complexity of these methods, shedding light on their practical applications. The only mathematical prerequisite is a first course in statistics and linear algebra, ensuring accessibility with rigorous proofs provided throughout the development.

Keywords

Bayesian inference, Gibbs sampling, Conjugate model, Alternating least squares (ALS), Multiplicative update, Real-valued matrix decomposition, Nonnegative matrix decomposition, Interpolative decomposition, Ordinal matrix decomposition, Poisson matrix decomposition.

Acknowledgment: We would like to express gratitude towards Ulrich Paquet for providing information on Bayesian ordinal matrix decomposition and towards Gilbert Strang for discussing the proof of the CUR decomposition. Additionally, we would like to thank Federico Poloni for his comment on the proof of alternating least squares. The author also wishes to acknowledge the cooperation of Joerg Osterrieder, Christine P. Chai, and Xuanyu Ye towards the Bayesian approach for nonnegative matrix factorization and interpolative decomposition. Their cooperation has helped enlighten the form of many discussions in the book.

Contents

I	Backgrounds	2
1	Introduction and Background	4
	Introduction and Background	5
	Chapter 1 Problems	18
2	Monte Carlo Methods	20
2.1	The Bayesian Approach	21
2.2	Approximate Inference	22
2.3	Monte Carlo (MC) Methods	23
2.3.1	Markov Chain Monte Carlo (MCMC)	24
2.3.2	MC V.S. MCMC	26
2.3.3	Gibbs Sampler	26
2.3.4	Adaptive Rejection Sampling (ARS)	27
2.4	Bayesian Appetizers	28
2.4.1	Beta-Bernoulli Model	29
2.4.2	Bayesian Linear Model with Zero-Mean Prior	32
2.4.3	Bayesian Linear Model with Semi-Conjugate Prior	34
2.4.4	Bayesian Linear Model with Full Conjugate Prior	36
	Chapter 2 Problems	37
3	Regular Probability Models and Conjugacy	38
3.1	Conjugate Priors	40
3.2	Regular Univariate Models and Conjugacy	40
3.3	Exponential and Conjugacy	56
3.4	Univariate Gaussian-Related Models	57
3.5	Multinomial Distribution and Conjugacy	66
3.5.1	Dirichlet Distribution	68
3.5.2	Posterior Distribution for Multinomial Distribution	69
3.6	Poisson and Multinomial	72

3.7	Multivariate Gaussian Distribution and Conjugacy	73
3.7.1	Multivariate Gaussian Distribution	74
3.7.2	Multivariate Student's t Distribution	77
3.7.3	Prior on Parameters of Multivariate Gaussian Distribution	78
3.7.4	Posterior Distribution of $\boldsymbol{\mu}$: Separated View	82
3.7.5	Posterior Distribution of $\boldsymbol{\Sigma}$: Separated View	83
3.7.6	Gibbs Sampling of the Mean and Covariance: Separated View	85
3.7.7	Posterior Distribution of $\boldsymbol{\mu}$ and $\boldsymbol{\Sigma}$ Under NIW: Unified View	85
3.7.8	Posterior Marginal Likelihood of Parameters	88
3.7.9	Posterior Marginal Likelihood of Data	89
3.7.10	Posterior Predictive for Data without Observations	89
3.7.11	Posterior Predictive for New Data with Observations	90
3.7.12	Further Optimization via the Cholesky Decomposition	91
	Chapter 3 Problems	92
II Non-Bayesian Matrix Decomposition		94
4	Alternating Least Squares	96
4.1	Preliminary: Least Squares Approximations	97
4.2	Netflix Recommender and Matrix Factorization	100
4.3	Regularization: Extension to General Matrices	105
4.4	Missing Entries and Rank-One Update	107
4.5	Vector Inner Product	109
4.6	Gradient Descent	109
4.7	Regularization: A Geometrical Interpretation	113
4.8	Stochastic Gradient Descent	115
4.9	Bias Term	117
4.10	Applications	119
4.10.1	Low-Rank Approximation	120
4.10.2	Movie Recommender	122
	Chapter 4 Problems	125
5	Nonnegative Matrix Factorization (NMF)	128
5.1	Nonnegative Matrix Factorization	129
5.2	NMF via Multiplicative Update (MU)	129
5.3	Regularization	131
5.4	Initialization	133
5.5	Movie Recommender Context	133
	Chapter 5 Problems	134
III Bayesian Matrix Decomposition		136
6	Bayesian Real Matrix Factorization	138
6.1	Introduction	139

6.2	All Gaussian (GGG) Model and Markov Blanket	141
6.3	All Gaussian Model with ARD Hierarchical Prior (GGGA)	148
6.4	All Gaussian Model with Wishart Hierarchical Prior (GGGW)	150
6.5	Gaussian Likelihood with Volume and Gaussian Priors (GVG)	153
	Chapter 6 Problems	154
7	Bayesian Nonnegative Matrix Factorization	156
7.1	Introduction	157
7.2	Gaussian Likelihood with Exponential Priors (GEE)	159
7.3	Gaussian Likelihood with Exponential Priors and ARD Hierarchical Prior (GEEA)	162
7.4	Gaussian Likelihood with Truncated-Normal Priors (GTT)	163
7.5	Gaussian Likelihood with Truncated-Normal and Hierarchical Priors (GTTN)	166
7.6	Gaussian Likelihood with Rectified-Normal Priors (GRR) and Hierarchical Prior (GRRN)	168
	7.6.1 Examples	173
7.7	Priors as Regularization	176
7.8	Gaussian ℓ_1^2 Norm (GL_1^2) Model	177
7.9	Gaussian ℓ_2^2 Norm (GL_2^2) and Gaussian ℓ_∞ Norm (GL_∞) Models	180
	7.9.1 Examples	184
7.10	Semi-Nonnegative Matrix Factorization	190
	7.10.1 Gaussian Likelihood with Exponential and Gaussian Priors (GEG)	190
	7.10.2 Gaussian Likelihood with Nonnegative Volume and Gaussian Priors (GnVG)	191
7.11	Nonnegative Matrix Tri-Factorization (NMTF)	191
	Chapter 7 Problems	195
8	Bayesian Poisson Matrix Factorization	196
8.1	Poisson Likelihood with Gamma Priors (PAA)	197
8.2	Poisson Likelihood with Gamma Priors and Hierarchical Gamma Priors (PAAA)	199
8.3	Properties of PAA or PAAA	200
8.4	Recommendation Systems	202
	Chapter 8 Problems	203
9	Bayesian Ordinal Matrix Factorization	204
9.1	Ordinal Likelihood with Gaussian Prior and Wishart Hierarchical Prior (OGGW)	205
	9.1.1 Ordinal Regression Likelihood	205
	9.1.2 Matrix Factorization Modeling on Latent Variables	207
	9.1.3 Gibbs Sampler	207
9.2	Properties of OGGW	209
	Chapter 9 Problems	210

10 Bayesian Interpolative Decomposition	212
10.1 Interpolative Decomposition (ID)	213
10.2 Existence of the Column Interpolative Decomposition	215
10.3 Skeleton/CUR Decomposition	219
10.4 Row ID and Two-Sided ID	220
10.5 Bayesian Low-Rank Interpolative Decomposition	221
10.5.1 Gibbs Sampler	225
10.5.2 Aggressive Update	227
10.5.3 Post-Processing	228
10.5.4 Bayesian ID with Automatic Relevance Determination	229
10.5.5 Examples for Bayesian ID	229
10.5.6 Hyper-parameters	231
10.5.7 Convergence and Comparative Analysis	232
10.6 Bayesian Intervened Interpolative Decomposition (IID)	233
10.6.1 Quantitative Problem Statement	234
10.6.2 Examples for Bayesian IID	235
Chapter 10 Problems	240
IV Appendix	242
A Appendix	244
A.1 Taylor's Expansion	245
A.2 Deriving the Dirichlet Distribution	246
A.2.1 Derivation	246
A.2.2 Properties of the Dirichlet Distribution	247
A.3 Existence of the Skeleton Decomposition	250

List of Figures

1.1	Two pairs of orthogonal subspaces in \mathbb{R}^n and \mathbb{R}^m . $\dim(\mathcal{C}(\mathbf{A}^\top)) + \dim(\mathcal{N}(\mathbf{A})) = n$ and $\dim(\mathcal{N}(\mathbf{A}^\top)) + \dim(\mathcal{C}(\mathbf{A})) = m$. The null space component goes to zero as $\mathbf{A}\mathbf{x}_n = \mathbf{0} \in \mathbb{R}^m$. The row space component goes to column space as $\mathbf{A}\mathbf{x}_r = \mathbf{A}(\mathbf{x}_r + \mathbf{x}_n) = \mathbf{b} \in \mathcal{C}(\mathbf{A})$	13
2.1	Rejection sampling. Figure is from Michael I. Jordan's lecture notes.	27
2.2	Adaptive rejection sampling. Figure is from Michael I. Jordan's lecture notes.	28
2.3	Beta probability density functions for different values of the parameters a and b . When $a = b = 1$, the beta distribution reduces to a <i>uniform distribution</i> in the support of $[0, 1]$. The mean, variance, and mode of the Beta distribution are $E[x] = \frac{a}{a+b}$, $\text{Var}[x] = \frac{ab}{(a+b+1)(a+b)^2}$, and $\text{mode}[x] = \frac{a-1}{(a-1)+(b-1)}$ if $a > 1, b > 1$, respectively.	29
2.4	The prior distribution is $\text{Beta}(x 2, 2)$. The posterior distributions for the three cases in Example 2.4.1 are $\text{Beta}(x 12, 2)$, $\text{Beta}(x 50, 4)$, and $\text{Beta}(x 188, 16)$, respectively.	31
3.1	Gaussian probability density functions for different values of the mean and variance parameters μ and σ^2	41
3.2	Student's t distribution for different values of the parameters ν and σ^2	43
3.3	Gamma and inverse-Gamma probability density functions for different values of the parameters r and λ	44
3.4	Normal-inverse-Gamma probability density functions by varying different parameters.	50
3.5	Chi-squared and inverse-Chi-squared probability density functions for different values of parameters.	51
3.6	Exponential probability density functions for different values of the rate parameter λ	57
3.7	Truncated-normal and general-truncated-normal probability density functions for different values of the parameters μ and τ	59

3.8 Mean of truncated-normal and general-truncated-normal distribution by varying $\mu, \tau, a,$ and b parameters. 59

3.9 Half-normal and normal probability density functions for different values of the parameters μ and τ . The probability density of any value $x \geq \mu$ in the half-normal distribution is twice as that in the normal distribution with the same parameters μ, τ 61

3.10 Truncated-normal and rectified-normal probability density functions for different values of the parameters $\mu, \tau,$ and λ 63

3.11 Inverse-Gaussian probability density functions for different values of the parameters μ and λ 64

3.12 Laplace and skew-Laplace probability density functions for different values of the parameters. 65

3.13 Binomial probability mass functions for different values of the parameters N, π . 68

3.14 Density plots (blue=low, red=high) for the Dirichlet distribution over the probability simplex in \mathbb{R}^3 for various values of the concentration parameter α . When $\alpha = [c, c, c]$, the distribution is called a *symmetric Dirichlet distribution*, and the density is symmetric about the uniform probability mass function (i.e., occurs in the middle of the simplex). When $0 < c < 1$, there are sharp peaks of density almost at the vertices of the simplex. When $c > 1$, the density becomes monomodal and concentrated in the center of the simplex. And when $c = 1$, it is uniform distributed over the simplex. Finally, if α is not a constant vector, the density is not symmetric. 70

3.15 Draw of 5,000 points from Dirichlet distribution over the probability simplex in \mathbb{R}^3 for various values of the concentration parameter α 71

3.16 Poisson probability mass functions for different values of the parameter λ . . 73

3.17 Density and contour plots (blue=low, yellow=high) for the multivariate Gaussian distribution over the \mathbb{R}^2 space for various values of the covariance/scale matrix with zero-mean vector. Fig 3.17(a) and 3.17(d): A spherical covariance matrix has a circular shape; Fig 3.17(b) and 3.17(e): A diagonal covariance matrix is an **axis aligned** ellipse; Fig 3.17(c) and 3.17(f): A full covariance matrix has an elliptical shape. 75

3.18 Density and contour plots (blue=low, yellow=high) for the multivariate Gaussian distribution and multivariate Student's t distribution over the \mathbb{R}^2 space for various values of the covariance/scale matrix with zero-mean vector. Fig 3.18(a): A spherical covariance matrix has a circular shape; Fig 3.18(b): A diagonal covariance matrix is an **axis aligned** ellipse; Fig 3.18(c): A full covariance matrix has a elliptical shape; Fig 3.18(d) to Fig 3.18(f) for the Student's t distribution with the same scale matrix and increasing ν such that the difference between (a) and (f) in Fig 3.18(i) is approaching zero. . 79

4.1 Three functions. 99

4.2 Figure 4.2(a) shows surface and contour plots for a specific function (blue=low, yellow=high), where the upper graph is the surface plot, and the lower one is the projection of it (i.e., contour). Figure 4.2(b): $-\nabla L(\mathbf{z})$ pushes the loss to decrease for the convex function $L(\mathbf{z})$ 113

4.3	Constrained gradient descent with $\mathbf{z}^\top \mathbf{z} \leq C$. The green vector \mathbf{w} represents the projection of \mathbf{v}_1 into $\mathbf{z}^\top \mathbf{z} \leq C$, where \mathbf{v}_1 is the component of $-\nabla l(\mathbf{z})$ that is perpendicular to \mathbf{z}_1 . The image on the right illustrates the next step after the update in the left picture. \mathbf{z}^* denotes the optimal solution of $\{\min l(\mathbf{z})\}$.	114
4.4	Unit ball of ℓ_p norm in two-dimensional space. The ℓ_p norm over a vector \mathbf{x} is defined as $L_p(\mathbf{x}) = (\sum_i x_i ^p)^{1/p}$. When $p < 1$, the metric is not a norm since it does not meet the triangle inequality property of a norm definition.	115
4.5	Unit ball of ℓ_p norm in three-dimensional space. When $p < 1$, the metric is not a norm since it does not meet the triangle inequality property of a norm definition.	115
4.6	Constrained gradient descent with $\ \mathbf{z}\ _1 \leq C$, where the red dot denotes the breakpoint in ℓ_1 norm. The right picture illustrates the next step after the update in the left picture. \mathbf{z}^* denotes the optimal solution of $\{\min l(\mathbf{z})\}$.	116
4.7	Bias terms in alternating least squares, where the yellow entries denote ones (which are fixed), and the cyan entries denote the added features to fit the bias terms. The dotted boxes provide an example of how the bias terms work.	118
4.8	A gray flag image to be compressed. The size of the image is 600×1200 with a rank of 402.	119
4.9	Image compression for gray flag image into a rank-5 matrix via the SVD, and decompose into 5 parts where $\sigma_1 \geq \sigma_2 \geq \dots \geq \sigma_5$, i.e., $F_1 \leq F_2 \leq \dots \leq F_5$ with $F_i = \ \sigma_i \mathbf{u}_i \mathbf{v}^\top - \mathbf{A}\ _F$ for $i \in \{1, 2, \dots, 5\}$. And reconstruct images by single singular value and its corresponding left and right singular vectors, $\mathbf{c}_i \mathbf{r}_i^\top$, $\mathbf{w}_i \mathbf{z}_i^\top$ respectively. Upper: SVD; Middle: Pseudoskeleton; Lower: ALS.	120
4.10	Comparison of reconstruction errors measured by Frobenius norm among the SVD, pseudoskeleton, and ALS, where the approximated rank ranges from 3 to 100. ALS with well-selected parameters works similarly to SVD.	122
4.11	Image compression for gray flag image with different ranks.	123
4.12	Comparison of training and validation error for “MovieLens 100K” data set with different reduction dimensions and regularization parameters.	124
4.13	Distribution of the insample and outsample using cosine and Pearson similarity, and the Precision-Recall curves for them.	125
6.1	Graphical model representation of the GGG model. Green circles denote prior variables, orange circles represent observed and latent variables, and plates represent repeated variables. The slash “/” in the variable represents “or.”	142
6.2	The Markov blanket of a directed acyclic graphical (DAG) model. In a Bayesian network, the Markov blanket of node A includes its parents, children, and the other parents of all of its children . That is, the nodes in the cycle are in the Markov blanket of node A . The figure is due to wikipedia page of Markov blanket.	143

6.3 Graphical model representation of GGGA and GGGW models. Green circles denote prior variables, orange circles represent observed and latent variables, and plates represent repeated variables. The slash “/” in the variable represents “or,” and the comma “,” in the variable represents “and.” 148

6.4 Graphical representation of GVG model. Green circles denote prior variables, orange circles represent observed and latent variables, and plates represent repeated variables. The slash “/” in the variable represents “or.” 153

7.1 Graphical model representation of GEE and GEEA models. Green circles denote prior variables, orange circles represent observed and latent variables, and plates represent repeated variables. The slash “/” in the variable represents “or.” 158

7.2 Graphical model representation of GTT and GTTN models. Green circles denote prior variables, orange circles represent observed and latent variables, and plates represent repeated variables. The slash “/” in the variable represents “or,” and the comma “,” in the variable represents “and.” 164

7.3 Graphical model representation of GTTN with same and different hyperparameters. Green circles denote prior variables, orange circles represent observed and latent variables, and plates represent repeated variables. The slash “/” in the variable represents “or,” and the comma “,” in the variable represents “and.” 167

7.4 Graphical representation of GRR and GRRN models. Green circles denote prior variables, orange circles represent observed and latent variables, and plates represent repeated variables. The slash “/” in the variable represents “or,” and the comma “,” in the variable represents “and.” 169

7.5 Data distribution of MovieLens 100K and MovieLens 1M data sets. The MovieLens 1M data set has a higher fraction of users who give a rate of 5 and a lower fraction for rates of 3. 173

7.6 Convergence of the models on the MovieLens 100K (upper) and the MovieLens 1M (lower) data sets, measuring the training data fit (mean squared error). When increasing latent dimension K , the GRRN continues to improve the performance; while other models start to decrease on the MovieLens 100K data set or stop increasing on the MovieLens 1M data set. 174

7.7 Ratio of the variance of data to the MSE of the predictions. The higher the better. All models perform similarly. Similar results can be found on the MovieLens 1M data set and other K values and we shall not repeat the details. 175

7.8 Predictive results on the MovieLens 100K (upper) and MovieLens 1M (lower) data sets with the least fractions of unobserved data being 0.928 and 0.953, respectively (see Table 7.2 for the data description). We measure the predictive performance (mean squared error) on a held-out data set for different fractions of unobserved data. The blue and red arrows compare the MSEs of GTTN and GRRN models when the fractions of unobserved data are 0.96 and 0.98, respectively. 176

7.9 Graphical model representation of GL_1^2 , GL_2^2 , GL_∞ , and $GL_{2,\infty}^2$ models. Green circles denote prior variables, orange circles represent observed and latent variables, and plates represent repeated variables. The slash “/” in the variable represents “or.” 178

7.10 Data distribution of GDSC IC_{50} and Gene Body Methylation data sets. . . 185

7.11 Convergence of the models on the GDSC IC_{50} (upper) and the distribution of factored \mathbf{W} (lower), measuring the training data fit (mean squared error). When we increase the latent dimension K , the GEE, GL_2^2 , and $GL_{2,\infty}^2$ algorithms continue to increase the performance; while GL_1^2 starts to decrease. The results of GL_∞ and $GL_{2,\infty}^2$ models are similar so we only present the results of the $GL_{2,\infty}^2$ model for brevity. 186

7.12 Convergence of the models on the Gene Body Methylation data set (upper) and the distribution of factored \mathbf{W} (lower), measuring the training data fit (mean squared error). When we increase the latent dimension K , all the models continue to improve the performance. 187

7.13 Predictive results on the **GDSC IC_{50}** (upper) and **Gene Body Methylation** (lower) data sets. We measure the predictive performance (mean squared error) on a held-out data set for different fractions of unobserved data. 189

7.14 Ratio of the variance of data to the MSE of the predictions, the higher the better. 190

7.15 Graphical model representation of GEG and GnVG models. Green circles denote prior variables, orange circles represent observed and latent variables, and plates represent repeated variables. The slash “/” in the variable represents “or.” 191

7.16 Graphical model representation of GEEE and GEEEA models. Green circles denote prior variables, orange circles represent observed and latent variables, and plates represent repeated variables. The slash “/” in the variable represents “or,” and the comma “,” in the variable represents “and.” 192

8.1 Graphical model representations of PAA and PAAA models. Green circles denote prior variables, orange circles represent observed and latent variables, and plates represent repeated variables. 198

8.2 Gamma probability density functions $\mathcal{G}(\alpha, \beta)$ by reducing the shape parameter α 201

8.3 User activity and item popularity for the “MovieLens 1M” data set (see data description in Table 7.2, p. 173). 202

9.1 Graphical representation of the ordinal regression model. 206

9.2 Ordinal probability of the ordinal regression model in Equation (9.3). . . . 206

9.3 Graphical representation of OGGW model. Green circles denote prior variables, orange circles represent observed and latent variables, and plates represent repeated variables. The slash “/” in the variable represents “or,” and the comma “,” in the variable represents “and.” 208

10.1	Demonstration of the column ID of a matrix, where the yellow vector denotes the linearly independent columns of \mathbf{A} , white entries denote zero, and purple entries denote one.	214
10.2	Demonstration of the skeleton decomposition of a matrix, where the yellow vectors denote the linearly independent columns of \mathbf{A} , and green vectors denote the linearly independent rows of \mathbf{A}	220
10.3	Demonstration of the interpolative decomposition of a matrix, where the yellow vector denotes the basis columns of matrix \mathbf{A} , white entries denote zero, purple entries denote one, blue and black entries denote elements that are not necessarily zero. The Bayesian ID models find the approximation $\mathbf{A} \approx \mathbf{XY}$, while the post-processing procedure calculates the approximation $\mathbf{A} \approx \mathbf{CW}$	223
10.4	Graphical representation of GBT and GBTN models. Orange circles represent observed and latent variables, green circles denote prior variables, and plates represent repeated variables. The slash “/” in the variable represents “or,” and the comma “,” in the variable represents “and.” Parameters a and b are fixed with $a = -1$ and $b = 1$ in our case; while a weaker construction can set them to $a = -2$ and $b = 2$	224
10.5	Data distribution of CCLE <i>EC50</i> , CCLE <i>IC50</i> , Gene Body Methylation, and Promoter Methylation data sets.	231
10.6	Convergence results (upper), sampling mixing analysis (middle), and reconstructive results (lower) on the CCLE <i>EC50</i> , CCLE <i>IC50</i> , Gene Body Methylation, and Promoter Methylation data sets for various latent dimensions.	232
10.7	Convergence results (upper), and sampling mixing analysis (lower) on the SH510050, SH510300, SH601939, SH601628, and SH601328 data sets for a latent dimension of $K = 10$	237
10.8	Portfolio values of the ten assets (left), and the portfolio values (right) of different methods, where we split by in-sample and out-of-sample periods, and initialize with a unitary value for each period. The IID performs better in the out-of-sample period (see also Table 10.5).	238

This section provides a concise reference describing notation used throughout this book. If you are unfamiliar with any of the corresponding mathematical concepts, the book describes most of these ideas in Chapter 1 (p. 4).

Numbers and Arrays

a	A scalar (integer or real)
\mathbf{a}	A vector
\mathbf{A}	A matrix
\mathbf{I}_n	Identity matrix with n rows and n columns
\mathbf{I}	Identity matrix with dimensionality implied by context
\mathbf{e}_i	Standard basis vector $[0, \dots, 0, 1, 0, \dots, 0]$ with a 1 at position i
$\text{diag}(\mathbf{a})$	A square, diagonal matrix with diagonal entries given by \mathbf{a}
a	A scalar random variable
\mathbf{a}	A vector-valued random variable
\mathbf{A}	A matrix-valued random variable

Sets

\mathbb{A}	A set
\emptyset	The null set
\mathbb{R}	The set of real numbers
\mathbb{N}	The set of natural numbers
\mathbb{C}	The set of complex numbers
$\{0, 1\}$	The set containing 0 and 1
$\{0, 1, \dots, n\}$	The set of all integers between 0 and n
$[a, b]$	The real interval including a and b
$(a, b]$	The real interval excluding a but including b
$\mathbb{A} \setminus \mathbb{B}$	Set subtraction, i.e., the set containing the elements of \mathbb{A} that are not in \mathbb{B}

Indexing

a_i	Element i of vector \mathbf{a} , with indexing starting at 1
\mathbf{a}_{-i}	All elements of vector \mathbf{a} except for element i
a_{ij}	Element i, j of matrix \mathbf{A}
$\mathbf{A}_{i,:}$	Row i of matrix \mathbf{A}
$\mathbf{A}_{:,i}, \mathbf{a}_i$	Column i of matrix \mathbf{A}

Linear Algebra Operations

\mathbf{A}^\top	Transpose of matrix \mathbf{A}
\mathbf{A}^+	Moore-Penrose pseudoinverse of \mathbf{A}
$\mathbf{A} \otimes \mathbf{B}$	Element-wise (Hadamard) product of \mathbf{A} and \mathbf{B}
$\det(\mathbf{A})$	Determinant of \mathbf{A}
$\text{rref}(\mathbf{A})$	Reduced row echelon form of \mathbf{A}
$\mathcal{C}(\mathbf{A})$	Column space of \mathbf{A}
$\mathcal{N}(\mathbf{A})$	Null space of \mathbf{A}
\mathcal{V}	A general subspace
$\text{rank}(\mathbf{A})$	Rank of \mathbf{A}
$\text{tr}(\mathbf{A})$	Trace of \mathbf{A}

Calculus

$\frac{dy}{dx}$	Derivative of y with respect to x
$\frac{\partial y}{\partial x}$	Partial derivative of y with respect to x
$\nabla_{\mathbf{x}}y$	Gradient of y with respect to \mathbf{x}
$\nabla_{\mathbf{X}}y$	Matrix derivatives of y with respect to \mathbf{X}
$\frac{\partial f}{\partial \mathbf{x}}$	Jacobian matrix $\mathbf{J} \in \mathbb{R}^{m \times n}$ of $f : \mathbb{R}^n \rightarrow \mathbb{R}^m$
$\nabla_{\mathbf{x}}^2 f(\mathbf{x})$ or $\mathbf{H}(f)(\mathbf{x})$	The Hessian matrix of f at input point \mathbf{x}
$\int f(\mathbf{x})d\mathbf{x}$	Definite integral over the entire domain of \mathbf{x}
$\int_{\mathbb{S}} f(\mathbf{x})d\mathbf{x}$	Definite integral with respect to \mathbf{x} over the set \mathbb{S}

Probability and Information Theory

$a \perp b$	The random variables a and b are independent
$a \perp b \mid c$	They are conditionally independent given c
$P(a)$	A probability distribution over a discrete variable
$p(a)$	A probability distribution over a continuous variable, or over a variable whose type has not been specified
$a \sim P$	Random variable a has distribution P
$E_{x \sim P}[f(x)]$ or $E[f(x)]$	Expectation of $f(x)$ with respect to $P(x)$
$\text{Var}[f(x)]$	Variance of $f(x)$ under $P(x)$
$\text{Cov}[f(x), g(x)]$	Covariance of $f(x)$ and $g(x)$ under $P(x)$
$H(x)$	Shannon entropy of the random variable x
$D_{\text{KL}}(P \parallel Q)$	Kullback-Leibler divergence of P and Q
$\mathcal{N}(\mathbf{x} \mid \boldsymbol{\mu}, \boldsymbol{\Sigma})$	Gaussian distribution over \mathbf{x} with mean $\boldsymbol{\mu}$ and covariance $\boldsymbol{\Sigma}$

Functions

$f : \mathbb{A} \rightarrow \mathbb{B}$	The function f with domain \mathbb{A} and range \mathbb{B}
$f \circ g$	Composition of the functions f and g
$f(\mathbf{x}; \boldsymbol{\theta})$	A function of \mathbf{x} parametrized by $\boldsymbol{\theta}$. (Sometimes we write $f(\mathbf{x})$ and omit the argument $\boldsymbol{\theta}$ to lighten notation)
$\log(x)$	Natural logarithm of x
$\sigma(x)$, Sigmoid(x)	Logistic sigmoid, i.e., $\frac{1}{1 + \exp\{-x\}}$
$\zeta(x)$	Softplus, $\log(1 + \exp\{x\})$
$\ \mathbf{x}\ _p$	ℓ_p norm of \mathbf{x}
$\ \mathbf{x}\ = \ \mathbf{x}\ _2$	ℓ_2 norm of \mathbf{x}
$\ \mathbf{x}\ = \ \mathbf{x}\ _1$	ℓ_1 norm of \mathbf{x}
$\ \mathbf{x}\ = \ \mathbf{x}\ _\infty$	ℓ_∞ norm of \mathbf{x}
x^+	Positive part of x , i.e., $\max(0, x)$
$u(x)$	Step function with value 1 when $x \geq 0$ and value 0 otherwise
$\mathbb{1}\{\text{condition}\}$	is 1 if the condition is true, 0 otherwise

Sometimes we use a function f whose argument is a scalar but apply it to a vector, matrix: $f(\mathbf{x})$, $f(\mathbf{X})$. This denotes the application of f to the array element-wise. For example, if $\mathbf{C} = \sigma(\mathbf{X})$, then $c_{ij} = \sigma(x_{ij})$ for all valid values of i and j .

Abbreviations

PD	Positive definite
PSD	Positive semidefinite
MCMC	Markov chain Monte Carlo
i.i.d.	Independently and identically distributed
p.d.f.	Probability density function
p.m.f.	Probability mass function
OLS	Ordinary least squares
NG	Normal-Gamma distribution
NIG	Normal-inverse-Gamma distribution
NIX	Normal-inverse-Chi-squared distribution
TN	Truncated-normal distribution
GTN	General-truncated-normal distribution
RN	Rectified-normal distribution
IW	Inverse-Wishart distribution
NIW	Normal-inverse-Wishart distribution
ALS	Alternating least squares
GD	Gradient descent
SGD	Stochastic gradient descent
MU	Multiplicative update
MSE	Mean squared error
NMF	Nonnegative matrix factorization
ID	Interpolative decomposition
IID	Intervened interpolative decomposition
BID	Bayesian interpolative decomposition

Part I

Backgrounds

1

Introduction and Background

Contents

Introduction and Background	5
Chapter 1 Problems	18

Introduction and Background

Matrix decomposition has become a core technology in various fields, including statistics (Banerjee and Roy, 2014; Gentle, 1998), optimization (Gill et al., 2021), clustering and classification (Li et al., 2009; Wang et al., 2013; Lu, 2021c), computer vision (Goel et al., 2020), and recommender system (Symeonidis and Zioupos, 2016). Its significance stems from its integration into machine learning applications (Goodfellow et al., 2016; Bishop, 2006). Machine learning algorithms, designed to uncover hidden patterns and relationships in data, often grapple with high-dimensional and complex datasets. Matrix decomposition techniques provide a way of reducing data dimensionality and representing it in a way that is easier for machine learning algorithms to process.

Matrix decomposition algorithms such as QR decomposition, singular value decomposition (SVD), alternating least squares (ALS), and nonnegative matrix factorization (NMF) provide a way of breaking down a matrix into a smaller set of constituent matrices that represent the underlying structure of data. These decomposed matrices can be used as features for machine learning algorithms, which can then learn the patterns and relationships in the data more effectively. This process can also help reduce the noise and redundancy in the data, making it easier for the machine learning algorithms to identify important patterns and relationships.

On the other hand, matrix decomposition can be applied to a variety of matrix-based problems, such as collaborative filtering and link prediction (Marlin, 2003; Lim and Teh, 2007; Mnih and Salakhutdinov, 2007; Raiko et al., 2007; Chen et al., 2009):

- In the context of collaborative filtering, matrix decomposition can be used to uncover hidden patterns in user-item matrices. For example, given a matrix of user ratings for different items, matrix decomposition algorithms can be used to infer the latent user preferences and item attributes. These latent variables can then be used to predict the ratings for unseen items, aiding in personalized suggestions for users (e.g., articles, movies, or musics).
- In link prediction problems, matrix decomposition algorithms can be used to uncover hidden patterns in networks. For example, given a network of users and their connections, matrix decomposition methods can be used to infer latent user preferences, which can then be used to predict new links in the network.

A (bilinear) matrix decomposition is a way of reducing a complex matrix into its constituent parts, which are in simpler forms and represent the original matrix as a product of two (or more) *factor matrices*. The underlying principle of the decompositional approach to matrix computation is that it is not the business of the matrix algorithmists to solve particular problems, but it is an approach that can simplify more complex matrix operations, which can be performed on the decomposed parts rather than on the original matrix itself. For example, a matrix decomposition, which though is usually expensive to compute, can be reused to solve new problems involving the original matrix in different scenarios, e.g., as long as the factorization of \mathbf{A} is obtained, it can be reused to solve the set of linear systems $\{\mathbf{b}_1 = \mathbf{A}\mathbf{x}_1, \mathbf{b}_2 = \mathbf{A}\mathbf{x}_2, \dots, \mathbf{b}_k = \mathbf{A}\mathbf{x}_k\}$.

There are two main approaches that have been applied to inference in the (low-rank) matrix factorization task. The first is to define a loss function and optimize over the factored components using alternating updates (Comon et al., 2009; Lee and Seung, 1999).

The second is to build a probabilistic model representing the matrix factorization and then to perform statistical inference to compute any desired components (Salakhutdinov and Mnih, 2008; Ari et al., 2012).

Another core application of matrix decomposition in machine learning is that it provides a way of incorporating prior knowledge into the machine learning algorithms. For example, in *Bayesian matrix decomposition (BMD, or Bayesian matrix factorization, BMF)*, prior information about sparsity or nonnegativity can be encoded into the model, allowing the algorithms to make more informed decisions and produce better results.

Traditional matrix factorization methods, such as SVD and NMF, have proven successful in capturing inherent structures. However, these methods often face challenges in handling missing or incomplete data, modeling uncertainties, and incorporating prior knowledge. Bayesian matrix factorization emerges as a powerful and flexible framework that addresses these challenges by integrating Bayesian principles into the factorization process.

Bayesian matrix decomposition is a probabilistic model that decomposes a matrix into its constituent parts. It was initially discussed in a factor analysis context (Canny, 2004; Dunson and Herring, 2005) and in a matrix completion context (Zhou et al., 2010). BMD is a generative graphical model that can be used to infer the low-dimensional latent factors from a matrix, such as user preferences and item attributes. It has been successfully applied to a variety of problems such as matrix completion, inpainting, denoising, and super-resolution. The model is based on a Bayesian framework, and the inference is mainly optimized using Markov chain Monte Carlo (MCMC) methods.

Given a data matrix \mathbf{A} , the bilinear matrix decomposition considers factoring it as $\mathbf{A} = \mathbf{W}\mathbf{Z}$. By Bayesian approaches, the minimization problem of finding factored matrices \mathbf{W} and \mathbf{Z} is described by probabilistic approaches as trying to infer the distributions over latent variables \mathbf{W} and \mathbf{Z} after observing the data matrix \mathbf{A} . Bayesian approaches extend this by placing prior distributions over latent variables \mathbf{W} and \mathbf{Z} , in which case we can either try to infer a *point estimate* of a *maximum likelihood estimator* by maximizing the likelihood $\max_{\mathbf{W}, \mathbf{Z}} p(\mathbf{A} | \mathbf{W}, \mathbf{Z})$; or of a *maximum a posteriori estimator* by $\max_{\mathbf{W}, \mathbf{Z}} p(\mathbf{W}, \mathbf{Z} | \mathbf{A})$; or find the full posterior distribution $p(\mathbf{W}, \mathbf{Z} | \mathbf{A})$.

Bayesian matrix decomposition approaches use a likelihood distribution to capture noise in the data, e.g., use a Poisson likelihood for count data, or a Gaussian likelihood for real-valued or nonnegative data. Based on the constraints, e.g., nonnegativity, count, sparsity, or ordinal values, different priors are placed over the entries in the factored components \mathbf{W} and \mathbf{Z} . In non-probabilistic matrix decomposition language, the likelihood can be regarded as a cost function (e.g., to minimize over the mean squared error), and the priors can be treated as a penalization term over the factored components (e.g., to favor a sparsity in \mathbf{W} and \mathbf{Z}). Situated within this book, our goal is to expand the repertoire of Bayesian matrix factorization algorithms.

In numerical matrix decomposition methods (Lu, 2021b), a matrix decomposition task on matrix \mathbf{A} can be cast as,

- $\mathbf{A} = \mathbf{Q}\mathbf{U}$: where \mathbf{Q} is an orthogonal matrix that contains the same column space as \mathbf{A} , and \mathbf{U} is a relatively simple and sparse matrix to reconstruct \mathbf{A} .

- $\mathbf{A} = \mathbf{Q}\mathbf{T}\mathbf{Q}^\top$: where \mathbf{Q} is orthogonal such that \mathbf{A} and \mathbf{T} are *similar matrices* that share the same properties such as same eigenvalues and sparsity. Moreover, working on \mathbf{T} is an easier task compared to that on \mathbf{A} .
- $\mathbf{A} = \mathbf{U}\mathbf{T}\mathbf{V}$: where \mathbf{U} and \mathbf{V} are orthogonal matrices such that the columns of \mathbf{U} and the rows of \mathbf{V} constitute an orthonormal basis for the column space and row space of \mathbf{A} , respectively.
- $\mathbf{A} = \mathbf{B} \mathbf{C}$: where \mathbf{B} and \mathbf{C} are full rank matrices that can reduce the memory storage of \mathbf{A} . In practice, a low-rank approximation $\mathbf{A} \approx \mathbf{D} \mathbf{F}$ can be employed, where $k < r$ is called the *numerical rank* of the matrix such that the matrix can be stored much more inexpensively and can be multiplied rapidly with vectors or other matrices. An approximation of the form $\mathbf{A} = \mathbf{D}\mathbf{F}$ is useful for storing the matrix \mathbf{A} more frugally (we can store \mathbf{D} and \mathbf{F} using $k(m+n)$ floating-point numbers, as opposed to mn numbers for storing \mathbf{A}), for efficiently computing a matrix-vector product $\mathbf{b} = \mathbf{A}\mathbf{x}$ (via $\mathbf{c} = \mathbf{F}\mathbf{x}$ and $\mathbf{b} = \mathbf{D}\mathbf{c}$), for data interpretation, and much more.

However, in Bayesian matrix decomposition, we consider simpler factorization forms, e.g., the (low-rank) real-valued factorization, nonnegative factorization, the factorization for count and ordinal data sets, and the Bayesian interpolative decomposition (ID).

The sole aim of this book is to provide a self-contained introduction to concepts and mathematical tools in Bayesian inference and matrix analysis in order to seamlessly introduce matrix decomposition (or factorization) techniques and their applications in subsequent sections. However, we clearly realize our inability to cover all the useful and interesting results concerning Bayesian matrix decomposition and given the paucity of scope to present this discussion, e.g., the separated analysis of the high-order Bayesian decomposition, nonparametric matrix factorization, and variational inference for Bayesian matrix decomposition. We refer the reader to literature in the field of Bayesian analysis for a more detailed introduction to the related fields. Some excellent examples include Rai et al. (2015); Qian et al. (2016); Lu (2021b); Takayama et al. (2022).

Notation and preliminaries. In the rest of this section, we will introduce and recap some basic knowledge about linear algebra related to matrix factorization. For the rest of the important concepts, we define and discuss them as per need for clarity. Readers with enough background in matrix analysis can skip this section. In the text, we simplify matters by considering only matrices that are real. Without special consideration, we assume throughout that $\|\cdot\| = \|\cdot\|_2$, i.e., the norm is an ℓ_2 norm or a Frobenius norm for vectors or matrices.

In all cases, scalars will be denoted in a non-bold font possibly with subscripts (e.g., a , α , α_i). We will use **boldface** lowercase letters possibly with subscripts to denote vectors (e.g., $\boldsymbol{\mu}$, \mathbf{x} , \mathbf{x}_n , \mathbf{z}) and **boldface** uppercase letters possibly with subscripts to denote matrices (e.g., \mathbf{A} , \mathbf{L}_j). The i -th element of a vector \mathbf{z} will be denoted by z_i in the non-bold font. In the meantime, the *normal fonts* of scalars denote **random variables** (e.g., a and b_1 are random variables, while italics a and b_1 are scalars); the normal fonts of **boldface** lowercase letters possibly with subscripts denote **random vectors** (e.g., \mathbf{a} and \mathbf{b}_1 are random vectors, while italics \mathbf{a} and \mathbf{b}_1 are vectors); and the normal fonts of **boldface** uppercase letters possibly

with subscripts denote **random matrices** (e.g., \mathbf{A} and \mathbf{B}_1 are random matrices, while italics \mathbf{A} and \mathbf{B}_1 are matrices).

Subarrays are formed when a subset of the indices is fixed. The i -th row and j -th column value of matrix \mathbf{A} (entry (i, j) of \mathbf{A}) will be denoted by a_{ij} . Furthermore, it will be helpful to utilize the **Matlab-style notation**, the i -th row to the j -th row and the k -th column to the m -th column submatrix of the matrix \mathbf{A} will be denoted by $\mathbf{A}_{i:j,k:m}$. A colon is used to indicate all elements of a dimension, e.g., $\mathbf{A}_{:,k:m}$ denotes the k -th column to the m -th column of the matrix \mathbf{A} , and $\mathbf{A}_{:,k}$ denotes the k -th column of \mathbf{A} . Alternatively, the k -th column of \mathbf{A} may be denoted more compactly by \mathbf{a}_k .

When the index is not continuous, given ordered subindex sets I and J , $\mathbf{A}[I, J]$ denotes the submatrix of \mathbf{A} obtained by extracting the rows and columns of \mathbf{A} indexed by I and J , respectively; and $\mathbf{A}[:, J]$ denotes the submatrix of \mathbf{A} obtained by extracting the columns of \mathbf{A} indexed by J , where the $[:, J]$ syntax in this expression selects all rows from \mathbf{A} and only the columns specified by the indices in J .

Definition 1.0.1 (Matlab Notation) Suppose $\mathbf{A} \in \mathbb{R}^{m \times n}$, and $I = [i_1, i_2, \dots, i_k]$ and $J = [j_1, j_2, \dots, j_l]$ are two index vectors, then $\mathbf{A}[I, J]$ denotes the $k \times l$ submatrix

$$\mathbf{A}[I, J] = \begin{bmatrix} a_{i_1, j_1} & a_{i_1, j_2} & \cdots & a_{i_1, j_l} \\ a_{i_2, j_1} & a_{i_2, j_2} & \cdots & a_{i_2, j_l} \\ \vdots & \vdots & \ddots & \vdots \\ a_{i_k, j_1} & a_{i_k, j_2} & \cdots & a_{i_k, j_l} \end{bmatrix}.$$

Whilst, $\mathbf{A}[I, :]$ denotes a $k \times n$ submatrix, and $\mathbf{A}[:, J]$ denotes a $m \times l$ submatrix analogously.

We note that it does not matter whether the index vectors I and J are row vectors or column vectors. It matters which axis they index (rows of \mathbf{A} or columns of \mathbf{A}). We should also notice the range of the index:

$$\begin{cases} 0 \leq \min(I) \leq \max(I) \leq m; \\ 0 \leq \min(J) \leq \max(J) \leq n. \end{cases}$$

And in all cases, vectors are formulated in a column rather than in a row. A row vector will be denoted by a transpose of a column vector such as \mathbf{a}^\top . A specific column vector with values is split by the semicolon symbol “;”, e.g., $\mathbf{x} = [1; 2; 3]$ is a column vector in \mathbb{R}^3 . Similarly, a specific row vector with values is split by the comma symbol “,”, e.g., $\mathbf{y} = [1, 2, 3]$ is a row vector with 3 values. Further, a column vector can be denoted by the transpose of a row vector e.g., $\mathbf{y} = [1, 2, 3]^\top$ is a column vector.

The transpose of a matrix \mathbf{A} will be denoted by \mathbf{A}^\top , and its inverse will be denoted by \mathbf{A}^{-1} . We will denote the $p \times p$ identity matrix by \mathbf{I}_p (or simply \mathbf{I} when the size can be determined from context). A vector or matrix of all zeros will be denoted by a **boldface** zero $\mathbf{0}$, whose size should be clear from context, or we denote $\mathbf{0}_p$ to be the vector of all zeros with p entries. Similarly, a vector or matrix of all ones will be denoted by a **boldface** one $\mathbf{1}$, whose size is clear from context, or we denote $\mathbf{1}_p$ to be the vector of all ones with p

entries. We will frequently omit the subscripts of these matrices when the dimensions are clear from context.

Linear Algebra

Definition 1.0.2 (Eigenvalue) *Given any vector space E and any linear map $\mathbf{A} : E \rightarrow E$ (or simply real matrix $\mathbf{A} \in \mathbb{R}^{m \times n}$), a scalar $\lambda \in K$ is called an eigenvalue, or proper value, or characteristic value of \mathbf{A} , if there exists some nonzero vector $\mathbf{u} \in E$ such that*

$$\mathbf{A}\mathbf{u} = \lambda\mathbf{u}.$$

In fact, real-valued matrices can have complex eigenvalues. However, all the eigenvalues of symmetric matrices are real (spectral theorem, see Lu (2021b)).

Definition 1.0.3 (Spectrum and Spectral Radius) *The set of all eigenvalues of \mathbf{A} is called the spectrum of \mathbf{A} and is denoted by $\Lambda(\mathbf{A})$. The largest magnitude of the eigenvalues is known as the spectral radius $\rho(\mathbf{A})$:*

$$\rho(\mathbf{A}) = \max_{\lambda \in \Lambda(\mathbf{A})} |\lambda|.$$

Definition 1.0.4 (Eigenvector) *A vector $\mathbf{u} \in E$ is called an eigenvector, or proper vector, or characteristic vector of \mathbf{A} , if $\mathbf{u} \neq 0$ and if there exists some $\lambda \in K$ such that*

$$\mathbf{A}\mathbf{u} = \lambda\mathbf{u},$$

where the scalar λ is then an eigenvalue. And we say that \mathbf{u} is an eigenvector associated with λ .

Moreover, the tuple (λ, \mathbf{u}) above is referred to as an **eigenpair**. Intuitively, these definitions imply that multiplying matrix \mathbf{A} by the vector \mathbf{u} results in a new vector that is in the same direction as \mathbf{u} , but only scaled by a factor λ . For any eigenvector \mathbf{u} , we can scale it by a scalar s such that $s\mathbf{u}$ remains an eigenvector of \mathbf{A} ; and for this reason we call the eigenvector an eigenvector of \mathbf{A} associated with eigenvalue λ . To avoid ambiguity, it is customary to assume that the eigenvector is normalized to have length 1 and the first entry is positive (or negative) since both \mathbf{u} and $-\mathbf{u}$ are eigenvectors.

In linear algebra, every vector space has a basis, and any vector within the space can be expressed as a linear combination of the basis vectors. We then define the span and dimension of a subspace via the basis.

Definition 1.0.5 (Subspace) *A nonempty subset \mathcal{V} of \mathbb{R}^n is called a subspace if $x\mathbf{a} + y\mathbf{b} \in \mathcal{V}$ for every $\mathbf{a}, \mathbf{b} \in \mathcal{V}$ and every $x, y \in \mathbb{R}$.*

Definition 1.0.6 (Span) *If every vector \mathbf{v} in subspace \mathcal{V} can be expressed as a linear combination of $\{\mathbf{a}_1, \mathbf{a}_2, \dots, \mathbf{a}_m\}$, then $\{\mathbf{a}_1, \mathbf{a}_2, \dots, \mathbf{a}_m\}$ is said to span \mathcal{V} .*

In this context, we will often use the idea of the linear independence of a set of vectors. Two equivalent definitions are given as follows.

Definition 1.0.7 (Linearly Independent) *A set of vectors $\{\mathbf{a}_1, \mathbf{a}_2, \dots, \mathbf{a}_m\}$ is called linearly independent if there is no combination that can yield $x_1\mathbf{a}_1 + x_2\mathbf{a}_2 + \dots + x_m\mathbf{a}_m = \mathbf{0}$ unless all x_i 's are equal to zero. An equivalent definition is that $\mathbf{a}_1 \neq \mathbf{0}$, and for every $k > 1$, the vector \mathbf{a}_k does not belong to the span of $\{\mathbf{a}_1, \mathbf{a}_2, \dots, \mathbf{a}_{k-1}\}$.*

Definition 1.0.8 (Basis and Dimension) *A set of vectors $\{\mathbf{a}_1, \mathbf{a}_2, \dots, \mathbf{a}_m\}$ is called a basis of \mathcal{V} if they are linearly independent and span \mathcal{V} . Every basis of a given subspace has the same number of vectors, and the number of vectors in any basis is called the dimension of the subspace \mathcal{V} . By convention, the subspace $\{\mathbf{0}\}$ is said to have a dimension of zero. Furthermore, every subspace of nonzero dimension has a basis that is orthogonal, i.e., the basis of a subspace can be chosen orthogonal.*

Definition 1.0.9 (Column Space (Range)) *If \mathbf{A} is an $m \times n$ real matrix, we define the column space (or range) of \mathbf{A} as the set spanned by its columns:*

$$\mathcal{C}(\mathbf{A}) = \{\mathbf{y} \in \mathbb{R}^m : \exists \mathbf{x} \in \mathbb{R}^n, \mathbf{y} = \mathbf{A}\mathbf{x}\}.$$

And the row space of \mathbf{A} is the set spanned by its rows, which is equivalent to the column space of \mathbf{A}^\top :

$$\mathcal{C}(\mathbf{A}^\top) = \{\mathbf{x} \in \mathbb{R}^n : \exists \mathbf{y} \in \mathbb{R}^m, \mathbf{x} = \mathbf{A}^\top \mathbf{y}\}.$$

Definition 1.0.10 (Null Space (Nullspace, Kernel)) *If \mathbf{A} is an $m \times n$ real matrix, we define the null space (or kernel, or nullspace) of \mathbf{A} as the set:*

$$\mathcal{N}(\mathbf{A}) = \{\mathbf{y} \in \mathbb{R}^n : \mathbf{A}\mathbf{y} = \mathbf{0}\}.$$

And the null space of \mathbf{A}^\top is defined as

$$\mathcal{N}(\mathbf{A}^\top) = \{\mathbf{x} \in \mathbb{R}^m : \mathbf{A}^\top \mathbf{x} = \mathbf{0}\}.$$

Both the column space of \mathbf{A} and the null space of \mathbf{A}^\top are subspaces of \mathbb{R}^m . In fact, every vector in $\mathcal{N}(\mathbf{A}^\top)$ is orthogonal to vectors in $\mathcal{C}(\mathbf{A})$, and vice versa.¹

Definition 1.0.11 (Rank) *The rank of a matrix $\mathbf{A} \in \mathbb{R}^{m \times n}$ is the dimension of its column space. That is, the rank of \mathbf{A} is equal to the maximum number of linearly independent columns of \mathbf{A} , and is also the maximum number of linearly independent rows of \mathbf{A} . The matrix \mathbf{A} and its transpose \mathbf{A}^\top have the same rank. A matrix \mathbf{A} is considered to have full rank if its rank equals $\min\{m, n\}$. Specifically, given a vector $\mathbf{u} \in \mathbb{R}^m$ and a vector $\mathbf{v} \in \mathbb{R}^n$, then the $m \times n$ matrix $\mathbf{u}\mathbf{v}^\top$ obtained by the outer product of vectors is of rank 1. In short, the rank of a matrix is equal to:*

1. Every vector in $\mathcal{N}(\mathbf{A})$ is also perpendicular to vectors in $\mathcal{C}(\mathbf{A}^\top)$, and vice versa.

- number of linearly independent columns;
- number of linearly independent rows.

And remarkably, these two quantities are always equal (see Theorem 1.1).

Definition 1.0.12 (Orthogonal Complement in General) The orthogonal complement \mathcal{V}^\perp of a subspace \mathcal{V} contains every vector that is perpendicular to \mathcal{V} . That is,

$$\mathcal{V}^\perp = \{\mathbf{v} : \mathbf{v}^\top \mathbf{u} = 0, \forall \mathbf{u} \in \mathcal{V}\}.$$

The two subspaces are disjoint that span the entire space. The dimensions of \mathcal{V} and \mathcal{V}^\perp add to the dimension of the entire space. Furthermore, $(\mathcal{V}^\perp)^\perp = \mathcal{V}$.

Definition 1.0.13 (Orthogonal Complement of Column Space) If \mathbf{A} is an $m \times n$ real matrix, the orthogonal complement of $\mathcal{C}(\mathbf{A})$, $\mathcal{C}^\perp(\mathbf{A})$, is the subspace defined as:

$$\begin{aligned} \mathcal{C}^\perp(\mathbf{A}) &= \{\mathbf{y} \in \mathbb{R}^m : \mathbf{y}^\top \mathbf{A}\mathbf{x} = \mathbf{0}, \forall \mathbf{x} \in \mathbb{R}^n\} \\ &= \{\mathbf{y} \in \mathbb{R}^m : \mathbf{y}^\top \mathbf{v} = \mathbf{0}, \forall \mathbf{v} \in \mathcal{C}(\mathbf{A})\}. \end{aligned}$$

Then we have the four fundamental spaces for any matrix $\mathbf{A} \in \mathbb{R}^{m \times n}$ of rank r , as delineated in Theorem 1.3. To establish the fundamental theorem of linear algebra, we first verify a crucial result: the equality between the row rank and the column rank of a matrix. This proof holds significance for subsequent developments.

Theorem 1.1: (Row Rank Equals Column Rank)

The dimension of the column space of a matrix $\mathbf{A} \in \mathbb{R}^{m \times n}$ is equal to the dimension of its row space, i.e., the row rank and the column rank of a matrix \mathbf{A} are equal.

Proof [of Theorem 1.1] We first notice that the null space of \mathbf{A} is orthogonal complementary to the row space of \mathbf{A} : $\mathcal{N}(\mathbf{A}) \perp \mathcal{C}(\mathbf{A}^\top)$ (where the row space of \mathbf{A} is exactly the column space of \mathbf{A}^\top), that is, vectors in the null space of \mathbf{A} are orthogonal to vectors in the row space of \mathbf{A} . To see this, suppose \mathbf{A} has rows $\{\mathbf{a}_1^\top, \mathbf{a}_2^\top, \dots, \mathbf{a}_m^\top\}$ and $\mathbf{A} = [\mathbf{a}_1^\top; \mathbf{a}_2^\top; \dots; \mathbf{a}_m^\top]$ is the row partition. For any vector $\mathbf{x} \in \mathcal{N}(\mathbf{A})$, we have $\mathbf{A}\mathbf{x} = \mathbf{0}$, that is, $[\mathbf{a}_1^\top \mathbf{x}; \mathbf{a}_2^\top \mathbf{x}; \dots; \mathbf{a}_m^\top \mathbf{x}] = \mathbf{0}$. And since the row space of \mathbf{A} is spanned by $\{\mathbf{a}_1^\top, \mathbf{a}_2^\top, \dots, \mathbf{a}_m^\top\}$. Then, \mathbf{x} is perpendicular to any vectors from $\mathcal{C}(\mathbf{A}^\top)$, which means $\mathcal{N}(\mathbf{A}) \perp \mathcal{C}(\mathbf{A}^\top)$.

Now suppose the dimension of row space of \mathbf{A} is r . Let $\{\mathbf{r}_1, \mathbf{r}_2, \dots, \mathbf{r}_r\}$ be a set of vectors in \mathbb{R}^n and form a basis for the row space. Then the r vectors $\{\mathbf{A}\mathbf{r}_1, \mathbf{A}\mathbf{r}_2, \dots, \mathbf{A}\mathbf{r}_r\}$ are in the column space of \mathbf{A} , which are linearly independent. To see this, suppose we have a linear combination of the r vectors: $x_1 \mathbf{A}\mathbf{r}_1 + x_2 \mathbf{A}\mathbf{r}_2 + \dots + x_r \mathbf{A}\mathbf{r}_r = \mathbf{0}$, that is, $\mathbf{A}(x_1 \mathbf{r}_1 + x_2 \mathbf{r}_2 + \dots + x_r \mathbf{r}_r) = \mathbf{0}$, and the vector $\mathbf{v} = x_1 \mathbf{r}_1 + x_2 \mathbf{r}_2 + \dots + x_r \mathbf{r}_r$ is in null space of \mathbf{A} . But since $\{\mathbf{r}_1, \mathbf{r}_2, \dots, \mathbf{r}_r\}$ is a basis for the row space of \mathbf{A} , \mathbf{v} is thus also in the row space of \mathbf{A} . We have shown that vectors from the null space of \mathbf{A} is perpendicular to vectors from the row space of \mathbf{A} ; thus, it holds that $\mathbf{v}^\top \mathbf{v} = 0$ and $x_1 = x_2 = \dots = x_r = 0$. Then $\mathbf{A}\mathbf{r}_1, \mathbf{A}\mathbf{r}_2, \dots, \mathbf{A}\mathbf{r}_r$ are in the column space of \mathbf{A} , and they are linearly independent, which means the dimension of the column space of \mathbf{A} is larger than r . This result shows that **row rank of $\mathbf{A} \leq$ column rank of \mathbf{A}** .

If we apply this process again for \mathbf{A}^\top . We will have **column rank of $\mathbf{A} \leq$ row rank of \mathbf{A}** . This completes the proof. \blacksquare

Additional insights from this proof reveal that if $\{\mathbf{r}_1, \mathbf{r}_2, \dots, \mathbf{r}_r\}$ constitutes a vector set in \mathbb{R}^n serving as a basis for the row space, then $\{\mathbf{A}\mathbf{r}_1, \mathbf{A}\mathbf{r}_2, \dots, \mathbf{A}\mathbf{r}_r\}$ forms a basis for the column space of \mathbf{A} . We formulate this finding into the following lemma.

Lemma 1.2: (Column Basis from Row Basis)

For any matrix $\mathbf{A} \in \mathbb{R}^{m \times n}$, suppose that $\{\mathbf{r}_1, \mathbf{r}_2, \dots, \mathbf{r}_r\}$ is a set of vectors in \mathbb{R}^n , which forms a basis for the row space, then $\{\mathbf{A}\mathbf{r}_1, \mathbf{A}\mathbf{r}_2, \dots, \mathbf{A}\mathbf{r}_r\}$ is a basis for the column space of \mathbf{A} .

For any matrix $\mathbf{A} \in \mathbb{R}^{m \times n}$, it can be easily verified that any vector in the row space of \mathbf{A} is orthogonal to any vector in the null space of \mathbf{A} . Suppose $\mathbf{x}_n \in \mathcal{N}(\mathbf{A})$, then $\mathbf{A}\mathbf{x}_n = \mathbf{0}$, indicating that \mathbf{x}_n is perpendicular to every row of \mathbf{A} , thus validating our assertion.

Similarly, we can also show that any vector in the column space of \mathbf{A} is perpendicular to any vector in the null space of \mathbf{A}^\top . Additionally, the column space of \mathbf{A} together with the null space of \mathbf{A}^\top span the entire \mathbb{R}^m , which is known as the fundamental theorem of linear algebra.

The fundamental theorem contains two parts, the dimension of the subspaces and the orthogonality of the subspaces. The orthogonality can be easily verified as shown above. Additionally, when the row space has dimension r , the null space has dimension $n - r$. This cannot be easily stated and we prove it in the following theorem.

Theorem 1.3: (The Fundamental Theorem of Linear Algebra)

Orthogonal Complement and Rank-Nullity Theorem: for any matrix $\mathbf{A} \in \mathbb{R}^{m \times n}$, we have

- $\mathcal{N}(\mathbf{A})$ is orthogonal complement to the row space $\mathcal{C}(\mathbf{A}^\top)$ in \mathbb{R}^n : $\dim(\mathcal{N}(\mathbf{A})) + \dim(\mathcal{C}(\mathbf{A}^\top)) = n$;
- $\mathcal{N}(\mathbf{A}^\top)$ is orthogonal complement to the column space $\mathcal{C}(\mathbf{A})$ in \mathbb{R}^m : $\dim(\mathcal{N}(\mathbf{A}^\top)) + \dim(\mathcal{C}(\mathbf{A})) = m$;
- For rank- r matrix \mathbf{A} , $\dim(\mathcal{C}(\mathbf{A}^\top)) = \dim(\mathcal{C}(\mathbf{A})) = r$, that is, $\dim(\mathcal{N}(\mathbf{A})) = n - r$ and $\dim(\mathcal{N}(\mathbf{A}^\top)) = m - r$.

Proof [of Theorem 1.3] Following from the proof of Theorem 1.1. Let $\mathbf{r}_1, \mathbf{r}_2, \dots, \mathbf{r}_r$ be a set of vectors in \mathbb{R}^n that form a basis for the row space, then $\mathbf{A}\mathbf{r}_1, \mathbf{A}\mathbf{r}_2, \dots, \mathbf{A}\mathbf{r}_r$ is a basis for the column space of \mathbf{A} . Let $\mathbf{n}_1, \mathbf{n}_2, \dots, \mathbf{n}_k \in \mathbb{R}^n$ form a basis for the null space of \mathbf{A} . Following again from the proof of Theorem 1.1, $\mathcal{N}(\mathbf{A}) \perp \mathcal{C}(\mathbf{A}^\top)$, thus, $\mathbf{r}_1, \mathbf{r}_2, \dots, \mathbf{r}_r$ are perpendicular to $\mathbf{n}_1, \mathbf{n}_2, \dots, \mathbf{n}_k$. Then, $\{\mathbf{r}_1, \mathbf{r}_2, \dots, \mathbf{r}_r, \mathbf{n}_1, \mathbf{n}_2, \dots, \mathbf{n}_k\}$ is linearly independent in \mathbb{R}^n .

For any vector $\mathbf{x} \in \mathbb{R}^n$, $\mathbf{A}\mathbf{x}$ is in the column space of \mathbf{A} . Then it can be represented as a linear combination of $\mathbf{A}\mathbf{r}_1, \mathbf{A}\mathbf{r}_2, \dots, \mathbf{A}\mathbf{r}_r$: $\mathbf{A}\mathbf{x} = \sum_{i=1}^r a_i \mathbf{A}\mathbf{r}_i$ which states that $\mathbf{A}(\mathbf{x} - \sum_{i=1}^r a_i \mathbf{r}_i) = \mathbf{0}$, and $\mathbf{x} - \sum_{i=1}^r a_i \mathbf{r}_i$ is thus in $\mathcal{N}(\mathbf{A})$. Since $\{\mathbf{n}_1, \mathbf{n}_2, \dots, \mathbf{n}_k\}$ is a basis for the null space of \mathbf{A} , $\mathbf{x} - \sum_{i=1}^r a_i \mathbf{r}_i$ can be represented by a linear combination of $\mathbf{n}_1, \mathbf{n}_2, \dots, \mathbf{n}_k$: $\mathbf{x} - \sum_{i=1}^r a_i \mathbf{r}_i = \sum_{j=1}^k b_j \mathbf{n}_j$, i.e., $\mathbf{x} = \sum_{i=1}^r a_i \mathbf{r}_i + \sum_{j=1}^k b_j \mathbf{n}_j$. That is, any vector $\mathbf{x} \in \mathbb{R}^n$ can be represented by $\{\mathbf{r}_1, \mathbf{r}_2, \dots, \mathbf{r}_r, \mathbf{n}_1, \mathbf{n}_2, \dots, \mathbf{n}_k\}$, and the set forms a basis for \mathbb{R}^n . Thus, the dimension sum to n : $r + k = n$, i.e., $\dim(\mathcal{N}(\mathbf{A})) + \dim(\mathcal{C}(\mathbf{A}^\top)) = n$.

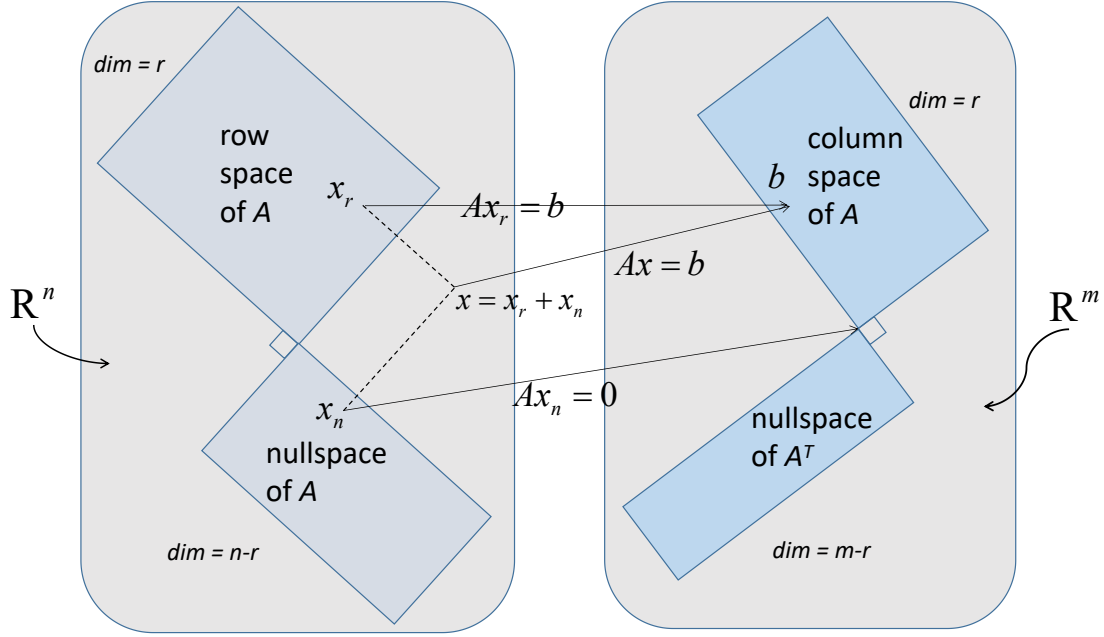


Figure 1.1: Two pairs of orthogonal subspaces in \mathbb{R}^n and \mathbb{R}^m . $\dim(\mathcal{C}(\mathbf{A}^\top)) + \dim(\mathcal{N}(\mathbf{A})) = n$ and $\dim(\mathcal{N}(\mathbf{A}^\top)) + \dim(\mathcal{C}(\mathbf{A})) = m$. The null space component goes to zero as $\mathbf{A}\mathbf{x}_n = \mathbf{0} \in \mathbb{R}^m$. The row space component goes to column space as $\mathbf{A}\mathbf{x}_r = \mathbf{A}(\mathbf{x}_r + \mathbf{x}_n) = \mathbf{b} \in \mathcal{C}(\mathbf{A})$.

Similarly, we can prove $\dim(\mathcal{N}(\mathbf{A}^\top)) + \dim(\mathcal{C}(\mathbf{A})) = m$. ■

Figure 1.1 demonstrates two pairs of such orthogonal subspaces and shows how \mathbf{A} takes \mathbf{x} into the column space. The dimensions of the row space of \mathbf{A} and the null space of \mathbf{A} add to n . And the dimensions of the column space of \mathbf{A} and the null space of \mathbf{A}^\top add to m . The null space component goes to zero as $\mathbf{A}\mathbf{x}_n = \mathbf{0} \in \mathbb{R}^m$, which is the intersection of the column space of \mathbf{A} and the null space of \mathbf{A}^\top . Conversely, the row space component goes to the column space as $\mathbf{A}\mathbf{x}_r = \mathbf{A}(\mathbf{x}_r + \mathbf{x}_n) = \mathbf{b} \in \mathbb{R}^m$.

Definition 1.0.14 (Orthogonal Matrix) A real square matrix \mathbf{Q} is an orthogonal matrix if the inverse of \mathbf{Q} equals the transpose of \mathbf{Q} , that is, $\mathbf{Q}^{-1} = \mathbf{Q}^\top$ and $\mathbf{Q}\mathbf{Q}^\top = \mathbf{Q}^\top\mathbf{Q} = \mathbf{I}$. In other words, suppose $\mathbf{Q} = [\mathbf{q}_1, \mathbf{q}_2, \dots, \mathbf{q}_n]$, where $\mathbf{q}_i \in \mathbb{R}^n$ for all $i \in \{1, 2, \dots, n\}$, then $\mathbf{q}_i^\top \mathbf{q}_j = \delta(i, j)$ with $\delta(i, j)$ being the Kronecker delta function. If \mathbf{Q} contains only γ of these columns with $\gamma < n$, then $\mathbf{Q}^\top\mathbf{Q} = \mathbf{I}_\gamma$ stills holds with \mathbf{I}_γ being the $\gamma \times \gamma$ identity matrix. But $\mathbf{Q}\mathbf{Q}^\top = \mathbf{I}$ will not be true. For any vector \mathbf{x} , the orthogonal matrix will preserve the length: $\|\mathbf{Q}\mathbf{x}\| = \|\mathbf{x}\|$.

Definition 1.0.15 (Permutation Matrix) A permutation matrix \mathbf{P} is a square binary matrix that has exactly one entry of 1 in each row and each column, and 0's elsewhere.

Row Point. That is, the permutation matrix \mathbf{P} has the rows of the identity \mathbf{I} in any order and the order decides the sequence of the row permutation. Suppose we want to permute the rows of matrix \mathbf{A} , we just multiply on the left by \mathbf{PA} .

Column Point. Or, equivalently, the permutation matrix \mathbf{P} has the columns of the identity \mathbf{I} in any order and the order decides the sequence of the column permutation. And now, the column permutation of \mathbf{A} is to multiply on the right by \mathbf{AP} .

The permutation matrix \mathbf{P} can be more efficiently represented via a vector $J \in \mathbb{Z}_+^n$ of indices such that $\mathbf{P} = \mathbf{I}[:, J]$, where \mathbf{I} is the $n \times n$ identity matrix, and notably, the elements in vector J sum to $1 + 2 + \dots + n = \frac{n^2+n}{2}$.

Example 1.1 (Permutation) Suppose,

$$\mathbf{A} = \begin{bmatrix} 1 & 2 & 3 \\ 4 & 5 & 6 \\ 7 & 8 & 9 \end{bmatrix} \quad \text{and} \quad \mathbf{P} = \begin{bmatrix} & 1 & \\ & & 1 \\ 1 & & \end{bmatrix}.$$

The row permutation is given by

$$\mathbf{PA} = \begin{bmatrix} 4 & 5 & 6 \\ 7 & 8 & 9 \\ 1 & 2 & 3 \end{bmatrix},$$

where the order of the rows of \mathbf{A} appearing in \mathbf{PA} matches the order of the rows of \mathbf{I} in \mathbf{P} . And the column permutation is given by

$$\mathbf{AP} = \begin{bmatrix} 3 & 1 & 2 \\ 6 & 4 & 5 \\ 9 & 7 & 8 \end{bmatrix},$$

where the order of the columns of \mathbf{A} appearing in \mathbf{AP} matches the order of the columns of \mathbf{I} in \mathbf{P} . □

Definition 1.0.16 (Positive Definite and Positive Semidefinite) A matrix $\mathbf{A} \in \mathbb{R}^{n \times n}$ is considered positive definite (PD) if $\mathbf{x}^\top \mathbf{A} \mathbf{x} > 0$ for all nonzero $\mathbf{x} \in \mathbb{R}^n$. And a matrix $\mathbf{A} \in \mathbb{R}^{n \times n}$ is called positive semidefinite (PSD) if $\mathbf{x}^\top \mathbf{A} \mathbf{x} \geq 0$ for all $\mathbf{x} \in \mathbb{R}^n$. ^{a b}

- a. In this book a positive definite or a semidefinite matrix is always assumed to be symmetric, i.e., the notion of a positive definite matrix or semidefinite matrix is only interesting for symmetric matrices.
- b. A symmetric matrix $\mathbf{A} \in \mathbb{R}^{n \times n}$ is called *negative definite* (ND) if $\mathbf{x}^\top \mathbf{A} \mathbf{x} < 0$ for all nonzero $\mathbf{x} \in \mathbb{R}^n$; a symmetric matrix $\mathbf{A} \in \mathbb{R}^{n \times n}$ is called *negative semidefinite* (NSD) if $\mathbf{x}^\top \mathbf{A} \mathbf{x} \leq 0$ for all $\mathbf{x} \in \mathbb{R}^n$; and a symmetric matrix $\mathbf{A} \in \mathbb{R}^{n \times n}$ is called *indefinite* (ID) if there exist \mathbf{x} and $\mathbf{y} \in \mathbb{R}^n$ such that $\mathbf{x}^\top \mathbf{A} \mathbf{x} < 0$ and $\mathbf{y}^\top \mathbf{A} \mathbf{y} > 0$.

We can establish that a matrix \mathbf{A} is positive definite if and only if it possesses exclusively *positive eigenvalues*. Similarly, a matrix \mathbf{A} is positive semidefinite if and only if it exhibits solely *nonnegative eigenvalues*. See Problem 1.1.

In conclusion, regarding the equivalent claims of nonsingular matrices, we have the following remark from an introductory course on linear algebra.

Remark 1.4: List of Equivalence of Nonsingularity for a Matrix

For a square matrix $\mathbf{A} \in \mathbb{R}^{n \times n}$, the following claims are equivalent:

- \mathbf{A} is nonsingular;
- \mathbf{A} is invertible, i.e., \mathbf{A}^{-1} exists;
- $\mathbf{A}\mathbf{x} = \mathbf{b}$ has a unique solution $\mathbf{x} = \mathbf{A}^{-1}\mathbf{b}$;
- $\mathbf{A}\mathbf{x} = \mathbf{0}$ has a unique, trivial solution: $\mathbf{x} = \mathbf{0}$;
- Columns of \mathbf{A} are linearly independent;
- Rows of \mathbf{A} are linearly independent;
- $\det(\mathbf{A}) \neq 0$;
- $\dim(\mathcal{N}(\mathbf{A})) = 0$;
- $\mathcal{N}(\mathbf{A}) = \{\mathbf{0}\}$, i.e., the null space is trivial;
- $\mathcal{C}(\mathbf{A}) = \mathcal{C}(\mathbf{A}^\top) = \mathbb{R}^n$, i.e., the column space or row space span the entire \mathbb{R}^n ;
- \mathbf{A} has full rank $r = n$;
- The reduced row echelon form is $\mathbf{R} = \mathbf{I}$;
- $\mathbf{A}^\top \mathbf{A}$ is symmetric positive definite;
- \mathbf{A} has n nonzero (positive) singular values;
- All eigenvalues are nonzero;

Keeping the above equivalence in mind is important to avoid confusion. On the other hand, the following remark also shows the equivalent claims for singular matrices.

Remark 1.5: List of Equivalence of Singularity for a Matrix

For a square matrix $\mathbf{A} \in \mathbb{R}^{n \times n}$ with eigenpair (λ, \mathbf{u}) , the following claims are equivalent:

- $(\mathbf{A} - \lambda\mathbf{I})$ is singular;
- $(\mathbf{A} - \lambda\mathbf{I})$ is not invertible;
- $(\mathbf{A} - \lambda\mathbf{I})\mathbf{x} = \mathbf{0}$ has nonzero $\mathbf{x} \neq \mathbf{0}$ solutions, and $\mathbf{x} = \mathbf{u}$ is one of such solutions;
- $(\mathbf{A} - \lambda\mathbf{I})$ has linearly dependent columns;
- $\det(\mathbf{A} - \lambda\mathbf{I}) = 0$;
- $\dim(\mathcal{N}(\mathbf{A} - \lambda\mathbf{I})) > 0$;
- Null space of $(\mathbf{A} - \lambda\mathbf{I})$ is nontrivial;
- Columns of $(\mathbf{A} - \lambda\mathbf{I})$ are linearly dependent;
- Rows of $(\mathbf{A} - \lambda\mathbf{I})$ are linearly dependent;
- $(\mathbf{A} - \lambda\mathbf{I})$ has rank $r < n$;
- Dimension of column space = dimension of row space = $r < n$;
- $(\mathbf{A} - \lambda\mathbf{I})^\top (\mathbf{A} - \lambda\mathbf{I})$ is symmetric semidefinite;
- $(\mathbf{A} - \lambda\mathbf{I})$ has $r < n$ nonzero (positive) singular values;
- Zero is an eigenvalue of $(\mathbf{A} - \lambda\mathbf{I})$.

Definition 1.0.17 (Vector ℓ_2 Norm) For a vector $\mathbf{x} \in \mathbb{R}^n$, the ℓ_2 vector norm is defined as $\|\mathbf{x}\|_2 = \sqrt{x_1^2 + x_2^2 + \dots + x_n^2}$.

For a matrix $\mathbf{A} \in \mathbb{R}^{m \times n}$, we define the (matrix) Frobenius norm as follows.

Definition 1.0.18 (Matrix Frobenius Norm) The *Frobenius norm* of a matrix $\mathbf{A} \in \mathbb{R}^{m \times n}$ is defined as

$$\|\mathbf{A}\|_F = \sqrt{\sum_{i=1, j=1}^{m, n} (a_{ij})^2} = \sqrt{\text{tr}(\mathbf{A}\mathbf{A}^\top)} = \sqrt{\text{tr}(\mathbf{A}^\top \mathbf{A})} = \sqrt{\sigma_1^2 + \sigma_2^2 + \dots + \sigma_r^2},$$

where $\sigma_1, \sigma_2, \dots, \sigma_r$ are nonzero singular values of \mathbf{A} .

The spectral norm is defined as follows.

Definition 1.0.19 (Matrix Spectral Norm) The *spectral norm* of a matrix $\mathbf{A} \in \mathbb{R}^{m \times n}$ is defined as

$$\|\mathbf{A}\|_2 = \max_{\mathbf{x} \neq \mathbf{0}} \frac{\|\mathbf{A}\mathbf{x}\|_2}{\|\mathbf{x}\|_2} = \max_{\mathbf{u} \in \mathbb{R}^n: \|\mathbf{u}\|_2=1} \|\mathbf{A}\mathbf{u}\|_2,$$

which is also the maximal singular value of \mathbf{A} , i.e., $\|\mathbf{A}\|_2 = \sigma_1(\mathbf{A})$.

We note that the Frobenius norm serves as the matrix counterpart of vector ℓ_2 norm. For simplicity, we do not give the full subscript of the norm for the vector ℓ_2 norm or Frobenius norm when it is clear from the context which one we are referring to: $\|\mathbf{A}\| = \|\mathbf{A}\|_F$ and $\|\mathbf{x}\| = \|\mathbf{x}\|_2$. However, for the spectral norm, the subscript $\|\mathbf{A}\|_2$ should **not** be omitted.

Given a specific norm definition, the concepts of an open ball and a closed ball are introduced as follows:

Definition 1.0.20 (Open Ball, Closed Ball) The *open ball* with center $\mathbf{c} \in \mathbb{R}^n$ and radius r is defined as

$$B(\mathbf{c}, r) = \{\mathbf{x} \in \mathbb{R}^n : \|\mathbf{x} - \mathbf{c}\| < r\}.$$

Similarly, the *closed ball* with center $\mathbf{c} \in \mathbb{R}^n$ and radius r is defined as

$$B[\mathbf{c}, r] = \{\mathbf{x} \in \mathbb{R}^n : \|\mathbf{x} - \mathbf{c}\| \leq r\}.$$

Differentiability and Differential Calculus

Definition 1.0.21 (Directional Derivative, Partial Derivative) Given a function f defined over a set $\mathbb{S} \subseteq \mathbb{R}^n$ and a nonzero vector $\mathbf{d} \in \mathbb{R}^n$. Then the *directional derivative* of f at \mathbf{x} w.r.t. the direction \mathbf{d} is given by, if the limit exists,

$$\lim_{t \rightarrow 0^+} \frac{f(\mathbf{x} + t\mathbf{d}) - f(\mathbf{x})}{t}.$$

And it is denoted by $f'(\mathbf{x}; \mathbf{d})$ or $D_{\mathbf{d}}f(\mathbf{x})$. The directional derivative is sometimes called the **Gâteaux derivative**.

For any $i \in \{1, 2, \dots, n\}$, the directional derivative at \mathbf{x} w.r.t. the direction of the i -th standard basis \mathbf{e}_i is called the i -th **partial derivative** and is denoted by $\frac{\partial f}{\partial x_i}(\mathbf{x})$, $D_{\mathbf{e}_i}f(\mathbf{x})$, or $\partial_i f(\mathbf{x})$.

If all the partial derivatives of a function f exist at a point $\mathbf{x} \in \mathbb{R}^n$, then the *gradient* of f at \mathbf{x} is defined as the column vector containing all the partial derivatives:

$$\nabla f(\mathbf{x}) = \begin{bmatrix} \frac{\partial f}{\partial x_1}(\mathbf{x}) \\ \frac{\partial f}{\partial x_2}(\mathbf{x}) \\ \vdots \\ \frac{\partial f}{\partial x_n}(\mathbf{x}) \end{bmatrix} \in \mathbb{R}^n.$$

A function f defined over an open set $\mathbb{S} \subseteq \mathbb{R}^n$ is called *continuously differentiable* over \mathbb{S} if all the partial derivatives exist and are continuous on \mathbb{S} . In the setting of continuous differentiability, the directional derivative and gradient have the following relationship:

$$f'(\mathbf{x}; \mathbf{d}) = \nabla f(\mathbf{x})^\top \mathbf{d}, \quad \text{for all } \mathbf{x} \in \mathbb{S} \text{ and } \mathbf{d} \in \mathbb{R}^n. \quad (1.1)$$

And in the setting of continuously differentiability, we also have

$$\lim_{\mathbf{d} \rightarrow \mathbf{0}} \frac{f(\mathbf{x} + \mathbf{d}) - f(\mathbf{x}) - \nabla f(\mathbf{x})^\top \mathbf{d}}{\|\mathbf{d}\|} = 0 \quad \text{for all } \mathbf{x} \in \mathbb{S}, \quad (1.2)$$

or

$$f(\mathbf{y}) = f(\mathbf{x}) + \nabla f(\mathbf{x})^\top (\mathbf{y} - \mathbf{x}) + o(\|\mathbf{y} - \mathbf{x}\|), \quad (1.3)$$

where $o(\cdot) : \mathbb{R}_+ \rightarrow \mathbb{R}$ is a one-dimensional function satisfying $\frac{o(t)}{t} \rightarrow 0$ as $t \rightarrow 0^+$.

The partial derivative $\frac{\partial f}{\partial x_i}(\mathbf{x})$ is also a real-valued function of $\mathbf{x} \in \mathbb{S}$ that can be partially differentiated. The j -th partial derivative of $\frac{\partial f}{\partial x_i}(\mathbf{x})$ is defined as

$$\frac{\partial^2 f}{\partial x_j \partial x_i}(\mathbf{x}) = \frac{\partial \left(\frac{\partial f}{\partial x_i}(\mathbf{x}) \right)}{\partial x_j}(\mathbf{x}).$$

This is called the (j, i) -th *second-order partial derivative* of function f . A function f defined over an open set $\mathbb{S} \subseteq \mathbb{R}^n$ is called *twice continuously differentiable* over \mathbb{S} if all the second-order partial derivatives exist and are continuous over \mathbb{S} . In the setting of twice continuously differentiability, the second-order partial derivatives are symmetric:

$$\frac{\partial^2 f}{\partial x_j \partial x_i}(\mathbf{x}) = \frac{\partial^2 f}{\partial x_i \partial x_j}(\mathbf{x}).$$

The *Hessian* of the function f at a point $\mathbf{x} \in \mathbb{S}$ is defined as the symmetric $n \times n$ matrix

$$\nabla^2 f(\mathbf{x}) = \begin{bmatrix} \frac{\partial^2 f}{\partial x_1^2}(\mathbf{x}) & \frac{\partial^2 f}{\partial x_1 \partial x_2}(\mathbf{x}) & \dots & \frac{\partial^2 f}{\partial x_1 \partial x_n}(\mathbf{x}) \\ \frac{\partial^2 f}{\partial x_2 \partial x_1}(\mathbf{x}) & \frac{\partial^2 f}{\partial x_2 \partial x_2}(\mathbf{x}) & \dots & \frac{\partial^2 f}{\partial x_2 \partial x_n}(\mathbf{x}) \\ \vdots & \vdots & \ddots & \vdots \\ \frac{\partial^2 f}{\partial x_n \partial x_1}(\mathbf{x}) & \frac{\partial^2 f}{\partial x_n \partial x_2}(\mathbf{x}) & \dots & \frac{\partial^2 f}{\partial x_n^2}(\mathbf{x}) \end{bmatrix}.$$

We provide a simple proof of Taylor's expansion in Appendix A.1 (p. 245) for one-dimensional functions. In the case of high-dimensional functions, we have the following two approximation results.

Theorem 1.6: (Linear Approximation Theorem)

Let $f(\mathbf{x}) : \mathbb{S} \rightarrow \mathbb{R}$ be a twice continuously differentiable function over an open set $\mathbb{S} \subseteq \mathbb{R}^n$, and given two points \mathbf{x}, \mathbf{y} . Then there exists $\mathbf{x}^* \in [\mathbf{x}, \mathbf{y}]$ such that

$$f(\mathbf{y}) = f(\mathbf{x}) + \nabla f(\mathbf{x})^\top (\mathbf{y} - \mathbf{x}) + \frac{1}{2} (\mathbf{y} - \mathbf{x})^\top \nabla^2 f(\mathbf{x}^*) (\mathbf{y} - \mathbf{x}).$$

Theorem 1.7: (Quadratic Approximation Theorem)

Let $f(\mathbf{x}) : \mathbb{S} \rightarrow \mathbb{R}$ be a twice continuously differentiable function over an open set $\mathbb{S} \subseteq \mathbb{R}^n$, and given two points \mathbf{x}, \mathbf{y} . Then it follows that

$$f(\mathbf{y}) = f(\mathbf{x}) + \nabla f(\mathbf{x})^\top (\mathbf{y} - \mathbf{x}) + \frac{1}{2} (\mathbf{y} - \mathbf{x})^\top \nabla^2 f(\mathbf{x}) (\mathbf{y} - \mathbf{x}) + o(\|\mathbf{y} - \mathbf{x}\|^2).$$

⌘ Chapter 1 Problems ⌘

1. **Eigenvalue Characterization Theorem:** Prove that a matrix \mathbf{A} is positive definite if and only if it possesses exclusively *positive eigenvalues*. Similarly, a matrix \mathbf{A} is positive semidefinite if and only if it exhibits solely *nonnegative eigenvalues*.
2. Prove Remark 1.4 and Remark 1.5.

Monte Carlo Methods

Contents

2.1	The Bayesian Approach	21
2.2	Approximate Inference	22
2.3	Monte Carlo (MC) Methods	23
2.3.1	Markov Chain Monte Carlo (MCMC)	24
2.3.2	MC V.S. MCMC	26
2.3.3	Gibbs Sampler	26
2.3.4	Adaptive Rejection Sampling (ARS)	27
	Rejection Sampling	27
	Adaptive Rejection Sampling	28
2.4	Bayesian Appetizers	28
2.4.1	Beta-Bernoulli Model	29
2.4.2	Bayesian Linear Model with Zero-Mean Prior	32
2.4.3	Bayesian Linear Model with Semi-Conjugate Prior	34
2.4.4	Bayesian Linear Model with Full Conjugate Prior	36
Chapter 2	Problems	37



This book focuses on Markov chain Monte Carlo (MCMC) methods for probabilistic inference, aiming to draw conclusions from a probabilistic model. This chapter provides a survey of the mathematical details related to probabilistic inference, emphasizing aspects that will establish the foundation for the subsequent chapters.

2.1. The Bayesian Approach

In the past decade, the Bayesian approach has been used in a wide variety of problems in data analysis, including economic forecasting, medical imaging, and population studies (Besag, 1986; Hill, 1994; Marseille et al., 1996). In modern statistics, Bayesian approaches have become increasingly more important and widely used. The inception of this idea is credited to *Thomas Bayes*, who came up with this idea but died before publishing it. Fortunately, his friend *Richard Price* carried on his work and published it in 1764. The same concept was later independently discovered by *Laplace* at the end of the 18-th century. In this section, we describe the basic ideas about the Bayesian approach and use the Beta-Bernoulli model and Bayesian linear model as an appetizer of the pros and prior information of Bayesian models.

Bayesian modeling and statistics are fundamentally driven by Bayes' theorem. Formally, the theorem is expressed as follows.

Theorem 2.1: (Bayes' Theorem)

Let \mathbb{S} be a sample space and let B_1, B_2, \dots, B_K be a partition of \mathbb{A} such that (1). $\cup_k B_k = \mathbb{S}$ and (2). $B_i \cap B_j = \emptyset$ for all $i \neq j$. Let further A be any event. Then it follows that

$$P(B_k | A) = \frac{P(A | B_k)P(B_k)}{P(A)} = \frac{P(A | B_k)P(B_k)}{\sum_{i=1}^K P(A | B_i)P(B_i)}.$$

In Bayesian modeling and statistics, Bayes' theorem provides us with a straightforward rule for updating probabilities when new information, such as observed data, becomes available. This allows us to adjust our prior beliefs regarding parameters of interest.

To be more specific, let $\mathcal{X} = \mathcal{X}(\mathbf{x}_{1:N}) = \{\mathbf{x}_1, \mathbf{x}_2, \dots, \mathbf{x}_N\}$ be the observations of N data points, and suppose they are independent and identically distributed (i.i.d.) with the probability parameterized by $\boldsymbol{\theta}$. Note that the parameters $\boldsymbol{\theta}$ might include hidden variables, such as latent variables in a mixture model indicating the cluster to which a data point belongs.

The idea of the Bayesian approach involves assuming a *prior* probability distribution for $\boldsymbol{\theta}$ with hyper-parameters $\boldsymbol{\alpha}$ (i.e., $p(\boldsymbol{\theta} | \boldsymbol{\alpha})$, also known as the probability of the model). This distribution represents the plausibility of each possible value of $\boldsymbol{\theta}$ before observing the data, and it captures our prior uncertainty regarding $\boldsymbol{\theta}$. The joint distribution of $\boldsymbol{\theta}$ and \mathcal{X} is given by

$$p(\boldsymbol{\theta}, \mathcal{X}) = p(\boldsymbol{\theta} | \boldsymbol{\alpha})p(\mathcal{X} | \boldsymbol{\theta}).$$

And we can integrate out $\boldsymbol{\theta}$ to obtain the marginal distribution of \mathcal{X} ,

$$p(\mathcal{X}) = \int_{\boldsymbol{\theta}} p(\boldsymbol{\theta} | \boldsymbol{\alpha})p(\mathcal{X} | \boldsymbol{\theta})d\boldsymbol{\theta}.$$

Then, to make inferences about θ , one simply considers the conditional distribution of θ given the observed data. This is referred to as the *posterior* distribution, since it represents the plausibility of each possible value of θ after seeing the data. The posterior distribution is the solution space for given problems, since it measures the probability of the present model in light of the data. Mathematically, this relationship is expressed via Bayes’ theorem,

$$\begin{aligned} p(\theta \mid \mathcal{X}, \alpha) &= \frac{p(\mathcal{X} \mid \theta)p(\theta \mid \alpha)}{p(\mathcal{X} \mid \alpha)} \\ &= \frac{p(\mathcal{X} \mid \theta)p(\theta \mid \alpha)}{\int_{\theta} p(\mathcal{X}, \theta \mid \alpha)} = \frac{p(\mathcal{X} \mid \theta)p(\theta \mid \alpha)}{\int_{\theta} p(\mathcal{X} \mid \theta)p(\theta \mid \alpha)} \propto p(\mathcal{X} \mid \theta)p(\theta \mid \alpha), \end{aligned} \tag{2.1}$$

where “ \propto ” means “proportional to” (see Problem 2.1.), \mathcal{X} is the observed data set, and $p(\mathcal{X} \mid \alpha)$ can be disregarded in this case since it acts as a scaling parameter (and we shall see the MCMC algorithm only needs relative probabilities). In other words, we say the posterior is proportional to the product of the likelihood and the prior. This means that the relative probability at a point in the solution space is determined completely by the likelihood, which is easily determined by comparing the model to the data, and the prior, which is the probability of the model independent of the data. The prior encodes any a priori knowledge of the solution irrespective of the observed data. For example, a prior for a system reducing over-clustering might assign a higher probability to a larger cluster than to a small cluster (Lu, 2021c).

More generally, the Bayesian approach—in a nutshell—is to assume a prior distribution for any unknowns (θ in our case), and then just follow the rules of probability to answer any questions of interest. For example, when we find the parameter based on the maximum posterior probability of θ , we turn to the *maximum a posteriori* (MAP) estimator.

Frequentists V.S. Bayesian. The *frequentist approach* to statistics, developed by Neyman, evaluates statistical procedures based on a probability distribution over all possible data sets. To be more specific, frequentists consider the parameter vector θ to be fixed (albeit unknown), while introducing uncertainty over possible data sets \mathcal{X} . Frequentist methods are often considered more objective as they avoid incorporating subjective prior information. In contrast, Bayesian methods allow for the incorporation of prior beliefs. The Bayesian approach treats the data set \mathcal{X} as given, while introducing uncertainty over θ . However, statisticians nowadays tend to move comfortably between these approaches and popular statistical procedures often combine both of them, incorporating Bayesian methods for certain aspects of the analysis while using frequentist methods for others. For instance, empirical Bayesian methods have a Bayesian spirit but are not strictly Bayesian; their analysis is frequently frequentist (Haugh, 2021).

2.2. Approximate Inference

In this book, our emphasis is on approximate probabilistic inference methods. In certain cases, it is computationally feasible to compute the posterior exactly. For example, exponential families with conjugate priors often enable analytical solutions. Although exact inference methods exist and they are precise and useful for certain classes of problems, exact inference methods in complicated models are usually intractable, because these methods

typically depend on integrals, summations, or intermediate representations that grow large and become impractical as the state space grows too large so as to make the computation inefficient. For instance, we may use conjugate priors in a Gaussian mixture model. However, the model is hierarchical and is too complicated to compute the exact posterior. Consequently, in such cases, approximate probabilistic inference methods are rather useful and necessary.

Generally, *variational methods* and *Monte Carlo methods* are two primary classes of approximate inference. We here give a brief comparison of the two methods (Bonawitz, 2008). In variational inference methods, we first approximate the full model with a simpler model, in which the inference questions are tractable. Then, the parameters of this simplified model are calculated by some methods (e.g., using optimization methods) to minimize a measure of the dissimilarity between the original model and the simplified version; this calculation usually performs deterministically because optimization methods are used. Finally, certain queries can be calculated and executed in the simplified model. In other words, the main idea behind variational methods is to pick a family of distributions over the parameters with its own *variational parameters*— $q(\boldsymbol{\theta} \mid \boldsymbol{\nu})$, where $\boldsymbol{\nu}$ represents the variable containing variational parameters. Then, find the setting of the parameters that makes q close to the posterior of interest. For a detailed example, refer to Ma et al. (2014). The main advantage of variational methods is deterministic; however, the corresponding results are in the form of a lower bound of the desired quantity, and the tightness of this bound depends on the degree to which the simplified distribution can model the original posterior distribution. The variational inference is an important tool for Bayesian deep learning (Jordan et al., 1999; Graves, 2011; Hoffman et al., 2013; Ranganath et al., 2014; Mandt and Blei, 2014).

On the contrary, in Monte Carlo methods, we first draw a sequence of samples from the true target posterior distribution. Then certain inference questions are then answered by using this set of samples as an approximation of the target distribution itself. Monte Carlo methods are guaranteed to converge—if you want a more accurate answer, you just need to run the inference for longer; in the limit of running the Monte Carlo algorithm forever, the approximation results from the samples converge to the target distribution (see Section 2.3).

2.3. Monte Carlo (MC) Methods

In Monte Carlo methods, we first draw N samples $\boldsymbol{\theta}_1, \boldsymbol{\theta}_2, \dots, \boldsymbol{\theta}_N$ from the posterior distribution $p(\boldsymbol{\theta} \mid \mathcal{X}, \boldsymbol{\alpha})$ in Equation (2.1). Subsequently, we approximate the distribution of interest by

$$p(\boldsymbol{\theta} \mid -) \approx \tilde{p}(\boldsymbol{\theta} \mid -) = \frac{1}{N} \sum_{n=1}^N \delta_{\boldsymbol{\theta}_n}(\boldsymbol{\theta}), \quad (2.2)$$

where $\delta_{\boldsymbol{\theta}_i}(\boldsymbol{\theta})$ is the Dirac delta function¹. As the number of samples increases, the approximation (almost surely) converges to the true target distribution, i.e., $\tilde{p}(\boldsymbol{\theta}) \xrightarrow[N \rightarrow \infty]{a.s.} p(\boldsymbol{\theta})$.

These kinds of sampling-based methods are extensively used in modern statistics due to their ease of use and the generality with which they can be applied. The fundamental

1. The Dirac delta function $\delta_{\mathbf{x}_0}(\mathbf{x})$ has the property that it is nonzero and equals 1 only at $\mathbf{x} = \mathbf{x}_0$.

problem solved by these methods is the approximation of expectations such as

$$Eh(\Theta) = \int_{\theta} h(\theta)p(\theta)d\theta, \quad (2.3)$$

in the case of a continuous random variable Θ with probability density function (p.d.f.) p . Or

$$Eh(\Theta) = \sum_{\theta} h(\theta)p(\theta), \quad (2.4)$$

in the case of a discrete random variable Θ with probability mass function (p.m.f.) p . The general principle at work is that such expectations can be approximated by

$$Eh(\Theta) \approx \sum_{n=1}^N h(\theta_n). \quad (2.5)$$

If it were generally easy to draw samples directly from $p(\theta | \mathcal{X}, \alpha)$, the Monte Carlo story would end here. Unfortunately, this is usually intractable. We can consider the posterior form $p(\theta | \mathcal{X}, \alpha) = \frac{p(\mathcal{X}|\theta)p(\theta|\alpha)}{p(\mathcal{X}|\alpha)}$, where in many problems $p(\mathcal{X} | \theta)p(\theta | \alpha)$ can be computed easily, but computing $p(\mathcal{X} | \alpha)$ is challenging due to integrals, summations, etc. In such cases, Markov chain Monte Carlo is especially useful.

2.3.1 Markov Chain Monte Carlo (MCMC)

Markov chain Monte Carlo (MCMC) algorithms, also called MCMC samplers, are numerical approximation algorithms. Since MCMC algorithms directly sample the solution space, uncertainty estimates are determined simultaneously with a “best” solution. Additionally, provided that the data support them, multiple solutions are feasible. Intuitively, it is a stochastic hill-climbing approach to inference, operating over the complete data set. This inference method is designed to spend most of the computational efforts to sample points from the high probability regions of true target posterior distribution $p(\theta | \mathcal{X}, \alpha)$ (Andrieu et al., 2003; Bonawitz, 2008; Hoff, 2009; Geyer, 2011).

In this sampler, a Markov chain stochastic walk is taken through the state space Θ such that the probability of being in a particular state θ_t at any point in the walk is $p(\theta_t | \mathcal{X}, \alpha)$. Therefore, samples from the true posterior distribution $p(\theta | \mathcal{X}, \alpha)$ can be approximated by recording the samples (states) visited by the stochastic walk and some other post-processing methods such as *thinning*. The stochastic walk is a Markov chain, i.e. the choice of state at time $t + 1$ depends only on its previous state—the state at time t . Formally, if θ_t is the state of the chain at time t , then it follows that $p(\theta_{t+1} | \theta_1, \theta_2, \dots, \theta_t) = p(\theta_{t+1} | \theta_t)$. That is, Markov chains are *history-free*. This history-free property of Markov chains provides two main advantages:

- Due to this history-free property, the Markov chain Monte Carlo methods can be run for an unlimited number of iterations without consuming additional memory space.
- The history-free property also indicates that the MCMC stochastic walk can be completely characterized by $p(\theta_{t+1} | \theta_t)$, known as the *transition kernel*.

We then focus on the discussion of the transition kernel. The transition kernel \mathbf{K} can also be expressed as a linear transform. If $p_t = p_t(\theta)$ is a row vector that encodes the probability

of the walk being in state θ at time t , then $p_{t+1} = p_t \mathbf{K}$. If the stochastic walk starts from state θ_0 , then the distribution from this initial state is the delta distribution $p_0 = \delta_{\theta_0}(\theta)$, and the state distribution for the chain after step t is $p_t = p_0 \mathbf{K}^t$. We can easily find that the key to Markov chain Monte Carlo lies in choosing a kernel \mathbf{K} such that $\lim_{t \rightarrow \infty} p_t = p(\theta | \mathcal{X}, \alpha)$, independent of the choice of θ_0 . Kernels exhibiting this property are said to converge to an **equilibrium distribution** $p_{eq} = p(\theta | \mathcal{X})$. Convergence is guaranteed if both of the following criteria are met (see Bonawitz (2008)):

- p_{eq} is an invariant (or stationary) distribution for \mathbf{K} . A distribution p_{inv} is considered an invariant distribution for \mathbf{K} if $p_{inv} = p_{inv} \mathbf{K}$;
- \mathbf{K} is *ergodic*. A kernel is called ergodic if it is *irreducible* (meaning that any state can be reached from any other state) and *aperiodic* (indicating that the stochastic walk never gets stuck in cycles).

There are a large number of MCMC algorithms, too extensive for comprehensive coverage in this context. Popular families include Gibbs sampling, Metropolis-Hastings (MH), slice sampling, Hamiltonian Monte Carlo, adaptive rejection sampling, and many others. Though the name is potentially misleading, Metropolis-within-Gibbs (MWG) was initially developed by Metropolis et al. (1953), and MH subsequently emerged as a generalization of MWG (Hastings, 1970). All MCMC algorithms are recognized as special instances of the MH algorithm. Regardless of the algorithm, the goal of Bayesian inference is to maximize the unnormalized joint posterior distribution and collect samples of the target distributions, which are marginal posterior distributions, later to be used for inference queries.

The most generalizable MCMC algorithm is the Metropolis-Hastings (MH) generalization (Metropolis et al., 1953; Hastings, 1970) of the MWG algorithm. The MH algorithm extended MWG to include asymmetric proposal distributions. In this method, it converts an arbitrary proposal kernel $q(\theta_* | \theta_t)$ into a transition kernel with the desired invariant distribution $p_{eq}(\theta)$. In order to generate a sample from a MH transition kernel, the process involves drawing a proposal $\theta_* \sim q(\theta_* | \theta_t)$ and subsequently evaluating the MH acceptance probability by

$$P[A(\theta_* | \theta_t)] = \min \left(1, \frac{p(\theta_* | \alpha) q(\theta_t | \theta_*)}{p(\theta_t | \alpha) q(\theta_* | \theta_t)} \right), \quad (2.6)$$

with probability $P[A(\theta_* | \theta_t)]$ the proposal is accepted and we set $\theta_{t+1} = \theta_*$; otherwise the proposal is rejected and we set $\theta_{t+1} = \theta_t$. That is

$$\theta_{t+1} = \begin{cases} \theta_*, & \text{with probability } P[A(\theta_* | \theta_t)]; \\ \theta_t, & \text{with probability } 1 - P[A(\theta_* | \theta_t)]. \end{cases} \quad (2.7)$$

Intuitively, we may find that the $\frac{p(\theta_* | \alpha)}{p(\theta_t | \alpha)}$ term tends to accept moves that lead to higher probability regions of the state space, while the $\frac{q(\theta_t | \theta_*)}{q(\theta_* | \theta_t)}$ term tends to accept moves that are easy to undo. Since in MH, we only evaluate $p(\theta)$ as a part of the ratio $\frac{p(\theta_* | \alpha)}{p(\theta_t | \alpha)}$, we do not need to compute $p(\mathcal{X} | \alpha)$ as mentioned in Section 2.3.

The key in MH is the proposal kernel $q(\theta_* | \theta_t)$. However, the transition kernel is not $q(\theta_* | \theta_t)$. Informally, the kernel $K(\theta_{t+1} | \theta_t)$ in MH is

$$p(\theta_{t+1} | \text{accept})P[\text{accept}] + p(\theta_{t+1} | \text{reject})P[\text{reject}].$$

While Tierney (1998) introduced that the precise transition kernel is

$$\begin{aligned} K(\boldsymbol{\theta}_t \rightarrow \boldsymbol{\theta}_{t+1}) &= p(\boldsymbol{\theta}_{t+1} \mid \boldsymbol{\theta}_t) \\ &= q(\boldsymbol{\theta}_{t+1} \mid \boldsymbol{\theta}_t)A(\boldsymbol{\theta}_{t+1} \mid \boldsymbol{\theta}_t) + \delta_{\boldsymbol{\theta}_t}(\boldsymbol{\theta}_{t+1}) \int_{\boldsymbol{\theta}_*} q(\boldsymbol{\theta}_* \mid \boldsymbol{\theta}_t)(1 - A(\boldsymbol{\theta}_* \mid \boldsymbol{\theta}_t)). \end{aligned} \quad (2.8)$$

2.3.2 MC V.S. MCMC

As shown in previous sections, the purpose of Monte Carlo or Markov chain Monte Carlo approximation is to obtain a sequence of parameter values $\{\boldsymbol{\theta}^{(1)}, \dots, \boldsymbol{\theta}^{(N)}\}$ such that

$$\frac{1}{N} \sum_{n=1}^N h(\boldsymbol{\theta}^{(n)}) \approx \int_{\boldsymbol{\theta}} h(\boldsymbol{\theta})p(\boldsymbol{\theta})d\boldsymbol{\theta}, \quad (2.9)$$

for any functions h of interest in the case of continuous random variables. In other words, we want the empirical average of $\{h(\boldsymbol{\theta}^{(1)}), \dots, h(\boldsymbol{\theta}^{(N)})\}$ to approximate the expected value of $h(\boldsymbol{\theta})$ under a target probability distribution $p(\boldsymbol{\theta})$. In order for this to be a good approximation for a wide range of functions h , we require the empirical distribution of the simulated sequence $\{\boldsymbol{\theta}^{(1)}, \dots, \boldsymbol{\theta}^{(N)}\}$ to look like the target distribution $p(\boldsymbol{\theta})$. MC and MCMC are two ways of generating such a sequence. MC simulation, in which we generate independent samples from the target distribution, is in some sense the “true situation.” Independent MC samples automatically create a sequence that is representative of $p(\boldsymbol{\theta})$, which means the probability that $\boldsymbol{\theta}^{(n)} \in A$ for any set A is

$$\int_A p(\boldsymbol{\theta})d\boldsymbol{\theta}, \quad (2.10)$$

where $n \in \{1, \dots, N\}$. However, this is not true for MCMC samples, in which case all we are sure of is that

$$\lim_{n \rightarrow \infty} Pr(\boldsymbol{\theta}^{(n)} \in A) = \int_A p(\boldsymbol{\theta})d\boldsymbol{\theta}. \quad (2.11)$$

2.3.3 Gibbs Sampler

Gibbs sampling was introduced by Turchin (Turchin, 1971) and later by brothers Geman and Geman (Geman and Geman, 1984) in the context of image restoration. The Geman brothers named the algorithm after the physicist J. W. Gibbs, some eight decades after his death, in reference to an analogy between the sampling algorithm and statistical physics.

Gibbs sampling is applicable when the joint distribution is not explicitly known or is challenging to sample from directly. Instead, it relies on the known and easily samplable conditional distribution of each variable. A Gibbs sampler sequentially generates a draw from the distribution of each parameter or variable in turn, conditional on the current values of the other parameters or variables. Therefore, a Gibbs sampler is a componentwise algorithm. In our example, given some data \mathcal{X} and a probability distribution $p(\boldsymbol{\theta} \mid \mathcal{X}, \boldsymbol{\alpha})$ parameterized by $\boldsymbol{\theta} = \{\theta_1, \theta_2, \dots, \theta_p\}$. We can successively draw samples from the distribution by sampling from

$$\theta_i^{(t)} \sim p(\theta_i \mid \boldsymbol{\theta}_{-i}^{(t-1)}, \mathcal{X}, \boldsymbol{\alpha}), \quad (2.12)$$

where $\boldsymbol{\theta}_{-i}^{(t-1)}$ is all current values of $\boldsymbol{\theta}$ in the $(t-1)$ -th iteration except for θ_i . If we sample sufficiently long, these θ_i values will be random samples from the distribution p . If we sample new values in turn for each parameter θ_i from Equation (2.12), we will eventually converge to draws from the posterior $p(\boldsymbol{\theta} \mid \mathcal{X}, \boldsymbol{\alpha})$. When doing this Gibbs sampler, we also have to discard the first k draws since it takes a while to converge (i.e., *burn-in*). And because the consecutive draws are correlated, we only use every j -th sample (i.e., *thinning*).

In deriving a Gibbs sampler, it is often helpful to observe that

$$p(\theta_i \mid \boldsymbol{\theta}_{-i}, \mathcal{X}) = \frac{p(\theta_1, \theta_2, \dots, \theta_p, \mathcal{X})}{p(\boldsymbol{\theta}_{-i}, \mathcal{X})} \propto p(\theta_1, \theta_2, \dots, \theta_p, \mathcal{X}). \quad (2.13)$$

That is, the conditional distribution is proportional to the joint distribution. We will get a lot of benefits from this simple observation by dropping constant terms from the joint distribution (relative to the parameters we are conditioned on).

Shortly, as a simplified example, given a joint probability distribution $p(\theta_1, \theta_2 \mid \mathcal{X})$, a Gibbs sampler would draw $p(\theta_1 \mid \theta_2, \mathcal{X})$, then $p(\theta_2 \mid \theta_1, \mathcal{X})$ iteratively. The procedure generates a sequence of realization for random variables θ_1 and θ_2 :

$$(\theta_1^0, \theta_2^0), (\theta_1^1, \theta_2^1), (\theta_1^2, \theta_2^2), \dots,$$

which converges to the joint distribution $p(\theta_1, \theta_2)$. Further details about Gibbs sampling can be found in Turchin (1971); Geman and Geman (1984); Hoff (2009); Gelman et al. (2013).

2.3.4 Adaptive Rejection Sampling (ARS)

The purpose of the adaptive rejection sampling algorithm is to provide a relatively efficient way to sample from a distribution from the large class of log-concave densities (Gilks and Wild, 1992; Wild and Gilks, 1993). We provide a brief overview of the algorithm here, with additional details available in Gilks and Wild (1992) and Wild and Gilks (1993).

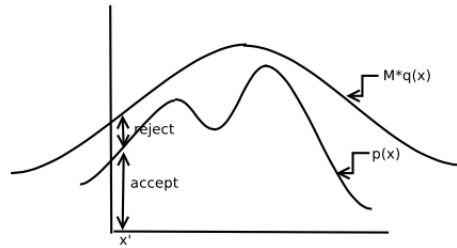


Figure 2.1: Rejection sampling. Figure is from Michael I. Jordan's lecture notes.

REJECTION SAMPLING

In rejection sampling, the objective is to sample from a target probability density function $p(x)$, given that we can sample from a probability density function $q(x)$ easily. Although the target density $p(x)$ is unknown, the approach relies on establishing an envelop by considering

$M \times q(x)$ such that it covers $p(x)$ for some $M > 1$, as illustrated in Figure 2.1. This is expressed as:

$$\frac{p(x)}{q(x)} < M, \text{ for all } x. \quad (2.14)$$

Subsequently, when sampling x_i from $q(x)$, and if $y_i = u \times M \times q(x_i)$ lies below the region under $p(x)$ for some $u \sim \text{Uniform}(0, 1)$, then we accept x_i ; otherwise, it is rejected.

In essence, the method involves sampling x_i from a distribution and making an acceptance or rejection decision based on the comparison with the envelope.

ADAPTIVE REJECTION SAMPLING

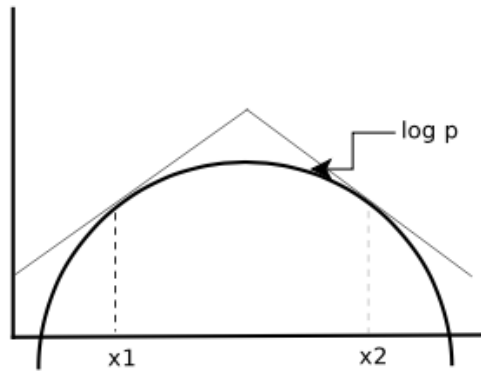


Figure 2.2: Adaptive rejection sampling. Figure is from Michael I. Jordan’s lecture notes.

The adaptive rejection sampling method, tailored for log-concave densities, is an extension of rejection sampling. The basic idea involves dynamically constructing an upper envelope (the upper bound on $p(x)$), serving as an adaptive replacement for $M \times q(x)$ in rejection sampling.

As shown in Figure 2.2, the logarithm of the density, $\log p(x)$, is considered. We then sample x_i from the upper envelope, and the sample is either accepted or rejected akin to rejection sampling. In case of rejection, a tangent is drawn passing through $x = x_i$ and $y = \log(p)$; and the tangent is used to reduce the upper envelope to decrease the number of rejected samples. The intersections of these tangent planes enable the formation of an envelope adaptively. To sample from the upper envelope, we need to transform from log space by exponentiating and using properties of the exponential distribution.

2.4. Bayesian Appetizers

This section delves into semi-conjugate priors with the Gibbs sampler and fully conjugate priors without approximate inference, offering an in-depth exploration of Bayesian approaches. Readers who already have a basic knowledge of Bayesian inference may choose to skip this section.

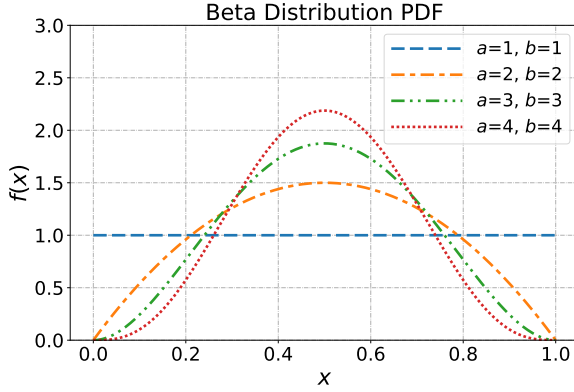


Figure 2.3: Beta probability density functions for different values of the parameters a and b . When $a = b = 1$, the beta distribution reduces to a *uniform distribution* in the support of $[0, 1]$. The mean, variance, and mode of the Beta distribution are $E[x] = \frac{a}{a+b}$, $\text{Var}[x] = \frac{ab}{(a+b+1)(a+b)^2}$, and $\text{mode}[x] = \frac{a-1}{(a-1)+(b-1)}$ if $a > 1, b > 1$, respectively.

2.4.1 Beta-Bernoulli Model

We formally introduce a *Beta-Bernoulli* model to illustrate how the Bayesian approach works. The Bernoulli distribution serves to model binary outcomes, i.e., outputting two possible values. The likelihood under this model corresponds to the probability mass function of the Bernoulli distribution with parameter θ :

$$\text{Bern}(x \mid \theta) = p(x \mid \theta) = \theta^x (1 - \theta)^{1-x} \mathbf{1}(x \in \{0, 1\}).$$

That is,

$$\text{Bern}(x \mid \theta) = p(x \mid \theta) = \begin{cases} 1 - \theta, & \text{if } x = 0; \\ \theta, & \text{if } x = 1, \end{cases}$$

where θ is the probability of outputting 1, and $1 - \theta$ is the probability of outputting 0. The mean of the Bernoulli distribution is θ . Suppose $\mathcal{X} = \{x_1, x_2, \dots, x_n\}$ are drawn i.i.d. from the Bernoulli distribution $\text{Bern}(\theta)$. Then the likelihood under the Bernoulli distribution with parameter θ is given by

$$\text{likelihood} = p(\mathcal{X} \mid \theta) = \theta^{\sum x_i} (1 - \theta)^{n - \sum x_i},$$

which is a distribution on \mathcal{X} and is called the *likelihood function* on \mathcal{X} .

And we will see the prior under this model is the probability density function of a *Beta distribution*:

$$\text{prior} = \text{Beta}(\theta \mid a, b) = p(\theta \mid a, b) = \frac{1}{B(a, b)} \theta^{a-1} (1 - \theta)^{b-1} \mathbf{1}(0 \leq \theta \leq 1),$$

where $B(a, b)$ denotes the *Euler's beta function* and it can be simply regarded as a constant normalization term, and $\mathbf{1}(a \leq x \leq b)$ is a step function that has a value of 1 when $a \leq x \leq b$ and 0 otherwise (when $x < a$ or $a > b$). Figure 2.3 compares different parameters for the Beta distribution. Specifically, when $a = b = 1$, the beta distribution reduces to a *uniform distribution* in the support of $[0, 1]$.

A Beta prior is assigned to the parameter θ of the Bernoulli distribution. The posterior is proportional to the product of the likelihood and prior densities, given by

$$\begin{aligned} \text{posterior} &= p(\theta \mid \mathcal{X}) \propto p(\mathcal{X} \mid \theta)p(\theta \mid a, b) \\ &= \theta^{\sum x_i} (1 - \theta)^{n - \sum x_i} \times \frac{1}{B(a, b)} \theta^{a-1} (1 - \theta)^{b-1} \cdot \mathbf{1}(0 \leq \theta \leq 1) \\ &\propto \theta^{a + \sum x_i - 1} (1 - \theta)^{b + n - \sum x_i - 1} \cdot \mathbf{1}(0 \leq \theta \leq 1) \\ &\propto \text{Beta} \left(\theta \mid a + \sum_{i=1}^n x_i, b + n - \sum_{i=1}^n x_i \right). \end{aligned}$$

We find that the posterior distribution shares the same form as the prior distribution; both stem from the Beta distribution, albeit with distinct parameters. When this happens, we call the prior a *conjugate prior*. A conjugate prior exhibits an advantageous structure, facilitating straightforward computations of the posterior probability density function, its derivatives, and the sampling process from the posterior. The advantage of using conjugate priors lies in their ability to preserve the mathematical form of the prior throughout the updating process. This results in closed-form expressions for the posterior distribution, avoiding the need for complex numerical methods.

Remark 2.2: Prior Information in Beta-Bernoulli Model

Upon comparing the prior and posterior formulations, it becomes evident that the hyperparameter a represents the prior count of occurrences of 1's in the output, while b corresponds to the prior count of 0's in the output. And the sum $a + b$ aggregates the prior information about the sample size. Uninformative prior parameters can then be characterized by $a = b = 1$, i.e., a uniform distribution.

Remark 2.3: Bayesian Estimator

From this Beta-Bernoulli model example, like the maximum likelihood estimator and method of moment (MoM, i.e., using the moment information to calculate the model parameter), Bayesian modeling also serves as a type of *point estimator*. However, Bayesian models output a probability of the parameter of interest, denoted as $p(\theta \mid \mathcal{X})$ in the example.

When predicting outcomes for new incoming data, instead of providing a direct model $p(x_{n+1} \mid \theta)$, the approach involves integration:

$$p(x_{n+1} \mid \mathcal{X}) = \int p(x_{n+1} \mid \theta)p(\theta \mid \mathcal{X})d\theta.$$

In other words, x_{n+1} depends on \mathcal{X} . The observed data \mathcal{X} provide insight into θ , which in turn provides information about x_{n+1} (i.e., $\mathcal{X} \rightarrow \theta \rightarrow x_{n+1}$).

Example 2.4.1 (Amount of Data Matters) *Suppose we have three observations for the success in the Bernoulli distribution:*

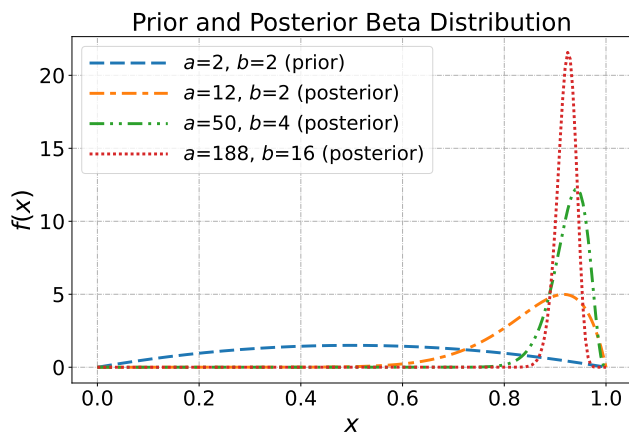


Figure 2.4: The prior distribution is $\text{Beta}(x \mid 2, 2)$. The posterior distributions for the three cases in Example 2.4.1 are $\text{Beta}(x \mid 12, 2)$, $\text{Beta}(x \mid 50, 4)$, and $\text{Beta}(x \mid 188, 16)$, respectively.

1. 10 out of 10 are observed to be success (1's);
2. 48 out of 50 are observed to be success (1's);
3. 186 out of 200 are observed to be success (1's).

So, what is the probability of success in the Bernoulli model? The normal answer to case 1, 2, and 3 are 100%, 96%, and 93%, respectively. But an observation of 10 inputs is rather a small amount of data, and the statistical significance may be limited due to potential noise.

To address this, we introduce a $\text{Beta}(1, 1)$ prior over the Bernoulli distribution. The posterior probability of success for each case would be $\frac{11}{12} = 91.6\%$, $\frac{49}{52} = 94.2\%$, and $\frac{187}{202} = 92.6\%$, respectively. Notably, case 1 now exhibits a lower probability of success compared to case 2.

A Bayesian perspective on the problem naturally incorporates the amount of data as well as its average. This special case shown here is also called Laplace's rate of succession (Ollivier, 2015). Laplace's "add-one" rule (i.e., employing a $\text{Beta}(1, 1)$ prior) of succession modifies the observed frequencies in a sequence of successes and failures by adding one to the observed counts. This modification improves prediction by avoiding zero probabilities and corresponds to a uniform Bayesian prior on the parameter. Suppose further the prior parameters are $a = b = 2$, Figure 2.4 compares the prior distribution and the posterior distributions for the three cases. \square

Why Bayes?

The presented example underscores that Bayesian models incorporate prior information on model parameters, making them particularly useful for regularizing regression problems with limited data information. This characteristic has propelled the Bayesian approach to global recognition over the decades.

In this framework, the prior information $p(\theta)$ and likelihood function $p(x \mid \theta)$ collectively represent a rational person's belief. And then the Bayes' rule emerges as the optimal method for updating this person's beliefs about parameter θ given new information from the data (Fahrmeir et al., 2007; Hoff, 2009).

The prior information given by $p(\theta)$ might be wrong if it does not accurately represent our prior beliefs. Nevertheless, this does not mean that the posterior $p(\theta \mid x)$ is

not useful. As encapsulated by the famous quote “all models are wrong, but some are useful” (Box and Draper, 1987). If the prior $p(\theta)$ approximates our beliefs, then the posterior $p(\theta | x)$ serves as a valuable approximation to posterior beliefs.

2.4.2 Bayesian Linear Model with Zero-Mean Prior

In the linear model, given the input data matrix $\mathbf{X} \in \mathbb{R}^{n \times p}$ and the observation vector $\mathbf{y} \in \mathbb{R}^n$, the model considers the overdetermined system $\mathbf{y} = \mathbf{X}\boldsymbol{\beta}$ when $n > p$, where the vector $\boldsymbol{\beta} \in \mathbb{R}^p$ represents a vector of weights. It often happens that $\mathbf{y} = \mathbf{X}\boldsymbol{\beta}$ has no solution since there are too many equations, i.e., the matrix \mathbf{X} has more rows than columns ($n > p$). Define the column space of \mathbf{X} by $\{\mathbf{X}\boldsymbol{\gamma} : \forall \boldsymbol{\gamma} \in \mathbb{R}^p\}$ and denoted by $\mathcal{C}(\mathbf{X})$. Thus the absence of a solution for the linear system $\mathbf{y} = \mathbf{X}\boldsymbol{\beta}$ implies that the observation vector \mathbf{y} is outside the column space of \mathbf{X} . Addressing this issue involves minimizing the mean squared error (MSE).

Instead of directly seeking the least MSE, we extend the analysis by introducing a Gaussian noise vector $\boldsymbol{\epsilon} \in \mathbb{R}^n$ such that $\mathbf{y} = \mathbf{X}\boldsymbol{\beta} + \boldsymbol{\epsilon}$, where $\boldsymbol{\epsilon} \sim \mathcal{N}(\mathbf{0}, \sigma^2 \mathbf{I})$ and σ^2 is **fixed** (where $\mathcal{N}(\mathbf{a}, \mathbf{B})$ denotes a multivariate Gaussian distribution² with mean \mathbf{a} and covariance \mathbf{B}). And a detailed analysis of this model can be found in Rasmussen (2003); Hoff (2009); Lu (2022a)), this additive Gaussian noise assumption gives rise to the likelihood. Let $\mathcal{X}(\mathbf{x}_{1:n}) = \{\mathbf{x}_1, \mathbf{x}_2, \dots, \mathbf{x}_n\}$ be the observations of n data points, the likelihood function under this Gaussian additive noise model is

$$\text{likelihood} = \mathbf{y} | \mathbf{X}, \boldsymbol{\beta}, \sigma^2 \sim \mathcal{N}(\mathbf{X}\boldsymbol{\beta}, \sigma^2 \mathbf{I}). \quad (2.15)$$

Suppose we specify a multivariate Gaussian prior with a zero-mean and a covariance matrix $\boldsymbol{\Sigma}_0$ over the weight parameter $\boldsymbol{\beta}$,

$$\text{prior} = \boldsymbol{\beta} \sim \mathcal{N}(\mathbf{0}, \boldsymbol{\Sigma}_0).$$

Applying Bayes’ theorem, “posterior \propto likelihood \times prior,” we obtain the posterior

$$\begin{aligned} \text{posterior} &= p(\boldsymbol{\beta} | \mathbf{y}, \mathbf{X}, \sigma^2) \\ &\propto p(\mathbf{y} | \mathbf{X}, \boldsymbol{\beta}, \sigma^2) \cdot p(\boldsymbol{\beta} | \boldsymbol{\Sigma}_0) \\ &= \frac{1}{(2\pi\sigma^2)^{n/2}} \exp\left\{-\frac{1}{2\sigma^2}(\mathbf{y} - \mathbf{X}\boldsymbol{\beta})^\top(\mathbf{y} - \mathbf{X}\boldsymbol{\beta})\right\} \times \frac{1}{(2\pi)^{n/2} |\boldsymbol{\Sigma}_0|^{1/2}} \exp\left(-\frac{1}{2}\boldsymbol{\beta}^\top \boldsymbol{\Sigma}_0^{-1} \boldsymbol{\beta}\right) \\ &\propto \exp\left\{-\frac{1}{2}(\boldsymbol{\beta} - \boldsymbol{\beta}_1)^\top \boldsymbol{\Sigma}_1^{-1}(\boldsymbol{\beta} - \boldsymbol{\beta}_1)\right\} \propto \mathcal{N}(\boldsymbol{\beta}_1, \boldsymbol{\Sigma}_1), \end{aligned}$$

where

$$\boldsymbol{\Sigma}_1 = \left(\frac{1}{\sigma^2} \mathbf{X}^\top \mathbf{X} + \boldsymbol{\Sigma}_0^{-1}\right)^{-1}, \quad \boldsymbol{\beta}_1 = \left(\frac{1}{\sigma^2} \mathbf{X}^\top \mathbf{X} + \boldsymbol{\Sigma}_0^{-1}\right)^{-1} \left(\frac{1}{\sigma^2} \mathbf{X}^\top \mathbf{y}\right).$$

Therefore, the posterior distribution is also a multivariate Gaussian distribution (same form as the prior distribution, i.e., a conjugate prior):

$$\text{posterior} = \boldsymbol{\beta} | \mathbf{y}, \mathbf{X}, \sigma^2 \sim \mathcal{N}(\boldsymbol{\beta}_1, \boldsymbol{\Sigma}_1).$$

². We delay the definition in Chapter 3, p. 38 when we discuss regular conjugate models, see Definition 3.7.1, p. 74.

A word on the notation. Note that we use $\{\boldsymbol{\beta}_1, \boldsymbol{\Sigma}_1\}$ to denote the posterior mean vector and posterior covariance matrix in the *zero-mean prior model*. Similarly, the posterior mean vector and posterior covariance matrix in *semi-conjugate prior* and *fully conjugate prior* models will be denoted as $\{\boldsymbol{\beta}_2, \boldsymbol{\Sigma}_2\}$ and $\{\boldsymbol{\beta}_3, \boldsymbol{\Sigma}_3\}$, respectively, for clarity (refer to the sections below).

Connection to ordinary least squares (OLS). In the Bayesian linear model, there is no general requirement for \mathbf{X} to have full rank. Note further that if we assume full rank for \mathbf{X} (i.e., $\mathbf{X}^\top \mathbf{X}$ is invertible when $n > p$), in the limit, when $\boldsymbol{\Sigma}_0^{-1} \rightarrow \mathbf{0}$, $\boldsymbol{\beta}_1 \rightarrow \hat{\boldsymbol{\beta}} = (\mathbf{X}^\top \mathbf{X})^{-1} \mathbf{X}^\top \mathbf{y}$, in which case, the *maximum a posteriori (MAP) estimator* from the Bayesian model reduces to the ordinary least squares (OLS) estimator. And the posterior is $\boldsymbol{\beta} \mid \mathbf{y}, \mathbf{X}, \sigma^2 \sim \mathcal{N}(\hat{\boldsymbol{\beta}}, \sigma^2 (\mathbf{X}^\top \mathbf{X})^{-1})$, which shares a similar form with the OLS estimator $\hat{\boldsymbol{\beta}} \sim \mathcal{N}(\boldsymbol{\beta}, \sigma^2 (\mathbf{X}^\top \mathbf{X})^{-1})$ under the Gaussian disturbance (see Lu (2022a)).

Remark 2.4: Ridge Regression

In the least squares approximation problem, we use $\mathbf{X}\boldsymbol{\beta}$ to approximate \mathbf{y} . However, two issues may arise: the model can potentially overfit and \mathbf{X} might not have full rank. To address these concerns, in a ridge regression model, we regularize large values of $\boldsymbol{\beta}$, prompting simpler models. Instead of minimizing $\|\mathbf{y} - \mathbf{X}\boldsymbol{\beta}\|^2$, we minimize $\|\mathbf{y} - \mathbf{X}\boldsymbol{\beta}\|^2 + \lambda \|\boldsymbol{\beta}\|^2$, where λ is a hyper-parameter that can be tuned accordingly, e.g., via cross-validation (CV):

$$\arg \min_{\boldsymbol{\beta}} (\mathbf{y} - \mathbf{X}\boldsymbol{\beta})^\top (\mathbf{y} - \mathbf{X}\boldsymbol{\beta}) + \lambda \boldsymbol{\beta}^\top \boldsymbol{\beta}.$$

By differentiating and setting the gradient to zero, we obtain

$$\hat{\boldsymbol{\beta}}_{\text{ridge}} = \left(\mathbf{X}^\top \mathbf{X} + \lambda \mathbf{I} \right)^{-1} \mathbf{X}^\top \mathbf{y},$$

in which case, $(\mathbf{X}^\top \mathbf{X} + \lambda \mathbf{I})$ is invertible even when \mathbf{X} does not have full rank. Further details on ridge regression will be left to the readers.

Connection to ridge regression. We realize that when we set $\boldsymbol{\Sigma}_0 = \mathbf{I}$, we obtain $\boldsymbol{\beta}_1 = (\mathbf{X}^\top \mathbf{X} + \sigma^2 \mathbf{I})^{-1} \mathbf{X}^\top \mathbf{y}$ and $\boldsymbol{\Sigma}_1 = \left(\frac{1}{\sigma^2} \mathbf{X}^\top \mathbf{X} + \mathbf{I} \right)^{-1}$. Since the posterior is $\boldsymbol{\beta} \mid \mathbf{y}, \mathbf{X}, \sigma^2 \sim \mathcal{N}(\boldsymbol{\beta}_1, \boldsymbol{\Sigma}_1)$. The MAP estimator of $\boldsymbol{\beta} = \boldsymbol{\beta}_1 = (\mathbf{X}^\top \mathbf{X} + \sigma^2 \mathbf{I})^{-1} \mathbf{X}^\top \mathbf{y}$, which shares the same form as the ridge regression by letting $\sigma^2 = \lambda$. This implies that the ridge regression estimator is a special instance of the Bayesian linear model with zero-mean prior. And the ridge regression has a nice interpretation from the Bayesian approach—finding the mode of the posterior.

An illustrative example of this Bayesian linear model is presented in Rasmussen (2003), where the “well determined” (i.e., the distribution around the slope is more compact) slope of $\boldsymbol{\beta}$ is almost unchanged after the posterior process while the intercept, which is more dispersed, is shrunk towards zero. This is actually a regularization effect on the parameter as the ridge regression does.

2.4.3 Bayesian Linear Model with Semi-Conjugate Prior

We will employ the *Gamma distribution* as the prior density for the inverse variance (precision) parameter of a Gaussian distribution. The rigorous definition of the Gamma distribution can be found in Chapter 3 (Definition 3.2.3, p. 43) when we discuss conjugate models. As for the reason of using the Gamma distribution as the prior for precision, we quote the description from Kruschke (2014):

Because of its role in conjugate priors for Gaussian likelihood functions, the Gamma distribution is routinely used as a prior for precision (i.e., inverse variance). But there is no logical necessity to do so, and modern MCMC methods permit more flexible specification of priors. Indeed, because precision is less intuitive than standard deviation, it can be more useful to give standard deviation a uniform prior that spans a wide range.

Same setting as Section 2.4.2, we now consider the case where the variance σ^2 of the Gaussian likelihood is **not fixed**. Again, The likelihood function is given by:

$$\text{likelihood} = \mathbf{y} \mid \mathbf{X}, \boldsymbol{\beta}, \sigma^2 \sim \mathcal{N}(\mathbf{X}\boldsymbol{\beta}, \sigma^2 \mathbf{I}).$$

We specify a **non-zero-mean** Gaussian prior over the weight parameter $\boldsymbol{\beta}$,

$$\begin{aligned} \text{prior} : \boldsymbol{\beta} &\sim \mathcal{N}(\boldsymbol{\beta}_0, \boldsymbol{\Sigma}_0) \\ \gamma &= 1/\sigma^2 \sim \mathcal{G}(a_0, b_0), \end{aligned}$$

where we differentiate from previous descriptions by blue text, and $\mathcal{G}(a, b) = \frac{b^a}{\Gamma(a)} x^{a-1} \exp(-bx)$ denotes a Gamma distribution with parameters a, b . And the function $\Gamma(a) = \int_0^\infty t^{a-1} \exp(-t) dt$ is the Gamma function.

Step 1, conditioned on σ^2 . Then, given σ^2 , by the Bayes' theorem “posterior \propto likelihood \times prior,” we get the conditional posterior density of $\boldsymbol{\beta}$:

$$\begin{aligned} \text{posterior} &= p(\boldsymbol{\beta} \mid \mathbf{y}, \mathbf{X}, \sigma^2) \propto p(\mathbf{y} \mid \mathbf{X}, \boldsymbol{\beta}, \sigma^2) \cdot p(\boldsymbol{\beta} \mid \boldsymbol{\beta}_0, \boldsymbol{\Sigma}_0) \\ &= \frac{1}{(2\pi\sigma^2)^{n/2}} \exp\left\{-\frac{1}{2\sigma^2}(\mathbf{y} - \mathbf{X}\boldsymbol{\beta})^\top (\mathbf{y} - \mathbf{X}\boldsymbol{\beta})\right\} \\ &\quad \times \frac{1}{(2\pi)^{n/2} |\boldsymbol{\Sigma}_0|^{1/2}} \exp\left\{-\frac{1}{2}(\boldsymbol{\beta} - \boldsymbol{\beta}_0)^\top \boldsymbol{\Sigma}_0^{-1}(\boldsymbol{\beta} - \boldsymbol{\beta}_0)\right\} \\ &\propto \exp\left\{-\frac{1}{2}(\boldsymbol{\beta} - \boldsymbol{\beta}_2)^\top \boldsymbol{\Sigma}_2^{-1}(\boldsymbol{\beta} - \boldsymbol{\beta}_2)\right\} \propto \mathcal{N}(\boldsymbol{\beta}_2, \boldsymbol{\Sigma}_2), \end{aligned}$$

where the parameters are

$$\begin{aligned} \boldsymbol{\Sigma}_2 &= \left(\frac{1}{\sigma^2} \mathbf{X}^\top \mathbf{X} + \boldsymbol{\Sigma}_0^{-1}\right)^{-1}, \\ \boldsymbol{\beta}_2 &= \boldsymbol{\Sigma}_2(\boldsymbol{\Sigma}_0^{-1}\boldsymbol{\beta}_0 + \frac{1}{\sigma^2} \mathbf{X}^\top \mathbf{y}) = \left(\frac{1}{\sigma^2} \mathbf{X}^\top \mathbf{X} + \boldsymbol{\Sigma}_0^{-1}\right)^{-1} \left(\boldsymbol{\Sigma}_0^{-1}\boldsymbol{\beta}_0 + \frac{1}{\sigma^2} \mathbf{X}^\top \mathbf{y}\right). \end{aligned}$$

Therefore, the conditional posterior follows from a Gaussian distribution:

$$\text{posterior} = \boldsymbol{\beta} \mid \mathbf{y}, \mathbf{X}, \sigma^2 \sim \mathcal{N}(\boldsymbol{\beta}_2, \boldsymbol{\Sigma}_2).$$

Connection to the zero-mean prior model. We highlight the connection between the zero-mean prior model and the semi-conjugate prior model as follows:

1. We note that β_1 in Section 2.4.2 is a special case of β_2 when $\beta_0 = \mathbf{0}$.
2. And if we assume further \mathbf{X} has full rank, when $\Sigma_0^{-1} \rightarrow \mathbf{0}$, we have $\beta_2 \rightarrow \hat{\beta} = (\mathbf{X}^\top \mathbf{X})^{-1} \mathbf{X}^\top \mathbf{y}$, which reduces to the OLS estimator.
3. When $\sigma^2 \rightarrow \infty$, β_2 is approximately approaching β_0 , the prior expectation of parameter. However, in the zero-mean prior model, $\sigma^2 \rightarrow \infty$ will make β_1 approach $\mathbf{0}$.
4. **Weighted average:** we reformulate β_2 by

$$\begin{aligned} \beta_2 &= \left(\frac{1}{\sigma^2} \mathbf{X}^\top \mathbf{X} + \Sigma_0^{-1} \right)^{-1} \left(\Sigma_0^{-1} \beta_0 + \frac{1}{\sigma^2} \mathbf{X}^\top \mathbf{y} \right) \\ &= \left(\frac{1}{\sigma^2} \mathbf{X}^\top \mathbf{X} + \Sigma_0^{-1} \right)^{-1} \Sigma_0^{-1} \beta_0 + \left(\frac{1}{\sigma^2} \mathbf{X}^\top \mathbf{X} + \Sigma_0^{-1} \right)^{-1} \frac{\mathbf{X}^\top \mathbf{X}}{\sigma^2} (\mathbf{X}^\top \mathbf{X})^{-1} \mathbf{X}^\top \mathbf{y} \\ &= (\mathbf{I} - \mathbf{A}) \beta_0 + \mathbf{A} \hat{\beta}, \end{aligned}$$

where $\hat{\beta} = (\mathbf{X}^\top \mathbf{X})^{-1} \mathbf{X}^\top \mathbf{y}$ is the OLS estimator of β , and $\mathbf{A} = \left(\frac{1}{\sigma^2} \mathbf{X}^\top \mathbf{X} + \Sigma_0^{-1} \right)^{-1} \frac{\mathbf{X}^\top \mathbf{X}}{\sigma^2}$. We observe that the posterior mean of β is a weighted average of the prior mean and the OLS estimator of β . Thus, if we set the prior parameter $\beta_0 = \hat{\beta}$, the posterior mean of β becomes precisely $\hat{\beta}$.

Step 2, conditioned on β . Given β , again, by Bayes' theorem, we obtain the conditional posterior density of $\gamma = \frac{1}{\sigma^2}$:

$$\begin{aligned} \text{posterior} &= p(\gamma = \frac{1}{\sigma^2} \mid \mathbf{y}, \mathbf{X}, \beta) \propto p(\mathbf{y} \mid \mathbf{X}, \beta, \gamma) \cdot p(\gamma \mid a_0, b_0) \\ &= \frac{\gamma^{n/2}}{(2\pi)^{n/2}} \exp \left\{ -\frac{\gamma}{2} (\mathbf{y} - \mathbf{X}\beta)^\top (\mathbf{y} - \mathbf{X}\beta) \right\} \\ &\quad \times \frac{b_0^{a_0}}{\Gamma(a_0)} \gamma^{a_0-1} \exp(-b_0\gamma) \\ &\propto \gamma^{(a_0 + \frac{n}{2} - 1)} \exp \left\{ -\gamma \left[b_0 + \frac{1}{2} (\mathbf{y} - \mathbf{X}\beta)^\top (\mathbf{y} - \mathbf{X}\beta) \right] \right\}, \end{aligned}$$

and the conditional posterior follows from a Gamma distribution:

$$\text{posterior of } \gamma \text{ given } \beta = \gamma \mid \mathbf{y}, \mathbf{X}, \beta \sim \mathcal{G} \left(a_0 + \frac{n}{2}, \left[b_0 + \frac{1}{2} (\mathbf{y} - \mathbf{X}\beta)^\top (\mathbf{y} - \mathbf{X}\beta) \right] \right).$$

Prior information on the noise/precision. We can find an intuitive prior interpretation as follows:

1. We notice that the prior mean and posterior mean of γ are $E[\gamma] = \frac{a_0}{b_0}$ and $E[\gamma \mid \beta] = \frac{a_0 + \frac{n}{2}}{b_0 + \frac{1}{2} (\mathbf{y} - \mathbf{X}\beta)^\top (\mathbf{y} - \mathbf{X}\beta)}$, respectively. So the latent meaning of $2a_0$ is the prior sample size for the noise $\sigma^2 = \frac{1}{\gamma}$.

2. As we assume $\mathbf{y} = \mathbf{X}\boldsymbol{\beta} + \boldsymbol{\epsilon}$ where $\boldsymbol{\epsilon} \sim \mathcal{N}(\mathbf{0}, \sigma^2 \mathbf{I})$, then $\frac{(\mathbf{y} - \mathbf{X}\boldsymbol{\beta})^\top (\mathbf{y} - \mathbf{X}\boldsymbol{\beta})}{\sigma^2} \sim \chi^2(n)$ and $E\left[\frac{1}{2}(\mathbf{y} - \mathbf{X}\boldsymbol{\beta})^\top (\mathbf{y} - \mathbf{X}\boldsymbol{\beta})\right] = \frac{n}{2}\sigma^2$ ³. So the latent meaning of $\frac{b_0}{a_0}$ is the prior variance of the noise.
3. Some textbooks would write $\gamma \sim \mathcal{G}(n_0/2, n_0\sigma_0^2/2)$ to make this explicit (in which case, n_0 is the prior sample size, and σ_0^2 is the prior variance). But a prior in this form seems coming from nowhere at first glance.

Gibbs sampler. By this Gibbs sampling method introduced in Section 2.3.3, we can construct a Gibbs sampler for the Bayesian linear model with semi-conjugate prior:

0. Set initial values to $\boldsymbol{\beta}$ and $\gamma = \frac{1}{\sigma^2}$;
1. update $\boldsymbol{\beta}$: posterior = $\boldsymbol{\beta} \mid \mathbf{y}, \mathbf{X}, \gamma \sim \mathcal{N}(\boldsymbol{\beta}_2, \boldsymbol{\Sigma}_2)$;
2. update γ : posterior = $\gamma \mid \mathbf{y}, \mathbf{X}, \boldsymbol{\beta} \sim \mathcal{G}\left(a_0 + \frac{n}{2}, [b_0 + \frac{1}{2}(\mathbf{y} - \mathbf{X}\boldsymbol{\beta})^\top (\mathbf{y} - \mathbf{X}\boldsymbol{\beta})]\right)$.

2.4.4 Bayesian Linear Model with Full Conjugate Prior

Introducing a Gamma prior over the inverse variance is equivalent to imposing an inverse-Gamma prior⁴ on the variance. Same setting as the semi-conjugate prior distribution in Section 2.4.3. We have the likelihood function:

$$\text{likelihood} = \mathbf{y} \mid \mathbf{X}, \boldsymbol{\beta}, \sigma^2 \sim \mathcal{N}(\mathbf{X}\boldsymbol{\beta}, \sigma^2 \mathbf{I}).$$

But now we specify a joint Gaussian and inverse-Gamma prior over the weight and variance parameters by

$$\begin{aligned} \text{prior} : \boldsymbol{\beta} \mid \sigma^2 &\sim \mathcal{N}(\boldsymbol{\beta}_0, \sigma^2 \boldsymbol{\Sigma}_0) \\ \sigma^2 &\sim \mathcal{G}^{-1}(a_0, b_0), \end{aligned}$$

where again we differentiate this description from the previous ones with blue text. Equivalently, we can formulate the prior into a joint one, which is called the *normal-inverse-Gamma* (*NIG*) distribution:

$$\text{prior} : \boldsymbol{\beta}, \sigma^2 \sim \mathcal{NIG}(\boldsymbol{\beta}_0, \boldsymbol{\Sigma}_0, a_0, b_0) = \mathcal{N}(\boldsymbol{\beta}_0, \sigma^2 \boldsymbol{\Sigma}_0) \cdot \mathcal{G}^{-1}(a_0, b_0).$$

Once again, applying Bayes' theorem, "posterior \propto likelihood \times prior," we obtain the posterior:

$$\begin{aligned} \text{posterior} &= p(\boldsymbol{\beta}, \sigma^2 \mid \mathbf{y}, \mathbf{X}) \propto p(\mathbf{y} \mid \mathbf{X}, \boldsymbol{\beta}, \sigma^2) \cdot p(\boldsymbol{\beta}, \sigma^2 \mid \boldsymbol{\beta}_0, \boldsymbol{\Sigma}_0, a_0, b_0) \\ &= \frac{1}{(2\pi\sigma^2)^{n/2}} \exp\left\{-\frac{1}{2\sigma^2}(\mathbf{y} - \mathbf{X}\boldsymbol{\beta})^\top (\mathbf{y} - \mathbf{X}\boldsymbol{\beta})\right\} \\ &\quad \times \frac{1}{(2\pi\sigma^2)^{p/2} |\boldsymbol{\Sigma}_0|^{1/2}} \exp\left\{-\frac{1}{2\sigma^2}(\boldsymbol{\beta} - \boldsymbol{\beta}_0)^\top \boldsymbol{\Sigma}_0^{-1}(\boldsymbol{\beta} - \boldsymbol{\beta}_0)\right\} \\ &\quad \times \frac{b_0^{a_0}}{\Gamma(a_0)} \frac{1}{(\sigma^2)^{a_0+1}} \exp\left(-\frac{b_0}{\sigma^2}\right) \\ &\propto \frac{1}{(2\pi\sigma^2)^{p/2}} \exp\left\{\frac{1}{2\sigma^2}(\boldsymbol{\beta} - \boldsymbol{\beta}_3)^\top \boldsymbol{\Sigma}_3^{-1}(\boldsymbol{\beta} - \boldsymbol{\beta}_3)\right\} \\ &\quad \times \frac{1}{(\sigma^2)^{a_0 + \frac{n}{2} + 1}} \exp\left\{-\frac{1}{\sigma^2} \left[b_0 + \frac{1}{2}(\mathbf{y}^\top \mathbf{y} + \boldsymbol{\beta}_0^\top \boldsymbol{\Sigma}_0^{-1} \boldsymbol{\beta}_0 - \boldsymbol{\beta}_3^\top \boldsymbol{\Sigma}_3^{-1} \boldsymbol{\beta}_3) \right]\right\}, \end{aligned}$$

3. $\chi^2(n)$ is a Chi-squared distribution with n degrees of freedom. See Definition 3.2.6 (p. 49).

4. We again delay the definition in Definition 3.2.4 (p. 47) when we discuss regular conjugate models.

where the parameters are

$$\begin{aligned}\boldsymbol{\Sigma}_3 &= \left(\mathbf{X}^\top \mathbf{X} + \boldsymbol{\Sigma}_0^{-1}\right)^{-1}, \\ \boldsymbol{\beta}_3 &= \boldsymbol{\Sigma}_3(\mathbf{X}^\top \mathbf{y} + \boldsymbol{\Sigma}_0^{-1}\boldsymbol{\beta}_0) = \left(\mathbf{X}^\top \mathbf{X} + \boldsymbol{\Sigma}_0^{-1}\right)^{-1}(\boldsymbol{\Sigma}_0^{-1}\boldsymbol{\beta}_0 + \mathbf{X}^\top \mathbf{y}).\end{aligned}$$

Let $a_n = a_0 + \frac{n}{2} + 1$ and $b_n = b_0 + \frac{1}{2}(\mathbf{y}^\top \mathbf{y} + \boldsymbol{\beta}_0^\top \boldsymbol{\Sigma}_0^{-1}\boldsymbol{\beta}_0 - \boldsymbol{\beta}_3^\top \boldsymbol{\Sigma}_3^{-1}\boldsymbol{\beta}_3)$. The posterior is thus a NIG distribution:

$$\text{posterior} = \boldsymbol{\beta}, \sigma^2 \mid \mathbf{y}, \mathbf{X} \sim \mathcal{NIG}(\boldsymbol{\beta}_3, \boldsymbol{\Sigma}_3, a_n, b_n).$$

Connection to zero-mean prior and semi-conjugate prior models. We highlight the connection of the fully conjugate model to the zero-mean prior and semi-conjugate prior models as follows:

1. If we assume further \mathbf{X} has full rank, when $\boldsymbol{\Sigma}_0^{-1} \rightarrow \mathbf{0}$, we have $\boldsymbol{\beta}_3 \rightarrow \hat{\boldsymbol{\beta}} = (\mathbf{X}^\top \mathbf{X})^{-1} \mathbf{X}^\top \mathbf{y}$, which reduces to the OLS estimator.
2. When $b_0 \rightarrow \infty$, then $\sigma^2 \rightarrow \infty$ and $\boldsymbol{\beta}_3$ is approximately approaching $\boldsymbol{\beta}_0$, the prior expectation of parameter. Compared to $\boldsymbol{\beta}_2$ in Section 2.4.3, $\sigma^2 \rightarrow \infty$ will make $\boldsymbol{\beta}_2$ approach to $\boldsymbol{\beta}_0$, where σ^2 is a fixed hyper-parameter.
3. **Weighted average:** we reformulate

$$\begin{aligned}\boldsymbol{\beta}_3 &= \left(\mathbf{X}^\top \mathbf{X} + \boldsymbol{\Sigma}_0^{-1}\right)^{-1}(\boldsymbol{\Sigma}_0^{-1}\boldsymbol{\beta}_0 + \mathbf{X}^\top \mathbf{y}) \\ &= \left(\mathbf{X}^\top \mathbf{X} + \boldsymbol{\Sigma}_0^{-1}\right)^{-1} \boldsymbol{\Sigma}_0^{-1}\boldsymbol{\beta}_0 + \left(\mathbf{X}^\top \mathbf{X} + \boldsymbol{\Sigma}_0^{-1}\right)^{-1}(\mathbf{X}^\top \mathbf{X})(\mathbf{X}^\top \mathbf{X})^{-1} \mathbf{X}^\top \mathbf{y} \\ &= (\mathbf{I} - \mathbf{C})\boldsymbol{\beta}_0 + \mathbf{C}\hat{\boldsymbol{\beta}},\end{aligned}$$

where $\hat{\boldsymbol{\beta}} = (\mathbf{X}^\top \mathbf{X})^{-1} \mathbf{X}^\top \mathbf{y}$ is the OLS estimator of $\boldsymbol{\beta}$, and $\mathbf{C} = (\mathbf{X}^\top \mathbf{X} + \boldsymbol{\Sigma}_0^{-1})^{-1}(\mathbf{X}^\top \mathbf{X})$. We observe that the posterior mean of $\boldsymbol{\beta}$ is a weighted average of the prior mean and the OLS estimator of $\boldsymbol{\beta}$. Thus, if we set $\boldsymbol{\beta}_0 = \hat{\boldsymbol{\beta}}$, the posterior mean of $\boldsymbol{\beta}$ will be exactly $\hat{\boldsymbol{\beta}}$.

4. From the relationship of $a_n = a_0 + \frac{n}{2} + 1$, we know that $2a_0$ is the prior sample size for σ^2 .
5. $\boldsymbol{\Sigma}_3^{-1} = \mathbf{X}^\top \mathbf{X} + \boldsymbol{\Sigma}_0^{-1}$: the posterior precision matrix (inverse covariance matrix) is equal to data precision $\mathbf{X}^\top \mathbf{X}$ + prior precision.

⌘ Chapter 2 Problems ⌘

1. Suppose both $p(x)$ and $q(x)$ are probability density functions with

$$p(x) \propto q(x).$$

Show that $p(x) = q(x)$ for all x .

Regular Probability Models and Conjugacy

Contents

3.1	Conjugate Priors	40
3.2	Regular Univariate Models and Conjugacy	40
3.3	Exponential and Conjugacy	56
3.4	Univariate Gaussian-Related Models	57
3.5	Multinomial Distribution and Conjugacy	66
3.5.1	Dirichlet Distribution	68
3.5.2	Posterior Distribution for Multinomial Distribution	69
3.6	Poisson and Multinomial	72
3.7	Multivariate Gaussian Distribution and Conjugacy	73
3.7.1	Multivariate Gaussian Distribution	74
3.7.2	Multivariate Student's t Distribution	77
3.7.3	Prior on Parameters of Multivariate Gaussian Distribution	78
3.7.4	Posterior Distribution of $\boldsymbol{\mu}$: Separated View	82
3.7.5	Posterior Distribution of $\boldsymbol{\Sigma}$: Separated View	83
3.7.6	Gibbs Sampling of the Mean and Covariance: Separated View	85
3.7.7	Posterior Distribution of $\boldsymbol{\mu}$ and $\boldsymbol{\Sigma}$ Under NIW: Unified View	85
	Parameter Choice	87
	Reducing Sampling Time by Maintaining Squared Sum of Customers	87
3.7.8	Posterior Marginal Likelihood of Parameters	88
3.7.9	Posterior Marginal Likelihood of Data	89
3.7.10	Posterior Predictive for Data without Observations	89
3.7.11	Posterior Predictive for New Data with Observations	90
3.7.12	Further Optimization via the Cholesky Decomposition	91
	Definition	91
	Rank One Update	91
	Speedup for Determinant	91

Update in NIW	91
Chapter 3 Problems	92

3.1. Conjugate Priors



In Section 2.4.1 (p. 29), we briefly discussed conjugate priors. Conjugate priors play a crucial role in Bayesian statistics, providing a convenient mathematical property that simplifies the computation of posterior distributions. We now present the formal definition as follows.

Definition 3.1.1 (Conjugate Prior) *Given a family $\{p(\mathcal{X} | \theta) : \theta \in \Theta\}$ of generating distributions, a collection of priors $p_\omega(\theta)$ indexed by $\omega \in \Omega$ is called a conjugate prior family if for any ω and any data, the resulting posterior equals to $p_{\omega'}(\theta | \mathcal{X})$ for some $\omega' \in \Omega$.*

In Bayesian inference, a prior distribution represents our beliefs about the parameters of a statistical model before observing any data. A prior is considered conjugate to a likelihood function if their combination results in a posterior distribution that belongs to the same family of distributions as the prior. This property facilitates analytical solutions, making the computation of the posterior more tractable. A toy example of the Beta-Bernoulli model can enhance our comprehension of conjugate priors.

Example 3.1 (Beta-Bernoulli) *Suppose $\mathcal{X} = \{x_1, x_2, \dots, x_N\}$ are drawn independently and identically distributed (i.i.d.) from a Bernoulli distribution with parameter θ , i.e., $\text{Bernoulli}(x | \theta)$. $\text{Beta}(\theta | a, b)$ distribution, with $a, b > 0$, is conjugate to $\text{Bernoulli}(x | \theta)$, since the posterior density is $p(\theta | \mathcal{X}) = \text{Beta}(\theta | a + \sum x_i, b + N - \sum x_i)$. \square*

Conjugate priors make it possible to do Bayesian reasoning in a computationally efficient manner, as well as having the philosophically satisfying interpretation of representing real or imaginary prior data. Generally, there are basically two reasons why models with conjugate priors are popular (Robert et al., 2007; Bernardo and Smith, 2009; Hoff, 2009; Gelman et al., 2013):

- They usually allow us to derive a closed-form expression for the posterior distribution.
- They are easy to interpret, as we can easily observe how the parameters of the prior change after the Bayesian updates.

3.2. Regular Univariate Models and Conjugacy

Gaussian, p. 41	Gamma, p. 43	Student's t , p. 43
Inverse-Gamma, p. 47	Truncated-Normal, p. 57	Inverse-Gaussian, p. 63
Chi-Square, p. 49	Normal-Inv-Gamma, p. 48	Inverse-Chi-Squared, p. 51
Nor-Inv-Chi-Squared, p. 52	General-Truncated-Nor, p. 60	Half-Normal, p. 61
Laplace, p. 64	Skew-Laplace, p. 66	Rectified-Normal, p. 62
Multinomial, p. 67	Dirichlet, p. 68	Poisson, p. 72
Exponential, p. 56	Multi Gaussian, p. 74	Multi Student's t , p. 77
Wishart, p. 78	Inverse-Wishart, p. 80	Normal-Inv-Wishart, p. 81

Table 3.1: Links for common distributions.

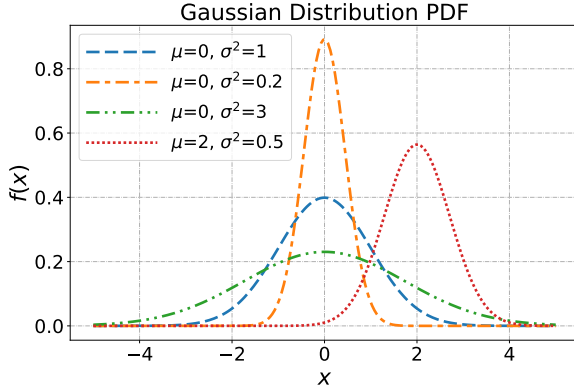


Figure 3.1: Gaussian probability density functions for different values of the mean and variance parameters μ and σ^2 .

In most of our Bayesian matrix decomposition developments, we express the models with univariate distributions. While in the Gaussian model, we also apply multivariate distributions. In this section, we provide rigorous definitions for common univariate distributions and their conjugate priors. Table 3.1 provides an overview of the topics covered in this section. Additionally, with special considerations, we also discuss the multivariate Gaussian distribution and its conjugacy in the next section.

Definition 3.2.1 (Gaussian or Normal Distribution) *A random variable x is said to follow the Gaussian distribution (a.k.a., a normal distribution) with mean and variance parameters μ and $\sigma^2 > 0$, denoted by $x \sim \mathcal{N}(\mu, \sigma^2)$ ^a, if*

$$f(x; \mu, \sigma^2) = \frac{1}{\sqrt{2\pi\sigma^2}} \exp\left\{-\frac{1}{2\sigma^2}(x - \mu)^2\right\} = \sqrt{\frac{\tau}{2\pi}} \exp\left\{-\frac{\tau}{2}(x - \mu)^2\right\}.$$

The mean and variance of $x \sim \mathcal{N}(\mu, \sigma^2)$ are given by

$$\mathbb{E}[x] = \mu, \quad \text{Var}[x] = \sigma^2 = \tau^{-1},$$

where τ is also known as the precision of the Gaussian distribution. Figure 3.1 illustrates the impact of different parameters μ, σ^2 for the Gaussian distribution.

a. Note if two random variables a and b have the same distribution, then we write $a \sim b$.

Suppose $\mathcal{X} = \{x_1, x_2, \dots, x_N\}$ are drawn i.i.d. from a Gaussian distribution of $\mathcal{N}(x | \mu, \sigma^2)$. For conjugate Bayesian analysis, we may rewrite the Gaussian probability density function as follows,

$$\begin{aligned} p(\mathcal{X} | \mu, \sigma^2) &= \prod_{i=1}^N \mathcal{N}(x_i | \mu, \sigma^2) \\ &= (2\pi)^{-N/2} (\sigma^2)^{-N/2} \exp\left\{-\frac{1}{2\sigma^2} \left[N(\bar{x} - \mu)^2 + N \sum_{n=1}^N (x_n - \bar{x})^2 \right]\right\} \quad (3.1) \\ &= (2\pi)^{-N/2} (\sigma^2)^{-N/2} \exp\left\{-\frac{1}{2\sigma^2} [N(\bar{x} - \mu)^2 + NS_{\bar{x}}]\right\}, \end{aligned}$$

where $S_{\bar{x}} = \sum_{n=1}^N (x_n - \bar{x})^2$ and $\bar{x} = \frac{1}{N} \sum_{i=1}^N x_i$. This form can help find the conditional posterior of Gaussian likelihood under *normal-inverse-Gamma* prior (Equation (3.11)).

Given fixed mean μ and variance σ^2 parameters, we have

$$p(x | \mu, \sigma^2) = \mathcal{N}(x | \mu, \sigma^2) \propto \exp \left\{ -\frac{1}{2\sigma^2} x^2 + \frac{\mu}{\sigma^2} x \right\}, \quad (3.2)$$

where “ \propto ” means “proportional to.” Therefore, if we find a form conforming to the above equation, we can say the random variable x follows the Gaussian distribution $x \sim \mathcal{N}(\mu, \sigma^2)$. Refer to the example of a Bayesian *GGG* matrix decomposition model in Equation (6.10) (p. 145).

While the product of two Gaussian variables remains an open problem, the sum of Gaussian variables follows from a new Gaussian distribution.

Remark 3.1: Sum of Gaussians

Let x and y be two Gaussian distributed variables with means μ_x, μ_y and variance σ_x^2, σ_y^2 , respectively.

- When there is no correlation between the two variables, then it follows that

$$x + y \sim \mathcal{N}(\mu_x + \mu_y, \sigma_x^2 + \sigma_y^2).$$

- When there exists a correlation of ρ between the two variables, then it follows that

$$x + y \sim \mathcal{N}(\mu_x + \mu_y, \sigma_x^2 + \sigma_y^2 + 2\rho\sigma_x\sigma_y).$$

Conjugate prior for mean of a Gaussian distribution and Normal-Normal model.

The Gaussian distribution serves as a conjugate prior for the mean parameter of a Gaussian distribution when the variance is fixed. To see this, suppose $\mathcal{X} = \{x_1, x_2, \dots, x_N\}$ are i.i.d. normal with mean θ and precision λ , i.e., the likelihood is $\mathcal{N}(x_i | \theta, \lambda^{-1})$, where the variance $\sigma^2 = \lambda^{-1}$ is fixed, and θ is given a $\mathcal{N}(\mu_0, \lambda_0^{-1})$ prior: $\theta \sim \mathcal{N}(\mu_0, \lambda^{-1})$. Using Bayes’ theorem, “posterior \propto likelihood \times prior,” the posterior density is

$$p(\theta | \mathcal{X}) \propto \prod_{i=1}^N \mathcal{N}(x_i | \theta, \lambda^{-1}) \times \mathcal{N}(\theta | \mu_0, \lambda_0^{-1}) \propto \mathcal{N}(\theta | \tilde{\mu}, \tilde{\lambda}^{-1}),$$

where, given $\bar{x} = \frac{1}{N} \sum_{i=1}^N x_i$,

$$\begin{aligned} \tilde{\mu} &= \frac{\lambda_0 \mu_0 + \lambda \sum_{i=1}^N x_i}{\lambda_0 + N\lambda} = \frac{\lambda_0}{\lambda_0 + N\lambda} \mu_0 + \frac{N\lambda}{\lambda_0 + N\lambda} \bar{x}, \\ \tilde{\lambda} &= \lambda_0 + N\lambda. \end{aligned} \quad (3.3)$$

Thus, the posterior mean is a weighted mean of the prior mean μ_0 and the sample average \bar{x} ; the posterior precision is the sum of the prior precision and sample precision $N\lambda$. We show that the Gaussian distribution is, itself, a conjugate prior for the mean parameter of a Gaussian distribution when fixing variance. This is often referred to as the *Normal-Normal model*, and this model can be used to provide evidence for the bimodal property of human heights (Schilling et al., 2002).

Definition 3.2.2 (Student’s t Distribution) A random variable x is said to follow the Student’s t distribution with parameters μ , $\sigma^2 > 0$, and ν , denoted by $x \sim \tau(\mu, \sigma^2, \nu)$, if

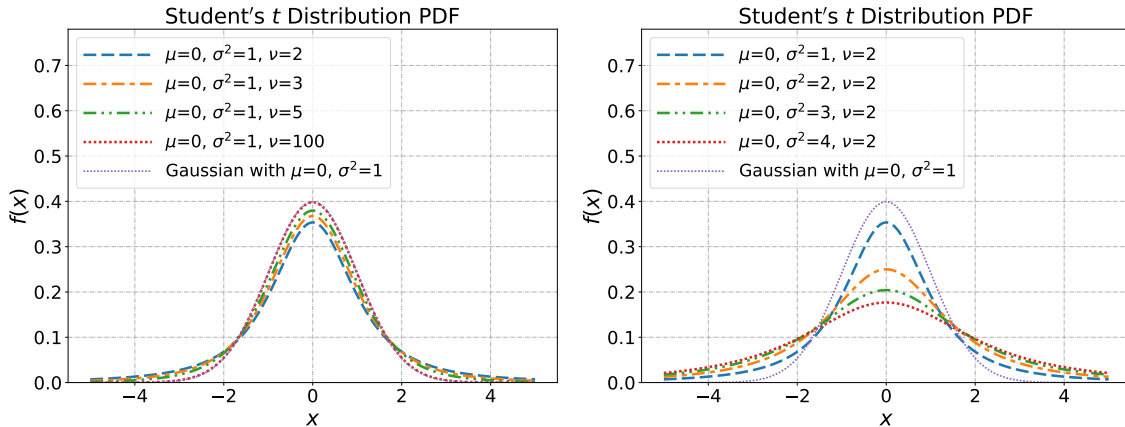
$$f(x; \mu, \sigma^2, \nu) = \frac{\Gamma(\frac{\nu+1}{2})}{\Gamma(\frac{\nu}{2})} \frac{1}{\sigma\sqrt{\nu\pi}} \times \left[1 + \frac{(x - \mu)^2}{\nu\sigma^2} \right]^{-\frac{(\nu+1)}{2}}, \tag{3.4}$$

where σ^2 is called the **scale parameter**, and ν is the **degree of freedom**. The distribution has fatter tails than a Gaussian distribution. The smaller ν is, the fatter the tail. As $\nu \rightarrow \infty$, the distribution converges towards a Gaussian. A particular case of the Student’s t distribution is the **Cauchy distribution**, $x \sim \mathcal{C}(\mu, \sigma^2)$ if $x \sim \tau(\mu, \sigma^2, 1)$, i.e., $\nu = 1$. The mean and variance of $x \sim \tau(\mu, \sigma^2, \nu)$ are given by

$$E[x] = \begin{cases} \mu, & \text{if } \nu > 1; \\ \text{undefined}, & \text{if } \nu \leq 1. \end{cases} \quad \text{Var}[x] = \begin{cases} \frac{\nu}{\nu - 2} \sigma^2, & \text{if } \nu > 2; \\ \infty, & \text{if } 1 < \nu \leq 2. \end{cases}$$

Figure 3.2 compares different parameters μ, σ^2, ν for the Student’s t distribution.

In Figure 3.2(a), we vary the ν parameter for the Student’s t distribution. As ν decreases, the distribution becomes more spread out, leading to fatter tails compared to a Gaussian distribution. This allows for more flexibility in modeling data with greater uncertainty or outliers since the Student’s t distribution has a greater probability of observing extreme values. In Bayesian modeling, the Student’s t distribution is often used as a prior for the mean parameter of a Gaussian likelihood, allowing for estimation of both the mean and precision of the data. This results in a *Student’s t -Normal* model.



(a) Student’s t distribution by varying parameter ν . (b) Student’s t distribution by varying parameter σ^2 . When $\nu = 100$, the distribution is very close to a Gaussian distribution.

Figure 3.2: Student’s t distribution for different values of the parameters ν and σ^2 .

Definition 3.2.3 (Gamma Distribution) A random variable x is said to follow the Gamma distribution with shape parameter $r > 0$ and rate parameter $\lambda > 0$ ^a, denoted by

$x \sim \mathcal{G}(r, \lambda)$, if

$$f(x; r, \lambda) = \begin{cases} \frac{\lambda^r}{\Gamma(r)} x^{r-1} \exp(-\lambda x), & \text{if } x \geq 0; \\ 0, & \text{if } x < 0, \end{cases}$$

where $\Gamma(x) = \int_0^\infty t^{x-1} \exp(-t) dt$ is the Gamma function, and we can just take it as a function to normalize the distribution into sum to 1. In special cases when y is a positive integer, $\Gamma(y) = (y - 1)!$. The mean and variance of $x \sim \mathcal{G}(r, \lambda)$ are given by

$$\mathbb{E}[x] = \frac{r}{\lambda}, \quad \text{Var}[x] = \frac{r}{\lambda^2}.$$

Specially, let x_1, x_2, \dots, x_n be i.i.d. random variables drawn from $\mathcal{G}(r_i, \lambda)$ for each $i \in \{1, 2, \dots, n\}$. Then $y = \sum_{i=1}^n x_i$ is a random variable following from $\mathcal{G}(\sum_{i=1}^n r_i, \lambda)$. Figure 3.3(a) compares different parameters r, λ for the Gamma distribution.

- a. Note the inverse rate parameter $1/\lambda$ is called the scale parameter. In probability theory and statistics, the **location** parameter shifts the entire distribution left or right, e.g., the mean parameter of a Gaussian distribution; the **shape** parameter compresses or stretches the entire distribution; the **scale** parameter changes the shape of the distribution in some manner.

It's crucial to keep in mind that the definition of the Gamma distribution does not restrict r to be a natural number and it allows for r to be any positive number. However, when r is a positive integer, the Gamma distribution can be interpreted as a sum of r exponentials of rate λ (see Definition 3.3.1). The summation property holds true more generally for Gamma variables with the same rate parameter. If x_1 and x_2 are random variables drawn from $\mathcal{G}(r_1, \lambda)$ and $\mathcal{G}(r_2, \lambda)$, respectively, then their sum $x_1 + x_2$ is a Gamma random variable from $\mathcal{G}(r_1 + r_2, \lambda)$.

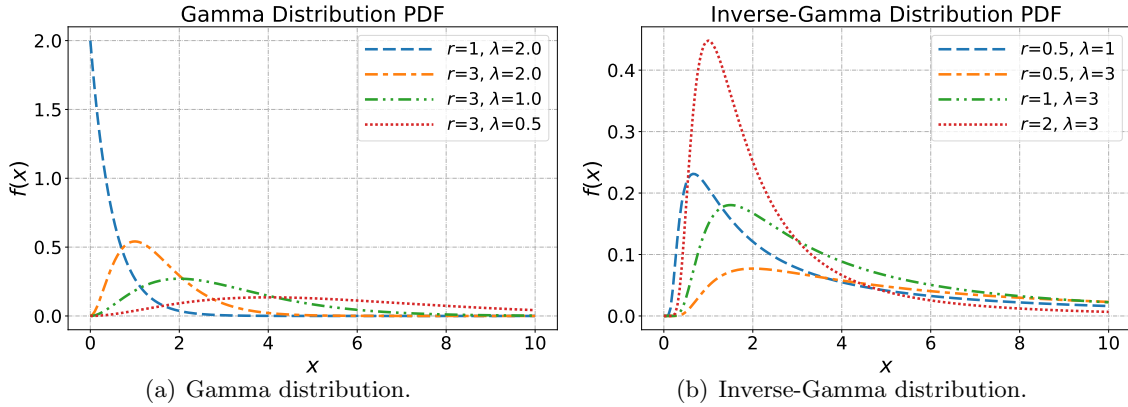


Figure 3.3: Gamma and inverse-Gamma probability density functions for different values of the parameters r and λ .

Conjugate prior for rate of a Gamma distribution and Gamma-Gamma model.

The Gamma distribution is a conjugate prior of the *rate* parameter of another Gamma distribution. Suppose data $\mathcal{X} = \{x_1, x_2, \dots, x_N\}$ follows i.i.d. from a Gamma distribution $x_i \sim \mathcal{G}(r, \lambda)$. Suppose further the rate parameter is given a Gamma prior $\lambda \sim \mathcal{G}(a, \frac{a}{b})$.

Using Bayes' theorem, the posterior density is

$$\begin{aligned}
 p(\lambda \mid \mathcal{X}) &\propto \prod_{i=1}^N \mathcal{G}(x_i \mid r, \lambda) \times \mathcal{G}(\lambda \mid a, \frac{a}{b}) \\
 &\propto \prod_{i=1}^N \frac{\lambda^r}{\Gamma(r)} x_i^{r-1} \exp(-\lambda x_i) \times \frac{(\frac{a}{b})^a}{\Gamma(a)} \lambda^{a-1} \exp(-\frac{a}{b} \lambda) \\
 &\propto \lambda^{Nr+a-1} \exp \left\{ - \left(\sum_{i=1}^N x_i + \frac{a}{b} \right) \lambda \right\} \propto \mathcal{G}(\lambda \mid \tilde{\alpha}, \tilde{\beta}),
 \end{aligned}$$

where

$$\tilde{\alpha} = Nr + a, \quad \tilde{\beta} = \sum_{i=1}^N x_i + \frac{a}{b}.$$

That is, the posterior density of rate λ follows from a Gamma distribution. We show that the Gamma distribution is, itself, a conjugate prior for the rate parameter of a Gamma distribution when fixing the shape parameter. This is often referred to as the *Gamma-Gamma model*.

Conjugate prior for precision of a Gaussian distribution. The Gamma distribution also serves as a conjugate prior for the *precision* parameter of a Gaussian distribution. To see this, suppose each entry a_{mn} of matrix \mathbf{A} is i.i.d. normal model with mean b_{mn} and precision τ , i.e., the likelihood is $p(\mathbf{A} \mid \mathbf{B}, \tau^{-1}) = \mathcal{N}(\mathbf{A} \mid \mathbf{B}, \tau^{-1})$, the prior of τ is $p(\tau) = \mathcal{G}(\tau \mid \alpha, \beta)$, where $\mathbf{A}, \mathbf{B} \in \mathbb{R}^{M \times N}$ are two matrices containing a_{mn} and b_{mn} , respectively (the result can be applied to vector or scalar cases). Using Bayes' theorem, it can be shown that

$$\begin{aligned}
 p(\tau \mid \mathbf{A}, \mathbf{B}, \alpha, \beta) &\propto \mathcal{N}(\mathbf{A} \mid \mathbf{B}, \tau^{-1}) \times \mathcal{G}(\tau \mid \alpha, \beta) \\
 &= \prod_{i,j=1}^{M,N} \mathcal{N}(a_{ij} \mid b_{ij}, (\tau)^{-1}) \times \frac{\beta^\alpha}{\Gamma(\alpha)} \tau^{\alpha-1} \exp(-\beta\tau) \\
 &\propto \tau^{\frac{MN}{2}} \exp \left\{ -\frac{\tau}{2} \sum_{i,j=1}^{M,N} (a_{ij} - b_{ij})^2 \right\} \cdot \tau^{\alpha-1} \exp(-\beta\tau) \quad (3.5) \\
 &= \tau^{\frac{MN}{2} + \alpha - 1} \exp \left\{ -\tau \left(\sum_{i,j=1}^{M,N} \frac{1}{2} (a_{ij} - b_{ij})^2 + \beta \right) \right\} \\
 &\propto \mathcal{G}(\tau \mid \tilde{\alpha}, \tilde{\beta}),
 \end{aligned}$$

where

$$\tilde{\alpha} = \frac{MN}{2} + \alpha, \quad \tilde{\beta} = \sum_{i,j=1}^{M,N} \frac{1}{2} (a_{ij} - b_{ij})^2 + \beta. \quad (3.6)$$

That is, the posterior density of precision τ follows from a Gamma distribution.

Joint conjugate prior for Gaussian mean and precision. Going further, when the variance/precision parameter of the Gaussian distribution is not fixed with x_1, x_2, \dots, x_N drawn i.i.d. from a normal distribution with mean θ and precision λ . The *normal-Gamma* distribution $\mathcal{NG}(\alpha, \beta, \mu, c)$, with $\mu \in \mathbb{R}$ and $\alpha, \beta, c \in \mathbb{R}_+$ is a joint distribution on (θ, λ) by letting

$$\begin{aligned}\lambda &\sim \mathcal{G}(\alpha, \beta); \\ \theta \mid \lambda &\sim \mathcal{N}(\mu, (c\lambda)^{-1}).\end{aligned}$$

That is, the joint p.d.f. is

$$p(\theta, \lambda) = \mathcal{N}(\theta \mid \mu, (c\lambda)^{-1}) \cdot \mathcal{G}(\lambda \mid \alpha, \beta) = \mathcal{NG}(\theta, \lambda \mid \alpha, \beta, \mu, c).$$

It turns out the posterior density is again a normal-Gamma distribution with

$$p(\theta, \lambda) \propto \prod_{i=1}^N \mathcal{N}(x_i \mid \theta, \lambda^{-1}) \cdot \mathcal{NG}(\theta, \lambda \mid \alpha, \beta, \mu, c) \propto \mathcal{NG}(\theta, \lambda \mid \tilde{\alpha}, \tilde{\beta}, \tilde{\mu}, \tilde{c}),$$

where

$$\begin{aligned}\tilde{\mu} &= \frac{c\mu + \sum_{i=1}^N x_i}{c + N}, & \tilde{c} &= c + N, \\ \tilde{\alpha} &= \alpha + \frac{N}{2}, & \tilde{\beta} &= \beta + \frac{1}{2} \left(c\mu^2 - \tilde{c}\tilde{\mu}^2 + \sum_{i=1}^N x_i \right).\end{aligned}$$

In contrast to the Normal-Normal, this model is often referred to as the *NormalGamma-Normal model*. The posterior mean for θ is a weighted average of the prior mean and the sample mean,

$$\tilde{\mu} = \frac{c\mu + \sum_{i=1}^N x_i}{c + N} = \frac{c}{c + N}\mu + \frac{N}{c + N}\bar{x},$$

where $\bar{x} = \frac{1}{N} \sum_{i=1}^N x_i$. From the posterior form of \tilde{c} , the prior interpretation of c can be described as the prior sample size for estimating mean parameter θ . The posterior shape parameter $\tilde{\alpha}$ grows linearly with the sample size. And the posterior rate parameter $\tilde{\beta}$ can be written as

$$\tilde{\beta} = \beta + \frac{1}{2} \left(c\mu^2 - \tilde{c}\tilde{\mu}^2 + \sum_{i=1}^N x_i \right) = \beta + \frac{1}{2} \sum_{i=1}^N (x_i - \bar{x})^2 + \frac{1}{2} \frac{cN}{c + N} (\bar{x} - \mu)^2.$$

In other words, it is decomposed into the sum of a prior variation, the observed variation (sample variance), and the variation between the prior mean and sample mean:

$$\tilde{\beta} = (\text{prior variation}) + \frac{1}{2}N(\text{observed variation}) + \frac{1}{2} \frac{cN}{c + N}(\text{variation between means}).$$

Putting a Gamma prior over the inverse variance of a Gaussian distribution is equivalent to placing an inverse-Gamma prior on the *variance*. We will now provide the formal definition of the inverse-Gamma distribution.

Definition 3.2.4 (Inverse-Gamma Distribution) A random variable x is said to follow the inverse-Gamma distribution with shape parameter $r > 0$ and scale parameter $\lambda > 0$, denoted by $x \sim \mathcal{G}^{-1}(r, \lambda)$, if

$$f(x; r, \lambda) = \begin{cases} \frac{\lambda^r}{\Gamma(r)} x^{-r-1} \exp\left(-\frac{\lambda}{x}\right), & \text{if } x > 0; \\ 0, & \text{if } x \leq 0. \end{cases}$$

And it is denoted by $x \sim \mathcal{G}^{-1}(r, \lambda)$. The mean and variance of inverse-Gamma distribution are given by

$$\mathbb{E}[x] = \begin{cases} \frac{\lambda}{r-1}, & \text{if } r \geq 1; \\ \infty, & \text{if } 0 < r < 1. \end{cases} \quad \text{Var}[x] = \begin{cases} \frac{\lambda^2}{(r-1)^2(r-2)}, & \text{if } r > 2; \\ \infty, & \text{if } 0 < r \leq 2. \end{cases}$$

Figure 3.3(b) illustrates the impact of different parameters r, λ for the inverse-Gamma distribution.

If x is Gamma distributed, then $y = 1/x$ is inverse-Gamma distributed. Note that the inverse-Gamma density is not simply the Gamma density with x replaced by $\frac{1}{y}$. There is an additional factor of y^{-2} .¹ The inverse-Gamma distribution is useful as a prior for positive parameters. It imparts a quite heavy tail and keeps probability further from zero than the Gamma distribution (see examples in Figure 3.3(b)).

Conjugate prior for variance of a Gaussian distribution. The inverse-Gamma distribution is a conjugate prior for the variance parameter of a Gaussian distribution with a fixed mean parameter. To see this, let the likelihood be $p(\mathbf{A} | \mathbf{B}, \sigma^2) = \mathcal{N}(\mathbf{A} | \mathbf{B}, \sigma^2)$, where $\mathbf{A}, \mathbf{B} \in \mathbb{R}^{M \times N}$ are two matrices containing elements of a_{mn} and b_{mn} , respectively (again the result can be applied to vector or scalar cases), and let the prior of σ^2 be $p(\sigma^2) = \mathcal{G}^{-1}(\sigma^2 | \alpha, \beta)$. Using Bayes' theorem, it can be shown that

$$\begin{aligned} p(\sigma^2 | \mathbf{A}, \mathbf{B}, \alpha, \beta) &\propto \mathcal{N}(\mathbf{A} | \mathbf{B}, \sigma^2) \times \mathcal{G}^{-1}(\sigma^2 | \alpha, \beta) \\ &= \prod_{i,j=1}^{M,N} \mathcal{N}(a_{ij} | b_{ij}, \sigma^2) \times \frac{\beta^\alpha}{\Gamma(\alpha)} (\sigma^2)^{-\alpha-1} \exp\left(-\frac{\beta}{\sigma^2}\right) \\ &\propto \frac{1}{\sigma^{MN}} \exp\left\{-\frac{1}{2\sigma^2} \sum_{i,j=1}^{M,N} (a_{ij} - b_{ij})^2\right\} \cdot (\sigma^2)^{-\alpha-1} \exp\left(-\frac{\beta}{\sigma^2}\right) \quad (3.7) \\ &= (\sigma^2)^{-\frac{MN}{2}-\alpha-1} \exp\left\{-\frac{1}{\sigma^2} \left(\sum_{i,j=1}^{M,N} \frac{1}{2}(a_{ij} - b_{ij})^2 + \beta\right)\right\} \\ &\propto \mathcal{G}^{-1}(\sigma^2 | \tilde{\alpha}, \tilde{\beta}), \end{aligned}$$

1. Which is from the *Jacobian in the change-of-variables formula*. A short proof is provided here. Let $y = \frac{1}{x}$ where $y \sim \mathcal{G}^{-1}(r, \lambda)$ and $x \sim \mathcal{G}(r, \lambda)$. Then, $f(y)|dy| = f(x)|dx|$, which results in $f(y) = f(x) \left| \frac{dx}{dy} \right| = f(x)x^2 \stackrel{y=\frac{1}{x}}{=} \frac{\lambda^r}{\Gamma(r)} y^{-r-1} \exp\left(-\frac{\lambda}{y}\right)$ for $y > 0$.

where

$$\tilde{\alpha} = \frac{MN}{2} + \alpha, \quad \tilde{\beta} = \sum_{i,j=1}^{M,N} \frac{1}{2} (a_{ij} - b_{ij})^2 + \beta. \quad (3.8)$$

That is, the posterior density of the variance σ^2 is also an inverse-Gamma distribution. And as claimed, we find the posterior parameters in Equation (3.8) are exactly the same as that in Equation (3.6) from a Gamma prior.

As we have seen that the normal-Gamma density is a joint conjugate prior for the mean and precision parameters of a Gaussian distribution. The *normal-inverse-Gamma* (NIG) distribution defined as follows is a joint conjugate prior for the mean and variance parameters of a Gaussian distribution.

Definition 3.2.5 (Normal-Inverse-Gamma (NIG) Distribution) *The joint density of normal-inverse-Gamma distribution is a density defined as*

$$\begin{aligned} \mathcal{NIG}(\mu, \sigma^2 \mid m, \kappa, r, \lambda) &= \mathcal{N}\left(\mu \mid m, \frac{\sigma^2}{\kappa}\right) \cdot \mathcal{G}^{-1}(\sigma^2 \mid r, \lambda) \\ &= \frac{1}{Z_{\mathcal{NIG}}(\kappa, r, \lambda)} (\sigma^2)^{-\frac{2r+3}{2}} \exp\left\{-\frac{1}{2\sigma^2} [\kappa(m - \mu)^2 + 2\lambda]\right\}, \end{aligned} \quad (3.9)$$

where $\sigma^2, r, \lambda > 0$, and $Z_{\mathcal{NIG}}(\kappa, r, \lambda)$ is a normalizing constant:

$$Z_{\mathcal{NIG}}(\kappa, r, \lambda) = \frac{\Gamma(r)}{\lambda^r} \sqrt{\frac{2\pi}{\kappa}}. \quad (3.10)$$

Figure 3.4 shows some normal-inverse-Gamma probability density functions by varying different parameters.

Joint conjugate prior for the Gaussian mean and variance (under NIG). The normal-inverse-Gamma defines an equivalent prior over the mean and variance parameters of a Gaussian distribution as the normal-Gamma prior, but is sometimes more convenient than the latter one. Similar to the normal-Gamma prior, when the variance and mean parameters of the Gaussian distribution are not fixed with N data points $\mathcal{X} = \{x_1, x_2, \dots, x_N\}$ drawn i.i.d. from a normal distribution with mean μ and variance σ^2 . The normal-inverse-Gamma $\mathcal{NIG}(m_0, \kappa_0, r_0, \lambda_0)$ with $m_0 \in \mathbb{R}$ and $r_0, \lambda_0, \kappa_0 \in \mathbb{R}_+$ is a joint distribution on μ, σ^2 by letting

$$\begin{aligned} \sigma^2 &\sim \mathcal{G}^{-1}(r_0, \lambda_0); \\ \mu \mid \sigma^2 &\sim \mathcal{N}\left(m_0, \frac{\sigma^2}{\kappa_0}\right). \end{aligned}$$

With this prior, μ and σ^2 decouple, and the posterior conditional densities of μ and σ^2 are Gaussian and inverse-Gamma, respectively. The joint p.d.f of NIG prior can be expressed as

$$p(\mu, \sigma^2) = \mathcal{N}\left(m_0, \frac{\sigma^2}{\kappa_0}\right) \cdot \mathcal{G}^{-1}(r_0, \lambda_0) = \mathcal{NIG}(\mu, \sigma^2 \mid m_0, \kappa_0, r_0, \lambda_0).$$

Again, by Bayes' theorem “posterior \propto likelihood \times prior,” the posterior of the μ and σ^2 parameters under the NIG prior is

$$\begin{aligned}
 & p(\mu, \sigma^2 \mid \mathcal{X}, \boldsymbol{\beta}) \\
 & \propto \mathcal{N}(\mathcal{X} \mid \mu, \sigma^2) \cdot \mathcal{NIG}(\mu, \sigma^2 \mid \boldsymbol{\beta}) \\
 & \propto \prod_{i=1}^N \mathcal{N}(x_i \mid \mu, \sigma^2) \cdot \mathcal{NIG}(\mu, \sigma^2 \mid m_0, \kappa_0, r_0, \lambda_0) \\
 & \stackrel{\star}{=} \frac{C}{(\sigma^2)^{\frac{2r_0+3+N}{2}}} \exp \left\{ -\frac{1}{2\sigma^2} [N(\bar{x} - \mu)^2 + NS_{\bar{x}}] \right\} \exp \left\{ -\frac{1}{2\sigma^2} [2\lambda_0 + \kappa_0(m_0 - \mu)^2] \right\} \\
 & \propto (\sigma^2)^{-\frac{2r_N+3}{2}} \exp \left\{ -\frac{1}{2\sigma^2} [\lambda_N + \kappa_N(m_N - \mu)^2] \right\} \\
 & \propto \mathcal{NIG}(\mu, \sigma^2 \mid m_N, \kappa_N, r_N, \lambda_N),
 \end{aligned} \tag{3.11}$$

where $\boldsymbol{\beta} = \{m_0, \kappa_0, r_0, \lambda_0\}$, $C = \frac{(2\pi)^{-N/2}}{Z_{\mathcal{NIG}(\kappa_0, r_0, \lambda_0)}}$, equality (\star) is from Equation (3.1), and

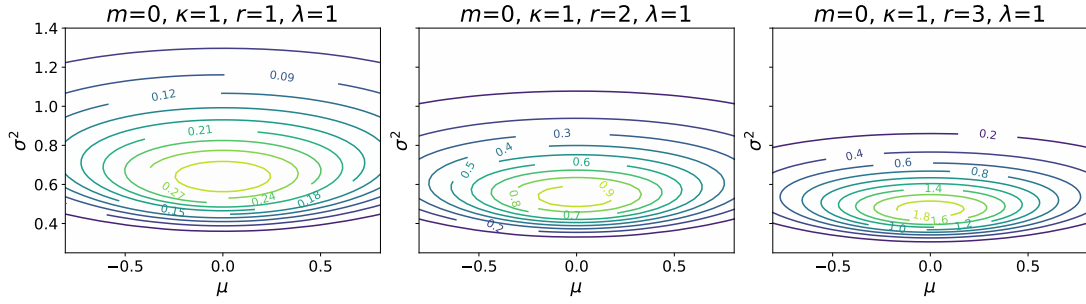
$$\begin{aligned}
 m_N &= \frac{\kappa_0 m_0 + N\bar{x}}{\kappa_N} = \frac{\kappa_0}{\kappa_N} m_0 + \frac{N}{\kappa_N} \bar{x}, \\
 \kappa_N &= \kappa_0 + N, \\
 r_N &= r_0 + \frac{N}{2}, \\
 \lambda_N &= \lambda_0 + \frac{1}{2} (NS_{\bar{x}} + N\bar{x}^2 + \kappa_0 m_0^2 - \kappa_N m_N^2) \\
 &= \lambda_0 + \frac{1}{2} \left(NS_{\bar{x}} + \frac{\kappa_0 N}{\kappa_0 + N} (\bar{x} - m_0)^2 \right),
 \end{aligned}$$

where $S_{\bar{x}} = \sum_{n=1}^N (x_n - \bar{x})^2$ and $\bar{x} = \frac{1}{N} \sum_{i=1}^N x_i$. Note in the above derivation, we use the fact about the likelihood under Gaussian in Equation (3.1). We will discuss the posterior marginal likelihood in the *normal-inverse-Chi-squared (NIX)* case. Further discussion on the posterior marginal likelihood for the NIG prior can be found in [Murphy \(2007\)](#). We will leave this to the readers as it is rather similar as that in the NIX prior.

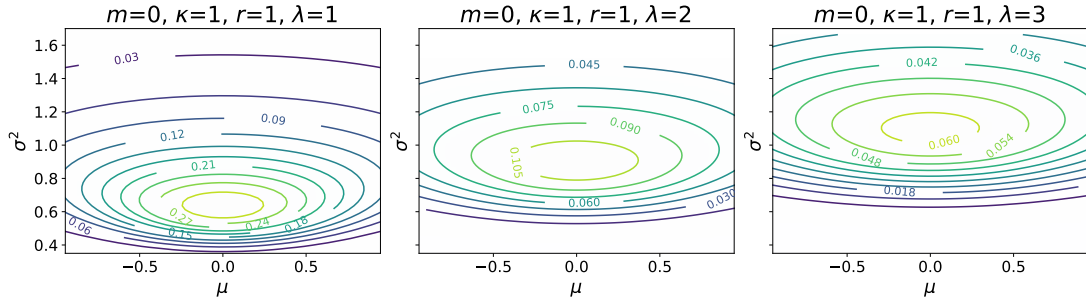
Another distribution that is closely related to the Gamma distribution is called the *Chi-squared* distribution, which is extensively used in the distribution theory of linear models ([Lu, 2022a](#)). The rigorous definition is given as follows.

Definition 3.2.6 (Chi-Squared Distribution) Let $\mathbf{A} \sim \mathcal{N}(\mathbf{0}, \mathbf{I}_p)$, where \mathbf{I}_p is a $p \times p$ identity matrix. Then $\mathbf{x} = \sum_i^p a_{ii}$ follows the Chi-squared distribution with p **degrees of freedom**. We write $\mathbf{x} \sim \chi^2(p)$, and we can see this is equivalent to $\mathbf{x} \sim \mathcal{G}(p/2, 1/2)$:

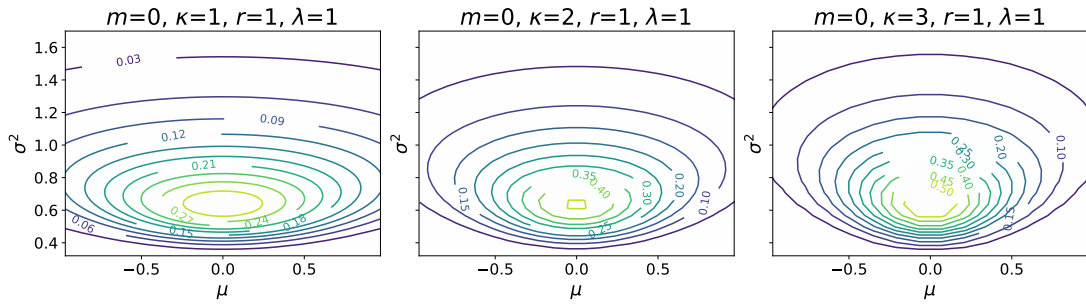
$$f(x; p) = \begin{cases} \frac{1}{2^{p/2} \Gamma(\frac{p}{2})} x^{\frac{p}{2}-1} \exp(-\frac{x}{2}), & \text{if } x \geq 0; \\ 0, & \text{if } x < 0. \end{cases}$$



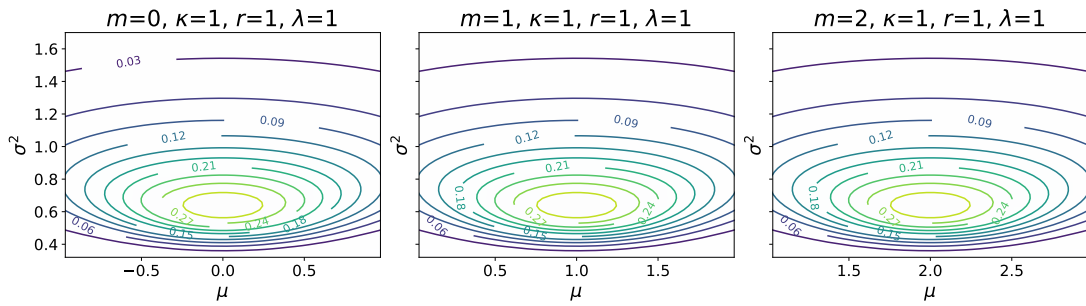
(a) Contour plot of normal-inverse-Gamma density by varying parameter r (purple=low, yellow=high).



(b) Contour plot of normal-inverse-Gamma density by varying parameter λ (purple=low, yellow=high).



(c) Contour plot of normal-inverse-Gamma density by varying parameter κ (purple=low, yellow=high).



(d) Contour plot of normal-inverse-Gamma density by varying parameter m (purple=low, yellow=high).

Figure 3.4: Normal-inverse-Gamma probability density functions by varying different parameters.

The mean, variance of $x \sim \chi^2(p)$ are given by

$$E[x] = p, \quad \text{Var}[x] = 2p.$$

Figure 3.5(a) compares different degrees of freedom p for the Chi-squared distribution.

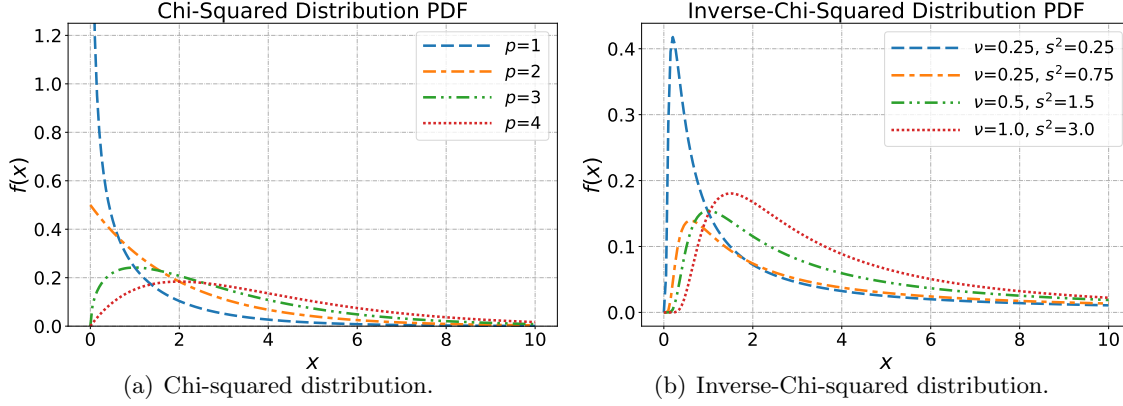


Figure 3.5: Chi-squared and inverse-Chi-squared probability density functions for different values of parameters.

An counterpart of the inverse-Gamma distribution is known as the *inverse-Chi-squared* distribution. Following the definition of the inverse-Gamma distribution in Definition 3.2.4, we provide the rigorous definition of the inverse-Chi-squared distribution as follows.

Definition 3.2.7 (Inverse-Chi-Squared Distribution) A random variable x is said to follow the inverse-Chi-squared distribution with parameter $\nu > 0$ and $s^2 > 0$, denoted by $x \sim \mathcal{G}^{-1}(\frac{\nu}{2}, \frac{\nu s^2}{2})$ if

$$f(x; \nu, s^2) = \begin{cases} \frac{(\frac{\nu s^2}{2})^{\frac{\nu}{2}}}{\Gamma(\frac{\nu}{2})} x^{-\frac{\nu}{2}-1} \exp(-\frac{\nu s^2}{2x}), & \text{if } x > 0; \\ 0, & \text{if } x \leq 0. \end{cases}$$

And it is also compactly denoted by $x \sim \chi^{-2}(\nu, s^2)$. The parameter $\nu > 0$ is called the **degrees of freedom**, and $s^2 > 0$ is the **scale parameter**. And it is also known as the **scaled inverse-Chi-squared** distribution. The mean and variance of the inverse-Chi-squared distribution are given by

$$E[x] = \begin{cases} \frac{\nu s^2}{\nu - 2}, & \text{if } \nu \geq 2; \\ \infty, & \text{if } 0 < \nu < 2. \end{cases} \quad \text{Var}[x] = \begin{cases} \frac{2\nu^2 s^4}{(\nu - 2)^2(\nu - 4)}, & \text{if } \nu \geq 4; \\ \infty, & \text{if } 0 < \nu < 4. \end{cases}$$

To establish a connection with the inverse-Gamma distribution, we can set $S = \nu s^2$. Then the inverse-Chi-squared distribution can also be denoted by $x \sim \mathcal{G}^{-1}(\frac{\nu}{2}, \frac{S}{2})$ if $x \sim \chi^{-2}(\nu, s^2)$, the form of which conforms to the univariate case of the inverse-Wishart

distribution (Definition 3.7.4). And we will observe the similarities in the posterior parameters as well. Figure 3.5(b) illustrates the impact of different parameters ν, s^2 for the inverse-Chi-squared distribution.

Exercise 3.1 (Conjugate prior for the variance of a Gaussian distribution) Show that the inverse-Chi-squared distribution is a conjugate prior for the Gaussian variance parameter when the mean parameter is fixed. Hint: the derivation follows the same procedure as in the inverse-Gamma case.

As we have seen that the normal-inverse-Gamma distribution is a joint conjugate prior for Gaussian mean and variance parameters. The *normal-inverse-Chi-squared (NIX)* distribution defined as follows is an alternative joint conjugate prior.

Definition 3.2.8 (Normal-Inverse-Chi-Squared (NIX) Distribution) Similar to the normal-inverse-Gamma distribution, the normal-inverse-Chi-squared (NIX) distribution is defined as (where again we set $S = \nu s^2$ as that in the inverse-Chi-square distribution to establish a connection with the normal-inverse-Gamma density)

$$\begin{aligned} \mathcal{NIX}(\mu, \sigma^2 \mid m, \kappa, \nu, S) &= \mathcal{N}\left(\mu \mid m, \frac{\sigma^2}{\kappa}\right) \cdot \chi^{-2}(\sigma^2 \mid \nu, s^2) \\ &= \frac{1}{Z_{\mathcal{NIX}}(\kappa, \nu, s^2)} (\sigma^2)^{-(\nu/2+3/2)} \exp\left\{-\frac{1}{2\sigma^2} [\nu s^2 + \kappa(m - \mu)^2]\right\} \\ &\stackrel{S=\nu s^2}{=} \frac{1}{Z_{\mathcal{NIX}}(\kappa, \nu, s^2)} (\sigma^2)^{-(\nu/2+3/2)} \exp\left\{-\frac{1}{2\sigma^2} [S + \kappa(m - \mu)^2]\right\}, \end{aligned} \quad (3.12)$$

where $\sigma^2, \nu, s^2 > 0$, and $Z_{\mathcal{NIX}}(\kappa, \nu, s^2)$ is a normalizing constant:

$$Z_{\mathcal{NIX}}(\kappa, \nu, s^2) = \Gamma\left(\frac{\nu}{2}\right) \left(\frac{2}{\nu s^2}\right)^{\nu/2} \sqrt{\frac{2\pi}{\kappa}} = \Gamma\left(\frac{\nu}{2}\right) \left(\frac{2}{S}\right)^{\nu/2} \sqrt{\frac{2\pi}{\kappa}}. \quad (3.13)$$

The normal-inverse-Chi-squared distribution can also be denoted by $\mathbf{x} \sim \mathcal{NIG}(m, \kappa, \frac{\nu}{2}, \frac{S}{2})$ if $\mathbf{x} \sim \mathcal{NIX}(m, \kappa, \nu, s^2)$, the form of which conforms to the univariate case of the normal-inverse-Wishart distribution (Equation (3.40)). And we will see the similarities in the posterior parameters as well.

Joint conjugate prior for the Gaussian mean and variance (under NIX). Similar to the normal-inverse-Gamma prior, when the variance and mean parameters of the Gaussian distribution are not fixed with N data points $\mathcal{X} = \{x_1, x_2, \dots, x_N\}$ drawn i.i.d. from a normal distribution with mean μ and variance σ^2 . The normal-inverse-Chi-squared $\mathcal{NIX}(m_0, \kappa_0, \nu_0, S_0 = \nu_0 \sigma_0^2)$ with $m_0 \in \mathbb{R}$ and $\kappa_0, \mu_0, S_0 \in \mathbb{R}_+$ is a joint distribution on μ, σ^2 by letting

$$\begin{aligned} \sigma^2 &\sim \chi^{-2}(\nu_0, \sigma_0^2); \\ \mu \mid \sigma^2 &\sim \mathcal{N}\left(m_0, \frac{\sigma^2}{\kappa_0}\right). \end{aligned}$$

Again, by Bayes' theorem “posterior \propto likelihood \times prior,” the conditional posterior of the μ and σ^2 parameters under the NIX prior is

$$\begin{aligned}
 & p(\mu, \sigma^2 \mid \mathcal{X}, \boldsymbol{\beta}) \\
 & \propto p(\mathcal{X} \mid \mu, \sigma^2) p(\mu, \sigma^2 \mid \boldsymbol{\beta}) = p(\mathcal{X}, \mu, \sigma^2 \mid \boldsymbol{\beta}) \\
 & = \frac{C}{(\sigma^2)^{\frac{\nu_0+3+N}{2}}} \exp \left\{ -\frac{1}{2\sigma^2} [N(\bar{x} - \mu)^2 + NS_{\bar{x}}] \right\} \exp \left\{ -\frac{1}{2\sigma^2} [S_0 + \kappa_0(m_0 - \mu)^2] \right\} \\
 & = C \times (\sigma^2)^{-\frac{\nu_N+3}{2}} \exp \left\{ -\frac{1}{2\sigma^2} [S_N + \kappa_N(m_N - \mu)^2] \right\} \\
 & \propto \mathcal{NIX}(\mu, \sigma^2 \mid m_N, \kappa_N, \nu_N, S_N) = \mathcal{N}\left(\mu \mid m_N, \frac{\sigma^2}{\kappa_N}\right) \cdot \chi^{-2}(\sigma^2 \mid \nu_N, \sigma_N^2),
 \end{aligned} \tag{3.14}$$

where $\boldsymbol{\beta} = \{m_0, \kappa_0, \nu_0, S_0 = \nu_0\sigma_0^2\}$, $C = \frac{(2\pi)^{-N/2}}{Z_{\mathcal{NIX}}(\kappa_0, \nu_0, \sigma_0^2)}$, and

$$\begin{aligned}
 m_N &= \frac{\kappa_0 m_0 + N\bar{x}}{\kappa_N} = \frac{\kappa_0}{\kappa_N} m_0 + \frac{N}{\kappa_N} \bar{x}, \\
 \kappa_N &= \kappa_0 + N, \\
 \nu_N &= \nu_0 + N, \\
 S_N &= S_0 + NS_{\bar{x}} + N\bar{x}^2 + \kappa_0 m_0^2 - \kappa_N m_N^2 \\
 &= S_0 + NS_{\bar{x}} + \frac{\kappa_0 N}{\kappa_0 + N} (\bar{x} - m_0)^2, \\
 \nu_N \sigma_N^2 &= S_N \quad \underline{\text{leads to}} \quad \sigma_N^2 = \frac{S_N}{\nu_N},
 \end{aligned}$$

Then the posterior density is a normal-inverse-Chi-squared density. ²

Suppose $\nu_0 \geq 2$, or $N \geq 2$ such that $\nu_N \geq 2$, the posterior expectations are given by

$$\mathbb{E}[\mu \mid \mathcal{X}, \boldsymbol{\beta}] = m_N, \quad \mathbb{E}[\sigma^2 \mid \mathcal{X}, \boldsymbol{\beta}] = \frac{S_N}{\nu_N - 2}.$$

Marginal posterior of σ^2 . Integrating out μ in the posterior, we have

$$\begin{aligned}
 p(\sigma^2 \mid \mathcal{X}, \boldsymbol{\beta}) &= \int_{\mu} p(\mu, \sigma^2 \mid \mathcal{X}, \boldsymbol{\beta}) d\mu \\
 &= \int_{\mu} \mathcal{N}\left(\mu \mid m_N, \frac{\sigma^2}{\kappa_N}\right) \cdot \chi^{-2}(\sigma^2 \mid \nu_N, \sigma_N^2) d\mu \\
 &= \chi^{-2}(\sigma^2 \mid \nu_N, \sigma_N^2),
 \end{aligned}$$

which is just an integral over a Gaussian distribution.

² This posterior shares the same form as that in the multivariate case from Equation (3.45) except the N in $NS_{\bar{x}}$, which results from the difference between the multivariate Gaussian distribution and the univariate Gaussian distribution. Similarly, in the inverse-Chi-squared language, we can show that $\nu_N \sigma_N^2 = S_N$.

Marginal posterior of μ . Integrating out σ^2 in the posterior, we have

$$\begin{aligned} p(\mu \mid \mathcal{X}, \boldsymbol{\beta}) &= \int_{\sigma^2} p(\mu, \sigma^2 \mid \mathcal{X}, \boldsymbol{\beta}) d\sigma^2 \\ &= \int_{\sigma^2} \mathcal{N}(\mu \mid m_N, \frac{\sigma^2}{\kappa_N}) \cdot \chi^{-2}(\sigma^2 \mid \nu_N, \sigma_N^2) d\sigma^2 \\ &= \int_{\sigma^2} C(\sigma^2)^{-\frac{\nu_N+3}{2}} \exp\left\{-\frac{1}{2\sigma^2} [S_N + \kappa_N(m_N - \mu)^2]\right\} d\sigma^2. \end{aligned}$$

Let $\phi = \sigma^2$ and $\alpha = (\nu_N + 1)/2$, $A = S_N + \kappa_N(m_N - \mu)^2$, and $x = \frac{A}{2\phi}$, we have

$$\frac{d\phi}{dx} = -\frac{A}{2}x^{-2},$$

where A can be easily verified to be positive and $\phi = \sigma^2 > 0$. It follows that

$$\begin{aligned} p(\mu \mid \mathcal{X}, \boldsymbol{\beta}) &= \int_0^\infty C(\phi)^{-\alpha-1} \exp\left(-\frac{A}{2\phi}\right) d\phi \\ &= \int_\infty^0 C\left(\frac{A}{2x}\right)^{-\alpha-1} \exp(-x) \left(-\frac{A}{2}x^{-2}\right) dx && \text{(since } x = \frac{A}{2\phi}\text{)} \\ &= \int_0^\infty C\left(\frac{A}{2x}\right)^{-\alpha-1} \exp(-x) \left(\frac{A}{2}x^{-2}\right) dx \\ &= \left(\frac{A}{2}\right)^{-\alpha} \int_x Cx^{\alpha-1} \exp(-x) dx \\ &= \left(\frac{A}{2}\right)^{-\alpha} (C \cdot \Gamma(1)) \int_x \mathcal{G}(x \mid \alpha, 1) dx && \text{(see Definition 3.2.3)} \\ &= (C \cdot \Gamma(1)) [\nu_N \sigma_N^2 + \kappa_N(m_N - \mu)^2]^{-\frac{\nu_N+1}{2}} \\ &\stackrel{(a)}{=} (C \cdot \Gamma(1)) (\nu_N \sigma_N^2)^{-\frac{\nu_N+1}{2}} \left[1 + \frac{\kappa_N}{\nu_N \sigma_N^2} (m_N - \mu)^2\right]^{-\frac{\nu_N+1}{2}} \end{aligned}$$

We notice that C is defined in Equation (3.14) (in terms of $\{\kappa_N, \nu_N, \sigma_N^2\}$) with

$$C \stackrel{(b)}{=} \frac{(2\pi)^{-N/2}}{Z_{N\mathcal{I}\mathcal{X}}(\kappa_N, \nu_N, \sigma_N^2)} = \frac{(2\pi)^{-N/2}}{\frac{\sqrt{(2\pi)}}{\sqrt{\kappa_N}} \Gamma\left(\frac{\nu_N}{2}\right) \left(\frac{2}{\nu_N \sigma_N^2}\right)^{\nu_N/2}} \propto (\nu_N \sigma_N^2)^{\nu_N/2}.$$

Combining equalities (a) and (b) above, we obtain

$$p(\mu \mid \mathcal{X}, \boldsymbol{\beta}) \propto \frac{1}{\sigma_N / \sqrt{\kappa_N}} \left[1 + \frac{\kappa_N}{\nu_N \sigma_N^2} (\mu - m_N)^2\right]^{-\frac{\nu_N+1}{2}} \propto \tau(\mu \mid m_N, \sigma_N^2 / \kappa_N, \nu_N),$$

which is a univariate Student's t distribution (Definition 3.2.2).

Marginal likelihood of data. By Equation (3.14), we can obtain the marginal likelihood of data under hyper-parameter $\beta = (m_0, \kappa_0, \nu_0, S_0 = \nu_0 \sigma_0^2)$

$$\begin{aligned}
 p(\mathcal{X} | \beta) &= \int_{\mu} \int_{\sigma^2} p(\mathcal{X}, \mu, \sigma^2 | \beta) d\mu d\sigma^2 \\
 &= \frac{(2\pi)^{-N/2}}{Z_{N\mathcal{I}\mathcal{X}}(\kappa_0, \nu_0, \sigma_0^2)} \int_{\mu} \int_{\sigma^2} (\sigma^2)^{-\frac{\nu_N+3}{2}} \exp\left\{-\frac{1}{2\sigma^2} [S_N + \kappa_N(m_N - \mu)^2]\right\} d\mu d\sigma^2 \\
 &= (2\pi)^{-N/2} \frac{Z_{N\mathcal{I}\mathcal{X}}(\kappa_N, \nu_N, \sigma_N^2)}{Z_{N\mathcal{I}\mathcal{X}}(\kappa_0, \nu_0, \sigma_0^2)} \\
 &= (\pi)^{-N/2} \frac{\Gamma(\nu_N/2)}{\Gamma(\nu_0/2)} \sqrt{\frac{\kappa_0}{\kappa_N}} \frac{(\nu_0 \sigma_0^2)^{\nu_0/2}}{(\nu_N \sigma_N^2)^{\nu_N/2}}.
 \end{aligned}$$

Posterior predictive for new data with observations. Let the number of samples for data set $\{x^*, \mathcal{X}\}$ be $N^* = N + 1$, we have

$$\begin{aligned}
 p(x^* | \mathcal{X}, \beta) &= \frac{p(x^*, \mathcal{X} | \beta)}{p(\mathcal{X} | \beta)} \\
 &= \left\{ (2\pi)^{-N^*/2} \frac{Z_{N\mathcal{I}\mathcal{X}}(\kappa_{N^*}, \nu_{N^*}, \sigma_{N^*}^2)}{Z_{N\mathcal{I}\mathcal{X}}(\kappa_0, \nu_0, \sigma_0^2)} \right\} / \left\{ (2\pi)^{-N/2} \frac{Z_{N\mathcal{I}\mathcal{X}}(\kappa_N, \nu_N, \sigma_N^2)}{Z_{N\mathcal{I}\mathcal{X}}(\kappa_0, \nu_0, \sigma_0^2)} \right\} \\
 &= (2\pi)^{-1/2} \frac{Z_{N\mathcal{I}\mathcal{X}}(\kappa_{N^*}, \nu_{N^*}, \sigma_{N^*}^2)}{Z_{N\mathcal{I}\mathcal{X}}(\kappa_N, \nu_N, \sigma_N^2)} \\
 &= (\pi)^{-1/2} \sqrt{\frac{\kappa_N}{\kappa_{N^*}} \frac{\Gamma(\frac{\nu_{N^*}}{2})}{\Gamma(\frac{\nu_N}{2})} \frac{(\nu_N \sigma_N^2)^{\frac{\nu_N}{2}}}{(\nu_{N^*} \sigma_{N^*}^2)^{\frac{\nu_{N^*}}{2}}}} \\
 &= \frac{\Gamma(\frac{\nu_N+1}{2})}{\Gamma(\frac{\nu_N}{2})} \sqrt{\frac{\kappa_N}{\kappa_N + 1} \frac{1}{(\pi \nu_N \sigma_N^2)}} \left[\frac{(\nu_{N^*} \sigma_{N^*}^2)}{(\nu_N \sigma_N^2)} \right]^{-\frac{\nu_N+1}{2}}.
 \end{aligned} \tag{3.15}$$

We realize that

$$\begin{aligned}
 m_N &= \frac{\kappa_{N^*} m_{N^*} - x^*}{\kappa_N} = \frac{(\kappa_0 + N + 1)m_{N^*} - x^*}{\kappa_0 + N}, \\
 m_{N^*} &= \frac{\kappa_N m_N + x^*}{\kappa_{N^*}} = \frac{(\kappa_0 + N)m_N + x^*}{\kappa_0 + N + 1}, \\
 S_{N^*} &= S_N + x^* x^{*T} - \kappa_{N^*} m_{N^*}^2 + \kappa_N m_N^2 \\
 &= S_N + \frac{\kappa_N + 1}{\kappa_N} (m_{N^*} - x^*)^2 \\
 &= S_N + \frac{\kappa_N}{\kappa_N + 1} (m_N - x^*)^2,
 \end{aligned}$$

Thus, we have

$$\left[\frac{(\nu_{N^*} \sigma_{N^*}^2)}{(\nu_N \sigma_N^2)} \right]^{-\frac{\nu_N+1}{2}} = \left(\frac{S_{N^*}}{S_N} \right)^{-\frac{\nu_N+1}{2}} = 1 + \frac{\kappa_N (m_N - x^*)^2}{(\kappa_N + 1) \nu_N \sigma_N^2}. \tag{3.16}$$

Substituting Equation (3.16) into Equation (3.15), it follows that

$$\begin{aligned} p(\mathbf{x}^* | \mathcal{X}, \boldsymbol{\beta}) &= \frac{\Gamma(\frac{\nu_N+1}{2})}{\Gamma(\frac{\nu_N}{2})} \sqrt{\frac{\kappa_N}{(\kappa_N+1)} \frac{1}{(\pi\nu_N\sigma_N^2)}} \left[1 + \frac{\kappa_N(m_N - \mathbf{x}^*)^2}{(\kappa_N+1)\nu_N\sigma_N^2} \right]^{-\frac{\nu_N+1}{2}} \\ &= \tau(\mathbf{x}^* | m_N, \frac{\kappa_N+1}{\kappa_N}\sigma_N^2, \nu_N). \end{aligned}$$

Posterior predictive for new data without observations. Similarly, considering the case without observations, we have

$$\begin{aligned} p(x^* | \boldsymbol{\beta}) &= \int_{\mu} \int_{\sigma^2} p(x^*, \mu, \sigma^2 | \boldsymbol{\beta}) d\mu d\sigma^2 \\ &= (2\pi)^{-1/2} \frac{Z_{N\mathcal{I}\mathcal{X}}(\kappa_1, \nu_1, \sigma_1^2)}{Z_{N\mathcal{I}\mathcal{X}}(\kappa_0, \nu_0, \sigma_0^2)} \\ &= (\pi)^{-1/2} \sqrt{\frac{\kappa_0}{\kappa_1} \frac{\Gamma(\frac{\nu_1}{2})}{\Gamma(\frac{\nu_0}{2})} \frac{(\nu_0\sigma_0^2)^{\frac{\nu_0}{2}}}{(\nu_1\sigma_1^2)^{\frac{\nu_1}{2}}}} \\ &= \frac{\Gamma(\frac{\nu_0+1}{2})}{\Gamma(\frac{\nu_0}{2})} \sqrt{\frac{\kappa_0}{(\kappa_0+1)} \frac{1}{(\pi\nu_0\sigma_0^2)}} \left[\frac{(\nu_1\sigma_1^2)}{(\nu_0\sigma_0^2)} \right]^{-\frac{\nu_0+1}{2}} \\ &= \tau(x^* | m_0, \frac{\kappa_0+1}{\kappa_0}\sigma_0^2, \nu_0). \end{aligned}$$

3.3. Exponential and Conjugacy

The *exponential* distribution is a probability distribution commonly used in modeling events occurring randomly over time, such as the time elapsed until the occurrence of a certain event, or the time between two consecutive events. It is a special Gamma distribution with support on nonnegative real values.

Definition 3.3.1 (Exponential Distribution) *A random variable x is said to follow the exponential distribution with rate parameter $\lambda > 0$, denoted by $x \sim \mathcal{E}(\lambda)$, if*

$$f(x; \lambda) = \begin{cases} \lambda \exp(-\lambda x), & \text{if } x \geq 0; \\ 0, & \text{if } x < 0. \end{cases}$$

We can see this is equivalent to $x \sim \mathcal{G}(1, \lambda)$. The mean and variance of $x \sim \mathcal{E}(\lambda)$ are given by

$$\mathbb{E}[x] = \lambda^{-1}, \quad \text{Var}[x] = \lambda^{-2}.$$

The support of an exponential distribution is on $(0, \infty)$. Figure 3.6 compares different parameters λ for the exponential distribution.

Note that the average λ^{-1} is the average time until the occurrence of the event of interest, interpreting λ as a rate parameter. An important property of the exponential distribution is that it is “memoryless,” meaning that the probability of waiting for an additional amount of time x depends only on x , not on the past waiting time.

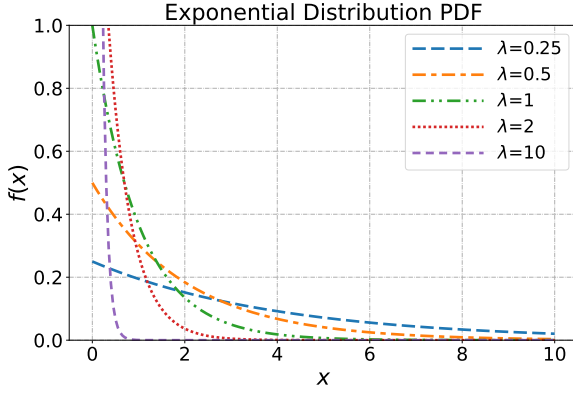


Figure 3.6: Exponential probability density functions for different values of the rate parameter λ .

Remark 3.2: Property of Exponential Distribution
 Let $x \sim \mathcal{E}(\lambda)$. Then we have $p(x \geq x + s \mid x \geq s) = p(x \geq x)$.

Conjugate prior for the exponential rate parameter. The Gamma distribution is a conjugate prior for the rate parameter of an exponential distribution. To see this, suppose $\mathcal{X} = \{x_1, x_2, \dots, x_N\}$ are drawn i.i.d. from an exponential distribution with rate λ , i.e., the likelihood is $\mathcal{E}(x \mid \lambda)$, and λ is given a $\mathcal{G}(\alpha_0, \beta_0)$ prior: $\lambda \sim \mathcal{G}(\alpha_0, \beta_0)$. Using Bayes’ theorem, the posterior is

$$p(\lambda \mid \mathcal{X}) \propto \prod_{i=1}^N \mathcal{E}(x_i \mid \lambda) \times \mathcal{G}(\lambda \mid \alpha_0, \beta_0) \propto \mathcal{G}(\lambda \mid \tilde{\alpha}, \tilde{\beta}),$$

where

$$\tilde{\alpha} = \alpha_0 + N, \quad \tilde{\beta} = \beta_0 + \sum_{i=1}^N x_i. \tag{3.17}$$

From this posterior form, the prior parameter α_0 can be interpreted as the number of prior observations, and β_0 as the sum of the prior observations. The posterior mean is

$$\frac{\tilde{\alpha}}{\tilde{\beta}} = \frac{\alpha_0 + N}{\beta_0 + \sum_{i=1}^N x_i}.$$

3.4. Univariate Gaussian-Related Models

The *truncated-normal (TN)* distribution is a variant of the normal distribution, excluding values smaller than zero. In other words, it is a normal distribution that is “cut off” at zero. The support of the distribution is nonnegative real such that it can be applied for application in a nonnegative matrix factorization context.

Definition 3.4.1 (Truncated-Normal (TN) Distribution) A random variable x is said to follow the truncated-normal distribution with “parent” mean μ and “parent” pre-

cision $\tau > 0$, denoted by $x \sim \mathcal{TN}(\mu, \tau^{-1})$, if

$$f(x; \mu, \tau^{-1}) = \begin{cases} \frac{\sqrt{\frac{\tau}{2\pi}} \exp\{-\frac{\tau}{2}(x - \mu)^2\}}{1 - \Phi(-\mu\sqrt{\tau})}, & \text{if } x \geq 0; \\ 0, & \text{if } x < 0, \end{cases}$$

where $\Phi(y) = \int_{-\infty}^y \mathcal{N}(u | 0, 1) du = \frac{1}{\sqrt{2\pi}} \int_{-\infty}^y \exp(-\frac{u^2}{2}) du$ is the cumulative distribution function (c.d.f.) of $\mathcal{N}(0, 1)$, the standard normal distribution. Generally, the cumulative density function of $y \sim \mathcal{N}(\mu, \sigma^2)$ can be written as

$$F(y) = p(y \leq y) = \Phi\left(\frac{y - \mu}{\sigma}\right) = \Phi((y - \mu) \cdot \sqrt{\tau}).^a$$

The mean and variance of $x \sim \mathcal{TN}(\mu, \tau^{-1})$ are given by

$$\begin{aligned} E[x] &= \mu - \frac{1}{\sqrt{\tau}} \cdot \frac{-\phi(\alpha)}{1 - \Phi(\alpha)}, \\ \text{Var}[x] &= \frac{1}{\tau} \left(1 + \frac{\alpha\phi(\alpha)}{1 - \Phi(\alpha)} + \left(\frac{\alpha\phi(\alpha)}{1 - \Phi(\alpha)} \right)^2 \right), \end{aligned}$$

where $\phi(y) = \frac{1}{\sqrt{2\pi}} \exp(-\frac{y^2}{2})$ is the p.d.f. of the standard normal distribution, and $\alpha = -\mu \cdot \sqrt{\tau}$ (Burkardt, 2014). Figure 3.7(a) compares different parameters μ, τ for the TN distribution. Figure 3.8(a) shows the mean value of the TN distribution by varying μ given fixed τ ; we can find when $\mu \rightarrow -\infty$, the mean is approaching zero.

a. Or equivalently, for general Gaussian distribution $y \sim \mathcal{N}(\mu, \sigma^2)$, the c.d.f. is $F(y) = \frac{1}{2} \left\{ 1 + \text{erf}\left(\frac{y - \mu}{\sigma\sqrt{2}}\right) \right\}$, where the error function is $\text{erf}(t) = \frac{2}{\sqrt{\pi}} \int_0^t \exp(-y^2) dy$.

Conjugate prior for the nonnegative mean parameter of a Gaussian. We have previously shown that a Gaussian distribution can serve as a conjugate prior for the mean parameter of another Gaussian distribution when the variance is fixed. The truncated-normal distribution also acts as a conjugate prior for the **nonnegative** mean parameter of a Gaussian distribution when the variance is fixed. To see this, suppose $\mathcal{X} = \{x_1, x_2, \dots, x_N\}$ are drawn i.i.d. from a normal distribution with mean θ and precision τ , i.e., the likelihood is $\mathcal{N}(x | \theta, \tau^{-1})$ with fixing the variance $\sigma^2 = \tau^{-1}$, and θ is given a $\mathcal{TN}(\mu_0, \tau_0^{-1})$ prior: $\theta \sim \mathcal{TN}(\mu_0, \tau_0^{-1})$. Using Bayes' theorem, the posterior is

$$\begin{aligned} p(\theta | \mathcal{X}) &\propto \prod_{i=1}^N \mathcal{N}(x_i | \theta, \tau^{-1}) \times \mathcal{TN}(\theta | \mu_0, \tau_0^{-1}) \\ &\propto \exp \left\{ -\frac{\tau_0 + N\tau}{2} \theta^2 + \left(\tau \sum_{i=1}^N x_i + \tau_0 \mu_0 \right) \theta \right\} \cdot u(\theta) \\ &\propto \mathcal{TN}(\theta | \tilde{\mu}, \tilde{\tau}^{-1}), \end{aligned} \tag{3.18}$$

where $u(y)$ is the step function with value 1 if $y \geq 0$ and value 0 if $y < 0$, and

$$\tilde{\mu} = \frac{\tau_0 \mu_0 + \tau \sum_{i=1}^N x_i}{\tau_0 + N\tau}, \quad \tilde{\tau} = \tau_0 + N\tau.$$

The posterior parameters are exactly the same as those in the Normal-Normal model (Equation (3.3)), and the posterior “parent” mean can also be expressed as a weighted mean of μ_0 and \bar{x} .

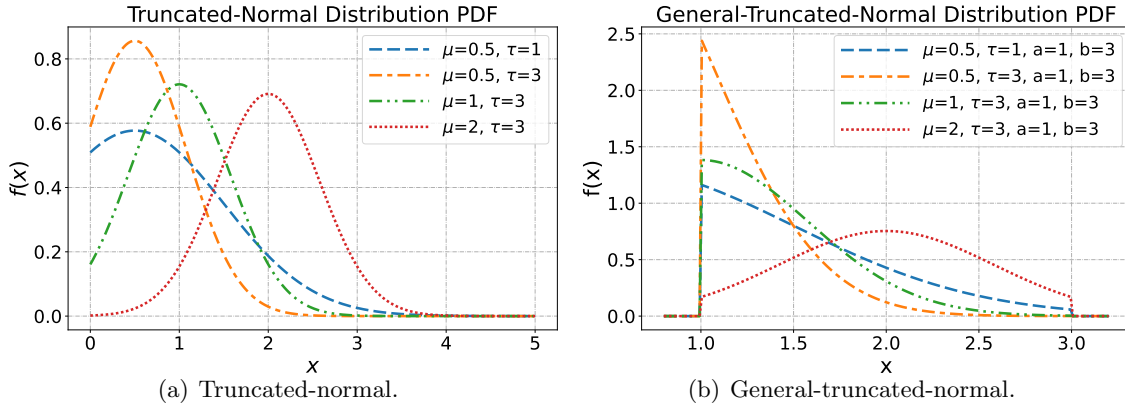


Figure 3.7: Truncated-normal and general-truncated-normal probability density functions for different values of the parameters μ and τ .

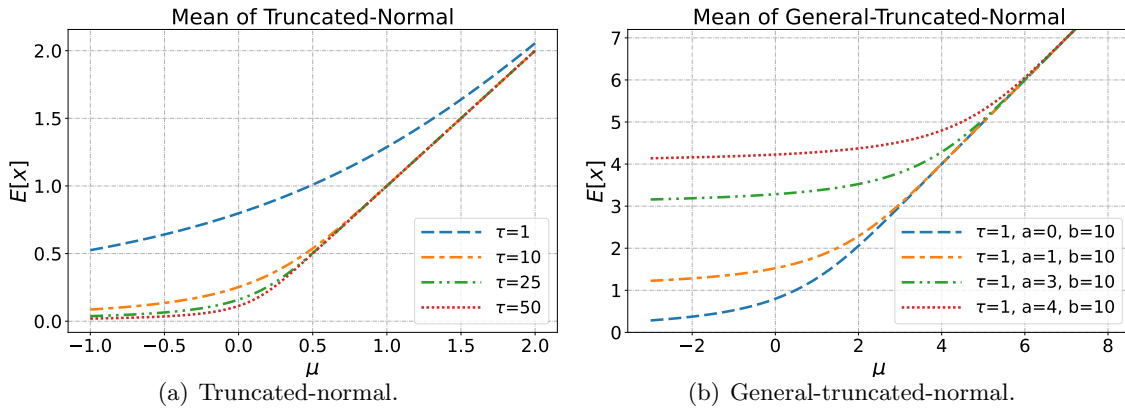


Figure 3.8: Mean of truncated-normal and general-truncated-normal distribution by varying μ, τ, a , and b parameters.

Expanding beyond the truncated-normal distribution, the *general-truncated-normal (GTN)* distribution is also a variant of the normal distribution, excluding values outside a specified range. In other words, it is a normal distribution that is “cut off” at some specified lower and/or upper bound. The range between the lower and upper bound is called the support of the distribution. ³

3. In some contexts, the general-truncated-normal distribution is named the truncated-normal directly. We here differentiate the two as the definitions describe.

Definition 3.4.2 (General-Truncated-Normal (GTN) Distribution) A random variable x is said to follow the general-truncated-normal distribution with “parent” mean μ and “parent” precision $\tau > 0$, denoted by $x \sim \mathcal{GTN}(\mu, \tau^{-1}, a, b)$, if

$$f(x; \mu, \tau^{-1}, a, b) = \begin{cases} 0, & \text{if } x < a; \\ \frac{\sqrt{\frac{\tau}{2\pi}} \exp\{-\frac{\tau}{2}(x - \mu)^2\}}{\Phi((b - \mu) \cdot \sqrt{\tau}) - \Phi((a - \mu) \cdot \sqrt{\tau})}, & \text{if } a \leq x \leq b; \\ 1, & \text{if } 0 > b, \end{cases}$$

where $\Phi(\cdot)$ is the c.d.f. of $\mathcal{N}(0, 1)$, the standard normal distribution. The mean and variance of $x \sim \mathcal{GTN}(\mu, \tau^{-1}, a, b)$ are given by

$$\begin{aligned} \mathbb{E}[x] &= \mu - \frac{1}{\sqrt{\tau}} \cdot \frac{\phi(\beta) - \phi(\alpha)}{\Phi(\beta) - \Phi(\alpha)}, \\ \text{Var}[x] &= \frac{1}{\tau} \left(1 - \frac{\beta\phi(\beta) - \alpha\phi(\alpha)}{\Phi(\beta) - \Phi(\alpha)} - \left(\frac{\beta\phi(\beta) - \alpha\phi(\alpha)}{\Phi(\beta) - \Phi(\alpha)} \right)^2 \right), \end{aligned}$$

where $\phi(\cdot)$ is the p.d.f. of the standard normal distribution, and

$$\alpha = (a - \mu) \cdot \sqrt{\tau}, \quad \beta = (b - \mu) \cdot \sqrt{\tau}.$$

Note that, the truncated-normal distribution is a special general-truncated-normal with $a = 0$ and $b = \infty$ (Burkardt, 2014). Figure 3.7(b) compares different parameters μ, τ for the GTN distribution. Figure 3.8(b) shows the mean value of the GTN distribution by varying μ given fixed τ, a, b ; we again find when $\mu \rightarrow -\infty$, the mean is approaching zero.

Conjugate prior for the constrained mean parameter of a Gaussian. We have previously shown that a Gaussian distribution can serve as a conjugate prior for the mean parameter of another Gaussian distribution when the variance is fixed. The truncated-normal distribution is also a conjugate prior for the **nonnegative** mean parameter of a Gaussian distribution when the variance is fixed. To see this, suppose $\mathcal{X} = \{x_1, x_2, \dots, x_N\}$ are drawn i.i.d. from a normal distribution with mean θ and precision τ , i.e., the likelihood is $\mathcal{N}(x | \theta, \tau^{-1})$, where the variance $\sigma^2 = \tau^{-1}$ is fixed, and θ is given a $\mathcal{GTN}(\mu_0, \tau_0^{-1}, a, b)$ prior: $\theta \sim \mathcal{GTN}(\mu_0, \tau_0^{-1}, a, b)$, with $a > 0$ for the nonnegativity constrain. Using Bayes’ theorem, the posterior is

$$\begin{aligned} p(\theta | \mathcal{X}) &\propto \prod_{i=1}^N \mathcal{N}(x_i | \theta, \tau^{-1}) \times \mathcal{GTN}(\theta | \mu_0, \tau_0^{-1}, a, b) \\ &\propto \exp \left\{ -\frac{\tau_0 + N\tau}{2} \theta^2 + \left(\tau \sum_{i=1}^N x_i + \tau_0 \mu_0 \right) \theta \right\} \cdot \mathbf{1}(a \leq \theta \leq b) \\ &\propto \mathcal{GTN}(\theta | \tilde{\mu}, \tilde{\tau}^{-1}, a, b), \end{aligned} \tag{3.19}$$

where $\mathbf{1}(a \leq y \leq b)$ is the step function with value 1 if $a \leq y \leq b$ and value 0 otherwise, and

$$\tilde{\mu} = \frac{\tau_0 \mu_0 + \tau \sum_{i=1}^N x_i}{\tau_0 + N\tau}, \quad \tilde{\tau} = \tau_0 + N\tau.$$

The posterior parameters are again exactly the same as those in the Normal-Normal model (Equation (3.3)).

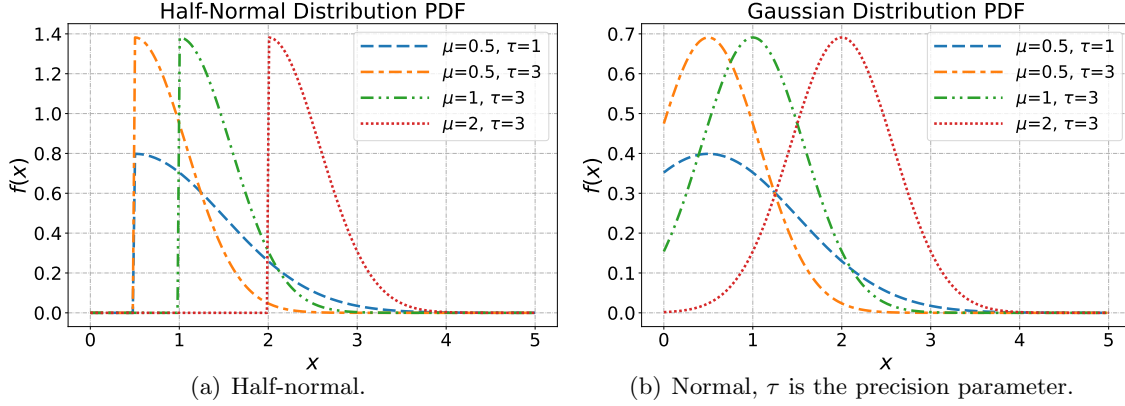


Figure 3.9: Half-normal and normal probability density functions for different values of the parameters μ and τ . The probability density of any value $x \geq \mu$ in the half-normal distribution is twice as that in the normal distribution with the same parameters μ, τ .

The half-normal distribution is a special case of the normal distribution, where the support is on the range with values larger than the mean parameter μ of a normal distribution (known as the “parent” mean parameter of the normal distribution) and the distribution is unsymmetrical around μ . This distribution is often used in modeling the scale or standard deviation of a process where the values cannot be smaller than μ .

Definition 3.4.3 (Half-Normal Distribution) A random variable x is said to follow the half-normal distribution with “parent” mean μ and “parent” precision $\tau > 0$, denoted by $x \sim \mathcal{HN}(\mu, \tau^{-1})$, if

$$f(x; \mu, \tau^{-1}) = \begin{cases} \sqrt{\frac{2\tau}{\pi}} \exp\left\{-\frac{\tau}{2}(x - \mu)^2\right\}, & \text{if } x \geq \mu; \\ 0, & \text{if } x < \mu. \end{cases}$$

The mean and variance of $x \sim \mathcal{HN}(\mu, \tau^{-1})$ are given by

$$E[x] = \mu + \sqrt{\frac{2}{\pi\tau}}, \quad \text{Var}[x] = \frac{1}{\tau} \left(1 - \frac{2}{\pi}\right).$$

Figure 3.9(a) compares different parameters μ, τ for the half-normal distribution.

In this text, the *rectified-normal (RN)* distribution is defined as proportional to the product of a Gaussian distribution and an exponential distribution. And it can also be called the *exponentially rectified-normal* distribution.

Definition 3.4.4 (Rectified-Normal (RN) Distribution) A random variable x is said to follow the rectified-normal distribution (or **exponentially rectified-normal** distribution) with “parent” mean μ , “parent” precision $\tau > 0$, and “parent” rate $\lambda > 0$, denoted by $x \sim \mathcal{RN}(\mu, \tau^{-1}, \lambda)$, if

$$\begin{aligned} f(x; \mu, \tau^{-1}, \lambda) &= \frac{1}{C} \cdot \mathcal{N}(x \mid \mu, \tau^{-1}) \cdot \mathcal{E}(x \mid \lambda) \\ &\propto \exp \left\{ -\frac{\tau}{2} \left(x - \frac{\tau\mu - \lambda}{\tau} \right)^2 \right\} \cdot u(x) \\ &\propto \mathcal{TN}(x \mid \frac{\tau\mu - \lambda}{\tau}, \tau^{-1}), \end{aligned}$$

where $\mathcal{TN}(\cdot)$ is the density function of a truncated-normal distribution, and C is a constant value,

$$C = C^{RN}(\mu, \tau, \lambda) = \lambda \left\{ 1 - \Phi \left(-\frac{\tau\mu - \lambda}{\sqrt{\tau}} \right) \right\} \cdot \exp \left(-\mu\lambda + \frac{\lambda^2}{2\tau} \right). \quad (3.20)$$

That is, the rectified-normal distribution is a special truncated-normal distribution with more flexibility. The mean and variance of $x \sim \mathcal{RN}(\mu, \tau^{-1}, \lambda)$ are given by

$$\begin{aligned} \mathbb{E}[x] &= \frac{\tau\mu - \lambda}{\tau} - \frac{1}{\sqrt{\tau}} \cdot \frac{-\phi(\alpha)}{1 - \Phi(\alpha)}, \\ \text{Var}[x] &= \frac{1}{\tau} \left\{ 1 + \frac{\alpha\phi(\alpha)}{1 - \Phi(\alpha)} + \left(\frac{\alpha\phi(\alpha)}{1 - \Phi(\alpha)} \right)^2 \right\}, \end{aligned}$$

where $\alpha = -\frac{\tau\mu - \lambda}{\tau} \cdot \sqrt{\tau}$. Figure 3.10(b) compares different parameters μ, τ for the RN distribution.

The comparison between the truncated-normal and rectified-normal distributions is presented in Figure 3.10.

Conjugate prior for the nonnegative mean parameter of a Gaussian by RN. Similar to the TN distribution, the RN distribution also serves to enforce nonnegative constraint, and is conjugate to the **nonnegative** mean parameter of a Gaussian likelihood. However, due to the extra parameter λ , the RN distribution is more flexible in this sense. And the derivation follows from Equation (3.18). To see this, suppose $\mathcal{X} = \{x_1, x_2, \dots, x_N\}$ are drawn i.i.d. from a normal distribution with mean θ and precision τ , i.e., the likelihood is $\mathcal{N}(x \mid \theta, \tau^{-1})$ where the variance $\sigma^2 = \tau^{-1}$ is fixed, and θ is given a $\mathcal{RN}(\mu_0, \tau_0^{-1}, \lambda_0)$

prior: $\theta \sim \mathcal{RN}(\mu_0, \tau_0^{-1}, \lambda_0)$. Using Bayes' theorem, the posterior is

$$\begin{aligned}
 p(\theta | \mathcal{X}) &\propto \prod_{i=1}^N \mathcal{N}(x_i | \theta, \tau^{-1}) \times \mathcal{RN}(\theta | \mu_0, \tau_0^{-1}, \lambda_0) \\
 &= \prod_{i=1}^N \mathcal{N}(x_i | \theta, \tau^{-1}) \times \mathcal{TN}(\theta | m_0, \tau_0^{-1}) \quad (m_0 = \frac{\tau_0 \mu_0 - \lambda_0}{\tau_0}) \\
 &\propto \mathcal{TN}(\theta | \tilde{\mu}, \tilde{\tau}^{-1}),
 \end{aligned} \tag{3.21}$$

where

$$\tilde{\mu} = \frac{\tau_0 m_0 + \tau \sum_{i=1}^N x_i}{\tau_0 + N\tau}, \quad \tilde{\tau} = \tau_0 + N\tau.$$

That is, the posterior density is a special RN or TN distribution.

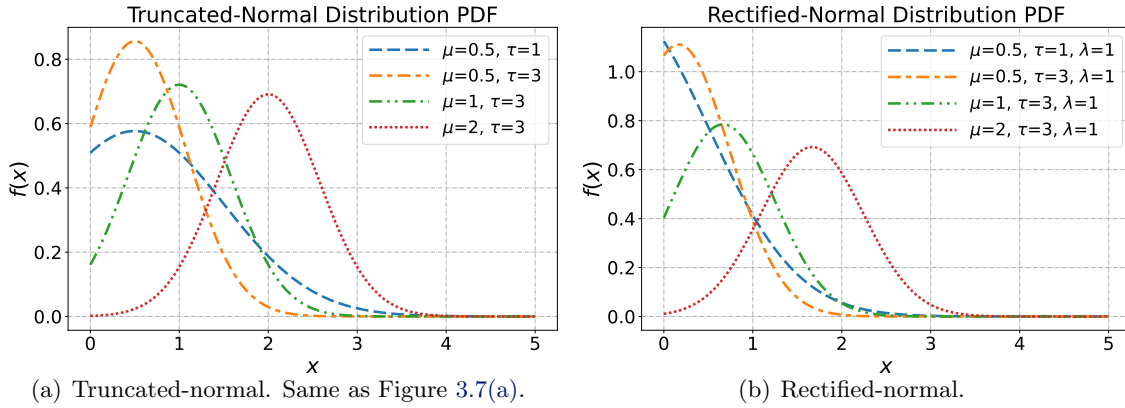


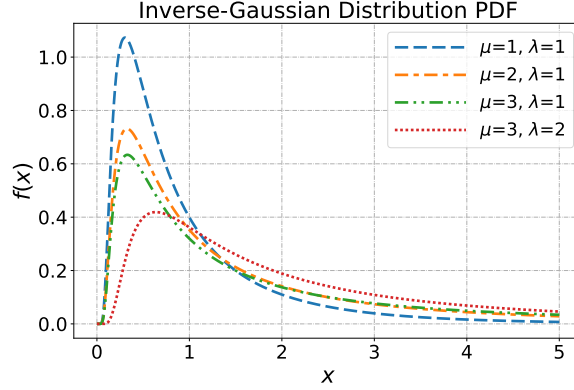
Figure 3.10: Truncated-normal and rectified-normal probability density functions for different values of the parameters μ , τ , and λ .

The *inverse-Gaussian* distribution, also known as the *Wald* distribution, is a continuous probability distribution with two parameters, $\mu > 0$ and $b > 0$. It is a versatile distribution that is used in various applications including modeling waiting times, stock prices, and lifetimes of mechanical systems. An important property of the distribution is that it is well-suited for modeling nonnegative, continuous, and positively skewed data with finite mean and variance.

Definition 3.4.5 (Inverse-Gaussian Distribution) A random variable x is said to follow the inverse-Gaussian distribution with parameters $\mu > 0$ and $b > 0$, denoted by $x \sim \mathcal{N}^{-1}(\mu, \lambda)$ ^a, if

$$f(x; \mu, \lambda) = \begin{cases} \sqrt{\frac{\lambda}{2\pi x^3}} \exp\left(-\frac{\lambda(x - \mu)^2}{2\mu^2 x}\right), & \text{if } x \geq 0; \\ 0, & \text{if } x < 0. \end{cases}$$

Figure 3.11: Inverse-Gaussian probability density functions for different values of the parameters μ and λ .



The mean and variance of $x \sim \mathcal{N}^{-1}(\mu, \lambda)$ are given by

$$E[x] = \mu, \quad \text{Var}[x] = \frac{\mu^3}{\lambda}.$$

The support of an inverse-Gaussian distribution is on $(0, \infty)$. Figure 3.11 compares different parameters μ, λ for the inverse-Gaussian distribution.

a. Note we use \mathcal{N}^{-1} to denote the inverse-Gaussian distribution and use \mathcal{G}^{-1} to denote the inverse-Gamma distribution.

The *Laplace* distribution, also known as the *double exponential* distribution, is named after *Pierre-Simon Laplace* (1749–1827), who obtained the distribution in 1774 (Kotz et al., 2001; Härdle and Simar, 2007). The Laplace distribution is useful in modeling heavy-tailed data since it has heavier tails than the normal distribution, and it is used extensively in sparse-favoring models since it expresses a high peak with heavy tails (same as the ℓ_1 regularization term in non-probabilistic or non-Bayesian optimization methods). When we have a prior belief that the parameter of interest is likely to be close to the mean with the potential for large deviations, the Laplace distribution is then used in Bayesian modeling as a prior distribution for this context.

Definition 3.4.6 (Laplace Distribution) A random variable x is said to follow the Laplace distribution with location and scale parameters μ and $b > 0$, respectively, denoted by $x \sim \mathcal{L}(\mu, b)$, if

$$f(x; \mu, b) = \frac{1}{2b} \exp\left(-\frac{|x - \mu|}{b}\right).$$

The mean and variance of $x \sim \mathcal{L}(\mu, b)$ are given by

$$E[x] = \mu, \quad \text{Var}[x] = 2b^2.$$

Figure 3.12(a) compares different parameters μ and b for the Laplace distribution.

Laplace as a mixture of normal distributions. Any Laplace random variable can be thought of as the integration of a Gaussian random variable with the same mean value and a *stochastic* variance that follows an exponential distribution. More formally, the Laplace

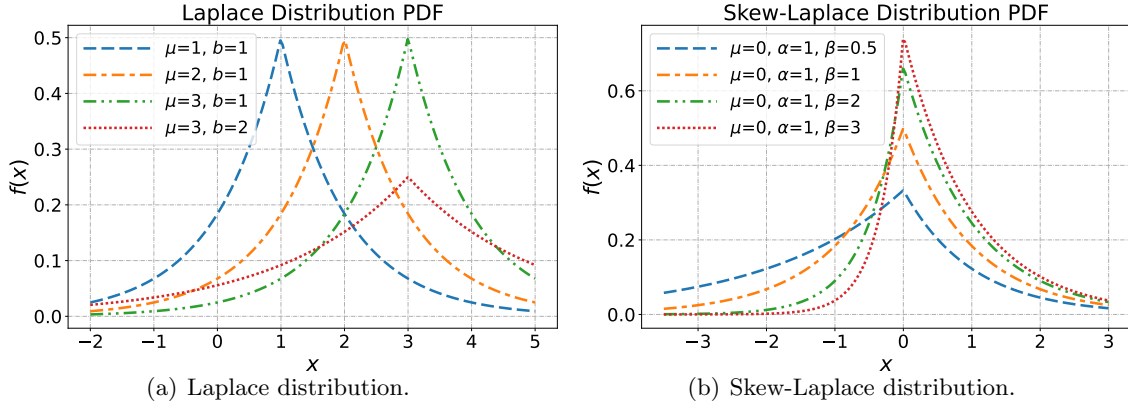


Figure 3.12: Laplace and skew-Laplace probability density functions for different values of the parameters.

distribution can be rewritten as:

$$\mathcal{L}(x \mid \mu, b) = \int_0^\infty \mathcal{N}(x \mid \mu, \epsilon) \cdot \mathcal{E}(\epsilon \mid \frac{1}{2b^2}) d\epsilon. \quad (3.22)$$

To see this, we have

$$\begin{aligned} & \int_0^\infty \mathcal{N}(x \mid \mu, \epsilon) \cdot \mathcal{E}(\epsilon \mid \frac{1}{2b^2}) d\epsilon \\ &= \int_0^\infty \frac{1}{\sqrt{2\pi\epsilon}} \exp\left\{-\frac{1}{2\epsilon}(x - \mu)^2\right\} \cdot \frac{1}{2b^2} \exp\left(-\frac{1}{2b^2}\epsilon\right) d\epsilon \\ &= \frac{1}{2b^2} \int_0^\infty \frac{1}{\sqrt{2\pi\epsilon}} \exp\left\{-\frac{(x - \mu)^2 + \frac{\epsilon^2}{b^2}}{2\epsilon}\right\} d\epsilon \\ &= \frac{1}{2b^2} \int_0^\infty \frac{\epsilon}{\sqrt{2\pi\epsilon^3}} \exp\left\{-\frac{(x - \mu - \frac{\epsilon}{b})^2 + 2|x - \mu|\frac{\epsilon}{b}}{2\epsilon}\right\} d\epsilon \\ &\stackrel{z:=|x-\mu|b}{=} \frac{1}{2b^2} \int_0^\infty \frac{\epsilon}{\sqrt{2\pi\epsilon^3}} \exp\left\{-\frac{(z - \epsilon)^2}{2\epsilon b^2}\right\} \exp\left\{\frac{|x - \mu|}{b}\right\} d\epsilon \\ &\stackrel{\lambda:=|x-\mu|}{=} \frac{1}{\sqrt{\lambda}} \frac{1}{2b^2} \exp\left\{\frac{|x - \mu|}{b}\right\} \int_0^\infty \epsilon \frac{\sqrt{\lambda}}{\sqrt{2\pi\epsilon^3}} \exp\left\{-\frac{\lambda(z - \epsilon)^2}{2\epsilon z^2}\right\} d\epsilon \\ &= \frac{1}{2b} \exp\left\{-\frac{|x - \mu|}{b}\right\}, \end{aligned}$$

where the last equality is from the mean value of an inverse-Gaussian distribution in Definition 3.4.5.

Conjugate prior for the Laplace scale parameter. Similar to the Gaussian case, the inverse-Gamma distribution is a conjugate prior for the scale parameter of a Laplace distribution. To see this, let the likelihood be $p(\mathbf{A} \mid \mathbf{B}, b) = \mathcal{L}(\mathbf{A} \mid \mathbf{B}, b)$, where $\mathbf{A}, \mathbf{B} \in$

$\mathbb{R}^{M \times N}$, the prior of b be $p(b) = \mathcal{G}^{-1}(b \mid \alpha, \beta)$. Using Bayes' theorem, it can be shown that

$$\begin{aligned}
 p(b \mid \mathbf{A}, \mathbf{B}, \alpha, \beta) &\propto \mathcal{L}(\mathbf{A} \mid \mathbf{B}, b) \times \mathcal{G}^{-1}(b \mid \alpha, \beta) \\
 &= \prod_{i,j=1}^{M,N} \mathcal{L}(a_{ij} \mid b_{ij}, b) \times \frac{\beta^\alpha}{\Gamma(\alpha)} (b)^{-\alpha-1} \exp\left(-\frac{\beta}{b}\right) \\
 &\propto \frac{1}{b^{MN}} \exp\left\{-\frac{1}{b} \sum_{i,j=1}^{M,N} |a_{ij} - b_{ij}|\right\} \cdot b^{-\alpha-1} \exp\left(-\frac{\beta}{b}\right) \\
 &= (b)^{-MN-\alpha-1} \exp\left\{-\frac{1}{b} \left(\sum_{i,j=1}^{M,N} \frac{1}{2} |a_{ij} - b_{ij}| + \beta\right)\right\} \\
 &\propto \mathcal{G}^{-1}(b \mid \tilde{\alpha}, \tilde{\beta}),
 \end{aligned} \tag{3.23}$$

where

$$\tilde{\alpha} = MN + \alpha, \quad \tilde{\beta} = \sum_{i,j=1}^{M,N} \frac{1}{2} |a_{ij} - b_{ij}| + \beta. \tag{3.24}$$

That is, the posterior density of the scale parameter b follows also from an inverse-Gamma distribution.

The skew-Laplace distribution is a type of heavy-tailed probability distribution that is similar to the Laplace distribution but allows for skewness (see Figure 3.12).

Definition 3.4.7 (Skew-Laplace Distribution) *A random variable x is said to follow the skew-Laplace (or the asymmetric Laplace) distribution with location and scale parameters μ and $\alpha, \beta > 0$, respectively, denoted by $x \sim \mathcal{SL}(\mu, \alpha, \beta)$, if*

$$f(x; \mu, \alpha, \beta) = \begin{cases} \frac{\alpha\beta}{\alpha + \beta} \exp\{-\alpha(x - \mu)\}, & \text{if } x \geq \mu; \\ \frac{\alpha\beta}{\alpha + \beta} \exp\{\beta(x - \mu)\}, & \text{if } x < \mu. \end{cases}$$

When $\alpha = \beta = \frac{1}{b}$, the skew-Laplace $x \sim \mathcal{SL}(\mu, \alpha, \beta)$ reduces to a Laplace density $x \sim \mathcal{L}(\mu, b)$. The mean and variance of $x \sim \mathcal{SL}(\mu, \alpha, \beta)$ are given by

$$\mathbb{E}[x] = \mu + \frac{\beta - \alpha}{\alpha\beta}, \quad \text{Var}[x] = \frac{\alpha^2 + \beta^2}{\alpha^2\beta^2}.$$

Figure 3.12(b) compares different parameters μ, α , and β for the skew-Laplace distribution. When $\alpha > \beta$, the distribution is skewed to the right.

3.5. Multinomial Distribution and Conjugacy

The multinomial distribution is widely used in the Bayesian mixture model to introduce latent variables. It is a discrete probability distribution that describes the probabilities of obtaining different outcomes from N independent trials, each with K different possible

outcomes and with probabilities of the K outcomes that are specified. It models the distribution of counts or frequencies of events among K categories. In specific, the multinomial distribution is parameterized by an integer N and a p.m.f. $\boldsymbol{\pi} = \{\pi_1, \pi_2, \dots, \pi_K\}$, and can be thought of as following: if we have N independent events, and for each event, the probability of outcome k is π_k , then the multinomial distribution specifies the probability that outcome k occurs N_k times, for $k = 1, 2, \dots, K$. Formally, we have the following definition of the multinomial distribution.

Definition 3.5.1 (Multinomial Distribution) A K -dimensional random vector $\mathbf{N} = [N_1, N_2, \dots, N_K] \in \{0, 1, 2, \dots, N\}^K$, where $\sum_{k=1}^K N_k = N$ is said to follow the multinomial distribution with parameter $N \in \mathbb{N}$, and $\boldsymbol{\pi} = [\pi_1, \pi_2, \dots, \pi_K] \in [0, 1]^K$ such that $\sum_{k=1}^K \pi_k = 1$. Denoted by $\mathbf{N} \sim \text{Multi}_K(N, \boldsymbol{\pi})$. Then its probability mass function is given by

$$p(N_1, N_2, \dots, N_K | N, \boldsymbol{\pi} = (\pi_1, \pi_2, \dots, \pi_K)) = \frac{N!}{N_1! N_2! \dots N_K!} \prod_{k=1}^K \pi_k^{N_k} \cdot \mathbb{1} \left\{ \sum_{k=1}^K N_k = N \right\},$$

where $\{0, 1, 2, \dots, N\}$ is a set of $N + 1$ elements and $[0, 1]$ is a closed set with values between 0 and 1. The mean, variance, and covariance of the multinomial distribution are

$$\mathbb{E}[N_k] = N\pi_k, \quad \text{Var}[N_k] = N\pi_k(1 - \pi_k), \quad \text{Cov}[N_k, N_m] = -N\pi_k\pi_m.$$

When $K = 2$, the multinomial distribution reduces to the **binomial** distribution.

Remark 3.3: Binomial Distribution

In the multinomial distribution, when $K = 2$, it is also known as a *binomial* distribution. A random variable x is said to follow the binomial distribution with parameter $\pi \in (0, 1)$ and $N \in \mathbb{N}$, denoted by $x \sim \text{Binom}(N, \pi)$, if

$$p(x | N, \pi) = \binom{N}{x} \pi^x (1 - \pi)^{N-x}.$$

The mean and variance of the binomial distribution are

$$\mathbb{E}[x] = N\pi, \quad \text{Var}[x] = N\pi(1 - \pi).$$

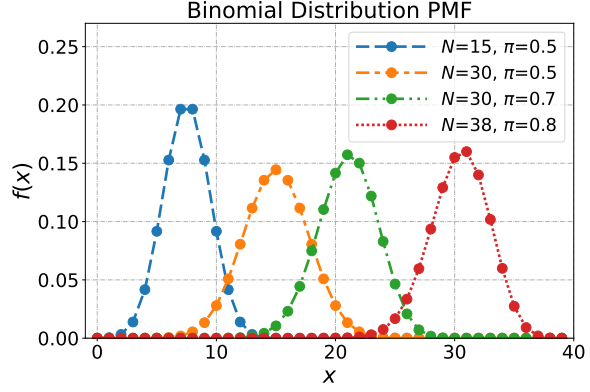
Figure 3.13 compares different parameters N and π for the binomial distribution.

A distribution that is closely related to the Binomial distribution is called the Bernoulli distribution. A random variable is said to follow the *Bernoulli* distribution with parameter $\pi \in (0, 1)$, denoted as $x \sim \text{Bern}(\pi)$, if

$$f(x; \pi) = \pi \mathbb{1}\{x = 1\} + (1 - \pi) \mathbb{1}\{x = 0\},$$

with mean $\mathbb{E}[x] = \pi$ and variance $\text{Var}[x] = \pi(1 - \pi)$, respectively.

Figure 3.13: Binomial probability mass functions for different values of the parameters N, π .



Exercise 3.2 (Bernoulli and Binomial) Show that if $\mathbf{x} = \sum_{i=1}^N y_i$ with $y_i \stackrel{i.i.d.}{\sim} \text{Bern}(\pi)$, then we have $\mathbf{x} \sim \text{Binom}(N, \pi)$.

3.5.1 Dirichlet Distribution

The Dirichlet distribution is a multi-dimensional probability distribution defined over the simplex. It takes a vector of positive real numbers as input and outputs a probability distribution over a set of probabilities that sum to 1. The Dirichlet distribution commonly serves as a prior distribution in Bayesian statistics, particularly in the context of discrete and categorical data, and it is a conjugate prior for the probability parameter $\boldsymbol{\pi}$ in the multinomial distribution.

Definition 3.5.2 (Dirichlet Distribution) A random vector $\mathbf{x} = [x_1, x_2, \dots, x_K] \in [0, 1]^K$ is said to follow the Dirichlet distribution with parameter $\boldsymbol{\alpha}$, denoted by $\mathbf{x} \sim \text{Dirichlet}(\boldsymbol{\alpha})$, if

$$f(\mathbf{x}; \boldsymbol{\alpha}) = \frac{1}{D(\boldsymbol{\alpha})} \prod_{k=1}^K x_k^{\alpha_k - 1}, \quad (3.25)$$

such that $\sum_{k=1}^K x_k = 1$, $x_k \in [0, 1]$ and

$$D(\boldsymbol{\alpha}) = \frac{\prod_{k=1}^K \Gamma(\alpha_k)}{\Gamma(\alpha_+)}, \quad (3.26)$$

where $\boldsymbol{\alpha} = [\alpha_1, \alpha_2, \dots, \alpha_K]$ is a vector of reals with $\alpha_k > 0, \forall k$, and $\alpha_+ = \sum_{k=1}^K \alpha_k$. The $\boldsymbol{\alpha}$ is also known as the **concentration parameter** in Dirichlet distribution. $\Gamma(\cdot)$ is the Gamma function, which is a generalization of the factorial function. The mean, variance, and covariance are

$$\mathbb{E}[x_k] = \frac{\alpha_k}{\alpha_+}, \quad \text{Var}[x_k] = \frac{\alpha_k(\alpha_+ - \alpha_k)}{\alpha_+^2(\alpha_+ + 1)}, \quad \text{Cov}[x_k, x_m] = \frac{-\alpha_k \alpha_m}{\alpha_+^2(\alpha_+ + 1)}.$$

When $K = 2$, the Dirichlet distribution reduces to the Beta distribution, The Beta distribution $\text{Beta}(\alpha, \beta)$ is defined on $[0, 1]$ with the probability density function given by

$$\text{Beta}(x \mid \alpha, \beta) = \frac{\Gamma(\alpha + \beta)}{\Gamma(\alpha)\Gamma(\beta)} x^{\alpha-1}(1-x)^{\beta-1}.$$

That is, if $x \sim \text{Beta}(\alpha, \beta)$, then $\mathbf{x} = [x, 1-x] \sim \text{Dirichlet}(\boldsymbol{\alpha})$, where $\boldsymbol{\alpha} = [\alpha, \beta]$.

Interesting readers can refer to Appendix A.2 (p. 246) for a derivation of the Dirichlet distribution. The sample space of the Dirichlet distribution lies on the $(K-1)$ -dimensional probability simplex, which is a surface in \mathbb{R}^K denoted by Δ_K . That is a set of vectors in \mathbb{R}^K whose components are nonnegative and sum to 1:

$$\Delta_K = \left\{ \boldsymbol{\pi} : 0 \leq \pi_k \leq 1, \sum_{k=1}^K \pi_k = 1 \right\}.$$

Notice that Δ_K lies on a $(K-1)$ -dimensional space since each component is nonnegative, and the components sum to 1.

Figure 3.14 shows various plots of the Dirichlet distribution’s density over the two-dimensional simplex in \mathbb{R}^3 for a handful of values of the parameter vector $\boldsymbol{\alpha}$, and Figure 3.15 shows the draw of 5,000 points for each setting. In specific, the density plots of Dirichlet in \mathbb{R}^3 is a surface plot in $4d$ -space. Figure 3.14(a) is a projection of a surface into $3d$ -space, where the z-axis is the probability density function, and Figure 3.14(b) is a projection of a surface into $3d$ -space, where the z-axis is π_3 . Figure 3.14(c) to Figure 3.14(f) are the projections into $2d$ -space.

When the concentration parameter is $\boldsymbol{\alpha} = [1, 1, 1]$, the Dirichlet distribution reduces to the uniform distribution over the simplex. This can be easily verified that $\text{Dirichlet}(\mathbf{x} \mid \boldsymbol{\alpha} = [1, 1, 1]) = \frac{\Gamma(3)}{(\Gamma(1))^3} = 2$, which is a constant that does not depend on the specific value of \mathbf{x} . When $\boldsymbol{\alpha} = [c, c, c]$ with $c > 1$, the density becomes monomodal and concentrated in the center of the simplex. This can be seen from $\text{Dirichlet}(\mathbf{x} \mid \boldsymbol{\alpha} = [c, c, c]) = \frac{\Gamma(3c)}{(\Gamma(c))^3} \prod_{k=1}^3 x_k^{c-1}$ such that a small value of x_k will make the probability density approach zero. On the contrary, when $\boldsymbol{\alpha} = [c, c, c]$ with $c < 1$, the density has sharp peaks almost at the vertices of the simplex.

More properties of the Dirichlet distribution are provided in Table 3.2, and the proof can be found in Appendix A.2 (p. 246). And the derivation on the Dirichlet distribution in Appendix A.2 (p. 246) can also be utilized to generate samples from the Dirichlet distribution by a set of samples from a set of Gamma distributions.

3.5.2 Posterior Distribution for Multinomial Distribution

For the conjugacy, that is, the Dirichlet distribution serves as a conjugate prior for the multinomial distribution. If $(\mathbf{N} \mid \boldsymbol{\pi}) \sim \text{Multi}_K(N, \boldsymbol{\pi})$, and $\boldsymbol{\pi}$ is given a Dirichlet prior with $\boldsymbol{\pi} \sim \text{Dirichlet}(\boldsymbol{\alpha})$, then it follows that $(\boldsymbol{\pi} \mid \mathbf{N}) \sim \text{Dirichlet}(\boldsymbol{\alpha} + \mathbf{N}) = \text{Dirichlet}(\alpha_1 + N_1, \dots, \alpha_K + N_K)$.

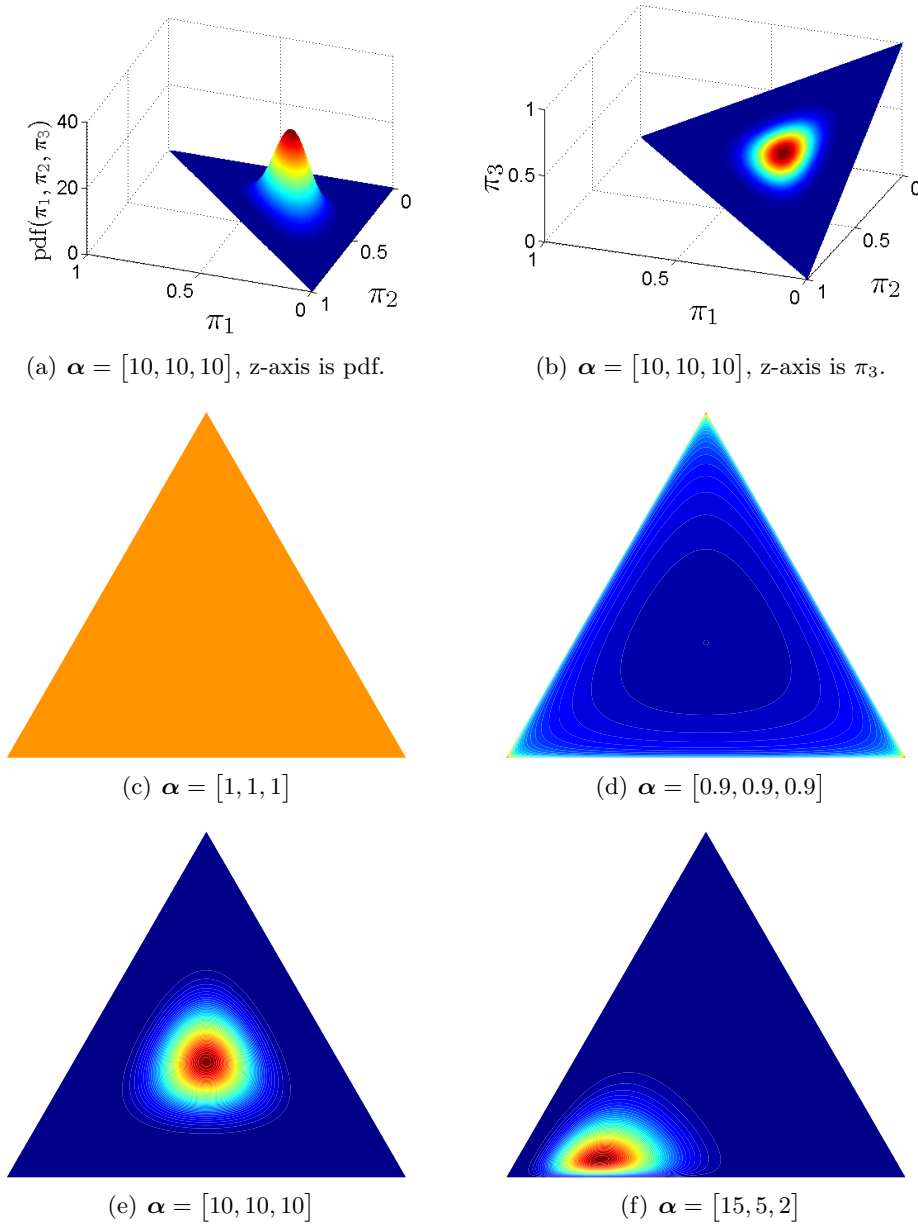


Figure 3.14: Density plots (blue=low, red=high) for the Dirichlet distribution over the probability simplex in \mathbb{R}^3 for various values of the concentration parameter α . When $\alpha = [c, c, c]$, the distribution is called a *symmetric Dirichlet distribution*, and the density is symmetric about the uniform probability mass function (i.e., occurs in the middle of the simplex). When $0 < c < 1$, there are sharp peaks of density almost at the vertices of the simplex. When $c > 1$, the density becomes monomodal and concentrated in the center of the simplex. And when $c = 1$, it is uniform distributed over the simplex. Finally, if α is not a constant vector, the density is not symmetric.

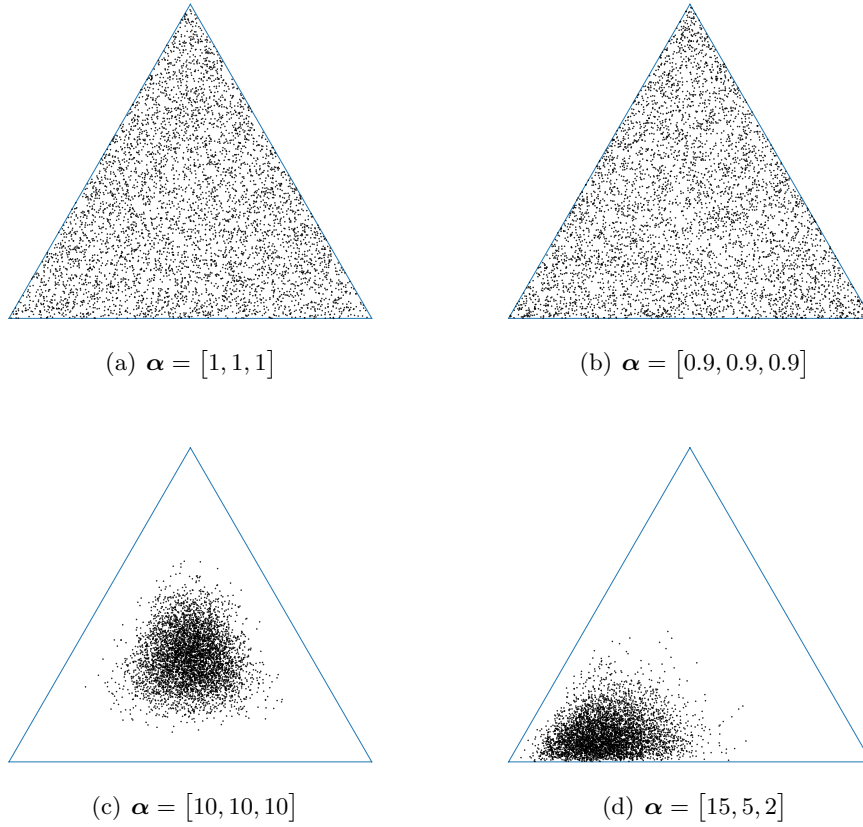


Figure 3.15: Draw of 5,000 points from Dirichlet distribution over the probability simplex in \mathbb{R}^3 for various values of the concentration parameter α .

Marginal Distribution	$x_i \sim \text{Beta}(\alpha_i, \alpha_+ - \alpha_i)$.
Conditional Distribution	$\mathbf{x}_{-i} \mid x_i \sim (1 - x_i)\text{Dirichlet}(\alpha_{-i})$, where \mathbf{x}_{-i} is a random vector excluding x_i .
Aggregation Property	If $M = x_i + x_j$, then $[x_1, \dots, x_{i-1}, x_{i+1}, \dots, x_{j-1}, x_{j+1}, \dots, x_K, M] \sim \text{Dirichlet}([\alpha_1, \dots, \alpha_{i-1}, \alpha_{i+1}, \dots, \alpha_{j-1}, \alpha_{j+1}, \dots, \alpha_K, \alpha_i + \alpha_j])$. In general, If $\{A_1, A_2, \dots, A_r\}$ is a partition of $\{1, 2, \dots, K\}$, then $[\sum_{i \in A_1} x_i, \sum_{i \in A_2} x_i, \dots, \sum_{i \in A_r} x_i] \sim \text{Dirichlet}([\sum_{i \in A_1} \alpha_i, \sum_{i \in A_2} \alpha_i, \dots, \sum_{i \in A_r} \alpha_i])$.

Table 3.2: Properties of the Dirichlet distribution.

Proof [of conjugate prior of multinomial distribution] Using Bayes' theorem “posterior \propto likelihood \times prior,” we obtain the posterior density

$$\begin{aligned} \text{posterior} &= p(\boldsymbol{\pi} \mid \boldsymbol{\alpha}, \mathbf{N}) \propto \text{Multi}_K(\mathbf{N} \mid N, \boldsymbol{\pi}) \cdot \text{Dirichlet}(\boldsymbol{\pi} \mid \boldsymbol{\alpha}) \\ &= \left(\frac{N!}{N_1! N_2! \dots N_K!} \prod_{k=1}^K \pi_k^{N_k} \right) \cdot \left(\frac{1}{D(\boldsymbol{\alpha})} \prod_{k=1}^K \pi_k^{\alpha_k - 1} \right) \\ &\propto \prod_{k=1}^K \pi_k^{\alpha_k + N_k - 1} \propto \text{Dirichlet}(\boldsymbol{\pi} \mid \boldsymbol{\alpha} + \mathbf{N}). \end{aligned}$$

Therefore, it follows that $(\boldsymbol{\pi} \mid \mathbf{N}) \sim \text{Dirichlet}(\boldsymbol{\alpha} + \mathbf{N}) = \text{Dirichlet}(\alpha_1 + N_1, \dots, \alpha_K + N_K)$. ■

A comparison between the prior and posterior distribution reveals that the relative sizes of the Dirichlet parameters α_k describe the mean of the prior distribution of $\boldsymbol{\pi}$, and the sum of α_k 's is a measure of the strength of the prior distribution. The prior distribution is mathematically equivalent to a likelihood resulting from $\sum_{k=1}^K (\alpha_k - 1)$ observations with $\alpha_k - 1$ observations for the k -th group.

Since the Dirichlet distribution is a multivariate generalization of the Beta distribution, the Beta distribution can be taken as a conjugate prior for binomial distribution (Hoff, 2009; Frigyik et al., 2010).

3.6. Poisson and Multinomial

The *Poisson* distribution is a discrete probability distribution that characterizes the number of events in a fixed interval of time or space, given the average number of events in that interval. The Poisson distribution is frequently employed for modeling count data, such as the number of calls received by a call center in an hour or the number of emails received in a day provided that the probability of a “success” for any given instance is “very small.”

Definition 3.6.1 (Poisson Distribution) A random variable x is said to follow the Poisson distribution with rate parameter $\lambda > 0$, denoted by $x \sim \mathcal{P}(\lambda)$, if

$$f(x; \lambda) = \frac{\lambda^x}{x!} \exp(-\lambda).$$

The mean and variance of $x \sim \mathcal{P}(\lambda)$ are given by

$$E[x] = \lambda, \quad \text{Var}[x] = \lambda.$$

The support of an exponential distribution is on $\{0, 1, 2, 3, \dots\} = \{0\} \cup \mathbb{N}$. Figure 3.16 compares probability mass functions of different parameter values λ for the Poisson distribution.

The mean and variance of the Poisson distribution are equal. Roughly speaking, a Poisson distribution is the limit of a binomial distribution when $N \rightarrow \infty$ and $\pi = \lambda/N$, i.e., the number of trials diverges to infinity but the probability of success decreases to zero linearly with respect to the number of trials. This is also known as the *law of rare events*.

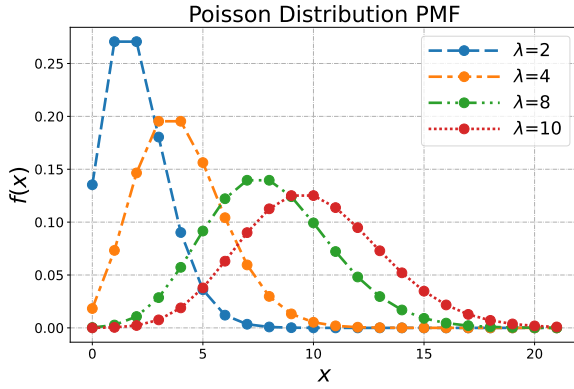


Figure 3.16: Poisson probability mass functions for different values of the parameter λ .

The sum of independently identical Poisson distributed random variables again follows a Poisson distribution.

Theorem 3.4: (Sum of Independently Distributed Poisson)

Let $x_i \sim \mathcal{P}(\lambda_i)$. Then $y = \sum_{i=1}^n x_i \sim \mathcal{P}(\sum_{i=1}^n \lambda_i)$.

For simplicity, we consider two independent Poisson random variables $x \sim \mathcal{P}(\lambda_1)$ and $y \sim \mathcal{P}(\lambda_2)$. Define $\lambda = \lambda_1 + \lambda_2$ and $z = x + y$. Then z is a Poisson random variable with parameter λ . To see this, we have

$$\begin{aligned} p(z) &= P(z = z) = \sum_{k=1}^z P(x = k) \cdot P(y = z - k) \\ &= \sum_{k=1}^z \frac{\lambda_1^k}{k!} \exp(-\lambda_1) \cdot \frac{\lambda_2^{z-k}}{(z-k)!} \exp(-\lambda_2) \\ &= \frac{\exp(-\lambda_1 - \lambda_2)}{z!} \sum_{k=1}^z \binom{z}{k} \lambda_1^k \lambda_2^{z-k} \\ &\stackrel{*}{=} \frac{\exp(-\lambda)}{z!} (\lambda_1 + \lambda_2)^z = \frac{\lambda^z}{z!} \exp(-\lambda), \end{aligned}$$

where the equality (*) is from the *binomial theorem*. Working for general, once we know the sum of two Poisson random variables, we can keep adding more and more of them to obtain another Poisson variable.

Theorem 3.5: (Poisson and Multinomial)

Let $x_i \sim \mathcal{P}(\lambda_i)$ be independent for $i \in \{1, 2, \dots, K\}$. Then the conditional distribution of $\mathbf{x} = [x_1, x_2, \dots, x_k]^\top$ given $\sum_{i=1}^K x_i = N$ is $\text{Multi}_K(N, \{p_1, p_2, \dots, p_K\})$ with

$$p_i = \frac{\lambda_i}{\lambda_1 + \lambda_2 + \dots + \lambda_K}, \quad \text{for all } i \in \{1, 2, \dots, K\}.$$

3.7. Multivariate Gaussian Distribution and Conjugacy

We have shown the conjugate prior for the mean parameter of a univariate Gaussian distribution when the variance (or precision) parameter is fixed; and the joint conjugate prior

for the mean and variance (or precision) parameters of a univariate Gaussian distribution. In this section, we further provide the conjugate analysis of the multivariate Gaussian distribution. See also discussion in Murphy (2007, 2012); Teh (2007); Kamper (2013); Das (2014).

3.7.1 Multivariate Gaussian Distribution

A multivariate Gaussian distribution (also known as a multivariate normal distribution) is a continuous probability distribution with jointly normal distribution over multiple variables. It is fully described by its mean vector (of size equal to the number of variables) and covariance matrix (a square matrix of size equal to the number of variables). The covariance matrix encodes the pairwise relationships between variables in terms of the covariance between them. The multivariate Gaussian can be used to model complex data distributions in various fields such as machine learning, statistics, and signal processing. We first present the rigorous definition of the multivariate Gaussian distribution as follows.

Definition 3.7.1 (Multivariate Gaussian Distribution) *A random vector $\mathbf{x} \in \mathbb{R}^D$ is said to follow the multivariate Gaussian distribution with parameters $\boldsymbol{\mu} \in \mathbb{R}^D$ and $\boldsymbol{\Sigma} \in \mathbb{R}^{D \times D}$, denoted by $\mathbf{x} \sim \mathcal{N}(\boldsymbol{\mu}, \boldsymbol{\Sigma})$, if*

$$f(\mathbf{x}; \boldsymbol{\mu}, \boldsymbol{\Sigma}) = (2\pi)^{-D/2} |\boldsymbol{\Sigma}|^{-1/2} \exp \left\{ -\frac{1}{2} (\mathbf{x} - \boldsymbol{\mu})^\top \boldsymbol{\Sigma}^{-1} (\mathbf{x} - \boldsymbol{\mu}) \right\},$$

where $\boldsymbol{\mu} \in \mathbb{R}^D$ is called the **mean vector**, and $\boldsymbol{\Sigma} \in \mathbb{R}^{D \times D}$ is positive definite and is called the **covariance matrix**. The mean, mode, and covariance of the multivariate Gaussian distribution are given by

$$\begin{aligned} \mathbb{E}[\mathbf{x}] &= \boldsymbol{\mu}, \\ \text{Mode}[\mathbf{x}] &= \boldsymbol{\mu}, \\ \text{Cov}[\mathbf{x}] &= \boldsymbol{\Sigma}. \end{aligned}$$

Figure 3.17 compares Gaussian density plots for different kinds of covariance matrices. The multivariate Gaussian variable can be drawn from a univariate Gaussian density; see Problem 3.3.

Similar to the likelihood under univariate Gaussian distribution (Equation (3.1)) for deriving the conjugate Bayesian result, the likelihood of N random observations $\mathcal{X} = \{\mathbf{x}_1, \mathbf{x}_2, \dots, \mathbf{x}_N\}$ generated by a multivariate Gaussian with mean vector $\boldsymbol{\mu}$ and covariance

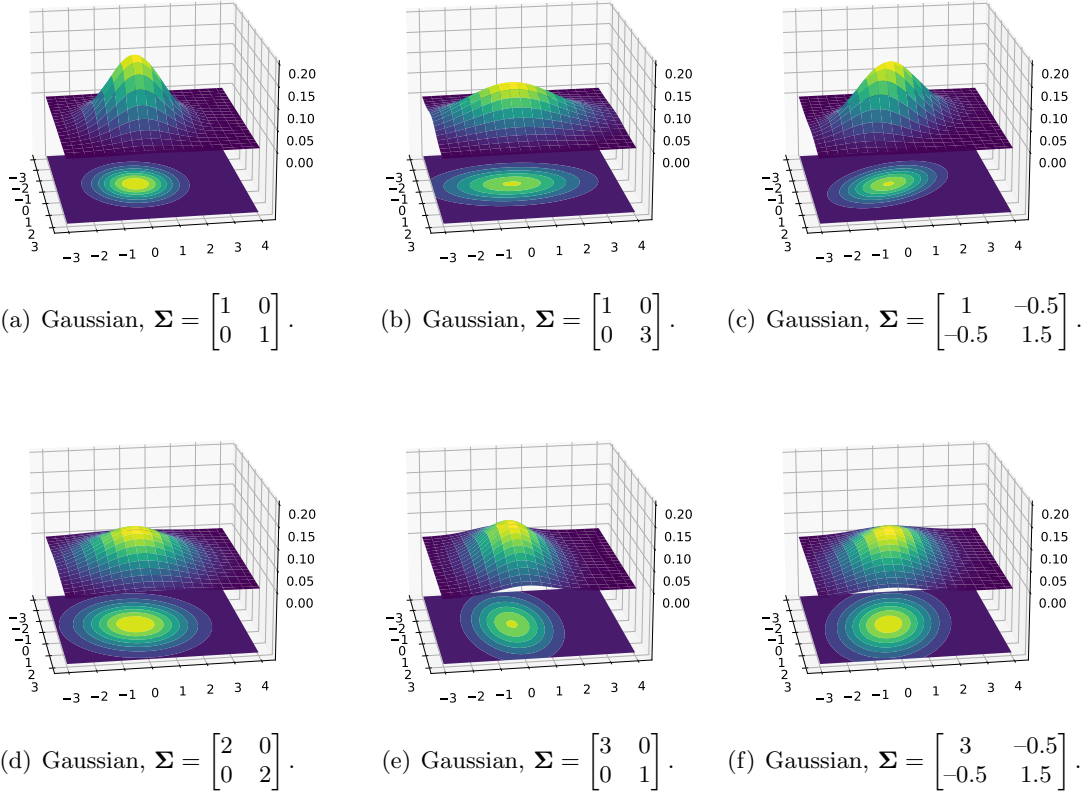


Figure 3.17: Density and contour plots (blue=low, yellow=high) for the multivariate Gaussian distribution over the \mathbb{R}^2 space for various values of the covariance/scale matrix with zero-mean vector. Fig 3.17(a) and 3.17(d): A spherical covariance matrix has a circular shape; Fig 3.17(b) and 3.17(e): A diagonal covariance matrix is an **axis aligned** ellipse; Fig 3.17(c) and 3.17(f): A full covariance matrix has an elliptical shape.

matrix Σ is given by

$$\begin{aligned}
 p(\mathcal{X} \mid \boldsymbol{\mu}, \Sigma) &= \prod_{n=1}^N \mathcal{N}(\mathbf{x}_n \mid \boldsymbol{\mu}, \Sigma) \\
 &\stackrel{(a)}{=} (2\pi)^{-ND/2} |\Sigma|^{-N/2} \exp \left\{ -\frac{1}{2} \sum_{n=1}^N (\mathbf{x}_n - \boldsymbol{\mu})^\top \Sigma^{-1} (\mathbf{x}_n - \boldsymbol{\mu}) \right\} \\
 &\stackrel{(b)}{=} (2\pi)^{-ND/2} |\Sigma|^{-N/2} \exp \left\{ -\frac{1}{2} \text{tr}(\Sigma^{-1} \mathbf{S}_\mu) \right\} \\
 &\stackrel{(c)}{=} (2\pi)^{-ND/2} |\Sigma|^{-N/2} \exp \left\{ -\frac{N}{2} (\boldsymbol{\mu} - \bar{\mathbf{x}})^\top \Sigma^{-1} (\boldsymbol{\mu} - \bar{\mathbf{x}}) \right\} \exp \left\{ -\frac{1}{2} \text{tr}(\Sigma^{-1} \mathbf{S}_{\bar{\mathbf{x}}}) \right\},
 \end{aligned} \tag{3.27}$$

where

$$\begin{aligned}\mathbf{S}_\mu &= \sum_{n=1}^N (\mathbf{x}_n - \boldsymbol{\mu})(\mathbf{x}_n - \boldsymbol{\mu})^\top, \\ \mathbf{S}_{\bar{\mathbf{x}}} &= \sum_{n=1}^N (\mathbf{x}_n - \bar{\mathbf{x}})(\mathbf{x}_n - \bar{\mathbf{x}})^\top, \\ \bar{\mathbf{x}} &= \frac{1}{N} \sum_{n=1}^N \mathbf{x}_n.\end{aligned}\tag{3.28}$$

The $\mathbf{S}_{\bar{\mathbf{x}}}$ is the *matrix of sum of squares* and is also known as the *scatter matrix*. The equivalence between equation (a) and equation (c) follows from the following identity (similar reasoning applies to the equivalence between equation (a) and equation (b)):

$$\sum_{n=1}^N (\mathbf{x}_n - \boldsymbol{\mu})^\top \boldsymbol{\Sigma}^{-1} (\mathbf{x}_n - \boldsymbol{\mu}) = \text{tr}(\boldsymbol{\Sigma}^{-1} \mathbf{S}_{\bar{\mathbf{x}}}) + N \cdot (\bar{\mathbf{x}} - \boldsymbol{\mu})^\top \boldsymbol{\Sigma}^{-1} (\bar{\mathbf{x}} - \boldsymbol{\mu}),\tag{3.29}$$

where the trace of a square matrix \mathbf{A} is defined to be the sum of the diagonal elements a_{ii} of \mathbf{A} :

$$\text{tr}(\mathbf{A}) = \sum_i a_{ii}.\tag{3.30}$$

The formulation in equation (b) is useful for the separated view of the conjugate prior for $\boldsymbol{\Sigma}$, and equation (c) is useful for the unified view of the joint conjugate prior for $\boldsymbol{\mu}, \boldsymbol{\Sigma}$ in the sequel.

Proof [Proof of Identity 3.29] There is a “trick” involving the trace that makes such calculations easy (see also Chapter 3 of Gentle (2007)):

$$\mathbf{x}^\top \mathbf{A} \mathbf{x} = \text{tr}(\mathbf{x}^\top \mathbf{A} \mathbf{x}) = \text{tr}(\mathbf{x} \mathbf{x}^\top \mathbf{A}) = \text{tr}(\mathbf{A} \mathbf{x} \mathbf{x}^\top),\tag{3.31}$$

where the first equality follows from the fact that $\mathbf{x}^\top \mathbf{A} \mathbf{x}$ is a scalar and the trace of a product is invariant under cyclical permutations of the factors⁴.

We can then rewrite $\sum_{n=1}^N (\mathbf{x}_n - \boldsymbol{\mu})^\top \boldsymbol{\Sigma}^{-1} (\mathbf{x}_n - \boldsymbol{\mu})$ as

$$\begin{aligned}& \sum_{n=1}^N (\mathbf{x}_n - \bar{\mathbf{x}})^\top \boldsymbol{\Sigma}^{-1} (\mathbf{x}_n - \bar{\mathbf{x}}) + \sum_{n=1}^N (\bar{\mathbf{x}} - \boldsymbol{\mu})^\top \boldsymbol{\Sigma}^{-1} (\bar{\mathbf{x}} - \boldsymbol{\mu}) \\ &= \text{tr}(\boldsymbol{\Sigma}^{-1} \mathbf{S}_{\bar{\mathbf{x}}}) + N \cdot (\bar{\mathbf{x}} - \boldsymbol{\mu})^\top \boldsymbol{\Sigma}^{-1} (\bar{\mathbf{x}} - \boldsymbol{\mu}).\end{aligned}\tag{3.32}$$

This concludes the proof. ■

Applying the equivalence established in Identity (3.29), we cannot reduce the complexity; however, this demonstration proves beneficial for establishing the conjugacy, as elucidated in Section 3.7.7 below.

4. Trace is invariant under cyclical permutations: $\text{tr}(\mathbf{ABC}) = \text{tr}(\mathbf{BCA}) = \text{tr}(\mathbf{CAB})$ if all \mathbf{ABC} , \mathbf{BCA} , and \mathbf{CAB} exist.

Similar to the univariate Gaussian likelihood in Equation (3.2), given fixed mean $\boldsymbol{\mu}$ and covariance $\boldsymbol{\Sigma}$ parameters, we have

$$p(\mathbf{x} \mid \boldsymbol{\mu}, \boldsymbol{\Sigma}) = \mathcal{N}(\mathbf{x} \mid \boldsymbol{\mu}, \boldsymbol{\Sigma}) \propto \exp \left\{ -\frac{1}{2} \mathbf{x}^\top \boldsymbol{\Sigma}^{-1} \mathbf{x} + \mathbf{x}^\top \boldsymbol{\Sigma}^{-1} \boldsymbol{\mu} \right\}. \quad (3.33)$$

Therefore, if we find the form of a random variable \mathbf{x} conforming to the above equation, we can assert that the random variable \mathbf{x} follows the Gaussian distribution $\mathbf{x} \sim \mathcal{N}(\boldsymbol{\mu}, \boldsymbol{\Sigma})$. See the example of a Bayesian *GGGM* matrix decomposition model in Equation (6.16) (p. 146).

3.7.2 Multivariate Student's t Distribution

The multivariate Student's t -distribution is a continuous probability distribution over multiple variables that generalizes the Gaussian distribution to allow for heavier tails, i.e., the probability of extreme values is higher than that in a Gaussian distribution. The multivariate Student's t distribution will be often used in the posterior predictive distribution of multivariate Gaussian parameters. We rigorously define the distribution as follows.

Definition 3.7.2 (Multivariate Student's t Distribution) *A random vector $\mathbf{x} \in \mathbb{R}^D$ is said to follow the multivariate Student's t distribution with parameters $\boldsymbol{\mu} \in \mathbb{R}^D$, $\boldsymbol{\Sigma} \in \mathbb{R}^{D \times D}$, and ν , denoted by $\mathbf{x} \sim \tau(\boldsymbol{\mu}, \boldsymbol{\Sigma}, \nu)$, if*

$$\begin{aligned} f(\mathbf{x}; \boldsymbol{\mu}, \boldsymbol{\Sigma}, \nu) &= \frac{\Gamma(\nu/2 + D/2)}{\Gamma(\nu/2)} \frac{|\boldsymbol{\Sigma}|^{-1/2}}{\nu^{D/2} \pi^{D/2}} \times \left[1 + \frac{1}{\nu} (\mathbf{x} - \boldsymbol{\mu})^\top \boldsymbol{\Sigma}^{-1} (\mathbf{x} - \boldsymbol{\mu}) \right]^{-\left(\frac{\nu+D}{2}\right)} \\ &= \frac{\Gamma(\nu/2 + D/2)}{\Gamma(\nu/2)} |\pi \mathbf{V}|^{-1/2} \times \left[1 + \frac{1}{\nu} (\mathbf{x} - \boldsymbol{\mu})^\top \mathbf{V}^{-1} (\mathbf{x} - \boldsymbol{\mu}) \right]^{-\left(\frac{\nu+D}{2}\right)}, \end{aligned}$$

where $\boldsymbol{\Sigma}$ is called the **scale matrix** and $\mathbf{V} = \nu \boldsymbol{\Sigma}$, and ν is the **degree of freedom**. This distribution has fatter tails than a Gaussian one. The smaller the ν is, the fatter the tails. As $\nu \rightarrow \infty$, the distribution converges towards a multivariate Gaussian. The mean, mode, and covariance of the multivariate Student's t distribution are given by

$$\begin{aligned} \mathbb{E}[\mathbf{x}] &= \boldsymbol{\mu}, \\ \text{Mode}[\mathbf{x}] &= \boldsymbol{\mu}, \\ \text{Cov}[\mathbf{x}] &= \frac{\nu}{\nu - 2} \boldsymbol{\Sigma}. \end{aligned}$$

Note that the $\boldsymbol{\Sigma}$ is called the scale matrix since it is not exactly the covariance matrix as that in a multivariate Gaussian distribution.

Specifically, When $D = 1$, it follows that (see Definition 3.2.2)

$$\tau(x \mid \mu, \sigma^2, \nu) = \frac{\Gamma(\frac{\nu+1}{2})}{\Gamma(\frac{\nu}{2})} \frac{1}{\sigma \sqrt{\nu \pi}} \times \left[1 + \frac{(x - \mu)^2}{\nu \sigma^2} \right]^{-\left(\frac{\nu+1}{2}\right)}. \quad (3.34)$$

When $D = 1$, $\boldsymbol{\mu} = 0$, $\boldsymbol{\Sigma} = 1$, then the *p.d.f.* defines the **univariate t distribution**.

$$\tau(x | \nu) = \frac{\Gamma(\frac{\nu+1}{2})}{\Gamma(\frac{\nu}{2})} \frac{1}{\sqrt{\nu\pi}} \times \left[1 + \frac{x^2}{\nu} \right]^{-\frac{(\nu+1)}{2}}.$$

Figure 3.18 compares the Gaussian and the Student's t distribution for various values such that when $\nu \rightarrow \infty$, the difference between the densities is approaching zero. Given the same parameters in the densities, the Student's t in general has longer “tails” than a Gaussian, which can be seen from the comparison between Figure 3.18(a) and Figure 3.18(d). This provides the Student's t distribution an important property known as **robustness**, which means that it is much less sensitive than the Gaussian in the presence of outliers (Bishop, 2006; Murphy, 2012).

A Student's t distribution can be written as a **Gaussian scale mixture**

$$\tau(\mathbf{x} | \boldsymbol{\mu}, \boldsymbol{\Sigma}, \nu) = \int_0^\infty \mathcal{N}(\mathbf{x} | \boldsymbol{\mu}, \boldsymbol{\Sigma}/z) \cdot \mathcal{G}(z | \frac{\nu}{2}, \frac{\nu}{2}) dz. \quad (3.35)$$

This can be thought of as an “infinite” mixture of Gaussians, each with a slightly different covariance matrix. In other words, a Student's t distribution is obtained by adding up an infinite number of Gaussian distributions having the same mean vector but different covariance matrices. From this Gaussian scale mixture view, when $\nu \rightarrow \infty$, the Gamma distribution becomes a degenerate random variable with all the nonzero mass at the point unity such that the multivariate Student's t distribution converges to a multivariate Gaussian distribution.

3.7.3 Prior on Parameters of Multivariate Gaussian Distribution

In Equation (3.7), we have shown that the inverse-Gamma distribution is a conjugate prior for the variance parameter of a Gaussian distribution. A generalization to this concept is the *inverse-Wishart* distribution, serving as a conjugate prior for the full covariance matrix of a multivariate Gaussian distribution. That is, the inverse-Wishart distribution is a probability distribution of random positive definite matrices that can be used to model random covariance matrices.

Before delving into the topic of the inverse-Wishart distribution, it's important to note that it originates from the Wishart distribution. As stated by Anderson (2003) in 1962, “The Wishart distribution ranks next to the (multivariate) normal distribution in order of importance and usefulness in multivariate statistics.”

Definition 3.7.3 (Wishart Distribution) A random symmetric positive definite matrix $\boldsymbol{\Lambda} \in \mathbb{R}^{D \times D}$ is said to follow the *Wishart distribution* with parameter $\mathbf{M} \in \mathbb{R}^{D \times D}$ and ν , denoted by $\boldsymbol{\Lambda} \sim \text{Wi}(\mathbf{M}, \nu)$, if

$$\begin{aligned} & f(\boldsymbol{\Lambda}; \mathbf{M}, \nu) \\ &= |\boldsymbol{\Lambda}|^{\frac{\nu-D-1}{2}} \exp \left\{ -\frac{1}{2} \text{tr}(\boldsymbol{\Lambda} \mathbf{M}^{-1}) \right\} \left[2^{\frac{\nu D}{2}} \pi^{D(D-1)/4} |\mathbf{M}|^{\nu/2} \prod_{d=1}^D \Gamma\left(\frac{\nu+1-d}{2}\right) \right]^{-1}, \end{aligned}$$

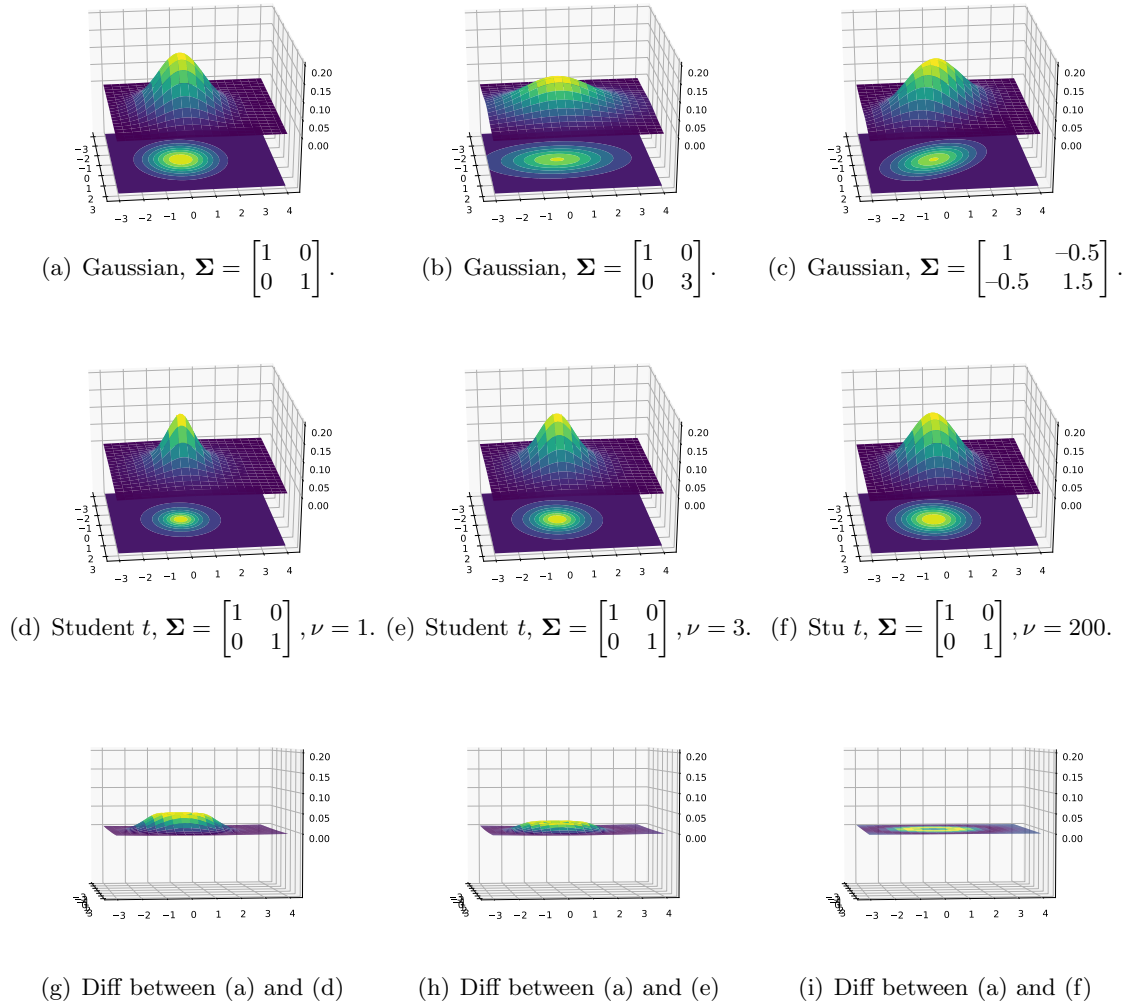


Figure 3.18: Density and contour plots (blue=low, yellow=high) for the multivariate Gaussian distribution and multivariate Student’s t distribution over the \mathbb{R}^2 space for various values of the covariance/scale matrix with zero-mean ν vector. Fig 3.18(a): A spherical covariance matrix has a circular shape; Fig 3.18(b): A diagonal covariance matrix is an **axis aligned** ellipse; Fig 3.18(c): A full covariance matrix has a elliptical shape; Fig 3.18(d) to Fig 3.18(f) for the Student’s t distribution with the same scale matrix and increasing ν such that the difference between (a) and (f) in Fig 3.18(i) is approaching zero.

where $\nu > D$ and \mathbf{M} is a $D \times D$ symmetric positive definite matrix, and $|\mathbf{\Lambda}| = \det(\mathbf{\Lambda})$ is the determinant of matrix $\mathbf{\Lambda}$. The ν is called the **number of degrees of freedom**, and \mathbf{M} is called the **scale matrix**. The mean and variance of the Wishart distribution

are given by

$$\begin{aligned} \mathbf{E}[\mathbf{\Lambda}] &= \nu \mathbf{M}, \\ \text{Var}[\mathbf{\Lambda}_{i,j}] &= \nu(m_{ij}^2 + m_{ii}m_{jj}), \end{aligned}$$

where m_{ij} is the (i, j) -th element of \mathbf{M} .

When $D = 1$ and $\mathbf{M} = 1$, the Wishart distribution reduces to the Chi-squared distribution (Definition 3.2.6) such that:

$$\text{Wi}(x \mid 1, \nu) = \chi^2(x \mid \nu).$$

An interpretation of the Wishart distribution is as follows. Suppose we independently sample vectors $\mathbf{z}_1, \mathbf{z}_2, \dots, \mathbf{z}_\nu \in \mathbb{R}^D$ from $\mathcal{N}(\mathbf{0}, \mathbf{M})$. The sum of squares matrix of the collection of multivariate vectors is given by

$$\sum_{i=1}^{\nu} \mathbf{z}_i \mathbf{z}_i^\top = \mathbf{Z}^\top \mathbf{Z},$$

where \mathbf{Z} is the $\nu \times D$ matrix with i -th row being \mathbf{z}_i^\top . It is evident that $\mathbf{Z}^\top \mathbf{Z}$ is positive semidefinite (PSD) and symmetric. If $\nu > D$ and the \mathbf{z}_i 's are linearly independent, then $\mathbf{Z}^\top \mathbf{Z}$ will be positive definite (PD) and symmetric. In other words, $\mathbf{Z}\mathbf{x} = \mathbf{0}$ only happens when $\mathbf{x} = \mathbf{0}$. We can repeat over and over again, generating matrices $\mathbf{Z}_1^\top \mathbf{Z}_1, \mathbf{Z}_2^\top \mathbf{Z}_2, \dots, \mathbf{Z}_l^\top \mathbf{Z}_l$. The population distribution of these matrices follows a Wishart distribution with parameters (\mathbf{M}, ν) . By definition,

$$\begin{aligned} \mathbf{\Lambda} &= \mathbf{Z}^\top \mathbf{Z} = \sum_{i=1}^{\nu} \mathbf{z}_i \mathbf{z}_i^\top; \\ \mathbf{E}[\mathbf{\Lambda}] &= \mathbf{E}[\mathbf{Z}^\top \mathbf{Z}] = \mathbf{E} \left[\sum_{i=1}^{\nu} \mathbf{z}_i \mathbf{z}_i^\top \right] = \nu \mathbf{E}[\mathbf{z}_i \mathbf{z}_i^\top] = \nu \mathbf{M}. \end{aligned}$$

When $D = 1$, this reduces to the case that if z is drawn from a zero-mean univariate normal random variable, then z^2 is drawn from a Gamma random variable. To be specific,

$$\text{suppose } z \sim \mathcal{N}(0, a), \quad \text{then } z^2 \sim \mathcal{G}(a/2, 1/2).$$

Just like the relationship between the inverse-Gamma distribution and the Gamma distribution that if $x \sim \mathcal{G}(r, \lambda)$, then $y = \frac{1}{x} \sim \mathcal{G}^{-1}(r, \lambda)$. There is a similar connection between the inverse-Wishart distribution and the Wishart distribution.

Since we often use the inverse-Wishart (IW) distribution as a prior distribution for a covariance matrix, it is often useful to replace \mathbf{M} in the Wishart distribution with $\mathbf{S} = \mathbf{M}^{-1}$. This results in that a random $D \times D$ symmetric positive definite matrix $\mathbf{\Sigma}$ follows an inverse-Wishart $\text{IW}(\mathbf{\Sigma} \mid \mathbf{S}, \nu)$ distribution if $\mathbf{\Sigma}^{-1} = \mathbf{\Lambda}$ follows a Wishart $\text{Wi}(\mathbf{\Lambda} \mid \mathbf{M}, \nu)$ distribution.

Definition 3.7.4 (Inverse-Wishart Distribution) A random symmetric positive definite matrix $\mathbf{\Sigma} \in \mathbb{R}^{D \times D}$ is said to follow the inverse-Wishart distribution with parameters

$\mathbf{S} \in \mathbb{R}^{D \times D}$ and ν , denoted by $\boldsymbol{\Sigma} \sim \text{IW}(\mathbf{S}, \nu)$, if

$$f(\boldsymbol{\Sigma}; \mathbf{S}, \nu) = |\boldsymbol{\Sigma}|^{-\frac{\nu+D+1}{2}} \exp\left\{-\frac{1}{2}\text{tr}(\boldsymbol{\Sigma}^{-1}\mathbf{S})\right\} \times \left[2^{\frac{\nu D}{2}} \pi^{D(D-1)/4} |\mathbf{S}|^{-\nu/2} \prod_{d=1}^D \Gamma\left(\frac{\nu+1-d}{2}\right)\right]^{-1},$$

where $\nu > D$ and \mathbf{S} is a $D \times D$ symmetric positive definite matrix, and $|\boldsymbol{\Sigma}| = \det(\boldsymbol{\Sigma})$. The ν is called the **number of degrees of freedom**, and \mathbf{S} is called the **scale matrix**. The mean and mode of the inverse-Wishart distribution are given by

$$\begin{aligned} \mathbb{E}[\boldsymbol{\Sigma}^{-1}] &= \nu \mathbf{S}^{-1} = \nu \mathbf{M}, \\ \mathbb{E}[\boldsymbol{\Sigma}] &= \frac{1}{\nu - D - 1} \mathbf{S}, \\ \text{Mode}[\boldsymbol{\Sigma}] &= \frac{1}{\nu + D + 1} \mathbf{S}. \end{aligned} \tag{3.36}$$

Note that, sometimes, we replace \mathbf{S} by $\mathbf{M} = \mathbf{S}^{-1}$ such that $\mathbb{E}[\boldsymbol{\Sigma}^{-1}] = \nu \mathbf{M}$, which does not involve the inverse of the matrix.

When $D = 1$, the inverse-Wishart distribution reduces to the inverse-Gamma such that $\frac{\nu}{2} = r$ and $\frac{\mathbf{S}}{2} = \lambda$ (see Definition 3.2.4):

$$\text{IW}(y | S, \nu) = \mathcal{G}^{-1}(y | r, \lambda).$$

Note that the Wishart density is not simply the inverse-Wishart density with $\boldsymbol{\Sigma}$ replaced by $\boldsymbol{\Lambda} = \boldsymbol{\Sigma}^{-1}$. There is an additional factor of $|\boldsymbol{\Sigma}|^{-(D+1)}$. See Theorem 7.7.1 in Anderson (2003) that the Jacobian of the transformation $\boldsymbol{\Lambda} = \boldsymbol{\Sigma}^{-1}$ is $|\boldsymbol{\Sigma}|^{-(D+1)}$. Substitution of $\boldsymbol{\Sigma}^{-1}$ in the definition of the Wishart distribution and multiplying by $|\boldsymbol{\Sigma}|^{-(D+1)}$ can yield the inverse-Wishart distribution. ⁵

The multivariate analog of the normal-inverse-Chi-squared distribution (Definition 3.2.8) is the *normal-inverse-Wishart (NIW) distribution* (Murphy, 2007). We will see that a sample drawn from a normal-inverse-Wishart distribution, a joint conjugate prior, provides a mean vector and a covariance matrix that can define a multivariate Gaussian distribution. Separately, we can first sample a matrix $\boldsymbol{\Sigma}$ from an inverse-Wishart distribution parameterized by $\{\mathbf{S}_0, \nu_0, \boldsymbol{\mu}\}$ (this is called a *semi-conjugate prior*), and then sample a mean vector from a Gaussian distribution parameterized by $\{\mathbf{m}_0, \mathbf{V}_0, \boldsymbol{\Sigma}\}$. ⁶

Definition 3.7.5 (Normal-Inverse-Wishart (NIW) Distribution) *Analog to the (univariate) normal-inverse-Chi-squared distribution, the multivariate counterpart, the normal-*

5. Which is from the Jacobian in the change-of-variables formula. A short proof is provided here. Let $\boldsymbol{\Lambda} = g(\boldsymbol{\Sigma}) = \boldsymbol{\Sigma}^{-1}$, where $\boldsymbol{\Sigma} \sim \text{IW}(\mathbf{S}, \nu)$ and $\boldsymbol{\Lambda} \sim \text{Wi}(\mathbf{S}, \nu)$. Then, $f(\boldsymbol{\Sigma}) = f(\boldsymbol{\Lambda})|J_g|$, where J_g is the Jacobian matrix, results in $f(\boldsymbol{\Sigma}) = f(\boldsymbol{\Lambda})|J_g| = f(\boldsymbol{\Lambda})|\boldsymbol{\Sigma}|^{-(D+1)}$.

6. Here we use a subscript value of 0 to indicate the parameters are used for prior density. However, in the Bayesian matrix decomposition analysis, things become more complex and the prior parameters could have other subscript values.

inverse-Wishart (NIW) distribution is defined as

$$\begin{aligned}
 \mathcal{N}\mathcal{I}\mathcal{W}(\boldsymbol{\mu}, \boldsymbol{\Sigma} \mid \mathbf{m}, \kappa, \nu, \mathbf{S}) &= \mathcal{N}(\boldsymbol{\mu} \mid \mathbf{m}, \frac{1}{\kappa}\boldsymbol{\Sigma}) \cdot \text{IW}(\boldsymbol{\Sigma} \mid \mathbf{S}, \nu) \\
 &= \frac{1}{Z_{\mathcal{N}\mathcal{I}\mathcal{W}}(D, \kappa, \nu, \mathbf{S})} |\boldsymbol{\Sigma}|^{-1/2} \exp \left\{ \frac{\kappa}{2} (\boldsymbol{\mu} - \mathbf{m})^\top \boldsymbol{\Sigma}^{-1} (\boldsymbol{\mu} - \mathbf{m}) \right\} \\
 &\quad \times |\boldsymbol{\Sigma}|^{-\frac{\nu+D+1}{2}} \exp \left\{ -\frac{1}{2} \text{tr}(\boldsymbol{\Sigma}^{-1} \mathbf{S}) \right\} \\
 &= \frac{1}{Z_{\mathcal{N}\mathcal{I}\mathcal{W}}(D, \kappa, \nu, \mathbf{S})} |\boldsymbol{\Sigma}|^{-\frac{\nu+D+2}{2}} \\
 &\quad \times \exp \left\{ -\frac{\kappa}{2} (\boldsymbol{\mu} - \mathbf{m})^\top \boldsymbol{\Sigma}^{-1} (\boldsymbol{\mu} - \mathbf{m}) - \frac{1}{2} \text{tr}(\boldsymbol{\Sigma}^{-1} \mathbf{S}) \right\},
 \end{aligned} \tag{3.37}$$

where the random vector $\boldsymbol{\mu} \in \mathbb{R}^D$ and the random positive definite matrix $\boldsymbol{\Sigma} \in \mathbb{R}^{D \times D}$ are said to follow NIW, denoted by $\boldsymbol{\mu}, \boldsymbol{\Sigma} \sim \mathcal{N}\mathcal{I}\mathcal{W}(\mathbf{m}, \kappa, \nu, \mathbf{S})$. And $Z_{\mathcal{N}\mathcal{I}\mathcal{W}}(D, \kappa, \nu, \mathbf{S})$ is a normalizing constant:

$$Z_{\mathcal{N}\mathcal{I}\mathcal{W}}(D, \kappa, \nu, \mathbf{S}) = 2^{\frac{(\nu+1)D}{2}} \pi^{D(D+1)/4} \kappa^{-D/2} |\mathbf{S}|^{-\nu/2} \prod_{d=1}^D \Gamma\left(\frac{\nu+1-d}{2}\right). \tag{3.38}$$

We then proceed to discuss the posterior density of the Gaussian model under the NIW or IW prior from two perspectives: a separated view and a unified view.

3.7.4 Posterior Distribution of $\boldsymbol{\mu}$: Separated View

Consider again N random observations $\mathcal{X} = \{\mathbf{x}_1, \mathbf{x}_2, \dots, \mathbf{x}_N\}$ generated by a multivariate Gaussian with mean vector $\boldsymbol{\mu}$ and covariance matrix $\boldsymbol{\Sigma}$. Suppose the covariance matrix $\boldsymbol{\Sigma}$ of a multivariate Gaussian distribution is known in Equation (3.27), the likelihood function is (equality (a) in Equation (3.27))

$$\begin{aligned}
 \text{likelihood} &= p(\mathcal{X} \mid \boldsymbol{\mu}) = \mathcal{N}(\mathcal{X} \mid \boldsymbol{\mu}, \boldsymbol{\Sigma}) = \prod_{n=1}^N \mathcal{N}(\mathbf{x}_n \mid \boldsymbol{\mu}, \boldsymbol{\Sigma}) \\
 &= (2\pi)^{-ND/2} |\boldsymbol{\Sigma}|^{-N/2} \exp \left\{ -\frac{1}{2} \sum_{n=1}^N (\mathbf{x}_n - \boldsymbol{\mu})^\top \boldsymbol{\Sigma}^{-1} (\mathbf{x}_n - \boldsymbol{\mu}) \right\} \\
 &\propto \exp \left(-\frac{1}{2} N \boldsymbol{\mu}^\top \boldsymbol{\Sigma}^{-1} \boldsymbol{\mu} + N \bar{\mathbf{x}}^\top \boldsymbol{\Sigma}^{-1} \boldsymbol{\mu} \right),
 \end{aligned}$$

where $\bar{\mathbf{x}} = \frac{1}{N} \sum_{n=1}^N \mathbf{x}_n$. The conjugate prior for the mean vector is also a Gaussian $p(\boldsymbol{\mu}) = \mathcal{N}(\boldsymbol{\mu} \mid \mathbf{m}_0, \mathbf{V}_0)$:

$$\begin{aligned} \text{prior} &= p(\boldsymbol{\mu}) = \mathcal{N}(\boldsymbol{\mu} \mid \mathbf{m}_0, \mathbf{V}_0) \\ &= (2\pi)^{-D/2} |\mathbf{V}_0|^{-1/2} \exp \left\{ -\frac{1}{2} (\boldsymbol{\mu} - \mathbf{m}_0)^\top \mathbf{V}_0^{-1} (\boldsymbol{\mu} - \mathbf{m}_0) \right\} \\ &= (2\pi)^{-D/2} |\mathbf{V}_0|^{-1/2} \exp \left(-\frac{1}{2} \boldsymbol{\mu}^\top \mathbf{V}_0^{-1} \boldsymbol{\mu} + \boldsymbol{\mu}^\top \mathbf{V}_0^{-1} \mathbf{m}_0 - \frac{1}{2} \mathbf{m}_0^\top \mathbf{V}_0^{-1} \mathbf{m}_0 \right) \\ &\propto \exp \left(-\frac{1}{2} \boldsymbol{\mu}^\top \mathbf{V}_0^{-1} \boldsymbol{\mu} + \boldsymbol{\mu}^\top \mathbf{V}_0^{-1} \mathbf{m}_0 \right). \end{aligned}$$

Using Bayes' theorem "posterior \propto likelihood \times prior," we can obtain a Gaussian posterior for $\boldsymbol{\mu}$:

$$\begin{aligned} \text{posterior} &= p(\boldsymbol{\mu} \mid \mathcal{X}, \boldsymbol{\Sigma}) \propto p(\mathcal{X} \mid \boldsymbol{\mu}, \boldsymbol{\Sigma}) \times p(\boldsymbol{\mu}) \\ &= \exp \left(N \bar{\mathbf{x}}^\top \boldsymbol{\Sigma}^{-1} \boldsymbol{\mu} - \frac{1}{2} N \boldsymbol{\mu}^\top \boldsymbol{\Sigma}^{-1} \boldsymbol{\mu} \right) \times \exp \left(-\frac{1}{2} \boldsymbol{\mu}^\top \mathbf{V}_0^{-1} \boldsymbol{\mu} + \boldsymbol{\mu}^\top \mathbf{V}_0^{-1} \mathbf{m}_0 \right) \\ &= \exp \left\{ -\frac{1}{2} \boldsymbol{\mu}^\top (\mathbf{V}_0^{-1} + N \boldsymbol{\Sigma}^{-1}) \boldsymbol{\mu} + \boldsymbol{\mu}^\top (\mathbf{V}_0^{-1} \mathbf{m}_0 + N \boldsymbol{\Sigma}^{-1} \bar{\mathbf{x}}) \right\} \\ &\propto \mathcal{N}(\boldsymbol{\mu} \mid \mathbf{m}_N, \mathbf{V}_N), \end{aligned}$$

where $\mathbf{V}_N^{-1} = \mathbf{V}_0^{-1} + N \boldsymbol{\Sigma}^{-1}$, and $\mathbf{m}_N = \mathbf{V}_N (\mathbf{V}_0^{-1} \mathbf{m}_0 + N \boldsymbol{\Sigma}^{-1} \bar{\mathbf{x}})$. In this case, **the posterior precision matrix is the sum of the prior precision matrix \mathbf{V}_0^{-1} and data precision matrix $N \boldsymbol{\Sigma}^{-1}$** . By letting $\mathbf{V}_0 \rightarrow \infty \mathbf{I}$, we can model *an uninformative prior* such that the posterior distribution of the mean is $p(\boldsymbol{\mu} \mid \mathcal{X}, \boldsymbol{\Sigma}) = \mathcal{N}(\boldsymbol{\mu} \mid \bar{\mathbf{x}}, \frac{1}{N} \boldsymbol{\Sigma})$.

3.7.5 Posterior Distribution of $\boldsymbol{\Sigma}$: Separated View

Suppose now the mean vector $\boldsymbol{\mu}$ of a multivariate Gaussian distribution is known in Equation (3.27), the likelihood is (equality (b) in Equation (3.27))

$$\text{likelihood} = p(\mathcal{X} \mid \boldsymbol{\mu}, \boldsymbol{\Sigma}) = \prod_{n=1}^N \mathcal{N}(\mathbf{x}_n \mid \boldsymbol{\mu}, \boldsymbol{\Sigma}) = (2\pi)^{-ND/2} |\boldsymbol{\Sigma}|^{-N/2} \exp \left\{ -\frac{1}{2} \text{tr}(\boldsymbol{\Sigma}^{-1} \mathbf{S}_\mu) \right\}.$$

The corresponding conjugate prior is the inverse-Wishart distribution:

$$\begin{aligned} \text{prior} &= \text{IW}(\boldsymbol{\Sigma} \mid \mathbf{S}_0, \nu_0) = |\boldsymbol{\Sigma}|^{-\frac{\nu_0 + D + 1}{2}} \exp \left\{ -\frac{1}{2} \text{tr}(\boldsymbol{\Sigma}^{-1} \mathbf{S}_0) \right\} \\ &\quad \times \left[2^{\frac{\nu_0 D}{2}} \pi^{D(D-1)/4} |\mathbf{S}_0|^{-\nu_0/2} \prod_{d=1}^D \Gamma\left(\frac{\nu_0 + 1 - d}{2}\right) \right]^{-1}. \end{aligned}$$

Again by Bayes' theorem, "posterior \propto likelihood \times prior," we obtain an inverse-Wishart posterior for Σ :

$$\begin{aligned}
 \text{posterior} &= p(\Sigma \mid \mathcal{X}, \boldsymbol{\mu}) \propto p(\mathcal{X} \mid \boldsymbol{\mu}, \Sigma) \times p(\Sigma) \\
 &\propto |\Sigma|^{-N/2} \exp\left\{-\frac{1}{2}\text{tr}(\Sigma^{-1}\mathbf{S}_\mu)\right\} \times |\Sigma|^{-\frac{\nu_0+D+1}{2}} \exp\left\{-\frac{1}{2}\text{tr}(\Sigma^{-1}\mathbf{S}_0)\right\} \\
 &= |\Sigma|^{-\frac{\nu_0+N+D+1}{2}} \exp\left\{-\frac{1}{2}\text{tr}(\Sigma^{-1}[\mathbf{S}_0 + \mathbf{S}_\mu])\right\} \\
 &\propto \text{IW}(\Sigma \mid \mathbf{S}_0 + \mathbf{S}_\mu, \nu_0 + N).
 \end{aligned}$$

The posterior degree of freedom is the sum of the prior degree of freedom ν_0 and the number of observations N . And the posterior scale matrix is the sum of the prior scale matrix \mathbf{S}_0 and the data scale matrix \mathbf{S}_μ . The mean of the posterior Σ is given by

$$\begin{aligned}
 \text{E}[\Sigma \mid \mathcal{X}, \boldsymbol{\mu}] &= \frac{1}{\nu_0 + N - D - 1} (\mathbf{S}_0 + \mathbf{S}_\mu) \\
 &= \frac{\nu_0 - D - 1}{\nu_0 + N - D - 1} \cdot \left(\frac{1}{\nu_0 - D - 1} \mathbf{S}_0\right) + \frac{N}{\nu_0 + N - D - 1} \cdot \left(\frac{1}{N} \mathbf{S}_\mu\right) \\
 &= \lambda \cdot \left(\frac{1}{\nu_0 - D - 1} \mathbf{S}_0\right) + (1 - \lambda) \cdot \left(\frac{1}{N} \mathbf{S}_\mu\right),
 \end{aligned}$$

where $\lambda = \frac{\nu_0 - D - 1}{\nu_0 + N - D - 1}$, $\left(\frac{1}{\nu_0 - D - 1} \mathbf{S}_0\right)$ is the prior mean of Σ , and $\left(\frac{1}{N} \mathbf{S}_\mu\right)$ is an unbiased estimator of the covariance such that $\left(\frac{1}{N} \mathbf{S}_\mu\right)$ converges to the true population covariance matrix when $N \rightarrow \infty$. Thus, **the posterior mean of the covariance matrix can be seen as the weighted average of the prior expectation and the unbiased estimator**. The unbiased estimator can be also shown to be equal to the maximum likelihood estimator (MLE) of Σ . As $N \rightarrow \infty$, it can be shown that the posterior expectation of Σ is a consistent ⁷ estimator of the population covariance. When we set $\nu_0 = D + 1$, $\lambda = 0$ and we recover the MLE.

Similarly, the mode of the posterior Σ is given by

$$\begin{aligned}
 \text{Mode}[\Sigma] &= \frac{1}{\nu_0 + N + D + 1} (\mathbf{S}_0 + \mathbf{S}_\mu) \\
 &= \frac{\nu_0 + D + 1}{\nu_0 + N + D + 1} \left(\frac{1}{\nu_0 + D + 1} \mathbf{S}_0\right) + \frac{N}{\nu_0 + N + D + 1} \left(\frac{1}{N} \mathbf{S}_\mu\right) \quad (3.39) \\
 &= \beta \left(\frac{1}{\nu_0 + D + 1} \mathbf{S}_0\right) + (1 - \beta) \left(\frac{1}{N} \mathbf{S}_\mu\right),
 \end{aligned}$$

where $\beta = \frac{\nu_0 + D + 1}{\nu_0 + N + D + 1}$, and $\left(\frac{1}{\nu_0 + D + 1} \mathbf{S}_0\right)$ is the prior mode of Σ . **The posterior mode is a weighted average of the prior mode and the unbiased estimator**. Again, the maximum a posterior (MAP) estimator in Equation (3.39) is a consistent estimator.

⁷. An estimator $\hat{\theta}_N$ of θ constructed on the basis of a sample of size N is said to be consistent if $\hat{\theta}_N \xrightarrow{p} \theta$ as $N \rightarrow \infty$. See also Lu (2022a).

3.7.6 Gibbs Sampling of the Mean and Covariance: Separated View

The separated view presented here is known as a **semi-conjugate prior** on the mean and covariance of a multivariate Gaussian distribution since both conditionals, $p(\boldsymbol{\mu} \mid \mathcal{X}, \boldsymbol{\Sigma})$ and $p(\boldsymbol{\Sigma} \mid \mathcal{X}, \boldsymbol{\mu})$, are individually conjugate. In the last two sections, we have shown

$$\begin{aligned}\boldsymbol{\mu} \mid \mathcal{X}, \boldsymbol{\Sigma} &\sim \mathcal{N}(\mathbf{m}_N, \mathbf{V}_N), \\ \boldsymbol{\Sigma} \mid \mathcal{X}, \boldsymbol{\mu} &\sim \text{IW}(\mathbf{S}_0 + \mathbf{S}_\mu, \nu_0 + N).\end{aligned}$$

The two full conditional distributions can be used to construct a Gibbs sampler. The Gibbs sampler generates the mean and covariance $\{\boldsymbol{\mu}^{t+1}, \boldsymbol{\Sigma}^{t+1}\}$ for $(t+1)$ -th step from $\{\boldsymbol{\mu}^t, \boldsymbol{\Sigma}^t\}$ in t -th step via the following two steps:

1. Sample $\boldsymbol{\mu}^{t+1}$ from its full conditional distribution: $\boldsymbol{\mu}^{t+1} \sim \mathcal{N}(\mathbf{m}_N, \mathbf{V}_N)$, where $\{\mathbf{m}_N, \mathbf{V}_N\}$ depend on $\boldsymbol{\Sigma}^t$.
2. Sample $\boldsymbol{\Sigma}^{t+1}$ from its full conditional distribution: $\boldsymbol{\Sigma}^{t+1} \sim \text{IW}(\mathbf{S}_0 + \mathbf{S}_\mu, \nu_0 + N)$, where $\{\mathbf{S}_0 + \mathbf{S}_\mu, \nu_0 + N\}$ depend on $\boldsymbol{\mu}^{t+1}$.

3.7.7 Posterior Distribution of $\boldsymbol{\mu}$ and $\boldsymbol{\Sigma}$ Under NIW: Unified View

The NIW, on the other hand, serves as a fully (joint) conjugate prior for the mean vector and covariance matrix of a multivariate Gaussian model.

Likelihood. The likelihood of N random observations $\mathcal{X} = \{\mathbf{x}_1, \mathbf{x}_2, \dots, \mathbf{x}_N\}$ generated by a multivariate Gaussian with mean vector $\boldsymbol{\mu}$ and covariance matrix $\boldsymbol{\Sigma}$ is (equality (c) in Equation (3.27))

$$p(\mathcal{X} \mid \boldsymbol{\mu}, \boldsymbol{\Sigma}) = \frac{1}{(2\pi)^{ND/2}} |\boldsymbol{\Sigma}|^{-N/2} \exp \left\{ -\frac{N}{2} (\boldsymbol{\mu} - \bar{\mathbf{x}})^\top \boldsymbol{\Sigma}^{-1} (\boldsymbol{\mu} - \bar{\mathbf{x}}) - \frac{1}{2} \text{tr}(\boldsymbol{\Sigma}^{-1} \mathbf{S}_{\bar{\mathbf{x}}}) \right\}.$$

Prior. A trivial prior is to combine the conjugate priors for $\boldsymbol{\mu}$ and $\boldsymbol{\Sigma}$ respectively in the above sections:

$$p(\boldsymbol{\mu}, \boldsymbol{\Sigma}) = \mathcal{N}(\boldsymbol{\mu} \mid \mathbf{m}_0, \mathbf{V}_0) \cdot \text{IW}(\boldsymbol{\Sigma} \mid \mathbf{S}_0, \nu_0).$$

However, this is not a conjugate prior of the likelihood with parameters $\{\boldsymbol{\mu}, \boldsymbol{\Sigma}\}$ since $\boldsymbol{\mu}$ and $\boldsymbol{\Sigma}$ appear together in a non-factorized way in the likelihood. For the full parameters of a multivariate Gaussian distribution (i.e., mean vector $\boldsymbol{\mu}$ and covariance matrix $\boldsymbol{\Sigma}$), the normal-inverse-Wishart (NIW) prior is fully conjugate:

$$\begin{aligned}\mathcal{NIW}(\boldsymbol{\mu}, \boldsymbol{\Sigma} \mid \mathbf{m}_0, \kappa_0, \nu_0, \mathbf{S}_0) &= \mathcal{N}(\boldsymbol{\mu} \mid \mathbf{m}_0, \frac{1}{\kappa_0} \boldsymbol{\Sigma}) \cdot \text{IW}(\boldsymbol{\Sigma} \mid \mathbf{S}_0, \nu_0) \\ &= \frac{|\boldsymbol{\Sigma}|^{-\frac{\nu_0 + D + 2}{2}}}{Z_{\mathcal{NIW}}(D, \kappa_0, \nu_0, \mathbf{S}_0)} \cdot \exp \left\{ -\frac{\kappa_0}{2} (\boldsymbol{\mu} - \mathbf{m}_0)^\top \boldsymbol{\Sigma}^{-1} (\boldsymbol{\mu} - \mathbf{m}_0) - \frac{1}{2} \text{tr}(\boldsymbol{\Sigma}^{-1} \mathbf{S}_0) \right\},\end{aligned}\tag{3.40}$$

where

$$Z_{\mathcal{NIW}}(D, \kappa_0, \nu_0, \mathbf{S}_0) = 2^{\frac{(\nu_0 + 1)D}{2}} \pi^{D(D+1)/4} \kappa_0^{-D/2} |\mathbf{S}_0|^{-\nu_0/2} \prod_{d=1}^D \Gamma\left(\frac{\nu_0 + 1 - d}{2}\right).\tag{3.41}$$

The specific form of the normalization term $Z_{\mathcal{NIW}}(D, \kappa_0, \nu_0, \mathbf{S}_0)$ will be useful to show the posterior marginal likelihood of the data in Section 3.7.9.

A “prior” interpretation for the NIW prior. The inverse-Wishart distribution will ensure that the resulting covariance matrix is positive definite when $\nu_0 > D$. And if we are confident that the true covariance matrix is near some covariance matrix Σ_0 , then we might choose a large value of ν_0 and set $\mathbf{S}_0 = (\nu_0 - D - 1)\Sigma_0$, making the distribution of the covariance matrix Σ concentrated around Σ_0 . On the other hand, choosing $\nu_0 = D + 2$ and $\mathbf{S}_0 = \Sigma_0$ will make Σ loosely concentrated around Σ_0 . More details can be referred to Chipman et al. (2001); Fraley and Raftery (2007); Hoff (2009); Murphy (2012).

An intuitive interpretation of the hyper-parameters is as follows (Murphy, 2012; Hoff, 2009): \mathbf{m}_0 is our prior mean for $\boldsymbol{\mu}$, κ_0 is how strongly we believe this prior for $\boldsymbol{\mu}$ (the larger the stronger we believe this prior mean), \mathbf{S}_0 is proportional to our prior mean for Σ , and ν_0 controls how strongly we believe this prior for Σ . Because the Gamma function is not defined for negative integers and zero, from Equation (3.41) we require $\nu_0 > D - 1$ (which can also be shown from the expectation of the covariance matrix Equation (3.36)). And also, \mathbf{S}_0 needs to be a positive definite matrix, where an intuitive reason can be shown from Equation (3.36). A more detailed reason can be found in Hoff (2009).

Posterior. By Bayes’ theorem, “posterior \propto likelihood \times prior,” the posterior of the $\boldsymbol{\mu}$ and Σ parameters under the NIW prior is

$$p(\boldsymbol{\mu}, \Sigma \mid \mathcal{X}, \boldsymbol{\beta}) \propto p(\mathcal{X} \mid \boldsymbol{\mu}, \Sigma)p(\boldsymbol{\mu}, \Sigma \mid \boldsymbol{\beta}) = p(\mathcal{X}, \boldsymbol{\mu}, \Sigma \mid \boldsymbol{\beta}), \quad (3.42)$$

where $\boldsymbol{\beta} = \{\mathbf{m}_0, \kappa_0, \nu_0, \mathbf{S}_0\}$ are the hyper-parameters, the right-hand side of Equation (3.42) is also known as the fully joint distribution $p(\mathcal{X}, \boldsymbol{\mu}, \Sigma \mid \boldsymbol{\beta})$, and it is given by

$$\begin{aligned} p(\mathcal{X}, \boldsymbol{\mu}, \Sigma \mid \boldsymbol{\beta}) &= p(\mathcal{X} \mid \boldsymbol{\mu}, \Sigma) \cdot p(\boldsymbol{\mu}, \Sigma \mid \boldsymbol{\beta}) \\ &= C \times |\Sigma|^{-\frac{\nu_0 + N + D + 2}{2}} \times \\ &\quad \exp \left\{ -\frac{N}{2}(\boldsymbol{\mu} - \bar{\mathbf{x}})^\top \Sigma^{-1}(\boldsymbol{\mu} - \bar{\mathbf{x}}) - \frac{\kappa_0}{2}(\boldsymbol{\mu} - \mathbf{m}_0)^\top \Sigma^{-1}(\boldsymbol{\mu} - \mathbf{m}_0) \right. \\ &\quad \left. - \frac{1}{2}\text{tr}(\Sigma^{-1}\mathbf{S}_{\bar{\mathbf{x}}}) - \frac{1}{2}\text{tr}(\Sigma^{-1}\mathbf{S}_0) \right\}, \end{aligned} \quad (3.43)$$

where $C = \frac{(2\pi)^{-ND/2}}{\mathbb{Z}_{NIW}(D, \kappa_0, \nu_0, \mathbf{S}_0)}$ is a constant normalization term. This can be reduced to

$$\begin{aligned} p(\mathcal{X}, \boldsymbol{\mu}, \Sigma \mid \boldsymbol{\beta}) &= C |\Sigma|^{-\frac{\nu_0 + N + D + 2}{2}} \times \\ &\quad \exp \left\{ -\frac{\kappa_0 + N}{2} \left(\boldsymbol{\mu} - \frac{\kappa_0 \mathbf{m}_0 + N \bar{\mathbf{x}}}{\kappa_N} \right)^\top \Sigma^{-1} \left(\boldsymbol{\mu} - \frac{\kappa_0 \mathbf{m}_0 + N \bar{\mathbf{x}}}{\kappa_N} \right) \right. \\ &\quad \left. - \frac{1}{2} \text{tr} \left[\Sigma^{-1} \left(\mathbf{S}_0 + \mathbf{S}_{\bar{\mathbf{x}}} + \frac{\kappa_0 N}{\kappa_0 + N} (\bar{\mathbf{x}} - \mathbf{m}_0)(\bar{\mathbf{x}} - \mathbf{m}_0)^\top \right) \right] \right\}, \end{aligned} \quad (3.44)$$

which is reformulated to compare with the NIW form in Equation (3.40), and we can see the reason why we rewrite the multivariate Gaussian distribution into Equation (3.29) by

the trace trick. It follows that the posterior is also a NIW density with updated parameters and gives the view of conjugacy for a multivariate Gaussian distribution:

$$p(\boldsymbol{\mu}, \boldsymbol{\Sigma} \mid \mathcal{X}, \boldsymbol{\beta}) = \mathcal{NIW}(\boldsymbol{\mu}, \boldsymbol{\Sigma} \mid \mathbf{m}_N, \kappa_N, \nu_N, \mathbf{S}_N), \quad (3.45)$$

where

$$\mathbf{m}_N = \frac{\kappa_0 \mathbf{m}_0 + N \bar{\mathbf{x}}}{\kappa_N} = \frac{\kappa_0}{\kappa_N} \mathbf{m}_0 + \frac{N}{\kappa_N} \bar{\mathbf{x}}, \quad (3.46)$$

$$\kappa_N = \kappa_0 + N, \quad (3.47)$$

$$\nu_N = \nu_0 + N, \quad (3.48)$$

$$\mathbf{S}_N = \mathbf{S}_0 + \mathbf{S}_{\bar{\mathbf{x}}} + \frac{\kappa_0 N}{\kappa_0 + N} (\bar{\mathbf{x}} - \mathbf{m}_0)(\bar{\mathbf{x}} - \mathbf{m}_0)^\top \quad (3.49)$$

$$= \mathbf{S}_0 + \sum_{n=1}^N \mathbf{x}_n \mathbf{x}_n^\top + \kappa_0 \mathbf{m}_0 \mathbf{m}_0^\top - \kappa_N \mathbf{m}_N \mathbf{m}_N^\top. \quad (3.50)$$

A “posterior” interpretation for the NIW prior. An intuitive interpretation of the parameters in NIW can be obtained from the updated parameters above. The parameter ν_0 is the prior number of samples to observe the covariance matrix, and $\nu_N = \nu_0 + N$ is the posterior number of samples. The posterior mean \mathbf{m}_N of the model mean $\boldsymbol{\mu}$ is a weighted average of the prior mean and the sample mean. The posterior scale matrix \mathbf{S}_N is the sum of the prior scale matrix, empirical covariance matrix $\mathbf{S}_{\bar{\mathbf{x}}}$, and an extra term due to the uncertainty in the mean.

PARAMETER CHOICE

In practice, it is often preferable to use a weakly informative data-dependent prior. A common choice is to set $\mathbf{S}_0 = \text{diag}(\mathbf{S}_{\bar{\mathbf{x}}})/N$ and $\nu_0 = D+2$ to ensure $\text{E}[\boldsymbol{\Sigma}] = \mathbf{S}_0$. Additionally, set $\mathbf{m}_0 = \bar{\mathbf{x}}$ and κ_0 to a small value, such as 0.01, where $\mathbf{S}_{\bar{\mathbf{x}}}$ is the sample covariance matrix, and $\bar{\mathbf{x}}$ is the sample mean vector as shown in Equation (3.28) (Chipman et al., 2001; Fraley and Raftery, 2007; Hoff, 2009; Murphy, 2012). Equivalently, we can also standardize the observation matrix \mathcal{X} first to have zero-mean and unit variance for every feature, and then let $\mathbf{S}_0 = \mathbf{I}_D$ and $\nu_0 = D + 2$ to ensure $\text{E}[\boldsymbol{\Sigma}] = \mathbf{I}_D$, and to set $\mathbf{m}_0 = \mathbf{0}$ and κ_0 to a small number, such as 0.01.

REDUCING SAMPLING TIME BY MAINTAINING SQUARED SUM OF CUSTOMERS

In this section, we introduce some tricks to implement NIW more efficiently. The trick is largely used in the Gaussian mixture models (Das, 2014; Lu, 2021c). While in our Bayesian matrix factorization context, this trick proves beneficial when we use cross-validation (CV) to down-sample matrix elements in each iteration (Section 6.4, p. 150). The readers will understand the Chinese restaurant process terminology better in this section after reading Lu (2021c). Feel free to skip this section.

We have seen the equivalence between Equation (3.49) and Equation (3.50). The reason why we make a step further to Equation (3.50) from Equation (3.49) is to reduce sampling time. Suppose now that the data is not fixed and some data points can be removed from

or added to \mathcal{X} . If we stick to the form in Equation (3.49), we need to calculate $\mathbf{S}_{\bar{x}}$ and \bar{x} over and over again whenever the data points are updated.

In Chinese restaurant process/clustering terminology, if we use Equation (3.49) instead of Equation (3.50), whenever a customer is removed from (or added to) a table, we have to compute the matrix $\mathbf{S}_{\bar{x}}$, which requires to go over each point in this cluster (or each customer in this table following the term from the Chinese restaurant process). Computing this term every time when a customer is removed or added could be computationally expensive.

We realize that the data terms in Equation (3.50) only involve a sum of the outer product, which does not contain any cross product (e.g., $\mathbf{x}_i \mathbf{x}_j^\top$ for $i \neq j$). By reformulating into Equation (3.50), whenever a customer (e.g., a customer represented by \mathbf{x}_n) is removed or added, we just have to subtract or add $\mathbf{x}_n \mathbf{x}_n^\top$. Thus for each table, we only have to maintain the squared sum of customer vectors $\sum_{n=1}^N \mathbf{x}_n \mathbf{x}_n^\top$ for \mathbf{S}_N .

Similarly, for \mathbf{m}_N , we need to maintain the sum of customer vectors $\sum_{n=1}^N \mathbf{x}_n$ for the same reason as Equation (3.46).

3.7.8 Posterior Marginal Likelihood of Parameters

The posterior marginal for Σ is given by

$$\begin{aligned} p(\Sigma \mid \mathcal{X}, \beta) &= \int_{\mu} p(\mu, \Sigma \mid \mathcal{X}, \beta) d\mu \\ &= \text{IW}(\Sigma \mid \mathbf{S}_N, \nu_N), \end{aligned}$$

where the mean and mode can be obtained by Equation (3.36):

$$\begin{aligned} \text{E}[\Sigma \mid \mathcal{X}, \beta] &= \frac{\mathbf{S}_N}{\nu_N - D - 1}, \\ \text{Mode}[\Sigma \mid \mathcal{X}, \beta] &= \frac{\mathbf{S}_N}{\nu_N + D + 1}. \end{aligned}$$

The posterior marginal for μ follows from a multivariate Student's t distribution (Definition 3.7.2). We can show the posterior marginal for μ is given by

$$\begin{aligned} p(\mu \mid \mathcal{X}, \beta) &= \int_{\Sigma} p(\mu, \Sigma \mid \mathcal{X}, \beta) d\Sigma \\ &= \int_{\Sigma} \mathcal{N}\mathcal{T}\mathcal{W}(\mu, \Sigma \mid \mathbf{m}_N, \kappa_N, \nu_N, \mathbf{S}_N) d\Sigma \\ &= \tau(\mu \mid \mathbf{m}_N, \frac{1}{\kappa_N(\nu_N - D + 1)} \mathbf{S}_N, \nu_N - D + 1), \end{aligned}$$

which is from the Gaussian scale mixture property of the Student's t distribution, see Equation (3.35) and further discussion in Murphy (2012).

3.7.9 Posterior Marginal Likelihood of Data

By integrating the full joint distribution in Equation (3.44), we can get the marginal likelihood of data under hyper-parameter $\beta = \{\mathbf{m}_0, \kappa_0, \nu_0, \mathbf{S}_0\}$:

$$\begin{aligned}
 p(\mathcal{X} | \beta) &= \int_{\boldsymbol{\mu}} \int_{\boldsymbol{\Sigma}} p(\mathcal{X}, \boldsymbol{\mu}, \boldsymbol{\Sigma} | \beta) d\boldsymbol{\mu} d\boldsymbol{\Sigma} \\
 &= \int_{\boldsymbol{\mu}} \int_{\boldsymbol{\Sigma}} \mathcal{N}(\mathcal{X} | \boldsymbol{\mu}, \boldsymbol{\Sigma}) \cdot \mathcal{NIW}(\boldsymbol{\mu}, \boldsymbol{\Sigma} | \beta) d\boldsymbol{\mu} d\boldsymbol{\Sigma} \\
 &= \frac{(2\pi)^{-ND/2}}{Z_{\mathcal{NIW}}(D, \kappa_0, \nu_0, \mathbf{S}_0)} \int_{\boldsymbol{\mu}} \int_{\boldsymbol{\Sigma}} |\boldsymbol{\Sigma}|^{-\frac{\nu_0 + N + D + 2}{2}} \\
 &\quad \times \exp\left(-\frac{\kappa_N}{2}(\boldsymbol{\mu} - \mathbf{m}_N)\boldsymbol{\Sigma}^{-1}(\boldsymbol{\mu} - \mathbf{m}_N) - \frac{1}{2}\text{tr}(\boldsymbol{\Sigma}^{-1}\mathbf{S}_N)\right) d\boldsymbol{\mu} d\boldsymbol{\Sigma} \\
 &\stackrel{(*)}{=} (2\pi)^{-ND/2} \frac{Z_{\mathcal{NIW}}(D, \kappa_N, \nu_N, \mathbf{S}_N)}{Z_{\mathcal{NIW}}(D, \kappa_0, \nu_0, \mathbf{S}_0)} \\
 &= \pi^{-\frac{ND}{2}} \cdot \frac{\kappa_0^{D/2} \cdot |\mathbf{S}_0|^{\nu_0/2}}{\kappa_N^{D/2} \cdot |\mathbf{S}_N|^{\nu_N/2}} \prod_{d=1}^D \frac{\Gamma(\frac{\nu_N + 1 - d}{2})}{\Gamma(\frac{\nu_0 + 1 - d}{2})},
 \end{aligned} \tag{3.51}$$

where the identity (*) is from the fact that the integral reduces to the normalizing constant of the NIW density given in Equation (3.45).

3.7.10 Posterior Predictive for Data without Observations

Similarly, suppose now we observe a data vector \mathbf{x}^* without observing any old data. Then the predictive for the data vector can be obtained by

$$\begin{aligned}
 p(\mathbf{x}^* | \beta) &= \int_{\boldsymbol{\mu}} \int_{\boldsymbol{\Sigma}} p(\mathbf{x}^*, \boldsymbol{\mu}, \boldsymbol{\Sigma} | \beta) d\boldsymbol{\mu} d\boldsymbol{\Sigma} \\
 &= \int_{\boldsymbol{\mu}} \int_{\boldsymbol{\Sigma}} \mathcal{N}(\mathbf{x}^* | \boldsymbol{\mu}, \boldsymbol{\Sigma}) \cdot \mathcal{NIW}(\boldsymbol{\mu}, \boldsymbol{\Sigma} | \beta) d\boldsymbol{\mu} d\boldsymbol{\Sigma} \\
 &= \pi^{-D/2} \frac{\kappa_0^{D/2} |\mathbf{S}_0|^{\nu_0/2}}{(\kappa_0 + 1)^{D/2} |\mathbf{S}_1|^{\nu_1/2}} \prod_{d=1}^D \frac{\Gamma(\frac{\nu_1 + 1 - d}{2})}{\Gamma(\frac{\nu_0 + 1 - d}{2})} \\
 &= \pi^{-D/2} \frac{\kappa_0^{D/2} |\mathbf{S}_0|^{\nu_0/2}}{(\kappa_0 + 1)^{D/2} |\mathbf{S}_1|^{\nu_1/2}} \frac{\Gamma(\frac{\nu_0 + 2 - D}{2})}{\Gamma(\frac{\nu_0}{2})},
 \end{aligned} \tag{3.52}$$

where $\nu_1 = \nu_0 + 1$, $\mathbf{S}_1 = \mathbf{S}_0 + \frac{\kappa_0}{\kappa_0 + 1}(\mathbf{x}^* - \mathbf{m}_0)(\mathbf{x}^* - \mathbf{m}_0)^\top$. An alternative form of Equation (3.52) is to rewrite by a multivariate Student's t distribution:

$$p(\mathbf{x}^* | \beta) = \tau(\mathbf{x}^* | \mathbf{m}_0, \frac{\kappa_0 + 1}{\kappa_0(\nu_0 - D + 1)} \mathbf{S}_0, \nu_0 - D + 1). \tag{3.53}$$

3.7.11 Posterior Predictive for New Data with Observations

Similar to posterior predictive for data without observation, now suppose we observe a new data vector \mathbf{x}^* given old observations \mathcal{X} . Then the posterior predictive for this vector is

$$p(\mathbf{x}^* | \mathcal{X}, \boldsymbol{\beta}) = \frac{p(\mathbf{x}^*, \mathcal{X} | \boldsymbol{\beta})}{p(\mathcal{X} | \boldsymbol{\beta})}. \quad (3.54)$$

The denominator of Equation (3.54) can be obtained directly from Equation (3.51). Its numerator can be obtained in a similar way from Equation (3.51) by considering the marginal likelihood of the new set $\{\mathcal{X}, \mathbf{x}^*\}$. We just need to replace N by $N^* = N + 1$ in Equation (3.46), Equation (3.47), and Equation (3.48), and replace \mathbf{S}_N by \mathbf{S}_{N^*} in Equation (3.49). Therefore, we obtain

$$\begin{aligned} p(\mathbf{x}^* | \mathcal{X}, \boldsymbol{\beta}) &= (2\pi)^{-D/2} \frac{Z_{NTW}(D, \kappa_{N^*}, \nu_{N^*}, \mathbf{S}_{N^*})}{Z_{NTW}(D, \kappa_N, \nu_N, \mathbf{S}_N)} \\ &= \pi^{-D/2} \frac{(\kappa_{N^*})^{-D/2} |\mathbf{S}_N|^{(\nu_N)/2}}{(\kappa_N)^{-D/2} |\mathbf{S}_{N^*}|^{(\nu_{N^*})/2}} \prod_{d=1}^D \frac{\Gamma(\frac{\nu_{N^*}+1-d}{2})}{\Gamma(\frac{\nu_N+1-d}{2})} \\ &= \pi^{-D/2} \frac{(\kappa_{N^*})^{-D/2} |\mathbf{S}_N|^{(\nu_N)/2}}{(\kappa_N)^{-D/2} |\mathbf{S}_{N^*}|^{(\nu_{N^*})/2}} \frac{\Gamma(\frac{\nu_0+N+2-D}{2})}{\Gamma(\frac{\nu_0+N}{2})}. \end{aligned} \quad (3.55)$$

Again, an alternative form of Equation (3.55) is to rewrite by a multivariate Student's t distribution:

$$p(\mathbf{x}^* | \mathcal{X}, \boldsymbol{\beta}) = \tau(\mathbf{x}^* | \mathbf{m}_N, \frac{\kappa_N + 1}{\kappa_N(\nu_N - D + 1)} \mathbf{S}_N, \nu_N - D + 1).$$

Thus, the mean and covariance of \mathbf{x}^* are given by

$$\begin{aligned} \mathbb{E}[\mathbf{x}^* | \mathcal{X}, \boldsymbol{\beta}] &= \mathbf{m}_N = \frac{\kappa_0}{\kappa_0 + N} \mathbf{m}_0 + \frac{N}{\kappa_0 + N} \bar{\mathbf{x}}, \\ \text{Cov}[\mathbf{x}^* | \mathcal{X}, \boldsymbol{\beta}] &= \frac{\kappa_N + 1}{\kappa_N(\nu_N - D - 1)} \mathbf{S}_N = \frac{\kappa_0 + N + 1}{(\kappa_0 + N)(\nu_0 + N - D - 1)} \mathbf{S}_N, \end{aligned}$$

where we can find, on average, the new coming data has an expectation of \mathbf{m}_N . We mentioned previously, κ_0 controls how strongly we believe this prior for $\boldsymbol{\mu}$. When κ_0 is large enough, $\mathbb{E}[\mathbf{x}^* | \mathcal{X}, \boldsymbol{\beta}]$ converges to \mathbf{m}_0 , the prior mean, and $\text{Cov}[\mathbf{x}^* | \mathcal{X}, \boldsymbol{\beta}]$ converges to $\frac{\mathbf{S}_N}{(\kappa_0 + N)(\nu_0 + N - D - 1)}$. In the meantime, if we set ν_0 large enough, the covariance matrix $\boldsymbol{\Sigma}$ is concentrated around $\boldsymbol{\Sigma}_0$, and

$$\mathbf{S}_N \rightarrow \frac{\mathbf{S}_{\bar{\mathbf{x}}}}{\nu_0} + \frac{\kappa_0 N}{\nu_0(\kappa_0 + N)} (\bar{\mathbf{x}} - \mathbf{m}_0)(\bar{\mathbf{x}} - \mathbf{m}_0)^\top,$$

which is largely controlled by data sample and data magnitude (rather than the prior hyperparameters), so as the posterior variance $\text{Cov}[\mathbf{x}^* | \mathcal{X}, \boldsymbol{\beta}]$.

3.7.12 Further Optimization via the Cholesky Decomposition

DEFINITION

The Cholesky decomposition of a symmetric positive definite matrix \mathbf{S} is its decomposition into the product of a lower triangular matrix \mathbf{L} and its transpose:

$$\mathbf{S} = \mathbf{L}\mathbf{L}^\top, \tag{3.56}$$

where \mathbf{L} is called the *Cholesky factor* of \mathbf{S} (see Problem 3.1.). We realize that an alternative form of the Cholesky decomposition is using its upper triangular $\mathbf{U} = \mathbf{L}^\top$, i.e., $\mathbf{S} = \mathbf{U}^\top\mathbf{U}$. A triangular matrix is a special kind of square matrices. Specifically, a square matrix is called lower triangular if all the entries above the main diagonal are zero. Similarly, a square matrix is called upper triangular if all the entries below the main diagonal are zero.

If the matrix has dimensionality D , the complexity of Cholesky decomposition is $O(D^3)$. In specific, it requires $\sim \frac{1}{3}D^3$ floating points operations (flops) to compute a Cholesky decomposition of a $D \times D$ positive definite matrix (Lu, 2021b), where the symbol “ \sim ” has the usual asymptotic meaning:

$$\lim_{D \rightarrow +\infty} \frac{\text{number of flops}}{(1/3)D^3} = 1.$$

RANK ONE UPDATE

A rank 1 update of matrix \mathbf{S} by vector \mathbf{x} is of the form (Seeger, 2004; Lu, 2021b):

$$\mathbf{S}' = \mathbf{S} + \mathbf{x}\mathbf{x}^\top.$$

If we have already calculated the Cholesky factor \mathbf{L} of \mathbf{S} , then the Cholesky factor \mathbf{L}' of \mathbf{S}' can be calculated efficiently. Note that \mathbf{S}' differs from \mathbf{S} only in the rank one matrix $\mathbf{x}\mathbf{x}^\top$. Hence we can compute \mathbf{L}' from \mathbf{L} using the rank one Cholesky update, which takes $O(D^2)$ operations each saving from $O(D^3)$ if we do know \mathbf{L} , the Cholesky decomposition of \mathbf{S} . See Lu (2021b) for more details.

SPEEDUP FOR DETERMINANT

The determinant of a positive definite matrix \mathbf{S} can be computed from its Cholesky factor \mathbf{L} :

$$|\mathbf{S}| = \prod_{d=1}^D l_{dd}^2, \quad \log(|\mathbf{S}|) = 2 \log(|\mathbf{L}|) = 2 \times \sum_{d=1}^D \log(l_{dd}),$$

where l_{dd} is the (d, d) -th entry of matrix \mathbf{L} . This is an $O(D)$ operation, i.e., given the Cholesky decomposition, the determinant is just the product of the diagonal terms.

UPDATE IN NIW

Now we consider computing the marginal likelihood of data in Equation (3.51) and the posterior predictive for new coming data in Equation (3.54) of which the two cases are similar.

Taking the latter as an example, consider that computing the posterior predictive for new coming data $p(\mathbf{x}^* | \mathcal{X}, \boldsymbol{\beta})$ in Equation (3.54), we just need to evaluate $\frac{p(\mathbf{x}^*, \mathcal{X} | \boldsymbol{\beta})}{p(\mathcal{X} | \boldsymbol{\beta})}$, in which we must calculate $|\mathbf{S}_N|$ and $|\mathbf{S}_{N^*}|$ efficiently with $N^* = N + 1$. We deal with computing the determinants $|\mathbf{S}_N|$ and $|\mathbf{S}_{N^*}|$ by representing \mathbf{S}_N and \mathbf{S}_{N^*} using their Cholesky decomposition forms. In particular, updates to \mathbf{S}_N and \mathbf{S}_{N^*} will be carried out by directly updating their Cholesky decompositions; given the Cholesky decomposition, the determinant is just the product of the diagonal terms. Write out \mathbf{S}_{N^*} by \mathbf{S}_N :

$$\mathbf{m}_N = \frac{\kappa_{N^*} \mathbf{m}_{N^*} - \mathbf{x}^*}{\kappa_N} = \frac{(\kappa_0 + N + 1) \mathbf{m}_{N^*} - \mathbf{x}^*}{\kappa_0 + N}, \quad (3.57)$$

$$\mathbf{m}_{N^*} = \frac{\kappa_N \mathbf{m}_N + \mathbf{x}^*}{\kappa_{N^*}} = \frac{(\kappa_0 + N) \mathbf{m}_N + \mathbf{x}^*}{\kappa_0 + N + 1}, \quad (3.58)$$

$$\mathbf{S}_{N^*} = \mathbf{S}_N + \mathbf{x}^* \mathbf{x}^{*T} - \kappa_{N^*} \mathbf{m}_{N^*} \mathbf{m}_{N^*}^\top + \kappa_N \mathbf{m}_N \mathbf{m}_N^\top \quad (3.59)$$

$$= \mathbf{S}_N + \frac{\kappa_0 + N + 1}{\kappa_0 + N} (\mathbf{m}_{N^*} - \mathbf{x}^*) (\mathbf{m}_{N^*} - \mathbf{x}^*)^\top, \quad (3.60)$$

where Equation (3.60) implies that Cholesky decomposition of \mathbf{S}_{N^*} can be obtained from Cholesky decomposition of \mathbf{S}_N by a rank 1 update. Therefore, if we know the Cholesky decomposition of \mathbf{S}_N , the Cholesky decomposition of \mathbf{S}_{N^*} can be obtained in $O(D^2)$ complexity.

⌘ Chapter 3 Problems ⌘

1. Prove the Cholesky decomposition: Every *positive definite* (PD) matrix $\mathbf{A} \in \mathbb{R}^{n \times n}$ can be factored as

$$\mathbf{A} = \mathbf{R}^\top \mathbf{R},$$

where $\mathbf{R} \in \mathbb{R}^{n \times n}$ is an upper triangular matrix **with positive diagonal elements**. This decomposition is known as the *Cholesky decomposition* of \mathbf{A} , and \mathbf{R} is called the *Cholesky factor* or *Cholesky triangle* of \mathbf{A} . Specifically, the Cholesky decomposition is **unique**. In cases where the diagonal elements of \mathbf{R} are not restricted to positive values, then the factorization $\mathbf{A} = \mathbf{R}^\top \mathbf{R}$ is **not unique**.⁸

2. **Poisson and conjugacy.** Let x_1, x_2, \dots, x_N be i.i.d. random variables drawn from the Poisson distribution $\mathcal{P}(\lambda)$. Suppose the prior for λ is

$$\mathcal{G}(\lambda | a, b) = \frac{b^a}{\Gamma(a)} \lambda^{a-1} \exp(-b\lambda) \mathbf{1}(\lambda > 0).$$

Derive the posterior distribution of λ .

3. Suppose we can generate the univariate Gaussian variable $\mathcal{N}(0, 1)$. Show a way to generate the multivariate Gaussian variable $\mathcal{N}(\boldsymbol{\mu}, \boldsymbol{\Sigma})$, where $\boldsymbol{\Sigma} = \mathbf{C}\mathbf{C}^\top$, $\boldsymbol{\mu} \in \mathbb{R}^n$, and $\boldsymbol{\Sigma} \in \mathbb{R}^{n \times n}$. *Hint: if x_1, x_2, \dots, x_n are i.i.d. from $\mathcal{N}(0, 1)$, and let $\mathbf{x} = [x_1, x_2, \dots, x_n]^\top$, then it follows that $\mathbf{C}\mathbf{x} + \boldsymbol{\mu} \sim \mathcal{N}(\boldsymbol{\mu}, \boldsymbol{\Sigma})$.*

⁸ The Cholesky decomposition also holds for *complex Hermitian positive definite* matrix $\mathbf{A} \in \mathbb{C}^{n \times n}$. In this case, $\mathbf{A} = \mathbf{R}^* \mathbf{R}$ for a unique upper triangular matrix \mathbf{R} with positive diagonal entries.

Part II

Non-Bayesian Matrix Decomposition

Alternating Least Squares

Contents

4.1	Preliminary: Least Squares Approximations	97
4.2	Netflix Recommender and Matrix Factorization	100
4.3	Regularization: Extension to General Matrices	105
4.4	Missing Entries and Rank-One Update	107
4.5	Vector Inner Product	109
4.6	Gradient Descent	109
4.7	Regularization: A Geometrical Interpretation	113
4.8	Stochastic Gradient Descent	115
4.9	Bias Term	117
4.10	Applications	119
4.10.1	Low-Rank Approximation	120
4.10.2	Movie Recommender	122
Chapter 4	Problems	125

4.1. Preliminary: Least Squares Approximations



The linear model stands as the primary technique in regression problems, utilizing the least squares approximation as the fundamental tool to minimize the sum of squared errors. This is a natural choice when seeking the regression function that minimizes the corresponding expected squared error. In recent decades, linear models have found wide-ranging applications, e.g., decision making (Dawes and Corrigan, 1974), time series (Christensen, 1991; Lu, 2017), quantitative finance (Menchero et al., 2011), and various fields of study such as production science, social science, and soil science (Fox, 1997; Lane, 2002; Schaeffer, 2004; Mrode, 2014).

To be more concrete, let's consider the overdetermined system $\mathbf{b} = \mathbf{A}\mathbf{x}$, where $\mathbf{A} \in \mathbb{R}^{m \times n}$ represents the input data matrix, $\mathbf{b} \in \mathbb{R}^m$ is the observation vector (or target vector), and the number of samples m exceeds the dimensionality n . The vector \mathbf{x} denotes a vector of weights for the linear model. Typically, \mathbf{A} will have full column rank since real-world data is often uncorrelated or becomes uncorrelated after post-processing. In practice, a bias term is introduced in the first column of \mathbf{A} to enable the least squares method to find the solution for:

$$\tilde{\mathbf{A}}\tilde{\mathbf{x}} = [\mathbf{1}, \mathbf{A}] \begin{bmatrix} x_0 \\ \mathbf{x} \end{bmatrix} = \mathbf{b}. \quad (4.1)$$

On the other hand, it often occurs that $\mathbf{b} = \mathbf{A}\mathbf{x}$ has no solution (the system is *inconsistent*). The usual reason is: too many equations, i.e., the matrix has more rows than columns. Define the column space of \mathbf{A} as $\{\mathbf{A}\boldsymbol{\gamma} : \forall \boldsymbol{\gamma} \in \mathbb{R}^n\}$, denoted by $\mathcal{C}(\mathbf{A})$. In essence, when we say $\mathbf{b} = \mathbf{A}\mathbf{x}$ has no solution, it implies that \mathbf{b} lies outside the column space of \mathbf{A} . In other words, the error $\mathbf{e} = \mathbf{b} - \mathbf{A}\mathbf{x}$ cannot be reduced to zero. When the error \mathbf{e} is minimized in terms of the mean squared error, \mathbf{x}_{LS} becomes a least squares solution, i.e., $\|\mathbf{b} - \mathbf{A}\mathbf{x}_{LS}\|^2$ is minimized. The method of least squares stands as one of the most powerful tools in mathematical sciences. There exist books dedicated entirely to this topic, and readers are also encouraged to refer to works by Trefethen and Bau III (1997); Strang (2019, 2021); Lu (2022a).

Least squares by calculus. When $\|\mathbf{b} - \mathbf{A}\mathbf{x}\|^2$ is differentiable, and the parameter space of \mathbf{x} covers the entire space \mathbb{R}^n ¹, the least squares estimator corresponds to the root of $\|\mathbf{b} - \mathbf{A}\mathbf{x}\|^2$. This leads us to the following lemma.

Lemma 4.1: (Least Squares by Calculus)

Assume the data matrix $\mathbf{A} \in \mathbb{R}^{m \times n}$ is fixed and has full rank (i.e., the columns of \mathbf{A} are linearly independent) with $m \geq n$. Considering the overdetermined system $\mathbf{b} = \mathbf{A}\mathbf{x}$, the least squares solution, obtained by employing calculus and setting the derivative in every direction of $\|\mathbf{b} - \mathbf{A}\mathbf{x}\|^2$ to be zero (i.e., the gradient is a zero vector), is $\mathbf{x}_{LS} = (\mathbf{A}^\top \mathbf{A})^{-1} \mathbf{A}^\top \mathbf{b}$ ^a. The value, $\mathbf{x}_{LS} = (\mathbf{A}^\top \mathbf{A})^{-1} \mathbf{A}^\top \mathbf{b}$, is commonly referred to as the *ordinary least squares (OLS)* estimator or simply the *least squares (LS)* estimator of \mathbf{x} .

a. This is known as the *first-order optimality condition* for local optima points.

1. In other words, the *domain* of the optimization problem $\min_{\mathbf{x}} \|\mathbf{b} - \mathbf{A}\mathbf{x}\|^2$ is the entire space \mathbb{R}^n .

To prove the lemma above, we need to demonstrate the invertibility of $\mathbf{A}^\top \mathbf{A}$. Since we assume \mathbf{A} has full rank and $m \geq n$, $\mathbf{A}^\top \mathbf{A} \in \mathbb{R}^{n \times n}$ is invertible if it has a rank of n , which is equivalent to the rank of \mathbf{A} .

Lemma 4.2: (Rank of $\mathbf{A}^\top \mathbf{A}$)

$\mathbf{A}^\top \mathbf{A}$ and \mathbf{A} share the same rank.

Proof [of Lemma 4.2] Let $\mathbf{x} \in \mathcal{N}(\mathbf{A})$, we have

$$\mathbf{A}\mathbf{x} = \mathbf{0} \quad \underline{\text{leads to}} \quad \mathbf{A}^\top \mathbf{A}\mathbf{x} = \mathbf{0},$$

i.e., $\mathbf{x} \in \mathcal{N}(\mathbf{A}) \underline{\text{leads to}} \mathbf{x} \in \mathcal{N}(\mathbf{A}^\top \mathbf{A})$. Therefore, $\mathcal{N}(\mathbf{A}) \subseteq \mathcal{N}(\mathbf{A}^\top \mathbf{A})$.

Further, let $\mathbf{x} \in \mathcal{N}(\mathbf{A}^\top \mathbf{A})$, we have

$$\mathbf{A}^\top \mathbf{A}\mathbf{x} = \mathbf{0} \underline{\text{leads to}} \mathbf{x}^\top \mathbf{A}^\top \mathbf{A}\mathbf{x} = 0 \underline{\text{leads to}} \|\mathbf{A}\mathbf{x}\|^2 = 0 \underline{\text{leads to}} \mathbf{A}\mathbf{x} = \mathbf{0},$$

i.e., $\mathbf{x} \in \mathcal{N}(\mathbf{A}^\top \mathbf{A}) \underline{\text{leads to}} \mathbf{x} \in \mathcal{N}(\mathbf{A})$. Therefore, $\mathcal{N}(\mathbf{A}^\top \mathbf{A}) \subseteq \mathcal{N}(\mathbf{A})$.

As a result, by “sandwiching,” it follows that

$$\mathcal{N}(\mathbf{A}) = \mathcal{N}(\mathbf{A}^\top \mathbf{A}) \quad \text{and} \quad \dim(\mathcal{N}(\mathbf{A})) = \dim(\mathcal{N}(\mathbf{A}^\top \mathbf{A})).$$

According to the fundamental theorem of linear algebra, $\mathbf{A}^\top \mathbf{A}$ and \mathbf{A} have the same rank. ■

Extending this observation to \mathbf{A}^\top , we can also prove that $\mathbf{A}\mathbf{A}^\top$ and \mathbf{A} share the same rank. This result gives rise to the ordinary least squares estimator, which can be expressed as follows.

Proof [of Lemma 4.1] Recalling from calculus that a function $f(\mathbf{x})$ attains a minimum at \mathbf{x}_{LS} when the gradient $\nabla f(\mathbf{x}) = \mathbf{0}$. The gradient of $\|\mathbf{b} - \mathbf{A}\mathbf{x}\|^2$ is given by $2\mathbf{A}^\top \mathbf{A}\mathbf{x} - 2\mathbf{A}^\top \mathbf{b}$. $\mathbf{A}^\top \mathbf{A}$ is invertible since we assume \mathbf{A} is fixed and has full rank with $m \geq n$. Consequently, the OLS solution for \mathbf{x} is $\mathbf{x}_{LS} = (\mathbf{A}^\top \mathbf{A})^{-1} \mathbf{A}^\top \mathbf{b}$, which completes the proof. ■

Definition 4.1.1 (Normal Equation) *The condition for the derivative of $\|\mathbf{b} - \mathbf{A}\mathbf{x}\|^2$ to be zero can be expressed as $\mathbf{A}^\top \mathbf{A}\mathbf{x}_{LS} = \mathbf{A}^\top \mathbf{b}$. The equation is also known as the **normal equation**. Under the assumption that \mathbf{A} has full rank with $m \geq n$, it follows that $\mathbf{A}^\top \mathbf{A}$ is invertible, implying $\mathbf{x}_{LS} = (\mathbf{A}^\top \mathbf{A})^{-1} \mathbf{A}^\top \mathbf{b}$.*

The least squares estimator derived in Lemma 4.1 does not guarantee whether it is the smallest, largest, or neither among achievable estimators. To illustrate this ambiguity, refer to Figure 4.1. While we can confidently affirm the existence of at least one root for the function $f(\mathbf{x}) = \|\mathbf{b} - \mathbf{A}\mathbf{x}\|^2$, it serves as a necessary condition for the minimum point, lacking sufficiency. Further clarification on this point is provided in the following remark.

Remark 4.3: Verification of Least Squares Solution

Why does the zero gradient imply the least mean squared error? The typical explanation stems from convex analysis, as we will see shortly. However, here we directly confirm

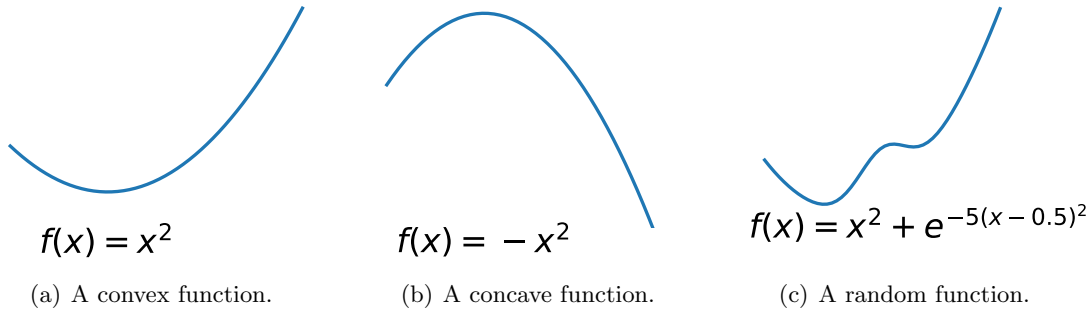


Figure 4.1: Three functions.

that the OLS solution indeed minimizes the mean squared error. For any $\mathbf{x} \neq \mathbf{x}_{LS}$, we have

$$\begin{aligned}
 \|\mathbf{b} - \mathbf{Ax}\|^2 &= \|\mathbf{b} - \mathbf{Ax}_{LS} + \mathbf{Ax}_{LS} - \mathbf{Ax}\|^2 = \|\mathbf{b} - \mathbf{Ax}_{LS} + \mathbf{A}(\mathbf{x}_{LS} - \mathbf{x})\|^2 \\
 &= \|\mathbf{b} - \mathbf{Ax}_{LS}\|^2 + \|\mathbf{A}(\mathbf{x}_{LS} - \mathbf{x})\|^2 + 2(\mathbf{A}(\mathbf{x}_{LS} - \mathbf{x}))^\top (\mathbf{b} - \mathbf{Ax}_{LS}) \\
 &= \|\mathbf{b} - \mathbf{Ax}_{LS}\|^2 + \|\mathbf{A}(\mathbf{x}_{LS} - \mathbf{x})\|^2 + 2(\mathbf{x}_{LS} - \mathbf{x})^\top (\mathbf{A}^\top \mathbf{b} - \mathbf{A}^\top \mathbf{Ax}_{LS}),
 \end{aligned}$$

where the third term is zero as a result of the normal equation, and $\|\mathbf{A}(\mathbf{x}_{LS} - \mathbf{x})\|^2 \geq 0$. Therefore,

$$\|\mathbf{b} - \mathbf{Ax}\|^2 \geq \|\mathbf{b} - \mathbf{Ax}_{LS}\|^2.$$

Thus, we demonstrate that the OLS estimator indeed corresponds to the minimum, rather than the maximum or a saddle point, using the calculus approach. As a matter of fact, this condition from the least squares estimator is also known as the *sufficiency of stationarity under convexity*. When \mathbf{x} is defined over the entire space \mathbb{R}^n , this condition is also known as the *necessity of stationarity under convexity*.

Another question that arises is: Why does this normal equation magically yield solutions for \mathbf{x} ? A simple example can shed light on the answer. The equation $x^2 = -1$ has no real solution. However, $x \cdot x^2 = x \cdot (-1)$ has a real solution $\hat{x} = 0$, in which case \hat{x} makes x^2 and -1 as close as possible.

Example 4.1 (Changing the Solution Set by Left Multiplication) Consider the following data matrix and target vector

$$\mathbf{A} = \begin{bmatrix} -3 & -4 \\ 4 & 6 \\ 1 & 1 \end{bmatrix} \quad \text{and} \quad \mathbf{b} = \begin{bmatrix} 1 \\ -1 \\ 0 \end{bmatrix}.$$

It can be easily verified that $\mathbf{Ax} = \mathbf{b}$ has no solution for \mathbf{x} . However, if we multiply on the left by

$$\mathbf{B} = \begin{bmatrix} 0 & -1 & 6 \\ 0 & 1 & -4 \end{bmatrix}.$$

Then we have $\mathbf{x}_{LS} = [1/2, -1/2]^\top$ as the solution to $\mathbf{BAx} = \mathbf{Bb}$. This specific example shows why the normal equation can give rise to the least squares solution. Multiplying on the left of a linear system will change the solution set. \square

Rank-Deficiency

Note here, we assume $\mathbf{A} \in \mathbb{R}^{m \times n}$ has full rank with $m \geq n$ to make $\mathbf{A}^\top \mathbf{A}$ invertible. However, when two or more columns of \mathbf{A} are perfectly correlated, the matrix \mathbf{A} becomes deficient and $\mathbf{A}^\top \mathbf{A}$ becomes singular. To address this issue, one can choose \mathbf{x} that minimizes $\mathbf{x}_{LS}^\top \mathbf{x}_{LS}$ in accordance with the normal equation. That is, we select the least squares solution with the smallest magnitude. However, this is not the main interest of the text, and we leave it for readers to explore further. In Lu (2021b), UTV decomposition and singular value decomposition (SVD) are applied to address the rank-deficient least squares problem.

4.2. Netflix Recommender and Matrix Factorization

In the Netflix Prize competition (Bennett et al., 2007), the goal is to predict the ratings of users for different movies, given the existing ratings of those users for other movies. We index M movies with $m = 1, 2, \dots, M$ and N users by $n = 1, 2, \dots, N$. We denote the rating of the n -th user for the m -th movie by a_{mn} . Define \mathbf{A} to be an $M \times N$ rating matrix with columns $\mathbf{a}_n \in \mathbb{R}^M$ containing ratings provided by the n -th user. Note that many ratings $\{a_{mn}\}$ are missing, and our goal is to predict these missing ratings accurately.

We formally consider algorithms for solving the following problem: The matrix \mathbf{A} is approximately factorized into an $M \times K$ matrix \mathbf{W} and a $K \times N$ matrix \mathbf{Z} . Typically, K is selected to be smaller than both M and N , ensuring that \mathbf{W} and \mathbf{Z} have reduced dimensions compared to the original matrix \mathbf{A} . This reduction in dimensionality results in a compressed version of the original data matrix. An appropriate decision on the value of K is critical in practice; but the choice of K is very often problem-dependent. The factorization is significant in the sense; suppose $\mathbf{A} = [\mathbf{a}_1, \mathbf{a}_2, \dots, \mathbf{a}_N]$ and $\mathbf{Z} = [\mathbf{z}_1, \mathbf{z}_2, \dots, \mathbf{z}_N]$ are the column partitions of \mathbf{A} and \mathbf{Z} , respectively. Then we have $\mathbf{a}_n = \mathbf{W}\mathbf{z}_n$, i.e., each column \mathbf{a}_n is approximated by a linear combination of the columns of \mathbf{W} , weighted by the components in \mathbf{z}_n . Therefore, the columns of \mathbf{W} can be thought of as containing the column basis of \mathbf{A} .

In order to obtain the approximation $\mathbf{A} \approx \mathbf{W}\mathbf{Z}$, we must establish a loss function such that the distance between \mathbf{A} and $\mathbf{W}\mathbf{Z}$ can be measured. In our discussion, the chosen loss function is the Frobenius norm (Definition 1.0.18, p. 16) between two matrices, which vanishes to zero if $\mathbf{A} = \mathbf{W}\mathbf{Z}$, and the advantage will be evident shortly.

To simplify the problem, let's first assume that there are no missing ratings. Project data vectors $\mathbf{a}_n \in \mathbb{R}^M$ into a lower dimension $\mathbf{z}_n \in \mathbb{R}^K$ with $K < \min\{M, N\}$ in a way that the *reconstruction error* as measured by the Frobenius norm is minimized (assume K is known):

$$\min_{\mathbf{W}, \mathbf{Z}} \sum_{n=1}^N \sum_{m=1}^M \left(a_{mn} - \mathbf{w}_m^\top \mathbf{z}_n \right)^2, \quad (4.2)$$

where $\mathbf{W} = [\mathbf{w}_1^\top; \mathbf{w}_2^\top; \dots; \mathbf{w}_M^\top] \in \mathbb{R}^{M \times K}$ and $\mathbf{Z} = [\mathbf{z}_1, \mathbf{z}_2, \dots, \mathbf{z}_N] \in \mathbb{R}^{K \times N}$ containing \mathbf{w}_m 's and \mathbf{z}_n 's as **rows and columns**, respectively. The loss formulation in Equation (4.2) is referred to as the *per-example loss*. It can be equivalently expressed as

$$L(\mathbf{W}, \mathbf{Z}) = \sum_{n=1}^N \sum_{m=1}^M (a_{mn} - \mathbf{w}_m^\top \mathbf{z}_n)^2 = \|\mathbf{W}\mathbf{Z} - \mathbf{A}\|^2.$$

Moreover, the loss function $L(\mathbf{W}, \mathbf{Z}) = \sum_{n=1}^N \sum_{m=1}^M (a_{mn} - \mathbf{w}_m^\top \mathbf{z}_n)$ is convex with respect to \mathbf{Z} given \mathbf{W} , and vice versa. Therefore, we can first minimize it with respect to \mathbf{Z} while keeping \mathbf{W} fixed, and subsequently minimize it with respect to \mathbf{W} with \mathbf{Z} fixed. This leads to two optimization problems, denoted by ALS1 and ALS2:

$$\begin{cases} \mathbf{Z} \leftarrow \arg \min_{\mathbf{Z}} L(\mathbf{W}, \mathbf{Z}); & \text{(ALS1)} \\ \mathbf{W} \leftarrow \arg \min_{\mathbf{W}} L(\mathbf{W}, \mathbf{Z}). & \text{(ALS2)} \end{cases}$$

This is known as the *coordinate descent algorithm*, where we alternate between optimizing the least squares with respect to \mathbf{W} and \mathbf{Z} . Hence, it is also called the *alternating least squares (ALS)* algorithm (Comon et al., 2009; Takács and Tikk, 2012; Giampouras et al., 2018). The convergence is guaranteed if the loss function $L(\mathbf{W}, \mathbf{Z})$ decreases at each iteration, and we shall discuss more on this in the sequel.

Remark 4.4: Convexity and Global Minimum

Although the loss function defined by Frobenius norm $\|\mathbf{W}\mathbf{Z} - \mathbf{A}\|^2$ is convex either with respect to \mathbf{W} when \mathbf{Z} is fixed or vice versa, it is not jointly convex in both variables simultaneously. Therefore, locating the global minimum is infeasible. However, the convergence is assured to find local minima.

Given \mathbf{W} , optimizing \mathbf{Z} . Now, let's examine the problem of $\mathbf{Z} \leftarrow \arg \min_{\mathbf{Z}} L(\mathbf{W}, \mathbf{Z})$. When there exists a unique minimum of the loss function $L(\mathbf{W}, \mathbf{Z})$ with respect to \mathbf{Z} , we refer to it as the *least squares* minimizer of $\arg \min_{\mathbf{Z}} L(\mathbf{W}, \mathbf{Z})$. Given \mathbf{W} fixed, $L(\mathbf{W}, \mathbf{Z})$ can be represented as $L(\mathbf{Z}|\mathbf{W})$ (or more compactly, as $L(\mathbf{Z})$) to emphasize the variable of \mathbf{Z} :

$$L(\mathbf{Z}|\mathbf{W}) = \|\mathbf{W}\mathbf{Z} - \mathbf{A}\|^2 = \|\mathbf{W}[\mathbf{z}_1, \mathbf{z}_2, \dots, \mathbf{z}_N] - [\mathbf{a}_1, \mathbf{a}_2, \dots, \mathbf{a}_N]\|^2 = \left\| \begin{bmatrix} \mathbf{W}\mathbf{z}_1 - \mathbf{a}_1 \\ \mathbf{W}\mathbf{z}_2 - \mathbf{a}_2 \\ \vdots \\ \mathbf{W}\mathbf{z}_N - \mathbf{a}_N \end{bmatrix} \right\|^2. \quad 2$$

2. The matrix norm employed in this context is the Frobenius norm (Definition 1.0.18, p. 16). It is defined as $\|\mathbf{A}\| = \sqrt{\sum_{i=1}^m \sum_{j=1}^n (a_{ij})^2}$ for $\mathbf{A} \in \mathbb{R}^{m \times n}$. And the vector norm used here is the ℓ_2 norm (Definition 1.0.17, p. 16), given by $\|\mathbf{x}\|_2 = \sqrt{\sum_{i=1}^n x_i^2}$ if $\mathbf{x} \in \mathbb{R}^n$.

Now, if we define

$$\widetilde{\mathbf{W}} = \begin{bmatrix} \mathbf{W} & \mathbf{0} & \dots & \mathbf{0} \\ \mathbf{0} & \mathbf{W} & \dots & \mathbf{0} \\ \vdots & \vdots & \ddots & \vdots \\ \mathbf{0} & \mathbf{0} & \dots & \mathbf{W} \end{bmatrix} \in \mathbb{R}^{MN \times KN}, \quad \widetilde{\mathbf{z}} = \begin{bmatrix} z_1 \\ z_2 \\ \vdots \\ z_N \end{bmatrix} \in \mathbb{R}^{KN}, \quad \widetilde{\mathbf{a}} = \begin{bmatrix} \mathbf{a}_1 \\ \mathbf{a}_2 \\ \vdots \\ \mathbf{a}_N \end{bmatrix} \in \mathbb{R}^{MN},$$

then the (ALS1) problem can be reduced to the ordinary least squares problem for minimizing $\|\widetilde{\mathbf{W}}\widetilde{\mathbf{z}} - \widetilde{\mathbf{a}}\|^2$ with respect to $\widetilde{\mathbf{z}}$. And the solution is given by

$$\widetilde{\mathbf{z}} = (\widetilde{\mathbf{W}}^\top \widetilde{\mathbf{W}})^{-1} \widetilde{\mathbf{W}}^\top \widetilde{\mathbf{a}}.$$

However, it is not advisable to obtain the result using this approach, as computing the inverse of $\widetilde{\mathbf{W}}^\top \widetilde{\mathbf{W}}$ requires $2(KN)^3$ flops (Lu, 2021b). Alternatively, a more direct way to solve the problem of (ALS1) is to find the gradient of $L(\mathbf{Z}|\mathbf{W})$ with respect to \mathbf{Z} (suppose all the partial derivatives of this function exist):

$$\begin{aligned} \nabla L(\mathbf{Z}|\mathbf{W}) &= \frac{\partial \operatorname{tr}((\mathbf{W}\mathbf{Z} - \mathbf{A})(\mathbf{W}\mathbf{Z} - \mathbf{A})^\top)}{\partial \mathbf{Z}} \\ &= \frac{\partial \operatorname{tr}((\mathbf{W}\mathbf{Z} - \mathbf{A})(\mathbf{W}\mathbf{Z} - \mathbf{A})^\top)}{\partial(\mathbf{W}\mathbf{Z} - \mathbf{A})} \frac{\partial(\mathbf{W}\mathbf{Z} - \mathbf{A})}{\partial \mathbf{Z}} \\ &\stackrel{*}{=} 2\mathbf{W}^\top(\mathbf{W}\mathbf{Z} - \mathbf{A}) \in \mathbb{R}^{K \times N}, \end{aligned} \quad (4.3)$$

where the first equality arises from the definition of the Frobenius norm (Definition 1.0.18, p. 16) such that $\|\mathbf{A}\| = \sqrt{\sum_{i=1}^m \sum_{j=1}^n (a_{ij})^2} = \sqrt{\operatorname{tr}(\mathbf{A}\mathbf{A}^\top)}$, and equality (*) is a consequence of the fact that $\frac{\partial \operatorname{tr}(\mathbf{A}\mathbf{A}^\top)}{\partial \mathbf{A}} = 2\mathbf{A}$. When the loss function is a differentiable function of \mathbf{Z} , we can determine the least squares solution using differential calculus. And a minimum of the function $L(\mathbf{Z}|\mathbf{W})$ must be a root of the equation:

$$\nabla L(\mathbf{Z}|\mathbf{W}) = \mathbf{0}.$$

By finding the root of the equation above, we obtain the “candidate” update for \mathbf{Z} that finds the minimizer of $L(\mathbf{Z}|\mathbf{W})$:

$$\boxed{\mathbf{Z} = (\mathbf{W}^\top \mathbf{W})^{-1} \mathbf{W}^\top \mathbf{A} \leftarrow \arg \min_{\mathbf{Z}} L(\mathbf{Z}|\mathbf{W})}. \quad (4.4)$$

This takes $2K^3$ flops to compute the inverse of $\mathbf{W}^\top \mathbf{W}$ as compared to $2(KN)^3$ flops to get the inverse of $\widetilde{\mathbf{W}}^\top \widetilde{\mathbf{W}}$. Before we declare a root of the equation above is actually a minimizer rather than a maximizer (that’s why we call the update a “candidate” update), we need to verify the function is convex. In the case where the function is twice differentiable, this verification can be equivalently achieved by confirming (see Problem 4.8.):

$$\nabla^2 L(\mathbf{Z}|\mathbf{W}) > 0. \quad 3$$

3. In short, a twice continuously differentiable function f over an open convex set \mathbb{S} is called *convex* if and only if $\nabla^2 f(\mathbf{x}) \geq \mathbf{0}$ for any $\mathbf{x} \in \mathbb{S}$ (sufficient and necessary for convex); and called *strictly convex* if $\nabla^2 f(\mathbf{x}) > \mathbf{0}$ for any $\mathbf{x} \in \mathbb{S}$ (only sufficient for strictly convex, e.g., $f(x) = x^6$ is strictly convex, but $f''(x) = 30x^4$ is equal to zero at $x = 0$). And when the convex function f is a continuously differentiable function over a convex set \mathbb{S} , the stationary point $\nabla f(\mathbf{x}^*) = \mathbf{0}$ of $\mathbf{x}^* \in \mathbb{S}$ is a *global minimizer* of f over \mathbb{S} . In our context, when given \mathbf{W} and updating \mathbf{Z} , the function is defined over the entire space $\mathbb{R}^{K \times N}$.

That is, the Hessian matrix is positive definite (recall the definition of positive definiteness, Definition 1.0.16, p. 14). To see this, we explicitly express the Hessian matrix as

$$\nabla^2 L(\mathbf{Z}|\mathbf{W}) = 2\widetilde{\mathbf{W}}^\top \widetilde{\mathbf{W}} \in \mathbb{R}^{KN \times KN}, \quad (4.5)$$

which has full rank if $\mathbf{W} \in \mathbb{R}^{M \times K}$ has full rank and $K < M$ (Lemma 4.2).

Remark 4.5: Positive Definite Hessian if \mathbf{W} Has Full Rank

We claim that if $\mathbf{W} \in \mathbb{R}^{M \times K}$ has full rank K with $K < M$, then $\nabla^2 L(\mathbf{Z}|\mathbf{W})$ is positive definite. This can be demonstrated by confirming that when \mathbf{W} has full rank, the equation $\mathbf{W}\mathbf{x} = \mathbf{0}$ only holds true when $\mathbf{x} = \mathbf{0}$, since the null space of \mathbf{W} is of dimension 0. Therefore,

$$\mathbf{x}^\top (2\mathbf{W}^\top \mathbf{W})\mathbf{x} > 0, \quad \text{for any nonzero vector } \mathbf{x} \in \mathbb{R}^K.$$

Now, the problem becomes that we need to verify **whether \mathbf{W} has full rank so that the Hessian of $L(\mathbf{Z}|\mathbf{W})$ is positive definite**; otherwise, we cannot claim the update of \mathbf{Z} in Equation (4.4) reduces the loss (due to convexity) so that the matrix decomposition progressively improves the approximation of the original matrix \mathbf{A} by $\mathbf{W}\mathbf{Z}$ in each iteration. We will shortly come back to the positive definiteness of the Hessian matrix in the sequel, relying on the following lemma.

Lemma 4.6: (Rank of \mathbf{Z} after Updating)

Suppose $\mathbf{A} \in \mathbb{R}^{M \times N}$ has full rank with $M \leq N$ and $\mathbf{W} \in \mathbb{R}^{M \times K}$ has full rank with $K < M$ (i.e., $K < M \leq N$), then the update of $\mathbf{Z} = (\mathbf{W}^\top \mathbf{W})^{-1} \mathbf{W}^\top \mathbf{A} \in \mathbb{R}^{K \times N}$ in Equation (4.4) has full rank.

Proof [of Lemma 4.6] Since $\mathbf{W}^\top \mathbf{W} \in \mathbb{R}^{K \times K}$ has full rank if \mathbf{W} has full rank (Lemma 4.2), it follows that $(\mathbf{W}^\top \mathbf{W})^{-1}$ has full rank.

Suppose $\mathbf{W}^\top \mathbf{x} = \mathbf{0}$, this implies that $(\mathbf{W}^\top \mathbf{W})^{-1} \mathbf{W}^\top \mathbf{x} = \mathbf{0}$. Thus, the following two null spaces satisfy:

$$\mathcal{N}(\mathbf{W}^\top) \subseteq \mathcal{N}\left((\mathbf{W}^\top \mathbf{W})^{-1} \mathbf{W}^\top\right).$$

Moreover, suppose \mathbf{x} is in the null space of $(\mathbf{W}^\top \mathbf{W})^{-1} \mathbf{W}^\top$ such that $(\mathbf{W}^\top \mathbf{W})^{-1} \mathbf{W}^\top \mathbf{x} = \mathbf{0}$. And since $(\mathbf{W}^\top \mathbf{W})^{-1}$ is invertible, this implies $\mathbf{W}^\top \mathbf{x} = (\mathbf{W}^\top \mathbf{W})\mathbf{0} = \mathbf{0}$, and

$$\mathcal{N}\left((\mathbf{W}^\top \mathbf{W})^{-1} \mathbf{W}^\top\right) \subseteq \mathcal{N}(\mathbf{W}^\top).$$

As a result, by “sandwiching,” it follows that

$$\mathcal{N}(\mathbf{W}^\top) = \mathcal{N}\left((\mathbf{W}^\top \mathbf{W})^{-1} \mathbf{W}^\top\right). \quad (4.6)$$

Therefore, $(\mathbf{W}^\top \mathbf{W})^{-1} \mathbf{W}^\top$ has full rank K . Let $\mathbf{T} = (\mathbf{W}^\top \mathbf{W})^{-1} \mathbf{W}^\top \in \mathbb{R}^{K \times M}$, and suppose $\mathbf{T}^\top \mathbf{x} = \mathbf{0}$. This implies $\mathbf{A}^\top \mathbf{T}^\top \mathbf{x} = \mathbf{0}$, and

$$\mathcal{N}(\mathbf{T}^\top) \subseteq \mathcal{N}(\mathbf{A}^\top \mathbf{T}^\top).$$

Similarly, suppose $\mathbf{A}^\top(\mathbf{T}^\top \mathbf{x}) = \mathbf{0}$. Since \mathbf{A} has full rank with the dimension of the null space being 0: $\dim(\mathcal{N}(\mathbf{A}^\top)) = 0$, $(\mathbf{T}^\top \mathbf{x})$ must be zero. The claim follows since \mathbf{A} has full rank M with the row space of \mathbf{A}^\top being equal to the column space of \mathbf{A} , where $\dim(\mathcal{C}(\mathbf{A})) = M$ and the $\dim(\mathcal{N}(\mathbf{A}^\top)) = M - \dim(\mathcal{C}(\mathbf{A})) = 0$. Therefore, \mathbf{x} is in the null space of \mathbf{T}^\top if \mathbf{x} is in the null space of $\mathbf{A}^\top \mathbf{T}^\top$:

$$\mathcal{N}(\mathbf{A}^\top \mathbf{T}^\top) \subseteq \mathcal{N}(\mathbf{T}^\top).$$

By “sandwiching” again,

$$\mathcal{N}(\mathbf{T}^\top) = \mathcal{N}(\mathbf{A}^\top \mathbf{T}^\top). \quad (4.7)$$

Since \mathbf{T}^\top has full rank $K < M \leq N$, it follows that $\dim(\mathcal{N}(\mathbf{T}^\top)) = \dim(\mathcal{N}(\mathbf{A}^\top \mathbf{T}^\top)) = 0$. Therefore, $\mathbf{Z}^\top = \mathbf{A}^\top \mathbf{T}^\top$ has full rank K . We complete the proof. \blacksquare

Given \mathbf{Z} , optimizing \mathbf{W} . Given \mathbf{Z} fixed, $L(\mathbf{W}, \mathbf{Z})$ can be expressed as $L(\mathbf{W}|\mathbf{Z})$ (or more compactly, as $L(\mathbf{W})$) to emphasize the variable of \mathbf{W} :

$$L(\mathbf{W}|\mathbf{Z}) = \|\mathbf{W}\mathbf{Z} - \mathbf{A}\|^2.$$

A direct approach to solve the optimization of (ALS2) is to find the gradient of $L(\mathbf{W}|\mathbf{Z})$ with respect to \mathbf{W} :

$$\begin{aligned} \nabla L(\mathbf{W}|\mathbf{Z}) &= \frac{\partial \operatorname{tr}((\mathbf{W}\mathbf{Z} - \mathbf{A})(\mathbf{W}\mathbf{Z} - \mathbf{A})^\top)}{\partial \mathbf{W}} \\ &= \frac{\partial \operatorname{tr}((\mathbf{W}\mathbf{Z} - \mathbf{A})(\mathbf{W}\mathbf{Z} - \mathbf{A})^\top)}{\partial(\mathbf{W}\mathbf{Z} - \mathbf{A})} \frac{\partial(\mathbf{W}\mathbf{Z} - \mathbf{A})}{\partial \mathbf{W}} \\ &= 2(\mathbf{W}\mathbf{Z} - \mathbf{A})\mathbf{Z}^\top \in \mathbb{R}^{M \times K}. \end{aligned}$$

Similarly, the “candidate” update for \mathbf{W} can be obtained by locating the root of the gradient $\nabla L(\mathbf{W}|\mathbf{Z})$:

$$\boxed{\mathbf{W}^\top = (\mathbf{Z}\mathbf{Z}^\top)^{-1} \mathbf{Z}\mathbf{A}^\top \leftarrow \arg \min_{\mathbf{W}} L(\mathbf{W}|\mathbf{Z})}. \quad (4.8)$$

Once more, we emphasize that the update is merely a “candidate” update. Further verification is required to determine whether the Hessian is positive definite or not. The Hessian matrix is expressed as follows:

$$\nabla^2 L(\mathbf{W}|\mathbf{Z}) = 2\tilde{\mathbf{Z}}\tilde{\mathbf{Z}}^\top \in \mathbb{R}^{KM \times KM}. \quad (4.9)$$

Therefore, by analogous analysis, if \mathbf{Z} has full rank with $K < N$, the Hessian matrix is positive definite.

Lemma 4.7: (Rank of \mathbf{W} after Updating)

Suppose $\mathbf{A} \in \mathbb{R}^{M \times N}$ has full rank with $M \geq N$ and $\mathbf{Z} \in \mathbb{R}^{K \times N}$ has full rank with $K < N$ (i.e., $K < N \leq M$), then the update of $\mathbf{W}^\top = (\mathbf{Z}\mathbf{Z}^\top)^{-1} \mathbf{Z}\mathbf{A}^\top$ in Equation (4.8) has full rank.

The proof of Lemma 4.7 is similar to that of Lemma 4.6, and we shall not repeat the details.

Key observation. Combine the observations in Lemma 4.6 and Lemma 4.7, as long as we initialize \mathbf{Z} and \mathbf{W} to have full rank, the updates in Equation (4.4) and Equation (4.8) are reasonable since the Hessians in Equation (4.5) and (4.9) are positive definite. Note that we need an additional condition to satisfy both Lemma 4.6 and Lemma 4.7: $M = N$, i.e., there must be an equal number of movies and users. We will relax this condition in the next section through regularization. We summarize the process in Algorithm 1.

Algorithm 1 Alternating Least Squares

Require: Matrix $\mathbf{A} \in \mathbb{R}^{M \times N}$ with $M = N$;

- 1: Initialize $\mathbf{W} \in \mathbb{R}^{M \times K}$, $\mathbf{Z} \in \mathbb{R}^{K \times N}$ with full rank and $K < M = N$;
 - 2: Choose a stop criterion on the approximation error δ ;
 - 3: Choose the maximal number of iterations C ;
 - 4: $iter = 0$; ▷ Count for the number of iterations
 - 5: **while** $\|\mathbf{A} - \mathbf{W}\mathbf{Z}\| > \delta$ and $iter < C$ **do**
 - 6: $iter = iter + 1$;
 - 7: $\mathbf{Z} = (\mathbf{W}^\top \mathbf{W})^{-1} \mathbf{W}^\top \mathbf{A} \leftarrow \arg \min_{\mathbf{Z}} L(\mathbf{Z}|\mathbf{W})$;
 - 8: $\mathbf{W}^\top = (\mathbf{Z}\mathbf{Z}^\top)^{-1} \mathbf{Z}\mathbf{A}^\top \leftarrow \arg \min_{\mathbf{W}} L(\mathbf{W}|\mathbf{Z})$;
 - 9: **end while**
 - 10: Output \mathbf{W}, \mathbf{Z} ;
-

4.3. Regularization: Extension to General Matrices

Regularization is a machine learning technique employed to prevent overfitting and improve model generalization. Overfitting occurs when a model is overly complex and fits the training data too closely, resulting in poor performance on unseen data. To address this issue, regularization introduces a constraint or penalty term into the loss function used for model optimization, discouraging the development of overly complex models. This results in a trade-off between having a simple, generalizable model and fitting the training data well. Common types of regularization include ℓ_1 regularization, ℓ_2 regularization, and elastic net regularization (a combination of ℓ_1 and ℓ_2 regularization). Regularization finds extensive application in machine learning algorithms such as linear regression, logistic regression, and neural networks.

In the context of the alternating least squares problem, we can add a ℓ_2 regularization term to minimize the following loss:

$$L(\mathbf{W}, \mathbf{Z}) = \|\mathbf{W}\mathbf{Z} - \mathbf{A}\|^2 + \lambda_w \|\mathbf{W}\|^2 + \lambda_z \|\mathbf{Z}\|^2, \quad \lambda_w > 0, \lambda_z > 0, \quad (4.10)$$

where the gradient with respect to \mathbf{Z} and \mathbf{W} are given respectively by

$$\begin{cases} \nabla L(\mathbf{Z}|\mathbf{W}) = 2\mathbf{W}^\top (\mathbf{W}\mathbf{Z} - \mathbf{A}) + 2\lambda_z \mathbf{Z} \in \mathbb{R}^{K \times N}; \\ \nabla L(\mathbf{W}|\mathbf{Z}) = 2(\mathbf{W}\mathbf{Z} - \mathbf{A})\mathbf{Z}^\top + 2\lambda_w \mathbf{W} \in \mathbb{R}^{M \times K}. \end{cases} \quad (4.11)$$

The Hessian matrices are given respectively by

$$\begin{cases} \nabla^2 L(\mathbf{Z}|\mathbf{W}) = 2\widetilde{\mathbf{W}}^\top \widetilde{\mathbf{W}} + 2\lambda_z \mathbf{I} \in \mathbb{R}^{KN \times KN}, \\ \nabla^2 L(\mathbf{W}|\mathbf{Z}) = 2\widetilde{\mathbf{Z}}\widetilde{\mathbf{Z}}^\top + 2\lambda_w \mathbf{I} \in \mathbb{R}^{KM \times KM}, \end{cases}$$

which are positive definite due to the perturbation by the regularization. To see this, we have

$$\begin{cases} \mathbf{x}^\top (2\widetilde{\mathbf{W}}^\top \widetilde{\mathbf{W}} + 2\lambda_z \mathbf{I}) \mathbf{x} = \underbrace{2\widetilde{\mathbf{x}}^\top \widetilde{\mathbf{W}}^\top \widetilde{\mathbf{W}} \mathbf{x}}_{\geq 0} + 2\lambda_z \|\mathbf{x}\|^2 > 0, & \text{for nonzero } \mathbf{x}; \\ \mathbf{x}^\top (2\widetilde{\mathbf{Z}}\widetilde{\mathbf{Z}}^\top + 2\lambda_w \mathbf{I}) \mathbf{x} = \underbrace{2\mathbf{x}^\top \widetilde{\mathbf{Z}}\widetilde{\mathbf{Z}}^\top \mathbf{x}}_{\geq 0} + 2\lambda_w \|\mathbf{x}\|^2 > 0, & \text{for nonzero } \mathbf{x}. \end{cases}$$

The regularization ensures that the Hessian matrices become positive definite, even if \mathbf{W} and \mathbf{Z} are rank-deficient. Consequently, matrix decomposition can be extended to any matrix, regardless of whether $M > N$ or $M < N$. In rare cases, K can be chosen as $K > \max\{M, N\}$ such that a *high-rank approximation* of \mathbf{A} is obtained. However, in most scenarios, we want to find the *low-rank approximation* of \mathbf{A} with $K < \min\{M, N\}$. For example, the ALS can be utilized to find the low-rank neural networks, reducing the memory usage of the neural networks while enhancing performance (Lu, 2021b). Therefore, the minimizers can be determined by identifying the roots of the gradient:

$$\begin{cases} \mathbf{Z} = (\mathbf{W}^\top \mathbf{W} + \lambda_z \mathbf{I})^{-1} \mathbf{W}^\top \mathbf{A}; \\ \mathbf{W}^\top = (\mathbf{Z}\mathbf{Z}^\top + \lambda_w \mathbf{I})^{-1} \mathbf{Z}\mathbf{A}^\top. \end{cases} \quad (4.12)$$

The regularization parameters $\lambda_z, \lambda_w \in \mathbb{R}$ are used to balance the trade-off between the accuracy of the approximation and the smoothness of the computed solution. The selection of these parameters is typically problem-dependent and can be obtained through *cross-validation*. Again, we summarize the process in Algorithm 2.

Algorithm 2 Alternating Least Squares with Regularization

Require: Matrix $\mathbf{A} \in \mathbb{R}^{M \times N}$;

- 1: Initialize $\mathbf{W} \in \mathbb{R}^{M \times K}$, $\mathbf{Z} \in \mathbb{R}^{K \times N}$ randomly without condition on the rank and the relationship between M, N, K ;
 - 2: Choose a stop criterion on the approximation error δ ;
 - 3: Choose regularization parameters λ_w, λ_z ;
 - 4: Choose the maximal number of iterations C ;
 - 5: $iter = 0$; ▷ Count for the number of iterations
 - 6: **while** $\|\mathbf{A} - \mathbf{W}\mathbf{Z}\| > \delta$ and $iter < C$ **do**
 - 7: $iter = iter + 1$;
 - 8: $\mathbf{Z} = (\mathbf{W}^\top \mathbf{W} + \lambda_z \mathbf{I})^{-1} \mathbf{W}^\top \mathbf{A} \leftarrow \arg \min_{\mathbf{Z}} L(\mathbf{Z}|\mathbf{W})$;
 - 9: $\mathbf{W}^\top = (\mathbf{Z}\mathbf{Z}^\top + \lambda_w \mathbf{I})^{-1} \mathbf{Z}\mathbf{A}^\top \leftarrow \arg \min_{\mathbf{W}} L(\mathbf{W}|\mathbf{Z})$;
 - 10: **end while**
 - 11: Output \mathbf{W}, \mathbf{Z} ;
-

4.4. Missing Entries and Rank-One Update

Since the matrix decomposition via the ALS is extensively used in the context of Netflix recommender data, where a substantial number of entries are missing due to users not having watched certain movies or choosing not to rate them for various reasons. To address this, we can introduce an additional mask matrix $\mathbf{M} \in \mathbb{R}^{M \times N}$, where $m_{mn} \in \{0, 1\}$ means if the user n has rated the movie m or not. Therefore, the loss function can be defined as

$$L(\mathbf{W}, \mathbf{Z}) = \|\mathbf{M} \circledast \mathbf{A} - \mathbf{M} \circledast (\mathbf{W}\mathbf{Z})\|^2,$$

where \circledast represents the *Hadamard product* between matrices. For example, the Hadamard product of a 3×3 matrix \mathbf{A} and a 3×3 matrix \mathbf{B} is

$$\mathbf{A} \circledast \mathbf{B} = \begin{bmatrix} a_{11} & a_{12} & a_{13} \\ a_{21} & a_{22} & a_{23} \\ a_{31} & a_{32} & a_{33} \end{bmatrix} \circledast \begin{bmatrix} b_{11} & b_{12} & b_{13} \\ b_{21} & b_{22} & b_{23} \\ b_{31} & b_{32} & b_{33} \end{bmatrix} = \begin{bmatrix} a_{11}b_{11} & a_{12}b_{12} & a_{13}b_{13} \\ a_{21}b_{21} & a_{22}b_{22} & a_{23}b_{23} \\ a_{31}b_{31} & a_{32}b_{32} & a_{33}b_{33} \end{bmatrix}.$$

To find the solution of the problem, we decompose the updates in Equation (4.12) into:

$$\begin{cases} \mathbf{z}_n = (\mathbf{W}^\top \mathbf{W} + \lambda_z \mathbf{I})^{-1} \mathbf{W}^\top \mathbf{a}_n, & \text{for } n \in \{1, 2, \dots, N\}; \\ \mathbf{w}_m = (\mathbf{Z}\mathbf{Z}^\top + \lambda_w \mathbf{I})^{-1} \mathbf{Z}\mathbf{b}_m, & \text{for } m \in \{1, 2, \dots, M\}, \end{cases} \quad (4.13)$$

where $\mathbf{Z} = [\mathbf{z}_1, \mathbf{z}_2, \dots, \mathbf{z}_N]$ and $\mathbf{A} = [\mathbf{a}_1, \mathbf{a}_2, \dots, \mathbf{a}_N]$ represent the column partitions of \mathbf{Z} and \mathbf{A} , respectively. Similarly, $\mathbf{W}^\top = [\mathbf{w}_1, \mathbf{w}_2, \dots, \mathbf{w}_M]$ and $\mathbf{A}^\top = [\mathbf{b}_1, \mathbf{b}_2, \dots, \mathbf{b}_M]$ are the column partitions of \mathbf{W}^\top and \mathbf{A}^\top , respectively. This decomposition of the updates indicates the updates can be performed in a column-by-column fashion (the rank-one update).

Given \mathbf{W} . Let $\mathbf{o}_n \in \mathbb{R}^M$ represent the movies rated by user n , where $o_{nm} = 1$ if user n has rated movie m , and $o_{nm} = 0$ otherwise. Then the n -th column of \mathbf{A} without missing entries can be denoted using the Matlab-style notation as $\mathbf{a}_n[\mathbf{o}_n]$. And we want to approximate the existing entries of the n -th column by $\mathbf{a}_n[\mathbf{o}_n] \approx \mathbf{W}[\mathbf{o}_n, :] \mathbf{z}_n$, which is actually a rank-one least squares problem:

$$\mathbf{z}_n = \left(\mathbf{W}[\mathbf{o}_n, :]^\top \mathbf{W}[\mathbf{o}_n, :] + \lambda_z \mathbf{I} \right)^{-1} \mathbf{W}[\mathbf{o}_n, :]^\top \mathbf{a}_n[\mathbf{o}_n], \quad \text{for } n \in \{1, 2, \dots, N\}. \quad (4.14)$$

Moreover, the loss function with respect to \mathbf{z}_n can be described by

$$L(\mathbf{z}_n | \mathbf{W}) = \sum_{m \in \mathbf{o}_n} \left(a_{mn} - \mathbf{w}_m^\top \mathbf{z}_n \right)^2,$$

and if we are concerned about the loss for all users:

$$L(\mathbf{Z} | \mathbf{W}) = \sum_{n=1}^N \sum_{m \in \mathbf{o}_n} \left(a_{mn} - \mathbf{w}_m^\top \mathbf{z}_n \right)^2.$$

Given \mathbf{Z} . Similarly, if $\mathbf{p}_m \in \mathbb{R}^N$ denotes the users who have rated movie m , with $p_{mn} = 1$ if the movie m has been rated by user n , and $p_{mn} = 0$ otherwise. Then the m -th row of \mathbf{A} without missing entries can be denoted by the Matlab-style notation as $\mathbf{b}_m[\mathbf{p}_m]$. And we want to approximate the existing entries of the m -th row by $\mathbf{b}_m[\mathbf{p}_m] \approx \mathbf{Z}[:, \mathbf{p}_m]^\top \mathbf{w}_m$,⁴ which is a rank-one least squares problem again:

$$\mathbf{w}_m = (\mathbf{Z}[:, \mathbf{p}_m] \mathbf{Z}[:, \mathbf{p}_m]^\top + \lambda_w \mathbf{I})^{-1} \mathbf{Z}[:, \mathbf{p}_m] \mathbf{b}_m[\mathbf{p}_m], \quad \text{for } m \in \{1, 2, \dots, M\}. \quad (4.15)$$

Moreover, the loss function with respect to \mathbf{w}_n can be described by

$$L(\mathbf{w}_n | \mathbf{Z}) = \sum_{n \in \mathbf{p}_m} \left(a_{mn} - \mathbf{w}_m^\top \mathbf{z}_n \right)^2,$$

and if we are concerned about the loss for all users:

$$L(\mathbf{W} | \mathbf{Z}) = \sum_{m=1}^M \sum_{n \in \mathbf{p}_m} \left(a_{mn} - \mathbf{w}_m^\top \mathbf{z}_n \right)^2.$$

The procedure is once again presented in Algorithm 3.

Algorithm 3 Alternating Least Squares with Missing Entries and Regularization

Require: Matrix $\mathbf{A} \in \mathbb{R}^{M \times N}$;

- 1: Initialize $\mathbf{W} \in \mathbb{R}^{M \times K}$, $\mathbf{Z} \in \mathbb{R}^{K \times N}$ randomly without condition on the rank and the relationship between M, N, K ;
 - 2: Choose a stop criterion on the approximation error δ ;
 - 3: Choose regularization parameters λ_w, λ_z ;
 - 4: Compute the mask matrix \mathbf{M} from \mathbf{A} ;
 - 5: Choose the maximal number of iterations C ;
 - 6: $iter = 0$; ▷ Count for the number of iterations
 - 7: **while** $\|\mathbf{M} \circledast \mathbf{A} - \mathbf{M} \circledast (\mathbf{W}\mathbf{Z})\|^2 > \delta$ and $iter < C$ **do**
 - 8: $iter = iter + 1$;
 - 9: **for** $n = 1, 2, \dots, N$ **do**
 - 10: $\mathbf{z}_n = (\mathbf{W}[\mathbf{o}_n, :]^\top \mathbf{W}[\mathbf{o}_n, :] + \lambda_z \mathbf{I})^{-1} \mathbf{W}[\mathbf{o}_n, :]^\top \mathbf{a}_n[\mathbf{o}_n]$; ▷ n -th column of \mathbf{Z}
 - 11: **end for**
 - 12: **for** $m = 1, 2, \dots, M$ **do**
 - 13: $\mathbf{w}_m = (\mathbf{Z}[:, \mathbf{p}_m] \mathbf{Z}[:, \mathbf{p}_m]^\top + \lambda_w \mathbf{I})^{-1} \mathbf{Z}[:, \mathbf{p}_m] \mathbf{b}_m[\mathbf{p}_m]$; ▷ m -th column of \mathbf{W}^\top
 - 14: **end for**
 - 15: **end while**
 - 16: Output $\mathbf{W}^\top = [\mathbf{w}_1, \mathbf{w}_2, \dots, \mathbf{w}_M]$, $\mathbf{Z} = [\mathbf{z}_1, \mathbf{z}_2, \dots, \mathbf{z}_N]$;
-

4. Note that $\mathbf{Z}[:, \mathbf{p}_m]^\top$ is the transpose of $\mathbf{Z}[:, \mathbf{p}_m]$, which is equal to $\mathbf{Z}^\top[\mathbf{p}_m, :]$, i.e., transposing first and then selecting.

4.5. Vector Inner Product

We have observed that the ALS algorithm seeks to find matrices \mathbf{W} and \mathbf{Z} such that their product \mathbf{WZ} can approximate $\mathbf{A} \approx \mathbf{WZ}$ in terms of squared loss:

$$\min_{\mathbf{W}, \mathbf{Z}} \sum_{n=1}^N \sum_{m=1}^M \left(a_{mn} - \mathbf{w}_m^\top \mathbf{z}_n \right)^2,$$

that is, each entry a_{mn} in \mathbf{A} can be approximated as the inner product of two vectors $\mathbf{w}_m^\top \mathbf{z}_n$. The geometric definition of the vector inner product is given by

$$\mathbf{w}_m^\top \mathbf{z}_n = \|\mathbf{w}\| \cdot \|\mathbf{z}\| \cos \theta,$$

where θ represents the angle between vectors \mathbf{w} and \mathbf{z} . So if the vector norms of \mathbf{w} and \mathbf{z} are determined, the smaller the angle, the larger the inner product.

Coming back to the Netflix data, the movie ratings range from 0 to 5 with higher ratings indicating a stronger user preference for the movie. If \mathbf{w}_m and \mathbf{z}_n fall sufficiently “close,” the value $\mathbf{w}_m^\top \mathbf{z}_n$ becomes larger. This concept elucidates the essence of ALS, where \mathbf{w}_m represents the features/attributes of movie m , while \mathbf{z}_n encapsulates the features/preferences of user n . In other words, the ALS associates each user with a *latent vector of preference*, and each movie with a *latent vector of attributes*. Furthermore, each element in \mathbf{w}_m and \mathbf{z}_n signifies a specific feature. For example, it could be that the second feature w_{m2} ⁵ represents whether the movie is an action movie or not, and z_{n2} denotes if the user n has a preference for action movies. When this holds true, then $\mathbf{w}_m^\top \mathbf{z}_n$ becomes large and provides a good approximation of a_{mn} .

In the decomposition $\mathbf{A} \approx \mathbf{WZ}$, it is established that the rows of \mathbf{W} contain the hidden features of the movies, and the columns of \mathbf{Z} contain the hidden features of the users. Nevertheless, the explicit meanings of the rows in \mathbf{W} or the columns in \mathbf{Z} remain undisclosed. Although they might correspond to categories or genres of the movies, fostering underlying connections between users and movies, their precise nature remains uncertain. It is precisely this ambiguity that gives rise to the terminology “latent” or “hidden.”

4.6. Gradient Descent

In Algorithm 1, 2, and 3, we reduce the loss via the inverse of matrices (e.g., algorithm by LU decomposition, see Lu (2021b)). The reality, however, is frequently far from straightforward, particularly in the big data era of today. As data volumes explode, the size of the inversion matrix will grow at a pace proportional to the cube of the number of samples, which poses a great challenge to the storage and computational resources. On the other hand, this leads to the creation of an ongoing development of the gradient-based optimization technique. The *gradient descent (GD)* method and its derivation, the *stochastic gradient descent (SGD)* method, are among them the simplest, fastest, and most efficient methods (Lu, 2022d). Convex loss function optimization problems are frequently solved using this type of approach. We now go into more details about its principle.

⁵. w_{m2} denotes the second element of vector \mathbf{w}_m .

In Equation (4.13), we derive the column-by-column update directly from the full matrix approach in Equation (4.12) (with regularization taken into account). Now let's see what's behind the idea. As per Equation (4.10), the loss function, considering the regularization, can be expressed as:

$$L(\mathbf{W}, \mathbf{Z}) = \|\mathbf{W}\mathbf{Z} - \mathbf{A}\|^2 + \lambda_w \|\mathbf{W}\|^2 + \lambda_z \|\mathbf{Z}\|^2, \quad \lambda_w > 0, \lambda_z > 0, \quad (4.16)$$

Since we are now considering the minimization of the above loss with respect to \mathbf{z}_n , we can decompose the loss into

$$\begin{aligned} L(\mathbf{z}_n) &= \|\mathbf{W}\mathbf{Z} - \mathbf{A}\|^2 + \lambda_w \|\mathbf{W}\|^2 + \lambda_z \|\mathbf{Z}\|^2 \\ &= \|\mathbf{W}\mathbf{z}_n - \mathbf{a}_n\|^2 + \lambda_z \|\mathbf{z}_n\|^2 + \underbrace{\sum_{i \neq n} \|\mathbf{W}\mathbf{z}_i - \mathbf{a}_i\|^2 + \lambda_z \sum_{i \neq n} \|\mathbf{z}_i\|^2 + \lambda_w \|\mathbf{W}\|^2}_{C_{z_n}}, \end{aligned} \quad (4.17)$$

where C_{z_n} represents a constant with respect to \mathbf{z}_n , and $\mathbf{Z} = [\mathbf{z}_1, \mathbf{z}_2, \dots, \mathbf{z}_N]$ and $\mathbf{A} = [\mathbf{a}_1, \mathbf{a}_2, \dots, \mathbf{a}_N]$ are the column partitions of \mathbf{Z} and \mathbf{A} , respectively. Taking the gradient

$$\nabla L(\mathbf{z}_n) = 2\mathbf{W}^\top \mathbf{W}\mathbf{z}_n - 2\mathbf{W}^\top \mathbf{a}_n + 2\lambda_z \mathbf{z}_n,$$

under which the root is exactly the first update of the column fashion in Equation (4.13):

$$\mathbf{z}_n = (\mathbf{W}^\top \mathbf{W} + \lambda_z \mathbf{I})^{-1} \mathbf{W}^\top \mathbf{a}_n, \quad \text{for } n \in \{1, 2, \dots, N\}.$$

Similarly, we can decompose the loss with respect to \mathbf{w}_m ,

$$\begin{aligned} L(\mathbf{w}_m) &= \|\mathbf{W}\mathbf{Z} - \mathbf{A}\|^2 + \lambda_w \|\mathbf{W}\|^2 + \lambda_z \|\mathbf{Z}\|^2 \\ &= \left\| \mathbf{Z}^\top \mathbf{W} - \mathbf{A}^\top \right\|^2 + \lambda_w \left\| \mathbf{W}^\top \right\|^2 + \lambda_z \|\mathbf{Z}\|^2 \\ &= \left\| \mathbf{Z}^\top \mathbf{w}_m - \mathbf{b}_n \right\|^2 + \lambda_w \|\mathbf{w}_m\|^2 + \underbrace{\sum_{i \neq m} \left\| \mathbf{Z}^\top \mathbf{w}_i - \mathbf{b}_i \right\|^2 + \lambda_w \sum_{i \neq m} \|\mathbf{w}_i\|^2 + \lambda_z \|\mathbf{Z}\|^2}_{C_{w_m}}, \end{aligned} \quad (4.18)$$

where C_{w_m} represents a constant with respect to \mathbf{w}_m , and $\mathbf{W}^\top = [\mathbf{w}_1, \mathbf{w}_2, \dots, \mathbf{w}_M]$ and $\mathbf{A}^\top = [\mathbf{b}_1, \mathbf{b}_2, \dots, \mathbf{b}_M]$ are the column partitions of \mathbf{W}^\top and \mathbf{A}^\top , respectively. Analogously, taking the gradient with respect to \mathbf{w}_m , it follows that

$$\nabla L(\mathbf{w}_m) = 2\mathbf{Z}\mathbf{Z}^\top \mathbf{w}_m - 2\mathbf{Z}\mathbf{b}_n + 2\lambda_w \mathbf{w}_m,$$

under which the root is exactly the second update of the column fashion in Equation (4.13):

$$\mathbf{w}_m = (\mathbf{Z}\mathbf{Z}^\top + \lambda_w \mathbf{I})^{-1} \mathbf{Z}\mathbf{b}_n, \quad \text{for } m \in \{1, 2, \dots, M\}.$$

Now suppose we express the iteration number ($k = 1, 2, \dots$) as the superscript, and we want to find the updates $\{\mathbf{z}_n^{(k+1)}, \mathbf{w}_m^{(k+1)}\}$ in the $(k+1)$ -th iteration base on $\{\mathbf{Z}^{(k)}, \mathbf{W}^{(k)}\}$ in the k -th iteration:

$$\begin{cases} \mathbf{z}_n^{(k+1)} \leftarrow \arg \min_{\mathbf{z}_n^{(k)}} L(\mathbf{z}_n^{(k)}); \\ \mathbf{w}_m^{(k+1)} \leftarrow \arg \min_{\mathbf{w}_m^{(k)}} L(\mathbf{w}_m^{(k)}). \end{cases}$$

For simplicity, we will only derive for $\mathbf{z}_n^{(k+1)} \leftarrow \arg \min_{\mathbf{z}_n^{(k)}} L(\mathbf{z}_n^{(k)})$, and the derivation for the update on $\mathbf{w}_m^{(k+1)}$ will be the same.

Approximation by linear update. Suppose we want to approximate $\mathbf{z}_n^{(k+1)}$ by a *linear update* on $\mathbf{z}_n^{(k)}$:

$$\text{Linear Update: } \boxed{\mathbf{z}_n^{(k+1)} = \mathbf{z}_n^{(k)} + \eta \mathbf{v}.}$$

The problem now turns to the solution of \mathbf{v} such that

$$\mathbf{v} = \arg \min_{\mathbf{v}} L(\mathbf{z}_n^{(k)} + \eta \mathbf{v}).$$

By Taylor's formula (Appendix A.1, p. 245), $L(\mathbf{z}_n^{(k)} + \eta \mathbf{v})$ can be approximated by

$$L(\mathbf{z}_n^{(k)} + \eta \mathbf{v}) \approx L(\mathbf{z}_n^{(k)}) + \eta \mathbf{v}^\top \nabla L(\mathbf{z}_n^{(k)}),$$

where η is a small value and $\nabla L(\mathbf{z}_n^{(k)})$ represents the gradient of $L(\mathbf{z})$ at $\mathbf{z}_n^{(k)}$. Then a search under the condition $\|\mathbf{v}\| = 1$ given positive η is shown as follows:

$$\mathbf{v} = \arg \min_{\|\mathbf{v}\|=1} L(\mathbf{z}_n^{(k)} + \eta \mathbf{v}) \approx \arg \min_{\|\mathbf{v}\|=1} \left\{ L(\mathbf{z}_n^{(k)}) + \eta \mathbf{v}^\top \nabla L(\mathbf{z}_n^{(k)}) \right\}.$$

This approach is known as the *greedy search*. The optimal \mathbf{v} can be obtained by

$$\mathbf{v} = - \frac{\nabla L(\mathbf{z}_n^{(k)})}{\|\nabla L(\mathbf{z}_n^{(k)})\|},$$

i.e., \mathbf{v} points in the opposite direction of $\nabla L(\mathbf{z}_n^{(k)})$. Therefore, it is reasonable to update $\mathbf{z}_n^{(k+1)}$ as follows:

$$\mathbf{z}_n^{(k+1)} = \mathbf{z}_n^{(k)} + \eta \mathbf{v} = \mathbf{z}_n^{(k)} - \eta \frac{\nabla L(\mathbf{z}_n^{(k)})}{\|\nabla L(\mathbf{z}_n^{(k)})\|},$$

which is usually called the *gradient descent* (GD). Similarly, the gradient descent for $\mathbf{w}_m^{(k+1)}$ is given by

$$\mathbf{w}_m^{(k+1)} = \mathbf{w}_m^{(k)} + \eta \mathbf{v} = \mathbf{w}_m^{(k)} - \eta \frac{\nabla L(\mathbf{w}_m^{(k)})}{\|\nabla L(\mathbf{w}_m^{(k)})\|}.$$

The revised procedure for Algorithm 2 employing a gradient descent approach is presented in Algorithm 4.

Geometrical interpretation of gradient descent.

Lemma 4.8: (Direction of Gradients)

An important fact is that gradients of variables given a loss function are perpendicular to level curves (a.k.a., level surfaces).

Algorithm 4 Alternating Least Squares with Full Entries and Gradient Descent**Require:** Matrix $\mathbf{A} \in \mathbb{R}^{M \times N}$;

- 1: Initialize $\mathbf{W} \in \mathbb{R}^{M \times K}$, $\mathbf{Z} \in \mathbb{R}^{K \times N}$ randomly without condition on the rank and the relationship between M, N, K ;
- 2: Choose a stop criterion on the approximation error δ ;
- 3: Choose regularization parameters λ_w, λ_z , and step size η_w, η_z ;
- 4: Choose the maximal number of iterations C ;
- 5: $iter = 0$; ▷ Count for the number of iterations
- 6: **while** $\|\mathbf{A} - (\mathbf{W}\mathbf{Z})\|^2 > \delta$ and $iter < C$ **do**
- 7: $iter = iter + 1$;
- 8: **for** $n = 1, 2, \dots, N$ **do**
- 9: $\mathbf{z}_n^{(k+1)} = \mathbf{z}_n^{(k)} - \eta_z \frac{\nabla L(\mathbf{z}_n^{(k)})}{\|\nabla L(\mathbf{z}_n^{(k)})\|}$; ▷ n -th column of \mathbf{Z}
- 10: **end for**
- 11: **for** $m = 1, 2, \dots, M$ **do**
- 12: $\mathbf{w}_m^{(k+1)} = \mathbf{w}_m^{(k)} - \eta_w \frac{\nabla L(\mathbf{w}_m^{(k)})}{\|\nabla L(\mathbf{w}_m^{(k)})\|}$; ▷ m -th column of \mathbf{W}^\top
- 13: **end for**
- 14: **end while**
- 15: Output $\mathbf{W}^\top = [\mathbf{w}_1, \mathbf{w}_2, \dots, \mathbf{w}_M]$, $\mathbf{Z} = [\mathbf{z}_1, \mathbf{z}_2, \dots, \mathbf{z}_N]$;

Proof [of Lemma 4.8] This is equivalent to proving that the gradient is orthogonal to the tangent of the level curve. For simplicity, let's first look at the two-dimensional case. Suppose the level curve takes the form $f(x, y) = c$. This implicitly establishes a relationship between x and y such that $y = y(x)$, where y can be regarded as a function of x . Therefore, the level curve can be expressed as

$$f(x, y(x)) = c.$$

The chain rule indicates

$$\frac{\partial f}{\partial x} \underbrace{\frac{dx}{dx}}_{=1} + \frac{\partial f}{\partial y} \frac{dy}{dx} = 0.$$

Therefore, the gradient is perpendicular to the tangent:

$$\left\langle \frac{\partial f}{\partial x}, \frac{\partial f}{\partial y} \right\rangle \cdot \left\langle \frac{dx}{dx}, \frac{dy}{dx} \right\rangle = 0.$$

In full generality, consider the level curve of a vector $\mathbf{x} \in \mathbb{R}^n$: $f(\mathbf{x}) = f(x_1, x_2, \dots, x_n) = c$. Each variable x_i can be regarded as a function of a variable t on the level curve $f(\mathbf{x}) = c$: $f(x_1(t), x_2(t), \dots, x_n(t)) = c$. Differentiate the equation with respect to t using chain rule:

$$\frac{\partial f}{\partial x_1} \frac{dx_1}{dt} + \frac{\partial f}{\partial x_2} \frac{dx_2}{dt} + \dots + \frac{\partial f}{\partial x_n} \frac{dx_n}{dt} = 0.$$

Therefore, the gradient is perpendicular to the tangent in the n -dimensional case:

$$\left\langle \frac{\partial f}{\partial x_1}, \frac{\partial f}{\partial x_2}, \dots, \frac{\partial f}{\partial x_n} \right\rangle \cdot \left\langle \frac{dx_1}{dt}, \frac{dx_2}{dt}, \dots, \frac{dx_n}{dt} \right\rangle = 0.$$

This completes the proof. ■

The lemma reveals the geometrical interpretation of gradient descent. When seeking a solution to minimize a convex function $L(\mathbf{z})$, gradient descent proceeds in the direction opposite to the gradient, which leads to a reduction in the loss. Figure 4.2 depicts a two-dimensional case, where $-\nabla L(\mathbf{z})$ pushes the loss to decrease for the convex function $L(\mathbf{z})$.

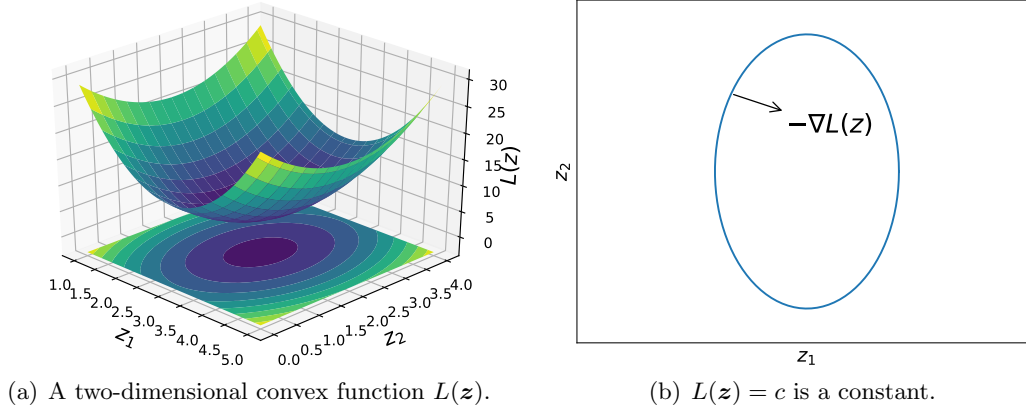


Figure 4.2: Figure 4.2(a) shows surface and contour plots for a specific function (blue=low, yellow=high), where the upper graph is the surface plot, and the lower one is the projection of it (i.e., contour). Figure 4.2(b): $-\nabla L(\mathbf{z})$ pushes the loss to decrease for the convex function $L(\mathbf{z})$.

4.7. Regularization: A Geometrical Interpretation

In Section 4.3, we discussed how regularization can extend the ALS algorithm to general matrices. Gradient descent can reveal the geometrical meaning of the regularization. To avoid confusion, we denote the loss function without regularization as $l(\mathbf{z})$ and the loss with regularization as $L(\mathbf{z}) = l(\mathbf{z}) + \lambda_z \|\mathbf{z}\|^2$, where $l(\mathbf{z}) : \mathbb{R}^n \rightarrow \mathbb{R}$. When minimizing $l(\mathbf{z})$, a descent method searches for a solution in \mathbb{R}^n . However, in machine learning, searching across the entire space \mathbb{R}^n can lead to overfitting. A partial solution is to search within a subset of the vector space, e.g., searching in $\mathbf{z}^\top \mathbf{z} \leq C$ for some constant C . That is,

$$\arg \min_{\mathbf{z}} l(\mathbf{z}), \quad \text{s.t.,} \quad \mathbf{z}^\top \mathbf{z} \leq C.$$

As demonstrated above, a basic gradient descent method will go further in the direction of $-\nabla l(\mathbf{z})$, i.e., update \mathbf{z} as $\mathbf{z} \leftarrow \mathbf{z} - \eta \nabla l(\mathbf{z})$ for a small step size η . When the level curve is $l(\mathbf{z}) = c_1$ and the current position of parameter \mathbf{z} is $\mathbf{z} = \mathbf{z}_1$, where \mathbf{z}_1 is the intersection of $\mathbf{z}^\top \mathbf{z} = C$ and $l(\mathbf{z}) = c_1$, the descent direction $-\nabla l(\mathbf{z}_1)$ will be perpendicular to the level curve of $l(\mathbf{z}_1) = c_1$, as shown in the left picture of Figure 4.3 (by Lemma 4.8). However, if we further restrict that the optimal value must lie within $\mathbf{z}^\top \mathbf{z} \leq C$, the trivial descent direction $-\nabla l(\mathbf{z}_1)$ will lead the update $\mathbf{z}_2 = \mathbf{z}_1 - \eta \nabla l(\mathbf{z}_1)$ beyond the boundary of $\mathbf{z}^\top \mathbf{z} \leq C$.

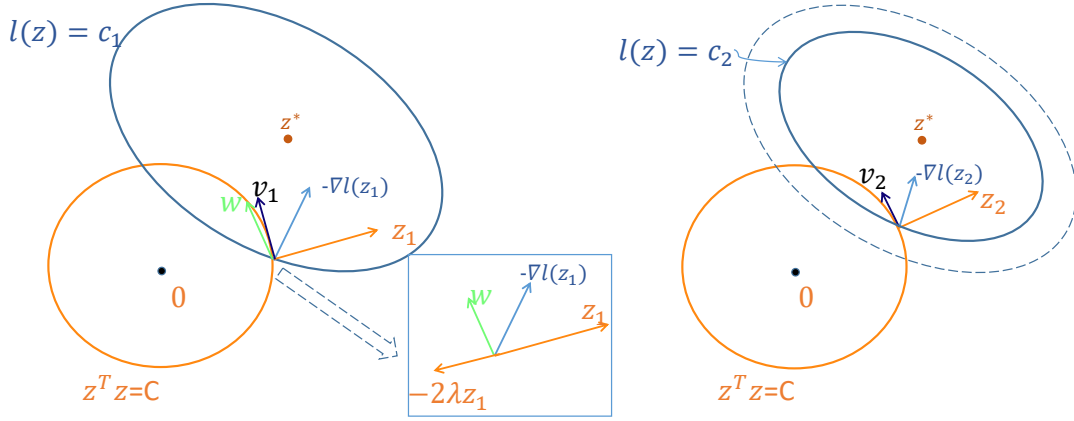


Figure 4.3: Constrained gradient descent with $\mathbf{z}^\top \mathbf{z} \leq C$. The green vector \mathbf{w} represents the projection of \mathbf{v}_1 into $\mathbf{z}^\top \mathbf{z} \leq C$, where \mathbf{v}_1 is the component of $-\nabla l(\mathbf{z})$ that is perpendicular to \mathbf{z}_1 . The image on the right illustrates the next step after the update in the left picture. \mathbf{z}^* denotes the optimal solution of $\{\min l(\mathbf{z})\}$.

One solution is to decompose the step $-\nabla l(\mathbf{z}_1)$ into

$$-\nabla l(\mathbf{z}_1) = a\mathbf{z}_1 + \mathbf{v}_1,$$

where $a\mathbf{z}_1$ represents the component perpendicular to the curve of $\mathbf{z}^\top \mathbf{z} = C$, and \mathbf{v}_1 is the component parallel to the curve of $\mathbf{z}^\top \mathbf{z} = C$. Keep only the step \mathbf{v}_1 , then the update is

$$\mathbf{z}_2 = \text{project}(\mathbf{z}_1 + \eta\mathbf{v}_1) = \text{project}\left(\mathbf{z}_1 + \eta \underbrace{(-\nabla l(\mathbf{z}_1) - a\mathbf{z}_1)}_{\mathbf{v}_1}\right),^6$$

which will lead to a smaller loss from $l(\mathbf{z}_1)$ to $l(\mathbf{z}_2)$, and it still matches the prerequisite of $\mathbf{z}^\top \mathbf{z} \leq C$. This approach is known as the *projection gradient descent*. It is not hard to see that the update $\mathbf{z}_2 = \text{project}(\mathbf{z}_1 + \eta\mathbf{v}_1)$ can be understood as finding a vector \mathbf{w} (represented by the green vector in the left picture of Figure 4.3) such that $\mathbf{z}_2 = \mathbf{z}_1 + \mathbf{w}$ lies inside the curve of $\mathbf{z}^\top \mathbf{z} \leq C$. Mathematically, the \mathbf{w} can be determined as $-\nabla l(\mathbf{z}_1) - 2\lambda\mathbf{z}_1$ for some λ , as shown in the middle picture of Figure 4.3. This is precisely the negative gradient of $L(\mathbf{z}) = l(\mathbf{z}) + \lambda\|\mathbf{z}\|^2$ such that

$$-\nabla L(\mathbf{z}) = -\nabla l(\mathbf{z}) - 2\lambda\mathbf{z},$$

and

$$\mathbf{w} = -\nabla L(\mathbf{z}) \quad \text{leads to} \quad \mathbf{z}_2 = \mathbf{z}_1 + \mathbf{w} = \mathbf{z}_1 - \nabla L(\mathbf{z}).$$

And in practice, a small step size η prevents the trajectory from moving outside the curve of $\mathbf{z}^\top \mathbf{z} \leq C$:

$$\mathbf{z}_2 = \mathbf{z}_1 - \eta\nabla L(\mathbf{z}),$$

which is exactly what we have discussed in Section 4.3, the regularization term.

6. where the operation $\text{project}(\mathbf{x})$ will project the vector \mathbf{x} to the closest point inside $\mathbf{z}^\top \mathbf{z} \leq C$. Notice here the unprojected update $\mathbf{z}_2 = \mathbf{z}_1 + \eta\mathbf{v}_1$ can still make \mathbf{z}_2 fall outside the curve of $\mathbf{z}^\top \mathbf{z} \leq C$.

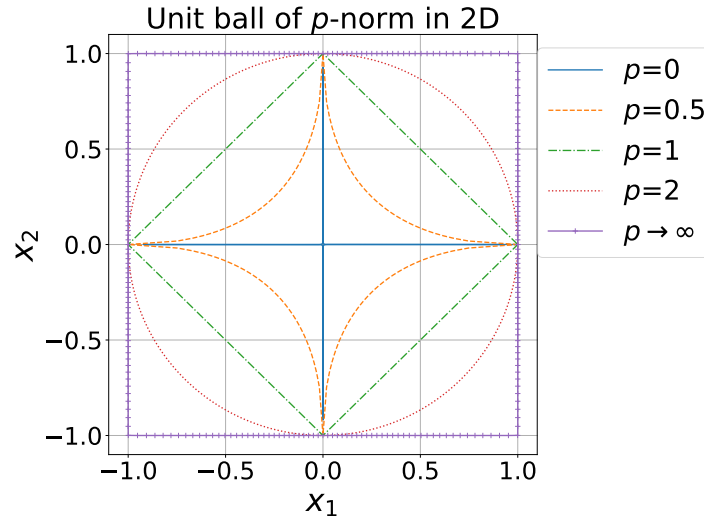


Figure 4.4: Unit ball of ℓ_p norm in two-dimensional space. The ℓ_p norm over a vector \mathbf{x} is defined as $L_p(\mathbf{x}) = (\sum_i |x_i|^p)^{1/p}$. When $p < 1$, the metric is not a norm since it does not meet the triangle inequality property of a norm definition.

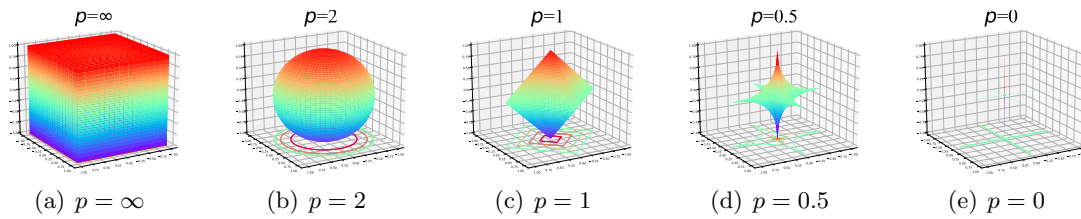


Figure 4.5: Unit ball of ℓ_p norm in three-dimensional space. When $p < 1$, the metric is not a norm since it does not meet the triangle inequality property of a norm definition.

Sparsity. In rare cases, we seek to identify a sparse solution \mathbf{z} such that $l(\mathbf{z})$ is minimized. Regularization to be constrained in $\|\mathbf{z}\|_1 \leq C$ exists to this purpose, where $\|\cdot\|_1$ is the ℓ_1 norm of a vector or a matrix. Visualizations of the ℓ_1 norm in two and three-dimensional spaces are shown in Figure 4.4 and 4.5, respectively. Similar to the previous case, the ℓ_1 constrained optimization pushes the gradient descent towards the border of the level of $\|\mathbf{z}\|_1 = C$. The situation in the two-dimensional case is shown in Figure 4.6. In a high-dimensional case, many elements in \mathbf{z} will be pushed towards the breakpoint of $\|\mathbf{z}\|_1 = C$, as shown in the right picture of Figure 4.6.

4.8. Stochastic Gradient Descent

The gradient descent method is a valuable optimization algorithm; however, it exhibits certain limitations in practical applications. To comprehend the issues associated with the gradient descent method, we consider the mean squared error (MSE) derived from

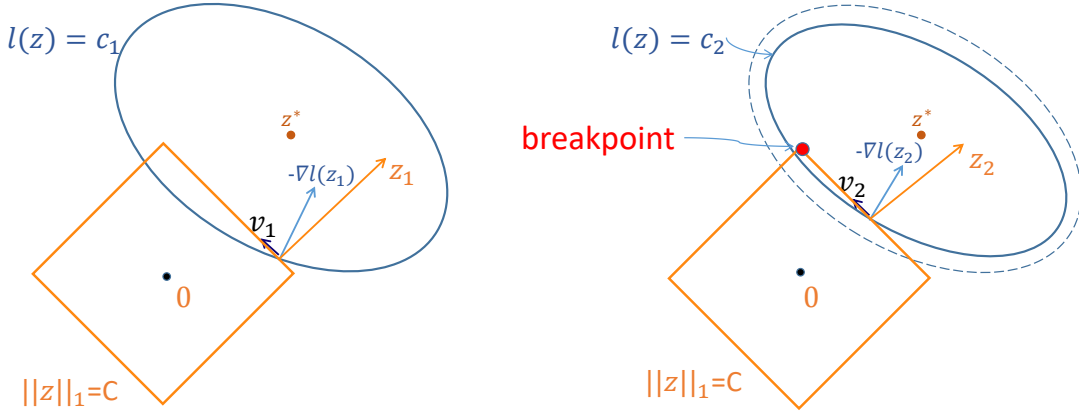


Figure 4.6: Constrained gradient descent with $\|z\|_1 \leq C$, where the red dot denotes the breakpoint in ℓ_1 norm. The right picture illustrates the next step after the update in the left picture. z^* denotes the optimal solution of $\{\min l(z)\}$.

Equation (4.2):

$$\frac{1}{MN} \min_{\mathbf{W}, \mathbf{Z}} \sum_{n=1}^N \sum_{m=1}^M (a_{mn} - \mathbf{w}_m^\top \mathbf{z}_n)^2. \quad (4.19)$$

The MSE needs to calculate the residual $e_{mn} = (a_{mn} - \mathbf{w}_m^\top \mathbf{z}_n)^2$ for each observed entry a_{mn} , representing the squared difference between predicted and actual values. The total sum of residual squares is denoted by $e = \sum_{m,n=1}^{MN} e_{mn}$. In cases with a substantial number of training entries (i.e., large MN), the entire computation process becomes notably slow. Additionally, the gradients from different input samples may cancel out, resulting in small changes in the final update. To address these challenges, researchers have enhanced the gradient descent method with the *stochastic gradient descent (SGD)* method (Lu, 2022d). The core idea of the stochastic gradient descent method is to randomly select a single sample from all training samples during each iteration.

We consider again the per-example loss:

$$L(\mathbf{W}, \mathbf{Z}) = \sum_{n=1}^N \sum_{m=1}^M (a_{mn} - \mathbf{w}_m^\top \mathbf{z}_n)^2 + \lambda_w \sum_{m=1}^M \|\mathbf{w}_m\|^2 + \lambda_z \sum_{n=1}^N \|\mathbf{z}_n\|^2.$$

As we iteratively reduce the per-example loss term $l(\mathbf{w}_m, \mathbf{z}_n) = (a_{mn} - \mathbf{w}_m^\top \mathbf{z}_n)^2$ for all $m \in \{1, 2, \dots, M\}, n \in \{1, 2, \dots, N\}$, the overall loss $L(\mathbf{W}, \mathbf{Z})$ decreases accordingly. This process is also known as the *stochastic coordinate descent*. The gradients with respect to

\mathbf{w}_m and \mathbf{z}_n , and their roots are given by

$$\left\{ \begin{array}{l} \nabla l(\mathbf{z}_n) = \frac{\partial l(\mathbf{w}_m, \mathbf{z}_n)}{\partial \mathbf{z}_n} = 2\mathbf{w}_m \mathbf{w}_m^\top \mathbf{z}_n + 2\lambda_w \mathbf{w}_m - 2a_{mn} \mathbf{w}_m \\ \quad \text{leads to } \mathbf{z}_n = a_{mn} (\mathbf{w}_m \mathbf{w}_m^\top + \lambda_z \mathbf{I})^{-1} \mathbf{w}_m; \\ \nabla l(\mathbf{w}_m) = \frac{\partial l(\mathbf{w}_m, \mathbf{z}_n)}{\partial \mathbf{w}_m} = 2\mathbf{z}_n \mathbf{z}_n^\top \mathbf{w}_m + 2\lambda_w \mathbf{z}_n - 2a_{mn} \mathbf{z}_n \\ \quad \text{leads to } \mathbf{w}_m = a_{mn} (\mathbf{z}_n \mathbf{z}_n^\top + \lambda_w \mathbf{I})^{-1} \mathbf{z}_n. \end{array} \right.$$

Or analogously, the update can be performed using gradient descent. Since we update based on the per-example loss, this approach is also known as the *stochastic gradient descent* (SGD):

$$\left\{ \begin{array}{l} \mathbf{z}_n = \mathbf{z}_n - \eta_z \frac{\nabla l(\mathbf{z}_n)}{\|\nabla l(\mathbf{z}_n)\|}; \\ \mathbf{w}_m = \mathbf{w}_m - \eta_w \frac{\nabla l(\mathbf{w}_m)}{\|\nabla l(\mathbf{w}_m)\|}. \end{array} \right.$$

The stochastic gradient descent update for ALS is formulated in Algorithm 5. And in practice, the values of m and n in the algorithm can be randomly generated, which is the reason for the term “*stochastic*.”

Algorithm 5 Alternating Least Squares with Full Entries and Stochastic Gradient Descent

Require: Matrix $\mathbf{A} \in \mathbb{R}^{M \times N}$;

- 1: Initialize $\mathbf{W} \in \mathbb{R}^{M \times K}$, $\mathbf{Z} \in \mathbb{R}^{K \times N}$ randomly without condition on the rank and the relationship between M, N, K ;
 - 2: Choose a stop criterion on the approximation error δ ;
 - 3: Choose regularization parameters λ_w, λ_z , and step size η_w, η_z ;
 - 4: Choose the maximal number of iterations C ;
 - 5: $iter = 0$; ▷ Count for the number of iterations
 - 6: **while** $\|\mathbf{A} - (\mathbf{W}\mathbf{Z})\|^2 > \delta$ and $iter < C$ **do**
 - 7: $iter = iter + 1$;
 - 8: **for** $n = 1, 2, \dots, N$ **do**
 - 9: **for** $m = 1, 2, \dots, M$ **do** ▷ in practice, m, n can be randomly produced
 - 10: $\mathbf{z}_n = \mathbf{z}_n - \eta_z \frac{\nabla l(\mathbf{z}_n)}{\|\nabla l(\mathbf{z}_n)\|}$; ▷ n -th column of \mathbf{Z}
 - 11: $\mathbf{w}_m = \mathbf{w}_m - \eta_w \frac{\nabla l(\mathbf{w}_m)}{\|\nabla l(\mathbf{w}_m)\|}$; ▷ m -th column of \mathbf{W}^\top
 - 12: **end for**
 - 13: **end for**
 - 14: **end while**
 - 15: Output $\mathbf{W}^\top = [\mathbf{w}_1, \mathbf{w}_2, \dots, \mathbf{w}_M]$, $\mathbf{Z} = [\mathbf{z}_1, \mathbf{z}_2, \dots, \mathbf{z}_N]$;
-

4.9. Bias Term

In ordinary least squares, a bias term is usually incorporated into the raw matrix, as illustrated in Equation (4.1). A similar idea can be applied to the ALS problem. We can

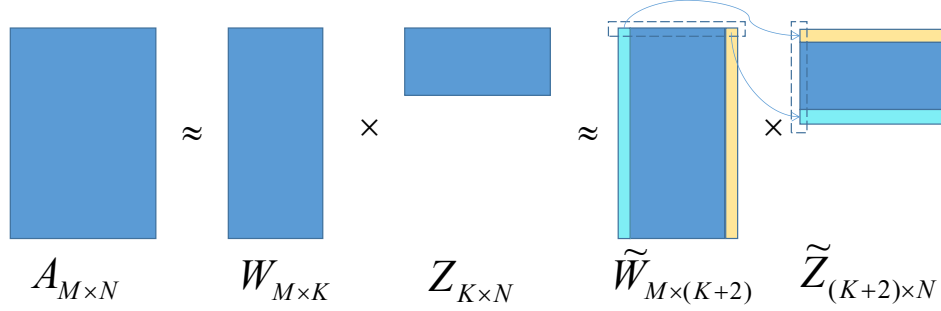


Figure 4.7: Bias terms in alternating least squares, where the **yellow** entries denote ones (which are fixed), and the **cyan** entries denote the added features to fit the bias terms. The dotted boxes provide an example of how the bias terms work.

append a fixed column filled with all 1's to the **last column** of \mathbf{W} , thus an extra row should be added to the last row of \mathbf{Z} to fit the features introduced by the bias term in \mathbf{W} . Analogously, a fixed row with all 1's can be added to the **first row** of \mathbf{Z} , and an extra column in the first column of \mathbf{W} can be added to fit the features. The situation is shown in Figure 4.7.

Following the loss with respect to the columns of \mathbf{Z} in Equation (4.17), suppose $\tilde{\mathbf{z}}_n = \begin{bmatrix} 1 \\ \mathbf{z}_n \end{bmatrix}$ is the n -th column of $\tilde{\mathbf{Z}}$, we have

$$\begin{aligned}
L(\mathbf{z}_n) &= \left\| \tilde{\mathbf{W}} \tilde{\mathbf{Z}} - \mathbf{A} \right\|^2 + \lambda_w \left\| \tilde{\mathbf{W}} \right\|^2 + \lambda_z \left\| \tilde{\mathbf{Z}} \right\|^2 \\
&= \left\| \tilde{\mathbf{W}} \begin{bmatrix} 1 \\ \mathbf{z}_n \end{bmatrix} - \mathbf{a}_n \right\|^2 + \underbrace{\lambda_z \|\tilde{\mathbf{z}}_n\|^2}_{=\lambda_z \|\mathbf{z}_n\|^2 + \lambda_z} + \sum_{i \neq n} \left\| \tilde{\mathbf{W}} \tilde{\mathbf{z}}_i - \mathbf{a}_i \right\|^2 + \lambda_z \sum_{i \neq n} \|\tilde{\mathbf{z}}_i\|^2 + \lambda_w \left\| \tilde{\mathbf{W}} \right\|^2 \\
&= \left\| \begin{bmatrix} \bar{\mathbf{w}}_0 & \bar{\mathbf{W}} \end{bmatrix} \begin{bmatrix} 1 \\ \mathbf{z}_n \end{bmatrix} - \mathbf{a}_n \right\|^2 + \lambda_z \|\mathbf{z}_n\|^2 + C_{z_n} = \left\| \bar{\mathbf{W}} \mathbf{z}_n - \underbrace{(\mathbf{a}_n - \bar{\mathbf{w}}_0)}_{\bar{\mathbf{a}}_n} \right\|^2 + \lambda_z \|\mathbf{z}_n\|^2 + C_{z_n},
\end{aligned} \tag{4.20}$$

where $\bar{\mathbf{w}}_0$ represents the first column of $\tilde{\mathbf{W}}$, $\bar{\mathbf{W}}$ denotes the last K columns of $\tilde{\mathbf{W}}$, and C_{z_n} is a constant with respect to \mathbf{z}_n . Let $\bar{\mathbf{a}}_n = \mathbf{a}_n - \bar{\mathbf{w}}_0$, the update for \mathbf{z}_n is just similar to the one in Equation (4.17), with the gradient given by

$$\nabla L(\mathbf{z}_n) = 2\bar{\mathbf{W}}^\top \bar{\mathbf{W}} \mathbf{z}_n - 2\bar{\mathbf{W}}^\top \bar{\mathbf{a}}_n + 2\lambda_z \mathbf{z}_n.$$

Therefore, the update for \mathbf{z}_n is given by determining the root of the gradient above:

$$\text{update for } \tilde{\mathbf{z}}_n \text{ is } \begin{cases} \mathbf{z}_n = (\bar{\mathbf{W}}^\top \bar{\mathbf{W}} + \lambda_z \mathbf{I})^{-1} \bar{\mathbf{W}}^\top \bar{\mathbf{a}}_n, & \text{for } n \in \{1, 2, \dots, N\}; \\ \tilde{\mathbf{z}}_n = \begin{bmatrix} 1 \\ \mathbf{z}_n \end{bmatrix}. \end{cases}$$



Figure 4.8: A gray flag image to be compressed. The size of the image is 600×1200 with a rank of 402.

Similarly, following the loss with respect to each row of \mathbf{W} in Equation (4.18), suppose $\tilde{\mathbf{w}}_m = \begin{bmatrix} \mathbf{w}_m \\ 1 \end{bmatrix}$ is the m -th row of $\tilde{\mathbf{W}}$ (or m -th column of $\tilde{\mathbf{W}}^\top$), we have

$$\begin{aligned}
& L(\mathbf{w}_m) \\
&= \left\| \tilde{\mathbf{Z}}^\top \tilde{\mathbf{W}} - \mathbf{A}^\top \right\|^2 + \lambda_w \left\| \tilde{\mathbf{W}}^\top \right\|^2 + \lambda_z \left\| \tilde{\mathbf{Z}} \right\|^2 \\
&= \left\| \tilde{\mathbf{Z}}^\top \tilde{\mathbf{w}}_m - \mathbf{b}_m \right\|^2 + \underbrace{\lambda_w \left\| \tilde{\mathbf{w}}_m \right\|^2}_{=\lambda_w \left\| \mathbf{w}_m \right\|^2 + \lambda_w} + \sum_{i \neq m} \left\| \tilde{\mathbf{Z}}^\top \tilde{\mathbf{w}}_i - \mathbf{b}_i \right\|^2 + \lambda_w \sum_{i \neq m} \left\| \tilde{\mathbf{w}}_i \right\|^2 + \lambda_z \left\| \tilde{\mathbf{Z}} \right\|^2 \\
&= \left\| \begin{bmatrix} \bar{\mathbf{Z}}^\top & \bar{z}_0 \end{bmatrix} \begin{bmatrix} \mathbf{w}_m \\ 1 \end{bmatrix} - \mathbf{b}_m \right\|^2 + \lambda_w \left\| \mathbf{w}_m \right\|^2 + C_{w_m} \\
&= \left\| \bar{\mathbf{Z}}^\top \mathbf{w}_m - (\mathbf{b}_m - \bar{z}_0) \right\|^2 + \lambda_w \left\| \mathbf{w}_m \right\|^2 + C_{w_m},
\end{aligned} \tag{4.21}$$

where \bar{z}_0 represents the last column of $\tilde{\mathbf{Z}}^\top$, $\bar{\mathbf{Z}}^\top$ contains the remaining columns of $\tilde{\mathbf{Z}}^\top$, C_{w_m} is a constant with respect to \mathbf{w}_m , and $\mathbf{W}^\top = [\mathbf{w}_1, \mathbf{w}_2, \dots, \mathbf{w}_M]$, $\mathbf{A}^\top = [\mathbf{b}_1, \mathbf{b}_2, \dots, \mathbf{b}_M]$ are the column partitions of \mathbf{W}^\top , \mathbf{A}^\top , respectively. Let $\bar{\mathbf{b}}_m = \mathbf{b}_m - \bar{z}_0$, the update for \mathbf{w}_m is again just similar to the one in Equation (4.18), with the gradient given by

$$\nabla L(\mathbf{w}_m) = 2\bar{\mathbf{Z}} \cdot \bar{\mathbf{Z}}^\top \mathbf{w}_m - 2\bar{\mathbf{Z}} \cdot \bar{\mathbf{b}}_m + 2\lambda_w \mathbf{w}_m.$$

Therefore, the update for \mathbf{w}_m is given by the root of the gradient above:

$$\text{update for } \tilde{\mathbf{w}}_m \text{ is } \begin{cases} \mathbf{w}_m = (\bar{\mathbf{Z}} \cdot \bar{\mathbf{Z}}^\top + \lambda_w \mathbf{I})^{-1} \bar{\mathbf{Z}} \cdot \bar{\mathbf{b}}_m, & \text{for } m \in \{1, 2, \dots, M\}; \\ \tilde{\mathbf{w}}_m = \begin{bmatrix} \mathbf{w}_m \\ 1 \end{bmatrix}. \end{cases}$$

Similar updates through gradient descent with the consideration of the bias terms or treatment on missing entries can be deduced, and we shall not repeat the details (see Section 4.6 and 4.4 for a reference).

4.10. Applications

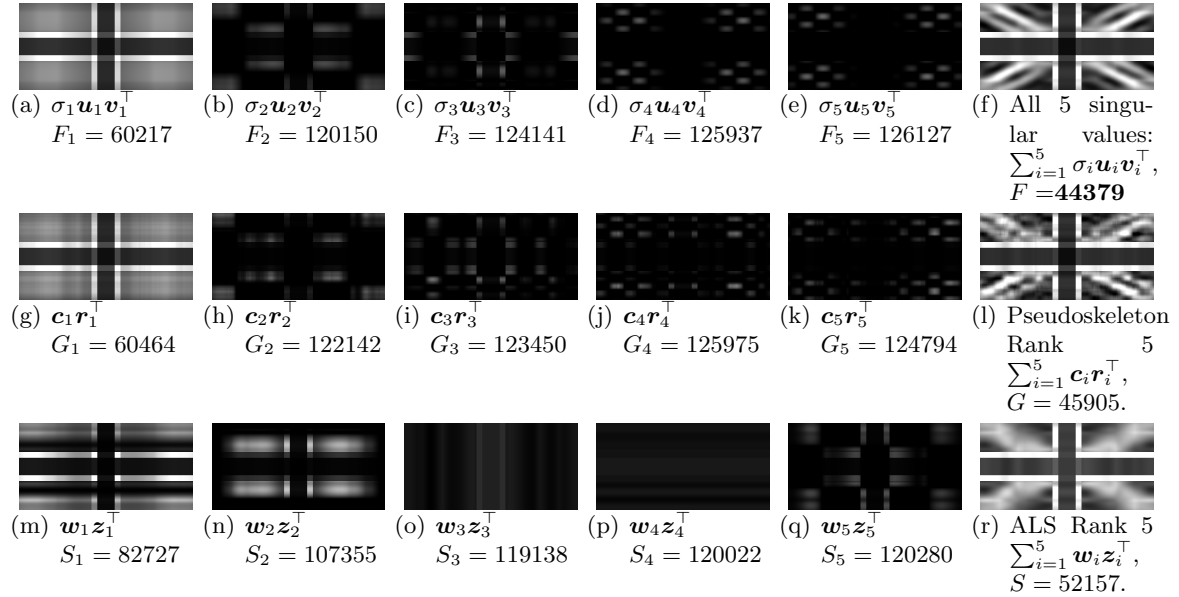


Figure 4.9: Image compression for gray flag image into a rank-5 matrix via the SVD, and decompose into 5 parts where $\sigma_1 \geq \sigma_2 \geq \dots \geq \sigma_5$, i.e., $F_1 \leq F_2 \leq \dots \leq F_5$ with $F_i = \|\sigma_i \mathbf{u}_i \mathbf{v}_i^\top - \mathbf{A}\|_F$ for $i \in \{1, 2, \dots, 5\}$. And reconstruct images by single singular value and its corresponding left and right singular vectors, $\mathbf{c}_i \mathbf{r}_i^\top$, $\mathbf{w}_i \mathbf{z}_i^\top$ respectively. **Upper:** SVD; **Middle:** Pseudoskeleton; **Lower:** ALS.

4.10.1 Low-Rank Approximation

Figure 4.8 shows an example of a gray image to be compressed. The size of the image is 600×1200 with a rank of 402. Low-rank approximation via the ALS decomposition, singular value decomposition (SVD), and Pseudoskeleton decomposition (Lu, 2021b) can be applied to find the compression.

In Figure 4.9(a) to 4.9(f), we approximate the image into a rank-5 matrix by *truncated SVD*: $\mathbf{A} \approx \sum_{i=1}^5 \sigma_i \mathbf{u}_i \mathbf{v}_i^\top$ (Lu, 2021b). It is known that the singular values contain the spectrum information with higher singular values containing lower-frequency information. And low-frequency contains more useful information (Leondes, 1995). We find that the image, $\sigma_1 \mathbf{u}_1 \mathbf{v}_1^\top$, reconstructed by the first singular value σ_1 , first left singular vector \mathbf{u}_1 , and first right singular vector \mathbf{v}_1 is very close to the original flag image; and second to the fifth images reconstructed by the corresponding singular values and singular vectors contains more details of the flag to reconstruct the raw image.

Similar results can be observed for the low-rank approximation via the pseudoskeleton decomposition (See Lu (2021b) for more details). At a high level, the pseudoskeleton decomposition finds the low-rank approximation by $\mathbf{A} \approx \mathbf{C}\mathbf{R}$, where $\mathbf{C} \in \mathbb{R}^{m \times \gamma}$ and $\mathbf{R} \in \mathbb{R}^{\gamma \times n}$ if

$\mathbf{A} \in \mathbb{R}^{m \times n}$ such that \mathbf{C} and \mathbf{R} are rank- γ matrices. Suppose $\gamma = 5$, and

$$\mathbf{C} = [\mathbf{c}_1, \mathbf{c}_2, \dots, \mathbf{c}_5], \quad \text{and} \quad \mathbf{R} = \begin{bmatrix} \mathbf{r}_1^\top \\ \mathbf{r}_2^\top \\ \vdots \\ \mathbf{r}_5^\top \end{bmatrix},$$

are the column and row partitions of \mathbf{C} and \mathbf{R} , respectively. Then \mathbf{A} can be approximated by $\sum_{i=1}^5 \mathbf{c}_i \mathbf{r}_i^\top$. The partitions are ordered such that

$$\underbrace{\|\mathbf{c}_1 \mathbf{r}_1^\top - \mathbf{A}\|_F}_{G_1} \leq \underbrace{\|\mathbf{c}_2 \mathbf{r}_2^\top - \mathbf{A}\|_F}_{G_2} \leq \dots \leq \underbrace{\|\mathbf{c}_5 \mathbf{r}_5^\top - \mathbf{A}\|_F}_{G_5}.$$

We observe (in Figure 4.9(g) to 4.9(l)) that $\mathbf{c}_1 \mathbf{r}_1^\top$ works similarly to that of $\sigma_1 \mathbf{u}_1 \mathbf{v}^\top$, where the reconstruction errors measured by the Frobenius norm are very close (60,464 in the pseudoskeleton case compared to that of 60,217 in the SVD case). This is partly because the pseudoskeleton decomposition relies on the SVD such that $\mathbf{c}_1 \mathbf{r}_1^\top$ internally has the largest “singular value” meaning in this sense (Lu, 2021b).

Similarly, the ALS approximation is given by $\mathbf{A} \approx \mathbf{WZ}$, where $\mathbf{W} \in \mathbb{R}^{m \times \gamma}$ and $\mathbf{Z} \in \mathbb{R}^{\gamma \times n}$ if $\mathbf{A} \in \mathbb{R}^{m \times n}$ such that \mathbf{W} and \mathbf{Z} are rank- γ matrices. Suppose

$$\mathbf{W} = [\mathbf{w}_1, \mathbf{w}_2, \dots, \mathbf{w}_5] \quad \text{and} \quad \mathbf{Z} = \begin{bmatrix} \mathbf{z}_1^\top \\ \mathbf{z}_2^\top \\ \vdots \\ \mathbf{z}_5^\top \end{bmatrix},$$

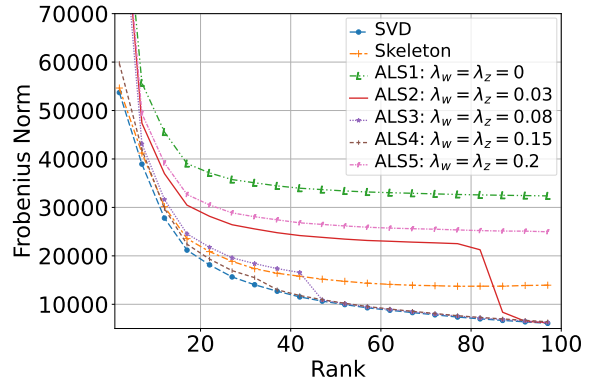
are the column and row partitions of \mathbf{W} and \mathbf{Z} , respectively⁷. Then \mathbf{A} can be approximated by $\sum_{i=1}^5 \mathbf{w}_i \mathbf{z}_i^\top$. The partitions are ordered such that

$$\underbrace{\|\mathbf{w}_1 \mathbf{z}_1^\top - \mathbf{A}\|_F}_{S_1} \leq \underbrace{\|\mathbf{w}_2 \mathbf{z}_2^\top - \mathbf{A}\|_F}_{S_2} \leq \dots \leq \underbrace{\|\mathbf{w}_5 \mathbf{z}_5^\top - \mathbf{A}\|_F}_{S_5}.$$

We observe (in Figure 4.9(m) to 4.9(r)) that $\mathbf{w}_1 \mathbf{z}_1^\top$ works slightly **differently** to that of $\sigma_1 \mathbf{u}_1 \mathbf{v}^\top$, where the reconstruction errors measured by Frobenius norm are not close as well (82,727 in the ALS case compared to that of 60,217 in the SVD case). As we mentioned previously, $\mathbf{c}_1 \mathbf{r}_1^\top$ works similarly to that of $\sigma_1 \mathbf{u}_1 \mathbf{v}^\top$ since the pseudoskeleton relies on the SVD. However, in ALS, the reconstruction is all from least squares optimization. The key difference between ALS and SVD is in the fact that, in SVD, the importance of each vector in the basis is relative to the value of the singular value associated with that vector. This usually means that the first vector of the basis dominates and is the most used vector to reconstruct data; then the second vector and so on. So the bases in SVD have an implicit hierarchy and that doesn’t happen in ALS, where we find the second component $\mathbf{w}_2 \mathbf{z}_2^\top$ via ALS in Figure 4.9(n) plays an important role in the reconstruction of the original figure; whereas the second component $\sigma_2 \mathbf{u}_2 \mathbf{v}_2^\top$ via SVD in Figure 4.9(b) plays a small role in the reconstruction.

7. For simplicity, note that this definition is different from what we have defined in Section 4.2, where we define \mathbf{w}_i ’s as the rows of \mathbf{W} .

Figure 4.10: Comparison of reconstruction errors measured by Frobenius norm among the SVD, pseudoskeleton, and ALS, where the approximated rank ranges from 3 to 100. ALS with well-selected parameters works similarly to SVD.



We finally compare low-rank approximation among the SVD, pseudoskeleton, and ALS with different ranks (3 to 100). Figure 4.11 shows the difference of each compression with rank 90, 60, 30, 10. We observe that the SVD reconstructs well with rank 90, 60, 30. The pseudoskeleton approximation compresses well in the black horizontal and vertical lines in the image. But it performs poorly in the details of the flag. ALS works similarly to the SVD in terms of visual expression and reconstruction errors measured by the Frobenius norm. Figure 4.10 shows the comparison of the reconstruction errors among the SVD, the pseudoskeleton, and the ALS approximations measured by the Frobenius norm ranging from rank 3 to 100, where we find in all cases, the truncated SVD performs best in terms of Frobenius norm. Similar results can be observed when applied to the spectral norm. The ALS works better than the pseudoskeleton decomposition when $\lambda_w = \lambda_z = 0.15$. An interesting cutoff happens when $\lambda_w = \lambda_z = \{0.03, 0.08, 0.15\}$. That is, when the value of rank increases, the ALS will be very close to the SVD in the sense of low-rank approximation.

4.10.2 Movie Recommender

The ALS is extensively developed for the movie recommender system. To see this, we obtain the “MovieLens 100K” data set from MovieLens (Harper and Konstan, 2015)⁸. It consists of 100,000 ratings from 943 users on 1,682 movies. The rating values go from 0 to 5. The data was collected through the MovieLens website during the seven-month period from September 19th, 1997 through April 22nd, 1998. This data has been cleaned up—users who had less than 20 ratings or did not have complete demographic information were removed from this data set such that simple demographic info for the users (age, gender, occupation, zip) can be obtained. However, we will only work on the trivial rating matrix⁹.

The data set is split into training and validation data, around 95,015 and 4,985 ratings, respectively. The error is measured by *root mean squared error (RMSE)*. The RMSE is frequently used as a measure of the difference between values. For a set of values

8. <http://grouplens.org>

9. In the next chapters, the data set is further cleaned by removing movies with less than 3 users such that 1,473 movies are kept accordingly.

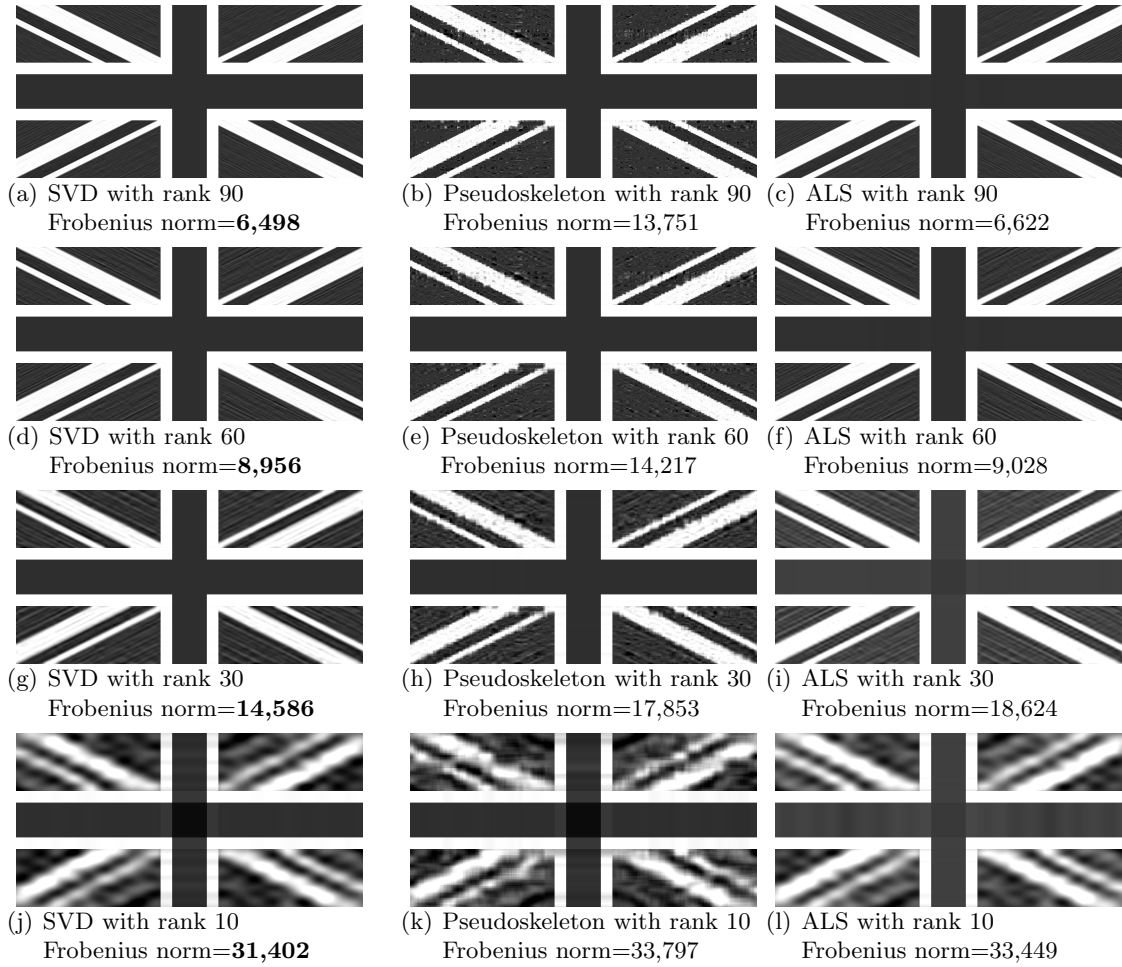


Figure 4.11: Image compression for gray flag image with different ranks.

$\{x_1, x_2, \dots, x_n\}$ and its predictions $\{\hat{x}_1, \hat{x}_2, \dots, \hat{x}_n\}$, the RMSE can be described as

$$\text{RMSE}(\mathbf{x}, \hat{\mathbf{x}}) = \sqrt{\frac{1}{n} \sum_{i=1}^n (x_i - \hat{x}_i)^2}.$$

The minimal RMSE for validation is obtained when $K = 185$ and $\lambda_w = \lambda_z = 0.15$, and it is equal to 0.806 as shown in Figure 4.12. Therefore, when the rating ranges from 0 to 5, the ALS at least can predict whether the user likes to watch the movie (e.g., ranges 4 to 5) or not (e.g., ranges 0 to 2).

Recommender 1. A recommender system can work simply by suggesting the movie m when $a_{mn} \geq 4$ if user n has not rated the movie m .

Recommender 2. Or in rare cases, it happens that the user n has rated all the movies he likes (say rates ≥ 4). Then a partial solution is to find out similar movies to the high-rated movies to recommend. Suppose user n likes movie m very much and he has rated the

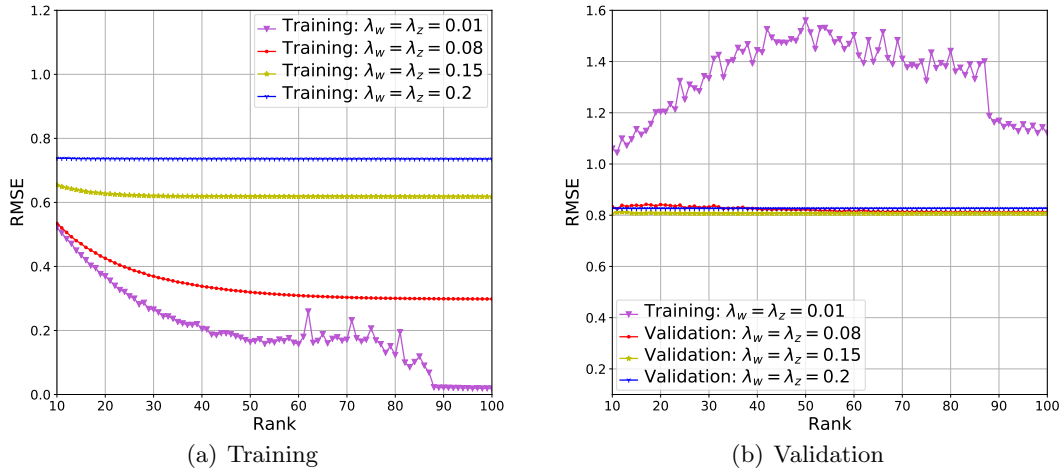


Figure 4.12: Comparison of training and validation error for “MovieLens 100K” data set with different reduction dimensions and regularization parameters.

movie m with 5: $a_{mn} = 5$. Under the ALS approximation $\mathbf{A} = \mathbf{W}\mathbf{Z}$, where each row of \mathbf{W} represents the hidden features of each movie (see Section 4.5 on the vector inner product), the solution is given by finding the most similar movies to movie m that user n has not rated (or watched). In mathematical language,

$$\arg \max_{\mathbf{w}_i} \text{similarity}(\mathbf{w}_i, \mathbf{w}_m), \quad \text{for all } i \notin \mathbf{o}_n,$$

where \mathbf{w}_i 's are the rows of \mathbf{W} representing the hidden feature of movie i , and \mathbf{o}_n is a mask vector indicating the movies that user n has rated.

The method above relies on the similarity function between two vectors. The *cosine similarity* is the most commonly used measure. It is defined as the cosine of the angle between the two vectors:

$$\cos(\mathbf{x}, \mathbf{y}) = \frac{\mathbf{x}^\top \mathbf{y}}{\|\mathbf{x}\| \cdot \|\mathbf{y}\|},$$

where the value ranges from -1 to 1 , with -1 representing perfectly dissimilar and 1 being perfectly similar. Based on this definition, it follows that the cosine similarity depends only on the angle between the two nonzero vectors, but not on their magnitudes since it can be regarded as the inner product between the normalized versions of these vectors. Another measure for calculating similarity is known as the *Pearson similarity*:

$$\text{Pearson}(\mathbf{x}, \mathbf{y}) = \frac{\text{Cov}(\mathbf{x}, \mathbf{y})}{\sigma_x \cdot \sigma_y} = \frac{\sum_{i=1}^n (x_i - \bar{x})(y_i - \bar{y})}{\sqrt{\sum_{i=1}^n (x_i - \bar{x})^2} \sqrt{\sum_{i=1}^n (y_i - \bar{y})^2}},$$

whose range varies between -1 and 1 , where -1 is perfectly dissimilar, 1 is perfectly similar, and 0 indicates no linear relationship. The Pearson similarity is usually used to measure the linear correlation between two sets of data. It is calculated as the ratio between the covariance of two variables and the product of their standard deviations.

Both Pearson correlation and cosine similarity are used in various fields, including machine learning and data analysis. Pearson correlation is commonly used in regression analysis, while cosine similarity is commonly used in recommendation systems and information

retrieval, as we will see the cosine similarity performs better in the *precision-recall (PR) curve* analysis.

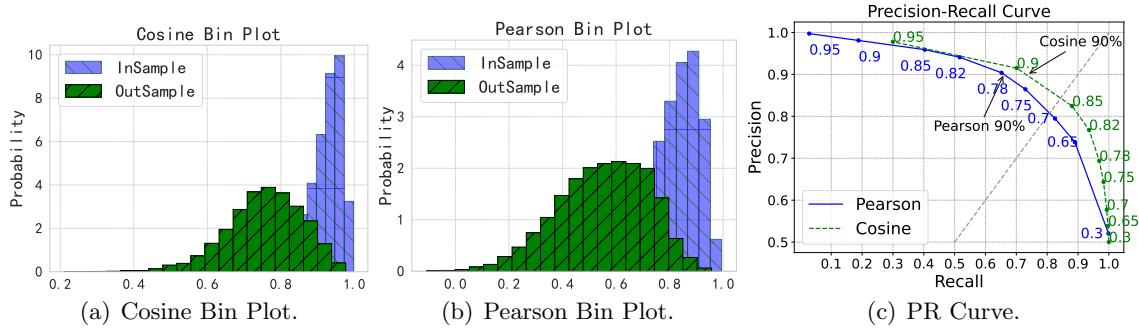


Figure 4.13: Distribution of the insample and outsample using cosine and Pearson similarity, and the Precision-Recall curves for them.

Building upon the previous example using the MovieLens 100K data set, we choose $\lambda_w = \lambda_z = 0.15$ for regularization and a rank of 62 to minimize RMSE. We want to look at the similarity between different movie hidden vectors, and the goal is to see whether the matrix factorization can help differentiate high-rated from low-rated movies, so that the system can recommend the movies correlated to the existing high-rated movies for each user. Define further the term “insample” as the similarity between the movies having rates 5 for each user, and “outsample” as the similarity between the movies having rates 5 and 1 for each user. Figure 4.13(a) and 4.13(b) depict the bin plots of the distributions of insample and outsample under cosine and Pearson similarities, respectively. In both scenarios, a clear distinction is observed between the distributions of the “insample” and “outsample” data, showing that the ALS decomposition can actually find the hidden features of different movies for each user. Figure 4.13(c) shows the *precision-recall (PR) curve* for these scenarios, where we find the cosine similarity works better such that it can find out more than 73% of the potential high-rated movies with a precision of 90%. However, Pearson similarity can identify only about 64% of the high-rated movies with the same precision. In practice, other measures can also be explored, such as the *negative Euclidean distance*, in which case the Euclidean distance can measure the “dissimilarity” between two vectors; and a negative one thus represents the similarity between them.

Chapter 4 Problems

1. Prove Lemma 4.7.
2. Find the update of column-by-column fashion for Algorithm 2.
3. **Constrained (Regularized) least squares (CLS).** Given $\mathbf{A} \in \mathbb{R}^{m \times n}$, $\mathbf{b} \in \mathbb{R}^n$, $\mathbf{B} \in \mathbb{R}^{p \times n}$, and $\lambda \in \mathbb{R}_{++}$, we consider the regularized least squares problem

$$\min_{\mathbf{x} \in \mathbb{R}^n} \|\mathbf{Ax} - \mathbf{b}\|^2 + \lambda \|\mathbf{Bx}\|^2.$$

Show that the constrained least squares (CLS) problem has a unique solution if and only if $\mathcal{N}(\mathbf{A}) \cap \mathcal{N}(\mathbf{B}) = \{\mathbf{0}\}$.

4. **Weighted least squares (WLS).** Going further from the assumptions in Lemma 4.1, we consider further that each data point $i \in \{1, 2, \dots, m\}$ (i.e., each row of \mathbf{A}) has a weight w_i . This means some data points may carry greater significance than others and there are ways to produce approximate minimizers that reflect this. Show that the value $\mathbf{x}_{WLS} = (\mathbf{A}^\top \mathbf{W}^2 \mathbf{A})^{-1} \mathbf{A}^\top \mathbf{W}^2 \mathbf{b}$ serves as the *weighted least squares (WLS)* estimator of \mathbf{x} , where $\mathbf{W} = \text{diag}([w_1, w_2, \dots, w_m]) \in \mathbb{R}^{m \times m}$. *Hint: find the normal equation for this problem.*
5. **Restricted least squares (RLS).** Going further from the assumptions in Lemma 4.1, we consider further the restriction $\mathbf{x} = \mathbf{C}\boldsymbol{\gamma} + \mathbf{c}$, where $\mathbf{C} \in \mathbb{R}^{n \times k}$ is a known matrix such that $\mathbf{A}\mathbf{C}$ has full rank, \mathbf{c} is a known vector, and $\boldsymbol{\gamma}$ is an unknown vector. Show that the value $\mathbf{x}_{RLS} = \mathbf{C}(\mathbf{C}^\top \mathbf{A}^\top \mathbf{A} \mathbf{C})^{-1} (\mathbf{C}^\top \mathbf{A}^\top)(\mathbf{b} - \mathbf{A}\mathbf{c}) + \mathbf{c}$ serves as the *restricted least squares (RLS)* estimator of \mathbf{x} .
6. Find the restricted weighted least squares estimator.
7. **First-order optimality condition for local optima points.** Consider the *Fermat's theorem*: for a one-dimensional function $g(\cdot)$ defined and differentiable over an interval (a, b) , if a point $x^* \in (a, b)$ is a local maximum or minimum, then $g'(x^*) = 0$. Prove the first-order optimality conditions for multivariate functions based on this Fermat's theorem for one-dimensional functions. That is, consider function $f : \mathbb{S} \rightarrow \mathbb{R}$ as a function defined on a set $\mathbb{S} \subseteq \mathbb{R}^n$. Suppose that $\mathbf{x}^* \in \text{int}(\mathbb{S})$, i.e., in the interior point of the set, is a local optimum point and that all the partial derivatives (Definition 1.0.21, p. 16) of f exist at \mathbf{x}^* . Then $\nabla f(\mathbf{x}^*) = \mathbf{0}$, i.e., the gradient vanishes at all local optimum points. (Note that, this optimality condition is a necessary condition; however, there could be vanished points which are not local maximum or minimum point.)
8. **Global minimum point.** Let function f be a twice continuously differentiable function defined over \mathbb{R}^n . Suppose that the Hessian $\nabla^2 f(\mathbf{x}) \geq 0$ for any $\mathbf{x} \in \mathbb{R}^n$. Then \mathbf{x}^* is a global minimum point of f if $\nabla f(\mathbf{x}^*) = \mathbf{0}$. *Hint: use linear approximation theorem in Theorem 1.6 (p. 18).*
9. **Two-sided matrix least squares.** Let \mathbf{B} be an $M \times K$ matrix and \mathbf{C} be a $P \times N$ matrix. Find the $K \times P$ matrix \mathbf{X} such that $L(\mathbf{X}) = \|\mathbf{A} - \mathbf{B}\mathbf{X}\mathbf{C}\|_F^2$ is minimized, where $\mathbf{A} \in \mathbb{R}^{M \times N}$ is known.
 - Derive the derivative of L with respect to \mathbf{X} and the optimality conditions.
 - Show that one possible solution to the optimality conditions is $\mathbf{X} = \mathbf{B}^+ \mathbf{A} \mathbf{C}^+$, where \mathbf{B}^+ and \mathbf{C}^+ are the pseudo-inverses of \mathbf{B} and \mathbf{C} , respectively.

5

Nonnegative Matrix Factorization (NMF)

Contents

5.1	Nonnegative Matrix Factorization	129
5.2	NMF via Multiplicative Update (MU)	129
5.3	Regularization	131
5.4	Initialization	133
5.5	Movie Recommender Context	133
	Chapter 5 Problems	134

5.1. Nonnegative Matrix Factorization



In the era of big data, extracting meaningful patterns and latent structures from high-dimensional data sets has become a central challenge in various scientific and technological domains. Nonnegative matrix factorization (NMF) has emerged as a powerful and interpretable tool for dimensionality reduction, feature extraction, and discovering latent structures within complex data. Early consideration of the NMF problem is due to Paatero and Tapper (1994); Cohen and Rothblum (1993), where they called it *positive matrix factorization*. While Lee and Seung (2001) later made the problem famous by the *multiplicative update*.

Following the matrix factorization via the ALS, we now consider algorithms for solving the nonnegative matrix factorization (NMF) problem:

- Given a nonnegative matrix $\mathbf{A} \in \mathbb{R}_+^{M \times N}$ with rank R , find nonnegative matrix factors $\mathbf{W} \in \mathbb{R}_+^{M \times K}$ and $\mathbf{Z} \in \mathbb{R}_+^{K \times N}$ such that:

$$\mathbf{A} \approx \mathbf{W}\mathbf{Z}.$$

The nonnegativity constraint imposes an inherent sparsity, enabling the factorization to capture additive features, which is especially advantageous in applications where parts-based representations are meaningful. This constraint make it find applications in diverse fields such as image processing, document analysis, and bioinformatics, where the identified components often correspond to distinct parts or features. For example, in image processing, NMF has proven valuable for tasks such as object detection, image segmentation, and facial recognition. The decomposition into nonnegative components aligns with the intuitive notion that images are composed of identifiable parts.

To measure the quality of the approximation, we evaluate the loss by computing the Frobenius norm of the difference between the original matrix and the approximation:

$$L(\mathbf{W}, \mathbf{Z}) = \|\mathbf{W}\mathbf{Z} - \mathbf{A}\|^2.$$

See also the applications of the NMF in the survey paper Berry et al. (2007). When we want to find two nonnegative matrices $\mathbf{W} \in \mathbb{R}_+^{M \times R}$ and $\mathbf{Z} \in \mathbb{R}_+^{R \times N}$ such that $\mathbf{A} = \mathbf{W}\mathbf{Z}$, the problem is known as the *Exact NMF* of \mathbf{A} of size R . Exact NMF is NP-hard (Gillis, 2020). Thus, we only consider the approximation of NMF here.

5.2. NMF via Multiplicative Update (MU)

We consider the NMF via an alternating update. The hidden features in \mathbf{W} and \mathbf{Z} are modeled as nonnegative vectors in low-dimensional space. These latent vectors are randomly initialized and iteratively updated via an alternating multiplicative update rule to minimize the Kullback-Leibler divergence between the observed and modeled matrices. Following Section 4.2 (p. 100), we consider the low-rank with K problem; given $\mathbf{W} \in \mathbb{R}_+^{M \times K}$, we want to update $\mathbf{Z} \in \mathbb{R}_+^{K \times N}$, the gradient with respect to \mathbf{Z} is given by Equation (4.3) (p. 102):

$$\frac{\partial L(\mathbf{Z}|\mathbf{W})}{\partial \mathbf{Z}} = 2\mathbf{W}^\top(\mathbf{W}\mathbf{Z} - \mathbf{A}) \in \mathbb{R}^{K \times N}.$$

Applying the gradient descent idea discussed in Section 4.6 (p. 109), the trivial update for \mathbf{Z} can be achieved by

$$(\text{GD on } \mathbf{Z}) \quad \mathbf{Z} \leftarrow \mathbf{Z} - \eta \left(\frac{\partial L(\mathbf{Z}|\mathbf{W})}{\partial \mathbf{Z}} \right) = \mathbf{Z} - \eta \left(2\mathbf{W}^\top \mathbf{W} \mathbf{Z} - 2\mathbf{W}^\top \mathbf{A} \right),$$

where η represents a small positive step size. Now if we impose a different step size for each entry of \mathbf{Z} and incorporate the constant 2 into the step size, the update can be obtained by

$$(\text{GD}' \text{ on } \mathbf{Z}) \quad \begin{aligned} z_{kn} &\leftarrow z_{kn} - \frac{\eta_{kn}}{2} \left(\frac{\partial L(\mathbf{Z}|\mathbf{W})}{\partial \mathbf{Z}} \right)_{kn} \\ &= z_{kn} - \eta_{kn} (\mathbf{W}^\top \mathbf{W} \mathbf{Z} - \mathbf{W}^\top \mathbf{A})_{kn}, \quad k \in \{1, \dots, K\}, n \in \{1, \dots, N\}, \end{aligned}$$

where z_{kn} denotes the (k, n) -th entry of \mathbf{Z} . To proceed, we further rescale the step size:

$$\eta_{kn} = \frac{z_{kn}}{(\mathbf{W}^\top \mathbf{W} \mathbf{Z})_{kn}}.$$

Then we obtain the update rule:

$$(\text{MU on } \mathbf{Z}) \quad z_{kn} \leftarrow z_{kn} \frac{(\mathbf{W}^\top \mathbf{A})_{kn}}{(\mathbf{W}^\top \mathbf{W} \mathbf{Z})_{kn}}, \quad k \in \{1, \dots, K\}, n \in \{1, \dots, N\},$$

which is known as the *multiplicative update (MU)*, and is first developed in Lee and Seung (2001) and further discussed in Pauca et al. (2006). Analogously, the multiplicative update for \mathbf{W} can be obtained by

$$(\text{MU on } \mathbf{W}) \quad w_{mk} \leftarrow w_{mk} \frac{(\mathbf{A} \mathbf{Z}^\top)_{mk}}{(\mathbf{W} \mathbf{Z} \mathbf{Z}^\top)_{mk}}, \quad m \in \{1, \dots, M\}, k \in \{1, \dots, K\}. \quad (5.1)$$

Theorem 5.1: (Convergence of Multiplicative Update)

The loss $L(\mathbf{W}, \mathbf{Z}) = \|\mathbf{W} \mathbf{Z} - \mathbf{A}\|^2$ remains non-increasing under the following multiplicative update rules:

$$\begin{cases} z_{kn} \leftarrow z_{kn} \frac{(\mathbf{W}^\top \mathbf{A})_{kn}}{(\mathbf{W}^\top \mathbf{W} \mathbf{Z})_{kn}}, & k \in \{1, \dots, K\}, n \in \{1, \dots, N\}; \\ w_{mk} \leftarrow w_{mk} \frac{(\mathbf{A} \mathbf{Z}^\top)_{mk}}{(\mathbf{W} \mathbf{Z} \mathbf{Z}^\top)_{mk}}, & m \in \{1, \dots, M\}, k \in \{1, \dots, K\}. \end{cases}$$

We refer the proof of the theorem above to Lee and Seung (2001). Clearly, the approximations \mathbf{W} and \mathbf{Z} remain nonnegative during the updates. It is generally better to update \mathbf{W} and \mathbf{Z} “simultaneously” rather than “sequentially,” i.e., updating each matrix completely before the other. In this case, after updating a row of \mathbf{Z} , we update the corresponding column of \mathbf{W} . In the implementation, it is advisable to introduce a small positive quantity, say the square root of the machine precision, to the denominators in the approximations of \mathbf{W} and \mathbf{Z} at each iteration. And a trivial value like $\epsilon = 10^{-9}$ suffices. The full procedure is shown in Algorithm 6.

Algorithm 6 NMF via Multiplicative Updates

Require: Matrix $\mathbf{A} \in \mathbb{R}^{M \times N}$;

- 1: Initialize $\mathbf{W} \in \mathbb{R}^{M \times K}$, $\mathbf{Z} \in \mathbb{R}^{K \times N}$ randomly with nonnegative entries;
- 2: Choose a stop criterion on the approximation error δ ;
- 3: Choose maximal number of iterations C ;
- 4: $iter = 0$; ▷ Count for the number of iterations
- 5: **while** $\|\mathbf{A} - (\mathbf{W}\mathbf{Z})\|^2 > \delta$ and $iter < C$ **do**
- 6: $iter = iter + 1$;
- 7: **for** $k = 1$ to K **do**
- 8: **for** $n = 1$ to N **do** ▷ update k -th row of \mathbf{Z}
- 9: $z_{kn} \leftarrow z_{kn} \frac{(\mathbf{W}^\top \mathbf{A})_{kn}}{(\mathbf{W}^\top \mathbf{W} \mathbf{Z})_{kn} + \epsilon}$;
- 10: **end for**
- 11: **for** $m = 1$ to M **do** ▷ update k -th column of \mathbf{W}
- 12: $w_{mk} \leftarrow w_{mk} \frac{(\mathbf{A} \mathbf{Z}^\top)_{mk}}{(\mathbf{W} \mathbf{Z} \mathbf{Z}^\top)_{mk} + \epsilon}$;
- 13: **end for**
- 14: **end for**
- 15: **end while**
- 16: Output \mathbf{W} , \mathbf{Z} ;

Algorithm 7 NMF via Regularized Multiplicative Updates

Require: Matrix $\mathbf{A} \in \mathbb{R}^{M \times N}$;

- 1: Initialize $\mathbf{W} \in \mathbb{R}^{M \times K}$, $\mathbf{Z} \in \mathbb{R}^{K \times N}$ randomly with nonnegative entries;
- 2: Choose a stop criterion on the approximation error δ ;
- 3: Choose maximal number of iterations C ;
- 4: Choose regularization parameter λ_z, λ_w ;
- 5: $iter = 0$; ▷ Count for the number of iterations
- 6: **while** $\|\mathbf{A} - (\mathbf{W}\mathbf{Z})\|^2 > \delta$ and $iter < C$ **do**
- 7: $iter = iter + 1$;
- 8: **for** $k = 1$ to K **do**
- 9: **for** $n = 1$ to N **do** ▷ update k -th row of \mathbf{Z}
- 10: $z_{kn} \leftarrow z_{kn} \frac{(\mathbf{W}^\top \mathbf{A})_{kn} - \lambda_z z_{kn}}{(\mathbf{W}^\top \mathbf{W} \mathbf{Z})_{kn} + \epsilon}$;
- 11: **end for**
- 12: **for** $m = 1$ to M **do** ▷ update k -th column of \mathbf{W}
- 13: $w_{mk} \leftarrow w_{mk} \frac{(\mathbf{A} \mathbf{Z}^\top)_{mk} - \lambda_w w_{mk}}{(\mathbf{W} \mathbf{Z} \mathbf{Z}^\top)_{mk} + \epsilon}$;
- 14: **end for**
- 15: **end for**
- 16: **end while**
- 17: Output \mathbf{W} , \mathbf{Z} ;

5.3. Regularization

Similar to the ALS with regularization discussed in Section 4.3 (p. 105), recall that the regularization can help extend the applicability of ALS to general matrices. Additionally,

a regularization term can be incorporated into the NMF framework to enhance its performance:

$$L(\mathbf{W}, \mathbf{Z}) = \|\mathbf{W}\mathbf{Z} - \mathbf{A}\|^2 + \lambda_w \|\mathbf{W}\|^2 + \lambda_z \|\mathbf{Z}\|^2, \quad \lambda_w > 0, \lambda_z > 0,$$

where the employed matrix norm is still the Frobenius norm. The gradient with respect to \mathbf{Z} given \mathbf{W} is the same as that in Equation (4.11) (p. 105):

$$\frac{\partial L(\mathbf{Z}|\mathbf{W})}{\partial \mathbf{Z}} = 2\mathbf{W}^\top(\mathbf{W}\mathbf{Z} - \mathbf{A}) + 2\lambda_z \mathbf{Z} \in \mathbb{R}^{K \times N}.$$

The gradient descent update can be obtained by

$$(\text{GD on } \mathbf{Z}) \quad \mathbf{Z} \leftarrow \mathbf{Z} - \eta \left(\frac{\partial L(\mathbf{Z}|\mathbf{W})}{\partial \mathbf{Z}} \right) = \mathbf{Z} - \eta \left(2\mathbf{W}^\top \mathbf{W} \mathbf{Z} - 2\mathbf{W}^\top \mathbf{A} + 2\lambda_z \mathbf{Z} \right),$$

Analogously, if we assume a different step size for each entry of \mathbf{Z} and incorporate the constant 2 into the step size, the update can be obtained by

$$\begin{aligned} (\text{GD}' \text{ on } \mathbf{Z}) \quad z_{kn} &\leftarrow z_{kn} - \frac{\eta_{kn}}{2} \left(\frac{\partial L(\mathbf{Z}|\mathbf{W})}{\partial \mathbf{Z}} \right)_{kn} \\ &= z_{kn} - \eta_{kn} (\mathbf{W}^\top \mathbf{W} \mathbf{Z} - \mathbf{W}^\top \mathbf{A} + \lambda_z \mathbf{Z})_{kn}, \quad k \in \{1, \dots, K\}, n \in \{1, \dots, N\}. \end{aligned}$$

Now if we rescale the step size:

$$\eta_{kn} = \frac{z_{kn}}{(\mathbf{W}^\top \mathbf{W} \mathbf{Z})_{kn}},$$

then we obtain the multiplicative update rule:

$$(\text{MU on } \mathbf{Z}) \quad z_{kn} \leftarrow z_{kn} \frac{(\mathbf{W}^\top \mathbf{A})_{kn} - \lambda_z z_{kn}}{(\mathbf{W}^\top \mathbf{W} \mathbf{Z})_{kn}}, \quad k \in \{1, \dots, K\}, n \in \{1, \dots, N\}.$$

Similarly, the multiplicative update on \mathbf{W} can be obtained by

$$(\text{MU on } \mathbf{W}) \quad w_{mk} \leftarrow w_{mk} \frac{(\mathbf{A} \mathbf{Z}^\top)_{mk} - \lambda_w w_{mk}}{(\mathbf{W} \mathbf{Z} \mathbf{Z}^\top)_{mk}}, \quad m \in \{1, \dots, M\}, k \in \{1, \dots, K\}.$$

The procedure is then formulated in Algorithm 7.

A nonnegative matrix factorization $\mathbf{A} \approx \mathbf{W}\mathbf{Z}$ can be applied for clustering algorithm. Specifically, the data vector \mathbf{a}_j is assigned to cluster i if z_{ij} is the largest element in column j of \mathbf{Z} (Brunet et al., 2004; Gao and Church, 2005).

In the context of collaborative filtering, it is recognized that the NMF via multiplicative update can result in overfitting despite favorable convergence results. The overfitting can be partially mitigated through regularization, but its out-of-sample performance remains low. Bayesian optimization through the use of generative models, on the other hand, can effectively prevent overfitting for nonnegative matrix factorization (Brouwer et al., 2017; Lu and Ye, 2022); see Chapter 7 (p. 156).

Readers are advised to consult the survey of Berry et al. (2007) for other issues in the NMF.

5.4. Initialization

A significant challenge in NMF is the absence of guaranteed convergence to a global minimum. It often happens that convergence is slow and a suboptimal approximation is reached. In the preceding discussion, we initialized \mathbf{W} and \mathbf{Z} randomly. To mitigate this issue, there are also alternative strategies designed to obtain better initial estimates in the hope of converging more rapidly to a good solution (Boutsidis and Gallopoulos, 2008; Gillis, 2014). We sketch the methods as follows for reference:

- *Clustering techniques.* Apply some clustering methods to the columns of \mathbf{A} , set the cluster means of the top K clusters as the columns of \mathbf{W} , and initialize \mathbf{Z} as a proper scaling of the cluster indicator matrix (that is, $z_{kn} \neq 0$ indicates \mathbf{a}_n belongs to the k -th cluster);
- *Subset selection.* Pick K columns of \mathbf{A} , and set those as the initial columns for \mathbf{W} . And analogously, K rows of \mathbf{A} are selected to form the rows of \mathbf{Z} ;
- *SVD-based approach.* Suppose the optimal rank- K approximation of \mathbf{A} via SVD is $\mathbf{A} = \sum_{i=1}^K \sigma_i \mathbf{u}_i \mathbf{v}_i^\top$, where each factor $\sigma_i \mathbf{u}_i \mathbf{v}_i^\top$ is a rank-one matrix with possible negative values in \mathbf{u}_i and \mathbf{v}_i , and nonnegative σ_i . Denote $[x]_+ = \max(x, 0)$, we notice

$$\mathbf{u}_i \mathbf{v}_i^\top = [\mathbf{u}_i]_+ [\mathbf{v}_i]_+^\top + [-\mathbf{u}_i]_+ [-\mathbf{v}_i]_+^\top - [-\mathbf{u}_i]_+ [\mathbf{v}_i]_+^\top - [\mathbf{u}_i]_+ [-\mathbf{v}_i]_+^\top,$$

where the first two rank-one factors in this decomposition are nonnegative. Then, either $[\mathbf{u}_i]_+ [\mathbf{v}_i]_+^\top$ or $[-\mathbf{u}_i]_+ [-\mathbf{v}_i]_+^\top$ can be selected to replace the factor $\mathbf{u}_i \mathbf{v}_i^\top$. Boutsidis and Gallopoulos (2008) suggests to replace each rank-one factor in $\sum_{i=1}^K \sigma_i \mathbf{u}_i \mathbf{v}_i^\top$ with either $[\mathbf{u}_i]_+ [\mathbf{v}_i]_+^\top$ or $[-\mathbf{u}_i]_+ [-\mathbf{v}_i]_+^\top$, selecting the one with larger norm and scaling it properly.¹ In other words, if we select $[\mathbf{u}_i]_+ [\mathbf{v}_i]_+^\top$, then $\sigma_i \cdot [\mathbf{u}_i]_+$ can be initialized as the i -th column of \mathbf{W} , and $[\mathbf{v}_i]_+^\top$ can be chosen as the i -th row of \mathbf{Z} .

However, these techniques are not guaranteed to yield better performance theoretically. We recommend referring to the aforementioned papers for more information.

5.5. Movie Recommender Context

Both the NMF and the ALS methods approximate the matrix and reconstruct the entries in the matrix with a set of basis vectors. The basis in the NMF is composed of vectors with nonnegative elements while the basis vectors in the ALS can have positive or negative values. The key distinction lies in how the approximation is carried out. In NMF, each vector is reconstructed as a positive summation of the basis vectors with a “relative” small component in the direction of each basis vector. Whereas, in the ALS approximation, the data is modeled as a linear combination of the basis such that we can add or subtract vectors as needed; and the components in the direction of each basis vector can be large positive values or negative values. Therefore, depending on the application, one or the other factorization can be utilized to describe the data with different meanings.

In the context of a movie recommender system, the rows of \mathbf{W} represent the hidden features of movies, while the columns of \mathbf{Z} represent the hidden features of users. In the NMF method, we can say that a movie is 0.5 comedy, 0.002 action, and 0.09 romantic.

1. Note here we consider general matrix \mathbf{A} . If \mathbf{A} is nonnegative, then \mathbf{u}_i and \mathbf{v}_i are nonnegative as well.

However, in the ALS approach, we can get combinations such as 4 comedy, -0.05 comedy, and -3 drama, i.e., a positive or negative component on that feature.

The ALS and NMF are similar in the sense that the importance of each basis vector is not ranked in a hierarchical manner. Whereas, the key difference between the ALS (or NMF) and the SVD is that, in the SVD, the importance of each vector in the basis is relative to the value of the singular value associated with that vector. In the SVD representation of $\mathbf{A} = \sum_{i=1}^r \sigma_i \mathbf{u}_i \mathbf{v}_i^\top$, this usually means that the reconstruction $\sigma_1 \mathbf{u}_1 \mathbf{v}_1^\top$ via the first set of basis vectors dominates and is the most used set to reconstruct data, followed by the second set, and so on. So the basis in the SVD has an implicit hierarchy and that doesn't happen in the ALS or the NMF approaches. Recall the low-rank approximation of the flag image in Section 4.10.1 (p. 120), where we find the second component $\mathbf{w}_2 \mathbf{z}_2^\top$ via the ALS in Figure 4.9(n) (p. 120) plays an important role in the reconstruction of the original figure. Conversely, the second component $\sigma_2 \mathbf{u}_2 \mathbf{v}_2^\top$ via the SVD in Figure 4.9(b) (p. 120) plays a less important role in the reconstruction.

Chapter 5 Problems

1. * Suppose $\mathbf{C} = P(\mathbf{A})$ is defined as the matrix obtained by setting each entry of \mathbf{C} as the absolute value of $\mathbf{A} \in \mathbb{R}^{n \times n}$. Suppose further that $\mathbf{B} - P(\mathbf{A}) \in \mathbb{R}_+^{n \times n}$, prove that

$$\rho(\mathbf{A}) \leq \rho(P(\mathbf{A})) \leq \rho(\mathbf{B}),$$

where $\rho(\mathbf{X})$ represents the spectral radius of matrix \mathbf{X} (Definition 1.0.3, p. 9).

2. * Given $\mathbf{A} \in \mathbb{R}_+^{n \times n}$, show that

$$\min_{1 \leq i \leq n} \sum_{j=1}^n a_{ij} \leq \rho(\mathbf{A}) \leq \max_{1 \leq i \leq n} \sum_{j=1}^n a_{ij};$$

$$\min_{1 \leq j \leq n} \sum_{i=1}^n a_{ij} \leq \rho(\mathbf{A}) \leq \max_{1 \leq j \leq n} \sum_{i=1}^n a_{ij}.$$

Part III

Bayesian Matrix Decomposition

6

Bayesian Real Matrix Factorization

Contents

6.1	Introduction	139
6.2	All Gaussian (GGG) Model and Markov Blanket	141
6.3	All Gaussian Model with ARD Hierarchical Prior (GGGA) .	148
6.4	All Gaussian Model with Wishart Hierarchical Prior (GGGW)	150
6.5	Gaussian Likelihood with Volume and Gaussian Priors (GVG)	153
	Chapter 6 Problems	154

6.1. Introduction



The explosion of data from advancements in sensor technology and computer hardware has presented new challenges for data analysis. The large volume of data often contains noise and other distortions, requiring pre-processing for deductive science to be applied. For example, signals received by antenna arrays often are contaminated by noise and other degradations. To effectively analyze the data, it is necessary to reconstruct or represent it in a way that reduces inaccuracies while maintaining certain feasibility conditions.

Additionally, in many cases, the data collected from complex systems is the result of multiple interrelated variables acting in unison. When these variables are not well defined, the information contained in the original data can be overlapping and unclear. By creating a reduced system model, we can achieve a level of accuracy that is close to the original system. The common approach in removing noise, reducing the model, and reconstructing feasibility, is to replace the original data with a lower-dimensional representation obtained through subspace approximation. Therefore, low-rank approximations or low-rank matrix decompositions play a crucial role in a wide range of applications.

Low-rank matrix decomposition is a powerful technique used in machine learning and data mining to represent a given matrix as the product of two or more matrices with lower dimensions. It is used to capture the essential structure of a matrix while ignoring noise and redundancies. The most common methods for low-rank matrix decomposition include singular value decomposition (SVD), principal component analysis (PCA), and multiplicative update nonnegative matrix factorization (NMF).

Bayesian low-rank decomposition is a variant of low-rank matrix decomposition that incorporates Bayesian modeling. It models the observed data as a low-rank matrix, where the low-rank approximation is assumed to be generated from a prior distribution. This incorporation allows for the inclusion of prior knowledge and uncertainty about the low-rank matrix into the decomposition. The use of priors can also lead to more interpretable results by providing a probabilistic representation of the uncertainty associated with the factor matrices. In addition, Bayesian methods allow for the quantification of uncertainty in the results, providing a measure of the confidence in the estimated factor matrices. Therefore, it can help to mitigate overfitting and produce more robust results, establishing it as a powerful method for modeling both predictive and explanatory data.

Given an observed data set, represented as an $M \times N$ matrix of results, \mathbf{A} , where rows represent the number of observations and columns represent the variables of interest. Following Chapter 4 (p. 96), the *real matrix factorization (RMF)* problem, a common bilinear decomposition problem, can be stated as $\mathbf{A} = \mathbf{W}\mathbf{Z} + \mathbf{E}$, where $\mathbf{A} = [\mathbf{a}_1, \mathbf{a}_2, \dots, \mathbf{a}_N] \in \mathbb{R}^{M \times N}$ is approximately factorized into an $M \times K$ matrix $\mathbf{W} \in \mathbb{R}^{M \times K}$ and a $K \times N$ matrix $\mathbf{Z} \in \mathbb{R}^{K \times N}$. The data set \mathbf{A} needs not to be complete such that the indices of observed entries can be represented by the mask matrix $\mathbf{M} \in \mathbb{R}^{M \times N}$, where a value of 1 indicates the entry is observed and a value of 0 indicates the entry is missing. Matrices \mathbf{W} and \mathbf{Z} represent the values of explanatory variables which, when multiplied, give a predictor of the values in \mathbf{A} . If entries in \mathbf{A} are missing, then \mathbf{W} and \mathbf{Z} can be used to give predictions of their values. When one of \mathbf{W} and \mathbf{Z} is observed, the factorization becomes a regression problem.

The factorization of the original data matrix \mathbf{A} is achieved by finding two such real matrices, one representing the *basis or dictionary* components and the other representing the *activations or coefficients*. Let \mathbf{z}_n denote the n -th column of \mathbf{Z} . Then the matrix multiplication of \mathbf{WZ} can be implemented as computing the column vectors of \mathbf{A} as linear combinations of the columns in \mathbf{W} using coefficients supplied by columns of \mathbf{Z} :

$$\mathbf{a}_n = \mathbf{W} \mathbf{z}_n.$$

In the Netflix context, the value of a_{mn} , the (m, n) -th element of \mathbf{A} , denotes the rating of the n -th user for the m -th movie (the larger the user more likes the movie). Then \mathbf{w}_m can represent the hidden features of the m -th movie, and \mathbf{z}_n contains the features of user n (Section 4.5, p. 109).

To simplify the problem, let us assume that there are no missing entries firstly. Project data vectors \mathbf{a}_n to a smaller dimension $\mathbf{z}_n \in \mathbb{R}^K$ with $K < M$, such that the *reconstruction error* measured by Frobenius norm is minimized (assume K is known):

$$\min_{\mathbf{W}, \mathbf{Z}} \sum_{n=1}^N \sum_{m=1}^M \left(a_{mn} - \mathbf{w}_m^\top \mathbf{z}_n \right)^2, \quad (6.1)$$

where $\mathbf{W} = [\mathbf{w}_1^\top; \mathbf{w}_2^\top; \dots; \mathbf{w}_M^\top] \in \mathbb{R}^{M \times K}$ and $\mathbf{Z} = [\mathbf{z}_1, \mathbf{z}_2, \dots, \mathbf{z}_N] \in \mathbb{R}^{K \times N}$ containing \mathbf{w}_m 's and \mathbf{z}_n 's as **rows and columns**, respectively ¹. The loss form in Equation (6.1) is known as the *per-example loss*. It can be equivalently written as

$$L(\mathbf{W}, \mathbf{Z}) = \sum_{n=1}^N \sum_{m=1}^M \left(a_{mn} - \mathbf{w}_m^\top \mathbf{z}_n \right)^2 = \|\mathbf{WZ} - \mathbf{A}\|^2 = \text{tr} \left\{ (\mathbf{WZ} - \mathbf{A})^\top (\mathbf{WZ} - \mathbf{A}) \right\}, \quad (6.2)$$

where $\text{tr}(\cdot)$ represents the trace of the quantity in the brackets. This matrix factorization problem is similar to a standard “inverse” problem, except that in the “inverse” problem, one of the factored components is known, and thus ordinary least squares or similar methods can be applied to find the other component, which minimizes the residuals between the reconstruction and the data. When neither \mathbf{W} nor \mathbf{Z} is known, the factorization problem is difficult even if the latent dimension K is only 2 or 3. We sample the space of potential solutions using the Markov chain Monte Carlo (MCMC) procedure to determine its properties because there are a vast number of possible solutions and no analytical approach to identify them.

We have discussed the Bayesian approach in Section 2.1 (p. 21). In the Bayesian matrix factorization context, the model leads to the specific form of Bayes' equation,

$$p(\mathbf{W}, \mathbf{Z} \mid \mathbf{A}) \propto p(\mathbf{A} \mid \mathbf{W}, \mathbf{Z}) \times p(\mathbf{W}, \mathbf{Z}), \quad (6.3)$$

where $p(\mathbf{W}, \mathbf{Z})$ captures the prior beliefs encoding the knowledge of the solution independent of the data, and $p(\mathbf{A} \mid \mathbf{W}, \mathbf{Z})$ denotes the likelihood comparing the model to the data.

1. Note in some contexts, \mathbf{Z} represents an $N \times K$ matrix such that \mathbf{A} is decomposed into $\mathbf{A} = \mathbf{WZ}^\top + \mathbf{E}$.

Name	Likelihood	Prior \mathbf{W}	Prior \mathbf{Z}	Hierarchical prior
GGG	$\mathcal{N}(a_{mn} \mathbf{w}_m^\top \mathbf{z}_n, \sigma^2)$	$\mathcal{N}(w_{mk} 0, (\lambda_{mk}^W)^{-1})$	$\mathcal{N}(z_{kn} 0, (\lambda_{kn}^Z)^{-1})$	/
GGGM	$\mathcal{N}(a_{mn} \mathbf{w}_m^\top \mathbf{z}_n, \sigma^2)$	$\mathcal{N}(\mathbf{w}_m \mathbf{0}, \lambda^{-1} \mathbf{I})$	$\mathcal{N}(\mathbf{z}_n \mathbf{0}, \lambda^{-1} \mathbf{I})$	/
GGGA	$\mathcal{N}(a_{mn} \mathbf{w}_m^\top \mathbf{z}_n, \sigma^2)$	$\mathcal{N}(w_{mk} 0, (\lambda_k)^{-1})$	$\mathcal{N}(z_{kn} 0, (\lambda_k)^{-1})$	$\mathcal{G}(\lambda_k \alpha_\lambda, \beta_\lambda)$
GGGW	$\mathcal{N}(a_{mn} \mathbf{w}_m^\top \mathbf{z}_n, \sigma^2)$	$\mathcal{N}(\mathbf{w}_m \boldsymbol{\mu}_w, \boldsymbol{\Sigma}_w)$	$\mathcal{N}(\mathbf{z}_n \boldsymbol{\mu}_z, \boldsymbol{\Sigma}_z)$	$\{\boldsymbol{\mu}_w, \boldsymbol{\Sigma}_w\}, \{\boldsymbol{\mu}_z, \boldsymbol{\Sigma}_z\} \sim \mathcal{NITW}(\mathbf{m}_0, \kappa_0, \nu_0, \mathbf{S}_0)$
GVG	$\mathcal{N}(a_{mn} \mathbf{w}_m^\top \mathbf{z}_n, \sigma^2)$	$\mathbf{W} \sim \exp\{-\gamma \mathbf{W}^\top \mathbf{W}\}$	$\mathcal{N}(z_{kn} 0, (\lambda_{kn}^Z)^{-1})$	/

Table 6.1: Overview of Bayesian real matrix factorization models.

Terminology. There are three types of choices we make that determine the specific type of matrix decomposition model we use, namely, the likelihood function, the priors we place over the factored matrices \mathbf{W} and \mathbf{Z} , and whether we use any further hierarchical priors. We will call the model by the density function in the order of the types of likelihood and priors. For example, if the likelihood function for the model is chosen to be a Gaussian density, and the two prior density functions are selected to be exponential density and Gaussian density functions, respectively, then the model will be denoted by the *Gaussian Exponential-Gaussian (GEG)* model. Sometimes, we will put a hyperprior over the parameters of the prior density functions, e.g., we put a Gamma prior over the exponential density, then it will further be termed as a *Gaussian Exponential-Gaussian Gamma (GEGA)* model (“A” is short for the Gamma density to avoid confusion with the Gaussian density). Table 6.1 summarizes the Bayesian models for real matrix factorization in this chapter.

6.2. All Gaussian (GGG) Model and Markov Blanket

The all Gaussian (GGG) model is perhaps the simplest approach for Bayesian RMF, where Gaussian priors are applied over factored matrices (Salakhutdinov and Mnih, 2008; Gönen, 2012; Virtanen et al., 2011, 2012). The model involves using Gaussian likelihood and Gaussian priors.

Likelihood. We view the data \mathbf{A} as being produced according to the probabilistic generative process shown in Figure 6.1. The observed (m, n) -th data entry a_{mn} of matrix \mathbf{A} is modeled using a Gaussian likelihood function with variance σ^2 and a mean determined by the latent decomposition $\mathbf{w}_m^\top \mathbf{z}_n$ (Equation (6.1)):

$$p(a_{mn} | \mathbf{w}_m^\top \mathbf{z}_n, \sigma^2) = \mathcal{N}(a_{mn} | \mathbf{w}_m^\top \mathbf{z}_n, \sigma^2). \quad (6.4)$$

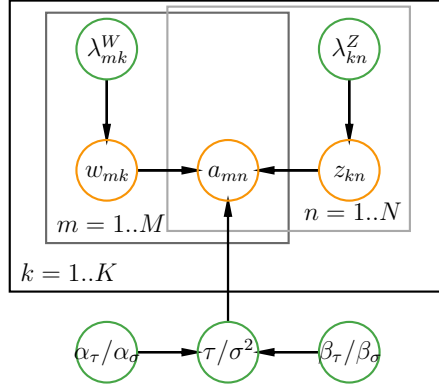


Figure 6.1: Graphical model representation of the GGG model. Green circles denote prior variables, orange circles represent observed and latent variables, and plates represent repeated variables. The slash “/” in the variable represents “or.”

This is equivalent to assuming the residuals, e_{mn} , are i.i.d. drawn from a zero-mean normal with variance σ^2 , which gives rise to the following likelihood function:

$$\begin{aligned} p(\mathbf{A} \mid \boldsymbol{\theta}) &= \prod_{m,n=1}^{M,N} \mathcal{N}(a_{mn} \mid (\mathbf{WZ})_{mn}, \sigma^2) \\ &= \prod_{m,n=1}^{M,N} \mathcal{N}(a_{mn} \mid (\mathbf{WZ})_{mn}, \tau^{-1}), \end{aligned} \quad (6.5)$$

where $\boldsymbol{\theta} = \{\mathbf{W}, \mathbf{Z}, \sigma^2\}$ denotes all parameters in the model, σ^2 is the variance, $\tau^{-1} = \sigma^2$ is the precision, and

$$\mathcal{N}(x \mid \mu, \sigma^2) = \frac{1}{(2\pi\sigma^2)^{1/2}} \exp\left\{-\frac{1}{2\sigma^2}(x - \mu)^2\right\} = \sqrt{\frac{\tau}{2\pi}} \exp\left\{-\frac{\tau}{2}(x - \mu)^2\right\}$$

is the normal density (Definition 3.2.1, p. 41).

Prior. We assume \mathbf{W} and \mathbf{Z} are independently Gaussian distributed with precisions λ_{mk}^W and λ_{kn}^Z , respectively,

$$\begin{aligned} w_{mk} &\sim \mathcal{N}(w_{mk} \mid 0, (\lambda_{mk}^W)^{-1}), & z_{kn} &\sim \mathcal{N}(z_{kn} \mid 0, (\lambda_{kn}^Z)^{-1}); \\ p(\mathbf{W}) &= \prod_{m,k=1}^{M,K} \mathcal{N}(w_{mk} \mid 0, (\lambda_{mk}^W)^{-1}), & p(\mathbf{Z}) &= \prod_{k,n=1}^{K,N} \mathcal{N}(z_{kn} \mid 0, (\lambda_{kn}^Z)^{-1}). \end{aligned} \quad (6.6)$$

The prior for the noise variance σ^2 is chosen as an inverse-Gamma density with shape α_σ and scale β_σ (Definition 3.2.4, p. 47),

$$p(\sigma^2) = \mathcal{G}^{-1}(\sigma^2 \mid \alpha_\sigma, \beta_\sigma) = \frac{\beta_\sigma^{\alpha_\sigma}}{\Gamma(\alpha_\sigma)} (\sigma^2)^{-\alpha_\sigma-1} \exp\left(-\frac{\beta_\sigma}{\sigma^2}\right).$$

By Bayes' rule (Equation (2.1), p. 22), the posterior is proportional to the product of likelihood and prior, it can be maximized to yield an estimate of \mathbf{W} and \mathbf{Z} .

Markov blanket. The most widely used posterior inference methods in Bayesian inference models are Markov chain Monte Carlo (MCMC) methods as described in Section 2.3 (p. 23). The concept behind MCMC methods is to define a Markov chain on the hidden variables that have the posterior as its equilibrium distribution (Andrieu et al., 2003). By drawing samples from this Markov chain, one eventually obtains samples from the posterior distribution. A simple form of MCMC sampling is Gibbs sampling, where the Markov chain is constructed by sampling the conditional distribution of each hidden variable given the values of other hidden variables and the observations. Gibbs sampling is widely used when these conditional distributions can be sampled from easily.

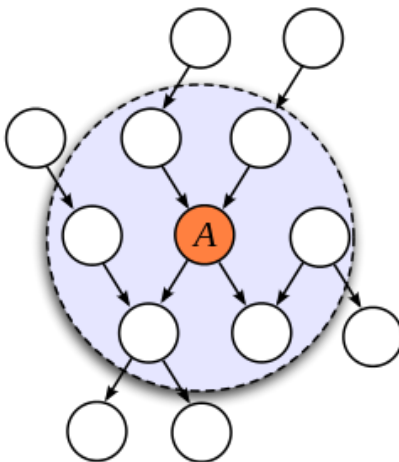


Figure 6.2: The Markov blanket of a directed acyclic graphical (DAG) model. In a Bayesian network, the Markov blanket of node A includes its **parents, children, and the other parents of all of its children**. That is, the nodes in the cycle are in the Markov blanket of node A . The figure is due to wikipedia page of Markov blanket.

To do Gibbs sampling, we need to derive the conditional posterior distributions for each parameter conditioned on all the other parameters $p(\theta_i | \boldsymbol{\theta}_{-i}, \mathcal{X})$, where \mathcal{X} is again the set of data points (here, the observed matrix \mathbf{A}), and θ_i 's are the variables for which we want to sample the distributions. But for a graphical model, this conditional distribution is a function only of the nodes in the *Markov blanket*. For the GGG model shown in Figure 6.1, which is a directed acyclic graphical (DAG) model, the Markov blanket of a node includes **the parents, the children, and the coparents** (Jordan and Bishop, 2004), as shown in Figure 6.2. The Markov blanket of node A is all nodes in the cycle.

An example for the Markov blanket. The idea of the Markov blanket might be mysterious at first glance. Suppose we want to sample the (m, k) -th element w_{mk} of \mathbf{W} for its distribution. From Figure 6.1, we find its parents, children, and coparents are $\{\lambda_{mk}^W\}$, $\{a_{mn}\}$, and $\{\sigma^2, \mathbf{Z}, \mathbf{W}_{-mk}\}$, respectively. Therefore, the conditional distribution of w_{mk}

only depends on the three pairs of parameters:

$$p(w_{mk} | -) = p(w_{mk} | \mathbf{A}, \mathbf{W}_{-mk}, \mathbf{Z}, \sigma^2, \lambda_{mk}^W).$$

More specifically, from this graphical representation, we can find the Markov blanket for each parameter in the GGG model, and then figure out their conditional posterior distributions to be derived:

$$p(w_{mk} | -) = p(w_{mk} | \mathbf{A}, \mathbf{W}_{-mk}, \mathbf{Z}, \sigma^2, \lambda_{mk}^W), \quad (6.7)$$

$$p(z_{kn} | -) = p(z_{kn} | \mathbf{A}, \mathbf{W}, \mathbf{Z}_{-kn}, \sigma^2, \lambda_{kn}^Z), \quad (6.8)$$

$$p(\sigma^2 | -) = p(\sigma^2 | \mathbf{A}, \mathbf{W}, \mathbf{Z}, \alpha_\sigma, \beta_\sigma). \quad (6.9)$$

We sequentially draw samples from the posterior of each parameter, conditioned on all other parameters. It can be shown that the sequence of samples computed constitutes a Markov chain, for which the stationary distribution is the posterior of interest. In other words, Gibbs sampler moves the chain forward by one step as follows:

- Sample the first component w_{mk} for each observation from Equation (6.7), which is known as the **conditional distribution of** w_{mk} ;
- Sample the second component z_{kn} for each observation from Equation (6.8), which is known as the **conditional distribution of** z_{kn} ;
- Sample the parameter σ^2 from Equation (6.9), which is known as the **conditional distribution of** data variance.

Posterior. Given the observed matrix \mathbf{A} , we want to estimate the conditional distribution of the latent structure $p(\mathbf{W}, \mathbf{Z} | \mathbf{A})$, termed the posterior. This estimation is the key to matrix decomposition-based applications. For example, in the Netflix context, we estimate the posterior expectation of each user's hidden feature/preferences and each movie's hidden attributes to perform predictions of which unconsumed movies each user will like. In this book, we apply Gibbs sampling to perform optimization since it tends to be very accurate at finding the true posterior. The advantage of the MCMC or Gibbs sampling methods lies in their ability to produce exact results asymptotically. Other than this method, variational Bayesian inference can be an alternative way, but we shall not go into the details. For RMF, following the Bayes' rule and MCMC, this means we need to be able to draw from distributions (by Markov blanket):

$$p(w_{mk} | \mathbf{A}, \mathbf{W}_{-mk}, \mathbf{Z}, \sigma^2, \lambda_{mk}^W),$$

$$p(z_{kn} | \mathbf{A}, \mathbf{W}, \mathbf{Z}_{-kn}, \sigma^2, \lambda_{kn}^Z),$$

$$p(\sigma^2 | \mathbf{A}, \mathbf{W}, \mathbf{Z}, \alpha_\sigma, \beta_\sigma),$$

where \mathbf{W}_{-mk} denotes all elements of \mathbf{W} except w_{mk} , and \mathbf{Z}_{-kn} denotes all elements of \mathbf{Z} except z_{kn} . Using Bayes' theorem, the conditional density of w_{mk} depends on its parents

(λ_{mk}^W) , children (a_{mn}) , and coparents $(\tau$ or $\sigma^2, \mathbf{W}_{-mk}, \mathbf{Z})$ ². And it can be obtained by

$$\begin{aligned}
& p(w_{mk} \mid \mathbf{A}, \mathbf{W}_{-mk}, \mathbf{Z}, \sigma^2, \lambda_{mk}^W) \propto p(\mathbf{A} \mid \mathbf{W}, \mathbf{Z}, \sigma^2) \times p(w_{mk} \mid \lambda_{mk}^W) \\
&= \prod_{i,j=1}^{M,N} \mathcal{N}(a_{ij} \mid \mathbf{w}_i^\top \mathbf{z}_j, \sigma^2) \times \mathcal{N}(w_{mk} \mid 0, (\lambda_{mk}^W)^{-1}) \\
&\propto \exp \left\{ -\frac{1}{2\sigma^2} \sum_{i,j=1}^{M,N} (a_{ij} - \mathbf{w}_i^\top \mathbf{z}_j)^2 \right\} \times \exp \left\{ -\frac{w_{mk}^2}{2} \lambda_{mk}^W \right\} \\
&\propto \exp \left\{ -\frac{1}{2\sigma^2} \sum_{j=1}^N (a_{mj} - \mathbf{w}_m^\top \mathbf{z}_j)^2 \right\} \times \exp \left\{ -\frac{w_{mk}^2}{2} \lambda_{mk}^W \right\} \\
&\propto \exp \left\{ -\frac{1}{2\sigma^2} \sum_{j=1}^N \left[w_{mk}^2 z_{kj}^2 + 2w_{mk} z_{kj} \left(\sum_{i \neq k}^K w_{mi} z_{ij} - a_{mj} \right) \right] \right\} \cdot \exp \left\{ -\frac{w_{mk}^2}{2} \lambda_{mk}^W \right\} \quad (6.10) \\
&\stackrel{\star}{\propto} \exp \left\{ -\underbrace{\left(\frac{\sum_{j=1}^N z_{kj}^2}{2\sigma^2} + \frac{\lambda_{mk}^W}{2} \right)}_{1/(2\widetilde{\sigma}_{mk}^2)} w_{mk}^2 + w_{mk} \underbrace{\left(\frac{1}{\sigma^2} \sum_{j=1}^N z_{kj} \left(a_{mj} - \sum_{i \neq k}^K w_{mi} z_{ij} \right) \right)}_{\widetilde{\sigma}_{mk}^2 - 1 \widetilde{\mu}_{mk}} \right\} \\
&\propto \mathcal{N}(w_{mk} \mid \widetilde{\mu}_{mk}, \widetilde{\sigma}_{mk}^2),
\end{aligned}$$

where the equality (\star) conforms to Equation (3.2) (p. 42) such that it follows from the normal distribution with variance $\widetilde{\sigma}_{mk}^2$,

$$\widetilde{\sigma}_{mk}^2 = 1 / \left(\frac{1}{\sigma^2} \sum_{j=1}^N z_{kj}^2 + \lambda_{mk}^W \right) \quad (6.11)$$

and mean $\widetilde{\mu}_{mk}$,

$$\widetilde{\mu}_{mk} = \frac{\widetilde{\sigma}_{mk}^2}{\sigma^2} \cdot \sum_{j=1}^N z_{kj} \left(a_{mj} - \sum_{i \neq k}^K w_{mi} z_{ij} \right). \quad (6.12)$$

In this case, the posterior precision $1/\widetilde{\sigma}_{mk}^2$ is the sum of prior precision λ_{mk}^W and “data precision” $\frac{1}{\sigma^2} \sum_{j=1}^N z_{kj}^2$. This also shows, in the Netflix context, that the conditional distribution over the movie feature vector \mathbf{w}_m , conditioned on the user features, observed rating matrix \mathbf{A} , and the values of the hyper-parameters, follows a Gaussian density.

Similarly, due to symmetry, a completely analogous derivation for parameter z_{kn} , where $k \in \{1, 2, \dots, K\}$ and $n \in \{1, 2, \dots, N\}$, is used for the factor \mathbf{Z} . See Problem 6.2.

The conditional density of σ^2 depends on its parents $(\alpha_\sigma, \beta_\sigma)$, children (\mathbf{A}) , and coparents (\mathbf{W}, \mathbf{Z}) . And it follows an inverse-Gamma distribution, as demonstrated by the

². See Figure 6.1 and Section 6.2.

conjugacy presented in Equation (3.7) (p. 47):

$$\begin{aligned}
 p(\sigma^2 \mid \mathbf{A}, \mathbf{W}, \mathbf{Z}, \alpha_\sigma, \beta_\sigma) &= \mathcal{G}^{-1}(\sigma^2 \mid \widetilde{\alpha}_\sigma, \widetilde{\beta}_\sigma), \\
 \widetilde{\alpha}_\sigma &= \frac{MN}{2} + \alpha_\sigma, \quad \widetilde{\beta}_\sigma = \frac{1}{2} \sum_{m,n=1}^{M,N} (\mathbf{A} - \mathbf{W}\mathbf{Z})_{mn}^2 + \beta_\sigma.
 \end{aligned} \tag{6.13}$$

Missing entries. In many cases, e.g., in the Netflix context, some entries of \mathbf{A} are missing. Let Ω denote the set containing all observed entries in data \mathbf{A} . Denote further $\Omega_m = \{n \mid (m, n) \in \Omega\}$, i.e., the observed entries in the m -th row; $\Omega_n = \{m \mid (m, n) \in \Omega\}$, i.e., the observed entries in the n -th column. The posterior density of w_{mk} can be obtained by

$$w_{mk} \sim \mathcal{N}(w_{mk} \mid \widetilde{\mu}_{mk}, \widetilde{\sigma}_{mk}^2), \tag{6.14}$$

where

$$\begin{aligned}
 \widetilde{\sigma}_{mk}^2 &= 1 / \left(\frac{1}{\sigma^2} \sum_{j \in \Omega_m} z_{kj}^2 + \lambda_{mk}^W \right), \\
 \widetilde{\mu}_{mk} &= \frac{\widetilde{\sigma}_{mk}^2}{\sigma^2} \cdot \sum_{j \in \Omega_m} z_{kj} \left(a_{mj} - \sum_{i \neq k} w_{mi} z_{ij} \right).
 \end{aligned} \tag{6.15}$$

In the following discussion, for the sake of simplicity, we only consider the data matrix \mathbf{A} with full observations. Analogous results for instances involving missing entries can be obtained in a similar manner.

GGG with shared prior (GGGM). When we set $\lambda = \lambda_{mk}^W$ for all $m \in \{1, 2, \dots, M\}$ and $k \in \{1, 2, \dots, K\}$, the conditional posterior distributions we obtain in the Gibbs sampling algorithm can be written as a multivariate Gaussian density (Definition 3.7.1, p. 74). In this case, we can place a multivariate Gaussian prior over each row \mathbf{w}_m of \mathbf{W} and each column \mathbf{z}_n of \mathbf{Z} :

$$\mathbf{w}_m \sim \mathcal{N}(\mathbf{w}_m \mid \mathbf{0}, \lambda^{-1} \mathbf{I}), \quad \mathbf{z}_n \sim \mathcal{N}(\mathbf{z}_n \mid \mathbf{0}, \lambda^{-1} \mathbf{I}),$$

i.e., each of the M or N item factors follows a multivariate normal distribution. Again by Bayes' rule, let \mathbf{W}_{-m} denote all elements of \mathbf{W} except the m -th row, the conditional posterior distribution we obtain in the Gibbs sampling algorithm can be obtained by

$$\begin{aligned}
 p(\mathbf{w}_m \mid \sigma^2, \mathbf{W}_{-m}, \mathbf{Z}, \lambda, \mathbf{A}) &\propto p(\mathbf{A} \mid \mathbf{W}, \mathbf{Z}, \sigma^2) \times \mathcal{N}(\mathbf{w}_m \mid \mathbf{0}, \lambda^{-1} \mathbf{I}) \\
 &\propto \mathcal{N}(\mathbf{A} \mid \mathbf{W}\mathbf{Z}, \sigma^2 \mathbf{I}) \times \mathcal{N}(\mathbf{w}_m \mid \mathbf{0}, \lambda^{-1} \mathbf{I}) \\
 &\propto \exp \left\{ -\frac{1}{2\sigma^2} \sum_{j=1}^N (a_{mj} - \mathbf{w}_m^\top \mathbf{z}_j)^2 \right\} \times \exp \left\{ -\frac{\lambda}{2} \mathbf{w}_m^\top \mathbf{w}_m \right\} \\
 &\stackrel{*}{\propto} \exp \left\{ -\frac{1}{2} \mathbf{w}_m^\top \left[\underbrace{\lambda \mathbf{I} + \frac{1}{\sigma^2} \sum_{j=1}^N \mathbf{z}_j \mathbf{z}_j^\top}_{\widetilde{\Sigma}^{-1}} \right] \mathbf{w}_m + \mathbf{w}_m^\top \underbrace{\frac{1}{\sigma^2} \sum_{j=1}^N a_{mj} \mathbf{z}_j}_{\widetilde{\Sigma}^{-1} \widetilde{\boldsymbol{\mu}}} \right\} \propto \mathcal{N}(\mathbf{w}_m \mid \widetilde{\boldsymbol{\mu}}, \widetilde{\Sigma}),
 \end{aligned} \tag{6.16}$$

where the equality (\star) conforms to Equation (3.33) (p. 77) such that it follows from the multivariate Gaussian distribution with covariance $\tilde{\Sigma}$,

$$\tilde{\Sigma} = \left[\lambda \mathbf{I} + \frac{1}{\sigma^2} \sum_{j=1}^N \mathbf{z}_j \mathbf{z}_j^\top \right]^{-1}$$

and mean vector $\tilde{\boldsymbol{\mu}}$,

$$\tilde{\boldsymbol{\mu}} = \frac{1}{\sigma^2} \tilde{\Sigma} \cdot \sum_{j=1}^N a_{mj} \mathbf{z}_j.$$

In this case, the **posterior precision matrix** $\tilde{\Sigma}^{-1}$ is the sum of the **prior precision matrix** $\lambda \mathbf{I}$ and “**data precision matrix**” $\frac{1}{\sigma^2} \sum_{j=1}^N \mathbf{z}_j \mathbf{z}_j^\top$. And due to symmetry, an analogous expression can be derived for each column \mathbf{z}_n of factor \mathbf{Z} , where $n \in \{1, 2, \dots, N\}$. See Problem 6.2.

Gibbs sampling. Because conjugate priors for both the parameters and hyper-parameters are used in the Bayesian matrix factorization model, it is easy to sample from the conditional distributions derived from the posterior distribution. By this Gibbs sampling method introduced in Section 2.3.3 (p. 26), we can construct a Gibbs sampler for the GGG model as formulated in Algorithm 8. Due to our choice of priors, we can sample from all conditional distributions directly using standard methods, which obviates slower sampling procedures such as rejection sampling. And also in practice, all the parameters of Gaussian priors are set to be the same value $\lambda = \{\lambda_{mk}^W\}'s = \{\lambda_{kn}^Z\}'s$ for all m, k, n . By default, uninformative hyper-parameters are $\alpha_\sigma = \beta_\sigma = 1$, $\{\lambda_{mk}^W\} = \{\lambda_{kn}^Z\} = 0.1$.

Algorithm 8 Gibbs sampler for GGG model in one iteration (prior on variance σ^2 here, similarly for the precision τ). The procedure presented here may not be efficient but is explanatory. A more efficient one can be implemented in a vectorized manner. By default, uninformative hyper-parameters are $\alpha_\sigma = \beta_\sigma = 1$, $\{\lambda_{mk}^W\} = \{\lambda_{kn}^Z\} = 0.1$.

Require: Choose initial $\alpha_\sigma, \beta_\sigma, \lambda_{mk}^W, \lambda_{kn}^Z$;

- 1: **for** $k = 1$ to K **do**
 - 2: **for** $m = 1$ to M **do**
 - 3: Sample w_{mk} from $p(w_{mk} \mid \mathbf{A}, \mathbf{W}_{-mk}, \mathbf{Z}, \sigma^2, \lambda_{mk}^W)$; ▷ Equation (6.10)
 - 4: **end for**
 - 5: **for** $n = 1$ to N **do**
 - 6: Sample z_{kn} from $p(z_{kn} \mid \mathbf{A}, \mathbf{W}, \mathbf{Z}_{-kn}, \sigma^2, \lambda_{kn}^Z)$; ▷ Symmetry of Eq. (6.10)
 - 7: **end for**
 - 8: **end for**
 - 9: Sample σ^2 from $p(\sigma^2 \mid \mathbf{A}, \mathbf{W}, \mathbf{Z}, \alpha_\sigma, \beta_\sigma)$; ▷ Equation (6.13)
 - 10: Report loss in Equation (6.2), stop if it converges.
-

Prior by Gamma distribution. We also notice that placing an inverse-Gamma prior on the variance parameter of a Gaussian density is equivalent to assigning a Gamma prior

on the precision parameter (the inverse of variance). In representing the precision $\tau = \sigma^{-2}$, we use a Gamma distribution with shape $\alpha_\tau > 0$ and rate $\beta_\tau > 0$ (Definition 3.2.3, p. 43):

$$p(\tau) \sim \mathcal{G}(\tau \mid \alpha_\tau, \beta_\tau) = \frac{\beta_\tau^{\alpha_\tau}}{\Gamma(\alpha_\tau)} \tau^{\alpha_\tau - 1} \exp(-\beta_\tau \cdot \tau), \quad (6.17)$$

The posterior is obtained similarly (Equation (3.5), p. 45),

$$p(\tau \mid \mathbf{W}, \mathbf{Z}, \mathbf{A}) = \mathcal{G}(\tau; \widetilde{\alpha}_\tau, \widetilde{\beta}_\tau),$$

$$\widetilde{\alpha}_\tau = \frac{MN}{2} + \alpha_\tau, \quad \widetilde{\beta}_\tau = \frac{1}{2} \sum_{m,n=1}^{M,N} (\mathbf{A} - \mathbf{W}\mathbf{Z})_{mn}^2 + \beta_\tau.$$

In practical applications, the prior parameters α_τ and β_τ can be chosen to be equal to α_σ and β_σ , respectively.

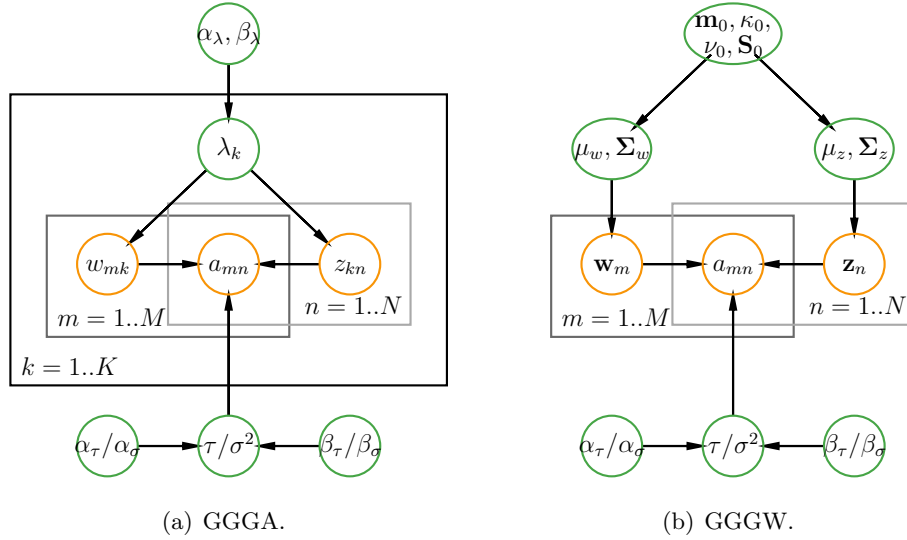


Figure 6.3: Graphical model representation of GGGA and GGGW models. Green circles denote prior variables, orange circles represent observed and latent variables, and plates represent repeated variables. The slash “/” in the variable represents “or,” and the comma “,” in the variable represents “and.”

6.3. All Gaussian Model with ARD Hierarchical Prior (GGGA)

The all Gaussian with hierarchical Gamma prior (GGGA) model is proposed by Virtanen et al. (2011, 2012) based on the GGG model. The distinction lies in the incorporation of a hyperprior over the Gaussian prior in the GGGA model. Moreover, the GGGA model favors an *automatic relevance determination* (ARD) that helps perform *automatic model selection* (Figure 6.3(a)).

Automatic relevance determination (ARD). *Automatic relevance determination* stands as a Bayesian technique employed in machine learning and statistical modeling to automatically discern the relevance or significance of input features. ARD is particularly applied in the context of Bayesian linear regression models.

In the Bayesian approach, we model the relationship between input features and the output using a probabilistic framework. In linear regression, this relationship is often represented as:

$$\mathbf{b} = \mathbf{A}\mathbf{x} + \boldsymbol{\epsilon},$$

where $\mathbf{A} \in \mathbb{R}^{M \times N}$ is the input data matrix, $\mathbf{x} \in \mathbb{R}^N$ is a vector of weights, and $\boldsymbol{\epsilon} \in \mathbb{R}^M$ is a noise term. ARD extends this framework by introducing a probabilistic prior distribution over the weights. The ARD method assigns a separate precision parameter (inverse variance) to each weight in the model.

The fundamental concept behind ARD is to automatically determine the relevance of input features by allowing the model to adaptively assign large precision (low variance) to irrelevant features and small precision (high variance) to relevant features. Features with small precision effectively become “shrunk” and contribute less to the model, allowing the algorithm to automatically select a subset of features.

In a Bayesian context, the ARD model involves placing a hyperprior over the precision parameters, and the optimization process aims to find the most probable values for these parameters given the observed data. This allows the model to effectively estimate the relevance of each feature while considering the uncertainty associated with the estimation.

The advantages of ARD include its ability to perform feature selection automatically, thereby reducing overfitting and improving the interpretability of the model. However, it’s essential to carefully choose appropriate prior distributions and hyper-parameters to achieve meaningful results.

Hyperprior. Going further from the GGG model, we consider the ARD prior, in which case we place a further Gamma prior (i.e., a hierarchical prior):

$$w_{mk} \sim \mathcal{N}(0, (\lambda_k)^{-1}), \quad z_{kn} \sim \mathcal{N}(0, (\lambda_k)^{-1}), \quad \lambda_k \sim \mathcal{G}(\alpha_\lambda, \beta_\lambda), \quad (6.18)$$

where $k \in \{1, 2, \dots, K\}$, and λ_k is shared by all entries in the same column of \mathbf{W} and the same row of \mathbf{Z} . The entire factor k is then either activated if λ_k has a low value or “turned off” if λ_k has a high value (see Figure 3.1, p. 41).

Posterior. For RMF, following the Bayes’ rule and MCMC, this means we need to be able to draw from distributions (again by Markov blanket, Section 6.2):

$$\begin{aligned} p(\sigma^2 \mid \mathbf{A}, \mathbf{W}, \mathbf{Z}, \alpha_\sigma, \beta_\sigma), & \quad p(w_{mk} \mid \mathbf{A}, \mathbf{W}_{-mk}, \mathbf{Z}, \sigma^2, \boldsymbol{\lambda}), \\ p(\lambda_k \mid \mathbf{W}, \mathbf{Z}, \boldsymbol{\lambda}_{-k}, \sigma^2, \alpha_\lambda, \beta_\lambda), & \quad p(z_{kn} \mid \mathbf{A}, \mathbf{W}, \mathbf{Z}_{-kn}, \sigma^2, \boldsymbol{\lambda}), \end{aligned}$$

where $\boldsymbol{\lambda} \in \mathbb{R}_+^K$ is a vector including all λ_k values, and $\boldsymbol{\lambda}_{-k}$ denotes all elements of $\boldsymbol{\lambda}$ except λ_k . The conditional posteriors for σ^2 , w_{mk} ’s, and z_{kn} ’s remain consistent with the GGG model, except now we replace λ_{mk}^W and λ_{kn}^Z for all $m \in \{1, 2, \dots, M\}$ and $n \in \{1, 2, \dots, N\}$ by λ_k . The conditional posterior density of λ_k depends on its parents ($\alpha_\lambda, \beta_\lambda$), children

(k -th row \mathbf{w}_k of \mathbf{W} , k -th column \mathbf{z}_k of \mathbf{Z} , see definition in Equation (6.1)), and coparents ($\boldsymbol{\lambda}_{-k}$)³. Then it follows that,

$$\begin{aligned}
 & p(\lambda_k \mid \mathbf{W}, \mathbf{Z}, \boldsymbol{\lambda}_{-k}, \sigma^2, \alpha_\lambda, \beta_\lambda) \\
 & \propto p(\mathbf{w}_k, \mathbf{z}_k \mid \lambda_k) \cdot p(\lambda_k) = \prod_{i=1}^M \mathcal{N}(w_{ik} \mid 0, (\lambda_k)^{-1}) \cdot \prod_{j=1}^N \mathcal{N}(z_{kj} \mid 0, (\lambda_k)^{-1}) \cdot \mathcal{G}(\lambda_k \mid \alpha_\lambda, \beta_\lambda) \\
 & = \prod_{i=1}^M \lambda_k^{1/2} \exp\left\{-\frac{\lambda_k w_{ik}^2}{2}\right\} \cdot \prod_{j=1}^N \lambda_k^{1/2} \exp\left\{-\frac{\lambda_k z_{kj}^2}{2}\right\} \cdot \frac{\beta_\lambda^{\alpha_\lambda}}{\Gamma(\alpha_\lambda)} \lambda_k^{\alpha_\lambda-1} \exp(-\lambda_k \beta_\lambda) \\
 & \propto \lambda_k^{\frac{M+N}{2} + \alpha_\lambda - 1} \exp\left\{-\lambda_k \cdot \left(\frac{1}{2} \sum_{i=1}^M w_{ik}^2 + \frac{1}{2} \sum_{j=1}^N z_{kj}^2 + \beta_\lambda\right)\right\} \\
 & \propto \mathcal{G}(\lambda_k \mid \widetilde{\alpha}_\lambda, \widetilde{\beta}_\lambda),
 \end{aligned} \tag{6.19}$$

where

$$\widetilde{\alpha}_\lambda = \frac{M+N}{2} + \alpha_\lambda, \quad \widetilde{\beta}_\lambda = \frac{1}{2} \sum_{i=1}^M w_{ik}^2 + \frac{1}{2} \sum_{j=1}^N z_{kj}^2 + \beta_\lambda.$$

According to the definition of the Gamma distribution (Definition 3.2.3, p. 43), we obtain the moments of the posterior density for λ_k :

$$\mathbb{E}[\lambda_k] = \frac{\widetilde{\alpha}_\lambda}{\widetilde{\beta}_\lambda}, \quad \text{Var}[\lambda_k] = \frac{\widetilde{\alpha}_\lambda}{\widetilde{\beta}_\lambda^2}.$$

Therefore, upon observing the posterior parameters, it is evident that with a larger shape of the raw matrix \mathbf{A} (i.e., $M+N$ is larger), there is a preference for a larger value of λ_k (during sampling, since $\widetilde{\alpha}_\lambda$ tends to be larger). As indicated in Equation (6.18), this preference imposes a larger and sparser regularization over the model. This is reasonable since a larger shape indicates the vector product for each entry of \mathbf{A} through \mathbf{W} and \mathbf{Z} involves more entries to sum up.

Moreover, if the elements of the factored components \mathbf{W} and \mathbf{Z} are larger, the value of $\widetilde{\beta}_\lambda$ tends to be larger as well. Consequently, a smaller value of λ_k will be drawn. This is reasonable in the sense that we want to explore in a larger space if the factored components have larger elements from previous Gibbs iterations.

Gibbs sampling. Again we can construct a Gibbs sampler for the GGGA model, as formulated in Algorithm 9. By default, uninformative hyper-parameters are $\alpha_\sigma = \beta_\sigma = 1$, $\alpha_\lambda = \beta_\lambda = 1$.

6.4. All Gaussian Model with Wishart Hierarchical Prior (GGGW)

The hierarchical prior with Wishart density is proposed by Salakhutdinov and Mnih (2008) to increase flexibility and calibration based on the GGG model. Instead of assuming independence of each entry in the factored components \mathbf{W} and \mathbf{Z} , we now assume each row

³. See Figure 6.3(a) and Section 6.2.

Algorithm 9 Gibbs sampler for GGGA model in one iteration (prior on variance σ^2 here, similarly for the precision τ). The procedure presented here may not be efficient but is explanatory. A more efficient one can be implemented in a vectorized manner. By default, uninformative hyper-parameters are $\alpha_\sigma = \beta_\sigma = 1$, $\alpha_\lambda = \beta_\lambda = 1$.

Require: Choose initial $\alpha_\sigma, \beta_\sigma, \alpha_\lambda, \beta_\lambda$;

- 1: **for** $k = 1$ to K **do**
 - 2: **for** $m = 1$ to M **do**
 - 3: Sample w_{mk} from $p(w_{mk} \mid \mathbf{A}, \mathbf{W}_{-mk}, \mathbf{Z}, \sigma^2, \lambda_k)$; ▷ Equation (6.10)
 - 4: **end for**
 - 5: **for** $n = 1$ to N **do**
 - 6: Sample z_{kn} from $p(z_{kn} \mid \mathbf{A}, \mathbf{W}, \mathbf{Z}_{-kn}, \sigma^2, \lambda_k)$; ▷ Symmetry of Eq. (6.10)
 - 7: **end for**
 - 8: Sample λ_k from $p(\lambda_k \mid \mathbf{W}, \mathbf{Z}, \sigma^2, \alpha_\lambda, \beta_\lambda)$; ▷ Equation (6.19)
 - 9: **end for**
 - 10: Sample σ^2 from $p(\sigma^2 \mid \mathbf{A}, \mathbf{W}, \mathbf{Z}, \alpha_\sigma, \beta_\sigma)$; ▷ Equation (6.13)
 - 11: Report loss in Equation (6.2), stop if it converges.
-

\mathbf{w}_m of \mathbf{W} and each column \mathbf{z}_n of \mathbf{Z} comes from a multivariate Gaussian density (Definition 3.7.1, p. 74), whose parameters are placed over a further normal-inverse-Wishart (NIW) prior (Definition 3.7.5, p. 81). Figure 6.3(b) shows the graphical representation of the GGGW model.

Prior and hyperprior. Same as the GGG model, we consider the Gaussian likelihood over the data matrix \mathbf{A} , and the variance parameter σ^2 is placed over an inverse-Gamma prior with shape α_σ and scale β_σ . Given the m -th row \mathbf{w}_m of \mathbf{W} and the n -th column \mathbf{z}_n of \mathbf{Z} , we consider the multivariate Gaussian density and the normal-inverse-Wishart prior as follows:

$$\mathbf{w}_m \sim \mathcal{N}(\mathbf{w}_m \mid \boldsymbol{\mu}_w, \boldsymbol{\Sigma}_w), \quad \boldsymbol{\mu}_w, \boldsymbol{\Sigma}_w \sim \mathcal{NIW}(\boldsymbol{\mu}_w, \boldsymbol{\Sigma}_w \mid \mathbf{m}_0, \kappa_0, \nu_0, \mathbf{S}_0); \quad (6.20)$$

$$\mathbf{z}_n \sim \mathcal{N}(\mathbf{z}_n \mid \boldsymbol{\mu}_z, \boldsymbol{\Sigma}_z), \quad \boldsymbol{\mu}_z, \boldsymbol{\Sigma}_z \sim \mathcal{NIW}(\boldsymbol{\mu}_z, \boldsymbol{\Sigma}_z \mid \mathbf{m}_0, \kappa_0, \nu_0, \mathbf{S}_0), \quad (6.21)$$

where $\mathcal{NIW}(\boldsymbol{\mu}, \boldsymbol{\Sigma} \mid \mathbf{m}_0, \kappa_0, \nu_0, \mathbf{S}_0) = \mathcal{N}(\boldsymbol{\mu} \mid \mathbf{m}_0, \frac{1}{\kappa_0} \boldsymbol{\Sigma}) \cdot \text{IW}(\boldsymbol{\Sigma} \mid \mathbf{S}_0, \nu_0)$ is the density of a normal-inverse-Wishart distribution, and $\text{IW}(\boldsymbol{\Sigma} \mid \mathbf{S}_0, \nu_0)$ is the inverse-Wishart distribution (Definition 3.7.4, p. 80). While we can also place normal and inverse-Wishart priors over the mean and covariance parameters separately, i.e., a semi-conjugate prior. We do not repeat the details here, see Section 3.7.4 and 3.7.5 (p. 82 and p. 82).

Following from the discussion in Section 3.7.7 (p. 85), the posterior density of $\{\boldsymbol{\mu}_w, \boldsymbol{\Sigma}_w\}$ also follows a NIW distribution with updated parameters:

$$\boldsymbol{\mu}_w, \boldsymbol{\Sigma}_w \sim \mathcal{NIW}(\boldsymbol{\mu}_w, \boldsymbol{\Sigma}_w \mid \mathbf{m}_M, \kappa_M, \nu_M, \mathbf{S}_M), \quad (6.22)$$

where

$$\mathbf{m}_M = \frac{\kappa_0 \mathbf{m}_0 + M \bar{\mathbf{w}}}{\kappa_M} = \frac{\kappa_0}{\kappa_M} \mathbf{m}_0 + \frac{M}{\kappa_M} \bar{\mathbf{w}}, \quad (6.23)$$

$$\kappa_M = \kappa_0 + M, \quad (6.24)$$

$$\nu_M = \nu_0 + M, \quad (6.25)$$

$$\mathbf{S}_M = \mathbf{S}_0 + \mathbf{S}_{\bar{\mathbf{w}}} + \frac{\kappa_0 M}{\kappa_0 + M} (\bar{\mathbf{w}} - \mathbf{m}_0)(\bar{\mathbf{w}} - \mathbf{m}_0)^\top \quad (6.26)$$

$$= \mathbf{S}_0 + \sum_{m=1}^M \mathbf{w}_m \mathbf{w}_m^\top + \kappa_0 \mathbf{m}_0 \mathbf{m}_0^\top - \kappa_M \mathbf{m}_M \mathbf{m}_M^\top, \quad (6.27)$$

$$\bar{\mathbf{w}} = \frac{1}{M} \sum_{m=1}^M \mathbf{w}_m, \quad (6.28)$$

$$\mathbf{S}_{\bar{\mathbf{w}}} = \sum_{m=1}^M (\mathbf{w}_m - \bar{\mathbf{w}})(\mathbf{w}_m - \bar{\mathbf{w}})^\top. \quad (6.29)$$

An intuitive interpretation for the parameters in NIW can be obtained from the updated parameters above. The parameter ν_0 is the prior number of samples to observe the covariance matrix, and $\nu_M = \nu_0 + M$ is the posterior number of samples. The posterior mean \mathbf{m}_M of the model mean $\boldsymbol{\mu}_w$ is a weighted average of the prior mean \mathbf{m}_0 and the sample mean $\bar{\mathbf{w}}$. The posterior scale matrix \mathbf{S}_M is the sum of the prior scale matrix \mathbf{S}_0 , empirical covariance matrix $\mathbf{S}_{\bar{\mathbf{w}}}$, and an extra term due to the uncertainty in the mean. And due to symmetry, a similar form for $\{\boldsymbol{\mu}_z, \boldsymbol{\Sigma}_z\}$ can be derived.

Gibbs sampling. Once again, we can construct a Gibbs sampler for the GGGW model as formulated in Algorithm 10. By default, uninformative hyper-parameters are $\alpha_\sigma = \beta_\sigma = 1$, $\mathbf{m}_0 = \mathbf{0}$, $\kappa_0 = 1$, $\nu_0 = K + 1$, $\mathbf{S}_0 = \mathbf{I}$.

Algorithm 10 Gibbs sampler for GGGW model in one iteration (prior on variance σ^2 here, similarly for the precision τ). By default, uninformative hyper-parameters are $\alpha_\sigma = \beta_\sigma = 1$, $\mathbf{m}_0 = \mathbf{0}$, $\kappa_0 = 1$, $\nu_0 = K + 1$, $\mathbf{S}_0 = \mathbf{I}$.

Require: Choose initial $\alpha_\sigma, \beta_\sigma, \mathbf{m}_0, \kappa_0, \nu_0, \mathbf{S}_0$;

- 1: **for** $m = 1$ to M **do**
 - 2: Sample \mathbf{w}_m from $p(\mathbf{w}_m \mid \boldsymbol{\mu}_w, \boldsymbol{\Sigma}_w)$; ▷ Equation (6.20)
 - 3: **end for**
 - 4: **for** $n = 1$ to N **do**
 - 5: Sample \mathbf{z}_n from $p(\mathbf{z}_n \mid \boldsymbol{\mu}_z, \boldsymbol{\Sigma}_z)$; ▷ Symmetry of Eq. (6.21)
 - 6: **end for**
 - 7: Sample $\boldsymbol{\mu}_w, \boldsymbol{\Sigma}_w$ from $p(\boldsymbol{\mu}_w, \boldsymbol{\Sigma}_w \mid \mathbf{m}_M, \kappa_M, \nu_M, \mathbf{S}_M)$ ▷ Equation (6.22)
 - 8: Sample $\boldsymbol{\mu}_z, \boldsymbol{\Sigma}_z$ from $p(\boldsymbol{\mu}_z, \boldsymbol{\Sigma}_z \mid \mathbf{m}_N, \kappa_N, \nu_N, \mathbf{S}_N)$ ▷ Symmetry of Eq. (6.22)
 - 9: Sample σ^2 from $p(\sigma^2 \mid \mathbf{A}, \mathbf{W}, \mathbf{Z}, \alpha_\sigma, \beta_\sigma)$; ▷ Equation (6.13)
 - 10: Report loss in Equation (6.2), stop if it converges.
-

6.5. Gaussian Likelihood with Volume and Gaussian Priors (GVG)

The Gaussian likelihood with volume and Gaussian prior (GVG) is introduced by Arngren et al. (2011). While the original paper applies the volume prior to unmix a set of pixels into *pure spectral signatures (endmembers)* and corresponding *fractional abundances* in hyper-spectral image analysis, in which case the factored components are nonnegative. However, it can also be applied in the real-valued applications.

In the GVG model, the prior over \mathbf{Z} is still a Gaussian density as that in the GGG model. Instead of assuming Gaussian prior over \mathbf{W} , Arngren et al. (2011) put a volume prior for the factored component \mathbf{W} with density $\mathbf{W} \propto \exp\{-\gamma \det(\mathbf{W}^\top \mathbf{W})\}$ (Figure 6.4). The prior has a single parameter γ that is manually determined.

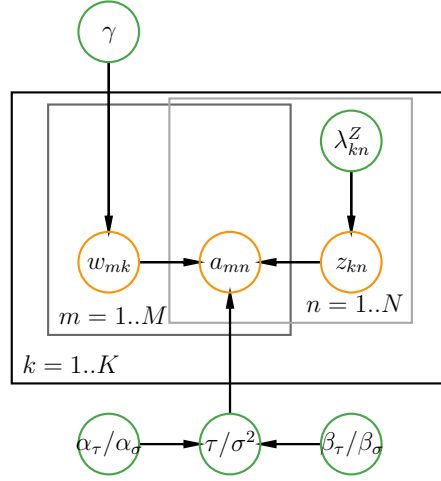


Figure 6.4: Graphical representation of GVG model. Green circles denote prior variables, orange circles represent observed and latent variables, and plates represent repeated variables. The slash “/” in the variable represents “or.”

Posterior. Denote vector $\mathbf{w}_{m,-k} \in \mathbb{R}^{K-1}$ as the m -th row of \mathbf{W} excluding column k ; vector $\mathbf{w}_{-m,k} \in \mathbb{R}^{M-1}$ as the k -th column of \mathbf{W} excluding row m ; matrix $\mathbf{W}_{-m,-k} \in \mathbb{R}^{(M-1) \times (K-1)}$ as \mathbf{W} excluding row m and column k ; matrix $\mathbf{W}_{:, -k} \in \mathbb{R}^{M \times (K-1)}$ as \mathbf{W} excluding column k ; scalar value $D_{-k,-k} = \det(\mathbf{W}_{:, -k}^\top \mathbf{W}_{:, -k})$; and the *matrix adjugate* of $(\mathbf{W}_{:, -k}^\top \mathbf{W}_{:, -k})$ as $\mathbf{A}_{-k,-k} = \det(\mathbf{W}_{:, -k}^\top \mathbf{W}_{:, -k}) (\mathbf{W}_{:, -k}^\top \mathbf{W}_{:, -k})^{-1} \in \mathbb{R}^{(K-1) \times (K-1)}$. Then the posterior density of w_{mk} can be obtained by

$$w_{mk} \sim \mathcal{N}(w_{mk} \mid \widetilde{\mu}_{mk}, \widetilde{\sigma}_{mk}^2), \quad (6.30)$$

where

$$\widetilde{\mu}_{mk} = \widetilde{\sigma}_{mk}^2 \left\{ \gamma \mathbf{w}_{m,-k}^\top \mathbf{A}_{-k,-k} (\mathbf{W}_{-m,-k}^\top \mathbf{w}_{-m,k}) + \frac{1}{\sigma^2} \sum_{j=1}^N (a_{mj} - \sum_{i \neq k} \mathbf{w}_{m,-k}^\top \mathbf{z}_{j,-k}) z_{kj} \right\},$$

and

$$\widetilde{\sigma}_{mk}^2 = 1 / \left(\frac{1}{\sigma^2} \sum_{j=1}^N z_{kj}^2 + \gamma \left(D_{-k,-k} - \mathbf{w}_{m,-k}^\top \mathbf{A}_{-k,-k} \mathbf{w}_{m,-k} \right) \right).$$

The above result can be obtained by extracting w_{mk} from $\exp\{-\gamma \det(\mathbf{W}^\top \mathbf{W})\}$ and from the fact that $\det(\mathbf{M}) = \det(\mathbf{D}) \det(\mathbf{A} - \mathbf{B}\mathbf{D}^{-1}\mathbf{C}) = \det(\mathbf{A}) \det(\mathbf{D} - \mathbf{C}\mathbf{A}^{-1}\mathbf{B})$ if the matrix \mathbf{M} has the block formulation $\mathbf{M} = \begin{bmatrix} \mathbf{A} & \mathbf{B} \\ \mathbf{C} & \mathbf{D} \end{bmatrix}$.

⌘ Chapter 6 Problems ⌘

1. Use the “MovieLens 100K” data set introduced in Section 4.10.2 (p. 122) to assess and compare the effectiveness of Bayesian real matrix factorization approaches introduced in this Chapter.
2. Following the derivation in Equation (6.10), derive the conditional distribution over the user feature z_{kn} for all $k \in \{1, 2, \dots, K\}$ and $n \in \{1, 2, \dots, N\}$ for the GGG model. Similarly, following the derivation in Equation (6.16), obtain the conditional distribution over the user feature z_n for all $n \in \{1, 2, \dots, N\}$ within the context of the GGGM model.
3. Derive the automatic relevance determination related results for the linear regression models based on the discussions in Section 6.3 and Section 2.4 (p. 28).

Bayesian Nonnegative Matrix Factorization

Contents

7.1	Introduction	157
7.2	Gaussian Likelihood with Exponential Priors (GEE)	159
7.3	Gaussian Likelihood with Exponential Priors and ARD Hierarchical Prior (GEEA)	162
7.4	Gaussian Likelihood with Truncated-Normal Priors (GTT) .	163
7.5	Gaussian Likelihood with Truncated-Normal and Hierarchical Priors (GTTN)	166
7.6	Gaussian Likelihood with Rectified-Normal Priors (GRR) and Hierarchical Prior (GRRN)	168
7.6.1	Examples	173
7.7	Priors as Regularization	176
7.8	Gaussian ℓ_1^2 Norm (GL$_1^2$) Model	177
7.9	Gaussian ℓ_2^2 Norm (GL$_2^2$) and Gaussian ℓ_∞ Norm (GL$_\infty$) Models	180
7.9.1	Examples	184
7.10	Semi-Nonnegative Matrix Factorization	190
7.10.1	Gaussian Likelihood with Exponential and Gaussian Priors (GEG)	190
7.10.2	Gaussian Likelihood with Nonnegative Volume and Gaussian Priors (GnVG)	191
7.11	Nonnegative Matrix Tri-Factorization (NMTF)	191
Chapter 7 Problems		195

7.1. Introduction



The nonnegative matrix factorization (NMF) method is employed for analyzing data matrices with nonnegative elements, which are common in data sets derived from texts and images (Berry et al., 2007). In cases where the entries in \mathbf{A} , \mathbf{W} , and \mathbf{Z} are nonnegative, NMF algorithms have frequently improved performance. Thus, the scope of NMF research has grown rapidly in recent years, particularly in the fields of machine learning (Lee and Seung, 1999, 2000).

Early work on nonnegative matrix factorizations was conducted by a Finnish group of researchers in the 1990s under the name *positive matrix factorization* (Paatero et al., 1991; Paatero and Tapper, 1994; Anttila et al., 1995). This work is rarely cited by later researchers partly due to the unfortunate phrasing of positive matrix factorization, which is misleading as Paatero and Tapper (1994) actually create a nonnegative matrix factorization. Since its introduction by Lee and Seung (1999, 2000), the NMF problem has received a significant amount of attention, both in published and unpublished work, in various fields such as science, engineering, and medicine. Different authors have also proposed alternative formulations for the NMF problem (Schmidt et al., 2009; Tan and Févotte, 2013; Brouwer and Lio, 2017; Lu and Ye, 2022).

The NMF problem can be stated as $\mathbf{A} = \mathbf{W}\mathbf{Z} + \mathbf{E}$, where $\mathbf{A} \in \mathbb{R}^{M \times N}$ is approximately factorized into an $M \times K$ nonnegative matrix $\mathbf{W} \in \mathbb{R}_+^{M \times K}$ and a $K \times N$ nonnegative matrix $\mathbf{Z} \in \mathbb{R}_+^{K \times N}$. The data set \mathbf{A} needs not be complete such that the indices of observed entries can be represented by the mask matrix $\mathbf{M} \in \mathbb{R}^{M \times N}$, where an entry of one indicates the element is observed, and zero indicates an unobserved element. This nonnegativity makes the resulting matrices easier to inspect and more intuitive to interpret, especially in the image analysis context.

To simplify the problem, let us assume that there are no missing entries firstly. Treating missing entries in the Bayesian NMF context is just the same as that in the Bayesian RMF cases (Section 6.2, p. 141). Projecting data vectors \mathbf{a}_n to a smaller dimension $\mathbf{z}_n \in \mathbb{R}^K$ with $K < M$, such that the *reconstruction error* measured by Frobenius norm is minimized (assume K is known):

$$\min_{\mathbf{W}, \mathbf{Z}} L(\mathbf{W}, \mathbf{Z}) = \min_{\mathbf{W}, \mathbf{Z}} \sum_{n=1}^N \sum_{m=1}^M \left(a_{mn} - \mathbf{w}_m^\top \mathbf{z}_n \right)^2, \quad (7.1)$$

where $\mathbf{W} = [\mathbf{w}_1^\top; \mathbf{w}_2^\top; \dots; \mathbf{w}_M^\top] \in \mathbb{R}^{M \times K}$ and $\mathbf{Z} = [\mathbf{z}_1, \mathbf{z}_2, \dots, \mathbf{z}_N] \in \mathbb{R}^{K \times N}$, containing \mathbf{w}_m 's and \mathbf{z}_n 's as **rows and columns**, respectively.

Terminology. Continuing the terminology established in Bayesian RMF, the Bayesian NMF models are denoted by their density functions, arranged in the order of likelihood, priors, and hyperpriors (Section 6.1, p. 139). Table 7.1 summarizes the Bayesian models for nonnegative matrix factorization in this chapter.

Name	Likelihood	Prior \mathbf{W}	Prior \mathbf{Z}	Hierarchical prior
GEE	$\mathcal{N}(a_{mn} \mathbf{w}_m^\top \mathbf{z}_n, \sigma^2)$	$\mathcal{E}(w_{mk} \lambda_{mk}^W)$	$\mathcal{E}(z_{kn} \lambda_{kn}^Z)$	/
GEEA	$\mathcal{N}(a_{mn} \mathbf{w}_m^\top \mathbf{z}_n, \sigma^2)$	$\mathcal{E}(w_{mk} \lambda_k)$	$\mathcal{E}(z_{kn} \lambda_k)$	$\mathcal{G}(\lambda_k \alpha_\lambda, \beta_\lambda)$
GTT	$\mathcal{N}(a_{mn} \mathbf{w}_m^\top \mathbf{z}_n, \sigma^2)$	$\mathcal{TN}(w_{mk} \mu_{mk}^W, \frac{1}{\tau_{mk}^W})$	$\mathcal{TN}(z_{kn} \mu_{kn}^Z, \frac{1}{\tau_{kn}^Z})$	/
GTTN	$\mathcal{N}(a_{mn} \mathbf{w}_m^\top \mathbf{z}_n, \sigma^2)$	$\mathcal{TN}(w_{mk} \mu_{mk}^W, \frac{1}{\tau_{mk}^W})$	$\mathcal{TN}(z_{kn} \mu_{kn}^Z, \frac{1}{\tau_{kn}^Z})$	$\{\mu_{mk}^W, \tau_{mk}^W\}, \{\mu_{kn}^Z, \tau_{kn}^Z\} \sim \mathcal{TNSNG}(\mu_\mu, \tau_\mu, a, b)$
GRR	$\mathcal{N}(a_{mn} \mathbf{w}_m^\top \mathbf{z}_n, \sigma^2)$	$\mathcal{RN}(\cdot \mu_{mk}^W, \frac{1}{\tau_{mk}^W}, \lambda_{mk}^W)$	$\mathcal{RN}(\cdot \mu_{kn}^Z, \frac{1}{\tau_{kn}^Z}, \lambda_{kn}^Z)$	/
GRRN	$\mathcal{N}(a_{mn} \mathbf{w}_m^\top \mathbf{z}_n, \sigma^2)$	$\mathcal{RN}(\cdot \mu_{mk}^W, \frac{1}{\tau_{mk}^W}, \lambda_{mk}^W)$	$\mathcal{RN}(\cdot \mu_{kn}^Z, \frac{1}{\tau_{kn}^Z}, \lambda_{kn}^Z)$	$\{\mu_{mk}^W, \tau_{mk}^W, \lambda_{mk}^W\}, \{\mu_{kn}^Z, \tau_{kn}^Z, \lambda_{kn}^Z\} \sim \mathcal{RNSNG}(\mu_\mu, \tau_\mu, a, b, \alpha_\lambda, \beta_\lambda)$
GL ₁ ²	$\mathcal{N}(a_{mn} \mathbf{w}_m^\top \mathbf{z}_n, \sigma^2)$	$\mathbf{W} \sim \exp \left\{ \frac{-\lambda_k^W}{2} \sum_m (\sum_k w_{mk})^2 \right\}$	$\mathbf{Z} \sim \exp \left\{ \frac{-\lambda_k^Z}{2} \sum_n (\sum_k z_{kn})^2 \right\}$	/
GL ₂ ²	$\mathcal{N}(a_{mn} \mathbf{w}_m^\top \mathbf{z}_n, \sigma^2)$	$\mathbf{W} \sim \exp \left\{ \frac{-\lambda_k^W}{2} \sum_m (\sum_k w_{mk}^2) \right\}$	$\mathbf{Z} \sim \exp \left\{ \frac{-\lambda_k^Z}{2} \sum_n (\sum_k z_{kn}^2) \right\}$	/
GL _∞	$\mathcal{N}(a_{mn} \mathbf{w}_m^\top \mathbf{z}_n, \sigma^2)$	$\mathbf{W} \sim \exp \left\{ -\lambda_k^W \sum_m (\max_k w_{mk}) \right\}$	$\mathbf{Z} \sim \exp \left\{ -\lambda_k^Z \sum_n (\max_k z_{kn}) \right\}$	/
GEG	$\mathcal{N}(a_{mn} \mathbf{w}_m^\top \mathbf{z}_n, \sigma^2)$	$\mathcal{E}(w_{mk} \lambda_{mk}^W)$	$\mathcal{N}(z_{kn} 0, (\lambda_{kn}^Z)^{-1})$	/
GnVG	$\mathcal{N}(a_{mn} \mathbf{w}_m^\top \mathbf{z}_n, \sigma^2)$	$\mathbf{W} \sim \exp \{-\gamma \mathbf{W}^\top \mathbf{W}\} u(\mathbf{W})$	$\mathcal{N}(z_{kn} 0, (\lambda_{kn}^Z)^{-1})$	/

Table 7.1: Overview of Bayesian nonnegative and semi-nonnegative matrix factorization models.

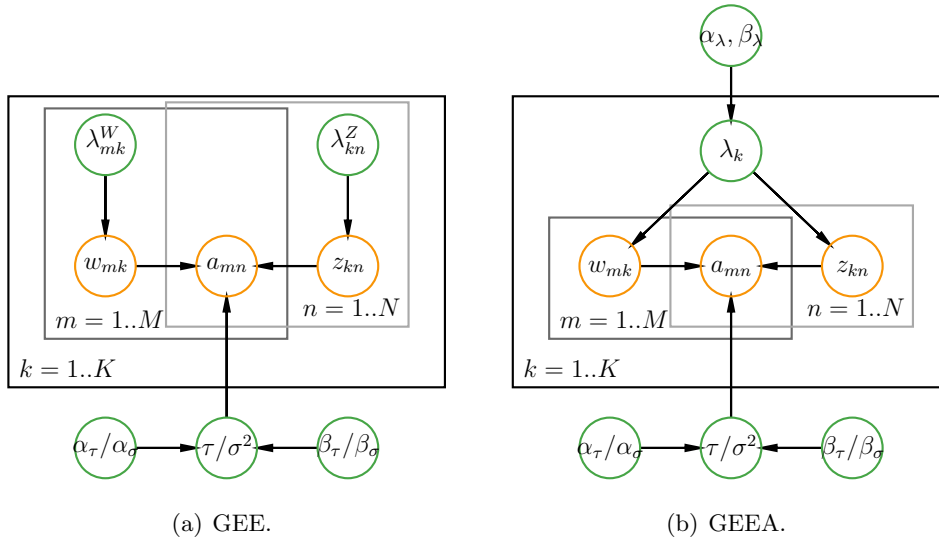


Figure 7.1: Graphical model representation of GEE and GEEA models. Green circles denote prior variables, orange circles represent observed and latent variables, and plates represent repeated variables. The slash “/” in the variable represents “or.”

7.2. Gaussian Likelihood with Exponential Priors (GEE)

The Gaussian likelihood with exponential priors (GEE) model stands out as one of the simplest Bayesian NMF models, employing a Gaussian likelihood for data elements and exponential priors over factor matrices (Schmidt et al., 2009).

Likelihood. Again, we view the data \mathbf{A} as being produced according to the probabilistic generative process shown in Figure 7.1(a). We assume the residuals, e_{mn} , are i.i.d. drawn from a zero-mean Gaussian distribution with variance σ^2 . This is equivalent to assuming the observed (m, n) -th data entry a_{mn} of matrix \mathbf{A} is modeled using a Gaussian likelihood with variance σ^2 and a mean given by the latent decomposition $\mathbf{w}_m^\top \mathbf{z}_n$ (Equation (7.1)). Consequently, this gives rise to the following likelihood function:

$$\begin{aligned} p(\mathbf{A} | \boldsymbol{\theta}) &= \prod_{m,n=1}^{M,N} \mathcal{N}(a_{mn} | (\mathbf{W}\mathbf{Z})_{mn}, \sigma^2) \\ &= \prod_{m,n=1}^{M,N} \mathcal{N}(a_{mn} | (\mathbf{W}\mathbf{Z})_{mn}, \tau^{-1}), \end{aligned} \quad (7.2)$$

where $\boldsymbol{\theta} = \{\mathbf{W}, \mathbf{Z}, \sigma^2\}$ denotes all parameters in the model, σ^2 is the variance, $\tau^{-1} = \sigma^2$ is the precision, and $\mathcal{N}(x | \mu, \sigma^2)$ is the normal density function.

Prior. We treat the latent variables w_{mk} 's (and z_{kn} 's) as random variables. And we need prior densities over these latent variables to express beliefs about their values, e.g., nonnegativity in this context, though there are many other possible constraints (semi-nonnegativity in Ding et al. (2008), discreteness in Gopalan et al. (2014, 2015)). Here, we assume w_{mk} 's and z_{kn} 's are independently drawn from exponential priors with rate parameters λ_{mk}^W and λ_{kn}^Z , respectively (Definition 3.3.1, p. 56):

$$\begin{aligned} w_{mk} &\sim \mathcal{E}(w_{mk} | \lambda_{mk}^W), & z_{kn} &\sim \mathcal{E}(z_{kn} | \lambda_{kn}^Z); \\ p(\mathbf{W}) &= \prod_{m,k=1}^{M,K} \mathcal{E}(w_{mk} | \lambda_{mk}^W), & p(\mathbf{Z}) &= \prod_{k,n=1}^{K,N} \mathcal{E}(z_{kn} | \lambda_{kn}^Z), \end{aligned} \quad (7.3)$$

where $\mathcal{E}(x | \lambda) = \lambda \exp(-\lambda x)u(x)$ is the exponential density with $u(x)$ being the unit step function. This prior serves to enforce the nonnegativity constraint on the components \mathbf{W} and \mathbf{Z} . Same as the GGG model, the prior for the noise variance σ^2 is chosen as an inverse-Gamma density with shape α_σ and scale β_σ (Definition 3.2.4, p. 47):

$$p(\sigma^2) = \mathcal{G}^{-1}(\sigma^2 | \alpha_\sigma, \beta_\sigma) = \frac{\beta_\sigma^{\alpha_\sigma}}{\Gamma(\alpha_\sigma)} (\sigma^2)^{-\alpha_\sigma-1} \exp\left(-\frac{\beta_\sigma}{\sigma^2}\right). \quad (7.4)$$

Again by Bayes' rule (Equation (2.1), p. 22), the posterior is proportional to the product of likelihood and prior, it can be maximized to yield an estimate of \mathbf{W} and \mathbf{Z} .

Posterior. For NMF, following the Bayes' rule and MCMC, this means we need to be able to draw from distributions (by Markov blanket, Section 6.2, p. 141):

$$\begin{aligned} p(w_{mk} \mid \mathbf{A}, \mathbf{W}_{-mk}, \mathbf{Z}, \sigma^2, \boldsymbol{\lambda}^W), \\ p(z_{kn} \mid \mathbf{A}, \mathbf{W}, \mathbf{Z}_{-kn}, \sigma^2, \boldsymbol{\lambda}^Z), \\ p(\sigma^2 \mid \mathbf{A}, \mathbf{W}, \mathbf{Z}, \boldsymbol{\lambda}^W, \boldsymbol{\lambda}^Z), \end{aligned}$$

where $\boldsymbol{\lambda}^W$ is an $M \times K$ matrix containing all $\{\lambda_{mk}^W\}$ entries, $\boldsymbol{\lambda}^Z$ is a $K \times N$ matrix including all $\{\lambda_{kn}^Z\}$ values, and \mathbf{W}_{-mk} denotes all elements of \mathbf{W} except w_{mk} . Using Bayes' theorem, the conditional density of w_{mk} depends on its parents (λ_{mk}^W), children (a_{mn}), and coparents (τ or σ^2 , \mathbf{W}_{-mk} , \mathbf{Z})¹. And it can be obtained by

$$\begin{aligned} & p(w_{mk} \mid \mathbf{A}, \mathbf{W}_{-mk}, \mathbf{Z}, \sigma^2, \lambda_{mk}^W) \\ & \propto p(\mathbf{A} \mid \mathbf{W}, \mathbf{Z}, \sigma^2) \times p(w_{mk} \mid \lambda_{mk}^W) = \prod_{i,j=1}^{M,N} \mathcal{N}(a_{ij} \mid \mathbf{w}_i^\top \mathbf{z}_j, \sigma^2) \times \mathcal{E}(w_{mk} \mid \lambda_{mk}^W) \\ & \propto \exp \left\{ -\frac{1}{2\sigma^2} \sum_{i,j=1}^{M,N} (a_{ij} - \mathbf{w}_i^\top \mathbf{z}_j)^2 \right\} \times \cancel{\lambda_{mk}^W} \exp(-\lambda_{mk}^W \cdot w_{mk}) u(w_{mk}) \\ & \propto \exp \left\{ -\frac{1}{2\sigma^2} \sum_{j=1}^N (a_{mj} - \mathbf{w}_m^\top \mathbf{z}_j)^2 \right\} \cdot \exp(-\lambda_{mk}^W \cdot w_{mk}) u(w_{mk}) \\ & \propto \exp \left\{ -\frac{1}{2\sigma^2} \sum_{j=1}^N \left(w_{mk}^2 z_{kj}^2 + 2w_{mk} z_{kj} \left(\sum_{i \neq k}^K w_{mi} z_{ij} - a_{mj} \right) \right) \right\} \cdot \exp(-\lambda_{mk}^W \cdot w_{mk}) u(w_{mk}) \\ & \propto \exp \left\{ -\underbrace{\left(\frac{\sum_{j=1}^N z_{kj}^2}{2\sigma^2} \right)}_{1/(2\widetilde{\sigma}_{mk}^2)} w_{mk}^2 + w_{mk} \underbrace{\left(-\lambda_{mk}^W + \frac{1}{\sigma^2} \sum_{j=1}^N z_{kj} \left(a_{mj} - \sum_{i \neq k}^K w_{mi} z_{ij} \right) \right)}_{\widetilde{\sigma}_{mk}^2 - 1 \widetilde{\mu}_{mk}} \right\} \cdot u(w_{mk}) \\ & \propto \mathcal{N}(w_{mk} \mid \widetilde{\mu}_{mk}, \widetilde{\sigma}_{mk}^2) \cdot u(w_{mk}) = \mathcal{TN}(w_{mk} \mid \widetilde{\mu}_{mk}, \widetilde{\sigma}_{mk}^2), \end{aligned} \tag{7.5}$$

where $u(x)$ is the unit function with value 1 if $x \geq 0$ and value 0 if $x < 0$,

$$\widetilde{\sigma}_{mk}^2 = \frac{\sigma^2}{\sum_{j=1}^N z_{kj}^2} \tag{7.6}$$

is the posterior ‘‘parent’’ variance of the normal distribution with ‘‘parent’’ mean $\widetilde{\mu}_{mk}$,

$$\widetilde{\mu}_{mk} = \left(-\lambda_{mk}^W + \frac{1}{\sigma^2} \sum_{j=1}^N z_{kj} \left(a_{mj} - \sum_{i \neq k}^K w_{mi} z_{ij} \right) \right) \cdot \widetilde{\sigma}_{mk}^2 \tag{7.7}$$

1. See Figure 7.1(a) and Section 6.2 (p. 141).

and $\mathcal{TN}(x | \mu, \sigma^2)$ is the *truncated-normal (TN) density* with “parent” mean μ and “parent” variance σ^2 (Definition 3.4.1, p. 57).

Interpretation of the Posterior: Sparsity Constraint

The exponential prior serves as an equivalent to imposing an ℓ_1 norm, introducing a sparsity constraint in the GEE model. The sparsity arises from the negative term $-\lambda_{mk}^W$ in Equation (7.7). When λ_{mk}^W becomes larger, the posterior “parent” mean becomes smaller, and the TN distribution will have a larger probability for smaller values since the draws of $\mathcal{TN}(w_{mk} | \widehat{\mu}_{mk}, \widehat{\sigma}_{mk}^2)$ will be around zero, thus imposing sparsity (see Figure 3.8(a), p. 59).

Or after rearrangement, the posterior density of w_{mk} can be equivalently described by

$$\begin{aligned}
 & p(w_{mk} | \mathbf{A}, \mathbf{W}_{-mk}, \mathbf{Z}, \sigma^2, \lambda^W) \\
 & \propto \exp \left\{ \left(\frac{-1}{2\sigma^2} \sum_{j=1}^N z_{kj}^2 \right) w_{mk}^2 + w_{mk} \underbrace{\left(\frac{1}{\sigma^2} \sum_{j=1}^N z_{kj} \left(a_{mj} - \sum_{i \neq k} w_{mi} z_{ij} \right) \right)}_{\widehat{\sigma}_{mk}^2 \widehat{\mu}_{mk}} \right\} \exp(-\lambda_{mk}^W w_{mk}) u(w_{mk}) \\
 & \propto \mathcal{N}(w_{mk} | \widehat{\mu}_{mk}, \widehat{\sigma}_{mk}^2) \cdot \mathcal{E}(w_{mk} | \lambda_{mk}^W) = \mathcal{RN}(w_{mk} | \widehat{\mu}_{mk}, \widehat{\sigma}_{mk}^2, \lambda_{mk}^W),
 \end{aligned}$$

where $\widehat{\sigma}_{mk}^2 = \widehat{\sigma}_{mk}^2 = \frac{\sigma^2}{\sum_{j=1}^N z_{kj}^2}$ is the posterior “parent” variance of the normal distribution with “parent” mean $\widehat{\mu}_{mk}$,

$$\widehat{\mu}_{mk} = \frac{1}{\sum_{j=1}^N z_{kj}^2} \cdot \sum_{j=1}^N z_{kj} \left(a_{mj} - \sum_{i \neq k} w_{mi} z_{ij} \right),$$

and $\mathcal{RN}(x | \mu, \sigma^2, \lambda) \propto \mathcal{N}(x | \mu, \sigma^2) \mathcal{E}(x | \lambda)$ is the *rectified-normal (RN) density* (Definition 3.4.4, p. 62). And due to symmetry, a similar expression for z_{kn} can be easily derived. The conditional density of σ^2 depends on its parents ($\alpha_\sigma, \beta_\sigma$), children (\mathbf{A}), and coparents (\mathbf{W}, \mathbf{Z}). And it is an inverse-Gamma distribution (by conjugacy in Equation (3.7), p. 47):

$$\begin{aligned}
 & p(\sigma^2 | \mathbf{A}, \mathbf{W}, \mathbf{Z}, \alpha_\sigma, \beta_\sigma) = \mathcal{G}^{-1}(\sigma^2 | \widetilde{\alpha}_\sigma, \widetilde{\beta}_\sigma), \\
 & \widetilde{\alpha}_\sigma = \frac{MN}{2} + \alpha_\sigma, \quad \widetilde{\beta}_\sigma = \frac{1}{2} \sum_{m,n=1}^{M,N} (\mathbf{A} - \mathbf{W}\mathbf{Z})_{mn}^2 + \beta_\sigma.
 \end{aligned} \tag{7.8}$$

Gibbs sampling. By this Gibbs sampling method introduced in Section 2.3.3 (p. 26), we can construct a Gibbs sampler for the GEE model as formulated in Algorithm 11. And also in practice, all the parameters of the exponential distribution are set to be the same value $\lambda = \{\lambda_{mk}^W\}'s = \{\lambda_{nk}^Z\}'s$ for all m, k, n . By default, uninformative hyper-parameters are $\alpha_\sigma = \beta_\sigma = 1$, $\{\lambda_{mk}^W\} = \{\lambda_{kn}^Z\} = 0.1$.

Algorithm 11 Gibbs sampler for GEE model in one iteration (prior on variance σ^2 here, similarly for the precision τ). The procedure presented here may not be efficient but is explanatory. A more efficient one can be implemented in a vectorized manner. By default, uninformative hyper-parameters are $\alpha_\sigma = \beta_\sigma = 1$, $\{\lambda_{mk}^W\} = \{\lambda_{kn}^Z\} = 0.1$.

Require: Choose initial $\alpha_\sigma, \beta_\sigma, \lambda_{mk}^W, \lambda_{kn}^Z$;

- 1: **for** $k = 1$ to K **do**
- 2: **for** $m = 1$ to M **do**
- 3: Sample w_{mk} from $p(w_{mk} \mid \mathbf{A}, \mathbf{W}_{-mk}, \mathbf{Z}, \sigma^2, \lambda_{mk}^W)$; ▷ Equation (7.5)
- 4: **end for**
- 5: **for** $n = 1$ to N **do**
- 6: Sample z_{kn} from $p(z_{kn} \mid \mathbf{A}, \mathbf{W}, \mathbf{Z}_{-kn}, \sigma^2 \lambda_{kn}^Z)$; ▷ Symmetry of Eq. (7.5)
- 7: **end for**
- 8: **end for**
- 9: Sample σ^2 from $p(\sigma^2 \mid \mathbf{A}, \mathbf{W}, \mathbf{Z}, \alpha_\sigma, \beta_\sigma)$; ▷ Equation (7.8)
- 10: Report loss in Equation (7.1), stop if it converges.

7.3. Gaussian Likelihood with Exponential Priors and ARD Hierarchical Prior (GEEA)

The Gaussian likelihood with exponential priors and hierarchical prior (GEEA) model is proposed by Tan and Févotte (2013) based on the GEE model. The difference lies in that the GEEA model applies a hyperprior on the exponential prior. Moreover, GEEA favors an *automatic relevance determination* (ARD) that helps perform *automatic model selection*. This ARD works by replacing the individual scale parameter of exponential prior for the factored components \mathbf{W} and \mathbf{Z} with one that is shared by all entries in the same column of \mathbf{W} and the same row of \mathbf{Z} . In other words, the parameters are shared for each factor.

Hyperprior. For each prior density in Equation (7.3), we assume a Gamma distribution on the parameters of exponential distributions in Equation (7.3):

$$w_{mk} \sim \mathcal{E}(w_{mk} \mid \lambda_k), \quad z_{kn} \sim \mathcal{E}(z_{kn} \mid \lambda_k), \quad \lambda_k \sim \mathcal{G}(\lambda_k \mid \alpha_\lambda, \beta_\lambda),$$

where λ_k is shared by all entries in the same column of \mathbf{W} and the same row of \mathbf{Z} . The entire factor k is then either activated if λ_k has a low value or “turned off” if λ_k has a high value (see Figure 3.6, p. 57). Therefore, we can establish an upper bound on the number of hidden factors, K , instead of choosing the precise value of K . The graphical model is shown in Figure 7.1(b).

Posterior. For NMF, following Bayes’ rule and MCMC, this means we need to be able to draw from distributions (again by Markov blanket, Section 6.2, p. 141):

$$\begin{aligned} p(\sigma^2 \mid \mathbf{A}, \mathbf{W}, \mathbf{Z}, \boldsymbol{\lambda}), & \quad p(w_{mk} \mid \mathbf{A}, \mathbf{W}_{-mk}, \mathbf{Z}, \sigma^2, \boldsymbol{\lambda}), \\ p(\lambda_k \mid \mathbf{W}, \mathbf{Z}, \boldsymbol{\lambda}_{-k}, \alpha_\lambda, \beta_\lambda), & \quad p(z_{kn} \mid \mathbf{A}, \mathbf{W}, \mathbf{Z}_{-kn}, \sigma^2, \boldsymbol{\lambda}), \end{aligned}$$

where $\boldsymbol{\lambda} \in \mathbb{R}_+^K$ is a vector including all λ_k values, and $\boldsymbol{\lambda}_{-k}$ denotes all elements of $\boldsymbol{\lambda}$ except λ_k . The posteriors for w_{mk} ’s and z_{kn} ’s are the same as those in the GEE model, except now

we replace λ_{mk}^W and λ_{kn}^Z by λ_k . The posteriors for λ_k can be obtained using Bayes' theorem. The conditional density of λ_k depends on its parents ($\alpha_\lambda, \beta_\lambda$), children (k -th column $\widehat{\mathbf{w}}_k$ or \mathbf{W} , k -th row $\widehat{\mathbf{z}}_k$ of \mathbf{Z} , note we define \mathbf{w}_m as the m -th row of \mathbf{W} and \mathbf{z}_n as the n -th column of \mathbf{Z} in Equation (7.1)), and coparents (none)². Then, it follows that,

$$\begin{aligned}
 & p(\lambda_k \mid \mathbf{W}, \mathbf{Z}, \alpha_\lambda, \beta_\lambda) \\
 & \propto p(\widehat{\mathbf{w}}_k, \widehat{\mathbf{z}}_k \mid \lambda_k) \times p(\lambda_k) = \prod_{i=1}^M \mathcal{E}(w_{ik} \mid \lambda_k) \cdot \prod_{j=1}^N \mathcal{E}(z_{kj} \mid \lambda_k) \times \mathcal{G}(\lambda_k \mid \alpha_\lambda, \beta_\lambda) \\
 & = \prod_{i=1}^M \lambda_k \exp(-\lambda_k w_{ik}) \cdot \prod_{j=1}^N \lambda_k \exp(-\lambda_k z_{kj}) \times \frac{\beta_\lambda^{\alpha_\lambda}}{\Gamma(\alpha_\lambda)} \lambda_k^{\alpha_\lambda - 1} \exp(-\lambda_k \beta_\lambda) \quad (7.9) \\
 & \propto \lambda_k^{M+N+\alpha_\lambda-1} \exp \left\{ -\lambda_k \cdot \left(\sum_{k=1}^K (w_{mk} + z_{kn}) + \beta_\lambda \right) \right\} \\
 & \propto \mathcal{G}(\lambda_k \mid \widetilde{\alpha}_\lambda, \widetilde{\beta}_\lambda),
 \end{aligned}$$

where

$$\widetilde{\alpha}_\lambda = M + N + \alpha_\lambda, \quad \widetilde{\beta}_\lambda = \sum_{k=1}^K (w_{mk} + z_{kn}) + \beta_\lambda.$$

From this posterior form, the prior parameter α_λ can be interpreted as the number of prior observations, and β_λ as the sum of the prior observations. Therefore, weak prior parameter can be chosen as $\alpha_\lambda = \beta_\lambda = 1$.

Gibbs sampling. Again we can construct a Gibbs sampler for the GEEA model as formulated in Algorithm 12. By default, uninformative hyper-parameters are $\alpha_\sigma = \beta_\sigma = 1$, $\alpha_\lambda = \beta_\lambda = 1$.

7.4. Gaussian Likelihood with Truncated-Normal Priors (GTT)

The Gaussian likelihood with truncated-normal priors (GTT) model is discussed in Brouwer and Lio (2017), where truncated-normal (TN) priors are used over factored matrices (Figure 7.2(a)). The truncated-normal distribution, a variant of the normal distribution, excludes values smaller than zero (Definition 3.4.1, p. 57), allowing it to impose nonnegativity in Bayesian models. The chosen likelihood function is identical to that of the GEE model (Equation (7.2)).

Prior. We assume \mathbf{W} and \mathbf{Z} are independently truncated-normal distributed with mean and precision given by $\{\boldsymbol{\mu}^W, \boldsymbol{\tau}^W\}$ and $\{\boldsymbol{\mu}^Z, \boldsymbol{\tau}^Z\}$, respectively:

$$w_{mk} \sim \mathcal{TN}(w_{mk} \mid \mu_{mk}^W, (\tau_{mk}^W)^{-1}), \quad z_{kn} \sim \mathcal{TN}(z_{kn} \mid \mu_{kn}^Z, (\tau_{kn}^Z)^{-1}), \quad (7.10)$$

where $\boldsymbol{\mu}^W$ is an $M \times K$ matrix containing all $\{\mu_{mk}^W\}$ entries, $\boldsymbol{\mu}^Z$ is a $K \times N$ matrix including all $\{\mu_{kn}^Z\}$ values, $\boldsymbol{\tau}^W$ is an $M \times K$ matrix containing all $\{\tau_{mk}^W\}$ entries, and $\boldsymbol{\tau}^Z$ is a $K \times N$ matrix including all $\{\tau_{kn}^Z\}$ values.

². See Figure 7.1(b) and Section 6.2 (p. 141).

Algorithm 12 Gibbs sampler for GEEA model in one iteration (prior on variance σ^2 here, similarly for the precision τ). The procedure presented here may not be efficient but is explanatory. A more efficient one can be implemented in a vectorized manner. By default, uninformative hyper-parameters are $\alpha_\sigma = \beta_\sigma = 1$, $\alpha_\lambda = \beta_\lambda = 1$.

Require: Choose initial $\alpha_\sigma, \beta_\sigma, \alpha_\lambda, \beta_\lambda$;

- 1: **for** $k = 1$ to K **do**
- 2: **for** $m = 1$ to M **do**
- 3: Sample w_{mk} from $p(w_{mk} \mid \mathbf{A}, \mathbf{W}_{-mk}, \mathbf{Z}, \sigma^2, \lambda_k)$; ▷ Equation (7.5)
- 4: **end for**
- 5: **for** $n = 1$ to N **do**
- 6: Sample z_{kn} from $p(z_{kn} \mid \mathbf{A}, \mathbf{W}, \mathbf{Z}_{-kn}, \sigma^2, \lambda_k)$; ▷ Symmetry of Eq. (7.5)
- 7: **end for**
- 8: Sample λ_k from $p(\lambda_k \mid \mathbf{W}, \mathbf{Z}, \alpha_\lambda, \beta_\lambda)$; ▷ Equation (7.9)
- 9: **end for**
- 10: Sample σ^2 from $p(\sigma^2 \mid \mathbf{A}, \mathbf{W}, \mathbf{Z}, \alpha_\sigma, \beta_\sigma)$; ▷ Equation (7.8)
- 11: Report loss in Equation (7.1), stop if it converges.

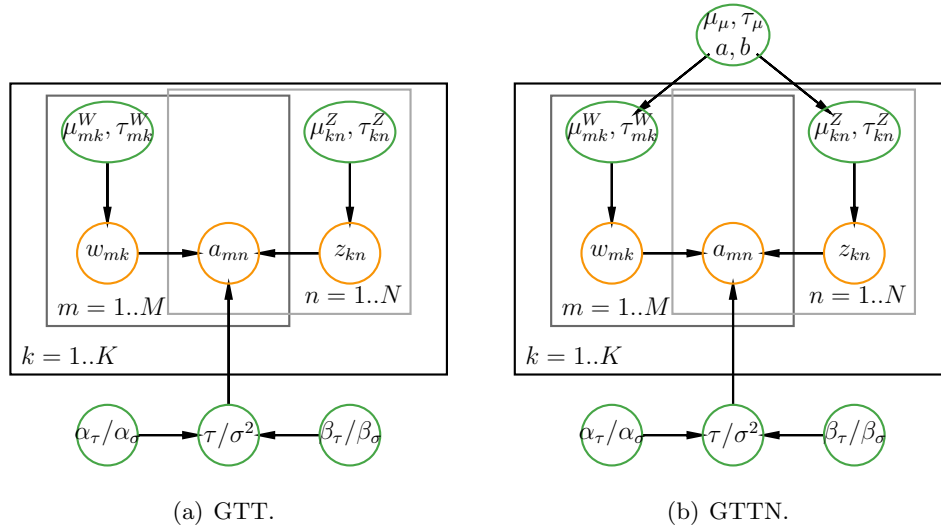


Figure 7.2: Graphical model representation of GTT and GTTN models. Green circles denote prior variables, orange circles represent observed and latent variables, and plates represent repeated variables. The slash “/” in the variable represents “or,” and the comma “,” in the variable represents “and.”

Posterior. Again, following Bayes’ rule and MCMC, this means we need to be able to draw from distributions (by Markov blanket, Section 6.2, p. 141):

$$\begin{aligned}
 & p(w_{mk} \mid \mathbf{A}, \mathbf{W}_{-mk}, \mathbf{Z}, \sigma^2, \mu_{mk}^W, \tau_{mk}^W), \\
 & p(z_{kn} \mid \mathbf{A}, \mathbf{W}, \mathbf{Z}_{-kn}, \sigma^2, \mu_{kn}^Z, \tau_{kn}^Z), \\
 & p(\sigma^2 \mid \mathbf{A}, \mathbf{W}, \mathbf{Z}, \alpha_\sigma, \beta_\sigma),
 \end{aligned}$$

where \mathbf{W}_{-mk} denotes all elements of \mathbf{W} except w_{mk} , and \mathbf{Z}_{-kn} denotes all elements of \mathbf{Z} except z_{kn} . Using Bayes' theorem, the conditional density of w_{mk} depends on its parents $(\mu_{mk}^W, \tau_{mk}^W)$, children (a_{mn}) , and coparents $(\tau$ or $\sigma^2, \mathbf{W}_{-mk}, \mathbf{Z})$ ³. And it can be obtained by (similar to computing the conditional density of w_{mk} in the GEE model, Equation (7.5))

$$\begin{aligned}
 & p(w_{mk} \mid \sigma^2, \mathbf{W}_{-mk}, \mathbf{Z}, \mu_{mk}^W, \tau_{mk}^W, \mathbf{A}) \propto p(\mathbf{A} \mid \mathbf{W}, \mathbf{Z}, \sigma^2) \cdot p(w_{mk} \mid \mu_{mk}^W, (\tau_{mk}^W)^{-1}) \\
 & = \prod_{i,j=1}^{M,N} \mathcal{N}(a_{ij} \mid \mathbf{w}_i^\top \mathbf{z}_j, \sigma^2) \times \mathcal{TN}(w_{mk} \mid \mu_{mk}^W, (\tau_{mk}^W)^{-1}) \\
 & \propto \exp \left\{ - \left(\frac{\sum_{j=1}^N z_{kj}^2}{2\sigma^2} + \frac{\tau_{mk}^W}{2} \right) w_{mk}^2 + w_{mk} \left\{ \frac{1}{\sigma^2} \sum_{j=1}^N z_{kj} (a_{mj} - \sum_{i \neq k} w_{mi} z_{ij}) + \tau_{mk}^W \mu_{mk}^W \right\} \right\} u(w_{mk}) \\
 & \propto \mathcal{N}(w_{mk} \mid \widetilde{\mu}_{mk}, \widetilde{\sigma}_{mk}^2) \cdot u(w_{mk}) = \mathcal{TN}(w_{mk} \mid \widetilde{\mu}_{mk}, \widetilde{\sigma}_{mk}^2),
 \end{aligned} \tag{7.11}$$

where $\widetilde{\sigma}_{mk}^2 = \frac{\sigma^2}{\sum_{j=1}^N z_{kj}^2 + \tau_{mk}^W \sigma^2}$ is the posterior ‘‘parent’’ variance of the normal distribution with ‘‘parent’’ mean $\widetilde{\mu}_{mk}$,

$$\widetilde{\mu}_{mk} = \left\{ \frac{1}{\sigma^2} \sum_{j=1}^N z_{kj} \left(a_{mj} - \sum_{i \neq k} w_{mi} z_{ij} \right) + \tau_{mk}^W \mu_{mk}^W \right\} \cdot \widetilde{\sigma}_{mk}^2.$$

Again, due to symmetry, a similar expression for z_{kn} can be immediately derived. Finally, the conditional density of σ^2 is the same as that in the GEE model (Equation (7.8)).

Algorithm 13 Gibbs sampler for GTT model in one iteration (prior on variance σ^2 here, similarly for the precision τ). The procedure presented here may not be efficient but is explanatory. A more efficient one can be implemented in a vectorized manner. By default, uninformative hyper-parameters are $\alpha_\sigma = \beta_\sigma = 1$, $\{\mu_{mk}^W\} = \{\mu_{kn}^Z\} = 0$, $\{\tau_{mk}^W\} = \{\tau_{kn}^Z\} = 0.1$.

Require: Choose initial $\alpha_\sigma, \beta_\sigma, \mu_{mk}^W, \tau_{mk}^W, \mu_{kn}^Z, \tau_{kn}^Z$;

- 1: **for** $k = 1$ to K **do**
 - 2: **for** $m = 1$ to M **do**
 - 3: Sample w_{mk} from $p(w_{mk} \mid \mathbf{A}, \mathbf{W}_{-mk}, \mathbf{Z}, \sigma^2, \mu_{mk}^W, \tau_{mk}^W)$; \triangleright Equation (7.11)
 - 4: **end for**
 - 5: **for** $n = 1$ to N **do**
 - 6: Sample z_{kn} from $p(z_{kn} \mid \mathbf{A}, \mathbf{W}, \mathbf{Z}_{-kn}, \sigma^2, \mu_{kn}^Z, \tau_{kn}^Z)$; \triangleright Symmetry of Eq. (7.11)
 - 7: **end for**
 - 8: **end for**
 - 9: Sample σ^2 from $p(\sigma^2 \mid \mathbf{A}, \mathbf{W}, \mathbf{Z}, \alpha_\sigma, \beta_\sigma)$; \triangleright Equation (7.8)
 - 10: Report loss in Equation (7.1), stop if it converges.
-

Gibbs sampling. We can again construct a Gibbs sampler for the GTT model as formulated in Algorithm 13. And also in practice, all the parameters of the truncated-normal priors are set to be the same value $\mu^W = \{\mu_{mk}^W\}'s$, $\mu^Z = \{\mu_{kn}^Z\}'s$, $\tau^W = \{\tau_{mk}^W\}'s$, $\tau^Z =$

³. See Figure 7.2(a) and Section 6.2 (p. 141).

$\{\tau_{nk}^Z\}$'s for all m, k, n . By default, uninformative hyper-parameters are $\alpha_\sigma = \beta_\sigma = 1$, $\{\mu_{mk}^W\} = \{\mu_{kn}^Z\} = 0$, $\{\tau_{mk}^W\} = \{\tau_{kn}^Z\} = 0.1$.

7.5. Gaussian Likelihood with Truncated-Normal and Hierarchical Priors (GTTN)

This hierarchical prior is proposed in Schmidt and Mohamed (2009) over a rectified-normal distribution originally, and further discussed in Brouwer and Lio (2017) based on the GTT model, where the difference lies in that the GTTN model puts a hyperprior on the two parameters of the truncated-normal distribution (Figure 7.2(b)).

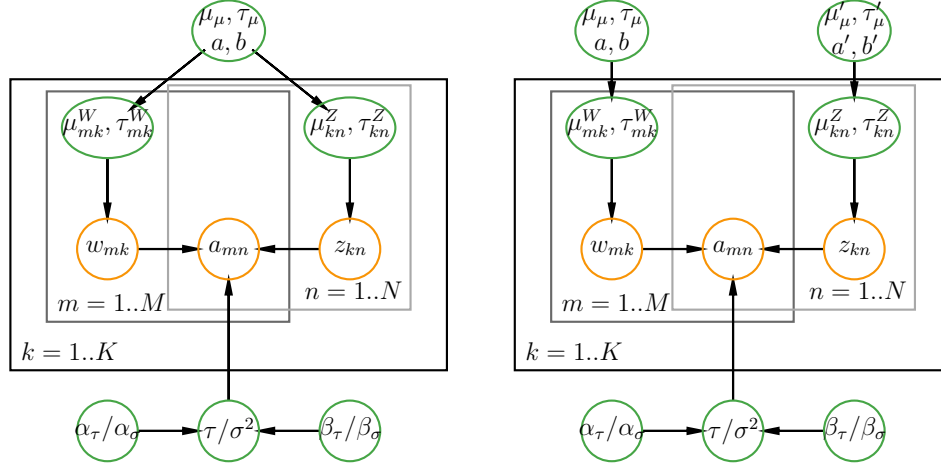
Hyperprior. We have shown in Equation (3.18) (p. 58) that the truncated-normal density is a conjugate prior over the nonnegative mean parameter of a Gaussian distribution that is favored in the GTT model. Moreover, if the prior over $\{w_{mk}\}$'s and $\{z_{kn}\}$'s had been a Gaussian, appropriate conjugate priors for the mean and variance would be a normal-inverse-Gamma or a normal-inverse-Chi-square distribution (Equation (3.11), p. 49; Equation (3.14), p. 53). However, these priors are not conjugate to the truncated-normal density. And instead, a convenient prior called *TN-scaled-normal-Gamma (TNSNG)* distribution is used (or a *TN-scaled-normal-inverse-Gamma* prior for “parent” mean and “parent” variance parameters)⁴:

$$\begin{aligned} \mu_{mk}^W, \tau_{mk}^W \mid \mu_\mu, \tau_\mu, a, b &\sim \mathcal{TNSNG}(\mu_{mk}^W, \tau_{mk}^W \mid \mu_\mu, \tau_\mu, a, b) \\ &\propto \frac{1}{\sqrt{\tau_{mk}^W}} \left(1 - \Phi\left(-\mu_{mk}^W \sqrt{\tau_{mk}^W}\right) \right) \cdot \mathcal{N}(\mu_{mk}^W \mid \mu_\mu, (\tau_\mu)^{-1}) \cdot \mathcal{G}(\tau_{mk}^W \mid a, b); \\ \mu_{kn}^Z, \tau_{kn}^Z \mid \mu_\mu, \tau_\mu, a, b &\sim \mathcal{TNSNG}(\mu_{kn}^Z, \tau_{kn}^Z \mid \mu_\mu, \tau_\mu, a, b). \end{aligned}$$

Here we use the same hyper-parameters $\{\mu_\mu, \tau_\mu, a, b\}$ over different entries $\{u_{mk}^W, \tau_{mk}^W\}$ and $\{u_{kn}^Z, \tau_{kn}^Z\}$. However, in rare cases, one may favor different behaviors over \mathbf{W} and \mathbf{Z} , e.g., small values in \mathbf{W} and large values in \mathbf{Z} ; the hyper-parameters can be chosen as different values accordingly (see the comparison in Figure 7.3). Note that the scaled-normal-Gamma distribution is not simply a product of a normal and a Gamma distribution. It is not easy to sample from this distribution. However, we will see the posteriors have simple forms due to this prior; that's the reason why we add scaled terms in the prior density. The prior can decouple parameters μ_{mk}^W and τ_{mk}^W , and the posterior conditional densities of them are normal and Gamma respectively due to this convenient scale.

Posterior. The posteriors for $\{w_{mk}\}$'s, $\{z_{kn}\}$'s, and σ^2 are the same as those in the GTT model. The posteriors for $\{u_{mk}^W, \tau_{mk}^W\}$ can be obtained using Bayes' rule, where the conditional density of $\{\mu_{mk}^W, \tau_{mk}^W\}$ depend on their parents $(\mu_\mu, \tau_\mu, a, b)$, children (w_{mk}) , and coparents (none). Then it follows from the likelihood in Equation (7.10) that the conditional

4. The original hyperprior in Schmidt and Mohamed (2009) is a rectified-normal (RN) scaled one. Here we scale it in the context of truncated-normal density.



(a) GTTN with same hyper-parameters. Same as Figure 7.2(b). (b) GTTN with different hyper-parameters.

Figure 7.3: Graphical model representation of GTTN with same and different hyperparameters. Green circles denote prior variables, orange circles represent observed and latent variables, and plates represent repeated variables. The slash “/” in the variable represents “or,” and the comma “,” in the variable represents “and.”

densities of μ_{mk}^W is

$$\begin{aligned}
& p(\mu_{mk}^W \mid \tau_{mk}^W, w_{mk}, \mu_\mu, \tau_\mu, a, b) \\
& \propto \mathcal{TN}(w_{mk} \mid \mu_{mk}^W, (\tau_{mk}^W)^{-1}) \cdot \frac{1}{\sqrt{\tau_{mk}^W}} \left(1 - \Phi(-\mu_{mk}^W \sqrt{\tau_{mk}^W}) \right) \mathcal{N}(\mu_{mk}^W \mid \mu_\mu, \tau_\mu) \mathcal{G}(\tau_{mk}^W \mid a, b) \\
& \propto \exp \left\{ - \underbrace{\frac{\tau_{mk}^W + \tau_\mu}{2}}_{\tilde{t}/2} (\mu_{mk}^W)^2 + \underbrace{\mu_{mk}^W (\tau_{mk}^W w_{mk} + \tau_\mu \mu_\mu)}_{\tilde{m} \cdot \tilde{t}} \right\} \propto \mathcal{N}(\mu_{mk}^W \mid \tilde{m}, \tilde{t}^{-1}),
\end{aligned} \tag{7.12}$$

where $\tilde{t} = \tau_{mk}^W + \tau_\mu$, $\tilde{m} = (\tau_{mk}^W w_{mk} + \tau_\mu \mu_\mu) / \tilde{t}$. And the conditional density of τ_{mk}^W is

$$\begin{aligned}
& p(\tau_{mk}^W \mid \mu_{mk}^W, w_{mk}, \mu_\mu, \tau_\mu, a, b) \\
& \propto \mathcal{TN}(w_{mk} \mid \mu_{mk}^W, (\tau_{mk}^W)^{-1}) \cdot \frac{1}{\sqrt{\tau_{mk}^W}} \left(1 - \Phi(-\mu_{mk}^W \sqrt{\tau_{mk}^W}) \right) \mathcal{N}(\mu_{mk}^W \mid \mu_\mu, \tau_\mu) \mathcal{G}(\tau_{mk}^W \mid a, b) \\
& \propto (\tau_{mk}^W)^{a-1} \exp \left\{ - \left(b + \frac{(w_{mk} - \mu_{mk}^W)^2}{2} \right) \tau_{mk}^W \right\} \propto \mathcal{G}(\tau_{mk}^W \mid \tilde{a}, \tilde{b}),
\end{aligned} \tag{7.13}$$

where $\tilde{a} = a$, $\tilde{b} = b + \frac{(w_{mk} - \mu_{mk}^W)^2}{2}$. And again due to symmetry, the expressions for μ_{kn}^Z and τ_{kn}^Z can be derived accordingly. The Gibbs sampler for the GTTN model is then

formulated in Algorithm 14. By default, uninformative hyper-parameters are $\alpha_\sigma = \beta_\sigma = 1$, $\mu_\mu = 0, \tau_\mu = 0.1, a = b = 1$.

Algorithm 14 GibbssSampler for GTTN model in one iteration (prior on variance σ^2 here, similarly for the precision τ). The procedure presented here may not be efficient but is explanatory. A more efficient one can be implemented in a vectorized manner. By default, uninformative hyper-parameters are $\alpha_\sigma = \beta_\sigma = 1, \mu_\mu = 0, \tau_\mu = 0.1, a = b = 1$.

Require: Choose initial $\alpha_\sigma, \beta_\sigma, \mu_\mu, \tau_\mu, a, b$;

- 1: **for** $k = 1$ to K **do**
- 2: **for** $m = 1$ to M **do**
- 3: Sample w_{mk} from $p(w_{mk} \mid \mathbf{A}, \mathbf{W}_{-mk}, \mathbf{Z}, \sigma^2, \mu_{mk}^W, \tau_{mk}^W)$; ▷ Equation (7.11)
- 4: Sample μ_{mk}^W from $p(\mu_{mk}^W \mid \tau_{mk}^W, w_{mk}, \mu_\mu, \tau_\mu, a, b)$; ▷ Equation (7.12)
- 5: Sample τ_{mk}^W from $p(\tau_{mk}^W \mid \mu_{mk}^W, w_{mk}, \mu_\mu, \tau_\mu, a, b)$; ▷ Equation (7.13)
- 6: **end for**
- 7: **for** $n = 1$ to N **do**
- 8: Sample z_{kn} from $p(z_{kn} \mid \mathbf{A}, \mathbf{W}, \mathbf{Z}_{-kn}, \sigma^2, \mu_{kn}^Z, \tau_{kn}^Z)$; ▷ Symmetry of Eq. (7.11)
- 9: Sample μ_{kn}^Z from $p(\mu_{kn}^Z \mid \tau_{kn}^Z, z_{kn}, \mu_\mu, \tau_\mu, a, b)$; ▷ Symmetry of Eq. (7.12)
- 10: Sample τ_{kn}^Z from $p(\tau_{kn}^Z \mid \mu_{kn}^Z, z_{kn}, \mu_\mu, \tau_\mu, a, b)$; ▷ Symmetry of Eq. (7.13)
- 11: **end for**
- 12: **end for**
- 13: Sample σ^2 from $p(\sigma^2 \mid \mathbf{A}, \mathbf{W}, \mathbf{Z}, \alpha_\sigma, \beta_\sigma)$; ▷ Equation (7.8)
- 14: Report loss in Equation (7.1), stop if it converges.

7.6. Gaussian Likelihood with Rectified-Normal Priors (GRR) and Hierarchical Prior (GRRN)

Going further, the Gaussian likelihood with rectified-normal and hierarchical priors (GRR and GRRN) models are proposed in Lu and Ye (2022) to enhance flexibility building upon the GTT and GTTN models. In this context, again, we view the data \mathbf{A} as being produced according to the probabilistic generative process shown in Figure 7.4(b). The observed (m, n) -th data entry a_{mn} of matrix \mathbf{A} is modeled using a Gaussian likelihood function with variance σ^2 and a mean given by the latent decomposition $\mathbf{w}_m^\top \mathbf{z}_n$ (Equation (7.1)). The chosen likelihood is consistent with that employed in the GEE model (Equation (7.2)).

Prior. We treat the latent variables w_{mk} 's (and z_{kn} 's) as random variables. And we need prior densities over these latent variables to express beliefs for their values, e.g., non-negativity in this context. Here, we assume further that the latent variables w_{mk} 's and z_{kn} 's are independently drawn from a *rectified-normal* (RN) priors (a.k.a., an *exponentially rectified-normal* distribution, Definition 3.4.4, p. 62),

$$\begin{aligned} p(w_{mk} \mid \cdot) &= \mathcal{RN}(w_{mk} \mid \mu_{mk}^W, (\tau_{mk}^W)^{-1}, \lambda_{mk}^W); \\ p(z_{kn} \mid \cdot) &= \mathcal{RN}(z_{kn} \mid \mu_{kn}^Z, (\tau_{kn}^Z)^{-1}, \lambda_{kn}^Z). \end{aligned} \tag{7.14}$$

This prior serves to enforce the nonnegativity constraint on the components \mathbf{W} and \mathbf{Z} , and it is conjugate to the Gaussian likelihood (Equation (3.21), p. 63). In some scenarios, the

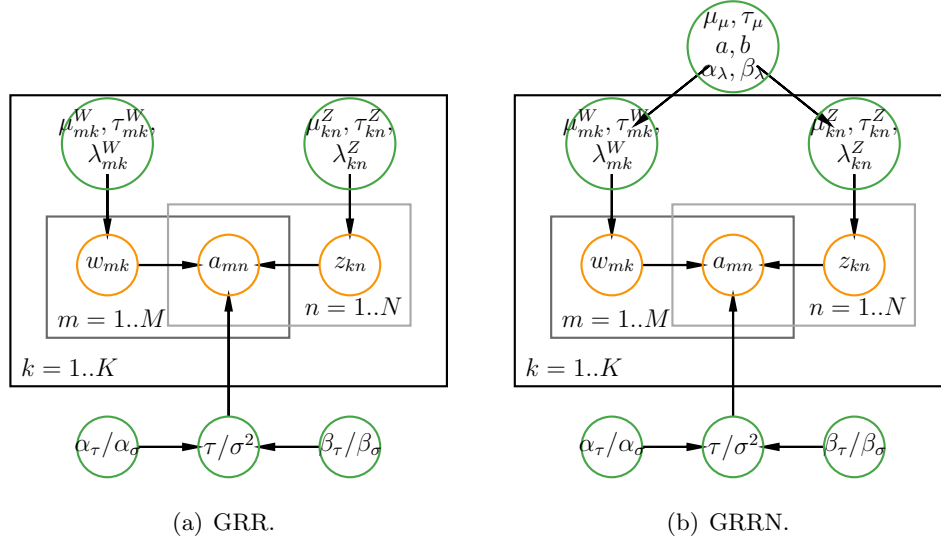


Figure 7.4: Graphical representation of GRR and GRRN models. Green circles denote prior variables, orange circles represent observed and latent variables, and plates represent repeated variables. The slash “/” in the variable represents “or,” and the comma “,” in the variable represents “and.”

two sets of latent variables can be drawn from two different rectified-normal priors, e.g., enforcing sparsity in \mathbf{W} while non-sparsity in \mathbf{Z} . And we shall not consider this case for our later examples as it is not the main interest of this book. The posterior density is a truncated-normal distribution, which is a special rectified-normal distribution. The model is then called a Gaussian likelihood with rectified-normal priors (GRR) model. Since the RN distribution is a special TN distribution, the GRR model is the same as the GTT model with a careful choice of prior parameters. What makes the RN prior important is from the hierarchical model that provides flexibility and guidance on the prior parameter choices; see discussion below.

Hierarchical prior. To further favor flexibility, we choose a convenient joint hyperprior density over the parameters $\{\mu_{mk}^W, \tau_{mk}^W, \lambda_{mk}^W\}$ of RN prior in Equation (7.14), namely, the *RN-scaled-normal-Gamma (RNSNG)* prior,

$$\begin{aligned}
 p(\mu_{mk}^W, \tau_{mk}^W, \lambda_{mk}^W \mid \cdot) &= \mathcal{RNSNG}(\mu_{mk}^W, \tau_{mk}^W, \lambda_{mk}^W \mid \mu_\mu, \tau_\mu, a, b, \alpha_\lambda, \beta_\lambda) \\
 &= C(\mu_{mk}^W, \tau_{mk}^W, \lambda_{mk}^W) \cdot \mathcal{N}(\mu_{mk}^W \mid \mu_\mu, (\tau_\mu)^{-1}) \cdot \mathcal{G}(\tau_{mk}^W \mid a, b) \cdot \mathcal{G}(\lambda_{mk}^W \mid \alpha_\lambda, \beta_\lambda),
 \end{aligned} \tag{7.15}$$

where $C(\mu_{mk}^W, \tau_{mk}^W, \lambda_{mk}^W)$ is a constant in terms of $\{\mu_{mk}^W, \tau_{mk}^W, \lambda_{mk}^W\}$. This prior can decouple parameters μ_{mk}^W, τ_{mk}^W , and λ_{mk}^W , and their posterior conditional densities are Gaussian, Gamma, and Gamma respectively due to this convenient scale. A similar RNSNG prior is given over $\{\mu_{kn}^Z, \tau_{kn}^Z, \lambda_{kn}^Z\}$.

Posterior. Again, following Bayes' rule and MCMC, this means we need to be able to draw from distributions (by Markov blanket, Section 6.2, p. 141):

$$\begin{aligned} p(w_{mk} \mid \mathbf{A}, \mathbf{W}_{-mk}, \mathbf{Z}, \sigma^2, \mu_{mk}^W, \tau_{mk}^W, \lambda_{mk}^W), \\ p(z_{kn} \mid \mathbf{A}, \mathbf{W}, \mathbf{Z}_{-kn}, \sigma^2, \mu_{kn}^Z, \tau_{kn}^Z, \lambda_{kn}^Z), \\ p(\sigma^2 \mid \mathbf{A}, \mathbf{W}, \mathbf{Z}, \alpha_\sigma, \beta_\sigma), \end{aligned}$$

where \mathbf{W}_{-mk} denotes all elements of \mathbf{W} except w_{mk} , and \mathbf{Z}_{-kn} denotes all elements of \mathbf{Z} except z_{kn} . Using Bayes' theorem, the conditional density of w_{mk} depends on its parents $(\mu_{mk}^W, \tau_{mk}^W, \lambda_{mk}^W)$, children (a_{mn}) , and coparents $(\tau$ or $\sigma^2, \mathbf{W}_{-mk}, \mathbf{Z})$ ⁵. The conditional density of w_{mk} follows a truncated-normal density. And it can be obtained by (similar to computing the conditional density of w_{mk} in the GEE model, Equation (7.5))

$$\begin{aligned} p(w_{mk} \mid \mathbf{A}, \mathbf{W}_{-mk}, \mathbf{Z}, \sigma^2, \mu_{mk}^W, \tau_{mk}^W, \lambda_{mk}^W) &\propto p(\mathbf{A} \mid \mathbf{W}, \mathbf{Z}, \sigma^2) \times p(w_{mk} \mid \mu_{mk}, \tau_{mk}, \lambda_{mk}) \\ &\propto \prod_{i,j=1}^{M,N} \mathcal{N}(a_{ij} \mid \mathbf{w}_i^\top \mathbf{z}_j, \sigma^2) \times \mathcal{RN}(\mu_{mk}, (\tau_{mk})^{-1}, \lambda_{mk}) \\ &\stackrel{*}{\propto} \prod_{i,j=1}^{M,N} \mathcal{N}(a_{ij} \mid \mathbf{w}_i^\top \mathbf{z}_j, \sigma^2) \times \mathcal{TN} \left(\underbrace{\frac{\tau_{mk}^W \mu_{mk}^W - \lambda_{mk}^W}{\tau_{mk}^W}}_{:=\mu'}, (\tau_{mk})^{-1} \right) \\ &\propto \exp \left\{ - \left(\frac{\sum_{j=1}^N z_{kj}^2}{2\sigma^2} + \frac{\tau_{mk}^W}{2} \right) w_{mk}^2 + w_{mk} \left(\frac{1}{\sigma^2} \sum_{j=1}^N z_{kj} (a_{mj} - \sum_{i \neq k} w_{mk} z_{ij}) + \tau_{mk}^W \mu' \right) \right\} u(w_{mk}) \\ &\propto \mathcal{N}(w_{mk} \mid \widetilde{\mu}_{mk}, \widetilde{\sigma}_{mk}^2) u(w_{mk}) = \mathcal{TN}(w_{mk} \mid \widetilde{\mu}_{mk}, \widetilde{\sigma}_{mk}^2), \end{aligned} \tag{7.16}$$

where the equality (\star) is from the equivalence between the RN and TN distributions (Definition 3.4.4, p. 62), $\widetilde{\sigma}_{mk}^2 = \frac{\sigma^2}{\sum_{j=1}^N z_{kj}^2 + \tau_{mk}^W \cdot \sigma^2}$ is the posterior ‘‘parent’’ variance of the normal distribution with posterior ‘‘parent’’ mean

$$\widetilde{\mu}_{mk} = \left(\frac{1}{\sigma^2} \sum_{j=1}^N z_{kj} (a_{mj} - \sum_{i \neq k} w_{mk} z_{ij}) + \tau_{mk}^W \mu' \right) \cdot \widetilde{\sigma}_{mk}^2.$$

The $\mu' = \frac{\tau_{mk}^W \mu_{mk}^W - \lambda_{mk}^W}{\tau_{mk}^W}$ is the ‘‘parent’’ mean of the truncated-normal density. Due to symmetry, the conditional posterior for z_{kn} can be derived similarly.

Extra update for GRRN. Following the graphical representation of the GRRN model in Figure 7.4(b), we need to draw samples iteratively from

$$\begin{aligned} p(\mu_{mk}^W \mid \tau_{mk}^W, \lambda_{mk}^W, \mu_\mu, \tau_\mu, a, b, \alpha_\lambda, \beta_\lambda, w_{mk}), \\ p(\tau_{mk}^W \mid \mu_{mk}^W, \lambda_{mk}^W, \mu_\mu, \tau_\mu, a, b, \alpha_\lambda, \beta_\lambda, w_{mk}), \\ p(\lambda_{mk}^W \mid \mu_{mk}^W, \tau_{mk}^W, \mu_\mu, \tau_\mu, a, b, \alpha_\lambda, \beta_\lambda, w_{mk}). \end{aligned}$$

5. See Figure 7.4(b) and Section 6.2 (p. 141).

The conditional density for μ_{mk}^W is a truncated-normal (a special rectified-normal):

$$\begin{aligned}
 & p(\mu_{mk}^W \mid \tau_{mk}^W, \lambda_{mk}^W, \mu_\mu, \tau_\mu, a, b, \alpha_\lambda, \beta_\lambda, w_{mk}) \\
 & \propto \mathcal{RN}(w_{mk} \mid \mu_{mk}^W, (\tau_{mk}^W)^{-1}, \lambda_{mk}^W) \cdot \mathcal{RN} \mathcal{SN} \mathcal{G}(\mu_{mk}^W, \tau_{mk}^W, \lambda_{mk}^W \mid \mu_\mu, \tau_\mu, a, b, \alpha_\lambda, \beta_\lambda) \\
 & \propto \mathcal{RN}(w_{mk} \mid \mu_{mk}^W, (\tau_{mk}^W)^{-1}, \lambda_{mk}^W) \cdot \mathcal{N}(\mu_{mk}^W \mid \mu_\mu, (\tau_\mu)^{-1}) \cdot \mathcal{G}(\tau_{mk}^W \mid a, b) \cdot \mathcal{G}(\lambda_{mk}^W \mid \alpha_\lambda, \beta_\lambda) \\
 & = \mathcal{N}(w_{mk} \mid \mu_{mk}^W, (\tau_{mk}^W)^{-1}) \cdot \cancel{\mathcal{E}(w_{mk} \mid \lambda_{mk}^W)} \cdot \mathcal{N}(\mu_{mk}^W \mid \mu_\mu, (\tau_\mu)^{-1}) \cdot \cancel{\mathcal{G}(\tau_{mk}^W \mid a, b)} \cdot \cancel{\mathcal{G}(\lambda_{mk}^W \mid \alpha_\lambda, \beta_\lambda)} \\
 & \propto \mathcal{N}(w_{mk} \mid \mu_{mk}^W, (\tau_{mk}^W)^{-1}) \mathcal{N}(\mu_{mk}^W \mid \mu_\mu, (\tau_\mu)^{-1}) \propto \mathcal{N}(\mu_{mk}^W \mid \tilde{m}, \tilde{t}^{-1}),
 \end{aligned} \tag{7.17}$$

where $\tilde{t} = \tau_{mk}^W + \tau_\mu$ and $\tilde{m} = (\tau_{mk}^W w_{mk} + \tau_\mu \mu_\mu) / \tilde{t}$ are the posterior precision and mean, respectively. The samples w_{mk} 's are nonnegative due to the rectification in the distribution (by exponential distribution with the density). However, this ‘‘parent’’ mean parameter μ_{mk}^W is not limited to be nonnegative.

The conditional density for τ_{mk}^W is a Gamma distribution:

$$\begin{aligned}
 & p(\tau_{mk}^W \mid \mu_{mk}^W, \lambda_{mk}^W, \mu_\mu, \tau_\mu, a, b, \alpha_\lambda, \beta_\lambda, w_{mk}) \\
 & \propto \mathcal{RN}(w_{mk} \mid \mu_{mk}^W, (\tau_{mk}^W)^{-1}, \lambda_{mk}^W) \cdot \mathcal{RN} \mathcal{SN} \mathcal{G}(\mu_{mk}^W, \tau_{mk}^W, \lambda_{mk}^W \mid \mu_\mu, \tau_\mu, a, b, \alpha_\lambda, \beta_\lambda) \\
 & \propto \mathcal{RN}(w_{mk} \mid \mu_{mk}^W, (\tau_{mk}^W)^{-1}, \lambda_{mk}^W) \cdot \mathcal{N}(\mu_{mk}^W \mid \mu_\mu, (\tau_\mu)^{-1}) \cdot \mathcal{G}(\tau_{mk}^W \mid a, b) \cdot \mathcal{G}(\lambda_{mk}^W \mid \alpha_\lambda, \beta_\lambda) \\
 & = \mathcal{N}(w_{mk} \mid \mu_{mk}^W, (\tau_{mk}^W)^{-1}) \cdot \cancel{\mathcal{E}(w_{mk} \mid \lambda_{mk}^W)} \cdot \cancel{\mathcal{N}(\mu_{mk}^W \mid \mu_\mu, (\tau_\mu)^{-1})} \cdot \mathcal{G}(\tau_{mk}^W \mid a, b) \cdot \cancel{\mathcal{G}(\lambda_{mk}^W \mid \alpha_\lambda, \beta_\lambda)} \\
 & \propto \mathcal{N}(w_{mk} \mid \mu_{mk}^W, (\tau_{mk}^W)^{-1}) \mathcal{G}(\tau_{mk}^W \mid a, b) \\
 & \propto (\tau_{mk}^W)^{a+\frac{1}{2}-1} \exp \left\{ - \left(b + \frac{(w_{mk} - \mu_{mk}^W)^2}{2} \right) \tau_{mk}^W \right\} \propto \mathcal{G}(\tau_{mk}^W \mid \tilde{a}, \tilde{b}),
 \end{aligned} \tag{7.18}$$

where $\tilde{a} = a + \frac{1}{2}$ and $\tilde{b} = b + \frac{(w_{mk} - \mu_{mk}^W)^2}{2}$ are the posterior shape and rate parameters, respectively.

Furthermore, the conditional density for λ_{mk}^W follows also a Gamma distribution:

$$\begin{aligned}
 & p(\lambda_{mk}^W \mid \mu_{mk}^W, \tau_{mk}^W, \mu_\mu, \tau_\mu, a, b, \alpha_\lambda, \beta_\lambda, w_{mk}) \\
 & \propto \mathcal{RN}(w_{mk} \mid \mu_{mk}^W, (\tau_{mk}^W)^{-1}, \lambda_{mk}^W) \cdot \mathcal{RN} \mathcal{SN} \mathcal{G}(\mu_{mk}^W, \tau_{mk}^W, \lambda_{mk}^W \mid \mu_\mu, \tau_\mu, a, b, \alpha_\lambda, \beta_\lambda) \\
 & \propto \mathcal{RN}(w_{mk} \mid \mu_{mk}^W, (\tau_{mk}^W)^{-1}, \lambda_{mk}^W) \cdot \mathcal{N}(\mu_{mk}^W \mid \mu_\mu, (\tau_\mu)^{-1}) \cdot \mathcal{G}(\tau_{mk}^W \mid a, b) \cdot \mathcal{G}(\lambda_{mk}^W \mid \alpha_\lambda, \beta_\lambda) \\
 & = \cancel{\mathcal{N}(w_{mk} \mid \mu_{mk}^W, (\tau_{mk}^W)^{-1})} \cdot \mathcal{E}(w_{mk} \mid \lambda_{mk}^W) \cdot \cancel{\mathcal{N}(\mu_{mk}^W \mid \mu_\mu, (\tau_\mu)^{-1})} \cdot \cancel{\mathcal{G}(\tau_{mk}^W \mid a, b)} \cdot \mathcal{G}(\lambda_{mk}^W \mid \alpha_\lambda, \beta_\lambda) \\
 & \propto \mathcal{E}(w_{mk} \mid \lambda_{mk}^W) \mathcal{G}(\lambda_{mk}^W \mid \alpha_\lambda, \beta_\lambda) \propto \mathcal{G}(\lambda_{mk}^W \mid \tilde{\alpha}_\lambda, \tilde{\beta}_\lambda),
 \end{aligned} \tag{7.19}$$

where $\tilde{\alpha}_\lambda = \alpha_\lambda + 1$ and $\tilde{\beta}_\lambda = \beta_\lambda + w_{mk}$.

Key observations. The importance of this hierarchical prior becomes evident through the interpretation of its conditional density. Here, **the prior parameter α_λ can be interpreted as the number of prior observations, and β_λ as the prior knowledge of w_{mk} .** On the one hand, an uninformative choice for α_λ is $\alpha_\lambda = 1$. On the other hand, if one prefers a sparse decomposition with a larger regularization on the model, β_λ can be chosen as a small value, e.g., $\beta_\lambda = 0.01$; or a large value, e.g., $\beta_\lambda = 100$, can be applied since we are in the NMF context, in which case, a large value in \mathbf{W} will enforce the counterparts

Algorithm 15 Gibbs sampler for GRRN in one iteration (prior on variance σ^2 here, similarly for the precision τ). The procedure presented here may not be efficient but is explanatory. A more efficient one can be implemented in a vectorized manner. By default, uninformative priors are $\alpha_\sigma = \beta_\sigma = 1$, $\mu_\mu = 0$, $\tau_\mu = 0.1$, $a = b = 1$, $\alpha_\lambda = 1$, $\beta_\lambda = \sqrt{\frac{m_0}{K}}$. One can even set $\beta_\lambda = 20 \cdot \sqrt{\frac{m_0}{K}}$ or $0.1 \cdot \sqrt{\frac{m_0}{K}}$ if one prefers a larger regularization.

```

1: Input: Choose parameters  $\alpha_\sigma, \beta_\sigma, \mu_\mu, \tau_\mu, a, b, \alpha_\lambda, \beta_\lambda$ ;
2: for  $k = 1$  to  $K$  do
3:   for  $m = 1$  to  $M$  do
4:     Sample  $w_{mk}$  from  $p(w_{mk} \mid \mathbf{A}, \mathbf{W}_{-mk}, \mathbf{Z}, \sigma^2, \mu_{mk}^W, \tau_{mk}^W, \lambda_{mk}^W)$ ;  $\triangleright$  Equation (7.16)
5:     Sample  $\mu_{mk}^W$  from  $p(\mu_{mk}^W \mid \tau_{mk}^W, \lambda_{mk}^W, \mu_\mu, \tau_\mu, a, b, \alpha_\lambda, \beta_\lambda, w_{mk})$ ;  $\triangleright$  Equation (7.17)
6:     Sample  $\tau_{mk}^W$  from  $p(\tau_{mk}^W \mid \mu_{mk}^W, \lambda_{mk}^W, \mu_\mu, \tau_\mu, a, b, \alpha_\lambda, \beta_\lambda, w_{mk})$ ;  $\triangleright$  Equation (7.18)
7:     Sample  $\lambda_{mk}^W$  from  $p(\lambda_{mk}^W \mid \mu_{mk}^W, \tau_{mk}^W, \mu_\mu, \tau_\mu, a, b, \alpha_\lambda, \beta_\lambda, w_{mk})$ ;  $\triangleright$  Equation (7.19)
8:   end for
9:   for  $n = 1$  to  $N$  do
10:    Sample  $z_{kn}$  from  $p(z_{kn} \mid \mathbf{A}, \mathbf{W}, \mathbf{Z}_{-kn}, \sigma^2, \mu_{kn}^Z, \tau_{kn}^Z, \lambda_{kn}^Z)$ ;  $\triangleright$  Sytry. of Eq. (7.16)
11:    Sample  $\mu_{kn}^Z$  from  $p(\mu_{kn}^Z \mid \tau_{kn}^Z, \lambda_{kn}^Z, \mu_\mu, \tau_\mu, a, b, \alpha_\lambda, \beta_\lambda, z_{kn})$ ;  $\triangleright$  Sytry. of Eq. (7.17)
12:    Sample  $\tau_{kn}^Z$  from  $p(\tau_{kn}^Z \mid \mu_{kn}^Z, \lambda_{kn}^Z, \mu_\mu, \tau_\mu, a, b, \alpha_\lambda, \beta_\lambda, z_{kn})$ ;  $\triangleright$  Sytry. of Eq. (7.18)
13:    Sample  $\lambda_{kn}^Z$  from  $p(\lambda_{kn}^Z \mid \mu_{kn}^Z, \tau_{kn}^Z, \mu_\mu, \tau_\mu, a, b, \alpha_\lambda, \beta_\lambda, z_{kn})$ ;  $\triangleright$  Sytry. of Eq. (7.19)
14:   end for
15: end for
16: Sample  $\sigma^2$  from  $p(\sigma^2 \mid \mathbf{A}, \mathbf{W}, \mathbf{Z}, \alpha_\sigma, \beta_\sigma)$ ;  $\triangleright$  Equation (7.8)
17: Report loss in Equation (7.1), stop if it converges.
    
```

in \mathbf{Z} to have small values. While an *uninformative choice* for β_λ is as follows. Suppose the mean value of all entries of matrix \mathbf{A} is m_0 , then β_λ can be set as $\beta_\lambda = \sqrt{\frac{m_0}{K}}$, where the value K is the latent dimension such that each prior entry $a_{mn} = \mathbf{w}_m^\top \mathbf{z}_n$ is equal to m_0 . After developing this hierarchical prior, we realize its similarity with the GTTN model (first introduced in a tensor decomposition context (Schmidt and Mohamed, 2009), and further discussed in Brouwer and Lio (2017)). However, the parameters in conditional densities of the GTTN model lack interpretation and flexibility so that there are no guidelines for parameter tuning when the performance is poor. The GRRN model, on the other hand, can work well generally when we select the uninformative prior $\beta_\lambda = \sqrt{\frac{m_0}{K}}$; moreover, one can even set $\beta_\lambda = 20 \cdot \sqrt{\frac{m_0}{K}}$ or $0.1 \cdot \sqrt{\frac{m_0}{K}}$ if one prefers a larger regularization as mentioned above.

Due to symmetry, the conditional expression for μ_{kn}^Z , τ_{kn}^Z , and λ_{kn}^Z can be easily derived similarly; and we shall not go into the details.

Gibbs sampling. The full procedure is formulated in Algorithm 15. By default, uninformative priors are $\alpha_\sigma = \beta_\sigma = 1$, $\mu_\mu = 0$, $\tau_\mu = 0.1$, $a = b = 1$, $\alpha_\lambda = 1$, $\beta_\lambda = \sqrt{\frac{m_0}{K}}$.

Computational complexity. The adopted Gibbs sampling method for the GRRN model has a complexity of $\mathcal{O}(MNK^2)$, where the most costs come from the update on the conditional density of w_{mk} and z_{kn} . In the meantime, all the methods we have introduced in the above sections (GEE, GTT, GTTN) have a complexity of $\mathcal{O}(MNK^2)$. Compared to the

GTTN model, the GRRN model only has an extra cost on the update of λ_{mk}^W , which does not constitute the bottleneck of the algorithm.

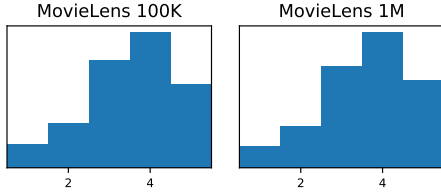


Figure 7.5: Data distribution of MovieLens 100K and MovieLens 1M data sets. The MovieLens 1M data set has a higher fraction of users who give a rate of 5 and a lower fraction for rates of 3.

Data set	Rows	Columns	Fraction obs.
MovieLens 100K	943	1473	0.072
MovieLens 1M	6040	3503	0.047

Table 7.2: Data set description. 99,723 and 999,917 observed entries for MovieLens 100K and MovieLens 1M data sets, respectively (user vectors or movie vectors with less than 3 observed entries are cleaned). MovieLens 100K is relatively a small data set and the MovieLens 1M tends to be large; while both of them are sparse.

7.6.1 Examples

To demonstrate the main advantages of the introduced GRRN method, we perform experiments with different analysis tasks; and different data sets including the MovieLens 100K and the MovieLens 1M from movie ratings for different users (Harper and Konstan, 2015). The data sets have a range from one to five stars with around 100,000 and 1,000,000 ratings, respectively. Our objective is to predict missing entries for users, enabling personalized movie recommendations (user vectors or movie vectors with less than 3 observed entries are cleaned). A summary of the two data sets can be seen in Table 7.2 and their distributions are shown in Figure 7.5. The MovieLens 1M data set has a higher fraction of users who give a rate of 5 and a lower fraction for rates of 3. We can see that the MovieLens 100K is relatively a small data set and the MovieLens 1M tends to be large; while both of them are sparse. On the other hand, the MovieLens 1M data set not only has a larger number of users, but also has an increased dimension (the number of movies) making it a harder task to evaluate.

Across all scenarios, the same parameter initialization is adopted when conducting different tasks. We compare the results in terms of convergence speed and generalization. In a wide range of scenarios across various models, GRRN improves convergence rates and achieves out-of-sample performances that are as good or better than other Bayesian NMF models.

Hyper-parameters. We follow the default hyper-parameter setups in Brouwer and Lio (2017). We use $\{\lambda_{mk}^W\} = \{\lambda_{kn}^Z\} = 0.1$ (GEE); $\{\mu_{mk}^Z\} = \{\mu_{kn}^Z\} = 0, \{\tau_{mk}^Z\} = \{\tau_{kn}^Z\} = 0.1$ (GTT); uninformative $\alpha_\sigma = \beta_\sigma = 1$ (Gaussian likelihood in GEE, GTT, GTTN, GRRN); $\mu_\mu = 0, \tau_\mu = 0.1, a = b = 1$ (hyperprior in GTTN, GRRN); $\alpha_\lambda = 1, \beta_\lambda = \sqrt{\frac{m_0}{K}}$ (hyperprior in GRRN). These are very weak prior choices and the models are not sensitive to them (Brouwer and Lio, 2017). As long as the hyper-parameters are set, the observed or unobserved variables are initialized from random draws as this initialization procedure provides a better initial guess of the right patterns in the matrices. In all experiments, we run the

Gibbs sampler 500 iterations with a burn-in of 400 iterations as the convergence analysis shows the algorithm can converge in less than 200 iterations.

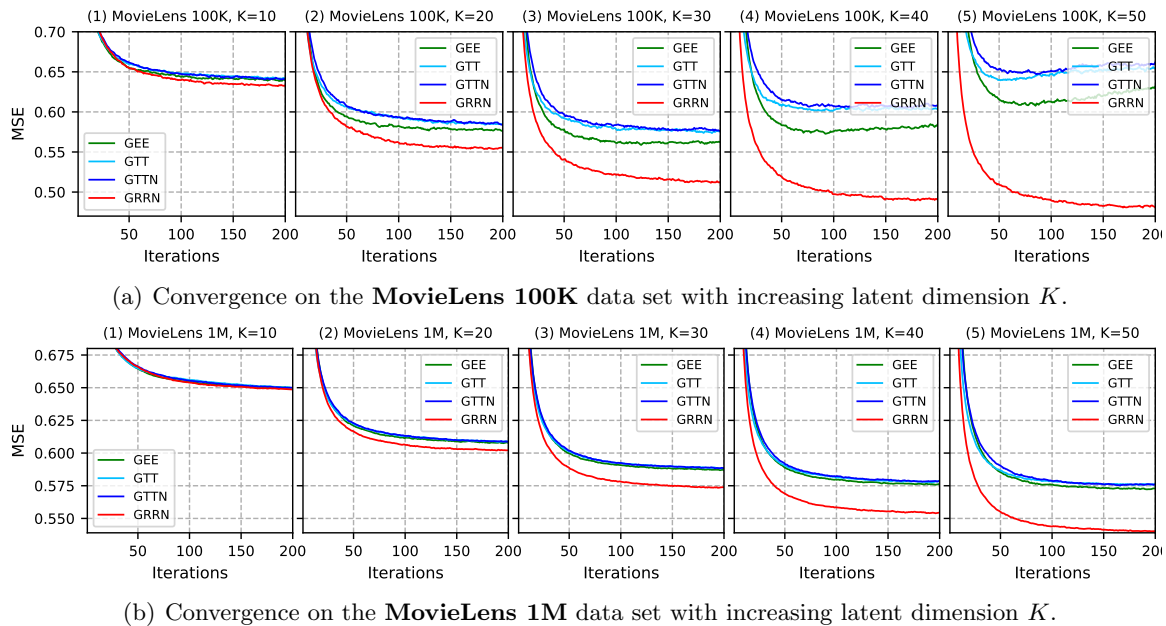
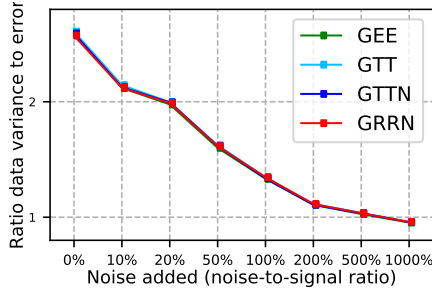


Figure 7.6: Convergence of the models on the MovieLens 100K (upper) and the MovieLens 1M (lower) data sets, measuring the training data fit (mean squared error). When increasing latent dimension K , the GRRN continues to improve the performance; while other models start to decrease on the MovieLens 100K data set or stop increasing on the MovieLens 1M data set.

Convergence analysis. Firstly, we compare the convergence in terms of iterations on the MovieLens 100K and MovieLens 1M data sets. We run each model with $K = 10, 20, 30, 40, 50$, and the loss is measured using mean squared error (MSE). Figure 7.6 shows the average convergence results of ten repeats. On the MovieLens 1M data set, all the methods converge to better performance with smaller MSE when increasing latent dimension K ; while the performance of GRRN is better than other models. Moreover, we observe that the convergence results of GTT and GTTN models are rather close since they share similar hidden structures, though GTTN is a hierarchical model. On the other hand, when conducting on the MovieLen 100K data set and increasing the feature dimension K , the GRRN model continues to converge to better performance with MSE continuing to decrease. However, GEE, GTT, and GTTN models first converge to better performance and then start to diverge with a larger MSE observed or stop improving at all when increasing latent dimension K . From this perspective, GRRN emerges as a better choice for data reduction compared to other Bayesian NMF models.

Noise sensitivity. We further assess the noise sensitivity of different models with predictive performance under noisy data sets. To see this, we add different levels of Gaussian noise to the data. We add levels of $\{0\%, 10\%, 20\%, 50\%, 100\%, 200\%, 500\%, 1000\%\}$ noise-

to-signal ratio noise (which is the ratio of the variance of the added Gaussian noise to the variance of the data). The results for the MovieLens 100K with $K = 50$ are shown in Figure 7.7. We observe that all models perform similarly. Moreover, similar results can be found on the MovieLens 1M data set and other K values and we shall not repeat the details.



$K \backslash$ Models	GEE	GTT	GTTN	GRRN
$K=20$	1.18	1.06	1.07	1.02
$K=30$	1.43	1.18	1.20	1.00
$K=40$	1.86	1.42	1.45	0.98
$K=50$	2.63	1.84	1.89	0.97
$K=20$	3.47	1.46	1.57	1.10
$K=30$	6.86	2.27	2.52	1.05
$K=40$	17056.27	4.07	4.79	1.04
$K=50$	236750.39	2650.21	5452.18	1.05

Figure 7.7: Ratio of the variance of data to the MSE of the predictions. The higher the better. All models perform similarly. Similar results can be found on the MovieLens 1M data set and other K values and we shall not repeat the details.

Table 7.3: Mean squared error measure when 97% (upper table) and 98% (lower table) of data is unobserved for the MovieLens 100K data set. The performance of the GRRN model exhibits only a marginal deterioration when increasing the fraction of unobserved from 97% to 98%. Similar situations can be observed in the MovieLens 1M experiment.

Predictive analysis. The training performance of the GRRN model steadily improves as the model complexity grows. Inspired by this result, we assess the predictive performance when the sparsity of the data increases to examine whether the models overfit or not. For different fractions of unobserved data, we randomly split the data based on that fraction, train the model on the observed data, and measure the performance on the held-out test data. Again, we increase K from $K = 20$ to $K = 30, 40, 50$ for all models. The average MSE of ten repeats is given in Figure 7.8. We observe that when $K = 20$ and the fraction of unobserved data is relatively a small value (e.g., fraction unobserved = 0.93 in Figure 7.8(a) and fraction unobserved = 0.96 in Figure 7.8(b)), all the models perform similarly (GRRN performs only slightly better). However, when the fraction of unobserved data increases or the latent dimension K increases, GRRN performs much better than the other models.

Table 7.3 shows MSE predictions of different models when the fraction of unobserved data is 97% and 98%. We observe that the performance of the GRRN model exhibits only a minor deterioration when increasing the fraction of unobserved from 97% to 98%, showing the GRRN model is more robust with less overfitting. While for other competitive models, the performances become extremely worse in this scenario. From Figure 7.6, we see that GEE can converge to a better in-sample performance generally; this leads to a worse out-of-sample performance as shown in Figure 7.8 (compared to GTT and GTTN). However, the GRRN has both better in-sample and out-of-sample performances from this experiment, making it a more robust choice in predicting missing entries. Similar situations can be observed in the MovieLens 1M case.

Furthermore, we also add a popular non-probabilistic NMF (NP-NMF) model to see the predictive results (Lee and Seung, 2000). Empirical results (grey lines in Figure 7.8) show

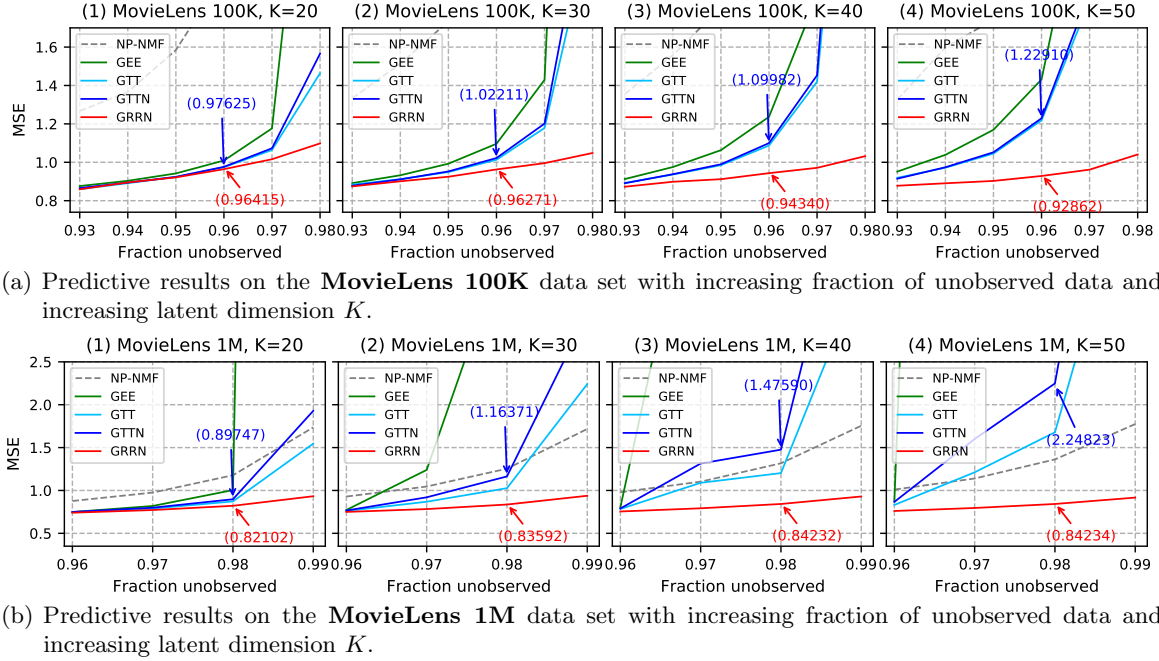


Figure 7.8: Predictive results on the MovieLens 100K (upper) and MovieLens 1M (lower) data sets with the least fractions of unobserved data being 0.928 and 0.953, respectively (see Table 7.2 for the data description). We measure the predictive performance (mean squared error) on a held-out data set for different fractions of unobserved data. The blue and red arrows compare the MSEs of GTTN and GRRN models when the fractions of unobserved data are 0.96 and 0.98, respectively.

that the NP-NMF can overfit easily compared to Bayesian NMF approaches, even when the fraction of unobserved data is relatively small and latent dimension K is small, though the issue is less severe in the MovieLens 1M data set.

7.7. Priors as Regularization

Denoting the prior parameters as θ and applying Bayes' rule, the posterior is proportional to the product of likelihood and prior density:

$$p(\theta | \mathbf{A}) \propto p(\mathbf{A} | \theta) \cdot p(\theta),$$

such that the log-likelihood follows

$$\begin{aligned} \log p(\theta | \mathbf{A}) &= \log p(\mathbf{A} | \theta) + \log p(\theta) + C_1 \\ &= \log \prod_{m,n=1}^{M,N} \mathcal{N}(a_{mn} | \mathbf{w}_m^\top \mathbf{z}_n, \sigma^2) + \log p(\mathbf{W}, \mathbf{Z}) + C_2 \\ &= -\frac{1}{2\sigma^2} (\mathbf{a}_{mn} - \mathbf{w}_m^\top \mathbf{z}_n)^2 + \log p(\mathbf{W}, \mathbf{Z}) + C_3, \end{aligned}$$

	Conditional w_{mk}	$\widetilde{\mu}_{mk}$ (mean)	$\widetilde{\sigma}_{mk}^2$ (variance)
GEE	$\mathcal{TN}(w_{mk} \widetilde{\mu}_{mk}, \widetilde{\sigma}_{mk}^2)$	$(-\lambda_{mk}^W + \frac{1}{\sigma^2} \sum_{j=1}^N z_{kj}(a_{mj} - \sum_{i \neq k}^K w_{mi}z_{ij})) \widetilde{\sigma}_{mk}^2$	$\frac{\sigma^2}{\sum_{j=1}^N z_{kj}^2}$
GL ₁ ²	$\mathcal{TN}(w_{mk} \widetilde{\mu}_{mk}, \widetilde{\sigma}_{mk}^2)$	$(-\lambda_k^W \sum_{j \neq k}^K w_{mj} + \frac{1}{\sigma^2} \sum_{j=1}^N z_{kj}(a_{mj} - \sum_{i \neq k}^K w_{mi}z_{ij})) \widetilde{\sigma}_{mk}^2$	$\frac{\sigma^2}{\sum_{j=1}^N z_{kj}^2 + \sigma^2 \lambda_k^W}$
GL ₂ ²	$\mathcal{TN}(w_{mk} \widetilde{\mu}_{mk}, \widetilde{\sigma}_{mk}^2)$	$(\frac{1}{\sigma^2} \sum_{j=1}^N z_{kj}(a_{mj} - \sum_{i \neq k}^K w_{mi}z_{ij})) \widetilde{\sigma}_{mk}^2$	$\frac{\sigma^2}{\sum_{j=1}^N z_{kj}^2 + \sigma^2 \lambda_k^W}$
GL _∞	$\mathcal{TN}(w_{mk} \widetilde{\mu}_{mk}, \widetilde{\sigma}_{mk}^2)$	$(-\lambda_k^W \cdot \mathbf{1}(w_{mk}) + \frac{1}{\sigma^2} \sum_{j=1}^N z_{kj}(a_{mj} - \sum_{i \neq k}^K w_{mi}z_{ij})) \widetilde{\sigma}_{mk}^2$	$\frac{\sigma^2}{\sum_{j=1}^N z_{kj}^2}$
GL _{2,∞} ²	$\mathcal{TN}(w_{mk} \widetilde{\mu}_{mk}, \widetilde{\sigma}_{mk}^2)$	$(-\lambda_k^W \cdot \mathbf{1}(w_{mk}) + \frac{1}{\sigma^2} \sum_{j=1}^N z_{kj}(a_{mj} - \sum_{i \neq k}^K w_{mi}z_{ij})) \widetilde{\sigma}_{mk}^2$	$\frac{\sigma^2}{\sum_{j=1}^N z_{kj}^2 + \sigma^2 \lambda_k^W}$

Table 7.4: Posterior conditional densities of w_{mk} 's for GEE, GL₁², GL₂², GL_∞, and GL_{2,∞}² models. The difference is highlighted in red. The conditional densities of z_{kn} 's are similar due to their symmetry to w_{mk} 's. $\mathcal{TN}(x|\mu, \tau^{-1}) = \frac{\sqrt{\frac{\tau}{2\pi}} \exp\{-\frac{\tau}{2}(x-\mu)^2\}}{1-\Phi(-\mu\sqrt{\tau})} u(x)$ is a truncated-normal (TN) density with zero density below $x = 0$ and renormalized to integrate to one. μ and τ are known as the ‘‘parent’’ mean and ‘‘parent’’ precision. $\Phi(\cdot)$ is the cumulative distribution function of standard normal density $\mathcal{N}(0, 1)$.

where C_1, C_2, C_3 are some constants. The ultimate equation is the sum of the negative squared loss of the training fit and a regularization term over the factored components \mathbf{W}, \mathbf{Z} . The prior distributions of \mathbf{W} and \mathbf{Z} then act as a regularization that can prevent the model from overfitting the data and increase the predictive performance. To be more concrete, the regularizers on \mathbf{W} can be categorized as follows:

$$\begin{aligned}
 \ell_1 &= \sum_{m=1}^M \sum_{k=1}^K w_{mk}, & \ell_2^{1/2} &= \sum_{m=1}^M \sqrt{\sum_{k=1}^K w_{mk}}, \\
 \ell_1^2 &= \sum_{m=1}^M \left(\sum_{k=1}^K w_{mk} \right)^2, & \ell_2^2 &= \sum_{m=1}^M \sum_{k=1}^K w_{mk}^2.
 \end{aligned} \tag{7.20}$$

We note that the ℓ_2^2 norm⁶ is equivalent to an independent Gaussian prior (GGG model); the ℓ_1 norm is equivalent to a Laplace prior in real-valued decomposition and is equivalently to an exponential prior (GEE model) in nonnegative matrix factorization. In the following sections, we will discuss some Bayesian nonnegative matrix factorization models that arise from different norms, the difference of the conditional posterior for latent variable w_{mk} is summarized in Table 7.4. The conditional densities of z_{kn} 's are similar due to their symmetry with w_{mk} 's.

7.8. Gaussian ℓ_1^2 Norm (GL₁²) Model

The Gaussian ℓ_1^2 norm (GL₁²) model is proposed by Brouwer and Lio (2017) based on the ℓ_1^2 norm in Equation (7.20) for both \mathbf{W} and \mathbf{Z} . We again view the data \mathbf{A} as being

6. To abuse the terminology, we call it a norm though it does not meet the criteria of a norm. A norm should satisfy nonnegativity ($\|\mathbf{A}\| \geq 0$), positive homogeneity ($\|\lambda\mathbf{A}\| = |\lambda| \cdot \|\mathbf{A}\|$), and triangle inequality ($\|\mathbf{A} + \mathbf{B}\| \leq \|\mathbf{A}\| + \|\mathbf{B}\|$), given matrices \mathbf{A}, \mathbf{B} and a scalar λ ; see Lu (2021b).

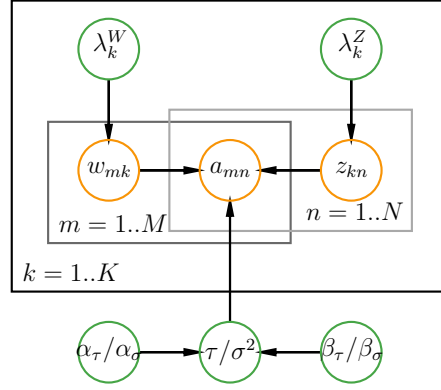


Figure 7.9: Graphical model representation of GL_1^2 , GL_2^2 , GL_∞ , and $GL_{2,\infty}^2$ models. Green circles denote prior variables, orange circles represent observed and latent variables, and plates represent repeated variables. The slash “/” in the variable represents “or.”

produced according to the probabilistic generative process shown in Figure 7.9. The (m, n) -th entry a_{mn} follows a Gaussian likelihood with variance σ^2 and a mean given by the latent decomposition $\mathbf{w}_m^\top \mathbf{z}_n$ (Equation (7.1)).

Prior. The ℓ_1^2 prior follows immediately by replacing the ℓ_1 norm with the ℓ_1^2 norm in the exponential prior. We assume \mathbf{W} and \mathbf{Z} are independently distributed with parameter λ_k^W and λ_k^Z proportional to an exponential function:

$$\begin{aligned}
 p(\mathbf{W} \mid \lambda_k^W) &\propto \begin{cases} \exp \left[-\frac{\lambda_k^W}{2} \sum_{m=1}^M \left(\sum_{k=1}^K w_{mk} \right)^2 \right], & \text{if } w_{mk} \geq 0 \text{ for all } m, k; \\ 0, & \text{if otherwise;} \end{cases} \\
 p(\mathbf{Z} \mid \lambda_k^Z) &\propto \begin{cases} \exp \left[-\frac{\lambda_k^Z}{2} \sum_{n=1}^N \left(\sum_{k=1}^K z_{kn} \right)^2 \right], & \text{if } z_{kn} \geq 0 \text{ for all } n, k; \\ 0, & \text{if otherwise.} \end{cases}
 \end{aligned} \tag{7.21}$$

Again, the prior for the noise variance $\sigma^2 = \frac{1}{\tau}$ is an inverse-Gamma density with shape α_σ and scale β_σ , respectively.

Posterior. Once again, following Bayes’ rule and MCMC, this means we need to be able to draw from distributions (by Markov blanket, Section 6.2, p. 141):

$$\begin{aligned}
 &p(w_{mk} \mid \mathbf{A}, \mathbf{W}_{-mk}, \mathbf{Z}, \sigma^2, \lambda_k^W, \lambda_k^Z), \\
 &p(z_{kn} \mid \mathbf{A}, \mathbf{W}, \mathbf{Z}_{-kn}, \sigma^2, \lambda_k^W, \lambda_k^Z), \\
 &p(\sigma^2 \mid \mathbf{A}, \mathbf{W}, \mathbf{Z}, \alpha_\sigma, \beta_\sigma),
 \end{aligned}$$

where \mathbf{W}_{-mk} denotes all elements of \mathbf{W} except w_{mk} , and \mathbf{Z}_{-kn} denotes all elements of \mathbf{Z} except z_{kn} . Using Bayes’ theorem, the conditional density of w_{mk} depends on its parents

(λ_k^W) , children (a_{mn}) , and coparents $(\tau$ or $\sigma^2, \mathbf{W}_{-mk}, \mathbf{Z})$ ⁷. Then, the conditional density of w_{mk} can be obtained by

$$\begin{aligned}
 p(w_{mk} | \mathbf{A}, \mathbf{W}_{-mk}, \mathbf{Z}, \sigma^2, \lambda_k^W) &\propto p(\mathbf{A} | \mathbf{W}, \mathbf{Z}, \sigma^2) \cdot p(\mathbf{W} | \lambda_k^W) = \prod_{i,j=1}^{M,N} \mathcal{N}(a_{ij} | \mathbf{w}_i^\top \mathbf{z}_j, \sigma^2) \cdot p(\mathbf{W} | \lambda_k^W) \\
 &\propto \exp \left\{ -\frac{1}{2\sigma^2} \sum_{i,j=1}^{M,N} (a_{ij} - \mathbf{w}_i^\top \mathbf{z}_j)^2 \right\} \times \exp \left\{ -\frac{\lambda_k^W}{2} \sum_{i=1}^M \left(\sum_{j=1}^K w_{ij} \right)^2 \right\} \cdot u(w_{mk}) \\
 &\propto \exp \left\{ -\frac{1}{2\sigma^2} \sum_{j=1}^N (a_{mj} - \mathbf{w}_m^\top \mathbf{z}_j)^2 \right\} \times \exp \left\{ -\frac{\lambda_k^W}{2} \left(w_{mk} + \sum_{j \neq k}^K w_{mj} \right)^2 \right\} \cdot u(w_{mk}) \\
 &\propto \exp \left\{ -\underbrace{\left(\frac{\sum_{j=1}^N z_{kj}^2 + \sigma^2 \lambda_k^W}{2\sigma^2} \right)}_{1/(2\widetilde{\sigma}_{mk}^2)} w_{mk}^2 + w_{mk} \underbrace{\left(-\lambda_k^W \sum_{j \neq k}^K w_{mj} + \sum_{j=1}^N \frac{z_{kj}}{\sigma^2} \left(a_{mj} - \sum_{i \neq k}^K w_{mi} z_{ij} \right) \right)}_{\widetilde{\sigma}_{mk}^{-2} \widetilde{\mu}_{mk}} \right\} u(w_{mk}) \\
 &\propto \mathcal{N}(w_{mk} | \widetilde{\mu}_{mk}, \widetilde{\sigma}_{mk}^2) \cdot u(w_{mk}) = \mathcal{TN}(w_{mk} | \widetilde{\mu}_{mk}, \widetilde{\sigma}_{mk}^2),
 \end{aligned} \tag{7.22}$$

where $u(x)$ is the unit function, taking the value 1 if $x \geq 0$ and 0 if $x < 0$, $\widetilde{\sigma}_{mk}^2 = \frac{\sigma^2}{\sum_{j=1}^N z_{kj}^2 + \sigma^2 \lambda_k^W}$ is the “parent” posterior variance of the normal distribution,

$$\widetilde{\mu}_{mk} = \left\{ -\lambda_k^W \cdot \sum_{j \neq k}^K w_{mj} + \frac{1}{\sigma^2} \sum_{j=1}^N z_{kj} \left(a_{mj} - \sum_{i \neq k}^K w_{mi} z_{ij} \right) \right\} \cdot \widetilde{\sigma}_{mk}^2$$

is the “parent” posterior mean of the normal distribution, and $\mathcal{TN}(x | \mu, \sigma^2)$ is the *truncated-normal density* with “parent” mean μ and “parent” variance σ^2 (Definition 3.4.1, p. 57). Note the posterior density of w_{mk} in Equation (7.22) is very similar to that of the GEE model in Equation (7.5), where we highlight the difference in red text. See also the comparison of conditional posteriors for w_{mk} in Table 7.4.

Or after rearrangement, the posterior density of w_{mk} can be equivalently described by a rectified-normal density (Definition 3.4.4, p. 62), and we shall not repeat the details.

And again, due to symmetry, a similar expression for z_{kn} can be easily derived. The conditional density of σ^2 in GL_1^2 is the same as that in Equation (7.8)

Connection between GEE and GL_1^2 models

We observe that there is an extra term in the denominator of the “parent” variance value such that when all else are held equal, the GL_1^2 has a smaller variance, and the distribution is more clustered in a smaller range. This implies that GL_1^2 acts as a stronger constraint/regularizer than the GEE model.

Moreover, when $\{\lambda_{mk}^W\}$ in the GEE model and $\{\lambda_k^W\}$ in the GL_1^2 model are equal (see Table 7.4), the extra term $\sum_{j \neq k}^K w_{mj}$ in the GL_1^2 model plays an important role in controlling the sparsity of factored components in the NMF context. To be more

7. See Figure 7.9 and Section 6.2 (p. 141).

concrete, when the distribution of elements in matrix \mathbf{A} has a large portion of big values, the extra term $\sum_{j \neq k}^K w_{mj}$ will be larger than 1, and thus enforcing the posterior “parent” mean $\widetilde{\mu_{mk}}$ of the truncated-normal density to be a small positive or even a negative value. This in turn constraints the draws of $\mathcal{TN}(w_{mk}|\cdot)$ to be around zero, thus favoring sparsity (see the expectation of the variable of a truncated-normal distribution for different “parent” mean values in Figure 3.8(a), p. 59, the smaller the “parent” mean value $\widetilde{\mu_{mk}}$, the smaller the expectation of the truncated-normal distributed variable w_{mk} ; see also the example in Section 7.9 for the experiment on the GDSC IC_{50} data set). On the contrary, when the entries in matrix \mathbf{A} are small, this extra term will be smaller than 1, the parameter λ_k^W has a little impact on the posterior “parent” mean $\widetilde{\mu_{mk}}$, which will possibly be a large value, and the factored component \mathbf{W} or \mathbf{Z} will be dense instead (also see Section 7.9 for the experiment on the Gene Body Methylation data set).

In this sense, the drawback of the GL_1^2 model is revealed that it is not consistent and not robust for different types of matrices \mathbf{A} . In contrast, the GL_2^2 and $GL_{2,\infty}^2$ models, introduced in the next section, are consistent and robust for different matrix types, and impose a larger regularization compared to the GEE model such that its predictive performance is better (when the data matrix \mathbf{A} has large values).

Algorithm 16 Gibbs sampler for GL_1^2 model in one iteration (prior on variance σ^2 here, similarly for the precision τ). The procedure presented here may not be efficient but is explanatory. A more efficient one can be implemented in a vectorized manner. By default, uninformative priors are $\alpha_\sigma = \beta_\sigma = 1$, $\{\lambda_k^W\} = \{\lambda_k^Z\} = 0.1$.

Require: Choose initial $\alpha_\sigma, \beta_\sigma, \{\lambda_k^W\}, \{\lambda_k^Z\}$;

- 1: **for** $k = 1$ to K **do**
- 2: **for** $m = 1$ to M **do**
- 3: Sample w_{mk} from $p(w_{mk} \mid \mathbf{A}, \mathbf{W}_{-mk}, \mathbf{Z}, \sigma^2, \lambda_k^W)$; ▷ Equation (7.22)
- 4: **end for**
- 5: **for** $n = 1$ to N **do**
- 6: Sample z_{kn} from $p(z_{kn} \mid \mathbf{A}, \mathbf{W}, \mathbf{Z}_{-kn}, \sigma^2, \lambda_k^Z)$; ▷ Symmetry of Equation (7.22)
- 7: **end for**
- 8: **end for**
- 9: Sample σ^2 from $p(\sigma^2 \mid \mathbf{A}, \mathbf{W}, \mathbf{Z}, \alpha_\sigma, \beta_\sigma)$; ▷ Equation (7.8)
- 10: Report loss in Equation (7.1), stop if it converges.

Gibbs sampling. By this Gibbs sampling method introduced in Section 2.3.3 (p. 26), we can construct a Gibbs sampler for the GL_1^2 model as formulated in Algorithm 16. And also in practice, all the parameters of the prior distribution are set to be the same value $\lambda = \{\lambda_k^W\} = \{\lambda_k^Z\}$. By default, uninformative priors are $\alpha_\sigma = \beta_\sigma = 1$, $\{\lambda_k^W\} = \{\lambda_k^Z\} = 0.1$.

7.9. Gaussian ℓ_2^2 Norm (GL_2^2) and Gaussian ℓ_∞ Norm (GL_∞) Models

After the development of the GL_1^2 model, more exploration of the behaviors for different “norms” are done in Lu and Chai (2022). The ℓ_p prior relies highly on the im-

plicit regularization in the GL_1^2 model. For any vector $\mathbf{x} \in \mathbb{R}^n$, the ℓ_p norm is given by $\ell_p(\mathbf{x}) = (\sum_{i=1}^n |x_i|^p)^{1/p}$, and the unit balls in two-dimensional space and three-dimensional space are illustrated in Figure 4.4 (p. 115) and Figure 4.5 (p. 115), respectively. The norms of a vector are quite useful in machine learning. In Chapter 4 (p. 96), we mentioned the least squares problem is applied to minimize the squared distance between observation \mathbf{b} and expected observation \mathbf{Ax} : $\|\mathbf{Ax} - \mathbf{b}\|_2^2$, i.e., the ℓ_2 norm of $\mathbf{Ax} - \mathbf{b}$. On the other hand, minimizing the ℓ_1 norm between the observation and the expected observation can result in a robust estimator of \mathbf{x} (Zoubir et al., 2012). While the ℓ_p norm over the matrix $\mathbf{W} \in \mathbb{R}^{M \times K}$ can be defined as

$$\ell_p = \sum_{m=1}^M \left(\sum_{k=1}^K |w_{mk}|^p \right)^{1/p}. \quad (7.23)$$

In the context of NMF, the ℓ_1 norm (for the GEE model) in Equation (7.20) can be regarded as an ℓ_p norm with $p = 1$ since $\{w_{mk}\}$'s are nonnegative. The ℓ_1 norm is known to have a sparse constraint (see discussion in Section 7.2). We can further extend the Bayesian models with ℓ_2^2 and ℓ_∞ norms. Again, we view the data \mathbf{A} as being produced according to the probabilistic generative process shown in Figure 7.9, the same graphical model as the GL_1^2 model. The (m, n) -th entry a_{mn} follows a Gaussian likelihood with variance σ^2 and a mean given by the latent decomposition $\mathbf{w}_m^\top \mathbf{z}_n$ (Equation (7.1)). Therefore, the posterior density of the Gaussian variance parameter σ^2 , given an inverse-Gamma prior with shape α_σ and scale β_σ parameters, is the same as the GEE model in Equation (7.8).

Prior for the GL_2^2 model. Based on the ℓ_2 norm, we assume \mathbf{W} and \mathbf{Z} are independently distributed with parameters λ_k^W and λ_k^Z proportional to an exponential function:

$$\begin{aligned}
 p(\mathbf{W} \mid \lambda_k^W) &\propto \begin{cases} \exp \left[-\frac{\lambda_k^W}{2} \sum_{m=1}^M \left(\sum_{k=1}^K w_{mk}^2 \right) \right], & \text{if } w_{mk} \geq 0 \text{ for all } m, k ; \\ 0, & \text{if otherwise;} \end{cases} \\
 p(\mathbf{Z} \mid \lambda_k^Z) &\propto \begin{cases} \exp \left[-\frac{\lambda_k^Z}{2} \sum_{n=1}^N \left(\sum_{k=1}^K z_{kn}^2 \right) \right], & \text{if } z_{kn} \geq 0 \text{ for all } n, k ; \\ 0, & \text{if otherwise.} \end{cases}
 \end{aligned} \quad (7.24)$$

Posterior for the GL_2^2 model. According to Bayes rule (Equation (2.1), p. 22), the posterior is proportional to the product of likelihood and prior, it can be maximized to yield an estimate of \mathbf{W} and \mathbf{Z} . Using Bayes' theorem, the conditional density of w_{mk} depends on its parents (λ^W), children (a_{mn}), and coparents (τ or σ^2 , \mathbf{W}_{-mk} , \mathbf{Z})⁸. And it can be obtained by

⁸. See Figure 7.9 and Section 6.2 (p. 141).

$$\begin{aligned}
 & p(w_{mk} \mid \mathbf{A}, \mathbf{W}_{-mk}, \mathbf{Z}, \sigma^2, \lambda_k^W) \\
 & \propto p(\mathbf{A} \mid \mathbf{W}, \mathbf{Z}, \sigma^2) \times p(\mathbf{W} \mid \lambda_k^W) = \prod_{i,j=1}^{M,N} \mathcal{N}(a_{ij} \mid \mathbf{w}_i^\top \mathbf{z}_j, \sigma^2) \times p(\mathbf{W} \mid \lambda_k^W) \cdot u(w_{mk}) \\
 & \propto \exp \left\{ -\frac{1}{2\sigma^2} \sum_{i,j=1}^{M,N} (a_{ij} - \mathbf{w}_i^\top \mathbf{z}_j)^2 \right\} \times \exp \left\{ -\frac{\lambda_k^W}{2} \sum_{i=1}^M \left(\sum_{j=1}^K w_{ij}^2 \right) \right\} \cdot u(w_{mk}) \\
 & \propto \exp \left\{ -\frac{1}{2\sigma^2} \sum_{j=1}^N (a_{mj} - \mathbf{w}_m^\top \mathbf{z}_j)^2 \right\} \times \exp \left\{ -\frac{\lambda_k^W}{2} w_{mk}^2 \right\} \cdot u(w_{mk}) \\
 & \propto \exp \left\{ -\underbrace{\left(\frac{\sum_{j=1}^N z_{kj}^2 + \sigma^2 \lambda_k^W}{2\sigma^2} \right)}_{1/(2\widetilde{\sigma}_{mk}^2)} w_{mk}^2 + w_{mk} \underbrace{\left(\frac{1}{\sigma^2} \sum_{j=1}^N z_{kj} \left(a_{mj} - \sum_{i \neq k} w_{mi} z_{ij} \right) \right)}_{\widetilde{\sigma}_{mk}^{-2} \widetilde{\mu}_{mk}} \right\} \cdot u(w_{mk}) \\
 & \propto \mathcal{N}(w_{mk} \mid \widetilde{\mu}_{mk}, \widetilde{\sigma}_{mk}^2) \cdot u(w_{mk}) = \mathcal{TN}(w_{mk} \mid \widetilde{\mu}_{mk}, \widetilde{\sigma}_{mk}^2), \tag{7.25}
 \end{aligned}$$

where $\widetilde{\sigma}_{mk}^2 = \frac{\sigma^2}{\sum_{j=1}^N z_{kj}^2 + \sigma^2 \lambda_k^W}$ is the posterior variance of the normal distribution,

$$\widetilde{\mu}_{mk} = \left\{ \frac{1}{\sigma^2} \sum_{j=1}^N z_{kj} \left(a_{mj} - \sum_{i \neq k} w_{mi} z_{ij} \right) \right\} \cdot \widetilde{\sigma}_{mk}^2$$

is the posterior mean of the normal distribution, and $\mathcal{TN}(x \mid \mu, \sigma^2)$ is the *truncated-normal density* with “parent” mean μ and “parent” variance σ^2 (Definition 3.4.1, p. 57). Note again the posterior density of w_{mk} in Equation (7.25) is very similar to that of the GEE model in Equation (7.5), where we highlight the difference in red text. See also the comparison of conditional posteriors for w_{mk} in Table 7.4.

Connection between GEE, GL_1^2 , and GL_2^2 models

We observe that the posterior “parent” mean $\widetilde{\mu}_{mk}$ in the GL_2^2 model is larger than that in the GEE model since it does not contain the negative term $-\lambda_{mk}^W$ (see Table 7.4). While the posterior “parent” variance is smaller than that in the GEE model; therefore, the conditional density of GL_2^2 model is more clustered and it imposes a larger regularization in the sense of data/entry distribution (see Figure 3.8(a), p. 59, the smaller the “parent” variance of the truncated-normal distribution, the larger the “parent” precision, and the smaller the expectation of the truncated-normal variable). This can induce sparsity in the context of nonnegative matrix factorization. Moreover, the GL_2^2 does not have the extra term $\sum_{j \neq k}^K w_{mj}$ in the GL_1^2 model, which causes the **inconsistency** for different types of matrix \mathbf{A} (as discussed previously), such that the introduced GL_2^2 model is more robust.

Prior for the \mathbf{GL}_∞ model. When $p \rightarrow \infty$, the ℓ_p norm defined over \mathbf{W} is

$$\ell_\infty = \sum_{m=1}^M \left(\sum_{k=1}^K |w_{mk}|^\infty \right)^{1/\infty} = \sum_{m=1}^M \max_k |w_{mk}|. \quad (7.26)$$

Based on the ℓ_p norm, we assume \mathbf{W} and \mathbf{Z} are independently exponentially distributed with scales λ_{mk} and λ_{kn} (Definition 3.3.1, p. 56):

$$\begin{aligned} p(\mathbf{W} \mid \lambda_k^W) &\propto \begin{cases} \exp \left[-\lambda_k^W \sum_{m=1}^M \max_k |w_{mk}| \right], & \text{if } w_{mk} \geq 0 \text{ for all } m, k; \\ 0, & \text{if otherwise;} \end{cases} \\ p(\mathbf{Z} \mid \lambda_k^Z) &\propto \begin{cases} \exp \left[-\lambda_k^Z \sum_{n=1}^N \max_k |z_{kn}| \right], & \text{if } z_{kn} \geq 0 \text{ for all } n, k; \\ 0, & \text{if otherwise.} \end{cases} \end{aligned} \quad (7.27)$$

Note we remove the 2 in the denominator of λ_k^W for consistency issues, which we will see shortly in the form of the conditional density in Equation (7.28).

Posterior for \mathbf{GL}_∞ model. Applying Bayes' rule (Equation (2.1), p. 22), the posterior is proportional to the product of likelihood and prior, it can be maximized to yield an estimate of \mathbf{W} and \mathbf{Z} . Using Bayes' theorem, the conditional density of w_{mk} depends on its parents (λ_k^W), children (a_{mn}), and coparents (τ or σ^2 , \mathbf{W}_{-mk} , \mathbf{Z})⁹. Denote $\mathbf{1}(w_{mk})$ as the indicator whether w_{mk} is the largest one for $k = 1, 2, \dots, K$, the conditional density can be obtained by

$$\begin{aligned} &p(w_{mk} \mid \mathbf{A}, \mathbf{W}_{-mk}, \mathbf{Z}, \sigma^2, \lambda_k^W) \\ &\propto p(\mathbf{A} \mid \mathbf{W}, \mathbf{Z}, \sigma^2) \times p(\mathbf{W} \mid \lambda_k^W) = \prod_{i,j=1}^{M,N} \mathcal{N}(a_{ij} \mid \mathbf{w}_i^\top \mathbf{z}_j, \sigma^2) \times p(\mathbf{W} \mid \lambda_k^W) \cdot u(w_{mk}) \\ &\propto \exp \left\{ -\frac{1}{2\sigma^2} \sum_{i,j=1}^{M,N} (a_{ij} - \mathbf{w}_i^\top \mathbf{z}_j)^2 \right\} \times \exp \left\{ -\lambda_k^W \cdot \sum_{i=1}^M \max_k |w_{ij}| \right\} \cdot u(w_{mk}) \\ &\propto \exp \left\{ -\frac{1}{2\sigma^2} \sum_{j=1}^N (a_{mj} - \mathbf{w}_m^\top \mathbf{z}_j)^2 \right\} \times \exp \left\{ -\lambda_k^W \cdot w_{mk} \right\} \cdot u(w_{mk}) \cdot \mathbf{1}(w_{mk}) \\ &\propto \exp \left\{ -\frac{1}{2\sigma^2} \sum_{j=1}^N \left[w_{mk}^2 z_{kj}^2 + 2w_{mk} z_{kj} \left(\sum_{i \neq k} w_{mi} z_{ij} - a_{mj} \right) \right] \right\} \cdot \exp \left\{ -w_{mk} \lambda_k^W \mathbf{1}(w_{mk}) \right\} \cdot u(w_{mk}) \\ &\propto \exp \left\{ -\underbrace{\left(\frac{\sum_{j=1}^N z_{kj}^2}{2\sigma^2} \right)}_{1/(2\widetilde{\sigma}_{mk}^2)} w_{mk}^2 + w_{mk} \underbrace{\left[-\lambda_k^W \mathbf{1}(w_{mk}) + \frac{1}{\sigma^2} \sum_{j=1}^N z_{kj} \left(a_{mj} - \sum_{i \neq k} w_{mi} z_{ij} \right) \right]}_{\widetilde{\sigma}_{mk}^2 - 1 \widetilde{\mu}_{mk}} \right\} \cdot u(w_{mk}) \\ &\propto \mathcal{N}(w_{mk} \mid \widetilde{\mu}_{mk}, \widetilde{\sigma}_{mk}^2) \cdot u(w_{mk}) = \mathcal{TN}(w_{mk} \mid \widetilde{\mu}_{mk}, \widetilde{\sigma}_{mk}^2), \end{aligned} \quad (7.28)$$

⁹. See Figure 7.9 and Section 6.2 (p. 141).

where $u(x)$ is the unit function with value 1 if $x \geq 0$ and value 0 if $x < 0$, $\widetilde{\sigma}_{mk}^2 = \frac{\sigma^2}{\sum_{j=1}^N z_{kj}^2}$ is the posterior “parent” variance of the normal distribution,

$$\widetilde{\mu}_{mk} = \left\{ -\lambda_k^W \cdot \mathbf{1}(w_{mk}) + \frac{1}{\sigma^2} \sum_{j=1}^N z_{kj} \left(a_{mj} - \sum_{i \neq k}^K w_{mi} z_{ij} \right) \right\} \cdot \widetilde{\sigma}_{mk}^2$$

is the posterior “parent” mean of the normal distribution, and $\mathcal{TN}(x | \mu, \sigma^2)$ is the *truncated normal density* with “parent” mean μ and “parent” variance σ^2 (Definition 3.4.1, p. 57).

Connection between GEE and GL_∞ models

The posterior “parent” variance $\widetilde{\sigma}_{mk}^2$ in the GL_∞ model is exactly the same as that in the GEE model (see Table 7.4). Denote $\mathbf{1}(w_{mk})$ as the indicator whether w_{mk} is the largest one among $k = 1, 2, \dots, K$. Suppose further the condition $\mathbf{1}(w_{mk})$ is satisfied, parameters $\{\lambda_{mk}^W\}$ in the GEE model and $\{\lambda_k^W\}$ in the GL_∞ model are equal, the “parent” mean parameter $\widetilde{\mu}_{mk}$ is the same as that in the GEE model as well. However, when w_{mk} is not the maximum value among $\{w_{m1}, w_{m2}, \dots, w_{mK}\}$, the “parent” mean $\widetilde{\mu}_{mk}$ is larger than that in the GEE model since the GL_∞ model excludes this negative term. The GL_∞ model then has the interpretation that it has a *sparsity constraint* when w_{mk} is the maximum value; and it has a *relatively loose constraint* when w_{mk} is not the maximum value. Overall, the GL_∞ favors a loose regularization compared to the GEE model.

Further extension: $\text{GL}_{2,\infty}^2$ model. The $\text{GL}_{2,\infty}^2$ model takes the advantages of both GL_2^2 and GL_∞ models, and the posterior parameters of $\text{GL}_{2,\infty}^2$ are shown in Table 7.4. The implicit prior of the $\text{GL}_{2,\infty}^2$ model can be obtained by

$$p(\mathbf{W} | \lambda_k^W) \propto \exp \left\{ \frac{-\lambda_k^W}{2} \sum_{m=1}^M \left(\sum_{k=1}^K w_{mk}^2 + 2 \max_k |w_{mk}| \right) \right\} u(\mathbf{W}). \quad (7.29)$$

Computational complexity and Gibbs sampler. The adopted Gibbs sampling methods for GEE, GL_1^2 , GL_2^2 , GL_∞ , and $\text{GL}_{2,\infty}^2$ models have complexity $\mathcal{O}(MNK^2)$, where the most expensive operation comes from the updates on the conditional density of w_{mk} ’s and z_{kn} ’s. The Gibbs sampler for the discussed models is formulated in Algorithm 17. By default, uninformative priors are $\{\lambda_k^W\} = \{\lambda_k^Z\} = 0.1$ (GL_1^2 , GL_2^2 , GL_∞ , $\text{GL}_{2,\infty}^2$); $\alpha_\sigma = \beta_\sigma = 1$ (inverse-Gamma prior in GL_1^2 , GL_2^2 , GL_∞ , $\text{GL}_{2,\infty}^2$).

7.9.1 Examples

We conduct experiments with various analysis tasks to demonstrate the main advantages of the GL_2^2 and $\text{GL}_{2,\infty}^2$ methods. We use two data sets from bioinformatics: The first one is the Genomics of Drug Sensitivity in Cancer data set ¹⁰ (GDSC IC_{50}) (Yang et al., 2012), which contains a wide range of drugs and their treatment outcomes on different cancer and

10. <https://www.cancerrxgene.org/>

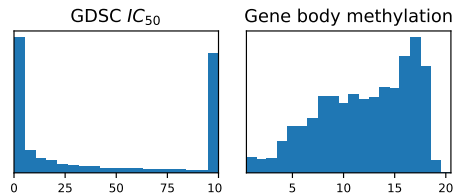
Algorithm 17 Gibbs sampler for GL_1^2 , GL_2^2 , and GL_∞ models (prior on variance σ^2 here, similarly for the precision τ). The procedure presented here is for explanatory purposes, and vectorization can expedite the procedure. By default, uninformative priors are $\{\lambda_k^W\} = \{\lambda_k^Z\} = 0.1$ (GL_1^2 , GL_2^2 , GL_∞ , $GL_{2,\infty}^2$); $\alpha_\sigma = \beta_\sigma = 1$ (inverse-Gamma prior in GL_1^2 , GL_2^2 , GL_∞ , $GL_{2,\infty}^2$).

```

1: for  $k = 1$  to  $K$  do
2:   for  $m = 1$  to  $M$  do
3:     Sample  $w_{mk}$  from  $p(w_{mk}|\cdot) = \mathcal{TN}(w_{mk}|\widetilde{\mu}_{mk}, \widetilde{\sigma}_{mk}^2)$  from Table 7.4;
4:   end for
5:   for  $n = 1$  to  $N$  do
6:     Sample  $z_{kn}$  from  $p(z_{kn}|\cdot) = \mathcal{TN}(w_{mk}|\widetilde{\mu}_{kn}, \widetilde{\sigma}_{kn}^2)$ ; ▷ symmetry of  $w_{mk}$ 
7:   end for
8: end for
9: Sample  $\sigma^2$  from  $p(\sigma^2 | \mathbf{A}, \mathbf{W}, \mathbf{Z}, \alpha_\sigma, \beta_\sigma)$ ; ▷ Equation (7.8)
10: Report loss in Equation (7.1), stop if it converges.

```

tissue types (cell lines). Following Brouwer and Lio (2017), we preprocess the GDSC IC_{50} data set by capping high values to 100, undoing the natural log transform, and casting them as integers. The second one is the Gene Body Methylation data set (Koboldt et al., 2012), which gives the amount of methylation measured in the body region of 160 breast cancer driver genes. We multiply the values in the Gene Body Methylation data set by 20 and cast them as integers as well. A summary of the two data sets can be seen in Table 7.5, and their distributions are shown in Figure 7.10. The GDSC IC_{50} data set has a larger range whose values are unbalanced (either small as 0 or large as 100); while the Gene Body Methylation data set has a smaller range whose values seem balanced. We can see that the GDSC IC_{50} is relatively a large data set, whose matrix rank is 139, and the Gene Body Methylation data tends to be small, possessing a matrix rank of 160.



Dataset	Rows	Columns	Fraction obs.
GDSC IC_{50}	707	139	0.806
Gene Body Meth.	160	254	1.000

Figure 7.10: Data distribution of IC_{50} and Gene Body Methylation data sets. **Table 7.5:** Dataset description. Gene Body Methylation is relatively a small data set, and the GDSC IC_{50} tends to be large. The description provides the number of rows, columns, and the fraction of entries that are observed.

The same parameter initialization is adopted in each scenario. We compare the results in terms of convergence speed and generalization. In a wide range of scenarios across various models, GL_2^2 and $GL_{2,\infty}^2$ improve convergence rates, and lead to out-of-sample performance that is as good or better than other Bayesian NMF models with implicit regularization meaning.

Hyper-parameters. We follow the default hyper-parameter setups in Brouwer and Lio (2017). We use $\{\lambda_{mk}^W\} = \{\lambda_{kn}^Z\} = 0.1$ (GEE); $\{\lambda_k^W\} = \{\lambda_k^Z\} = 0.1$ (GL_1^2 , GL_2^2 , $GL_{2,\infty}^2$); uninformative $\alpha_\sigma = \beta_\sigma = 1$ (inverse-Gamma prior in GEE, GL_1^2 , GL_2^2 , $GL_{2,\infty}^2$). These are very weak prior choices and the models are insensitive to them (Brouwer and Lio, 2017). As long as the hyper-parameters are set, the observed or unobserved variables are initialized from random draws as this initialization procedure provides a better initial guess of the right patterns in the matrices. In all experiments, we run the Gibbs sampler 500 iterations with a burn-in of 300 iterations as the convergence analysis shows the algorithm can converge in fewer than 200 iterations.

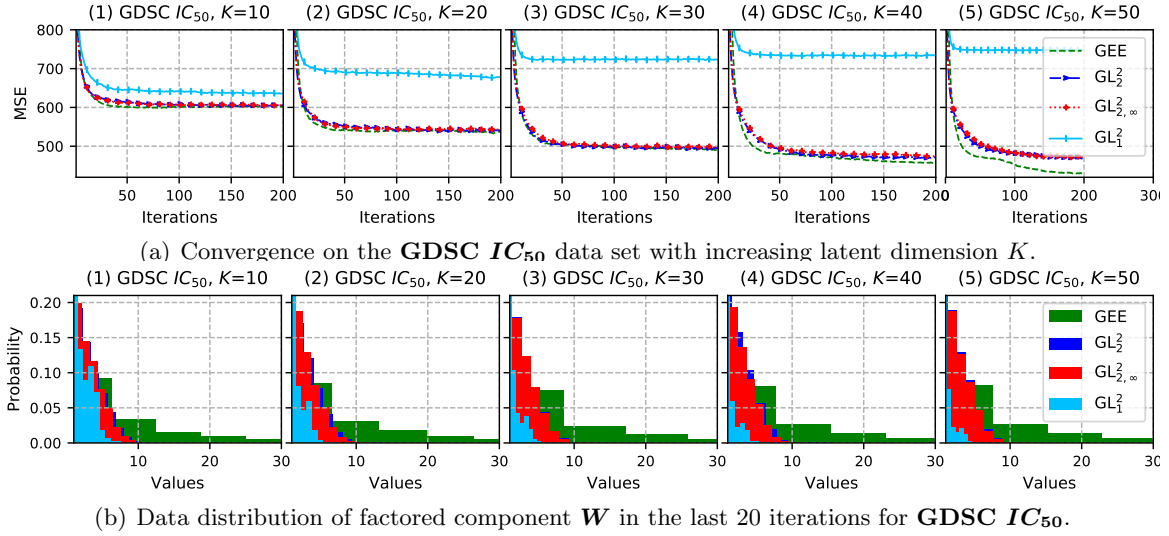


Figure 7.11: Convergence of the models on the GDSC IC_{50} (upper) and the distribution of factored \mathbf{W} (lower), measuring the training data fit (mean squared error). When we increase the latent dimension K , the GEE, GL_2^2 , and $GL_{2,\infty}^2$ algorithms continue to increase the performance; while GL_1^2 starts to decrease. The results of GL_∞ and $GL_{2,\infty}^2$ models are similar so we only present the results of the $GL_{2,\infty}^2$ model for brevity.

Convergence analysis for GDSC IC_{50} with relatively large entries. Firstly, we compare the convergence in terms of iterations on the GDSC IC_{50} and Gene Body Methylation data sets. We run each model with $K = \{10, 20, 30, 40, 50\}$, and the loss is measured by mean squared error (MSE). Figure 7.11(a) shows the average convergence results of ten repeats, and Figure 7.11(b) shows the distribution of entries of the factored \mathbf{W} for the last 20 iterations on the GDSC IC_{50} data set. The result is consistent with our analysis (see the connection between different models). Since the values of the data matrix for GDSC IC_{50} data set is large, the posterior “parent” mean $\widetilde{\mu}_{mk}$ in the GL_1^2 model is approaching zero or even negative; thus, it has a larger regularization than GEE model. This makes the GL_1^2 model converge to a worse performance. GL_2^2 and $GL_{2,\infty}^2$ models, on the contrary, impose a looser regularization than the GL_1^2 model, and the convergence performances are close to that of the GEE model.

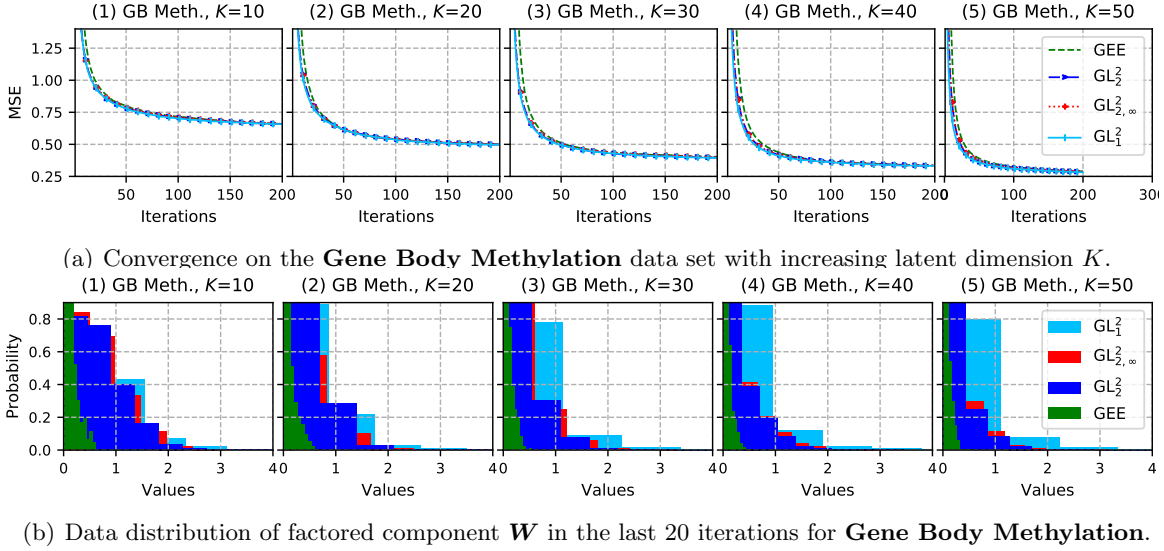


Figure 7.12: Convergence of the models on the Gene Body Methylation data set (upper) and the distribution of factored \mathbf{W} (lower), measuring the training data fit (mean squared error). When we increase the latent dimension K , all the models continue to improve the performance.

Convergence analysis for Gene Body Methylation with relatively small entries. Figure 7.12(a) further shows the average convergence results of ten repeats, and Figure 7.12(b) shows the distribution of the entries of the factored \mathbf{W} for the last 20 iterations on the Gene Body Methylation data set. The situation is different for the GL_1^2 model since the range of the entries of the Gene Body Methylation data set is smaller than that of the GDSC IC_{50} data set (see Figure 7.10). This makes the $-\lambda_k^W \cdot \sum_{j \neq k}^K w_{mj}$ term of posterior “parent” mean $\widetilde{\mu}_{mk}$ in the GL_1^2 model approach zero (see Table 7.4), and the model then favors a looser regularization than the GEE model.

The situation can be further presented by the distribution of the factored component \mathbf{W} on the GDSC IC_{50} (Figure 7.11(b)) and the Gene Body Methylation (Figure 7.12(b)). The GEE model has larger values of \mathbf{W} on the former data set and smaller values on the latter; while GL_1^2 has smaller values of \mathbf{W} on the former data set and larger values on the latter. In other words, the regularization of the GEE and GL_1^2 is **inconsistent** on the two different data matrices. In comparison, the GL_2^2 and $GL_{2,\infty}^2$ models are **consistent** on different data sets, making them more robust algorithms to compute the nonnegative matrix factorization of the observed data.

Table 7.6 shows the mean values of the factored component \mathbf{W} in the last 20 iterations for GDSC IC_{50} (upper table) and Gene Body Methylation (lower table), where the value in the parentheses is the sparsity evaluated by taking the percentage of values smaller than 0.1. The **inconsistency** of GEE for different matrices can be observed (either large sparsity or small sparsity), while the results for the GL_2^2 and $GL_{2,\infty}^2$ models are more **consistent**.

Predictive analysis. The training performances of the GEE, GL_2^2 , and $GL_{2,\infty}^2$ models steadily improve as the model complexity grows. Inspired by this result, we measure the

K	GEE	GL_1^2	GL_2^2	$GL_{2,\infty}^2$	Unobs.	K	GEE	GL_1^2	GL_2^2	$GL_{2,\infty}^2$
10	8.1 (1.9)	1.3 (10.3)	2.4 (3.8)	2.4 (4.5)	60%	20	787.60	880.36	769.24	768.27
20	8.6 (1.5)	0.8 (14.7)	2.3 (4.1)	2.2 (4.4)		30	810.39	888.47	774.53	773.27
30	8.7 (1.4)	0.7 (17.3)	2.2 (4.3)	2.2 (4.4)		40	802.39	892.01	783.26	784.30
40	8.3 (1.5)	0.6 (19.4)	2.2 (4.4)	2.2 (4.4)		50	795.72	895.05	806.14	807.44
50	8.0 (1.6)	0.5 (21.2)	2.2 (4.1)	2.2 (4.2)	70%	20	841.74	895.77	798.44	796.15
20	0.1 (80.4)	0.7 (11.4)	0.7 (11.5)	0.7 (12.7)		30	830.45	902.48	807.37	806.61
30	0.1 (87.8)	0.6 (16.2)	0.5 (21.3)	0.5 (21.0)		40	842.70	907.65	832.67	835.89
40	0.0 (90.2)	0.6 (18.2)	0.3 (37.1)	0.3 (36.4)		50	846.83	1018.97 \uparrow	864.58	869.15
50	0.0 (92.2)	0.6 (20.8)	0.3 (48.9)	0.3 (49.1)	80%	20	904.39	926.72	842.24	841.84
20	0.0 (93.0)	0.5 (22.8)	0.2 (58.4)	0.2 (58.4)		30	887.63	938.92	879.30	883.57
30						40	942.44	2634.69	935.09	939.77
40						50	952.45	2730.30 \uparrow	974.01	973.75

Table 7.6: Mean values of the factored component \mathbf{W} in the last 20 iterations, where the value in the (parentheses) is the sparsity evaluated by taking the percentage of values smaller than 0.1, for GDSC IC_{50} (upper table) and Gene Body Methylation (lower table). The **inconsistency** of GEE and GL_1^2 for different matrices can be observed.

Table 7.7: Mean squared error measure when the percentage of unobserved data is 60% (upper table), 70% (middle table), or 80% (lower table) for the GDSC IC_{50} data set. The performance of the GL_2^2 and $GL_{2,\infty}^2$ models is only slightly worse when we increase the fraction of unobserved from 60% to 80%; while the performance of GL_1^2 becomes extremely poor. Similar observations occur in the Gene Body Methylation experiment. The symbol \uparrow means the performance becomes extremely worse.

predictive performance when the sparsity of the data increases to see whether the models overfit or not. For different fractions of unobserved data, we randomly split the data based on that fraction, train the model on the observed data, and measure the performance on the held-out test data. Again, we increase the latent dimension K from $K = 20$ to $K = 30, 40, 50$ for all models. The average MSE of ten repeats is given in Figure 7.13. We still observe the **inconsistency** issue in the GL_1^2 model, its predictive performance is as good as that of the introduced GL_2^2 and $GL_{2,\infty}^2$ models on the Gene Body Methylation data set; while the predictive results of the GL_1^2 model are extremely poor on the GDSC IC_{50} data set.

For the GDSC IC_{50} data set, the GL_2^2 and $GL_{2,\infty}^2$ models perform best when the latent dimensions are $K = 20, 30, 40$; when $K = 50$ and the fraction of unobserved data increases, the GEE model is slightly better. As aforementioned, the GL_1^2 performs the worst on this data set; and when the fraction of unobserved data increases or K increases, the predictive results of GL_1^2 deteriorate quickly.

For the Gene Body Methylation data set, the predictive performance of GL_1^2 , GL_2^2 , and $GL_{2,\infty}^2$ models are close (GL_1^2 has a slightly larger error). The GEE model performs the worst on this data set.

The comparison of the results on the two sets shows the GL_2^2 and $GL_{2,\infty}^2$ models have both better in-sample and out-of-sample performance, making them a more robust choice in predicting missing entries.

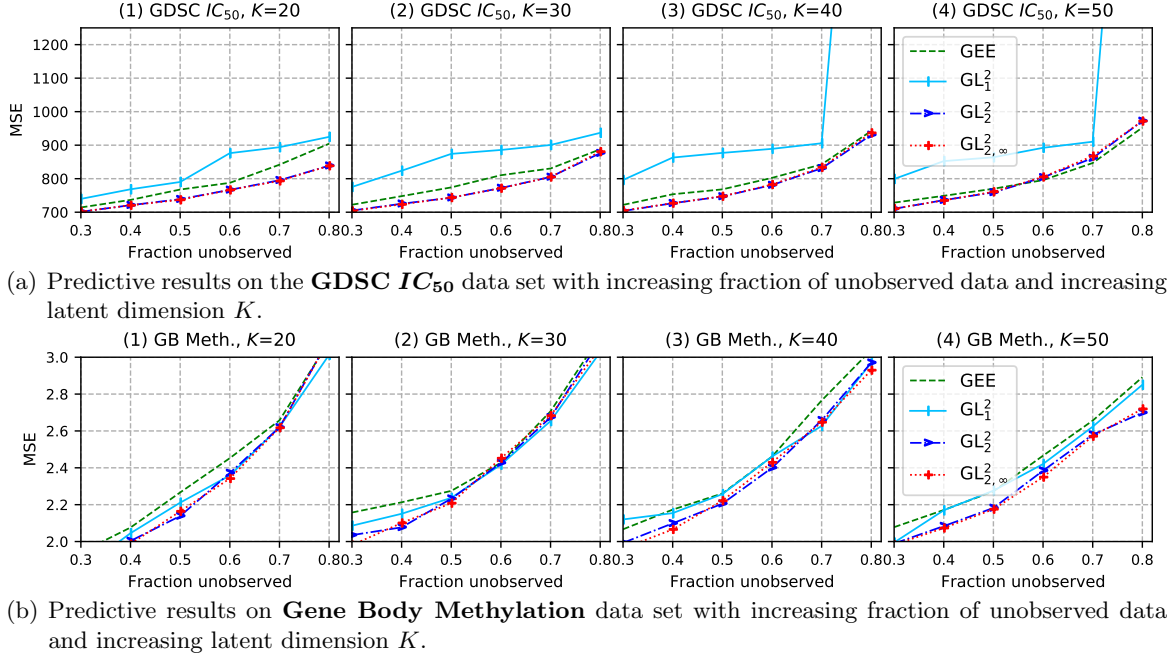


Figure 7.13: Predictive results on the **GDSC IC_{50}** (upper) and **Gene Body Methylation** (lower) data sets. We measure the predictive performance (mean squared error) on a held-out data set for different fractions of unobserved data.

Table 7.7 shows MSE predictions of different models when the fractions of unobserved data are 60%, 70%, and 80%, respectively. We observe that the performance of the GL_2^2 and $GL_{2,\infty}^2$ models are only slightly worse when we increase the fraction of unobserved from 60% to 80%. This, again, indicates that the GL_2^2 and $GL_{2,\infty}^2$ models are more robust with less overfitting. While for the GL_1^2 model, the performance becomes extremely poor in this scenario.

Noise sensitivity. Finally, we measure the noise sensitivity of different models with predictive performance when the data sets are noisy. To see this, we add different levels of Gaussian noise to the data. We add levels of $\{0\%, 10\%, 20\%, 50\%, 100\%\}$ noise-to-signal ratio noise (which is the ratio of the variance of the added Gaussian noise to the variance of the data). The results for the GDSC IC_{50} with $K = 10$ are shown in Figure 7.14. The results are the average performance over 10 repeats. We observe that the GL_2^2 and $GL_{2,\infty}^2$ models perform slightly better than other Bayesian NMF models (with implicit regularization meaning). The GL_2^2 and $GL_{2,\infty}^2$ models perform notably better when the noise-to-signal ratio is smaller than 10% and slightly better when the ratio is larger than 20%. Similar results can be found on the Gene Body Methylation data set and other K values, and we shall not repeat the details.

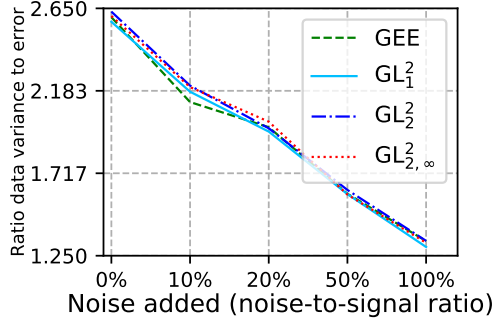


Figure 7.14: Ratio of the variance of data to the MSE of the predictions, the higher the better.

7.10. Semi-Nonnegative Matrix Factorization

Instead of forcing nonnegativity constraints on both factored matrices, an alternative approach, as suggested by Ding et al. (2008) and Fei et al. (2008), involves applying this constraint to only one of them. Through the Bayesian framework, we can place a real-valued prior over one component, and a nonnegative prior over the other. As previously discussed, NMF is well-suited for nonnegative data sets, such as those derived from images and texts. Nevertheless, the main advantage of the semi-nonnegative matrix factorization (semi-NMF) is that it allows us to handle real-valued data sets while still maintaining some nonnegative constraints, allowing more flexibility in capturing the underlying structure of the data.

7.10.1 Gaussian Likelihood with Exponential and Gaussian Priors (GEG)

The Gaussian likelihood with exponential and Gaussian priors (GEG) model places an exponential prior over the component \mathbf{W} and a Gaussian prior over the component \mathbf{Z} as those were done in GEE and GGG models, respectively (Section 7.2 and Section 6.2, p. 141). The likelihood is chosen to be the same as that in the GEE model (Equation (7.2)). The graphical representation of GEG model is shown in Figure 7.15(a).

Prior. We assume \mathbf{W} is independently exponentially distributed with scales λ_{mk}^W , and \mathbf{Z} is Gaussian distributed with precisions λ_{kn}^Z ,

$$\begin{aligned}
 w_{mk} &\sim \mathcal{E}(w_{mk} \mid \lambda_{mk}^W), & z_{kn} &\sim \mathcal{N}(z_{kn} \mid 0, (\lambda_{kn}^Z)^{-1}); \\
 p(\mathbf{W}) &= \prod_{m,k=1}^{M,K} \mathcal{E}(w_{mk} \mid \lambda_{mk}^W), & p(\mathbf{Z}) &= \prod_{k,n=1}^{K,N} \mathcal{N}(z_{kn} \mid 0, (\lambda_{kn}^Z)^{-1}),
 \end{aligned} \tag{7.30}$$

where $\mathcal{E}(x \mid \lambda) = \lambda \exp(-\lambda x)u(x)$ is the exponential density with $u(x)$ being the unit step function. The prior for the noise variance σ^2 is again chosen as an inverse-Gamma density with shape α_σ and scale β_σ (Equation (7.4)). The conditional posterior densities for w_{mk} 's and z_{kn} 's are already provided in the GEE and GGG models, respectively.

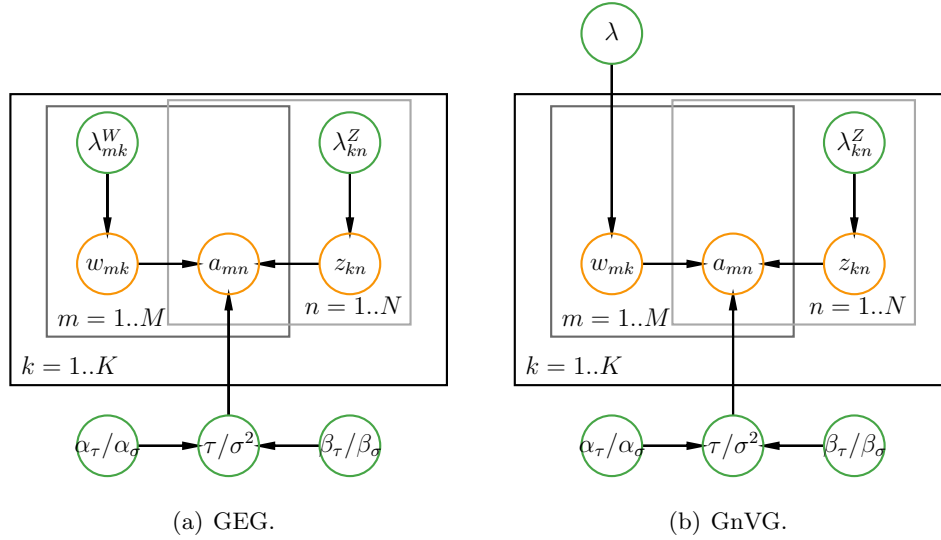


Figure 7.15: Graphical model representation of GEG and GnVG models. Green circles denote prior variables, orange circles represent observed and latent variables, and plates represent repeated variables. The slash “/” in the variable represents “or.”

7.10.2 Gaussian Likelihood with Nonnegative Volume and Gaussian Priors (GnVG)

The volume prior discussed in the GVG model (Section 6.5, p. 153) can be formulated to be nonnegative so as to enforce nonnegativity (Figure 7.15(b)).

Prior. Same as the GGG and GEG models, we place a Gaussian density with precision λ_{kn}^Z over \mathbf{Z} :

$$z_{kn} \sim \mathcal{N}(z_{kn} \mid 0, (\lambda_{kn}^Z)^{-1});$$

$$p(\mathbf{Z}) = \prod_{k,n=1}^{K,N} \mathcal{N}(z_{kn} \mid 0, (\lambda_{kn}^Z)^{-1}). \quad (7.31)$$

The nonnegative volume prior is constructed as follows:

$$\mathbf{W} \sim \begin{cases} \exp\{-\gamma \det(\mathbf{W}^\top \mathbf{W})\}, & \text{if } w_{mk} \geq 0 \text{ for all } m, k; \\ 0, & \text{if any } w_{mk} < 0. \end{cases} \quad (7.32)$$

The posterior density for z_{kn} is the same as those in the GEG and GGG models. And the posterior density for w_{mk} is similar to that of the GVG model; in this case, we draw the samples from a truncated-normal rather than a normal density.

7.11. Nonnegative Matrix Tri-Factorization (NMTF)

Similar to the *bilinear* nonnegative matrix factorization, in which case we reduce the observed matrix into a product of two factor matrices, the nonnegative matrix tri-factorization (NMTF) extends the components into three, i.e., we factor the data matrix \mathbf{A} into three matrices $\mathbf{A} = \mathbf{W}\mathbf{F}\mathbf{Z} + \mathbf{E}$, where $\mathbf{W} \in \mathbb{R}_+^{M \times K}$, $\mathbf{F} \in \mathbb{R}_+^{K \times L}$, and $\mathbf{Z} \in \mathbb{R}_+^{L \times N}$.

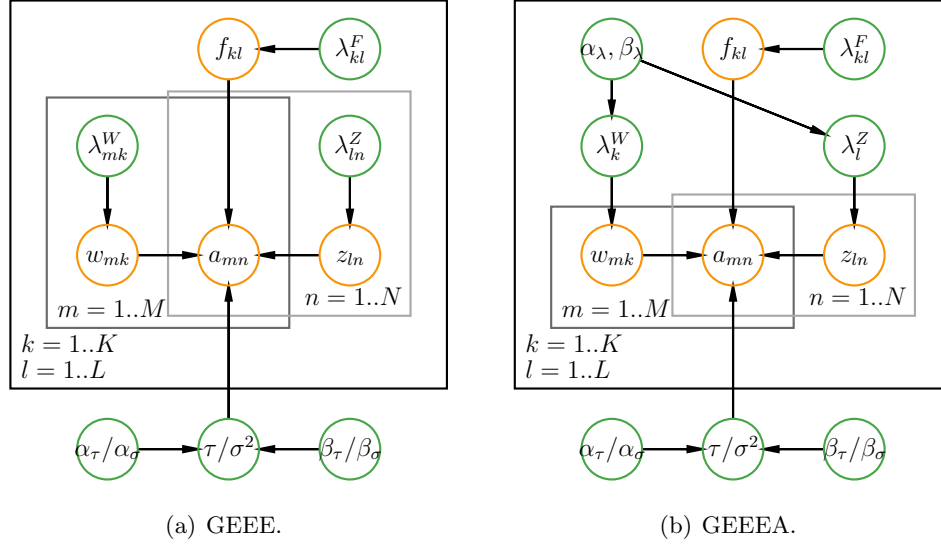


Figure 7.16: Graphical model representation of GEEE and GEEEA models. Green circles denote prior variables, orange circles represent observed and latent variables, and plates represent repeated variables. The slash “/” in the variable represents “or,” and the comma “,” in the variable represents “and.”

Likelihood. We again assume the residuals, e_{mn} , are i.i.d. zero-mean normal with variance σ^2 , which gives rise to the likelihood:

$$\begin{aligned}
 p(\mathbf{A} \mid \boldsymbol{\theta}) &= \prod_{m,n=1}^{M,N} \mathcal{N}(a_{mn} \mid \mathbf{w}_m^\top \mathbf{F} \mathbf{z}_n, \sigma^2) \\
 &= \prod_{m,n=1}^{M,N} \mathcal{N}(a_{mn} \mid \mathbf{w}_m^\top \mathbf{F} \mathbf{z}_n, \tau^{-1}),
 \end{aligned} \tag{7.33}$$

where $\boldsymbol{\theta} = \{\mathbf{W}, \mathbf{F}, \mathbf{Z}, \sigma^2\}$ denotes all parameters in the model, σ^2 is the variance, and $\tau^{-1} = \sigma^2$ is the precision. And now we want the reconstruction error measured by Frobenius norm to be minimized:

$$\min_{\mathbf{W}, \mathbf{Z}} L(\mathbf{W}, \mathbf{Z}) = \min_{\mathbf{W}, \mathbf{Z}} \sum_{n=1}^N \sum_{m=1}^M (a_{mn} - \mathbf{w}_m^\top \mathbf{F} \mathbf{z}_n)^2. \tag{7.34}$$

Prior. We assume \mathbf{W} and \mathbf{Z} are independently exponentially distributed with scales λ_{mk}^W and λ_{kn}^Z (Definition 3.3.1, p. 56):

$$\begin{aligned}
 w_{mk} &\sim \mathcal{E}(w_{mk} \mid \lambda_{mk}^W), & f_{kl} &\sim \mathcal{E}(f_{kl} \mid \lambda_{kl}^F), & z_{ln} &\sim \mathcal{E}(z_{ln} \mid \lambda_{ln}^Z); \\
 p(\mathbf{W}) &= \prod_{m,k=1}^{M,K} \mathcal{E}(w_{mk} \mid \lambda_{mk}^W), & p(\mathbf{F}) &= \prod_{k,l=1}^{K,L} \mathcal{E}(f_{kl} \mid \lambda_{kl}^F), & p(\mathbf{Z}) &= \prod_{l,n=1}^{L,N} \mathcal{E}(z_{ln} \mid \lambda_{ln}^Z),
 \end{aligned} \tag{7.35}$$

where $\mathcal{E}(x | \lambda) = \lambda \exp(-\lambda x)u(x)$ is the exponential density with $u(x)$ being the unit step function. Hence, we call this approach a *GEEE model*. See Figure 7.16(a).

The prior for the noise variance σ^2 is chosen as an inverse-Gamma density with shape α_σ and scale β_σ (Definition 3.2.4, p. 47):

$$p(\sigma^2) = \mathcal{G}^{-1}(\sigma^2 | \alpha_\sigma, \beta_\sigma) = \frac{\beta_\sigma^{\alpha_\sigma}}{\Gamma(\alpha_\sigma)} (\sigma^2)^{-\alpha_\sigma-1} \exp\left(-\frac{\beta_\sigma}{\sigma^2}\right). \quad (7.36)$$

Therefore, the posterior density of σ^2 is still from Equation (7.8).

Posterior. For NMF, following Bayes' rule and MCMC, this means we need to be able to draw from distributions (by Markov blanket, Section 6.2, p. 141):

$$\begin{aligned} & p(w_{mk} | \mathbf{A}, \mathbf{W}_{-mk}, \mathbf{F}, \mathbf{Z}, \sigma^2, \boldsymbol{\lambda}^W, \boldsymbol{\lambda}^F, \boldsymbol{\lambda}^Z), \\ & p(f_{kl} | \mathbf{A}, \mathbf{W}, \mathbf{F}_{-kl}, \mathbf{Z}, \sigma^2, \boldsymbol{\lambda}^W, \boldsymbol{\lambda}^F, \boldsymbol{\lambda}^Z), \\ & p(z_{ln} | \mathbf{A}, \mathbf{W}, \mathbf{F}, \mathbf{Z}_{-ln}, \sigma^2, \boldsymbol{\lambda}^W, \boldsymbol{\lambda}^F, \boldsymbol{\lambda}^Z), \\ & p(\sigma^2 | \mathbf{A}, \mathbf{W}, \mathbf{Z}, \alpha_\sigma, \beta_\sigma), \end{aligned}$$

where $\boldsymbol{\lambda}^W$ is an $M \times K$ matrix containing all $\{\lambda_{mk}^W\}$ entries, $\boldsymbol{\lambda}^Z$ is a $L \times N$ matrix including all $\{\lambda_{ln}^Z\}$ values, and \mathbf{W}_{-mk} denotes all elements of \mathbf{W} except w_{mk} . The conditional density of w_{mk} is just similar to that in the GEE model in Equation (7.5). For simplicity, we denote the k -th row of \mathbf{F} as \mathbf{r}_k , and l -th column of \mathbf{F} as \mathbf{c}_l . The conditional density of w_{mk} is the same as that in Equation (7.5), except now we replace z_{kj} with $\mathbf{r}_k^\top \mathbf{z}_j$ in the variance parameter of Equation (7.6), and replace z_{kj} with $\mathbf{r}_k^\top \mathbf{z}_j$ and replace z_{ij} with $\mathbf{r}_i^\top \mathbf{z}_j$ in Equation (7.7). The reason is obvious as, when considering the conditional density of w_{mk} , we can treat \mathbf{FZ} as a single matrix, and the problem becomes a bilinear decomposition. Similarly, the conditional posterior density of z_{ln} can be derived due to its symmetry to w_{mk} .

Using Bayes' theorem, the conditional density of f_{kl} depends on its parents (λ_{kl}^F), children (a_{mn}), and coparents (τ or σ^2 , $\mathbf{W}, \mathbf{F}_{kl}, \mathbf{Z}$)¹¹. And it can be obtained by

$$\begin{aligned} & p(f_{kl} | \mathbf{A}, \mathbf{W}, \mathbf{F}_{-kl}, \mathbf{Z}, \sigma^2, \boldsymbol{\lambda}^W, \boldsymbol{\lambda}^Z, \boldsymbol{\lambda}^F, \mathbf{A}) = p(f_{kl} | \mathbf{A}, \mathbf{W}, \mathbf{F}_{-kl}, \mathbf{Z}, \sigma^2, \lambda_{kl}^F) \\ & \propto p(\mathbf{A} | \mathbf{W}, \mathbf{F}, \mathbf{Z}, \sigma^2) \times p(f_{kl} | \lambda_{kl}^F) = \prod_{i,j=1}^{M,N} \mathcal{N}(a_{ij} | \mathbf{w}_i^\top \mathbf{F} \mathbf{z}_j, \sigma^2) \times \mathcal{E}(w_{kl} | \lambda_{kl}^F) \\ & \propto \exp\left\{-\frac{1}{2\sigma^2} \sum_{i,j=1}^{M,N} (a_{ij} - \mathbf{w}_i^\top \mathbf{F} \mathbf{z}_j)^2\right\} \times \cancel{\lambda_{kl}^F} \exp(-\lambda_{kl}^F \cdot f_{kl}) u(f_{kl}) \\ & \propto \exp\left\{-\frac{1}{2\sigma^2} \sum_{i,j=1}^{M,N} \left(-2a_{ij}(\mathbf{w}_i^\top \mathbf{F} \mathbf{z}_j) + (\mathbf{w}_i^\top \mathbf{F} \mathbf{z}_j)^2\right)\right\} \cdot \exp(-\lambda_{kl}^F \cdot f_{kl}) u(f_{kl}). \end{aligned} \quad (7.37)$$

To express the conditional density of $\{f_{kl} | \mathbf{A}, \mathbf{W}, \mathbf{F}_{-kl}, \mathbf{Z}, \sigma^2, \lambda_{kl}^F\}$ in terms of f_{kl} , we write out $\mathbf{w}_i^\top \mathbf{F} \mathbf{z}_j$ in the above equation as

$$\mathbf{w}_i^\top \mathbf{F} \mathbf{z}_j = \sum_{s,t=1}^{K,L} w_{is} f_{st} z_{tj} = f_{kl} (w_{ik} z_{lj}) + C,$$

11. See Figure 7.16(a) and Section 6.2 (p. 141).

where

$$C = \sum_{(s,t) \neq (k,l)}^{K,L} w_{is} f_{st} z_{tj}$$

is a constant when considering f_{kl} . Therefore, Equation (7.37) can be expressed as, by excluding terms non-relevant to f_{kl} ,

$$\begin{aligned} & p(f_{kl} \mid \mathbf{A}, \mathbf{W}, \mathbf{F}_{-kl}, \mathbf{Z}, \sigma^2, \lambda_{kl}^F) \\ & \propto \exp \left\{ - \underbrace{\frac{\sum_{i,j=1}^{M,N} (w_{ik} z_{lj})^2}{2\sigma^2}}_{1/(2\widetilde{\sigma}_{kl}^2)} f_{kl}^2 + f_{kl} \underbrace{\left[-\lambda_{kl}^F + \sum_{i,j=1}^{M,N} (w_{ik} z_{lj}) \left(\frac{a_{ij} - C}{\sigma^2} \right) \right]}_{\widetilde{\sigma}_{kl}^{-2} \widetilde{\mu}_{kl}} \right\} \cdot u(f_{kl}) \quad (7.38) \\ & \propto \mathcal{N}(f_{kl} \mid \widetilde{\mu}_{kl}, \widetilde{\sigma}_{kl}^2) \cdot u(w_{kl}) = \mathcal{TN}(f_{kl} \mid \widetilde{\mu}_{kl}, \widetilde{\sigma}_{kl}^2), \end{aligned}$$

where $u(x)$ is the unit function with a value 1 if $x \geq 0$ and 0 if $x < 0$,

$$\widetilde{\sigma}_{kl}^2 = \frac{\sigma^2}{\sum_{i,j=1}^{M,N} (w_{ik} z_{lj})^2} \quad (7.39)$$

is the “parent” posterior variance of the normal distribution with posterior “parent” mean $\widetilde{\mu}_{kl}$,

$$\widetilde{\mu}_{kl} = \left[-\lambda_{kl}^F + \sum_{i,j=1}^{M,N} (w_{ik} z_{lj}) \left(\frac{a_{ij} - C}{\sigma^2} \right) \right] \cdot \widetilde{\sigma}_{kl}^2, \quad (7.40)$$

and $\mathcal{TN}(x \mid \mu, \sigma^2)$ is the truncated-normal density with “parent” mean μ and “parent” variance σ^2 (Definition 3.4.1, p. 57).

Sparsity. Similar to the GEE model on the factored component w_{mk} , the posterior parameters have a similar sparsity constraint on the component f_{kl} . The sparsity comes from the negative term $-\lambda_{kl}^F$ in Equation (7.40). When λ_{kl}^F becomes larger, the posterior “parent” mean becomes smaller, and the TN distribution will have a larger probability for smaller values (or even approaching zero) since the draws of $\mathcal{TN}(f_{kl} \mid \widetilde{\mu}_{kl}, \widetilde{\sigma}_{kl}^2)$ will be around zero, thus imposing sparsity (see Figure 3.8(a), p. 59).

Gibbs sampling. Once again, by this Gibbs sampling method introduced in Section 2.3.3 (p. 26), we can construct a Gibbs sampler for the GEEE model as formulated in Algorithm 18. And also in practice, all the parameters of the exponential distribution are set to be the same value $\lambda = \{\lambda_{mk}^W\}'s = \{\lambda_{kl}^F\}'s = \{\lambda_{ln}^Z\}'s$ for all m, k, l, n . By default, uninformative hyper-parameters are $\alpha_\sigma = \beta_\sigma = 1$, $\{\lambda_{mk}^W\} = \{\lambda_{kl}^F\} = \{\lambda_{ln}^Z\} = 0.1$.

Automatic relevance determination. Similar to the GEEA model (Section 7.3), we can use ARD to share the scale parameter of exponential priors for each row of \mathbf{W} and each

Algorithm 18 Gibbs sampler for GEEE Model in one iteration (prior on variance σ^2 here, similarly for the precision τ). The procedure presented here may not be efficient but is explanatory. A more efficient one can be implemented in a vectorized manner. By default, uninformative hyper-parameters are $\alpha_\sigma = \beta_\sigma = 1$, $\{\lambda_{mk}^W\} = \{\lambda_{kl}^F\} = \{\lambda_{ln}^Z\} = 0.1$.

Require: Choose initial $\alpha_\sigma, \beta_\sigma, \lambda_{mk}^W, \lambda_{kl}^F, \lambda_{ln}^Z$:

- 1: **for** $k = 1$ to K **do**
- 2: **for** $m = 1$ to M **do**
- 3: Sample w_{mk} from $p(w_{mk} \mid \mathbf{A}, \mathbf{W}_{-mk}, \mathbf{F}, \mathbf{Z}, \sigma^2, \lambda_{mk}^W)$; \triangleright Equation (7.5)
- 4: **end for**
- 5: **for** $l = 1$ to L **do**
- 6: Sample f_{kl} from $p(f_{kl} \mid \mathbf{A}, \mathbf{W}, \mathbf{F}_{-kl}, \mathbf{Z}, \sigma^2, \lambda_{kl}^F)$; \triangleright Equation (7.38)
- 7: **end for**
- 8: **end for**
- 9: **for** $l = 1$ to L **do**
- 10: **for** $n = 1$ to N **do**
- 11: Sample z_{ln} from $p(z_{ln} \mid \mathbf{A}, \mathbf{W}, \mathbf{F}, \mathbf{Z}_{-ln}, \sigma^2, \lambda_{ln}^Z)$; \triangleright Symmetry of Equation (7.5)
- 12: **end for**
- 13: **end for**
- 14: Sample σ^2 from $p(\sigma^2 \mid \mathbf{A}, \mathbf{W}, \mathbf{Z}, \alpha_\sigma, \beta_\sigma)$; \triangleright Equation (7.8)
- 15: Report loss in Equation (7.34), stop if it converges.

column of \mathbf{Z} so as to perform automatic model selection. The graphical representation is shown in Figure 7.16(b):

$$\begin{aligned} w_{mk} &\sim \mathcal{E}(w_{mk} \mid \lambda_k^W), & z_{ln} &\sim \mathcal{E}(z_{ln} \mid \lambda_l^Z), \\ \lambda_k^W &\sim \mathcal{G}(\lambda_k^W \mid \alpha_\lambda, \beta_\lambda), & \lambda_l^Z &\sim \mathcal{G}(\lambda_l^Z \mid \alpha_\lambda, \beta_\lambda). \end{aligned}$$

In this case, there is no parameter sharing among the entries of \mathbf{F} . For brevity, we do not go into the details of this model here.

Chapter 7 Problems

1. Following the derivation in Equation (7.5), derive the conditional distribution over the user feature z_{kn} for all $k \in \{1, 2, \dots, K\}$ and $n \in \{1, 2, \dots, N\}$ for the GEE model. Similarly, following the derivation in Equation (7.11), obtain the conditional distribution over the user feature z_{kn} for all $k \in \{1, 2, \dots, K\}$ and $n \in \{1, 2, \dots, N\}$ within the context of the GTT model.
2. Following the derivation of nonnegative matrix tri-factorization in Section 7.11, find a way of real-valued matrix tri-factorization, in which case, we factor the data matrix \mathbf{A} into three matrices $\mathbf{A} = \mathbf{W}\mathbf{F}\mathbf{Z} + \mathbf{E}$, where $\mathbf{W} \in \mathbb{R}^{M \times K}$, $\mathbf{F} \in \mathbb{R}^{K \times L}$, and $\mathbf{Z} \in \mathbb{R}^{L \times N}$.

Bayesian Poisson Matrix Factorization

Contents

8.1	Poisson Likelihood with Gamma Priors (PAA)	197
8.2	Poisson Likelihood with Gamma Priors and Hierarchical Gamma Priors (PAAA)	199
8.3	Properties of PAA or PAAA	200
8.4	Recommendation Systems	202
	Chapter 8 Problems	203

8.1. Poisson Likelihood with Gamma Priors (PAA)



The Poisson likelihood with Gamma priors (PAA) model is proposed by Gopalan et al. (2013, 2015) in the context of recommendation systems, specifically addressing the challenges posed by nonnegative count data, such as those prevalent in movie recommendation datasets like the Netflix Prize challenge. The PAA model extends the Poisson factorization (Canny, 2004; Dunson and Herring, 2005; Cemgil, 2009) and has been further discussed in Gopalan et al. (2014); Hu et al. (2015). The model is working on nonnegative count data, $\mathbf{A} \in \mathbb{N}^{M \times N}$, e.g., a data matrix about users and items¹, where each user has consumed and possibly rated a set of items. The observation a_{mn} is the rating that user n gave to item m , or zero if no rating was given. We again assume the matrix is factored as the product of $\mathbf{W} \in \mathbb{R}_+^{M \times K}$ and $\mathbf{Z} \in \mathbb{R}_+^{K \times N}$.

To be more specific, the PAA model considers to minimize the following loss:

$$\min_{\mathbf{W}, \mathbf{Z}} L(\mathbf{W}, \mathbf{Z}) = \min_{\mathbf{W}, \mathbf{Z}} \sum_{n=1}^N \sum_{m=1}^M \left(a_{mn} - \mathbf{w}_m^\top \mathbf{z}_n \right)^2, \quad (8.1)$$

where $\mathbf{W} = [\mathbf{w}_1^\top; \mathbf{w}_2^\top; \dots; \mathbf{w}_M^\top] \in \mathbb{R}^{M \times K}$ and $\mathbf{Z} = [\mathbf{z}_1, \mathbf{z}_2, \dots, \mathbf{z}_N] \in \mathbb{R}^{K \times N}$ containing \mathbf{w}_m 's and \mathbf{z}_n 's as **rows and columns**, respectively. Therefore, each item m is represented by a vector of K *latent attributes* \mathbf{w}_m and each user n by a vector of K *latent preferences* \mathbf{z}_n . In the Netflix context, the PAA model is specifically designed to accommodate the *heterogeneous interests of users* (some users tend to consume more than others), the different types of items (some items/movies are more popular than others), and the realistic distribution of limited resources that users have to consume these items as the recommendation system literature suggests that an effective model should consider the *heterogeneity* among both users and items (Koren et al., 2009).

Likelihood. Given a data matrix \mathbf{A} about users and items, where each user has consumed and possibly rated a set of items. We assume each element a_{mn} is Poisson distributed with a mean given by the factored component $\mathbf{w}_m^\top \mathbf{z}_n$ (see Figure 8.1(a)):

$$a_{mn} \sim \mathcal{P}(\mathbf{w}_m^\top \mathbf{z}_n),$$

where $\mathcal{P}(\cdot)$ is a Poisson distribution with its parameter being a linear combination of the corresponding user preferences and item attributes, denoted as $\mathbf{w}_m^\top \mathbf{z}_n$. This is just like the Gaussian likelihood, where the expectation of a_{mn} is also given by $\mathbf{w}_m^\top \mathbf{z}_n$ (Definition 3.6.1, p. 72). Suppose further we decompose a_{mn} by K components,

$$a_{mn} = \sum_{k=1}^K o_{mnk}.$$

The prior over a_{mn} then can be decomposed into

$$o_{mnk} \sim \mathcal{P}(w_{mk} z_{kn}).$$

1. The items can be any of movies, songs, articles, or products. We also refer to movies in the Netflix context.

Since, by Theorem 3.4 (p. 73), the sum of Poisson random variables is itself a Poisson random variable, we obtain the presumed Poisson likelihood by

$$a_{mn} = \sum_{k=1}^K o_{mnk} \sim \mathcal{P}(\mathbf{w}_m^\top \mathbf{z}_n). \quad (8.2)$$

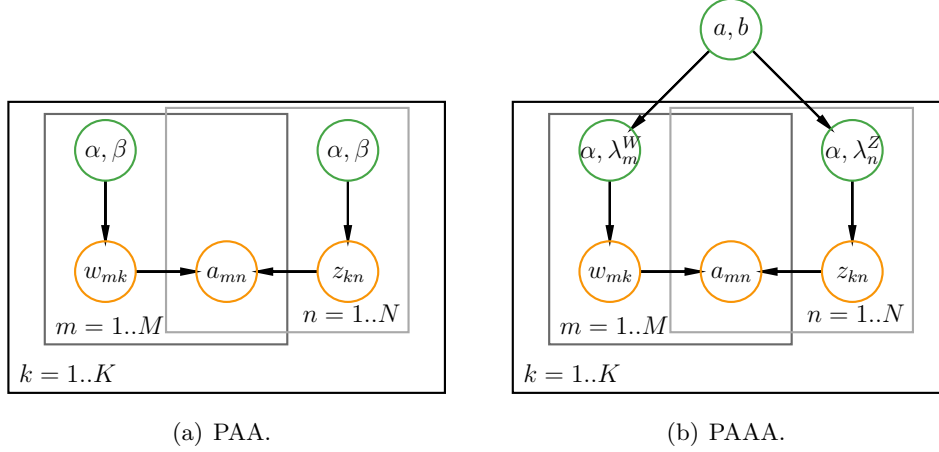


Figure 8.1: Graphical model representations of PAA and PAAA models. Green circles denote prior variables, orange circles represent observed and latent variables, and plates represent repeated variables.

Prior. We assume \mathbf{W} and \mathbf{Z} are independently Gamma distributed with shape and rate parameters α and β , respectively (Definition 3.2.3, p. 43):

$$w_{mk} \sim \mathcal{G}(w_{mk} \mid \alpha, \beta), \quad z_{kn} \sim \mathcal{G}(z_{kn} \mid \alpha, \beta). \quad (8.3)$$

This Gamma prior on the latent attributes and the latent preferences can drive the model towards a **sparse representation** of users and items (see Figure 3.3(a), p. 44 for examples of the Gamma distribution), which is more representative of real-world behavior.

Posterior. Let $\mathbf{o}^{mn} = [o_{mn1}, o_{mn2}, \dots, o_{mnK}]^\top \in \mathbb{R}^K$, by Theorem 3.5 (p. 73), the conditional distribution of \mathbf{o}^{mn} , given $a_{mn} = \sum_{k=1}^K o_{mnk}$, is

$$\text{Multi}_K(\mathbf{o}^{mn} \mid a_{mn}, \mathbf{p}), \quad (8.4)$$

where $\mathbf{p} = \frac{1}{\mathbf{w}_m^\top \mathbf{z}_n} [w_{m1}z_{1n}, w_{m2}z_{2n}, \dots, w_{mK}z_{Kn}]^\top \in [0, 1]^K$ such that $\mathbf{1}^\top \mathbf{p} = 1$, and each element p_i in \mathbf{p} is in the range of $[0, 1]$.

The conditional posterior of w_{mk} is again from Bayes's rule:

$$\begin{aligned} p(w_{mk} \mid \mathbf{A}, \mathbf{W}_{-mk}, \mathbf{Z}, \alpha, \beta) &\propto \prod_{j=1}^N \mathcal{P}(o_{mj k} \mid w_{mk} z_{kj}) \cdot \mathcal{G}(w_{mk} \mid \alpha, \beta) \\ &\propto w_{mk}^{(\sum_{j=1}^N o_{mj k})} \exp \left\{ -w_{mk} \left(\sum_{j=1}^N z_{kj} \right) \right\} \cdot w_{mk}^{\alpha-1} \exp(-\beta w_{mk}) \\ &\propto \mathcal{G}(w_{mk} \mid \tilde{\alpha}, \tilde{\beta}), \end{aligned} \quad (8.5)$$

where

$$\tilde{\alpha} = \alpha + \sum_{j=1}^N o_{mjk}, \quad \tilde{\beta} = \beta + \sum_{j=1}^N z_{kj}.$$

According to the definition of the Gamma distribution (Definition 3.2.3, p. 43), the posterior mean of w_{mk} is given by

$$\mathbb{E}[w_{mk} \mid \mathbf{A}, \mathbf{W}_{-mk}, \mathbf{Z}, \alpha, \beta] = \frac{\alpha + \sum_{j=1}^N o_{mjk}}{\beta + \sum_{j=1}^N z_{kj}}.$$

This is reasonable in the sense that when $\sum_{j=1}^N o_{mjk}$ is large, we are dealing with a large value of a_{mn} , thus favoring a large value of w_{mk} . Conversely, when the value of $\sum_{j=1}^N z_{kj}$ is large from the last iteration of the Gibbs sampling procedure, we expect a small value of w_{mk} to compensate for this. By symmetry, a similar conditional density for z_{kn} can be derived.

Algorithm 19 Gibbs sampler for PAA model in one iteration. By default, uninformative hyper-parameters are $\alpha = \beta = 1$.

Require: Choose initial α, β ;

```

1: for  $m = 1$  to  $M$  do
2:   for  $n = 1$  to  $N$  do
3:     Sample  $\mathbf{o}^{mn}$  from  $p(\mathbf{o}^{mn} \mid a_{mn}, \mathbf{p})$ ; ▷ Equation (8.4)
4:   end for
5: end for
6: for  $k = 1$  to  $K$  do
7:   for  $m = 1$  to  $M$  do
8:     Sample  $w_{mk}$  from  $p(w_{mk} \mid \mathbf{A}, \mathbf{W}_{-mk}, \mathbf{Z}, \alpha, \beta)$ ; ▷ Equation (8.5)
9:   end for
10:  for  $n = 1$  to  $N$  do
11:    Sample  $z_{kn}$  from  $p(z_{kn} \mid \mathbf{A}, \mathbf{W}, \mathbf{Z}_{-kn}, \alpha, \beta)$ ; ▷ Symmetry of Eq. (8.5)
12:  end for
13: end for

```

Gibbs sampling. By this Gibbs sampling method introduced in Section 2.3.3 (p. 26), we can construct a Gibbs sampler for the PAA model as formulated in Algorithm 19. In practice, the initial hyper-parameters can be set to a weak prior with $\alpha = \beta = 1$.

8.2. Poisson Likelihood with Gamma Priors and Hierarchical Gamma Priors (PAAA)

Extending the PAA model, the Poisson likelihood with Gamma priors and hierarchical Gamma priors (PAAA) model is introduced in Gopalan et al. (2015).

Prior. Going further from the PAA model, we put a hierarchical Gamma prior over the Gamma parameter:

$$\begin{aligned} a_{mn} &\sim \mathcal{P}(a_{mn} \mid \mathbf{w}_m^\top \mathbf{z}_n), \\ w_{mk} &\sim \mathcal{G}(w_{mk} \mid \alpha, \lambda_m^W), & z_{kn} &\sim \mathcal{G}(z_{kn} \mid \alpha, \lambda_n^Z), \\ \lambda_m^W &\sim \mathcal{G}(a, \frac{a}{b}), & \lambda_n^Z &\sim \mathcal{G}(a, \frac{a}{b}). \end{aligned} \quad (8.6)$$

The hierarchical structure allows us to capture the *diversity of users*, i.e., some users tend to consume more than others; and the *diversity of items*, i.e., some items are more popular than others.

Posterior. The conditional posteriors for w_{mk} , z_{kn} , and \mathbf{o}^{mn} are identical to those in the PAA model except we replace β with λ_m^W in the expression for $\tilde{\beta}$. For the conditional posterior of λ_m^W , the hierarchical part, we again follow Bayes' rule,

$$\begin{aligned} p(\lambda_m^W \mid \mathbf{W}, \alpha, a, b) &\propto \prod_{k=1}^K \mathcal{G}(w_{mk} \mid \alpha, \lambda_m^W) \cdot \mathcal{G}(\lambda_m^W \mid a, \frac{a}{b}) \\ &\propto \prod_{k=1}^K \frac{(\lambda_m^W)^\alpha}{\Gamma(\alpha)} w_{mk}^{\alpha-1} \exp(-\lambda_m^W w_{mk}) \cdot \frac{(\frac{a}{b})^a}{\Gamma(a)} (\lambda_m^W)^{a-1} \exp(-\frac{a}{b} \lambda_m^W) \\ &\propto (\lambda_m^W)^{K\alpha+a-1} \exp\left\{-\lambda_m^W \left(\frac{a}{b} + \sum_{k=1}^K w_{mk}\right)\right\} \\ &\propto \mathcal{G}(\lambda_m^W \mid \tilde{a}_m, \tilde{b}_m), \end{aligned} \quad (8.7)$$

where

$$\tilde{a}_m = K\alpha + a, \quad \tilde{b}_m = \frac{a}{b} + \sum_{k=1}^K w_{mk}.$$

Gibbs sampling. We can construct a Gibbs sampler for the PAA model as formulated in Algorithm 20. In practice, the initial parameters can be set to a weak prior with $\alpha = a = b = 1$.

8.3. Properties of PAA or PAAA

After introducing the modeling details, we outline some statistical features of the PAA or PAAA approaches. These characteristics offer benefits over the Gaussian likelihood matrix factorization methods we have discussed in previous chapters when considering the Netflix context.

PAA or PAAA captures sparse factors. As mentioned previously, the Gamma priors on the factored components, i.e., on the user preferences and item attributes, can encourage sparse representations of users and items. A small shape parameter in the Gamma prior results in most weights being close to zero, leaving only a few large ones (see Figure 8.2 for examples of the Gamma distribution $\mathcal{G}(\alpha, \beta)$ where we reduce the shape parameter α from 3 to 1, given $\beta = 1$. The density drives to zero.). This leads to a simpler and more easily interpretable model.

Algorithm 20 Gibbs sampler for PAAA model in one iteration. By default, uninformative hyper-parameters are $\alpha = a = b = 1$.

Require: Choose initial α, a, b ;

```

1: for  $m = 1$  to  $M$  do
2:   for  $n = 1$  to  $N$  do
3:     Sample  $\sigma^{mn}$  from  $p(\sigma^{mn} \mid a_{mn}, \mathbf{p})$ ; ▷ Equation (8.4)
4:   end for
5: end for
6: for  $k = 1$  to  $K$  do
7:   for  $m = 1$  to  $M$  do
8:     Sample  $w_{mk}$  from  $p(w_{mk} \mid \mathbf{A}, \mathbf{W}_{-mk}, \mathbf{Z}, \alpha, \lambda_m^W)$ ; ▷ Eq. (8.5), replace  $\beta$  by  $\lambda_m^W$ 
9:     Sample  $\lambda_m^W$  from  $p(\lambda_m^W \mid \mathbf{W}, \alpha, a, b)$ ; ▷ Equation (8.7)
10:  end for
11:  for  $n = 1$  to  $N$  do
12:    Sample  $z_{kn}$  from  $p(z_{kn} \mid \mathbf{A}, \mathbf{W}, \mathbf{Z}_{-kn}, \alpha, \lambda_n^Z)$ ; ▷ Eq. (8.5), replace  $\beta$  by  $\lambda_n^Z$ 
13:    Sample  $\lambda_n^Z$  from  $p(\lambda_n^Z \mid \mathbf{Z}, \alpha, a, b)$ ; ▷ Symmetry of Eq. (8.7)
14:  end for
15: end for

```

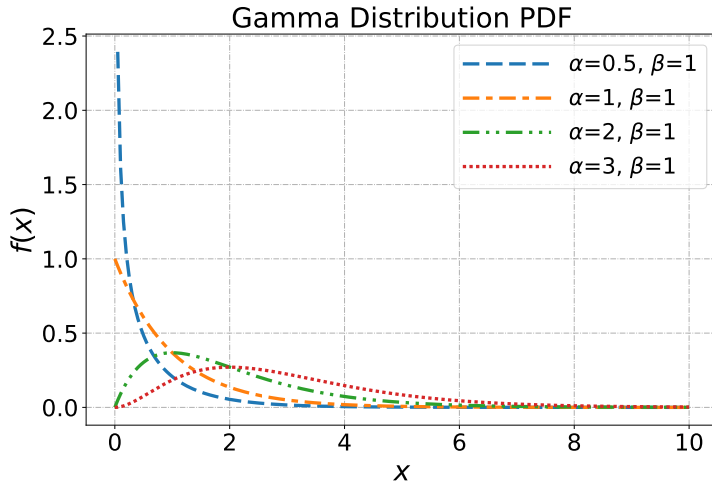


Figure 8.2: Gamma probability density functions $\mathcal{G}(\alpha, \beta)$ by reducing the shape parameter α .

PAA or PAAA models the long-tail of users and items. In the “*implicit*” consumer data that we consider a_{mn} equals one if user n consumed item m and zero otherwise², the distribution of *user activity* (i.e., how many items a user consumed) and *item popularity* (i.e., how many users consumed an item) in real-world user behavior data is characterized by a long-tail distribution, where the majority of users consume only a few items, while a small number of “tail users” consume a large amount. To see this, we consider the “MovieLens 1M” data set (see Table 7.2, p. 173), which contains movie ratings for 6,040 movies from 3,503 users. Figure 8.3(a) shows that only a small portion of users have consumed more than 1,500 movies; and Figure 8.3(b) shows that only a small portion of items have been consumed by more than 500 users, indicating the long-tail behavior.

². In contrast, the “explicit” consumer data contains a matrix of integer ratings.

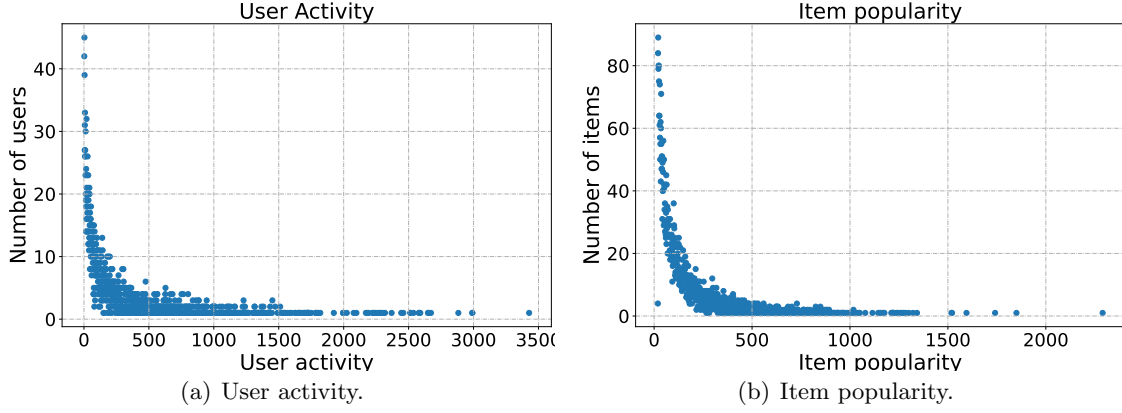


Figure 8.3: User activity and item popularity for the “MovieLens 1M” data set (see data description in Table 7.2, p. 173).

The PAA or PAAA model can capture this property easily via a two-stage process. From Equation (8.2), for each user n , again by Theorem 3.4 (p. 73) and Theorem 3.5 (p. 73), we have

$$u_n = \sum_{i=1}^M a_{in} \sim \mathcal{P} \left(\sum_{i=1}^M \mathbf{w}_i^\top \mathbf{z}_n \right),$$

$$[a_{1n}, a_{2n}, \dots, a_{Mn}]^\top \sim \text{Multi}_M(u_n, \mathbf{q}),$$

where $\mathbf{q} = \frac{1}{\sum_{i=1}^M \mathbf{w}_i^\top \mathbf{z}_n} [\mathbf{w}_1^\top \mathbf{z}_n, \mathbf{w}_2^\top \mathbf{z}_n, \dots, \mathbf{w}_M^\top \mathbf{z}_n]^\top \in [0, 1]^M$ such that $\mathbf{1}^\top \mathbf{q} = 1$. Therefore, the PAA or PAAA model first learns a *budget* u_n for each user n , and then learns how to distribute the budget across items. Learning this budget value is important for modeling the long-tail behavior of user activity.

Similar for each item m , we have

$$v_m = \sum_{i=1}^N a_{mi} \sim \mathcal{P} \left(\sum_{i=1}^N \mathbf{w}_m^\top \mathbf{z}_i \right),$$

$$[a_{m1}, a_{m2}, \dots, a_{mN}]^\top \sim \text{Multi}_N(v_m, \mathbf{s}),$$

where $\mathbf{s} = \frac{1}{\sum_{i=1}^N \mathbf{w}_m^\top \mathbf{z}_i} [\mathbf{w}_m^\top \mathbf{z}_1, \mathbf{w}_m^\top \mathbf{z}_2, \dots, \mathbf{w}_m^\top \mathbf{z}_N]^\top \in [0, 1]^N$ such that $\mathbf{1}^\top \mathbf{s} = 1$. The PAA or PAAA model finds the *popularity* of item m by v_m , and then learns how the popularity is distributed across users.

8.4. Recommendation Systems

In Section 4.10.2 (p. 122), we introduce two recommendation systems based on matrix factorization. We shortly discuss in the following two paragraphs, and we consider a new recommender via this Bayesian matrix factorization model.

Recommender 1. A recommender system can work simply by suggesting the unconsumed movie m when a_{mn} for user n by the posterior expected Poisson parameters:

$$\text{score}_{mn} = \mathbb{E}[\mathbf{w}_m^\top \mathbf{z}_n \mid \mathbf{A}]. \quad (8.8)$$

The score $\mathbb{E}[\mathbf{w}_m^\top \mathbf{z}_n \mid \mathbf{A}]$ can be obtained by averaging the values during the Gibbs sampling iterations.

Recommender 2. After obtaining the item attributes $\{\mathbf{w}_1, \mathbf{w}_2, \dots, \mathbf{w}_M\}$, we compare the similar matrix (with different measures, e.g., Pearson similarity or cosine similarity) of movies and suggest the movie with high similarity to the consumed item for each user n . The precision-recall curve can help find out a threshold to decide the final recommendation.

Recommender 3. In the movie recommendation case, the uncertainty about each entry in \mathbf{A} can be measured by its predictive standard deviation. A practical system can exploit this to only suggest items with a high confidence. Since we can also model uncertainty via the Bayesian approach. Absorbing the idea of the *Sharpe ratio* in quantitative finance. The Sharpe ratio is a measure of the risk-adjusted return of an investment, calculated as the ratio of its average return and its standard deviation. It measures the excess return per unit of risk, and is widely used in finance to evaluate the performance of an investment relative to its volatility. The higher the Sharpe ratio, the better the risk-adjusted return of the investment is considered to be. Embracing the concept of the Sharpe ratio, we can suggest the unconsumed item m when a_{mn} for user n by the *uncertainty-adjusted score* of posterior expected Poisson parameters:

$$\text{score}_{mn} = \frac{\mathbb{E}[\mathbf{w}_m^\top \mathbf{z}_n \mid \mathbf{A}]}{\sqrt{\text{Var}[\mathbf{w}_m^\top \mathbf{z}_n \mid \mathbf{A}]}}.$$

⌘ Chapter 8 Problems ⌘

1. Following the derivation in Equation (8.5), derive the conditional distribution over the user feature z_{kn} for all $k \in \{1, 2, \dots, K\}$ and $n \in \{1, 2, \dots, N\}$ for the PAA model.
2. Use the “MovieLens 100K” data set introduced in Section 4.10.2 (p. 122) to assess and compare the effectiveness of PAA and PAAA models introduced in this Chapter with Bayesian real matrix factorization approaches.

Bayesian Ordinal Matrix Factorization

Contents

9.1	Ordinal Likelihood with Gaussian Prior and Wishart Hierarchical Prior (OGGW)	205
9.1.1	Ordinal Regression Likelihood	205
9.1.2	Matrix Factorization Modeling on Latent Variables	207
9.1.3	Gibbs Sampler	207
9.2	Properties of OGGW	209
Chapter 9	Problems	210

9.1. Ordinal Likelihood with Gaussian Prior and Wishart Hierarchical Prior (OGGW)



The properties of the Poisson factorization models (PF, e.g., PAA and PAAA models) show that their primary objective is to provide recommendations by predicting future interactions between users and items. Therefore, the PF is often applied to the implicit consumer data, where the data $\mathbf{A} \in \{0, 1\}^{M \times N}$, i.e., the data contains only the information that a user is interacting with an item or not.

In many applications, the data matrix \mathbf{A} will be further constrained. The ordinal matrix factorization (OMF) deals with ordinal data (Stevens, 1946), where entries in \mathbf{A} are restricted to a finite ordered (ranked) set of values such that a judgment of preference is made. For example, in collaborate filtering, we seek to predict a consumer's rating of a novel item on an ordinal scale such as *good* > *average* > *bad*; the temperature of a day is *hot* > *warm* > *cold*; a teacher always rates his/her students by giving grades on their overall performance having the ordering $A > B > C > D > F$ (Paquet et al., 2005; Chu et al., 2005; Gouvert et al., 2020). Although real-valued or nonnegative matrix factorization techniques introduced in previous chapters can be used to find the decomposition, a specific approach that explicitly models this ordinal data can be more efficient.

Instead of factoring $\mathbf{A} = \mathbf{WZ} + \mathbf{E}$ directly as those were done in real-valued matrix factorization and nonnegative matrix factorization, Bayesian ordinary matrix factorization introduces an additional *hidden* matrix $\mathbf{H} = \mathbf{WZ} + \mathbf{E} \in \mathbb{R}^{M \times N}$, which is then used as an unobserved input to an ordinal regression model to obtain the data matrix \mathbf{A} (see Figure 9.3). Therefore, ordinary matrix factorization is also called a hierarchical Bayesian model.

9.1.1 Ordinal Regression Likelihood

We now consider the data matrix $\mathbf{A} \in \mathbb{A}^{M \times N}$, where \mathbb{A} is a finite set of A -ordered categories. Without loss of generality, these categories can be denoted as consecutive integers $\mathbb{A} = \{1, 2, \dots, A\}$ that conserve the known ordering information. The real number line is divided into a set of contiguous intervals with boundaries $\{b_a\}$,

$$-\infty = b_1 < b_2 < \dots < b_{A+1} = \infty,$$

such that the interval $[b_a, b_{a+1})$ corresponds to the discrete category $a \in \mathbb{A}$. To model the hidden variable h , we introduce an additional hidden variable f (see Figure 9.1). The value of the variable f implies the rank a if f falls in the rank a 's interval:

$$p(a | f) = \begin{cases} 1, & \text{if } b_a \leq f < b_{a+1} \\ 0, & \text{otherwise} \end{cases} = u(f - b_a) - u(f - b_{a+1}), \quad (9.1)$$

where $u(y)$ is the step function with a value 1 if $y \geq 0$ and 0 if $y < 0$.

Given the hidden value h , uncertainty about the exact location of f can be modeled by a unit variance Gaussian:

$$p(f | h) = \mathcal{N}(f | h, 1). \quad (9.2)$$

Averaging over f in $p(a, f | h) = p(a | f)p(f | h)$, we have

$$p(a | h) = \int p(a, f | h)df = \Phi(h - b_a) - \Phi(h - b_{a+1}), \quad (9.3)$$

where $\Phi(y) = \int_{-\infty}^y \mathcal{N}(u | 0, 1)du = \frac{1}{\sqrt{2\pi}} \int_{-\infty}^y \exp(-\frac{u^2}{2})du$ is the cumulative distribution function of $\mathcal{N}(0, 1)$. In Equation (9.3), we use the fact that

$$\Phi(h - b) = \int \mathcal{N}(f | h, 1) u(f - b)df$$

(see Albert and Chib (1993)). Figure 9.2 shows the probability functions for $p(a | h)$ by varying h . We observe when h falls outside of the interval $[b_a, b_{a+1}]$, the probability is not exactly zero. And when the interval $b_{a+1} - b_a$ is small, the probability tends to be small (in a sense, a small interval of $b_{a+1} - b_a$ indicates there are a large number of categories such that the probability tends to be small for falling into each interval).

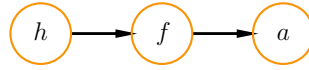


Figure 9.1: Graphical representation of the ordinal regression model.

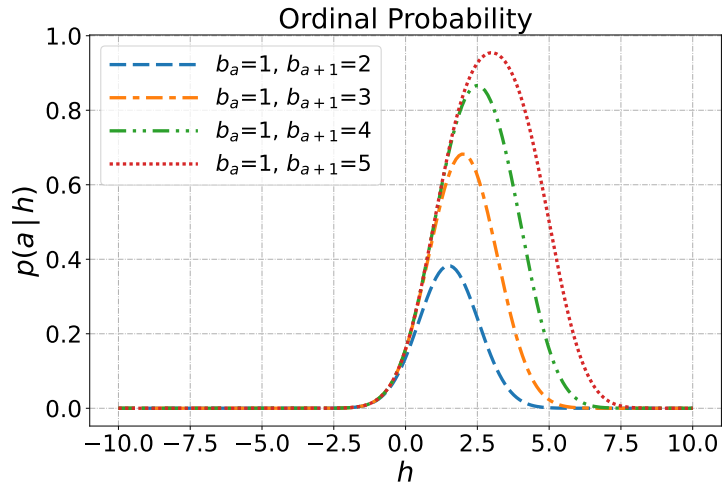
Full likelihood. The ordinal regression model then maps continuous latent variables h_{mn} in \mathbf{H} to probabilities $p(a_{mn} | h_{mn})$:

$$p(a_{mn} | h_{mn}) = \prod_{a=1}^A [\Phi(h_{mn} - b_a) - \Phi(h_{mn} - b_{a+1})]^{1(a_{mn}=a)}. \quad (9.4)$$

Suppose the set of observed entries or the training set is denoted by $\mathcal{X} = \{a_{mn} | (m, n) \in \text{training set}\}$, the likelihood of observed entries under the ordinal regression model is

$$p(\mathcal{X} | \mathbf{H}) = \prod_{(m,n)} p(a_{mn} | h_{mn}), \quad (9.5)$$

Figure 9.2: Ordinal probability of the ordinal regression model in Equation (9.3).



where the product is over all the observed entries or training set entries (m, n) .

9.1.2 Matrix Factorization Modeling on Latent Variables

The Bayesian modeling is identical to that of the GGGW model (Section 6.4, p. 150), with the only difference being the consideration of Gaussian likelihoods over the hidden variables $\{h_{mn}\}$ instead of the observed ratings $\{a_{mn}\}$. The full graphical representation of the model is then shown in Figure 9.3, referred to as the ordinal likelihood with Gaussian and hierarchical normal-inverse-Wishart priors (OGGW) model.

Likelihood. We assume the residuals, e_{mn} , are i.i.d. zero-mean normal with precision $\tau = \frac{1}{\sigma^2}$, which gives rise to the following likelihood function:

$$\begin{aligned} p(\mathbf{H} \mid \mathbf{W}, \mathbf{Z}, \tau) &= \prod_{m,n=1}^{M,N} \mathcal{N}(h_{mn} \mid (\mathbf{W}\mathbf{Z})_{mn}, \sigma^2) \\ &= \prod_{m,n=1}^{M,N} \mathcal{N}(h_{mn} \mid (\mathbf{W}\mathbf{Z})_{mn}, \tau^{-1}), \end{aligned} \quad (9.6)$$

where σ^2 is the variance, and $\tau^{-1} = \sigma^2$ is the precision.

Prior. Given the m -th row \mathbf{w}_m of \mathbf{W} and the n -th column \mathbf{z}_n of \mathbf{Z} , we consider the multivariate Gaussian density and the normal-inverse-Wishart prior as follows:

$$\begin{aligned} \mathbf{w}_m &\sim \mathcal{N}(\mathbf{w}_m \mid \boldsymbol{\mu}_w, \boldsymbol{\Sigma}_w), & \boldsymbol{\mu}_w, \boldsymbol{\Sigma}_w &\sim \mathcal{NIW}(\boldsymbol{\mu}_w, \boldsymbol{\Sigma}_w \mid \mathbf{m}_0, \kappa_0, \nu_0, \mathbf{S}_0); \\ \mathbf{z}_n &\sim \mathcal{N}(\mathbf{z}_n \mid \boldsymbol{\mu}_z, \boldsymbol{\Sigma}_z), & \boldsymbol{\mu}_z, \boldsymbol{\Sigma}_z &\sim \mathcal{NIW}(\boldsymbol{\mu}_z, \boldsymbol{\Sigma}_z \mid \mathbf{m}_0, \kappa_0, \nu_0, \mathbf{S}_0), \end{aligned} \quad (9.7)$$

where $\mathcal{NIW}(\boldsymbol{\mu}, \boldsymbol{\Sigma} \mid \mathbf{m}_0, \kappa_0, \nu_0, \mathbf{S}_0) = \mathcal{N}(\boldsymbol{\mu} \mid \mathbf{m}_0, \frac{1}{\kappa_0} \boldsymbol{\Sigma}) \cdot \text{IW}(\boldsymbol{\Sigma} \mid \mathbf{S}_0, \nu_0)$ is the density of a normal-inverse-Wishart distribution, and $\text{IW}(\boldsymbol{\Sigma} \mid \mathbf{S}_0, \nu_0)$ is the inverse-Wishart distribution (Equation (3.40), p. 85).

The prior for the noise variance σ^2 is chosen as a conjugate inverse-Gamma density with shape α_σ and scale β_σ (Definition 3.2.4, p. 47),

$$p(\sigma^2) = \mathcal{G}^{-1}(\sigma^2 \mid \alpha_\sigma, \beta_\sigma) = \frac{\beta_\sigma^{\alpha_\sigma}}{\Gamma(\alpha_\sigma)} (\sigma^2)^{-\alpha_\sigma-1} \exp\left(-\frac{\beta_\sigma}{\sigma^2}\right).$$

Or placing an inverse-Gamma prior on the variance is equivalent to applying a Gamma prior on the precision parameter. For the precision $\tau = \sigma^{-2}$, we use a Gamma distribution with shape $\alpha_\tau > 0$ and rate $\beta_\tau > 0$ (Definition 3.2.3, p. 43),

$$p(\tau) \sim \mathcal{G}(\tau \mid \alpha_\tau, \beta_\tau) = \frac{\beta_\tau^{\alpha_\tau}}{\Gamma(\alpha_\tau)} \tau^{\alpha_\tau-1} \exp(-\beta_\tau \cdot \tau),$$

9.1.3 Gibbs Sampler

To construct the Gibbs sampler, we need to obtain the conditional posterior for each variable.

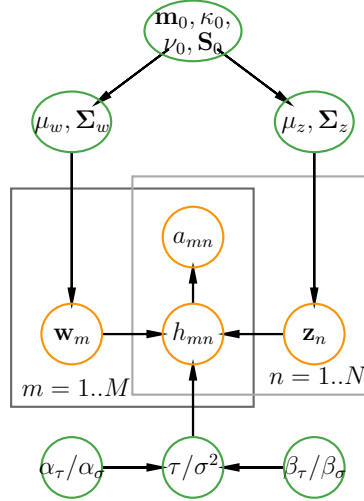


Figure 9.3: Graphical representation of OGGW model. Green circles denote prior variables, orange circles represent observed and latent variables, and plates represent repeated variables. The slash “/” in the variable represents “or,” and the comma “,” in the variable represents “and.”

Latent variables. The conditional density for latent variables h_{mn} is

$$p(h_{mn} | a_{mn}, \mathbf{w}_m, \mathbf{z}_n, \tau) \propto p(a_{mn} | h_{mn}) p(h_{mn} | \mathbf{w}_m, \mathbf{z}_n, \tau). \quad (9.8)$$

To sample from this conditional density, we introduce back the hidden variable f_{mn} . For brevity, we omit the subscript m, n . The density $f, h | a, \mathbf{w}, \mathbf{z}, \tau$ then can be sampled from in two steps, $f | a, \mathbf{w}, \mathbf{z}, \tau$ and $h | f, \mathbf{w}, \mathbf{z}, \tau$. The joint marginal distribution of a, f , and h , given $m = \mathbf{w}^\top \mathbf{z}$ and τ , is

$$p(a | f) p(f | h) p(h | m, \tau) = [u(f - b_a) - u(f - b_{a+1})] \mathcal{N}(f | h, 1) \mathcal{N}(h | m, \tau^{-1}). \quad (9.9)$$

The conditional density of $p(f | a, m, \tau)$ follows from

$$p(f | a, m, \tau) = \mathcal{GTN}(f | m, 1 + \tau^{-1}, b_a, b_{a+1}),$$

a general-truncated-normal density (Definition 3.4.2, p. 60). Therefore, the sample h can be obtained by

$$\begin{aligned} p(h | f, m, \tau) &\propto p(f | h) p(h | m, \tau^{-1}) = \mathcal{N}(f | h, 1) \mathcal{N}(h | m, \tau^{-1}) \\ &\propto \mathcal{N}\left(h \mid \frac{f + m\tau}{1 + \tau}, (1 + \tau)^{-1}\right). \end{aligned} \quad (9.10)$$

Multivariate Gaussian parameters. Same as the GGGW model, from the discussion in Section 3.7.7 (p. 85), the posterior density of $\{\boldsymbol{\mu}_w, \boldsymbol{\Sigma}_w\}$ also follows a NIW distribution with updated parameters:

$$\boldsymbol{\mu}_w, \boldsymbol{\Sigma}_w \sim \mathcal{NIW}(\boldsymbol{\mu}_w, \boldsymbol{\Sigma}_w | \mathbf{m}_M, \kappa_M, \nu_M, \mathbf{S}_M), \quad (9.11)$$

where

$$\mathbf{m}_M = \frac{\kappa_0 \mathbf{m}_0 + M \bar{\mathbf{w}}}{\kappa_M} = \frac{\kappa_0}{\kappa_M} \mathbf{m}_0 + \frac{M}{\kappa_M} \bar{\mathbf{w}} \quad (9.12)$$

$$\kappa_M = \kappa_0 + M \quad (9.13)$$

$$\nu_M = \nu_0 + M \quad (9.14)$$

$$\mathbf{S}_M = \mathbf{S}_0 + \mathbf{S}_{\bar{\mathbf{w}}} + \frac{\kappa_0 M}{\kappa_0 + M} (\bar{\mathbf{w}} - \mathbf{m}_0)(\bar{\mathbf{w}} - \mathbf{m}_0)^\top \quad (9.15)$$

$$= \mathbf{S}_0 + \sum_{m=1}^M \mathbf{w}_m \mathbf{w}_m^\top + \kappa_0 \mathbf{m}_0 \mathbf{m}_0^\top - \kappa_M \mathbf{m}_M \mathbf{m}_M^\top \quad (9.16)$$

$$\bar{\mathbf{w}} = \frac{1}{M} \sum_{m=1}^M \mathbf{w}_m. \quad (9.17)$$

$$\mathbf{S}_{\bar{\mathbf{w}}} = \sum_{m=1}^M (\mathbf{w}_m - \bar{\mathbf{w}})(\mathbf{w}_m - \bar{\mathbf{w}})^\top \quad (9.18)$$

Gaussian variance parameter. The conditional density of σ^2 depends on its parents $(\alpha_\sigma, \beta_\sigma)$, children (\mathbf{A}) , and coparents (\mathbf{W}, \mathbf{Z}) . And it is an inverse-Gamma distribution (by conjugacy in Equation (3.7), p. 47),

$$p(\sigma^2 \mid \mathbf{W}, \mathbf{Z}, \mathbf{A}) = p(\sigma^2 \mid \mathbf{W}, \mathbf{Z}, \mathbf{A}) = \mathcal{G}^{-1}(\sigma^2 \mid \tilde{\alpha}_\sigma, \tilde{\beta}_\sigma), \quad (9.19)$$

$$\tilde{\alpha}_\sigma = \frac{MN}{2} + \alpha_\sigma, \quad \tilde{\beta}_\sigma = \frac{1}{2} \sum_{m,n=1}^{M,N} (\mathbf{A} - \mathbf{W}\mathbf{Z})_{mn}^2 + \beta_\sigma.$$

Gaussian precision parameter. Alternatively, the conditional posterior density of $\tau = \frac{1}{\sigma^2}$ is obtained similarly (Equation (3.5), p. 45) by

$$p(\tau \mid \mathbf{W}, \mathbf{Z}, \mathbf{A}) = p(\tau \mid \mathbf{W}, \mathbf{Z}, \mathbf{A}) = \mathcal{G}(\tau \mid \tilde{\alpha}_\tau, \tilde{\beta}_\tau), \quad (9.20)$$

$$\tilde{\alpha}_\tau = \frac{MN}{2} + \alpha_\tau, \quad \tilde{\beta}_\tau = \frac{1}{2} \sum_{m,n=1}^{M,N} (\mathbf{A} - \mathbf{W}\mathbf{Z})_{mn}^2 + \beta_\tau.$$

In practice, the prior parameters α_τ and β_τ are chosen to be equal to α_σ and β_σ , respectively.

Gibbs sampling. We can construct a Gibbs sampler for the OGGW model as formulated in Algorithm 21 based on Gibbs sampling method introduced in Section 2.3.3 (p. 26). A specific choice of hyper-parameters for the normal-inverse-Wishart prior on the mean and covariance is not significant in practice since there is a large amount of data for learning that will override any reasonable weak prior. The weak prior can be chosen as $\mathbf{m}_0 = \mathbf{0}$, $\kappa_0 = 1$, $\nu_0 = K + 1$, $\mathbf{S}_0 = \mathbf{I}$. While the choice for α_τ and β_τ rather depends on the data sets. A weak prior choice is $\alpha_\tau = \beta_\tau = 1$.

9.2. Properties of OGGW

The OGGW model's significant feature is that it is not limited to offering only the expected value of missing entries in \mathbf{A} ; it can also provide a probability distribution over feasible

Algorithm 21 Gibbs sampler for OGGW model in one iteration (prior on $\tau = \frac{1}{\sigma^2}$). By default, uninformative hyper-parameters are $\mathbf{m}_0 = \mathbf{0}$, $\kappa_0 = 1$, $\nu_0 = K + 1$, $\mathbf{S}_0 = \mathbf{I}$, $\alpha_\tau = \beta_\tau = 1$.

Require: Choose initial $\alpha_\tau, \beta_\tau, \mathbf{m}_0, \kappa_0, \nu_0, \mathbf{S}_0$;

- 1: **for** $m = 1$ to M **do**
 - 2: Sample \mathbf{w}_m from $p(\mathbf{w}_m \mid \boldsymbol{\mu}_m, \boldsymbol{\Sigma}_m)$; ▷ Equation (9.7)
 - 3: Sample h_{mn} from $p(h_{mn} \mid a_{mn}, \mathbf{w}_m, \mathbf{z}_n, \tau)$ for each n ; ▷ Equation (9.10)
 - 4: **end for**
 - 5: **for** $n = 1$ to N **do**
 - 6: Sample \mathbf{z}_n from $p(\mathbf{z}_n \mid \boldsymbol{\mu}_z, \boldsymbol{\Sigma}_z)$; ▷ Equation (9.7)
 - 7: Sample h_{mn} from $p(h_{mn} \mid a_{mn}, \mathbf{w}_m, \mathbf{z}_n, \tau)$ for each m ; ▷ Equation (9.10)
 - 8: **end for**
 - 9: Sample τ from $p(\tau \mid \mathbf{W}, \mathbf{Z}, \mathbf{A})$; ▷ Equation (9.20)
 - 10: Sample $\boldsymbol{\mu}_w, \boldsymbol{\Sigma}_w$ from $p(\boldsymbol{\mu}_w, \boldsymbol{\Sigma}_w \mid \mathbf{W}, M)$; ▷ Equation (9.11)
 - 11: Sample $\boldsymbol{\mu}_z, \boldsymbol{\Sigma}_z$ from $p(\boldsymbol{\mu}_z, \boldsymbol{\Sigma}_z \mid \mathbf{Z}, N)$; ▷ Symmetry of Eq. (9.11)
-

discrete values. Though this extra information cannot enhance root mean squared error (RMSE) performance, other measurements, such as mean absolute error (MAE), can profit from it.

Given the hidden variables $\{h_{mn}\}$ and using the likelihood in Equation (9.3), the expected value of the category value for (m, n) -th entry is

$$\begin{aligned} \sum_{a=1}^A a \cdot p(a \mid h_{mn}) &= \sum_{a=1}^A a \cdot (\Phi(h_{mn} - b_a) - \Phi(h_{mn} - b_{a+1})) \\ &= \sum_{a=1}^A \Phi(h_{mn} - b_a) - A\Phi(h_{mn} - b_{A+1}). \end{aligned}$$

Following the likelihood in Equation (9.6) and integrating out h_{mn} , we have

$$y_{mn} := \sum_{a=1}^A a \cdot p(a \mid \mathbf{w}_m, \mathbf{z}_n, \tau) = \sum_{a=1}^A \Phi\left(\frac{\mathbf{w}_m^\top \mathbf{z}_n - b_a}{\sqrt{1 + \tau^{-1}}}\right). \quad (9.21)$$

Therefore, instead of using the score in Equation (8.8) (p. 203), the score $E[y_{mn} \mid \mathbf{A}]$ can be obtained by averaging the values of Equation (9.21) during the Gibbs sampling process.

Similar to the third recommendation system introduced in Section 8.4 (p. 202), the OGGW model can also provide uncertainty about each entry in \mathbf{A} . Adopting again the idea of the Sharpe ratio, we can suggest the unconsumed movie m (in the Netflix context) when a_{mn} for user n by the uncertainty-adjusted score of posterior expected Poisson parameters:

$$\text{score}_{mn} = \frac{E[y_{mn} \mid \mathbf{A}]}{\sqrt{\text{Var}[y_{mn} \mid \mathbf{A}]}}.$$

1. Use the “MovieLens 100K” data set introduced in Section 4.10.2 (p. 122) to assess and compare the effectiveness of OGGW model introduced in this Chapter with PAA and PAAA models.


10

Bayesian Interpolative Decomposition

Contents

10.1	Interpolative Decomposition (ID)	213
10.2	Existence of the Column Interpolative Decomposition	215
10.3	Skeleton/CUR Decomposition	219
10.4	Row ID and Two-Sided ID	220
10.5	Bayesian Low-Rank Interpolative Decomposition	221
10.5.1	Gibbs Sampler	225
10.5.2	Aggressive Update	227
10.5.3	Post-Processing	228
10.5.4	Bayesian ID with Automatic Relevance Determination	229
10.5.5	Examples for Bayesian ID	229
10.5.6	Hyper-parameters	231
10.5.7	Convergence and Comparative Analysis	232
10.6	Bayesian Intervened Interpolative Decomposition (IID)	233
10.6.1	Quantitative Problem Statement	234
	Formulaic Alphas	235
	Evaluation Metrics	235
10.6.2	Examples for Bayesian IID	235
	Convergence and Comparative Analysis	237
	Quantitative Strategy	238
Chapter 10	Problems	240

10.1. Interpolative Decomposition (ID)

 Low-rank real-valued or nonnegative matrix factorization is essential in modern data science. Low-rank matrix approximation with respect to the Frobenius norm—minimizing the sum squared differences to the target matrix—can be easily solved with singular value decomposition (SVD) or the Bayesian real-valued/nonnegative matrix decomposition methods. For many applications, however, it is sometimes advantageous to work with a basis that consists of a subset of the columns from the observed matrix itself (Halko et al., 2011; Martinsson et al., 2011). The interpolative decomposition (ID) is one such approach that stands out by allowing the reuse of columns from the original matrix. This enables it to preserve matrix properties such as sparsity and nonnegativity that also help reduce memory usage.

ID is widely used as a feature selection tool that extracts the essence and allows dealing with big data that may originally be too large to fit into RAM. In addition, we can remove the non-relevant parts of the data, which consist of errors and redundant information, via these methods (Liberty et al., 2007; Halko et al., 2011; Martinsson et al., 2011; Ari et al., 2012; Lu, 2022b; Lu and Osterrieder, 2022). Locating the indices associated with the spanning columns is frequently valuable for the purpose of data interpretation and analysis. It can be very useful to identify a subset of the columns that distills the information in the matrix. When the columns of the observed matrix have some specific interpretations, e.g., they are transactions in a transaction data set, the columns of the factored matrix in ID will retain the same meaning as well.

The column ID ¹ factors a matrix into the product of two matrices, one of which consists of selected columns from the original matrix, and the other of which contains a subset of columns consisting of the identity matrix with all its values having absolute values no greater than 1. We first state and demonstrate the existence of the *exact ID* in the following theorem, and we will later describe the *low-rank ID* through Bayesian approaches.

Theorem 10.1: (Column Interpolative Decomposition)

Any rank- R matrix $\mathbf{A} \in \mathbb{R}^{m \times n}$ can be factored as

$$\mathbf{A}_{M \times N} = \mathbf{C}_{M \times R} \mathbf{W}_{R \times N},$$

where $\mathbf{C} \in \mathbb{R}^{M \times R}$ is some R linearly independent columns of \mathbf{A} , $\mathbf{W} \in \mathbb{R}^{R \times N}$ represents the matrix used to reconstruct \mathbf{A} . The factor \mathbf{W} contains an $R \times R$ identity submatrix (under a mild column permutation). Specifically, the entries in \mathbf{W} have values no larger than 1 in magnitude:

$$\max |w_{ij}| \leq 1, \quad \forall i \in [1, R], j \in [1, N].$$

The storage required for the decomposition is then reduced or potentially increased from MN floating-point numbers to MR and $(N - R)R$ floats for storing \mathbf{C} and \mathbf{W} , respectively. Additionally, extra R integers are required to remember the position of each column of \mathbf{C} within \mathbf{A} .

1. The *column ID* will simply be referred to as *ID* without further clarification.

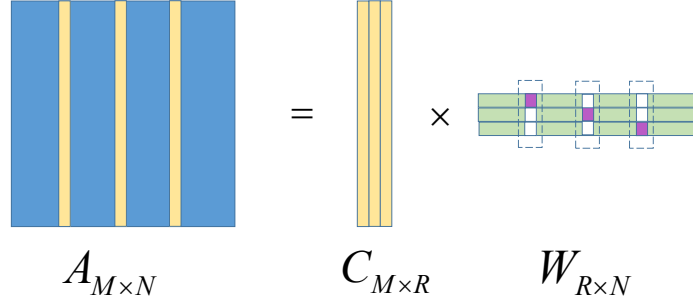


Figure 10.1: Demonstration of the column ID of a matrix, where the **yellow** vector denotes the linearly independent columns of \mathbf{A} , white entries denote zero, and **purple** entries denote one.

While we claim that entries in \mathbf{W} have magnitudes no greater than 1, a weaker construction assumes that no entry of \mathbf{W} has an absolute value exceeding 2. The illustration of the column ID is shown in Figure 10.1, where the **yellow** vectors denote the linearly independent columns of \mathbf{A} , and the **purple** vectors in \mathbf{W} form an $R \times R$ identity submatrix. The positions of the **purple** vectors inside \mathbf{W} are identical to the placements of the corresponding **yellow** vectors within \mathbf{A} . The column ID is very similar to the *CR decomposition*, both select R linearly independent columns into the first factor, and the second factor comprises an $R \times R$ identity submatrix (Strang, 2021; Strang and Moler, 2022; Lu, 2021b). The difference between the two is that the CR decomposition precisely selects the first R linearly independent columns into the first factor, and the identity submatrix appears in the pivot positions. And more importantly, the second factor in the CR decomposition comes from the *reduced row echelon form (RREF)*. Therefore, the column ID can also be utilized in the same applications as the CR decomposition, say proving the rank equals trace property in idempotent matrices (Lu, 2021b), and demonstrating the elementary theorem in linear algebra that the column rank equals row rank of a matrix (Lu, 2021a). Moreover, the column ID is also a special case of the *rank decomposition* and is not unique (Lu, 2021b).

Notations that will be extensively used in the sequel. Following again the Matlab-style notation, if J is an index vector with size R that contains the indices of columns selected from \mathbf{A} into \mathbf{C} , then \mathbf{C} can be denoted as $\mathbf{C} = \mathbf{A}[:, J]$ (Definition 1.0.1, p. 8). The matrix \mathbf{C} contains “skeleton” columns of \mathbf{A} . From the “skeleton” index vector J , the $R \times R$ identity matrix inside \mathbf{W} can be recovered by

$$\mathbf{W}[:, J] = \mathbf{I}_R \in \mathbb{R}^{R \times R}.$$

Suppose further we put the remaining indices of \mathbf{A} into an index vector I with

$$J \cap I = \emptyset \quad \text{and} \quad J \cup I = \{1, 2, \dots, N\}.$$

The remaining $N - R$ columns in \mathbf{W} consist of an $R \times (N - R)$ *expansion matrix* since the matrix contains *expansion coefficients* to reconstruct the columns of \mathbf{A} from \mathbf{C} :

$$\mathbf{E} = \mathbf{W}[:, I] \in \mathbb{R}^{R \times (N - R)},$$

where the entries of \mathbf{E} are known as the *expansion coefficients*. Moreover, let $\mathbf{P} \in \mathbb{R}^{N \times N}$ be a (column) permutation matrix (Definition 1.0.15, p. 14) defined by $\mathbf{P} = \mathbf{I}_N[:, (J, I)]$ such that

$$\mathbf{A}\mathbf{P} = \mathbf{A}[:, (J, I)] = [\mathbf{C}, \mathbf{A}[:, I]],$$

and

$$\mathbf{W}\mathbf{P} = \mathbf{W}[:, (J, I)] = [\mathbf{I}_R, \mathbf{E}] \quad \underline{\text{leads to}} \quad \mathbf{W} = [\mathbf{I}_R, \mathbf{E}] \mathbf{P}^\top. \quad (10.1)$$

10.2. Existence of the Column Interpolative Decomposition

Cramer's rule. The proof of the existence of the column ID relies on Cramer's rule, which will be briefly covered in the following discussion. Cramer's rule is an explicit formula for the solution of a system of linear equations with as many equations as unknowns, and it is valid whenever the system has a unique solution, i.e., the underlying matrix is nonsingular. Consider a system of n linear equations for n unknowns, represented in the following matrix multiplication form:

$$\mathbf{M}\mathbf{x} = \mathbf{l},$$

where $\mathbf{M} \in \mathbb{R}^{n \times n}$ is nonsingular, and $\mathbf{x}, \mathbf{l} \in \mathbb{R}^n$. Then the theorem states that, in this case, the system has a unique solution, whose individual values for the unknowns are given by:

$$x_i = \frac{\det(\mathbf{M}_i)}{\det(\mathbf{M})}, \quad \text{for all } i \in \{1, 2, \dots, n\},$$

where \mathbf{M}_i is the matrix formed by replacing the i -th column of \mathbf{M} with the column vector \mathbf{l} . In full generality, Cramer's rule considers the matrix equation

$$\mathbf{M}\mathbf{X} = \mathbf{L},$$

where $\mathbf{M} \in \mathbb{R}^{n \times n}$ is nonsingular, and $\mathbf{X}, \mathbf{L} \in \mathbb{R}^{n \times m}$. Let $I_c = [i_1, i_2, \dots, i_k]$ and $J_c = [j_1, j_2, \dots, j_k]$ be two index vectors satisfying $1 \leq i_1 \leq i_2 \leq \dots \leq i_k \leq n$ and $1 \leq j_1 \leq j_2 \leq \dots \leq j_k \leq m$. Then $\mathbf{X}[I_c, J_c]$ is a $k \times k$ submatrix of \mathbf{X} . Let further $\mathbf{M}_\mathbf{L}(I_c, J_c)$ be the $n \times n$ matrix formed by replacing the (i_s) -th column of \mathbf{M} with (j_s) -th column of \mathbf{L} for all $s \in \{1, 2, \dots, k\}$. Then we have

$$\det(\mathbf{X}[I_c, J_c]) = \frac{\det(\mathbf{M}_\mathbf{L}(I_c, J_c))}{\det(\mathbf{M})}.$$

When I_c and J_c are of size 1, it follows that

$$x_{ij} = \frac{\det(\mathbf{M}_\mathbf{L}(i, j))}{\det(\mathbf{M})}. \quad (10.2)$$

Now we are ready to prove the existence of the column ID.

Proof [of Theorem 10.1] We have mentioned previously that the proof relies on Cramer's rule. If we can show the entries of \mathbf{W} can be denoted by the Cramer's rule equality in Equation (10.2), and furthermore, establish that the numerator is smaller than the denominator, then we can complete the proof. However, we notice that the matrix in the denominator of Equation (10.2) is a square matrix. Here comes the trick.

Step 1: column ID for full row rank matrix. For a start, we first consider the full row rank matrix \mathbf{A} (which implies $R = M$, $M \leq N$, and $\mathbf{A} \in \mathbb{R}^{R \times N}$ such that the matrix $\mathbf{C} \in \mathbb{R}^{R \times R}$ is a square matrix in the column ID $\mathbf{A} = \mathbf{C}\mathbf{W}$ that we want). Determine the “skeleton” index vector J by

$$J = \arg \max_{J_t} \{ |\det(\mathbf{A}[:, J_t])| : J_t \text{ is a subset of } \{1, 2, \dots, N\} \text{ with size } R = M \}, \quad (10.3)$$

i.e., J is the index vector that is determined by maximizing the magnitude of the determinant of $\mathbf{A}[:, J]$. As we have discussed in the last section, there exists a (column) permutation matrix satisfying

$$\mathbf{A}\mathbf{P} = [\mathbf{A}[:, J] \quad \mathbf{A}[:, I]].$$

Since $\mathbf{C} = \mathbf{A}[:, J]$ has full column rank $R = M$, it is then nonsingular. The above equation can be rewritten as

$$\begin{aligned} \mathbf{A} &= [\mathbf{A}[:, J] \quad \mathbf{A}[:, I]] \mathbf{P}^\top \\ &= \mathbf{A}[:, J] \begin{bmatrix} \mathbf{I}_R & \mathbf{A}[:, J]^{-1} \mathbf{A}[:, I] \end{bmatrix} \mathbf{P}^\top \\ &= \mathbf{C} \underbrace{[\mathbf{I}_R \quad \mathbf{C}^{-1} \mathbf{A}[:, I]]}_{\mathbf{W}} \mathbf{P}^\top, \end{aligned}$$

where the matrix \mathbf{W} is given by $[\mathbf{I}_R \quad \mathbf{C}^{-1} \mathbf{A}[:, I]] \mathbf{P}^\top = [\mathbf{I}_R \quad \mathbf{E}] \mathbf{P}^\top$ by Equation (10.1). To prove the claim that the magnitude of \mathbf{W} is no larger than 1 is equivalent to proving that entries in $\mathbf{E} = \mathbf{C}^{-1} \mathbf{A}[:, I] \in \mathbb{R}^{R \times (N-R)}$ are no greater than 1 in absolute value.

Define the index vector $[j_1, j_2, \dots, j_N]$ as a permutation of $[1, 2, \dots, N]$ such that

$$[j_1, j_2, \dots, j_N] = [1, 2, \dots, N] \mathbf{P} = [J, I]. \quad 2$$

Thus, it follows from $\mathbf{C}\mathbf{E} = \mathbf{A}[:, I]$ that

$$\underbrace{[\mathbf{a}_{j_1}, \mathbf{a}_{j_2}, \dots, \mathbf{a}_{j_R}]}_{=\mathbf{C}=\mathbf{A}[:, J]} \mathbf{E} = \underbrace{[\mathbf{a}_{j_{R+1}}, \mathbf{a}_{j_{R+2}}, \dots, \mathbf{a}_{j_N}]}_{=\mathbf{A}[:, I]=\mathbf{B}},$$

where \mathbf{a}_i is the i -th column of \mathbf{A} , and we let $\mathbf{B} = \mathbf{A}[:, I]$. Therefore, by Cramer’s rule in Equation (10.2), we have

$$e_{kl} = \frac{\det(\mathbf{C}_B(k, l))}{\det(\mathbf{C})}, \quad (10.4)$$

where e_{kl} is the entry (k, l) of \mathbf{E} , and $\mathbf{C}_B(k, l)$ is the $R \times R$ matrix formed by replacing the k -th column of \mathbf{C} with the l -th column of \mathbf{B} . For example,

$$\begin{aligned} e_{11} &= \frac{\det([\mathbf{a}_{j_{R+1}}, \mathbf{a}_{j_2}, \dots, \mathbf{a}_{j_r}])}{\det([\mathbf{a}_{j_1}, \mathbf{a}_{j_2}, \dots, \mathbf{a}_{j_r}])}, & e_{12} &= \frac{\det([\mathbf{a}_{j_{R+2}}, \mathbf{a}_{j_2}, \dots, \mathbf{a}_{j_r}])}{\det([\mathbf{a}_{j_1}, \mathbf{a}_{j_2}, \dots, \mathbf{a}_{j_r}])}, \\ e_{21} &= \frac{\det([\mathbf{a}_{j_1}, \mathbf{a}_{j_{R+1}}, \dots, \mathbf{a}_{j_r}])}{\det([\mathbf{a}_{j_1}, \mathbf{a}_{j_2}, \dots, \mathbf{a}_{j_r}])}, & e_{22} &= \frac{\det([\mathbf{a}_{j_1}, \mathbf{a}_{j_{R+2}}, \dots, \mathbf{a}_{j_r}])}{\det([\mathbf{a}_{j_1}, \mathbf{a}_{j_2}, \dots, \mathbf{a}_{j_r}])}. \end{aligned}$$

Since J is chosen to maximize the magnitude of $\det(\mathbf{C})$ in Equation (10.3), it follows that

$$|e_{kl}| \leq 1, \quad \text{for all } k \in \{1, 2, \dots, R\}, \quad l \in \{1, 2, \dots, N - R\}.$$

2. Note here $[j_1, j_2, \dots, j_N]$, $[1, 2, \dots, N]$, J , and I are row vectors.

Step 2: apply to general matrices. To summarize what we have proved above and to abuse the notation. For any matrix $\mathbf{F} \in \mathbb{R}^{R \times N}$ with **full rank** $R \leq N$, the column ID exists such that $\mathbf{F} = \mathbf{C}_0 \mathbf{W}$, where the values in \mathbf{W} are no greater than 1 in absolute value.

Applying the finding to the full general matrix $\mathbf{A} \in \mathbb{R}^{M \times N}$ with $\text{rank } R \leq \{M, N\}$, it is trivial that the matrix \mathbf{A} admits a *rank decomposition* (see Problem 10.3.):

$$\mathbf{A} = \underset{M \times N}{\mathbf{D}} = \underset{M \times R}{\mathbf{D}} \underset{R \times N}{\mathbf{F}},$$

where \mathbf{D} and \mathbf{F} have full column rank R and full row rank R , respectively (Lu, 2021b). For the column ID of $\mathbf{F} = \mathbf{C}_0 \mathbf{W}$, where $\mathbf{C}_0 = \mathbf{F}[:, J]$ contains R linearly independent columns of \mathbf{F} . We notice by $\mathbf{A} = \mathbf{D}\mathbf{F}$ such that

$$\mathbf{A}[:, J] = \mathbf{D}\mathbf{F}[:, J],$$

i.e., the columns indexed by J of $(\mathbf{D}\mathbf{F})$ can be obtained by $\mathbf{D}\mathbf{F}[:, J]$, which in turn are the columns of \mathbf{A} indexed by J . This makes

$$\underbrace{\mathbf{A}[:, J]}_{\mathbf{C}} = \underbrace{\mathbf{D}\mathbf{F}[:, J]}_{\mathbf{D}\mathbf{C}_0}$$

and

$$\mathbf{A} = \mathbf{D}\mathbf{F} = \mathbf{D}\mathbf{C}_0\mathbf{W} = \underbrace{\mathbf{D}\mathbf{F}[:, J]}_{\mathbf{C}}\mathbf{W} = \mathbf{C}\mathbf{W}.$$

This completes the proof. ■

The above proof reveals an intuitive way for computing the optimal column ID of matrix \mathbf{A} as shown in Algorithm 22. Nevertheless, any algorithm that is guaranteed to find such an optimally-conditioned factorization must have combinatorial complexity (Martinsson, 2019). In the next sections, we will consider alternative ways to find a relatively well-conditioned ID factorization.

Example 10.1 (Compute the Column ID) *Given a matrix*

$$\mathbf{A} = \begin{bmatrix} 56 & 41 & 30 \\ 32 & 23 & 18 \\ 80 & 59 & 42 \end{bmatrix}$$

with rank 2, the trivial process for computing the column ID of \mathbf{A} is shown as follows. We first find a rank decomposition

$$\mathbf{A} = \mathbf{D}\mathbf{F} = \begin{bmatrix} 1 & 0 \\ 0 & 1 \\ 2 & -1 \end{bmatrix} \begin{bmatrix} 56 & 41 & 30 \\ 32 & 23 & 18 \end{bmatrix}.$$

Since rank $R = 2$, J is one of $[1, 2], [0, 2], [0, 1]$, where the absolute determinant of $\mathbf{F}[:, J]$ are 48, 48, 24, respectively. We proceed by choosing $J = [0, 2]$:

$$\tilde{\mathbf{C}} = \mathbf{F}[:, J] = \begin{bmatrix} 56 & 30 \\ 32 & 18 \end{bmatrix}, \quad \mathbf{M} = \mathbf{F}[:, I] = \begin{bmatrix} 41 \\ 23 \end{bmatrix}.$$

Algorithm 22 An *Intuitive* Method to Compute the Column ID

Require: Rank- R matrix \mathbf{A} with size $M \times N$;

1: Compute the rank decomposition $\mathbf{A} = \mathbf{D} \mathbf{F}$ such as from a UTV decomposition (Lu, 2021b);

2: Compute column ID of \mathbf{F} : $\mathbf{F} = \mathbf{F}[:, J] \mathbf{W} = \tilde{\mathbf{C}} \mathbf{W}$:

$$2.1. \begin{cases} J = \arg \max_J \{ |\det(\mathbf{F}[:, J])| : J \text{ is a subset of } \{1, 2, \dots, N\} \text{ with size } R \}; \\ I = \{1, 2, \dots, N\} \setminus J; \end{cases}$$

$$2.2. \begin{cases} \tilde{\mathbf{C}} = \mathbf{F}[:, J]; \\ \mathbf{M} = \mathbf{F}[:, I]; \end{cases}$$

2.3. $\mathbf{F} \mathbf{P} = \mathbf{F}[:, (J, I)]$ to obtain permutation matrix \mathbf{P} ;

$$2.4. e_{kl} = \frac{\det(\tilde{\mathbf{C}}_{M(k,l)})}{\det(\tilde{\mathbf{C}})}, \quad \text{for all } k \in [1, R], l \in [1, N - R] \text{ (Equation (10.4))};$$

2.5. $\mathbf{W} = [\mathbf{I}_R, \mathbf{E}] \mathbf{P}^\top$ (Equation (10.1)).

3: $\mathbf{C} = \mathbf{A}[:, J]$;

4: Output the column ID $\mathbf{A} = \mathbf{C} \mathbf{W}$;

And

$$\mathbf{F} \mathbf{P} = \mathbf{F}[:, (J, I)] = \mathbf{F}[:, (0, 2, 1)] \quad \underline{\text{leads to}} \quad \mathbf{P} = \begin{bmatrix} 1 & & \\ & 1 & \\ & & 1 \end{bmatrix}.$$

In this example, $\mathbf{E} \in \mathbb{R}^{2 \times 1}$:

$$e_{11} = \det \left(\begin{bmatrix} 41 & 30 \\ 23 & 18 \end{bmatrix} \right) / \det \left(\begin{bmatrix} 56 & 30 \\ 32 & 18 \end{bmatrix} \right) = 1;$$

$$e_{21} = \det \left(\begin{bmatrix} 56 & 41 \\ 32 & 23 \end{bmatrix} \right) / \det \left(\begin{bmatrix} 56 & 30 \\ 32 & 18 \end{bmatrix} \right) = -\frac{1}{2}.$$

This makes

$$\mathbf{E} = \begin{bmatrix} 1 \\ -\frac{1}{2} \end{bmatrix} \quad \underline{\text{leads to}} \quad \mathbf{W} = [\mathbf{I}_2, \mathbf{E}] \mathbf{P}^\top = \begin{bmatrix} 1 & 1 & 0 \\ 0 & -\frac{1}{2} & 1 \end{bmatrix}.$$

The final selected columns are

$$\mathbf{C} = \mathbf{A}[:, J] = \begin{bmatrix} 56 & 30 \\ 32 & 18 \\ 80 & 42 \end{bmatrix}.$$

The net result is given by

$$\mathbf{A} = \mathbf{C} \mathbf{W} = \begin{bmatrix} 56 & 30 \\ 32 & 18 \\ 80 & 42 \end{bmatrix} \begin{bmatrix} 1 & 1 & 0 \\ 0 & -\frac{1}{2} & 1 \end{bmatrix},$$

where entries of \mathbf{W} are no greater than 1 in absolute value as we want. \square

To end up this section, we discuss the source of the non-uniqueness in the column ID.

Remark 10.2: Non-uniqueness of the Column ID

In the above specific Example 10.1, we notice that both $\mathbf{F}[:, (1, 2)]$ and $\mathbf{F}[:, (0, 2)]$ yield the maximum absolute determinant. Therefore, both of them can result in a column ID of \mathbf{A} . Whilst, we only select J from $[1, 2]$, $[0, 2]$, and $[0, 1]$. When the J is fixed from the maximum absolute determinant search, any permutation of it can also be selected, e.g., $J = [0, 2]$ or $J = [2, 0]$ are both good. The two choices on the selection of the column index search yield the non-uniqueness of the column ID.

10.3. Skeleton/CUR Decomposition

To delve deeper into the topic of ID, we first present the rigorous form of a related decomposition known as the *CUR* or *skeleton* decomposition.

Theorem 10.3: (Skeleton Decomposition)

Any rank- R matrix $\mathbf{A} \in \mathbb{R}^{M \times N}$ can be decomposed as

$$\mathbf{A}_{M \times N} = \mathbf{C}_{M \times R} \mathbf{U}_{R \times R}^{-1} \mathbf{R}_{R \times N},$$

where \mathbf{C} contains some R linearly independent columns of \mathbf{A} , \mathbf{R} contains some R linearly independent rows of \mathbf{A} , and \mathbf{U} is the nonsingular submatrix on the intersection of \mathbf{C} and \mathbf{R} .

- The storage for the decomposition is then reduced or potentially increased from MN floating-point numbers (floats) to $R(M + N) + R^2$ floating-point numbers.
- Alternatively, if we only record the position of the indices, it requires MR and NR floating-point numbers for storing \mathbf{C} and \mathbf{R} , respectively. Additionally, extra $2R$ integers are required to remember the position of each column of \mathbf{C} in that of \mathbf{A} and each row of \mathbf{R} in that of \mathbf{A} (i.e., construct \mathbf{U} from \mathbf{C} and \mathbf{R}).

We note in the case where \mathbf{A} is square and invertible, we have the skeleton decomposition $\mathbf{A} = \mathbf{C}\mathbf{U}^{-1}\mathbf{R}$, where $\mathbf{C} = \mathbf{R} = \mathbf{U} = \mathbf{A}$ such that the decomposition reduces to $\mathbf{A} = \mathbf{A}\mathbf{A}^{-1}\mathbf{A}$. The proof of the skeleton decomposition is provided in Appendix A.3 (p. 250).

The skeleton decomposition is also referred to as the CUR decomposition following from the notation in the decomposition. Compared to singular value decomposition (SVD), CUR is better in terms of reification issues since it uses the actual columns (rows) of the matrix, whereas SVD uses some artificial singular vectors that may not represent physical reality (Mahoney and Drineas, 2009). Moreover, same as ID, CUR maintains sparsity if the data is sparse. On the other hand, similar to SVD, CUR decomposition can be used as a tool for data compression, feature extraction, or data analysis in many application areas (Mahoney and Drineas, 2009; An et al., 2012; Lee and Choi, 2008). The illustration of the skeleton

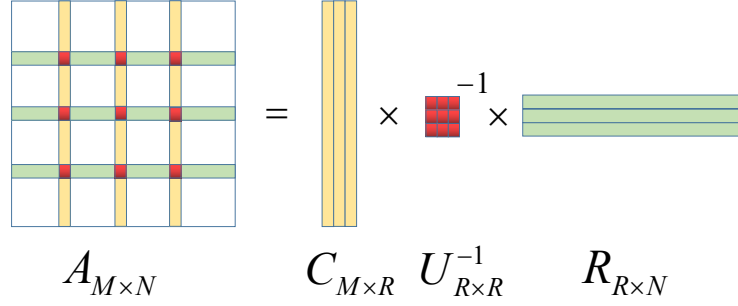


Figure 10.2: Demonstration of the skeleton decomposition of a matrix, where the yellow vectors denote the linearly independent columns of \mathbf{A} , and green vectors denote the linearly independent rows of \mathbf{A} .

decomposition is shown in Figure 10.2, where yellow vectors denote the linearly independent columns of \mathbf{A} , and green vectors denote the linearly independent rows of \mathbf{A} . Specifically, given index vectors I and J both with size R that contain the indices of rows and columns selected from \mathbf{A} into \mathbf{R} and \mathbf{C} , respectively, then \mathbf{U} can be denoted by $\mathbf{U} = \mathbf{A}[I, J]$ (see Definition 1.0.1, p. 8).

10.4. Row ID and Two-Sided ID

We term the interpolative decomposition above as column ID. This is no coincidence since it has its siblings.

Theorem 10.4: (The Whole Interpolative Decomposition)

Any rank- R matrix $\mathbf{A} \in \mathbb{R}^{M \times N}$ can be factored as

$$\begin{aligned} \text{Column ID: } \mathbf{A}_{M \times N} &= \begin{bmatrix} \mathbf{C} \\ M \times R \end{bmatrix} \mathbf{W}_{R \times N}; \\ \text{Row ID: } &= \mathbf{Z}_{M \times R} \begin{bmatrix} \mathbf{R} \\ R \times N \end{bmatrix}; \\ \text{Two-Sided ID: } &= \mathbf{Z}_{M \times R} \begin{bmatrix} \mathbf{U} \\ R \times R \end{bmatrix} \mathbf{W}_{R \times N}, \end{aligned}$$

where

- $\mathbf{C} = \mathbf{A}[:, J] \in \mathbb{R}^{M \times R}$ is some R linearly independent columns of \mathbf{A} , $\mathbf{W} \in \mathbb{R}^{R \times N}$ is the matrix to reconstruct \mathbf{A} and it contains an $R \times R$ identity submatrix (under a mild column permutation): $\mathbf{W}[:, J] = \mathbf{I}_R$;
- $\mathbf{R} = \mathbf{A}[S, :] \in \mathbb{R}^{R \times N}$ is some R linearly independent rows of \mathbf{A} , $\mathbf{Z} \in \mathbb{R}^{M \times R}$ is the matrix to reconstruct \mathbf{A} and it contains an $R \times R$ identity submatrix (under a mild row permutation): $\mathbf{Z}[S, :] = \mathbf{I}_R$;
- Entries in \mathbf{W} and \mathbf{Z} have values no larger than 1 in magnitude: $\max |w_{ij}| \leq 1$ and $\max |z_{ij}| \leq 1$;

- $\mathbf{U} = \mathbf{A}[S, J] \in \mathbb{R}^{R \times R}$ is the nonsingular submatrix on the intersection of \mathbf{C} and \mathbf{R} ;
- **Skeleton decomposition:** the three matrices \mathbf{C} , \mathbf{R} , and \mathbf{U} in the boxed texts share same notation as the skeleton decomposition (Theorem 10.3), where they even have same meanings such that the three matrices make the skeleton decomposition of \mathbf{A} : $\mathbf{A} = \mathbf{C}\mathbf{U}^{-1}\mathbf{R}$.

The proof of the row ID is just similar to that of the column ID. Suppose the column ID of \mathbf{A}^\top is given by $\mathbf{A}^\top = \mathbf{C}_0\mathbf{W}_0$, where \mathbf{C}_0 contains R linearly independent columns of \mathbf{A}^\top (i.e., R linearly independent rows of \mathbf{A}). Let $\mathbf{R} = \mathbf{C}_0^\top$ and $\mathbf{Z} = \mathbf{W}_0^\top$, the row ID is obtained by $\mathbf{A} = \mathbf{Z}\mathbf{R}$.

For the two-sided ID, recall from the skeleton decomposition. When \mathbf{U} is the intersection of \mathbf{C} and \mathbf{R} , it follows that $\mathbf{A} = \mathbf{C}\mathbf{U}^{-1}\mathbf{R}$. Thus, we have $\mathbf{C}\mathbf{U}^{-1} = \mathbf{Z}$ by the row ID. And this implies $\mathbf{C} = \mathbf{Z}\mathbf{U}$. By column ID, it follows that $\mathbf{A} = \mathbf{C}\mathbf{W} = \mathbf{Z}\mathbf{U}\mathbf{W}$, which proves the existence of the two-sided ID.

Data storage. For the data storage of each ID, we summarize as follows:

- *Column ID.* It requires MR and $(N - R)R$ floats to store \mathbf{C} and \mathbf{W} , respectively, and R integers to store the indices of the selected columns in \mathbf{A} ;
- *Row ID.* It requires NR and $(M - R)R$ floats to store \mathbf{R} and \mathbf{Z} , respectively, and R integers to store the indices of the selected rows in \mathbf{A} ;
- *Two-Sided ID.* It requires $(M - R)R$, $(N - R)R$, and R^2 floats to store \mathbf{Z} , \mathbf{W} , and \mathbf{U} , respectively. And extra $2R$ integers are required to store the indices of the selected rows and columns in \mathbf{A} .

Further reduction on the storage of two-sided ID for sparse matrix \mathbf{A} . Suppose the column ID of $\mathbf{A} = \mathbf{C}\mathbf{W}$, where $\mathbf{C} = \mathbf{A}[:, J]$, and a good spanning rows index S set of \mathbf{C} could be found:

$$\mathbf{A}[S, :] = \mathbf{C}[S, :]\mathbf{W}.$$

We observe that $\mathbf{C}[S, :] = \mathbf{A}[S, J] \in \mathbb{R}^{R \times R}$, which is nonsingular (since full rank R in the sense of both row rank and column rank). It follows that

$$\mathbf{W} = (\mathbf{A}[S, J])^{-1}\mathbf{A}[S, :].$$

Therefore, there is no need to store the matrix \mathbf{W} explicitly. We only need to store $\mathbf{A}[S, :]$ and $(\mathbf{A}[S, J])^{-1}$. Alternatively, when we are able to compute the inverse of $\mathbf{A}[S, J]$ on the fly, it only requires R integers to store J , and we can recover $\mathbf{A}[S, J]$ from $\mathbf{A}[S, :]$. The storage of $\mathbf{A}[S, :]$ is inexpensive if \mathbf{A} is sparse.

10.5. Bayesian Low-Rank Interpolative Decomposition

The low-rank ID problem of the observed matrix \mathbf{A} can be stated as $\mathbf{A} = \mathbf{C}\mathbf{W} + \mathbf{E}$, where $\mathbf{A} = [\mathbf{a}_1, \mathbf{a}_2, \dots, \mathbf{a}_N] \in \mathbb{R}^{M \times N}$ is approximately factorized into an $M \times K$ matrix $\mathbf{C} \in \mathbb{R}^{M \times K}$ containing K basis columns of \mathbf{A} and a $K \times N$ matrix $\mathbf{W} \in \mathbb{R}^{K \times N}$ with entries no larger than 1 in magnitude; the noise is captured by matrix $\mathbf{E} \in \mathbb{R}^{M \times N}$. The value of K is smaller than the rank R , hence the term low-rank ID.

Various methods exist for computing the low-rank ID of a matrix. The most popular algorithm to compute the low-rank ID approximation is the randomized ID (RID) algorithm

(Liberty et al., 2007). At a high level, the algorithm randomly samples $S > K$ columns from \mathbf{A} , uses column-pivoted QR (CPQR) to select K of those S columns for basis matrix \mathbf{C} , and then computes \mathbf{W} via least squares (Lu, 2021b). S is usually set to $S = 1.2K$ to oversample the columns so as to capture a large portion of the range of \mathbf{A} .

The drawback of the randomized algorithm is that the maximum magnitude of the factored component \mathbf{W} may exceed 1. Though this is not a big issue in many applications, it has potential problems for other applications that have a high requirement for numerical stability. Advani and O’Hagan (2021) even report that the randomized ID may have a magnitude larger than 167, making it less numerically stable. While probabilistic models can easily accommodate constraints on the specific range of the factored matrix. In this light, we focus on the Bayesian ID (BID) of underlying matrices. The Bayesian ID algorithms are proposed in Lu (2022b,c) and is further adapted in a feature selection context by Lu and Osterrieder (2022). Training such models amounts to finding the best rank- K approximation to the observed $M \times N$ target matrix \mathbf{A} under the given loss function. Let $\mathbf{r} \in \{0, 1\}^N$ be the *state vector* with each element indicating the type of the corresponding column, i.e., basis column or interpolated (remaining) column: if $r_n = 1$, then the n -th column \mathbf{a}_n is a basis column; if $r_n = 0$, then \mathbf{a}_n is interpolated using the basis columns plus some error term. Suppose further J is the set of the indices of the selected basis columns (with size K now), I is the set of the indices of the interpolated columns (with size $N - K$) such that

$$\begin{aligned} J \cap I &= \emptyset, & J \cup I &= \{1, 2, \dots, N\}; \\ J = J(\mathbf{r}) &= \{n \mid r_n = 1\}_{n=1}^N, & I = I(\mathbf{r}) &= \{n \mid r_n = 0\}_{n=1}^N. \end{aligned}$$

Then, \mathbf{C} can be described as $\mathbf{C} = \mathbf{A}[:, J]$, where the colon operator implies all indices. The approximation $\mathbf{A} \approx \mathbf{C}\mathbf{W}$ can be equivalently stated that

$$\underset{M \times N}{\mathbf{A}} \approx \underset{M \times K}{\mathbf{C}} \underset{K \times N}{\mathbf{W}} = \underset{M \times N}{\mathbf{X}} \underset{N \times N}{\mathbf{Y}},$$

where $\mathbf{X} \in \mathbb{R}^{M \times N}$ and $\mathbf{Y} \in \mathbb{R}^{N \times N}$ with

$$\begin{aligned} \mathbf{X}[:, J] &= \mathbf{C} \in \mathbb{R}^{M \times K}, & \mathbf{X}[:, I] &= \mathbf{0} \in \mathbb{R}^{M \times (N-K)}; \\ \mathbf{Y}[J, :] &= \mathbf{W} \in \mathbb{R}^{K \times N}, & \mathbf{Y}[I, :] &= \text{random matrix} \in \mathbb{R}^{(N-K) \times N}. \end{aligned}$$

We also notice that there exists an identity matrix $\mathbf{I}_K \in \mathbb{R}^{K \times K}$ in \mathbf{W} and \mathbf{Y} :

$$\mathbf{I}_K = \mathbf{W}[:, J] = \mathbf{Y}[J, J]. \quad (10.5)$$

To find the low-rank ID of $\mathbf{A} \approx \mathbf{C}\mathbf{W}$ then can be transformed into the problem of finding the $\mathbf{A} \approx \mathbf{X}\mathbf{Y}$ with state vector \mathbf{r} recovering the submatrix \mathbf{C} (see Figure 10.3). To evaluate the approximation, *reconstruction error* measured by mean squared error (MSE or Frobenius norm) is minimized:

$$\min_{\mathbf{W}, \mathbf{Z}} \frac{1}{MN} \sum_{n=1}^N \sum_{m=1}^M \left(a_{mn} - \mathbf{x}_m^\top \mathbf{y}_n \right)^2, \quad (10.6)$$

where \mathbf{x}_m and \mathbf{y}_n are the m -th **row** of \mathbf{X} and n -th **column** of \mathbf{Y} , respectively. We approach the magnitude constraint in \mathbf{W} and \mathbf{Y} by considering the Bayesian ID model as a latent

factor model. And we describe a fully specified graphical model for the problem and employ Bayesian learning methods to infer the latent factors. In this sense, explicit magnitude constraints are not required on the latent factors, since this is naturally taken care of by the appropriate choice of prior distribution; here we use a general-truncated-normal (GTN) prior (Definition 3.4.2, p. 60).

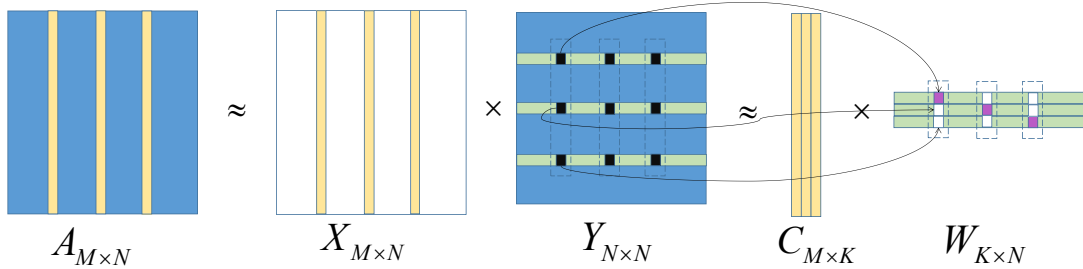


Figure 10.3: Demonstration of the interpolative decomposition of a matrix, where the yellow vector denotes the basis columns of matrix A , white entries denote zero, purple entries denote one, blue and black entries denote elements that are not necessarily zero. The Bayesian ID models find the approximation $A \approx XY$, while the post-processing procedure calculates the approximation $A \approx CW$.

Bayesian GBT and GBTN models for ID. We then introduce the Bayesian ID model called the *GBT* model. To further promote flexibility and insensitivity in the hyperparameter choices, we also introduce the hierarchical model known as the *GBTN* algorithm, which has simple conditional density forms with a little extra computation. We further provide an example to show that the method can be successfully applied to the large, sparse, and very imbalanced Movie-User data set, containing 100,000 user/movie ratings.

Likelihood. We view the data A as being produced according to the probabilistic generative process shown in Figure 10.4. The observed (m, n) -th entry a_{mn} of matrix A is modeled using a Gaussian likelihood function with variance σ^2 and a mean given by the latent decomposition $\mathbf{x}_m^\top \mathbf{y}_n$ (Equation (10.6)):

$$p(a_{mn} | \mathbf{x}_m^\top \mathbf{y}_n, \sigma^2) = \mathcal{N}(a_{mn} | \mathbf{x}_m^\top \mathbf{y}_n, \sigma^2);$$

$$p(\mathbf{A} | \boldsymbol{\theta}) = \prod_{m,n=1}^{M,N} \mathcal{N}(a_{mn} | (\mathbf{XY})_{mn}, \sigma^2) = \prod_{m,n=1}^{M,N} \mathcal{N}(a_{mn} | (\mathbf{XY})_{mn}, \tau^{-1}), \quad (10.7)$$

where $\boldsymbol{\theta} = \{\mathbf{X}, \mathbf{Y}, \sigma^2\}$ denotes all parameters in the model, $\mathcal{N}(\cdot | \cdot)$ is a Gaussian distribution, σ^2 is the variance, and $\tau^{-1} = \sigma^2$ is the precision.

Prior. We choose a conjugate prior over the data variance, an inverse-Gamma distribution with shape α_σ and scale β_σ ,

$$p(\sigma^2 | \alpha_\sigma, \beta_\sigma) = \mathcal{G}^{-1}(\sigma^2 | \alpha_\sigma, \beta_\sigma). \quad (10.8)$$

While it can also be equivalently given a conjugate Gamma prior $\mathcal{G}(\tau | \alpha_\tau, \beta_\tau)$ over the precision $\tau = \frac{1}{\sigma^2}$, and we shall not repeat the details (see Equation (6.17), p. 148 in GGG model).

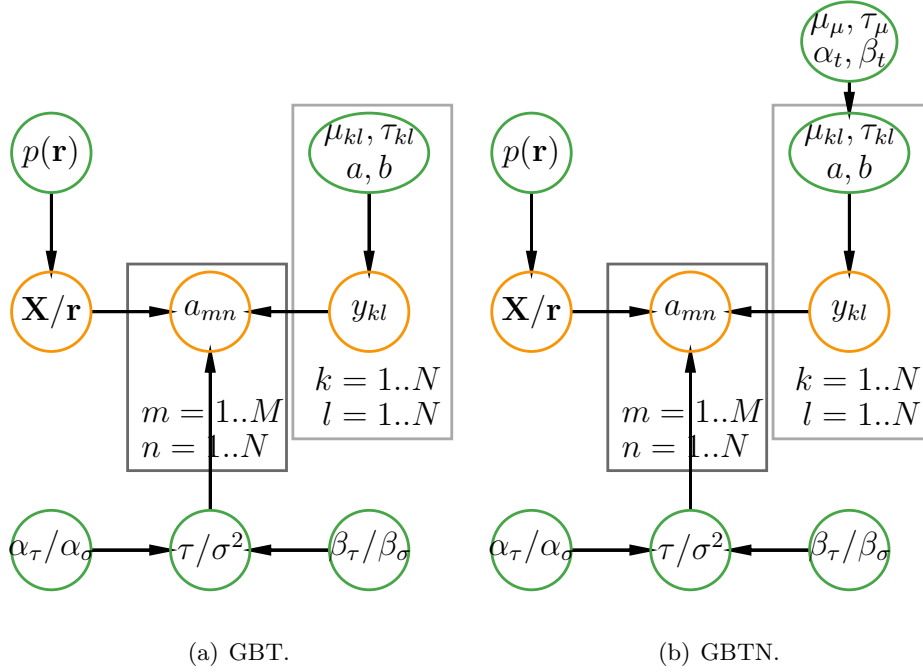


Figure 10.4: Graphical representation of GBT and GBTN models. Orange circles represent observed and latent variables, green circles denote prior variables, and plates represent repeated variables. The slash “/” in the variable represents “or,” and the comma “,” in the variable represents “and.” Parameters a and b are fixed with $a = -1$ and $b = 1$ in our case; while a weaker construction can set them to $a = -2$ and $b = 2$.

We treat the latent variables y_{kl} ’s as random variables (with $k, l \in \{1, 2, \dots, N\}$, see Figure 10.4). And we need prior densities over these latent variables to express beliefs for their values, e.g., constraint with magnitudes smaller than 1 in this context. Here we assume further that the latent variable y_{kl} ’s are independently drawn from a general-truncated-normal (GTN) prior (Definition 3.4.2, p. 60):

$$\begin{aligned}
 p(y_{kl} | \cdot) &= \mathcal{GTN}(y_{kl} | \mu_{kl}, (\tau_{kl})^{-1}, a = -1, b = 1) \\
 &= \frac{\sqrt{\frac{\tau_{kl}}{2\pi}} \exp\{-\frac{\tau_{kl}}{2}(y_{kl} - \mu_{kl})^2\}}{\Phi((b - \mu_{kl}) \cdot \sqrt{\tau_{kl}}) - \Phi((a - \mu_{kl}) \cdot \sqrt{\tau_{kl}})} \cdot \mathbf{1}(a \leq y_{kl} \leq b), \tag{10.9}
 \end{aligned}$$

where $\mathbf{1}(a \leq x \leq b)$ is a step function that has a value of 1 when $a \leq x \leq b$, and 0 when $x < a$ or $a > b$. This prior serves to enforce the constraint on the components \mathbf{Y} with no entry of \mathbf{Y} having an absolute value greater than 1, and is conjugate to the Gaussian likelihood (Equation (3.19), p. 60). The posterior density is also a GTN distribution. While in a weaker construction of interpolative decomposition, the constraint on the magnitude can be relaxed to 2; the GTN prior is flexible in that the parameters can adapt to this change by adjusting to $a = -2$ and $b = 2$ accordingly.

Hierarchical prior. To further favor flexibility, we choose a convenient joint hyperprior density over the parameters $\{\mu_{kl}, \tau_{kl}\}$ of GTN prior in Equation (10.9), namely, the GTN-scaled-normal-Gamma (GTNSNG) prior,

$$\begin{aligned} p(\mu_{kl}, \tau_{kl} \mid \cdot) &= \mathcal{GTNSNG}(\mu_{kl}, \tau_{kl} \mid \mu_\mu, \frac{1}{\tau_\mu}, \alpha_t, \beta_t) \\ &= \left\{ \Phi((b - \mu_\mu) \cdot \sqrt{\tau_\mu}) - \Phi((a - \mu_\mu) \cdot \sqrt{\tau_\mu}) \right\} \cdot \mathcal{N}(\mu_{kl} \mid \mu_\mu, (\tau_\mu)^{-1}) \cdot \mathcal{G}(\tau_{kl} \mid \alpha_t, \beta_t). \end{aligned} \quad (10.10)$$

See Figure 10.4(b). This prior can decouple parameters $\{\mu_{kl}\}$ and $\{\tau_{kl}\}$, and their posterior conditional densities are normal and Gamma, respectively, due to this convenient scale.

Terminology. Following again the Bayesian matrix factorization terminology in Section 6.1 (p. 139), the Bayesian ID models are referred to as the *GBT* and *GBTN* models, where the letter “*B*” stands for Beta-Bernoulli density intrinsically.

10.5.1 Gibbs Sampler

In this section, we provide the derivation of the Gibbs sampler for the discussed Bayesian ID models.

Update of latent variables. The conditional posterior density of y_{kl} is a GTN distribution. Denote all elements of \mathbf{Y} except y_{kl} by \mathbf{Y}_{-kl} , and following the graphical representation of the GBT (or the GBTN) model shown in Figure 10.4, the conditional posterior density of y_{kl} can be obtained by

$$\begin{aligned} & p(y_{kl} \mid \mathbf{A}, \mathbf{X}, \mathbf{Y}_{-kl}, \mu_{kl}, \tau_{kl}, \sigma^2) \propto p(\mathbf{A} \mid \mathbf{X}, \mathbf{Y}, \sigma^2) \cdot p(y_{kl} \mid \mu_{kl}, \tau_{kl}) \\ &= \prod_{i,j=1}^{M,N} \mathcal{N}(a_{ij} \mid \mathbf{x}_i^\top \mathbf{y}_j, \sigma^2) \times \mathcal{GTN}(y_{kl} \mid \mu_{kl}, (\tau_{kl})^{-1}, a = -1, b = 1) \\ &\propto \exp \left\{ -\frac{1}{2\sigma^2} \sum_{i,j=1}^{M,N} (a_{ij} - \mathbf{x}_i^\top \mathbf{y}_j)^2 \right\} \exp \left\{ -\frac{\tau_{kl}}{2} (y_{kl} - \mu_{kl})^2 \right\} u(y_{kl} \mid a, b) \\ &\propto \exp \left\{ -\frac{1}{2\sigma^2} \sum_i^M (a_{il} - \mathbf{x}_i^\top \mathbf{y}_l)^2 \right\} \exp \left\{ -\frac{\tau_{kl}}{2} (y_{kl} - \mu_{kl})^2 \right\} u(y_{kl} \mid a, b) \\ &\propto \exp \left\{ -\frac{1}{2\sigma^2} \sum_i^M \left(x_{ik}^2 y_{kl}^2 + 2x_{ik} y_{kl} \left(\sum_{j \neq k}^N x_{ij} y_{jl} - a_{il} \right) \right) \right\} \exp \left\{ -\frac{\tau_{kl}}{2} (y_{kl} - \mu_{kl})^2 \right\} u(y_{kl} \mid a, b) \\ &\propto \exp \left\{ -y_{kl}^2 \underbrace{\left(\frac{\sum_i^M x_{ik}^2}{2\sigma^2} + \frac{\tau_{kl}}{2} \right)}_{\frac{1}{2} \tilde{\tau}} + y_{kl} \underbrace{\left(\frac{1}{\sigma^2} \sum_i^M x_{ik} (a_{il} - \sum_{j \neq k}^N x_{ij} y_{jl}) + \tau_{kl} \mu_{kl} \right)}_{\tilde{\tau} \tilde{\mu}} \right\} u(y_{kl} \mid a, b) \\ &\propto \mathcal{N}(y_{kl} \mid \tilde{\mu}, (\tilde{\tau})^{-1}) u(y_{kl} \mid a, b) \propto \mathcal{GTN}(y_{kl} \mid \tilde{\mu}, (\tilde{\tau})^{-1}, a = -1, b = 1), \end{aligned} \quad (10.11)$$

where again, for simplicity, we assume the **rows** of \mathbf{X} are denoted by \mathbf{x}_i 's and **columns** of \mathbf{Y} are denoted by \mathbf{y}_j 's, $\tilde{\tau} = \frac{\sum_i^M x_{ik}^2}{\sigma^2} + \tau_{kl}$ is the posterior ‘‘parent’’ precision of the GTN density, and the posterior ‘‘parent’’ mean of the GTN density is

$$\tilde{\mu} = \left(\frac{1}{\sigma^2} \sum_i^M x_{ik} (a_{il} - \sum_{j \neq k}^N x_{ij} y_{jl}) + \tau_{kl} \mu_{kl} \right) / \tilde{\tau}.$$

Update of variance parameter. The conditional density of σ^2 is an inverse-Gamma distribution by conjugacy:

$$p(\sigma^2 \mid \mathbf{X}, \mathbf{Y}, \mathbf{A}) = \mathcal{G}^{-1}(\sigma^2 \mid \tilde{\alpha}_\sigma, \tilde{\beta}_\sigma), \quad (10.12)$$

where $\tilde{\alpha}_\sigma = \frac{MN}{2} + \alpha_\sigma$, $\tilde{\beta}_\sigma = \frac{1}{2} \sum_{i,j=1}^{M,N} (a_{ij} - \mathbf{x}_i^\top \mathbf{y}_j)^2 + \beta_\sigma$.

Update of state vector for GBT and GBTN without ARD. Suppose further that $\mathbf{r} \in \{0, 1\}^N$ is the state vector with each element indicating the type of the corresponding column. If $r_n = 1$, then \mathbf{a}_n is a basis column; otherwise, \mathbf{a}_n is interpolated using the basis columns plus some error term. Given the state vector $\mathbf{r} = [r_1, r_2, \dots, r_N]^\top \in \mathbb{R}^N$, the relation between \mathbf{r} and the index sets J is simple; $J = J(\mathbf{r}) = \{n \mid r_n = 1\}_{n=1}^N$ and $I = I(\mathbf{r}) = \{n \mid r_n = 0\}_{n=1}^N$. A new value of state vector \mathbf{r} is to select one index j from index set J and another index i from index set I (we note that $r_j = 1$ and $r_i = 0$ for the old state vector \mathbf{r}) such that

$$\begin{aligned} & j \in J, \\ & i \in I; \\ o_j &= \frac{p(r_j = 0, r_i = 1 \mid \mathbf{A}, \sigma^2, \mathbf{Y}, \mathbf{r}_{-ji})}{p(r_j = 1, r_i = 0 \mid \mathbf{A}, \sigma^2, \mathbf{Y}, \mathbf{r}_{-ji})} \\ &= \frac{p(r_j = 0, r_i = 1)}{p(r_j = 1, r_i = 0)} \times \frac{p(\mathbf{A} \mid \sigma^2, \mathbf{Y}, \mathbf{r}_{-ji}, r_j = 0, r_i = 1)}{p(\mathbf{A} \mid \sigma^2, \mathbf{Y}, \mathbf{r}_{-ji}, r_j = 1, r_i = 0)}, \end{aligned} \quad (10.13)$$

where \mathbf{r}_{-ji} denotes all elements of \mathbf{r} except j -th and i -th entries. Under a weak construction, we can set $p(r_j = 0, r_i = 1) = p(r_j = 1, r_i = 0)$. Then, the full conditional probability of $p(r_j = 0, r_i = 1 \mid \mathbf{A}, \sigma^2, \mathbf{Y}, \mathbf{r}_{-ji})$ can be calculated by

$$p(r_j = 0, r_i = 1 \mid \mathbf{A}, \sigma^2, \mathbf{Y}, \mathbf{r}_{-ji}) = \frac{o_j}{1 + o_j}. \quad (10.14)$$

Extra update for GBTN model. Following the conceptual representation of the GBTN model in Figure 10.4, the conditional density of μ_{kl} can be obtained by

$$\begin{aligned}
& p(\mu_{kl} \mid \tau_{kl}, \mu_\mu, \tau_\mu, \alpha_t, \beta_t, y_{kl}) \\
& \propto \mathcal{GTN}(y_{kl} \mid \mu_{kl}, (\tau_{kl})^{-1}, a = -1, b = 1) \cdot \mathcal{GTNSNG}(\mu_{kl}, \tau_{kl} \mid \mu_\mu, (\tau_\mu)^{-1}, \alpha_t, \beta_t) \\
& \propto \mathcal{GTN}(y_{kl} \mid \mu_{kl}, (\tau_{kl})^{-1}, a = -1, b = 1) \cdot \left\{ \Phi((b - \mu_\mu) \cdot \sqrt{\tau_\mu}) - \Phi((a - \mu_\mu) \cdot \sqrt{\tau_\mu}) \right\} \\
& \quad \cdot \mathcal{N}(\mu_{kl} \mid \mu_\mu, (\tau_\mu)^{-1}) \cdot \mathcal{G}(\tau_{kl} \mid \alpha_t, \beta_t) \\
& \propto \sqrt{\tau_{kl}} \cdot \exp \left\{ -\frac{\tau_{kl}}{2} (y_{kl} - \mu_{kl})^2 \right\} \cdot \exp \left\{ -\frac{\tau_\mu}{2} (\mu_\mu - \mu_{kl})^2 \right\} \\
& \propto \exp \left\{ -\mu_{kl}^2 \underbrace{\frac{\tau_{kl} + \tau_\mu}{2}}_{\frac{1}{2}\tilde{t}} + \mu_{kl} \underbrace{(\tau_{kl}y_{kl} + \tau_\mu\mu_\mu)}_{\tilde{m}\tilde{t}} \right\} \propto \mathcal{N}(\mu_{kl} \mid \tilde{m}, (\tilde{t})^{-1}),
\end{aligned} \tag{10.15}$$

where $\tilde{t} = \tau_{kl} + \tau_\mu$ and $\tilde{m} = (\tau_{kl}y_{kl} + \tau_\mu\mu_\mu)/\tilde{t}$ are the posterior precision and mean of the normal density, respectively. Similarly, the conditional density of τ_{kl} is,

$$\begin{aligned}
& p(\tau_{kl} \mid \mu_{kl}, \mu_\mu, \tau_\mu, \alpha_t, \beta_t, y_{kl}) \\
& \propto \mathcal{GTN}(y_{kl} \mid \mu_{kl}, (\tau_{kl})^{-1}, a = -1, b = 1) \cdot \mathcal{GTNSNG}(\mu_{kl}, \tau_{kl} \mid \mu_\mu, (\tau_\mu)^{-1}, \alpha_t, \beta_t) \\
& \propto \mathcal{GTN}(y_{kl} \mid \mu_{kl}, (\tau_{kl})^{-1}, a = -1, b = 1) \cdot \left\{ \Phi((b - \mu_\mu) \cdot \sqrt{\tau_\mu}) - \Phi((a - \mu_\mu) \cdot \sqrt{\tau_\mu}) \right\} \\
& \quad \cdot \mathcal{N}(\mu_{kl} \mid \mu_\mu, (\tau_\mu)^{-1}) \cdot \mathcal{G}(\tau_{kl} \mid \alpha_t, \beta_t) \\
& \propto \exp \left\{ -\tau_{kl} \frac{(y_{kl} - \mu_{kl})^2}{2} \right\} \tau_{kl}^{1/2} \tau_{kl}^{\alpha_t - 1} \exp \{-\beta_t \tau_{kl}\} \\
& \propto \exp \left\{ -\tau_{kl} \left[\beta_t + \frac{(y_{kl} - \mu_{kl})^2}{2} \right] \right\} \cdot \tau_{kl}^{(\alpha_t + 1/2) - 1} \propto \mathcal{G}(\tau_{kl} \mid \tilde{a}, \tilde{b}),
\end{aligned} \tag{10.16}$$

where $\tilde{a} = \alpha_t + 1/2$ and $\tilde{b} = \beta_t + \frac{(y_{kl} - \mu_{kl})^2}{2}$ are the posterior parameters of the Gamma density. The full procedure is then formulated in Algorithm 23 for GBT and GBTN models.

10.5.2 Aggressive Update

In Algorithm 23, we notice that we set $\mathbf{X}[:, I] = \mathbf{0}$ when the new state vector \mathbf{r} is sampled. However, in the next iteration step, the index set I may be updated, in which case one entry i of I may be altered to have a value of 1:

$$r_i = 0 \rightarrow r_i = 1.$$

This may cause problems in the update of y_{kl} in Equation (10.11), a zero i -th column in \mathbf{X} cannot update \mathbf{Y} accordingly. One solution is to record a proposal state vector \mathbf{r}_2 and a proposal factor matrix \mathbf{X}_2 from the \mathbf{r}_2 vector. When the update in the next iteration selects the old state vector \mathbf{r} , the factor matrix \mathbf{X} is adopted to finish the updates; while the algorithm chooses the proposal state vector \mathbf{r}_2 , the proposal factor matrix \mathbf{X}_2 is applied to do the updates. We call this procedure the *aggressive* update. The *aggressive* sampler for the GBT model is formulated in Algorithm 24. For the sake of simplicity, we don't include the sampler for the GBTN model because it may be done in a similar way.

Algorithm 23 Gibbs sampler for GBT and GBTN ID models. The procedure presented here may not be efficient but is explanatory. A more efficient one can be implemented in a vectorized manner. By default, uninformative priors are $a = -1, b = 1, \alpha_\sigma = 0.1, \beta_\sigma = 1, (\{\mu_{kl}\} = 0, \{\tau_{kl}\} = 1)$ for GBT, $(\mu_\mu = 0, \tau_\mu = 0.1, \alpha_t = \beta_t = 1)$ for GBTN.

```

1: for  $t = 1$  to  $T$  do ▷  $T$  iterations
2:   Sample state vector  $\mathbf{r}$  from Equation (10.14);
3:   Update matrix  $\mathbf{X}$  by  $\mathbf{A}[:, J]$  where index vector  $J$  is the index of  $\mathbf{r}$  with value 1 and
   set  $\mathbf{X}[:, I] = \mathbf{0}$  where index vector  $I$  is the index of  $\mathbf{r}$  with value 0;
4:   Sample  $\sigma^2$  from  $p(\sigma^2 \mid \mathbf{X}, \mathbf{Y}, \mathbf{A})$  in Equation (10.12);
5:   for  $k = 1$  to  $N$  do
6:     for  $l = 1$  to  $N$  do
7:       Sample  $y_{kl}$  from Equation (10.11);
8:       (GBTN only) Sample  $\mu_{kl}$  from Equation (10.15);
9:       (GBTN only) Sample  $\tau_{kl}$  from Equation (10.16);
10:    end for
11:  end for
12:  Report loss in Equation (10.6), stop if it converges.
13: end for
14: Report mean loss in Equation (10.6) after burn-in iterations.

```

Algorithm 24 *Aggressive* Gibbs sampler for GBT ID model. The procedure presented here may not be efficient but is explanatory. A more efficient one can be implemented in a vectorized manner. By default, uninformative priors are $a = -1, b = 1, \alpha_\sigma = 0.1, \beta_\sigma = 1, (\{\mu_{kl}\} = 0, \{\tau_{kl}\} = 1)$ for GBT.

```

1: for  $t = 1$  to  $T$  do ▷  $T$  iterations
2:   Sample state vector  $\mathbf{r}$  from  $\{\mathbf{r}_1, \mathbf{r}_2\}$  by Equation (10.14);
3:   Decide  $\mathbf{Y}$ :  $\mathbf{Y} = \mathbf{Y}_1$  if  $\mathbf{r}$  is  $\mathbf{r}_1$ ;  $\mathbf{Y} = \mathbf{Y}_2$  if  $\mathbf{r}$  is  $\mathbf{r}_2$ ;
4:   Update state vector  $\mathbf{r}_1 = \mathbf{r}$ ;
5:   Sample proposal state vector  $\mathbf{r}_2$  based on  $\mathbf{r}$ ;
6:   Update matrix  $\mathbf{X}$  by  $\mathbf{r} = \mathbf{r}_1$ ;
7:   Update proposal  $\mathbf{X}_2$  by  $\mathbf{r}_2$ ;
8:   Sample  $\sigma^2$  from  $p(\sigma^2 \mid \mathbf{X}, \mathbf{Y}, \mathbf{A})$  in Equation (10.12);
9:   Sample  $\mathbf{Y}_1 = \{y_{kl}\}$  using  $\mathbf{X}$ ;
10:  Sample  $\mathbf{Y}_2 = \{y_{kl}\}$  using  $\mathbf{X}_2$ ;
11:  Report loss in Equation (10.6), stop if it converges.
12: end for
13: Report mean loss in Equation (10.6) after burn-in iterations.

```

10.5.3 Post-Processing

The Gibbs sampling algorithm finds the approximation $\mathbf{A} \approx \mathbf{X}\mathbf{Y}$, where $\mathbf{X} \in \mathbb{R}^{M \times N}$ and $\mathbf{Y} \in \mathbb{R}^{N \times N}$. As stated above, the redundant columns in \mathbf{X} and redundant rows in \mathbf{Y} can

be removed by the index vector J :

$$\begin{aligned}\mathbf{C} &= \mathbf{X}[:, J] = \mathbf{A}[:, J], \\ \mathbf{W} &= \mathbf{Y}[J, :].\end{aligned}$$

Since the submatrix $\mathbf{Y}[J, J] = \mathbf{W}[:, J]$ (Equation (10.5)) from the Gibbs sampling procedure is not enforced to be an identity matrix (as required in the interpolative decomposition). We need to set it to be an identity matrix manually. This will basically reduce the reconstructive error further. The post-processing procedure is shown in Figure 10.3.

10.5.4 Bayesian ID with Automatic Relevance Determination

We further extend the Bayesian models with automatic relevance determination (ARD) to eliminate the need for model selection. Given the state vector $\mathbf{r} = [r_1, r_2, \dots, r_N]^\top \in \mathbb{R}^N$ whose index sets are $J = J(\mathbf{r}) = \{n \mid r_n = 1\}_{n=1}^N$ and $I = I(\mathbf{r}) = \{n \mid r_n = 0\}_{n=1}^N$. A new value of state vector \mathbf{r} is to select one index j from either the index set J or the index set I such that

$$\begin{aligned}j &\in J \cup I; \\ o_j &= \frac{p(r_j = 0 \mid \mathbf{A}, \sigma^2, \mathbf{Y}, \mathbf{r}_{-j})}{p(r_j = 1 \mid \mathbf{A}, \sigma^2, \mathbf{Y}, \mathbf{r}_{-j})} = \frac{p(r_j = 0)}{p(r_j = 1)} \times \frac{p(\mathbf{A} \mid \sigma^2, \mathbf{Y}, \mathbf{r}_{-j}, r_j = 0)}{p(\mathbf{A} \mid \sigma^2, \mathbf{Y}, \mathbf{r}_{-j}, r_j = 1)},\end{aligned}\quad (10.17)$$

where \mathbf{r}_{-j} denotes all elements of \mathbf{r} except the j -th element. Comparing Equation (10.17) with Equation (10.13), we may find that in the former equation, the number of selected columns is not fixed now. Therefore, we let the inference decide the number of columns in basis matrix \mathbf{C} of interpolative decomposition. Again, we can set $p(r_j = 0) = p(r_j = 1) = 0.5$. Then the full conditional probability of $p(r_j = 0, r_i = 1 \mid \mathbf{A}, \sigma^2, \mathbf{Y}, \mathbf{r}_{-ji})$ can be calculated by

$$p(r_j = 0 \mid \mathbf{A}, \sigma^2, \mathbf{Y}, \mathbf{r}_{-j}) = \frac{o_j}{1 + o_j}.\quad (10.18)$$

The full algorithm of GBT and GBTN with ARD is described in Algorithm 25, where the difference lies in that we need to iterate over all elements of the state vector rather than just one or two elements of it. We aware that many elements in the state vector can change their signs, making the update of matrix \mathbf{Y} unstable. Therefore, we also define a number of *critical steps* ν : after sampling the whole state vector \mathbf{r} , we update several times (here we repeat ν times) for the matrix \mathbf{Y} and its related parameters (the difference is highlighted in blue of Algorithm 25).

10.5.5 Examples for Bayesian ID

To evaluate the strategy and demonstrate the main advantages of the Bayesian ID method, we conduct experiments with different analysis tasks; and different data sets including Cancer Cell Line Encyclopedia (CCLE *EC50* and CCLE *IC50* data sets (Barretina et al., 2012)), cancer driver genes (Gene Body Methylation (Koboldt et al., 2012)), and the promoter region (Promoter Methylation (Koboldt et al., 2012)) from bioinformatics. Following Brouwer and Lio (2017), we preprocess these data sets by capping high values to 100 and undoing the natural log transform for the former three data sets. Then we standardize to

Algorithm 25 Gibbs sampler for GBT and GBTN ID with *ARD* models. The procedure presented here can be inefficient but is explanatory. While a vectorized manner can be implemented to find a more efficient algorithm. By default, weak priors are $a = -1, b = 1, \alpha_\sigma = 0.1, \beta_\sigma = 1, (\{\mu_{kl}\} = 0, \{\tau_{kl}\} = 1)$ for GBT, $(\mu_\mu = 0, \tau_\mu = 0.1, \alpha_t = \beta_t = 1)$ for GBTN. **Number of critical steps:** ν .

```

1: for  $t = 1$  to  $T$  do ▷  $T$  iterations
2:   for  $j = 1$  to  $N$  do
3:     Sample state vector element  $r_j$  from Equation (10.18);
4:   end for
5:   Update matrix  $\mathbf{X}$  by  $\mathbf{A}[:, J]$  where index vector  $J$  is the index of  $\mathbf{r}$  with value 1 and
   set  $\mathbf{X}[:, I] = \mathbf{0}$  where index vector  $I$  is the index of  $\mathbf{r}$  with value 0;
6:   Sample  $\sigma^2$  from  $p(\sigma^2 | \mathbf{X}, \mathbf{Y}, \mathbf{A})$  in Equation (10.12);
7:   for  $n = 1$  to  $\nu$  do
8:     for  $k = 1$  to  $N$  do
9:       for  $l = 1$  to  $N$  do
10:        Sample  $y_{kl}$  from Equation (10.11);
11:        (GBTN only) Sample  $\mu_{kl}$  from Equation (10.15);
12:        (GBTN only) Sample  $\tau_{kl}$  from Equation (10.16);
13:      end for
14:    end for
15:  end for
16:  Output loss in Equation (10.6), stop iteration if it converges.
17: end for
18: Output averaged loss in Equation (10.6) for evaluation after burn-in iterations.

```

Data set	Num. Rows	Num. Columns	Fraction observed	Matrix rank
CCLC <i>EC50</i>	502	48	0.632	24
CCLC <i>IC50</i>	504	48	0.965	24
Gene Body Methylation	160	254	1.000	160
Promoter Methylation	160	254	1.000	160

Table 10.1: Overview of the CCLC *EC50*, CCLC *IC50*, Gene Body Methylation, and Promoter Methylation data sets, giving the number of rows, columns, the fraction of entries that are observed, and the matrix rank.

have zero-mean and unit variance for all data sets, and fill missing entries by 0. Finally, we copy every column twice (for the CCLC *EC50* and CCLC *IC50* data sets) in order to **increase redundancy** in the matrix; while for the latter two (Gene Body Methylation and Promoter Methylation data sets), the number of columns is already larger than the matrix rank such that we do not increase any redundancy. A summary of the four data sets is reported in Table 10.1, and their distributions are presented in Figure 10.5.

In all scenarios, the same parameter initialization is adopted when conducting different tasks. Experimental evidence reveals that post-processing procedure can increase performance to a minor extent, and that the outcomes of the GBT and GBTN models are

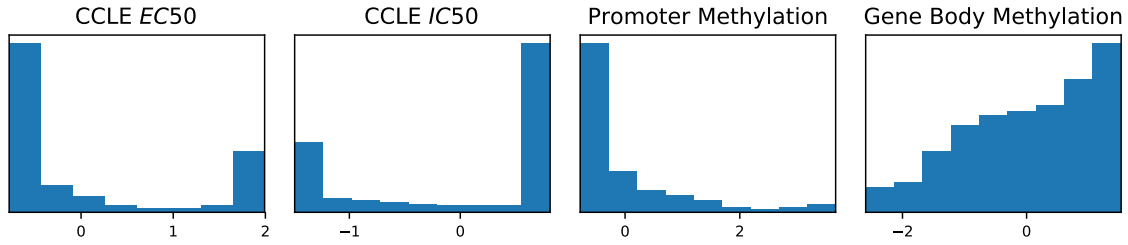


Figure 10.5: Data distribution of CCLE *EC50*, CCLE *IC50*, Gene Body Methylation, and Promoter Methylation data sets.

	K_1	K_2	K_3	K_4	GBT (ARD)	GBTN (ARD)
CCLE <i>EC50</i>	0.354	0.218	0.131	0.046	0.034	0.031
CCLE <i>IC50</i>	0.301	0.231	0.161	0.103	0.035	0.031
Gene Body Methylation	0.433	0.443	0.466	0.492	0.363	0.372
Promoter Methylation	0.323	0.319	0.350	0.337	0.252	0.263

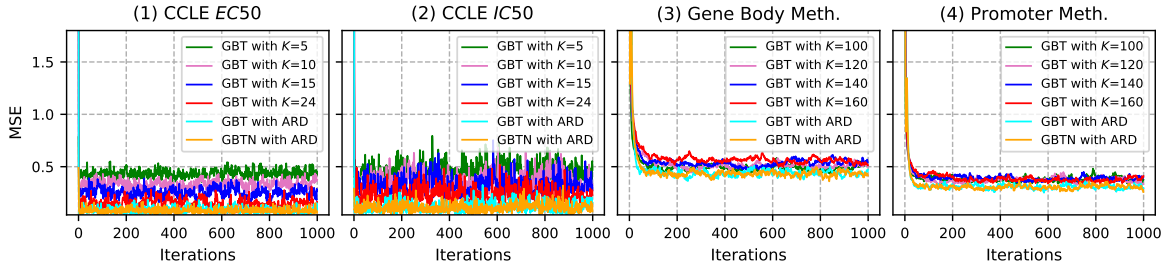
Table 10.2: Mean squared error measure with various latent dimension K parameters for CCLE *EC50*, CCLE *IC50*, Gene Body Methylation, and Promoter Methylation data sets. In all cases, K_4 is the full rank of each matrix, $K_1 = 5, K_2 = 10, K_3 = 15$ for the former two data sets, and $K_1 = 100, K_2 = 120, K_3 = 140$ for the latter two data sets. Results of GBT and GBTN with ARD surpass those of the GBT and GBTN with full rank K_4 .

relatively similar (Lu, 2022b). For clarification, we only provide the findings of the GBT model after post-processing. We compare the results of ARD versions of GBT and GBTN with vanilla GBT and GBTN algorithms. In a wide range of experiments across various data sets, the GBT or GBTN with ARD models improve reconstructive error and lead to performance that is as good or better than the vanilla GBT or GBTN methods in low-rank ID approximation.

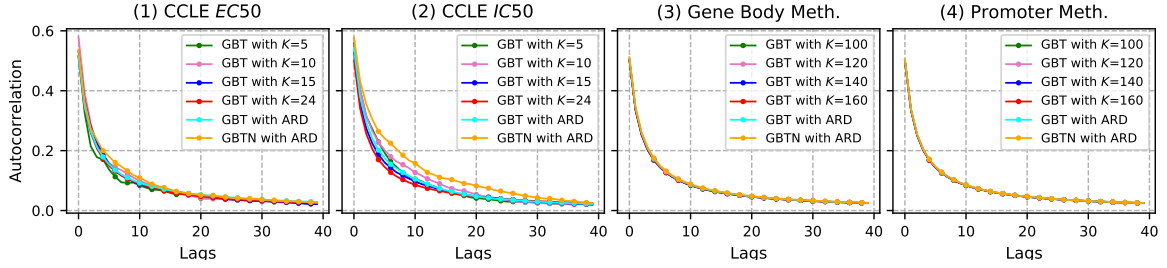
In order to measure overall decomposition performance, we use mean squared error (MSE, Equation (10.6)), which measures the similarity between the true and reconstructive; the smaller the better performance.

10.5.6 Hyper-parameters

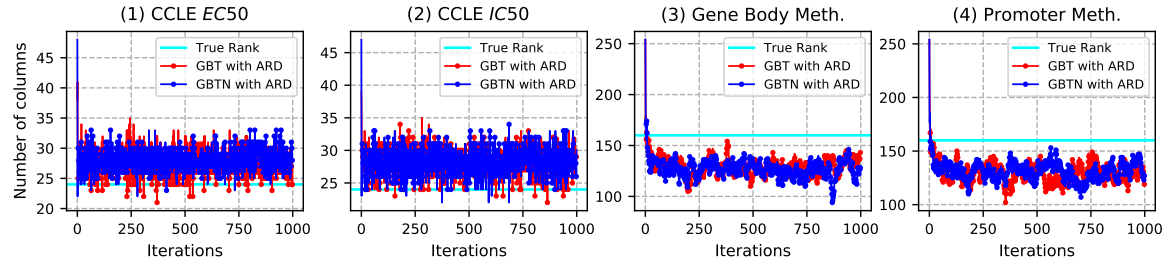
In this experiments, we use $a = -1, b = 1, \alpha_\sigma = 0.1, \beta_\sigma = 1, (\{\mu_{kl}\} = 0, \{\tau_{kl}\} = 1)$ for GBT, $(\mu_\mu = 0, \tau_\mu = 0.1, \alpha_t = \beta_t = 1)$ for GBTN, and critical steps $\nu = 5$ for GBT and GBTN with ARD. The adopted parameters are very uninformative and weak prior choices, and the models are insensitive to them. The observed or unobserved variables are initialized from random draws as long as these hyper-parameters are fixed since this initialization method provides a better initial guess of the correct patterns in the matrices. In all scenarios, we run the Gibbs sampling 1,000 iterations with a burn-in of 100 iterations and a thinning of 5 iterations, as the convergence analysis shows the algorithm can converge in less than 100 iterations.



(a) Convergence of the models on the CCLE *EC50*, CCLE *IC50*, Gene Body Methylation, and Promoter Methylation data sets, measured by the data fit (MSE). The algorithm almost converges in less than 500 iterations.



(b) Averaged autocorrelation coefficients of samples of y_{kl} computed using Gibbs sampling on the CCLE *EC50*, CCLE *IC50*, Gene Body Methylation, and Promoter Methylation data sets.



(c) Convergence of the number of selected columns on the CCLE *EC50*, CCLE *IC50*, Gene Body Methylation, and Promoter Methylation data sets, measured by the data fit (MSE). The algorithm almost converges in less than 100 iterations.

Figure 10.6: Convergence results (upper), sampling mixing analysis (middle), and reconstructive results (lower) on the CCLE *EC50*, CCLE *IC50*, Gene Body Methylation, and Promoter Methylation data sets for various latent dimensions.

10.5.7 Convergence and Comparative Analysis

We first show the rate of convergence over iterations on the CCLE *EC50*, CCLE *IC50*, Gene Body Methylation, and Promoter Methylation data sets. We run the GBT model with $K = 5, 10, 15, 24$ for the CCLE *EC50* and CCLE *IC50* data sets, where $K = 24$ is the full rank of the matrices³, and $K = 100, 120, 140, 160$ for the Gene Body Methylation and Promoter Methylation data sets, where $K = 160$ is the full rank of the matrices; and the error is measured by MSE. Figure 10.6(a) shows the rate of convergence over iterations. Figure 10.6(b) shows the autocorrelation coefficients of samples computed using Gibbs sampling. We observe that the mixings of the GBT and GBTN with ARD are close to those

3. The results of GBT and GBTN without ARD are close so here we only provide the results of GBT for clarity.

without ARD. The coefficients are less than 0.1 when the lags are more than 10, showing the mixing of the Gibbs sampler is good. In all experiments, the algorithm converges in less than 50 iterations. The results on the CCLE *EC50*, Gene Body Methylation, and Promoter Methylation data sets show less noise in the sampling; while on the CCLE *IC50* data set, the sampling of GBT without ARD seems to be noisier than those of GBT and GBTN with ARD.

Comparative results for the GBT and GBTN with ARD and those without ARD on the four data sets are again shown in Figure 10.6(a) and Table 10.2. In all experiments, the GBT and GBTN with ARD achieve the smallest MSE, even compared to the non-ARD versions with latent dimension K setting to the full matrix rank ($K = 24$ for the CCLE *EC50* and CCLE *IC50* data sets, and $K = 160$ for the Gene Body Methylation and Promoter Methylation data sets). Figure 10.6(c) shows the convergence of the number of selected columns for GBT and GBTN with ARD models on each data set. We observe that the samples are walking around 27 for the CCLE *EC50* and CCLE *IC50* data sets; and around 130 for the Gene Body Methylation and Promoter Methylation data sets. These samples are close to the true rank of each matrix. The GBT and GBTN with ARD thus can determine the number of columns inside the factored component \mathbf{X} automatically.

10.6. Bayesian Intervened Interpolative Decomposition (IID)

Expanding on the GBT model, we introduce the the intervened interpolative decomposition (IID) algorithm (Lu and Osterrieder, 2022). The IID algorithm shares the same generative process as expressed in Equation (10.7). It applies an inverse-Gamma prior over the variance parameter σ^2 in Equation (10.8) and a GTN prior over the latent variables y_{kl} 's in Equation (10.9). However, we consider further that some columns of the observed matrix \mathbf{A} are more significant and important, and they *should* be given a higher priority over other columns.

Suppose the importance of each column in the observed matrix \mathbf{A} is captured by a *raw importance vector* $\hat{\mathbf{p}} \in \mathbb{R}^N$, where $\hat{p}_i \in [-\infty, \infty]$ for all i in $\{1, 2, \dots, N\}$. To bring the raw importance vector into the range 0 to 1, we apply the Sigmoid function:

$$\mathbf{p} = \text{Sigmoid}(\hat{\mathbf{p}}),$$

where $\text{Sigmoid}(\cdot)$ represents the function $f(x) = \frac{1}{1+\exp\{-x\}}$ that can return a value in the range of 0 to 1. The Sigmoid function acts as a squashing function because its domain is the set of all real numbers, and its range is $(0, 1)$. Then we take the \mathbf{p} vector as the final *importance vector* to indicate the importance of each column in matrix \mathbf{A} .

Going further from Equation (10.13), the intermediate variable o_j is calculated instead by

$$\begin{aligned} o_j &= \frac{p(r_j = 0, r_i = 1)}{p(r_j = 1, r_i = 0)} \times \frac{p(\mathbf{A} \mid \sigma^2, \mathbf{Y}, \mathbf{r}_{-ji}, r_j = 0, r_i = 1)}{p(\mathbf{A} \mid \sigma^2, \mathbf{Y}, \mathbf{r}_{-ji}, r_j = 1, r_i = 0)} \\ &= \frac{1 - p_j}{p_j} \frac{p_i}{1 - p_i} \times \frac{p(\mathbf{A} \mid \sigma^2, \mathbf{Y}, \mathbf{r}_{-ji}, r_j = 0, r_i = 1)}{p(\mathbf{A} \mid \sigma^2, \mathbf{Y}, \mathbf{r}_{-ji}, r_j = 1, r_i = 0)}. \end{aligned} \quad (10.19)$$

And again, the conditional probability of $p(r_j = 0, r_i = 1 \mid \mathbf{A}, \sigma^2, \mathbf{Y}, \mathbf{r}_{-ji})$ can be obtained by

$$p(r_j = 0, r_i = 1 \mid \mathbf{A}, \sigma^2, \mathbf{Y}, \mathbf{r}_{-ji}) = \frac{o_j}{1 + o_j}. \quad (10.20)$$

Since we intervene in the procedure of the Gibbs sampling outlined in Equation (10.19), hence the name *intervened interpolative decomposition (IID)*.

10.6.1 Quantitative Problem Statement

After the presentation of the algorithms for the intervened interpolative decomposition, the significance and potential practical applications come into focus. It is well known that large quantitative hedge funds and asset managers have been recruiting a significant number of data miners and financial engineers in order to construct effective alphas. The number of alpha components ⁴ might reach into millions or perhaps billions (Tulchinsky, 2019). As a result, creating a meta-alpha (that contains the true trading signals) from all of the alphas or a large fraction of the alpha pool might be troublesome for the following reasons:

1. **Trading volume issues:** if we use the same alphas as others, some illiquid alphas with low volume will be traded heavily. This will make the strategy meaningless due to capacity constraints.
2. **Overfitting concerns:** using too many alphas may result in overfitting, leading to poor out-of-sample (OS) performance.
3. **Dependence challenges:** many alphas might be mutually dependent, and certain machine learning algorithms, such as neural networks and XGBoost models, might uncover their limits caused by multi-linear difficulties while attempting to determine the meta-strategy from the entire set of alphas.
4. **Computational limitations:** finding trading signals from the full alpha pool can be time-consuming because of limited computing resources.
5. **Risk mitigation:** to minimize market risks, we constantly aim to discover a distinct subset of alphas to test alternative methods with low correlation.

For the five reasons stated above, there is an urgent need to design algorithms that choose a small subset of alphas from a large pool of them in order to prevent overfitting, make the final approach more scalable, and obtain the findings in a reasonable amount of time. It is trivial to select an appropriate subset by the *RankIC* metric (see definition below), i.e., we select the alphas having the highest RankIC values. However, the problems still remain that the selected subset will not represent the whole pool of alphas, and the selected alphas may be mutually dependent.

Our objective is to identify as many representative alpha factors as possible with optimal performance. The selected subset of alphas is representative in the sense that the small subset of alphas can be used to reconstruct other alphas with a small replication error. The traditional ID algorithm, either using a *Randomized algorithm* (Liberty et al., 2007) or a Bayesian approach we have discussed above, can only help to find the representative ones. However, the end choices may seem to select alphas with low performance. Using the discussed IID method, on the other hand, can help find the representative (that can

4. Which can be simply treated as features in quantitative finance.

reconstruct other alphas with small error) and the desirable (high RankIC scores) alphas at the same time.

FORMULAIC ALPHAS

WorldQuant, a quantitative investment management firm, previously disclosed 101 formulaic short-term alpha determinants in 2016 (Kakushadze, 2016). Since then, the 191 alpha factors from Guotai Junan Securities (GuotaiJunan, 2017) have also been welcomed by many investors and institutions. These formulaic alpha components are derived from several stock data elements, including, among others, volumes, prices, volatilities, and volume-weighted average prices (vwap). As the name implies, a formulaic alpha is a type of alpha that can be expressed as a formula or a mathematical expression. For example, a *mean-reversion* alpha can be expressed in terms of a mathematical expression as follows:

$$\text{Alpha} = -(\text{close}(\text{today}) - \text{close}(\text{5_days_ago})) / \text{close}(\text{5_days_ago}).$$

In this sense, we take the opposite action as indicated by the closing price: we go short if the price has risen during the previous five days, and we go long otherwise. At a high level, the alpha value indicates the trend of the price in the days to come; the higher the alpha value for each stock, the more likely it is that the stock's price will rise in the next few days.

EVALUATION METRICS

Let r_t denote the yield rate of stock s on the t -th day. Suppose further p_t is the closing price of the asset at time t for all $t \in \{1, 2, \dots, T\}$, the return of the asset at time t can be obtained by the following equation:

$$r_t = \frac{p_t - p_{t-1}}{p_t}. \quad (10.21)$$

We use the *Rank information coefficient* (*RankIC*) to evaluate the effectiveness of an alpha:

$$\text{RankIC}(\mathbf{a}, \mathbf{r}^h) = \text{Spearman}(\mathbf{a}, \mathbf{r}^h), \quad (10.22)$$

where $\text{Spearman}(\cdot)$ indicates the *Spearman correlation*, \mathbf{a} is the sequence of an alpha, and \mathbf{r}^h is the sequence of the return value with holding period h such that the i -th element of \mathbf{r}^h represent the daily return of h days later on the i -th day. The RankIC then can be used as an indicator of the importance of each alpha factor and plugged into Equation (10.19) directly.

10.6.2 Examples for Bayesian IID

For each stock s (i.e., $s \in \{1, 2, \dots, S\}$, where S is the total number of stocks), we have a matrix \mathbf{A}_s with shape $\mathbf{A}_s \in \mathbb{R}^{N \times D}$, where N is the number of alphas and D is the number of dates so that each row of \mathbf{A}_s is regarded as an alpha series. We want to select a subset of the alphas (here we assume M out of the N alphas are selected). The RankIC between each alpha series and the delayed return series with horizon $h = 1$ is then taken as the *important value* directly, a higher RankIC indicates a higher priority.

Ticker	Type	Sector	Company	Avg. Amount
SH601988	Share	Bank	Bank of China Limited	427,647,786
SH601601	Share	Public Utility	China Pacific Insurance (Group)	819,382,926
SH600028	Share	Public Utility	China Petroleum & Chemical Corporation	748,927,952
SH600016	Share	Bank	China Minsheng Banking Corporation	285,852,414
SH601186	Share	Public Utility	China Railway Construction Corporation	594,970,588
SH601328	Share	Bank	Bank of Communications Corporation	484,445,915
SH601628	Share	Public Utility	China Life Insurance Company Limited	368,179,861
SH601939	Share	Bank	China Construction Bank Corporation	527,876,669
SH510300	ETF	CSI 300	Huatai-PineBridge CSI 300 ETF	1,960,687,059
SH510050	ETF	CSI 50	ChinaAMC China CSI 50 ETF	2,020,385,879

Table 10.3: Summary of the underlying portfolios in the China market, ten assets in total. The average amount (in the currency of RMB) is calculated in the period of the test set.

Data set. To assess the discussed algorithm and highlight the primary benefits of the IID technique, we perform experiments with several analytical tasks and use data for ten assets from the China market and diverse industrial areas, including Bank, Public Utility, and ETF. We obtain publicly available data from tushare ⁵. The data covers a three-year period, i.e., 2018-07-18 to 2021-07-05 (720 trading days), where the data between 2018-07-18 and 2020-07-09 is considered the training set (480 calendar days); while data between 2020-07-10 and 2021-07-05 is taken as the test set (240 trading days). The underlying portfolios are summarized in Table 10.3. And Figure 10.8(a) shows the series of different assets, where we initialize each portfolio with a unitary value for clarity. The assets are chosen by selecting the ones with high amount values (random ten assets among the fifty assets with the highest average amounts in China market during the selected period) so that there are fewer trading restrictions.

We obtain 78 alphas from the 101 formulaic alphas (Kakushadze, 2016), 94 alphas from the 191 formulaic alphas (GuotaiJunan, 2017), and 19 proprietary alphas. The alphas are chosen to have a value that is neither too large nor too small. In this sense, the alpha matrix \mathbf{A}_s is of shape 214×720 for each asset.

In all scenarios, the same parameter initialization is adopted when conducting different tasks. Experimental evidence demonstrates that post-processing can marginally improve performance. For clarification, we only provide the findings of the GBT (without ARD) and IID models after post-processing. The IID model can select the important features (alphas) with a higher priority while keeping the reconstructive error as small as possible, resulting in performance that is as good as or better than the vanilla GBT method in low-rank ID approximations across a wide range of experiments on different data sets.

We again use the mean squared error (MSE, Equation (10.6)), which measures the similarity between the observed and reconstructive matrices, to evaluate the overall decomposition performance; the smaller the value, the better the performance.

⁵. <https://tushare.pro/>.

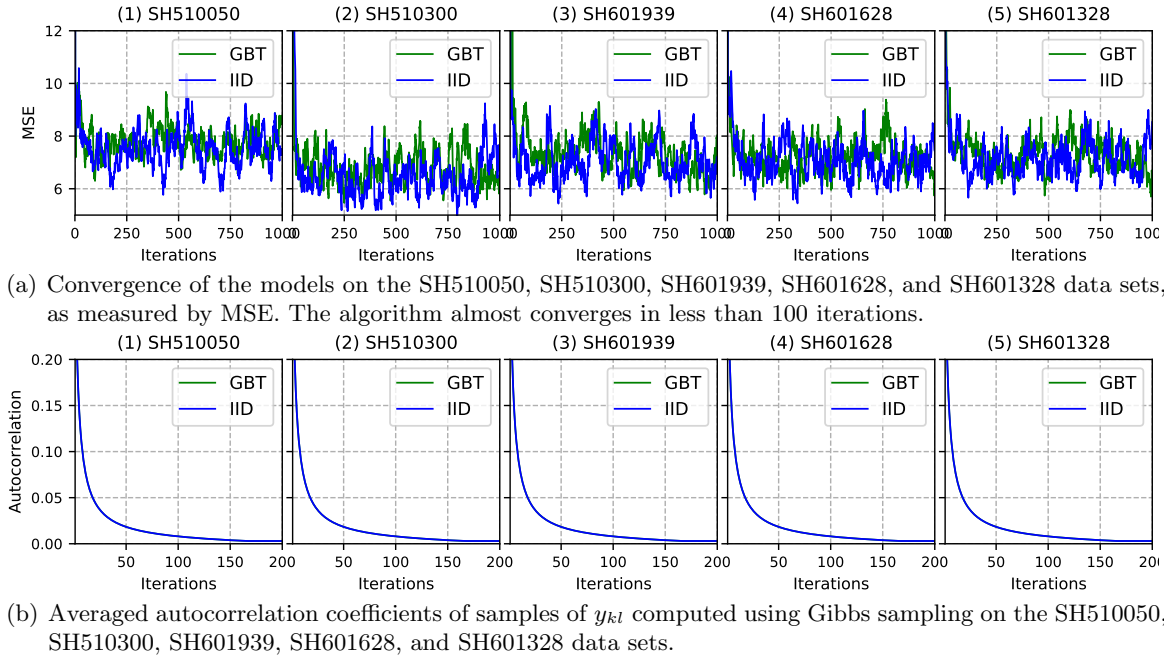


Figure 10.7: Convergence results (upper), and sampling mixing analysis (lower) on the SH510050, SH510300, SH601939, SH601628, and SH601328 data sets for a latent dimension of $K = 10$.

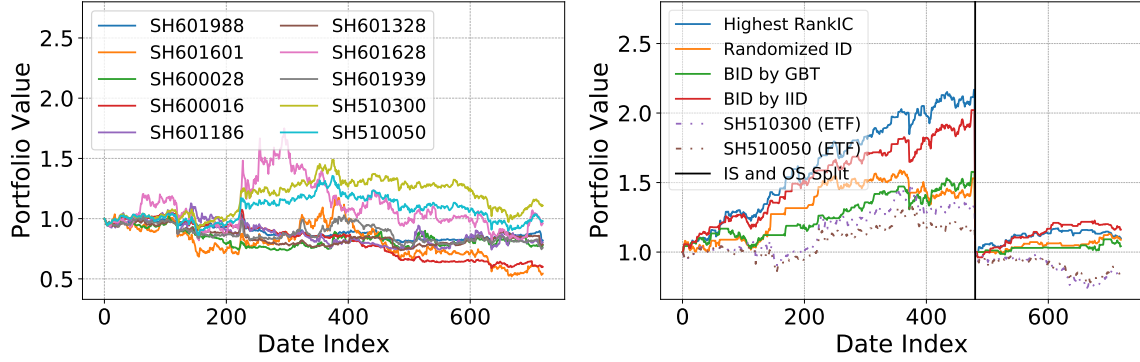
	SH601988	SH601601	SH600028	SH600016	SH601186	SH601328	SH601628	SH601939	SH510300	SH510050
GBT Min.	5.235	5.814	5.235	6.381	5.819	5.700	5.734	5.785	5.462	6.297
IID Min.	4.567	5.700	4.843	6.490	5.104	5.658	5.445	5.435	4.876	5.767
GBT Mean	6.476	7.367	6.764	8.053	7.066	7.250	7.206	7.242	6.769	7.776
IID Mean	6.239	7.449	6.664	7.831	6.558	7.081	7.002	7.031	6.450	7.492

Table 10.4: Minimal and mean MSE measures after burn-in across different iterations for GBT and IID models on the 10 alpha matrices from 10 assets. In all cases, $K = 10$ is set as the latent dimension. In most cases, the results of IID converge to a smaller value than the GBT model.

Hyper-parameters. In those experiments, we use $a = -1, b = 1, \alpha_\sigma = 0.1, \beta_\sigma = 1, (\{\mu_{kl}\} = 0, \{\tau_{kl}\} = 1)$ for both GBT and IID models. The adopted parameters are uninformative and weak prior choices, and the models are insensitive to them. The observed or unobserved variables are initialized from random draws as long as those hyper-parameters are fixed since this initialization method provides a better initial guess of the correct patterns in the matrices. In all cases, we execute 1,000 iterations of Gibbs sampling with a burn-in of 100 iterations and a thinning of 5 iterations, since the convergence analysis indicates the algorithm can converge in fewer than 100 iterations.

CONVERGENCE AND COMPARATIVE ANALYSIS

We first show the rate of convergence over iterations on different assets. Due to space constraints, we omit convergence results for the first five assets and only present those for portfolios SH510050, SH510300, SH601939, SH601628, and SH601328. Results for the other assets are quantitatively similar.



(a) Ten different portfolios, where we initialize each portfolio with a unitary value for clarity. (b) Portfolio values with the same strategy by using different alphas via comparative selection models.

Figure 10.8: Portfolio values of the ten assets (left), and the portfolio values (right) of different methods, where we split by in-sample and out-of-sample periods, and initialize with a unitary value for each period. The IID performs better in the out-of-sample period (see also Table 10.5).

We run GBT and IID models with $K = 10$ for the five data sets, where 214 is the full rank of the matrices, and the error is measured by MSE. Figure 10.7(a) shows the rate of convergence over iterations. Figure 10.7(b) shows the autocorrelation coefficients of samples computed using Gibbs sampling. We observe that the mixings of the IID are close to those of GBT. When the lags are greater than ten, the coefficients are less than 0.1, indicating that the Gibbs sampler mixes well. In all experiments, the algorithm converges in less than 100 iterations. We also observe that the IID model does not converge to a larger error than the vanilla GBT model, though we put more emphasis on selecting the columns with high RankIC. Table 10.4 presents the minimal MSE and mean MSE after burn-in across different iterations for GBT and IID models on the ten alpha matrices from ten assets. In most cases, the IID can even converge to a smaller MSE value.

QUANTITATIVE STRATEGY

After executing the GBT and IID algorithms for computing the interpolative decomposition of each asset's alpha matrix, the state vector \mathbf{r} for each asset is saved, and the ten alphas with the largest mean selection during the 1,000 iterations are chosen (with a burn-in of 100 iterations, and a thinning of 5 iterations).

Then we follow the quantitative strategy in Algorithm 26 (in which case, $h = 1$, $N = 214$ alphas, $M = 10$ alphas, $D = 720$ trading days, and $D_{\text{in}} = 480$ trading days). The procedure shown in Algorithm 26 is a very simple quantitative strategy. However, the algorithm can show precisely how the IID method can work in practice.

The strategy using the alphas selected by the IID method is only slightly worse than the one selecting the *highest RankIC* alphas for the in-sample (IS) performance in terms of Sharpe ratio, annual return, and maximum drawdown; however, the IID performs better in the out-of-sample (OS) scenario, and this is what we actually want (see Table 10.5 and Figure 10.8(b)). To evaluate the strategy, we also adopt the Randomized algorithm

Algorithm 26 Alpha selection for portfolio allocation. Select holding period h , number of alphas to select is M . D_{in} is the in-sample number of days, D is the total number of days, N is the total number of alphas. We then select M alphas out of the N alphas.

1: Split the alpha matrix for in-sample (IS) and out-of-sample (OS) evaluations:

$$\mathbf{A}_{in} = \mathbf{A}_s[:, 0 : D_{in}] \in \mathbb{R}^{N \times D_{in}}, \quad \mathbf{A}_{out} = \mathbf{A}_s[:, D_{in} + 1 : D] \in \mathbb{R}^{N \times (D - D_{in})};$$

2: Using (column) ID to decide the alphas to be selected on matrix \mathbf{A}_{in}^\top , with the selected indices \mathbf{m} :

$$\hat{\mathbf{A}}_{in} = \mathbf{A}_s[\mathbf{m}, 0 : D_{in}] \in \mathbb{R}^{M \times D_{in}}, \quad \hat{\mathbf{A}}_{out} = \mathbf{A}_s[\mathbf{m}, D_{in} + 1 : D] \in \mathbb{R}^{M \times (D - D_{in})};$$

3: **for** $m = 1$ to M **do**

4: Using the m -th IS alpha vector $\mathbf{a}_m = \hat{\mathbf{A}}_{in}[m, :] \in \mathbb{R}^{D_{in}}$ to decide the weight \mathbf{w}_m and interception b_m via ordinary least squares (OLS) so that the MSE between the prediction $\mathbf{a}_m^\top \mathbf{w}_m + b_m$ and the shifted return vector \mathbf{r}^h is minimized, i.e., minimizing $\text{MSE}(\mathbf{a}_m^\top \mathbf{w}_m + b_m, \mathbf{r}^h)$. The weight and interception are then used in OS evaluation.

5: **end for**

6: **for** $d = 1$ to $D - D_{in}$ **do**

7: On each day in the OS period, we use the mean evaluation of each prediction from the M alphas to decide to go long or not, i.e., to go long if $\sum_{m=1}^M \mathbf{a}_m^\top \mathbf{w}_m + b_m > 0$; and do nothing otherwise since we restrict the analysis to long-only portfolios.

8: Though we employ a long-only portfolio, we can favor a *market-neutral strategy*: we open long positions only when we anticipate that at least half of the stocks will rise on the following h day, and we weight each stock equally.

9: **end for**

Methods	Highest RankIC	Randomized ID	BID with GBT	BID with IID
Mean RankIC	0.1035	0.0651	0.0553	0.0752
Mean Correlation	0.2276↓	0.5741↓	0.1132	0.1497
Sharpe Ratio (OS)	1.0276	1.0544	0.5045	1.5721
Sharpe Ratio (IS)	2.6511	1.3019	1.4965	2.3231
Annual Return (OS)	0.1043	0.0932	0.0484	0.1633
Annual Return (IS)	0.4390	0.2281	0.2425	0.3805
Max Drawdown (OS)	0.0632	0.0373	0.0484	0.0552
Max Drawdown (IS)	0.0892	0.1548	0.1232	0.0975

Table 10.5: Mean RankIC and correlation of the selected alphas across various assets for different methods. A higher mean RankIC and a lower mean correlation are better. The IID method can find the trade-off between the mean RankIC and the mean correlation. In all cases, *IS* means in-sample measurements, and *OS* means out-of-sample measurements. The symbol “↓” means the performance is extremely poor.

to compute the ID for comparison (Liberty et al., 2007), termed *Randomized ID*. The Randomized ID performs even worse than BID with GBT (see Table 10.5). Though the IID

does not select alphas with the highest RankIC values, this does not mean that the alpha selection procedure is meaningless for the following reasons:

1. *Pool size*: We only use a small alpha pool that only contains 214 alpha factors. When the number of alphas is approaching millions or even billions, the alpha selection procedure is expected to work better.
2. *Correlation*: The mean correlation of selected alphas across the ten assets of the IID method is smaller than the highest RankIC method. In this sense, the alphas of the latter method have high correlations and a low diversity. If the correlated alphas have low liquidity or perform poorly during a given period, the strategy's risk might increase.
3. *Machine learning models*: In our test, we only use OLS to find the weight of each alpha. For more complex models, e.g., neural networks or XGBoost models, the correlated alphas can cause multi-linear problems so that the performance and interpretability are hampered.
4. *Diversification*: Even if selecting the alphas with the highest RankIC can work well in practice, we also want to diversify the strategies so that we are not exposed to specific risks. The IID method can help find different strategies.

⌘ Chapter 10 Problems ⌘

1. Determine the column ID for the matrix

$$\mathbf{A} = \begin{bmatrix} 1 & 3 & 2 \\ 3 & 7 & 6 \\ 4 & 5 & 8 \end{bmatrix}.$$

2. Identify an example that demonstrates the effectiveness of the post-processing method described in Section 10.5.3 in reducing reconstruction errors.
3. Prove the rank decomposition: Any rank- R matrix $\mathbf{A} \in \mathbb{R}^{M \times N}$ admits the factorization

$$\underset{M \times N}{\mathbf{A}} = \underset{M \times R}{\mathbf{D}} \underset{R \times N}{\mathbf{F}},$$

where $\mathbf{D} \in \mathbb{R}^{M \times R}$ has rank R , and $\mathbf{F} \in \mathbb{R}^{R \times N}$ also has rank R , i.e., \mathbf{D} and \mathbf{F} have full rank R . The storage for the decomposition is then reduced or potentially increased from MN floating-point numbers to $R(M + N)$ floating-point numbers. *Hint: use elementary transformation.*

Part IV
Appendix

A

Appendix

Contents

A.1	Taylor's Expansion	245
A.2	Deriving the Dirichlet Distribution	246
A.2.1	Derivation	246
A.2.2	Properties of the Dirichlet Distribution	247
A.3	Existence of the Skeleton Decomposition	250

A.1. Taylor's Expansion

Theorem A.1: (Taylor's Expansion with Lagrange Remainder)

Let $f(x) : \mathbb{R} \rightarrow \mathbb{R}$ be k -times continuously differentiable on the closed interval I with endpoints x and y , for some $k \geq 0$. If $f^{(k+1)}$ exists on the interval I , then there exists a $x^* \in (x, y)$ such that

$$\begin{aligned} f(x) &= f(y) + f'(y)(x-y) + \frac{f''(y)}{2!}(x-y)^2 + \dots + \frac{f^{(k)}(y)}{k!}(x-y)^k + \frac{f^{(k+1)}(x^*)}{(k+1)!}(x-y)^{k+1} \\ &= \sum_{i=0}^k \frac{f^{(i)}(y)}{i!}(x-y)^i + \frac{f^{(k+1)}(x^*)}{(k+1)!}(x-y)^{k+1}. \end{aligned}$$

The Taylor's expansion can be extended to a function of vector $f(\mathbf{x}) : \mathbb{R}^n \rightarrow \mathbb{R}$ or a function of matrix $f(\mathbf{X}) : \mathbb{R}^{m \times n} \rightarrow \mathbb{R}$.

The Taylor's expansion, or also known as the *Taylor's series*, approximates the function $f(x)$ around the value of y by a polynomial in a single indeterminate x . To see where this series comes from, we recall from the elementary calculus course that the approximated function around $\theta = 0$ for $\cos(\theta)$ is given by

$$\cos(\theta) \approx 1 - \frac{\theta^2}{2}.$$

That is, the $\cos(\theta)$ is approximated by a polynomial with a degree of 2. Suppose we want to approximate $\cos(\theta)$ by the more general polynomial with a degree of 2 by $f(\theta) = c_1 + c_2\theta + c_3\theta^2$. An intuitive idea is to match the gradients around the 0 point. That is,

$$\begin{cases} \cos(0) = f(0); \\ \cos'(0) = f'(0); \\ \cos''(0) = f''(0); \end{cases} \quad \text{leads to} \quad \begin{cases} 1 = c_1; \\ -\sin(0) = 0 = c_2; \\ -\cos(0) = -1 = 2c_3. \end{cases}$$

This makes $f(\theta) = c_1 + c_2\theta + c_3\theta^2 = 1 - \frac{\theta^2}{2}$ and agrees with our claim that $\cos(\theta) \approx 1 - \frac{\theta^2}{2}$ around the 0 point. We shall not give the details of the proof.

A.2. Deriving the Dirichlet Distribution

We derive the Dirichlet distribution and its properties in this appendix.

A.2.1 Derivation

Let x_1, x_2, \dots, x_K be i.i.d. random variables drawn from the Gamma distribution such that $x_k \sim \mathcal{G}(\alpha_k, 1)$ for $k \in \{1, 2, \dots, K\}$. The joint p.d.f. of x_1, x_2, \dots, x_K is given by

$$f_{x_1, x_2, \dots, x_K}(x_1, x_2, \dots, x_K) = \begin{cases} \prod_{k=1}^K \frac{1}{\Gamma(\alpha_k)} x_k^{\alpha_k-1} \exp(-x_k), & \text{if all } x_k \geq 0. \\ 0, & \text{if otherwise.} \end{cases}$$

Define variables y_k 's as follows:

$$\begin{aligned} y_k &= \frac{x_k}{\sum_{k=1}^K x_k}, \quad \forall k \in \{1, 2, \dots, K-1\} \\ y_K &= \frac{x_K}{\sum_{k=1}^K x_k} = 1 - \sum_{k=1}^{K-1} y_k, \end{aligned} \tag{A.1}$$

and variable z_K as

$$z_K = \sum_{k=1}^K x_k. \tag{A.2}$$

Let random variables $\mathbf{X} = [x_1, x_2, \dots, x_K]$, $\mathbf{Y} = [y_1, y_2, \dots, y_{K-1}, z_K]$, and their draws $\mathbf{x} = [x_1, x_2, \dots, x_K]$, $\mathbf{y} = [y_1, y_2, \dots, y_{K-1}, z_K]$. By *multidimensional transformation of variables*, we have

$$f_{\mathbf{Y}}(\mathbf{y}) = f_{\mathbf{X}}(g^{-1}(\mathbf{y})) |\det [J_{g^{-1}}(\mathbf{y})]|,$$

where

$$\begin{bmatrix} x_1 \\ x_2 \\ \vdots \\ x_{K-1} \\ x_K \end{bmatrix} = g^{-1}(\mathbf{y}) = g^{-1} \left(\begin{bmatrix} y_1 \\ y_2 \\ \vdots \\ y_{K-1} \\ z_K \end{bmatrix} \right) = \begin{bmatrix} y_1 \cdot z_K \\ y_2 \cdot z_K \\ \vdots \\ y_{K-1} \cdot z_K \\ y_K \cdot z_K \end{bmatrix},$$

and the Jacobian matrix is given by

$$\begin{aligned} J_{g^{-1}}(\mathbf{y}) &= \begin{bmatrix} \frac{\partial}{\partial y_1} g_1^{-1}(\mathbf{y}) & \cdots & \frac{\partial}{\partial y_{K-1}} g_1^{-1}(\mathbf{y}) & \frac{\partial}{\partial z_K} g_1^{-1}(\mathbf{y}) \\ \vdots & \ddots & \cdots & \vdots \\ \frac{\partial}{\partial y_1} g_K^{-1}(\mathbf{y}) & \cdots & \frac{\partial}{\partial y_{K-1}} g_K^{-1}(\mathbf{y}) & \frac{\partial}{\partial z_K} g_K^{-1}(\mathbf{y}) \end{bmatrix} \\ &= \begin{bmatrix} z_K & 0 & \cdots & 0 & y_1 \\ 0 & z_K & \cdots & 0 & y_2 \\ \vdots & \vdots & \ddots & \vdots & \vdots \\ 0 & 0 & \cdots & z_K & y_{K-1} \\ -z_K & -z_K & \cdots & -z_K & (1 - \sum_{k=1}^{K-1} y_k) \end{bmatrix} = z_K^{K-1}. \end{aligned}$$

This implies the joint p.d.f of \mathbf{Y} is

$$f_{\mathbf{Y}}(\mathbf{y}) = f_{\mathbf{X}}(g^{-1}(\mathbf{y}))z_K^{K-1} = \frac{y_1^{\alpha_1-1}y_2^{\alpha_2-1}\cdots y_{K-1}^{\alpha_{K-1}-1}y_K^{\alpha_K-1}}{\prod_{k=1}^K \Gamma(\alpha_k)} \exp(-z_K)z_K^{\alpha_1+\alpha_2+\dots+\alpha_K-1}.$$

We realize that the right-hand side of the above equation is proportional to a p.d.f. of a Gamma distribution and

$$\int \exp(-z_K)z_K^{\alpha_1+\alpha_2+\dots+\alpha_K-1}dz_K = \Gamma(\alpha_1 + \alpha_2 + \dots + \alpha_K).$$

Let $\alpha_+ = \alpha_1 + \alpha_2 + \dots + \alpha_K$, this implies

$$f(y_1, y_2, \dots, y_{K-1}) = \frac{\Gamma(\alpha_+)}{\prod_{k=1}^K \Gamma(\alpha_k)} \prod_{k=1}^K y_k^{\alpha_k-1}.$$

We notice that y_k 's are defined that $0 < y_k < 1$ for all $k \in \{1, 2, \dots, K\}$, and $\sum_{k=1}^K y_k = 1$. This implies the above equation is the p.d.f. of the Dirichlet distribution. The construction shown above can be utilized to generate random variables from the Dirichlet distribution.

A.2.2 Properties of the Dirichlet Distribution

Suppose $\mathbf{Y} = [y_1, y_2, \dots, y_K] \sim \text{Dirichlet}(\boldsymbol{\alpha})$ with $\boldsymbol{\alpha} = [\alpha_1, \alpha_2, \dots, \alpha_K]$, we here show the moments and properties of the Dirichlet distribution.

Mean of Dirichlet distribution. Write out the expectation,

$$\begin{aligned} \mathbb{E}[y_1] &= \int \cdots \int y_1 \cdot \text{Dirichlet}(\mathbf{y} \mid \boldsymbol{\alpha}) dy_1 dy_2 \cdots dy_K \\ &= \int \cdots \int y_1 \frac{\Gamma(\alpha_+)}{\prod_{k=1}^K \Gamma(\alpha_k)} \prod_{k=1}^K y_k^{\alpha_k-1} dy_1 dy_2 \cdots dy_K \\ &= \frac{\Gamma(\alpha_+)}{\prod_{k=1}^K \Gamma(\alpha_k)} \int \cdots \int y_1^{\alpha_1+1-1} \prod_{k=2}^K y_k^{\alpha_k-1} dy_1 dy_2 \cdots dy_K \\ &= \frac{\Gamma(\alpha_+)}{\prod_{k=1}^K \Gamma(\alpha_k)} \frac{\Gamma(\alpha_1 + 1) \prod_{k=2}^K \Gamma(\alpha_k)}{\Gamma(\alpha_+ + 1)} \\ &= \frac{\Gamma(\alpha_+) \Gamma(\alpha_1 + 1)}{\Gamma(\alpha_1) \Gamma(\alpha_+ + 1)} = \frac{\alpha_1}{\alpha_+}, \end{aligned}$$

where the last equality comes from the fact that $\Gamma(x + 1) = x\Gamma(x)$.

Variance of Dirichlet distribution. Write out the variance $\text{Var}[y_i] = \mathbb{E}[y_i^2] - \mathbb{E}[y_i]^2$. Similarly, from the proof of the mean, we have

$$\mathbb{E}[y_i^2] = \frac{\Gamma(\alpha_+)}{\Gamma(\alpha_+ + 2)} \frac{\Gamma(\alpha_i + 2)}{\Gamma(\alpha_i)} = \frac{(\alpha_i + 1)\alpha_i}{(\alpha_+ + 1)\alpha_+}.$$

This implies

$$\text{Var}[y_i] = \mathbb{E}[y_i^2] - \mathbb{E}[y_i]^2 = \frac{(\alpha_i + 1)\alpha_i}{(\alpha_+ + 1)\alpha_+} - \left(\frac{\alpha_i}{\alpha_+}\right)^2 = \frac{\alpha_i(\alpha_+ - \alpha_i)}{\alpha_+^2(\alpha_+ + 1)}.$$

Covariance of Dirichlet distribution. Write out the covariance $\text{Cov}[y_i y_j] = \text{E}[y_i y_j] - \text{E}[y_i]\text{E}[y_j]$. Again, similar to the proof of the mean, for $i \neq j$, we have

$$\text{E}[y_i y_j] = \frac{\Gamma(\alpha_+) \Gamma(\alpha_i + 1) \Gamma(\alpha_j + 1)}{\Gamma(\alpha_+ + 2) \Gamma(\alpha_i) \Gamma(\alpha_j)} = \frac{\alpha_i \alpha_j}{\alpha_+ (\alpha_+ + 1)}.$$

This implies

$$\text{Cov}[y_i y_j] = \text{E}[y_i y_j] - \text{E}[y_i]\text{E}[y_j] = \frac{\alpha_i \alpha_j}{\alpha_+ (\alpha_+ + 1)} - \frac{\alpha_i \alpha_j}{\alpha_+^2} = \frac{-\alpha_i \alpha_j}{\alpha_+^2 (\alpha_+ + 1)}.$$

Marginal distribution of y_i . By definitions in Equation (A.1) and Equation (A.2), we have $z_K - x_i \sim \mathcal{G}(\alpha_+ - \alpha_i, 1)$. This implies

$$y_i = \frac{x_i}{z_K} = \frac{x_i}{x_i + (z_K - x_i)} \sim \text{Beta}(\alpha_i, \alpha_+ - \alpha_i).$$

which is from the fact about the p.d.f. of two independent Gamma random variables. ¹

Aggregation property. Suppose $[y_1, y_2, \dots, y_K] \sim \text{Dirichlet}([\alpha_1, \alpha_2, \dots, \alpha_K])$. Then, let $M = y_i + y_j$, it follows that

$$\begin{aligned} & [y_1, \dots, y_{i-1}, y_{i+1}, \dots, y_{j-1}, y_{j+1}, \dots, y_K, M] \\ & \sim \text{Dirichlet}([\alpha_1, \dots, \alpha_{i-1}, \alpha_{i+1}, \dots, \alpha_{j-1}, \alpha_{j+1}, \dots, \alpha_K, \alpha_i + \alpha_j]). \end{aligned}$$

Proof We realize that $M \sim \mathcal{G}(\alpha_i + \alpha_j, 1)$. Again by the multidimensional transformation of variables as shown at the beginning of this section, we conclude the result. \blacksquare

The results can be extended to a more general case. If $\{A_1, A_2, \dots, A_r\}$ is a partition of $\{1, 2, \dots, K\}$, then

$$\left[\sum_{i \in A_1} y_i, \sum_{i \in A_2} y_i, \dots, \sum_{i \in A_r} y_i \right] \sim \text{Dirichlet} \left(\left[\sum_{i \in A_1} \alpha_i, \sum_{i \in A_2} \alpha_i, \dots, \sum_{i \in A_r} \alpha_i \right] \right).$$

Conditional distribution. Let $y_0 = \sum_{k=3}^K y_k$ and $\alpha_0 = \alpha_+ - \alpha_1 - \alpha_2$, then $[y_1, y_2, y_0] \sim \text{Dirichlet}([\alpha_1, \alpha_2, \alpha_0])$. Therefore, it follows that

$$f_{y_1, y_2}(y_1, y_2) = \frac{\Gamma(\alpha_1 + \alpha_2 + \alpha_0)}{\Gamma(\alpha_1)\Gamma(\alpha_2)\Gamma(\alpha_0)} y_1^{\alpha_1-1} y_2^{\alpha_2-1} (1 - y_1 - y_2)^{\alpha_0-1}.$$

Similarly, we have

$$f_{y_2}(y_2) = \frac{\Gamma(\alpha_1 + \alpha_2 + \alpha_0)}{\Gamma(\alpha_2)\Gamma(\alpha_1 + \alpha_0)} y_2^{\alpha_2-1} (1 - y_2)^{\alpha_1 + \alpha_0 - 1} = \text{Beta}(y_2 \mid \alpha_2, \alpha_1 + \alpha_0),$$

which is a p.d.f. of a Beta distribution. Therefore, the conditional p.d.f. of $y_1 \mid y_2 = y_2$ is given by

$$f_{y_1|y_2=y_2}(y_1 \mid y_2) = \frac{f_{y_1, y_2}(y_1, y_2)}{f_{y_2}(y_2)} = \frac{\Gamma(\alpha_1 + \alpha_0)}{\Gamma(\alpha_1)\Gamma(\alpha_0)} \left(\frac{y_1}{1 - y_2} \right)^{\alpha_1-1} \left(1 - \frac{y_1}{1 - y_2} \right)^{\alpha_0-1} \frac{1}{1 - y_2},$$

1. Suppose $x \sim \mathcal{G}(a, \lambda)$ and $y \sim \mathcal{G}(b, \lambda)$, then $\frac{x}{x+y} \sim \text{Beta}(a, b)$.

which implies

$$\frac{1}{1 - y_2} y_1 \mid y_2 = y_2 \sim \text{Beta}(\alpha_1, \alpha_0).$$

Apply this procedure, we will have

$$\mathbf{Y}_{-i} \mid y_i \sim (1 - y_i) \text{Dirichlet}(\boldsymbol{\alpha}_{-i}),$$

where \mathbf{Y}_{-i} contains all the $K - 1$ variables except y_i ; and similarly for $\boldsymbol{\alpha}_{-i}$.

A.3. Existence of the Skeleton Decomposition

In linear algebra, the row rank and the column rank of a matrix are equal. In other words, we can also claim that the dimension of the column space and the dimension of the row space are equal (Lu, 2021a). This property is essential for proving the existence of the skeleton decomposition. The proof is rather elementary.

Proof [of Theorem 10.3, p. 219] The proof relies on the existence of such a nonsingular matrix \mathbf{U} , which is central to this decomposition method.

Existence of such nonsingular matrix \mathbf{U} . Since matrix \mathbf{A} is of rank R , we can pick R columns from \mathbf{A} such that they are linearly independent. Suppose we put the specific R linearly independent columns $\mathbf{a}_{i1}, \mathbf{a}_{i2}, \dots, \mathbf{a}_{iR}$ into the columns of an $M \times R$ matrix $\mathbf{N} = [\mathbf{a}_{i1}, \mathbf{a}_{i2}, \dots, \mathbf{a}_{iR}] \in \mathbb{R}^{M \times R}$. The dimension of the column space of \mathbf{N} is R so that the dimension of the row space of \mathbf{N} is also R . Again, we can pick R linearly independent rows $\mathbf{n}_{j1}^\top, \mathbf{n}_{j2}^\top, \dots, \mathbf{n}_{jR}^\top$ from \mathbf{N} and put the specific R rows into rows of an $R \times R$ matrix $\mathbf{U} = [\mathbf{n}_{j1}^\top; \mathbf{n}_{j2}^\top; \dots; \mathbf{n}_{jR}^\top] \in \mathbb{R}^{R \times R}$. The dimension of the column space of \mathbf{U} is also R , which means there are R linearly independent columns from \mathbf{U} . So \mathbf{U} is such a nonsingular matrix with size $R \times R$.

Main proof. As long as we find the nonsingular $R \times R$ matrix \mathbf{U} inside \mathbf{A} , we can find the existence of the skeleton decomposition as follows.

Suppose $\mathbf{U} = \mathbf{A}[I, J]$, where I and J are index vectors of size R . Since \mathbf{U} is a nonsingular matrix, the columns of \mathbf{U} are linearly independent. Thus the columns of matrix \mathbf{C} based on the columns of \mathbf{U} are also linearly independent (i.e., select the R columns of \mathbf{A} with the same entries of the matrix \mathbf{U} . Here \mathbf{C} is equal to the matrix \mathbf{N} we construct above, and $\mathbf{C} = \mathbf{A}[:, J]$).

As the rank of the matrix \mathbf{A} is R , if we take any other column \mathbf{a}_i of \mathbf{A} , \mathbf{a}_i can be represented as a linear combination of the columns of \mathbf{C} , i.e., there exists a vector \mathbf{x} such that $\mathbf{a}_i = \mathbf{C}\mathbf{x}$ for all $i \in \{1, 2, \dots, N\}$. Let R rows (entries) of $\mathbf{a}_i \in \mathbb{R}^N$ corresponding to the row entries of \mathbf{U} be $\mathbf{r}_i \in \mathbb{R}^R$ for all $i \in \{1, 2, \dots, N\}$ (i.e., \mathbf{r}_i contains R entries of \mathbf{a}_i). That is, select the R entries of \mathbf{a}_i 's corresponding to the entries of \mathbf{U} as follows:

$$\mathbf{A} = [\mathbf{a}_1, \mathbf{a}_2, \dots, \mathbf{a}_N] \in \mathbb{R}^{M \times N} \quad \longrightarrow \quad \mathbf{A}[I, :] = [\mathbf{r}_1, \mathbf{r}_2, \dots, \mathbf{r}_N] \in \mathbb{R}^{R \times N}.$$

Since $\mathbf{a}_i = \mathbf{C}\mathbf{x}$, \mathbf{U} is a submatrix inside \mathbf{C} , and \mathbf{r}_i is a subvector inside \mathbf{a}_i , we have $\mathbf{r}_i = \mathbf{U}\mathbf{x}$, which states that $\mathbf{x} = \mathbf{U}^{-1}\mathbf{r}_i$. Thus, for every $i \in \{1, 2, \dots, N\}$, we have $\mathbf{a}_i = \mathbf{C}\mathbf{U}^{-1}\mathbf{r}_i$. Combining the n columns of such \mathbf{r}_i into $\mathbf{R} = [\mathbf{r}_1, \mathbf{r}_2, \dots, \mathbf{r}_N]$, we obtain

$$\mathbf{A} = [\mathbf{a}_1, \mathbf{a}_2, \dots, \mathbf{a}_N] = \mathbf{C}\mathbf{U}^{-1}\mathbf{R},$$

from which the result follows.

In short, we first find R linearly independent columns of \mathbf{A} into $\mathbf{C} \in \mathbb{R}^{M \times R}$. From \mathbf{C} , we find an $R \times R$ nonsingular submatrix \mathbf{U} . The R rows of \mathbf{A} corresponding to entries of \mathbf{U} can help to reconstruct the columns of \mathbf{A} . ■

Bibliography

- Rishi Advani and Sean O’Hagan. Efficient algorithms for constructing an interpolative decomposition. *arXiv preprint arXiv:2105.07076*, 2021. 222
- James H Albert and Siddhartha Chib. Bayesian analysis of binary and polychotomous response data. *Journal of the American statistical Association*, 88(422):669–679, 1993. 206
- İsmail An, Umut Şimşekli, Ali Taylan Cemgil, and Laie Akarun. Large scale polyphonic music transcription using randomized matrix decompositions. In *2012 Proceedings of the 20th European Signal Processing Conference (EUSIPCO)*, pages 2020–2024. IEEE, 2012. 219
- Theodore Wilbur Anderson. An introduction to multivariate statistical analysis. Technical report, Wiley New York, 2003. 78, 81
- Christophe Andrieu, Nando De Freitas, Arnaud Doucet, and Michael I Jordan. An introduction to MCMC for machine learning. *Machine learning*, 50(1):5–43, 2003. 24, 143
- Pia Anttila, Pentti Paatero, Unto Tapper, and Olli Järvinen. Source identification of bulk wet deposition in Finland by positive matrix factorization. *Atmospheric Environment*, 29(14):1705–1718, 1995. 157
- Ismail Arı, A Taylan Cemgil, and Lale Akarun. Probabilistic interpolative decomposition. In *2012 IEEE International Workshop on Machine Learning for Signal Processing*, pages 1–6. IEEE, 2012. 6, 213
- Morten Arngren, Mikkel N Schmidt, and Jan Larsen. Unmixing of hyperspectral images using Bayesian non-negative matrix factorization with volume prior. *Journal of Signal Processing Systems*, 65(3):479–496, 2011. 153
- Sudipto Banerjee and Anindya Roy. *Linear algebra and matrix analysis for statistics*, volume 181. CRC Press Boca Raton, FL, USA:, 2014. 5

- Jordi Barretina, Giordano Caponigro, Nicolas Stransky, Kavitha Venkatesan, Adam A Margolin, Sungjoon Kim, Christopher J Wilson, Joseph Lehár, Gregory V Kryukov, Dmitriy Sonkin, et al. The Cancer Cell Line Encyclopedia enables predictive modelling of anti-cancer drug sensitivity. *Nature*, 483(7391):603–607, 2012. 229
- James Bennett, Stan Lanning, et al. The Netflix prize. In *Proceedings of KDD cup and workshop*, volume 2007, page 35. New York, NY, USA., 2007. 100
- José M Bernardo and Adrian FM Smith. *Bayesian theory*, volume 405. John Wiley & Sons, 2009. 40
- Michael W Berry, Murray Browne, Amy N Langville, V Paul Pauca, and Robert J Plemmons. Algorithms and applications for approximate nonnegative matrix factorization. *Computational statistics & data analysis*, 52(1):155–173, 2007. 129, 132, 157
- Julian Besag. On the statistical analysis of dirty pictures. *Journal of the Royal Statistical Society: Series B (Methodological)*, 48(3):259–279, 1986. 21
- Christopher M Bishop. Pattern recognition. *Machine learning*, 128(9), 2006. 5, 78
- Keith Allen Bonawitz. *Composable Probabilistic Inference with Blaise*. PhD thesis, Massachusetts Institute of Technology, 2008. 23, 24, 25
- Christos Boutsidis and Efstratios Gallopoulos. SVD based initialization: A head start for nonnegative matrix factorization. *Pattern recognition*, 41(4):1350–1362, 2008. 133
- George EP Box and Norman R Draper. *Empirical model-building and response surfaces*. John Wiley & Sons, 1987. 32
- Thomas Brouwer and Pietro Lio. Prior and likelihood choices for Bayesian matrix factorization on small datasets. *arXiv preprint arXiv:1712.00288*, 2017. 157, 163, 166, 172, 173, 177, 185, 186, 229
- Thomas Brouwer, Jes Frelsen, and Pietro Lió. Comparative study of inference methods for Bayesian nonnegative matrix factorisation. In *Joint European Conference on Machine Learning and Knowledge Discovery in Databases*, pages 513–529. Springer, 2017. 132
- Jean-Philippe Brunet, Pablo Tamayo, Todd R Golub, and Jill P Mesirov. Metagenes and molecular pattern discovery using matrix factorization. *Proceedings of the national academy of sciences*, 101(12):4164–4169, 2004. 132
- John Burkardt. The truncated normal distribution. *Department of Scientific Computing Website, Florida State University*, 1:35, 2014. 58, 60
- John Canny. GaP: a factor model for discrete data. In *Proceedings of the 27th annual international ACM SIGIR conference on Research and development in information retrieval*, pages 122–129, 2004. 6, 197
- Ali Taylan Cemgil. Bayesian inference for nonnegative matrix factorisation models. *Computational intelligence and neuroscience*, 2009, 2009. 197

- Gang Chen, Fei Wang, and Changshui Zhang. Collaborative filtering using orthogonal nonnegative matrix tri-factorization. *Information Processing & Management*, 45(3):368–379, 2009. 5
- Hugh Chipman, Edward I George, Robert E McCulloch, Merlise Clyde, Dean P Foster, and Robert A Stine. The practical implementation of Bayesian model selection. *Lecture Notes-Monograph Series*, pages 65–134, 2001. 86, 87
- Ronald Christensen. *Linear models for multivariate, time series, and spatial data*, volume 1. Springer, 1991. 97
- Wei Chu, Zoubin Ghahramani, and Christopher KI Williams. Gaussian processes for ordinal regression. *Journal of machine learning research*, 6(7), 2005. 205
- Joel E Cohen and Uriel G Rothblum. Nonnegative ranks, decompositions, and factorizations of nonnegative matrices. *Linear Algebra and its Applications*, 190:149–168, 1993. 129
- Pierre Comon, Xavier Luciani, and André LF De Almeida. Tensor decompositions, alternating least squares and other tales. *Journal of Chemometrics: A Journal of the Chemometrics Society*, 23(7-8):393–405, 2009. 5, 101
- Rajarshi Das. Collapsed Gibbs sampler for Dirichlet process Gaussian mixture models (DPGMM). *Talk*, 2014. 74, 87
- Robyn M Dawes and Bernard Corrigan. Linear models in decision making. *Psychological bulletin*, 81(2):95, 1974. 97
- Chris HQ Ding, Tao Li, and Michael I Jordan. Convex and semi-nonnegative matrix factorizations. *IEEE transactions on pattern analysis and machine intelligence*, 32(1):45–55, 2008. 159, 190
- David B Dunson and Amy H Herring. Bayesian latent variable models for mixed discrete outcomes. *Biostatistics*, 6(1):11–25, 2005. 6, 197
- Ludwig Fahrmeir, Thomas Kneib, Stefan Lang, and Brian Marx. *Regression*. Springer, 2007. 31
- Wang Fei, Li Tao, and Zhang Changshui. Semi-supervised clustering via matrix factorization. In *Proc. SIAM Int. Conf. on Data Mining*, 2008. 190
- John Fox. *Applied regression analysis, linear models, and related methods*. Sage Publications, Inc, 1997. 97
- Chris Fraley and Adrian E Raftery. Bayesian regularization for normal mixture estimation and model-based clustering. *Journal of classification*, 24(2):155–181, 2007. 86, 87
- Bela A Frigiyik, Amol Kapila, and Maya R Gupta. Introduction to the Dirichlet distribution and related processes. Department of electrical engineering, university of Washington. Technical report, UWEETR-2010-0006, 2010. 72

- Yuan Gao and George Church. Improving molecular cancer class discovery through sparse non-negative matrix factorization. *Bioinformatics*, 21(21):3970–3975, 2005. 132
- Andrew Gelman, John B Carlin, Hal S Stern, David B Dunson, Aki Vehtari, and Donald B Rubin. *Bayesian data analysis*. CRC press, 2013. 27, 40
- Stuart Geman and Donald Geman. Stochastic relaxation, Gibbs distributions, and the Bayesian restoration of images. *IEEE Transactions on pattern analysis and machine intelligence*, (6):721–741, 1984. 26, 27
- James E Gentle. *Numerical linear algebra for applications in statistics*. Springer Science & Business Media, 1998. 5
- James E Gentle. *Matrix algebra: theory, computations, and applications in statistics*. Springer Science & Business Media, 2007. 76
- Charles Geyer. Introduction to Markov chain Monte Carlo. *Handbook of markov chain monte carlo*, pages 3–48, 2011. 24
- Paris V Giampouras, Athanasios A Rontogiannis, and Konstantinos D Koutroumbas. Alternating iteratively reweighted least squares minimization for low-rank matrix factorization. *IEEE Transactions on Signal Processing*, 67(2):490–503, 2018. 101
- Walter R Gilks and Pascal Wild. Adaptive rejection sampling for Gibbs sampling. *Applied Statistics*, pages 337–348, 1992. 27
- Philip E Gill, Walter Murray, and Margaret H Wright. *Numerical linear algebra and optimization*. SIAM, 2021. 5
- Nicolas Gillis. The why and how of nonnegative matrix factorization. *Connections*, 12:2–2, 2014. 133
- Nicolas Gillis. *Nonnegative matrix factorization*. SIAM, 2020. 129
- Abhinav Goel, Caleb Tung, Yung-Hsiang Lu, and George K Thiruvathukal. A survey of methods for low-power deep learning and computer vision. In *2020 IEEE 6th World Forum on Internet of Things (WF-IoT)*, pages 1–6. IEEE, 2020. 5
- Mehmet Gönen. Predicting drug–target interactions from chemical and genomic kernels using Bayesian matrix factorization. *Bioinformatics*, 28(18):2304–2310, 2012. 141
- Ian Goodfellow, Yoshua Bengio, and Aaron Courville. *Deep learning*. MIT press, 2016. 5
- Prem Gopalan, Jake M Hofman, and David M Blei. Scalable recommendation with Poisson factorization. *arXiv preprint arXiv:1311.1704*, 2013. 197
- Prem Gopalan, Francisco J Ruiz, Rajesh Ranganath, and David Blei. Bayesian nonparametric Poisson factorization for recommendation systems. In *Artificial Intelligence and Statistics*, pages 275–283. PMLR, 2014. 159, 197

- Prem Gopalan, Jake M Hofman, and David M Blei. Scalable recommendation with hierarchical Poisson factorization. In *UAI*, pages 326–335, 2015. 159, 197, 199
- Olivier Gouvert, Thomas Oberlin, and Cédric Févotte. Ordinal non-negative matrix factorization for recommendation. In *International Conference on Machine Learning*, pages 3680–3689. PMLR, 2020. 205
- Alex Graves. Practical variational inference for neural networks. *Advances in neural information processing systems*, 24, 2011. 23
- Securities GuotaiJunan. Multi factor stock selection system based on the characteristics of short cycle price. 2017. 235, 236
- Nathan Halko, Per-Gunnar Martinsson, and Joel A Tropp. Finding structure with randomness: Probabilistic algorithms for constructing approximate matrix decompositions. *SIAM review*, 53(2):217–288, 2011. 213
- Wolfgang Karl Härdle and Léopold Simar. *Applied multivariate statistical analysis*. Springer Nature, 2007. 64
- F Maxwell Harper and Joseph A Konstan. The movielens datasets: History and context. *Acm transactions on interactive intelligent systems (tiis)*, 5(4):1–19, 2015. 122, 173
- W Keith Hastings. Monte Carlo sampling methods using Markov chains and their applications. *Biometrika*, 57(1):97–109, 1970. 25
- Martin B Haugh. A tutorial on Markov chain Monte Carlo and Bayesian modeling. *Available at SSRN 3759243*, 2021. 22
- Bruce M Hill. Bayesian forecasting of economic time series. *Econometric theory*, 10(3-4): 483–513, 1994. 21
- Peter D Hoff. *A first course in Bayesian statistical methods*. Springer Science & Business Media, 2009. 24, 27, 31, 32, 40, 72, 86, 87
- Matthew D Hoffman, David M Blei, Chong Wang, and John Paisley. Stochastic variational inference. *Journal of Machine Learning Research*, 14(5), 2013. 23
- Changwei Hu, Piyush Rai, and Lawrence Carin. Zero-truncated Poisson tensor factorization for massive binary tensors. *arXiv preprint arXiv:1508.04210*, 2015. 197
- Michael I Jordan and Chris Bishop. An introduction to graphical models, 2004. 143
- Michael I Jordan, Zoubin Ghahramani, Tommi S Jaakkola, and Lawrence K Saul. An introduction to variational methods for graphical models. *Machine learning*, 37(2):183–233, 1999. 23
- Zura Kakushadze. 101 formulaic alphas. *Wilmott*, 2016(84):72–81, 2016. 235, 236
- Herman Kamper. Gibbs sampling for fitting finite and infinite Gaussian mixture models, 2013. 74

- Daniel C Koboldt, Robert S Fulton, Michael D McLellan, Heather Schmidt, Joelle Kalicki-Veizer, Joshua F McMichael, Lucinda L Fulton, David J Dooling, Li Ding, Elaine R Mardis, et al. Comprehensive molecular portraits of human breast tumours. *Nature*, 490 (7418):61–70, 2012. 185, 229
- Yehuda Koren, Robert Bell, and Chris Volinsky. Matrix factorization techniques for recommender systems. *Computer*, 42(8):30–37, 2009. 197
- Samuel Kotz, Tomasz Kozubowski, and Krzysztof Podgórski. *The Laplace distribution and generalizations: A revisit with applications to communications, economics, engineering, and finance*. Number 183. Springer Science & Business Media, 2001. 64
- John Kruschke. Doing Bayesian data analysis: A tutorial with R, JAGS, and Stan. 2014. 34
- PW Lane. Generalized linear models in soil science. *European Journal of Soil Science*, 53 (2):241–251, 2002. 97
- Daniel Lee and H Sebastian Seung. Algorithms for non-negative matrix factorization. *Advances in neural information processing systems*, 13, 2000. 157, 175
- Daniel D Lee and H Sebastian Seung. Learning the parts of objects by non-negative matrix factorization. *Nature*, 401(6755):788–791, 1999. 5, 157
- Daniel D Lee and Hyunjun Sebastian Seung. Algorithms for non-negative matrix factorization. In *14th Annual Neural Information Processing Systems Conference, NIPS 2000*. Neural information processing systems foundation, 2001. 129, 130
- Hyekeyoung Lee and Seungjin Choi. CUR+NMF for learning spectral features from large data matrix. In *2008 IEEE International Joint Conference on Neural Networks (IEEE World Congress on Computational Intelligence)*, pages 1592–1597. IEEE, 2008. 219
- Cornelius T Leondes. *Multidimensional Systems: Signal Processing and Modeling Techniques: Advances in Theory and Applications*. Elsevier, 1995. 120
- Tao Li, Yi Zhang, and Vikas Sindhwani. A non-negative matrix tri-factorization approach to sentiment classification with lexical prior knowledge. In *Proceedings of the Joint Conference of the 47th Annual Meeting of the ACL and the 4th International Joint Conference on Natural Language Processing of the AFNLP*, pages 244–252, 2009. 5
- Edo Liberty, Franco Woolfe, Per-Gunnar Martinsson, Vladimir Rokhlin, and Mark Tygert. Randomized algorithms for the low-rank approximation of matrices. *Proceedings of the National Academy of Sciences*, 104(51):20167–20172, 2007. 213, 222, 234, 239
- Yew Jin Lim and Yee Whye Teh. Variational Bayesian approach to movie rating prediction. In *Proceedings of KDD cup and workshop*, volume 7, pages 15–21. Citeseer, 2007. 5
- Jun Lu. Machine learning modeling for time series problem: Predicting flight ticket prices. *arXiv preprint arXiv:1705.07205*, 2017. 97

- Jun Lu. On the column and row ranks of a matrix. *arXiv preprint arXiv:2112.06638*, 2021a. 214, 250
- Jun Lu. Numerical matrix decomposition. *arXiv preprint arXiv:2107.02579*, 2021b. 6, 7, 9, 91, 100, 102, 106, 109, 120, 121, 177, 214, 217, 218, 222
- Jun Lu. A survey on Bayesian inference for Gaussian mixture model. *arXiv preprint arXiv:2108.11753*, 2021c. 5, 22, 87
- Jun Lu. *A rigorous introduction to linear models*. Eliva Press, 2022a. 32, 33, 49, 84, 97
- Jun Lu. Bayesian low-rank interpolative decomposition for complex datasets. *arXiv preprint arXiv:2205.14825*, 2022b. 213, 222, 231
- Jun Lu. Comparative study of inference methods for interpolative decomposition. *arXiv preprint arXiv:2206.14542*, 2022c. 222
- Jun Lu. Gradient descent, stochastic optimization, and other tales. *arXiv preprint arXiv:2205.00832*, Eliva Press, 2022d. 109, 116
- Jun Lu and Christine P Chai. Robust Bayesian nonnegative matrix factorization with implicit regularizers. *arXiv preprint arXiv:2208.10053*, 2022. 180
- Jun Lu and Joerg Osterrieder. Feature selection via the intervened interpolative decomposition and its application in diversifying quantitative strategies. *arXiv preprint arXiv:2209.14532*, 2022. 213, 222, 233
- Jun Lu and Xuanyu Ye. Flexible and hierarchical prior for Bayesian nonnegative matrix factorization. *arXiv preprint arXiv:2205.11025*, 2022. 132, 157, 168
- Zhanyu Ma, Pravin Kumar Rana, Jalil Taghia, Markus Flierl, and Arne Leijon. Bayesian estimation of Dirichlet mixture model with variational inference. *Pattern Recognition*, 47(9):3143–3157, 2014. 23
- Michael W Mahoney and Petros Drineas. CUR matrix decompositions for improved data analysis. *Proceedings of the National Academy of Sciences*, 106(3):697–702, 2009. 219
- Stephan Mandt and David Blei. Smoothed gradients for stochastic variational inference. *arXiv preprint arXiv:1406.3650*, 2014. 23
- Benjamin M Marlin. Modeling user rating profiles for collaborative filtering. *Advances in neural information processing systems*, 16, 2003. 5
- GJ Marseille, R de Beer, M Fuderer, AF Mehlkopf, and D van Ormondt. Bayesian estimation of MR images from incomplete raw data. In *Maximum Entropy and Bayesian Methods*, pages 13–22. Springer, 1996. 21
- Per-Gunnar Martinsson. Randomized methods for matrix computations. *The Mathematics of Data*, 25(4):187–231, 2019. 217

- Per-Gunnar Martinsson, Vladimir Rokhlin, and Mark Tygert. A randomized algorithm for the decomposition of matrices. *Applied and Computational Harmonic Analysis*, 30(1): 47–68, 2011. 213
- Jose Menchero, D Orr, and Jun Wang. The Barra US equity model (USE4), methodology notes. *English, MSCI (May, 2011)*. 97
- Nicholas Metropolis, Arianna W Rosenbluth, Marshall N Rosenbluth, Augusta H Teller, and Edward Teller. Equation of state calculations by fast computing machines. *The journal of chemical physics*, 21(6):1087–1092, 1953. 25
- Andriy Mnih and Russ R Salakhutdinov. Probabilistic matrix factorization. *Advances in neural information processing systems*, 20, 2007. 5
- Raphael A Mrode. *Linear models for the prediction of animal breeding values*. Cabi, 2014. 97
- Kevin P Murphy. Conjugate Bayesian analysis of the Gaussian distribution. *def*, 1(2 σ 2): 16, 2007. 49, 74, 81
- Kevin P Murphy. *Machine learning: A probabilistic perspective*. MIT press, 2012. 74, 78, 86, 87, 88
- Yann Ollivier. Laplace’s rule of succession in information geometry. In *International Conference on Geometric Science of Information*, pages 311–319. Springer, 2015. 31
- Pentti Paatero and Unto Tapper. Positive matrix factorization: A non-negative factor model with optimal utilization of error estimates of data values. *Environmetrics*, 5(2): 111–126, 1994. 129, 157
- Pentti Paatero, Unto Tapper, Pasi Aalto, and Markku Kulmala. Matrix factorization methods for analysing diffusion battery data. *Journal of Aerosol Science*, 22:S273–S276, 1991. 157
- Ulrich Paquet, Sean Holden, and Andrew Naish-Guzman. Bayesian hierarchical ordinal regression. In *International Conference on Artificial Neural Networks*, pages 267–272. Springer, 2005. 205
- V Paul Pauca, Jon Piper, and Robert J Plemmons. Nonnegative matrix factorization for spectral data analysis. *Linear algebra and its applications*, 416(1):29–47, 2006. 130
- Dong Qian, Bei Wang, Xiangyun Qing, Tao Zhang, Yu Zhang, Xingyu Wang, and Masatoshi Nakamura. Bayesian nonnegative CP decomposition-based feature extraction algorithm for drowsiness detection. *IEEE Transactions on neural systems and rehabilitation engineering*, 25(8):1297–1308, 2016. 7
- Piyush Rai, Yingjian Wang, and Lawrence Carin. Leveraging features and networks for probabilistic tensor decomposition. In *Proceedings of the AAAI Conference on Artificial Intelligence*, volume 29, 2015. 7

- Tapani Raiko, Alexander Ilin, and Juha Karhunen. Principal component analysis for large scale problems with lots of missing values. In *European Conference on Machine Learning*, pages 691–698. Springer, 2007. 5
- Rajesh Ranganath, Sean Gerrish, and David Blei. Black box variational inference. In *Artificial intelligence and statistics*, pages 814–822. PMLR, 2014. 23
- Carl Edward Rasmussen. Gaussian processes in machine learning. In *Summer school on machine learning*, pages 63–71. Springer, 2003. 32, 33
- Christian P Robert et al. *The Bayesian choice: from decision-theoretic foundations to computational implementation*, volume 2. Springer, 2007. 40
- Ruslan Salakhutdinov and Andriy Mnih. Bayesian probabilistic matrix factorization using Markov chain Monte Carlo. In *Proceedings of the 25th international conference on Machine learning*, pages 880–887, 2008. 6, 141, 150
- Lawrence R Schaeffer. Application of random regression models in animal breeding. *Livestock Production Science*, 86(1-3):35–45, 2004. 97
- Mark F Schilling, Ann E Watkins, and William Watkins. Is human height bimodal? *The American Statistician*, 56(3):223–229, 2002. 42
- Mikkel N Schmidt and Shakir Mohamed. Probabilistic non-negative tensor factorization using Markov chain Monte Carlo. In *2009 17th European Signal Processing Conference*, pages 1918–1922. IEEE, 2009. 166, 172
- Mikkel N Schmidt, Ole Winther, and Lars Kai Hansen. Bayesian non-negative matrix factorization. In *International Conference on Independent Component Analysis and Signal Separation*, pages 540–547. Springer, 2009. 157, 159
- Matthias Seeger. Low rank updates for the Cholesky decomposition. Technical report, 2004. 91
- Stanley Smith Stevens. On the theory of scales of measurement. *Science*, 103(2684):677–680, 1946. 205
- Gilbert Strang. *Linear algebra and learning from data*. Wellesley-Cambridge Press Cambridge, 2019. 97
- Gilbert Strang. *Linear algebra for everyone*. Wellesley-Cambridge Press Wellesley, 2021. 97, 214
- Gilbert Strang and Cleve Moler. LU and CR elimination. *SIAM Review*, 64(1):181–190, 2022. 214
- Panagiotis Symeonidis and Andreas Zioupos. *Matrix and Tensor Factorization Techniques for Recommender Systems*, volume 1. Springer, 2016. 5

- Gábor Takács and Domonkos Tikk. Alternating least squares for personalized ranking. In *Proceedings of the sixth ACM conference on Recommender systems*, pages 83–90, 2012. 101
- Hiromu Takayama, Qibin Zhao, Hidekata Hontani, and Tatsuya Yokota. Bayesian tensor completion and decomposition with automatic CP rank determination using MGP shrinkage prior. *SN Computer Science*, 3(3):1–17, 2022. 7
- VY Tan and C Févotte. Automatic relevance determination in nonnegative matrix factorization with the β -divergence. *IEEE Transactions on Pattern Analysis and Machine Intelligence*, 35(7):1592–1605, 2013. 157, 162
- Yee Whye Teh. Exponential families: Gaussian, Gaussian-Gamma, Gaussian-Wishart, multinomial, 2007. 74
- Luke Tierney. A note on Metropolis-Hastings kernels for general state spaces. *Annals of applied probability*, pages 1–9, 1998. 26
- Lloyd N Trefethen and David Bau III. *Numerical linear algebra*, volume 50. SIAM, 1997. 97
- Igor Tulchinsky. *Finding Alphas: A quantitative approach to building trading strategies*. John Wiley & Sons, 2019. 234
- Valentin F Turchin. On the computation of multidimensional integrals by the Monte-Carlo method. *Theory of Probability & Its Applications*, 16(4):720–724, 1971. 26, 27
- Seppo Virtanen, Arto Klami, and Samuel Kaski. Bayesian CCA via group sparsity. In *Proceedings of the 28th International Conference on International Conference on Machine Learning*, pages 457–464, 2011. 141, 148
- Seppo Virtanen, Arto Klami, Suleiman Khan, and Samuel Kaski. Bayesian group factor analysis. In *Artificial Intelligence and Statistics*, pages 1269–1277. PMLR, 2012. 141, 148
- Jim Jing-Yan Wang, Xiaolei Wang, and Xin Gao. Non-negative matrix factorization by maximizing correntropy for cancer clustering. *BMC bioinformatics*, 14(1):1–11, 2013. 5
- Pascal Wild and WR Gilks. Algorithm AS 287: Adaptive rejection sampling from log-concave density functions. *Journal of the Royal Statistical Society. Series C (Applied Statistics)*, 42(4):701–709, 1993. 27
- Wanjuan Yang, Jorge Soares, Patricia Greninger, Elena J Edelman, Howard Lightfoot, Simon Forbes, Nidhi Bindal, Dave Beare, James A Smith, I Richard Thompson, et al. Genomics of drug sensitivity in cancer (GDSC): A resource for therapeutic biomarker discovery in cancer cells. *Nucleic Acids Research*, 41(D1):D955–D961, 2012. 184
- Mingyuan Zhou, Chunping Wang, Minhua Chen, John Paisley, David Dunson, and Lawrence Carin. Nonparametric Bayesian matrix completion. In *2010 IEEE Sensor Array and Multichannel Signal Processing Workshop*, pages 213–216. IEEE, 2010. 6

Abdelhak M Zoubir, Visa Koivunen, Yacine Chakhchoukh, and Michael Muma. Robust estimation in signal processing: A tutorial-style treatment of fundamental concepts. *IEEE Signal Processing Magazine*, 29(4):61–80, 2012. 181

Alphabetical Index

- l_1 constraint, 161
- l_1 norm, 115, 161, 176
- l_2 norm, 115
- l_∞ norm, 115
- l_p norm, 115, 176

- ALS, 101
- Alternating update, 129
- Aoordinate descent algorithm, 101
- Automatic relevance determination, 148, 161, 194, 229

- Basis, 10
- Bayes' theorem, 21
- Bayesian inference, 132
- Bayesian linear regression, 148
- Bayesian matrix decomposition, 132
- Bayesian optimization, 132
- Binomial distribution, 67

- Chi-squared distribution, 49
- Collaborative filtering, 5
- Column space, 10
- Conditional independence, xx
- Conjugacy, 161
- Conjugate prior, 40
- Consistency, 184, 186
- Continuously differentiability, 16
- Contour plot, 113
- Convex function, 113

- Convexity, 101
- Covariance, xx
- Cramer's rule, 215

- Decomposition: ALS, 100
- Decomposition: CUR, 219
- Decomposition: GBT, 223
- Decomposition: GBT with ARD, 229
- Decomposition: GBTN, 223
- Decomposition: GEE, 157
- Decomposition: GEEA, 161
- Decomposition: GEG, 190
- Decomposition: GGG, 141
- Decomposition: GGGA, 148
- Decomposition: GGGM, 146
- Decomposition: GGGW, 150
- Decomposition: GL_1^2 , 177
- Decomposition: GL_2^2 , 180
- Decomposition: GL_∞ , 180
- Decomposition: G_nVG , 190
- Decomposition: GRR, 168
- Decomposition: GRRN, 168
- Decomposition: GTT, 163
- Decomposition: GTTN, 166
- Decomposition: GVG, 152
- Decomposition: IID, 233
- Decomposition: NMF, 129
- Decomposition: NMTF, 191
- Decomposition: OGGW, 205

- Decomposition: PAA, 197
 Decomposition: PAAA, 199
 Decomposition: Skeleton, 219
 Derivative, xx
 Determinant, xix
 Dimension, 10
- Eigenvalue, 9
 Eigenvector, 9
 Element-wise product, *see* Hadamard product
 Exponential distribution, 56, 189
 Exponentially rectified-normal distribution, 61, 168
- Frobenius norm, 16
 Fundamental spaces, 12
 Fundamental theorem of linear algebra, 12
- Gamma distribution, 43, 162
 Gaussian distribution, 41
 General-truncated-normal distribution, 59, 223
 Geometrical interpretation, 113
 Global minimum, 101
 Gradient descent, 109, 111
 Graph, xix
 Greedy search, 111
- Hadamard product, xix, 106
 Half-normal distribution, 61
 Hessian matrix, xx
 Hidden features, 108
 Hierarchical prior, 166, 168
 Hyperprior, 149, 162, 166
- Implicit hierarchy, 133
 Independence, xx
 Inner product, 108
 Integral, xx
 Inverse-Gamma distribution, 46, 143, 161, 223
 Inverse-Gaussian distribution, 63
 Inverse-Wishart distribution, 207
- Jacobian matrix, xx
- Joint conjugate prior, 52
- Kullback-Leibler divergence, xx, 129
- Laplace distribution, 64
 Least squares, 97
 Level curves, 111
 Level surfaces, 111
 Linear approximation, 111
 Linear model, 148
 Linear regression, 148
 Linear update, 111
 Linearly independent, 9
 Link prediction, 5
 LU decomposition, 109
- Machine precision, 130
 Markov blanket, 149, 159, 161, 163, 169, 178
 Markov chain Monte Carlo, 21
 Matlab-style notation, 8
 Matrix, xviii, xix
 Matrix indexing, xix
 Matrix inverse, 109
 Matrix norm, 15
 Matrix rank, 11
 Missing entries, 106
 Multinomial distribution, 67
 Multiplicative update, 129
 Multivariate Student's t distribution, 77
- Netflix, 100
 Netflix recommender, 106
 NMF, 128
 Nonnegativity constraint, 129
 Norm, xxi
 Normal-inverse-Chi-squared distribution, 52
 Normal-inverse-Gamma distribution, 48
 Normal-inverse-Wishart distribution, 81
 Notation, xviii
 Null space, 10
 Numerical rank, 6
- Orthogonal matrix, 13
 Overfitting, 113, 132

- Poisson distribution, 72
Positive definite, 14
Positive semidefinite, 14
Projection gradient descent, 113
- Rank, 10, 11
Rectified-normal distribution, 61, 161, 166, 168
Regularization, 105, 113, 130
RN-scaled-normal-Gamma prior, 168
- Scalar, xviii, xix
Second-order partial derivative, 16
Semi-nonnegative matrix factorization, 189
Set, xix
Sets, xviii
Shannon entropy, xx
Sigmoid, xxi, 233
Skew-Laplace distribution, 66
Softplus, xxi
Span, 9
Sparsity, 115, 129, 161, 176
- Spectral radius, 9
Spectrum, 9
Stochastic coordinate descent, 115
Stochastic gradient descent, 109, 115
Student's t distribution, 42
Subspace, 9
- Taylor's expansion, 245
Taylor's formula, 245
Tensor, xviii, xix
TN-scaled-normal-Gamma (TNSNG) prior, 166
Transpose, xix
Truncated, 122
Truncated SVD, 122
Truncated-normal distribution, 57, 163
- Unit ball, 115
- Variance, xx
Vector, xviii, xix
Vector norm, 15
- Wishart distribution, 78